John J. Qu • William T. Sommers
Ruixin Yang • Allen R. Riebau
Editors

Remote Sensing and Modeling Applications to Wildland Fires

TSINGHUA UNIVERSITY PRESS

Springer

John J. Qu William T. Sommers
Ruixin Yang Allen R. Riebau *Editors*

Remote Sensing and Modeling Applications to Wildland Fires

John J. Qu   William T. Sommers
Ruixin Yang   Allen R. Riebau   *Editors*

Remote Sensing and Modeling Applications to Wildland Fires

With 109 figures

TSINGHUA UNIVERSITY PRESS   Springer

Editors:
Prof. John J. Qu
Environmental Science and Technology Center,
Department of Geography and Geoinformation Science,
College of Science, George Mason University,
4400 University Drive, Fairfax, VA 22030, USA
Email: jqu@gmu.edu

Prof. Ruixin Yang
Department of Geography and Geoinformation Science,
College of Science, MS 6C3, George Mason University, 4400 University Drive,
Fairfax, VA 22030, USA
Email: ryang@gmu.edu

Dr. William T. Sommers
Environmental Science and Technology Center,
College of Science, George Mason University,
4400 University Drive, Fairfax, VA 22030, USA
Email: wsommers@gmu.edu

Dr. Allen R. Riebau
Nine Points South Technical Pty, Ltd.,
P.O.Box 2419, Clarkson, Western Australia 6030, Australia
Email: ariebau@ninepointsouth.com.au

ISBN 978-7-302-28861-9
Tsinghua University Press, Beijing

ISBN 978-3-642-32529-8 ISBN 978-3-642-32530-4 (eBook)
Springer Heidelberg Dordrecht London New York

Library of Congress Control Number: 2012944169

Printed on acid-free paper

Springer is part of Springer Science+Business Media (www.springer.com)

John J. Qu   William T. Sommers
Ruixin Yang   Allen R. Riebau

遥感及模式在森林火灾中的应用

Remote Sensing and Modeling Applications to Wildland Fires

John J. Qu　William T. Sommers
Ruixin Yang　Allen R. Riebau

遥感及模式在森林火灾中的应用

Remote Sensing and Modeling Applications to Wildland Fires

With 109 figures

TSINGHUA UNIVERSITY PRESS

Springer

图书在版编目(CIP)数据

遥感及模式在森林火灾中的应用= Remote Sensing and Modeling Applications to Wildland Fires 英文/(美)曲(Qu), (美)萨默斯(Sommers, W.), 杨瑞新等主编. --北京：清华大学出版社，2013. 1

ISBN 978-7-302-28861-9

Ⅰ.①野…　Ⅱ.①曲… ②萨… ③杨…　Ⅲ.①遥感技术–应用–火灾监测–英文 Ⅳ.①TU998.12

中国版本图书馆 CIP 数据核字(2012)第 104727 号

责任编辑：薛　慧
责任校对：王淑云
责任印制：

出版发行：清华大学出版社　　地　　址：北京清华大学学研大厦 A 座
http://www.tup.com.cn　　邮　　编：100084
社 总 机：010-62770175　　邮　　购：010-62786544
投稿与读者服务：010-62776969, c-service@tup.tsinghua.edu.cn
质量反馈：010-62772015, zhiliang@tup.tsinghua.edu.cn
印 装 者：
经　　销：全国新华书店
开　　本：153mm×235mm　　印张：24.75　　字数：560 千字
版　　次：2013 年 1 月第 1 版　　印次：2013 年 1 月第 1 次印刷
印　　数：1～0000
定　　价：00.00 元

产品编号：

Foreword

Wildfires intrude on public awareness only periodically, when blazes in particular parts of the United States, mainly in the West, cause a level of destruction and disruption that wins attention from the national news. But particular groups of American, and particular professional categories, pay more consistent attention to the incidence and impact of wild fires. And there is some general understanding the wildfires risk becoming more devastating in future, because of climate changes and because expansion of urban sprawls put more and more communities in the midst of potential hazards.

In this context, it is important to recognize that expanding branches of science are available to help explore the phenomenon, facilitating prediction and management alike. This book, building on the expansion of computational facilities at George Mason University's EastFIRE Lab and on other research contributions, provides important evidence of the relevance of remote sensing and modeling to understanding wildland fires and to the provision of effective management decisions. The issue is national and international alike, and the contributions of a growing global community of scholars to this focus for remote sensing provides a vigorous basis for further research and for advanced training. This book deals principally with the eastern United States, where issues are less familiar to a wider public but the potential problems are acute. However, the findings and procedures have broader applicability, as an important sub-discipline steadily gains in maturity and visibility.

Peter N. Stearns
Provost, George Mason University
June 16, 2011

Contents

List of Contributors

Dr. Gary L. Achtemeier
Center for Forest Disturbance Science, USDA Forest Service, 320 Green Street, Athens, GA 30602, USA
Email: gachtemeier@fs.fed.us

Mr. Stephen Ambrose
NASA Headquarters, Washington, DC 20546, USA
Email: sambrose@nasa.gov

Mr. Thomas Bobbe
Remote Sensing Applications Center, USDA Forest Service, 2222 West 2300 South, Salt Lake City, UT 84119, USA
Email: tbobbe@fs.fed.us

Mr. Johnny L. Boggs
Eastern Forest Environmental Treat Assessment Center, USDA Forest Service, Raleigh, NC 27606, USA
Email: jboggs@fs.fed.us

Dr. Kirk Borne
George Mason University, Fairfax, Virginia 22030, USA
Email: kborne@gmu.edu

Dr. Luigi Boschetti
Department of Geography, University of Maryland, 2181 LeFrak Hall, College Park, MD 20742, USA
Email: luigi.boschetti@hermes.geog.umd.edu

Mr. Robert A. Carr
Eastern Regional Office, USDA Forest Service, 626 E. Wisconsin Avenue, Milwaukee, WI 53202, USA
Email:racarr@fs.fed.us

Dr. Joseph Charney
Northern Research Station, USDA Forest Service, East Lansing, MI, USA
Email: jcharney@fs.fed.us

Dr. Jiquan Chen
Department of Environmental Sciences, University of Toledo, Bowman-Oddy Laboratories, Mail Stop 604, Toledo, OH 43606, USA
Email: Jiquan.Chen@utoledo.edu

Mr. Phil Cheney
Australian Commonwealth Scientific Research Organization ACT, Australia
Email: phil.cheney@gmail.com

Mr. Yuechen Chi
George Mason University, Fairfax, Virginia 22030, USA
Email: ychi@mason.gmu.edu

Dr. David C. Chojnacky
Department of Forestry, Virginia Tech., Falls Church, VA 22046, USA
Email: dchoj@cox.net

Dr. Kenneth Clark
Northern Research Station, USDA Forest Service, Newtown Square, PA 19073, USA
Email: kennethclark@fs.fed.us

Ms. Erika Cohen
Eastern Forest Environmental Treat Assessment Center, USDA Forest Service, Raleigh, NC 27606, USA
Email: erika_cohen@ncsu.edu

Dr. Ivan A. Csiszar
NOAA/NESDIS Center for Satellite Applications and Research, 5200 Auth Road, Camp Springs, MD 20746, USA
Email: ivan.csiszar@noaa.gov

Dr. Philip Cunningham
Earth and Environmental Sciences Division, Los Alamos National Laboratory, Los Alamos, New Mexico 87545, USA
Email: pcunning@lanl.gov

Dr. Diane Davies
Department of Geography, University of Maryland, 2181 LeFrak Hall, College Park, MD 20742, USA
Email: ddavies@hermes.geog.umd.edu

Dr. Christopher D. Elvidge
NOAA National Geophysical Data Center, 325 Broadway, Boulder, CO 80303, USA
E-mail: Chris.Elvidge@noaa.gov

Dr. David D. Evans
Home Safety Foundation, 3 Magnolia Parkway, Chevy Chase, MD 20815, USA
Email: devans@smartsafety.org

Dr. Douglas G. Fox
Nine Points South Technical Pty, Ltd., P.O. Box 2419, Clarkson, Western Australia 6030, Australia
Email: dgfox@comcast.net

Mr. Michael J. Gavazzi
Eastern Forest Environmental Treat Assessment Center, USDA Forest Service, Raleigh, NC 27606, USA
Email:mgavazzi@fs.fed.us

Dr. Johann G. Goldammer
Global Fire Monitoring Center, Max Planck Institute for Chemistry c/o Freiburg University, Georges-Koehler-Allee 75 D – 79110, Freiburg, Germany
Email: johann.goldammer@fire.uni-freiburg.de

Dr. Scott L. Goodrick
Center for Forest Disturbance Science, USDA Forest Service, Athens, Georgia 30602, USA
Email: sgoodrick@fs.fed.us

Mr. Jim Gould
Australian Commonwealth Scientific Research Organization ACT, Australia
Email: Jim.Gould@csiro.au

Dr. William J. de Groot
Natural Resources Canada, Canadian Forest Service Great Lakes Forestry Centre, 1219 Queen Street East, Sault Ste. Marie, ON P6A 2E5, Canada
Email: bill.degroot@NRCan.gc.ca

Dr. Deborah E. Hanley
AWS Truepower, LLC, 463 New Karner Road, Albany, NY 12205, USA
Email: dhanley@awstruepower.com

Dr. Xianjun Hao
Environmental Science and Technology Center, Department of Geography and Geoinformation Science, College of Science, George Mason University, 4400 University Drive, Fairfax, VA 22030, USA
Email: xhao1@gmu.edu

Dr. Heath Hockenberry
Office of Climate, Water, and Weather Services, NOAA National Weather Service, 1325 East West Highway, Silver Spring, MD 20910, USA
Email: Heath.Hockenberry@noaa.gov

Dr. John L. Hom
Northern Research Station, USDA Forest Service, Newtown Square, PA 19073, USA
Email: jhom@fs.fed.us

Dr. Zhenping Huang
University of Virginia, Charlottesville, Virginia 22904, USA
Email: zh2a@virginia.edu

Dr. Elliot Jacks
Office of Climate, Water, and Weather Services, NOAA National Weather Service, 1325 East West Highway, Silver Spring, MD 20910, USA
Email: Elliot.Jacks@noaa.gov

Dr. Mary Ann Jenkins
Department of Earth and Space Science and Engineering, York University, Toronto, Canada
Email: maj@yorku.ca

Dr. Yimin Ji
Wyle Information System, 1651 Old Meadow RD, McLean, VA 22102, USA
Email: yimin.ji-1@nasa.gov

Dr. W. Matt Jolly
Rocky Mountain Research Station Fire Sciences Laboratory, US Forest Service, 5775 Hwy 10 W, Missoula, MT 59808, USA
Email: mjolly@fs.fed.us

Dr. Christopher O. Justice
Department of Geography, University of Maryland, 2181 LeFrak Hall, College Park, MD 20742, USA
Email: justice@hermes.geog.umd.edu

Dr. Stefania Korontzi
Department of Geography, University of Maryland, 2181 LeFrak Hall, College Park, MD 20742, USA
Email: stef@hermes.geog.umd.edu

Dr. Jacob J. LaCroix
Scenarios Network for Alaska and Arctic Planning, University of Alaska, Fairbanks, 3352 College Road, Fairbanks, Alaska 99709, USA
Email: jlacroix@alaska.edu

Dr. Qinglin Li
Forest Analysis and Inventory Branch, Ministry of Forests and Range, 6th 727 Fisgard St, Victoria, BC V8T 9W3, Canada
Email: Qinglin.li@gov.bc.ca

Dr. Yongqiang Liu
Center for Forest Disturbance Science, USDA Forest Service, 320 Green Street, Athens, GA 30602, USA
Email: yliu@fs.fed.us

Dr. Eckehard Lorenz
Deutsches Zentrum für Luft- und Raumfahrt Optical Information Systems, Rutherfordstrasse 2, Berlin D-12489, Germany
Email: eckehard.lorenz@dlr.de

Mr. Timothy Lynham
Natural Resources Canada, Canadian Forest Service Great Lakes Forestry Centre, 1219 Queen Street East, Sault Ste. Marie, ON P6A 2E5, Canada
Email: tim.lynham@nrcan.gc.ca

Dr. Steven G. McNulty
Eastern Forest Environmental Treat Assessment Center, USDA Forest Service, Raleigh, NC 27606, USA
Email: smcnulty@fs.fed.us

Dr. William Mell
Pacific Wildland Fire Sciences Laboratory, US Forest Service, 400 N 34th St., Suite 201, Seattle, WA 98103
Email: wemell@fs.fed.us

Dr. Jerome Miller
NASA/Goddard Space Flight Center, Greenbelt, Maryland 20771, USA
Email: Jerome.Miller-1@nasa.gov

Mr. Bill Millinor
Jones Edmunds & Associates Inc., 730 Northeast Waldo Road, Gainesville, FL 32641-5699, USA
Email: wmillinor@jonesedmunds.com

Ms. Jennifer A. Moore Myers
Eastern Forest Environmental Treat Assessment Center, USDA Forest Service, Raleigh, NC 27606, USA
Email: jmooremyers@fs.fed.us

Dr. Gregory J. Nowacki
Eastern Regional Office, USDA Forest Service, 626 E. Wisconsin Avenue, Milwaukee, WI 53202, USA
Email: gnowacki@fs.fed.us

Dr. Dieter Oertel
Deutsches Zentrum für Luft- und Raumfahrt Optical Information Systems, Rutherfordstrasse 2, Berlin D-12489, Germany
Email: Dieter.Oertel@dlr.de

Dr. Elaine M. Prins
Cooperative Institute for Meteorological Satellite Studies, University of Wisconsin-Madison, 1225 W. Dayton St., Madison, WI 53706, USA
Email: elaine.prins@ssec.wisc.edu

Prof. John J. Qu
Environmental Science and Technology Center, Department of Geography and Geoinformation Science, College of Science, George Mason University, 4400 University Drive, Fairfax, VA 22030, USA
Email: jqu@gmu.edu

Mr. Brad Quayle
Remote Sensing Applications Center, USDA Forest Service, 2222 West 2300 South, Salt Lake City, UT 84119, USA
Email: bquayle@fs.fed.us

Dr. Ronald G. Rehm
RGR Consulting, LLC, 405 W. Montgomery Ave., Rockville, MD 20850, USA
Email: rehmro@comcast.net

Dr. Allen R. Riebau
Nine Points South Technical Pty, Ltd., P.O. Box 2419, Clarkson, Western Australia 6030, Australia
Email: ariebau@ninepointsouth.com.au

Prof. David P. Roy
Geographic Information Science Center of Excellence, South Dakota State University, Wecota Hall, Box 506B, Brookings, SD 57007, USA
Email: david.roy@sdstate.edu

Dr. Soung-Ryoul Ryu
Department of Renewable Resources, University of Alberta, 713C General Services, Edmonton, AB T6G 2H1, Canada
Email: soung.ryu@ualberta.ca

Dr. William T. Sommers
Environmental Science and Technology Center, College of Science, George Mason University, 4400 University Drive, Fairfax, VA 22030, USA
Email: wsommers@gmu.edu

Ms. Christine M. Stalling
Missoula Forestry Sciences Lab, Rocky Mountain Research Station, 800 East Beckwith, Missoula, MT 59801, USA
Email: cstalling@fs.fed.us

Dr. John A. Stanturf
Center for Forest Disturbance Science, US Forest Service, 320 Green St., Athens, GA 30602, USA
Email: jstanturf@fs.fed.us

Dr. George Stephens
NOAA NESDIS (ret.), 511 Deerfield Ave., Silver Spring, MD 20910, USA
Email: George.stephens@verizon.net

Dr. Erich Franz Stocker
NASA/GSFC, Code 610.2, Greenbelt, MD 20771, USA
Email: Erich.F.Stocker@nasa.gov

Ms. Sara E. Strickland
Eastern Forest Environmental Treat Assessment Center, USDA Forest Service, Raleigh, NC 27606, USA
Email: sstrickland@fs.fed.us

Dr. Brian Thomas
University of Maryland, College Park, Maryland 20742, USA
Email: thomas@astro.umd.edu

Dr. Wanting Wang
Environmental Science and Technology Center, Department of Geography and GeoInformation Science, College of Science, George Mason University, 4400 University Drive, Fairfax, VA 22030, USA
Email: wwang1797@gmail.com

Prof. Michael C. Wimberly
GISc Center of Excellence, South Dakota State University, Brookings, SD 57007-3510, USA
Email: michael.wimberly@sdstate.edu

Prof. Ruixin Yang
Department of Geography and Geoinformation Science, College of Science, MS 6C3, George Mason University, 4400 University Drive, Fairfax, VA 22030, USA
Email: ryang@gmu.edu

Dr. Daolan Zheng
Department of Natural Resources & the Environment, University of New Hampshire, Durham, NH 03824, USA
Email: daolan.zheng@unh.edu

1 Introduction to Remote Sensing and Modeling Applications to Wildland Fires

John J. Qu and Xianjun Hao

Environmental Science and Technology Center, Department of Geography and Geoinformation Science, College of Science, George Mason University, Fairfax, VA 22030, USA

Email: jqu@gmu.edu, xhao1@gmu.edu

Abstract Wildland fire is one of the most disastrous natural hazards threatening life and properties. The rapid growth of wildland-urban interface since last century has increased the complexity of fire management. It is important to exploit new technologies for fire risk assessment, fuel management, wildland fire detection, fire behavior modeling, smoke emissions estimation, and analysis of fire impacts on air quality. This book contains 23 chapters, covering various topics related wildland fires, including satellite remote sensing applications for fire detection and monitoring, fire behavior simulation, smoke emissions and monitoring, and fuel managements. It can be used as a reference book for graduate students and researchers interested in wildland fire study.

Keywords Wildland fires, Remote sensing, Fire behavior model, Air quality, Fire management

Wildland fire is one of major natural hazards. For the last century, North American forest communities have been vitally concerned with wildland fires. They have tried to eliminate wildland fires entirely, to reduce fire intensity, to thin and burn, and even to return to a more naturally occurring wildland fire regime. Urban and suburban growth through the 20th century has dramatically increased the association of housing and people with wildlands, increasing the complexity of fuel management and fire fighting activities. Since topography, climate, ecosystems, and development patterns are all so different in east and west, it is time for a focused look at these issues from an eastern perspective. The EastFIRE conference brings together researchers, subject matter experts, technicians, vendors, and decision makers to share information on using remote sensing (RS), decision support systems and simulation to better manage wildland fire in the eastern United States. Planned products of this conference will capture the significant outcomes for determining future plans of action.

The core of this book arose from the EastFIRE conference held at George Mason university May 11 – 13, 2005 (http://eastfire.gmu.edu/workshop). The primary objectives of the conference are: ① Develop bridging approaches that link ecology and the physical sciences at local, landscape, state, and regional scales for wildland fire in the east. ② Suggest decision support views of integrated data for policy makers and front-line decision-makers. ③ Share information on new technologies and techniques which address eastern states fire management issues. ④ Create new understanding of the challenges ahead for eastern states wildland fire management and how RS might better address them. ⑤ Create appreciation for geographic scale issues in wildland fire management and rehabilitation in the east, and descriptions of experiences in applying RS and simulation modeling to these issues. The Conference would accelerate coalescence of scientists and managers around a strategy aimed at providing timely, cost effective, and technically appropriate fire related information to the broad and diverse fire community of the Eastern United States. We believe that the conference was largely successful in providing that acceleration. Over 111 papers were delivered at the conference covering, by over 100 authors representing a diverse area of public and private institutions. Based on session chairs' suggestions, the EastFIRE conference editorial board selected 28 tentative chapters for the book.

We proposed five sessions: ① research needs and programs; ② fire-atmosphere, ③ fire-RS; ④ fire-modeling, and ⑤ Fuels and impacts. This book can be use a reference book for graduate and under graduate students. This book includes 23 chapters in total.

In Chapter 2, Dr. William T. Sommers discusses "Wildland Fire and Eastern states diversity" (Sommers, 2010), provides an introduction of wildland fires in the Eastern United States. Much of wildland fire management, research and resource allocation in the United States is focused on the Western states, while the Eastern states are different from the west in terms of ecosystems, climate, land use, and demographics etc., it is necessary to study the characteristics of wildland fires in the eastern states so as to meet the diverse needs of eastern fire managements.

In Chapter 3, Dr. John A. Stanturf and Dr. Michael C. Wimberly analyze demographic trends in the Eastern United States and the impacts on fire management (Stanturf et al., 2010). The changing demographics and growing wildland urban interface (WUI) of the Eastern United States were characterized, and the implications for the land manager of the expansion of dense human settlements into fire-affected forests were discussed. To improve the capability of fire risk estimation and fire monitoring, land managers and policy makers need to exploit new approaches, such as RS and geographic information systems, to monitor land use change and update the WUI.

Dr. LeRoy Spayd provides an overview of NOAA's fire weather, climate and air quality forecast products and services in Chapter 4 (Spayd, 2010). NOAA's national weather service's (NWS) fire weather program provides timely fire weather data and forecasts, which are critical to wildland firefighting and resource management. NWS climate services provide data products of major drought indicators, as well as services for drought monitoring and prediction. For air quality forecast, NOAA and the environmental protection agency (EPA) have teamed together to develop a national air quality forecasting (AQF) system.

Dr. Douglas G. Fox, Dr. Allen R. Riebau, and Dr. Pete Lahm review wildland fire and air quality management in Chapter 5 (Fox et al., 2010). Wildland fire and smoke can make significant contribution to air pollution. Smoke emissions from fires that are not "natural", such as prescribed fire and agricultural burning, need to be planned, managed, and mitigated in the same way as other air pollution sources. US regional Haze rule and national ambient air quality standard for particulate material are described, as well as recommendations for strategic and tactical planning, operations and evaluation of smoke management activities.

High resolution numerical models for smoke transport in plumes from wildland fires are discussed by Dr. Philip Cunningham and Dr. Scott L. Goodrick in Chapter 6 (Cunningham et al., 2010). It is a critical problem to predict the impacts of wildland fires and prescribed burnings on air quality, especially in the Eastern United States where wildfire-prone regions are often located near populated areas. While various models are available for modeling the air quality impacts of smoke from wildland fires, it is of particular interest, to explore the fundamental dynamics of buoyant plumes arising from intense heat sources to assess the utility and accuracy of the models and identify situations in which these models may have significant errors. The details of a high-resolution large-eddy simulation (LES) model are described, and the basic time-averaged properties of the simulated plumes and their dependence on the heat source strength and the ambient wind are analyzed.

Weather is one of key factors leading to extreme wildfire behavior, and may have significant impact on fire intensity. In Florida, sea-breeze circulations are frequently observed to have a significant impact on fire behavior, but the interaction between wildfires and the sea-breeze is still poorly understood. In Chapter 7, Dr. Deborah E. Hanley, Dr. Philip Cunningham, and Dr. Scott L. Goodrick conduct insight analysis based on radar observations and numerical simulations to explore the interaction between a buoyant plume and a density current (Hanley et al., 2010).

In Chapter 8, Dr. Gary L. Achtemeier, Dr. Yongqiang Liu, and Dr. Scott L. Goodrick review efforts in investigating the air quality impacts of prescribed fires in the southern United States (Achtemeier et al., 2010). Tools for smoke transport and the regional air quality modeling of prescribed burns, SHRMC-4S and Daysmoke, are described. SHRMC-4S is a framework for smoke and air quality modeling focused on prescribed fires in the southern United States. Daysmoke is a plume model that incorporates a human factor to assist land managers in prescribed burning. Applications of SHRMC-4S and Daysmoke are illustrated with case studies.

As one of the major natural disasters, wildland fires release large amount of particulate matter (PM) and ozone precursors that adversely affect regional air quality. Emissions from wildland fires can cause severe environmental consequences. Dr. Yongqiang Liu, Dr. John J. Qu, Dr. Wanting Wang, and Dr. Xianjun Hao discuss calculation and analysis of fire emissions (Liu et al., 2010) in Chapter 9. Approaches for fire emission calculation and techniques for fuel and fire properties estimation are reviewed briefly. Uncertainty in fire emission estimation is analyzed. And future works for fire emission research are discussed.

Foliar phenology significantly influences the exchange of mass, energy and momentum between the Earth's surface and its atmosphere (Jolly, 2010). In Chapter 10, Dr. Jolly presents a phenology monitoring system that combines satellite-derived vegetation indices from the advanced very high resolution radiometer (AVHRR) and surface weather data (Jolly, 2010). It is the first of its kind to integrate RS and surface weather-based models to determine green up dates and green factors. The system provides friendly web-based user interface that is suitable for use by land managers and general public.

In Chapter 11, Dr. Bill Millinor, Dr. Hugh Devine, and Dr. Elizabeth Eastman present the development of a comprehensive database that can be used to crosswalk formation-level vegetation maps to NFFL fuel-model maps (Millinor, 2010). Fuel type and fuel load are critical to the performance of fire behavior models. Current fire models reply heavily on national fire fuel laboratory (NFFL) fuel-classification procedures. It is found that there was a one-to-one relationship between vegetation type and NFFL fuel models for mid-Atlantic Eastern United States forests. This chapter investigates the vegetation type-fuel model relationship in eight additional Northeastern national parks, with focus on the development of a comprehensive database.

Although the primary objective of the tropical rainfall measuring mission (TRMM) is to improve observations and understanding of the tropical rainfall variability, the visible infrared scanner (VIRS) on board TRMM has the capability of producing continuous global fire data set over tropics and subtropics. In Chapter 12, Dr. Yimin Ji and Dr. Erich Stocker summarize the algorithm for detecting land fires with TRMM/VIRS measurements, and discuss the diurnal and seasonal cycles of land fires based on TRMM fire products (Ji et al., 2010).

In Chapter 13, Dr. John Hom, Dr. Kenneth Clark, Dr. Yude Pan, Dr. Steve Van Tuyl, Dr. Nick Skowronski and Dr. Warren Heilman introduce an interdisciplinary research program to enhance fire research in New Jersey and the Eastern coastal plain. Research products and applications of the program are described, including network of observation towers, mesoscale fire weather modeling and validation, vegetation mapping by RS and validation, and estimation of forest productivity and fuel dynamics.

Dead fuel load is one of the major factors associated with wildfire risk, but there is still little data available for local and regional applications. For better quantification of wildland fire risks, it is critically important to develop the capability to estimate dead fuel load and investigate uncertainties of the estimates.

In Chapter 14, Dr. Michael J. Gavazzi, Dr. Steven G. McNulty, Dr. Johnny L. Boggs, Dr. Sara E. Strickland, and Dr. David C. Chojnacky compare dead fuel load estimates across six North Carolina forest communities with different management objectives and assess the accuracy of NFDRS dead fuel load estimates for these forest types (Gavazzi et al., 2010).

In Chapter 15, by numerical simulations of grassland fires, Dr. William E. Mell, Dr. Joseph J. Charney, Dr. Mary Ann Jenkins, Dr. Phil Cheney, and Dr. Jim Gould review and compare FIRETEC and WFDS, two physics-based fire models capable of predicting time dependent fire behavior and fire-atmosphere interactions in 3D (Mell et al., 2010). Although these two models are still in their initial stages of development, they have the potential to provide reliable and detailed predictions of the behavior and effects of fire over a much wider range of conditions than operational models. Case studies show that FIRETEC and WFDS can produce similar results qualitatively, although there are some differences.

In WUI, since structures and vegetation are intermixed, fire behaviors are different from pure wildland. Dr. R.G. Rehm and Dr. D. D. Evans discuss the mechanisms and major features of WUI fires, and physics-based modeling of fires in WUI in Chapter 16 (Rehm et al., 2010). To build a complete and accurate model of the WUI fire, methods of fire propagation, including spread by brands, need to be quantified.

The impacts of climate change, and the associated increase in wild fire frequency and severity will very likely increase in coming years and decades. It is important to investigate the impacts of climate change and fires on ecosystem health. In Chapter 17, Dr. Steven G. McNulty, Dr. Sara E. Strickland, and Dr. Jennifer A. Moore Myers assess the climate change and fire impacts on ecosystem critical nitrogen load (Strickland et al., 2010). Change of ecosystem parameters due to drought, climate change shifts in water availability, increases aire temperature, as well as wildfires and prescribed burns, are exmined. The combined impacts of climate change and fire on critical nitrogen load are discussed.

Understanding fuel structure in a landscape and its potential influence on fire spread is helpful in fire and land management. In Chapter 18, Dr. Jacob J. LaCroix, Dr. Qinglin Li, Dr. Soung-Ryoul Ryu, Dr. Daolan Zheng, and Dr. Jiquan Chen investigate the impacts of fuels in AEI (LaCroix et al., 2010). Through simulating fire spread with landscape level edge fuel scenarios using the FARSITE model, it is found that separating AEI from other landscape elements clearly produced different projections of fire spread, fuel loading around edges plays significant role in determining the rate of fire spread and the total size of burns in the landscape. The results suggest that fuel management around edge sould be considered seriously.

Because of the interdependent nature of the variables on which sustainable forestry depends, sustainable forest management requires knowledges from multiple disciplines. In Chapter 19, Dr. Christine M. Stalling discusses integrating social and biophysical processes using SIMulating patterns and processes at Landscape scales (SIMPPLLE), which is a management tool developed to help land managers integrate the best available knowledge of vegetation change caused by disturbances, including fire, insects and disease, fire suppression, and fuel treatment. Criteria and indicators from the Montreal process, combined with modeling techniques and cooperative efforts will provide the capability to help land managers in protecting and maintaining sustainable forests.

Satellite RS has become the primary technique for wildland fire detection and monitoring. Although there exist automatic algorithms for various space-borne measurements, such as data from the geostationary operational environmental satellite (GOES), the AVHRR and the moderate resolution imaging spectroradiometer (MODIS), human element is still important for accurate fire detection and analysis. The NASA goddard space flight center (GSFC) has been collaborating with NOAA national environmental satellite, data and information service (NESDIS) to automate hazard mapping system by training neural networks to mimic the decision-making process of fire experts (Miller et al., 2010). In Chapter 20, Dr. Jerry Miller, Dr. Kirk Borne, Dr. Brian Thomas, Dr. Zhenping Huang, and Dr. Yuechen Chi describe these efforts for automated wildfire detection using artificial networks, including data reduction, architecture of neural network, traing and testing of the neural network, as well as classification and analysis.

Wildland fire is not only a natural disaster, but also an essential process for maintaining ecosystem health. Prescribed burning is an important approach for land management. It is important to analyze fire regimes and related ecological changes. In Chapter 21, Dr. Gregory J. Nowacki and Dr. Robert A. Carr compare the past and current fire regimes in the Eastern United States using GIS and remote technology, illustrate the distainct difference between the past and current fire regimes across the Eastern United States, and investigate the ecological consequences (Nowacki et al., 2010).

The prediction of fire spread behavior and burned area across landscape is very important in fire suppression planning. In Chapter 22, Dr. Zheng, Dr. LaCroix, Dr. Ryu, Dr. Chen, Dr. Hom, and Dr. Clark investigate the effects of weather, landscape structure and land management on fire spread (Zhang et al., 2010) by combining simulations with 3 models. The results demonstrate that landscape structure and fuel type composition can significantly affect fire spread behavior. Roads can remarkabley reduce burned area and thus function as fire barriers. Surface temperature and moisture conditions are the weather factors having most significant impacts on fire spread.

In the last chapter, Chapter 23, Csiszar et al. introduce the fire mapping and monitoring theme of global observation of forest cover-global observation of landcover dynamics (GOFC-GOLD) program (Csiszar et al., 2010), including GOFC-GOLD fire goals, current implementation status, and future plans. Contributory activities from US Agencies are also discussed.

Contributed by many scientists and experts from areas related to wildland fire, this book covers various topics related to wildland fire, including fire detection and monitoring, fire behavior modeling and analysis, smoke emissions and air quality, as well as fire management. It can be used as reference book, and readers can get more details from the chapters and references.

References

Achtemeier, GA, Liu, Y, Goodrick, SL, (2010), A Review of Conflicting Interests and a Technique for Incorporating the Land Manager into Regional Air Quality Modeling. In: Qu, J. J., Sommers, W. T., Wang, R. and Reban, A. Remote Sensing and Modeling Applications to Wildland Fires. Springer-Verlag, Tsinghua University Press

Bachelet D, Neilson RP, Lenihan JM, Drapek RJ, (2004), Regional Differences in the Carbon Source-Sink Potential of Natural Vegetation in the USA. Environmental Management Vol. 33, Supplement 1, S23 – S43 Springer

Bailey RG, (1995), Description of Ecoregions of the United States. http://www.fs.fed.us/land/ecosysmgmt/ecoreg1_home.html

Breshears DD, Cobb NS, Rich PM, Price KP, Allen CD, Balice RG, Romme WH, Kastens JH, Floyd ML, Belnap J, Anderson JJ, Myers OB, Myer CW, (2005), Regional vegetation die-off in response to global-change-type drought. Proc. Natl. Acad. Sci. USA 102, 15144 – 15148 (www.pnas.org/doi/10.1073/pnas.0505734102)

Cunningham, P, Goodrick, SL, (2010), High-Resolution Numerical Models for Smoke Transport in Plumes from Wildland Fires. In: Qu, Rebau, Yang, And Sommers (eds) Remote Sensing and Modeling Applications to Wildland Fires. Springer-Verlag, Tsinghua University Press (this publication)

Csiszar, IA, Justice, CO, Goldammer, JG, Lynham, T, Groot, WJ, Prins, EM, Elvidge, CD, Oertel, D, Lorenz, E, Bobbe, T, Quayle, B, Davies, D, Roy, DP, Boschetti, L, Korontzi, S, Ambrose, S, Stephens, G, (2010), The GOFC-GOLD Fire Mapping and Monitoring Theme: Assessment and Strategic Plans. In: Qu, Rebau, Yang, And Sommers (eds) Remote Sensing and Modeling Applications to Wildland Fires. Springer-Verlag, Tsinghua University Press (this publication)

Fox, DG, Riebau AR, Lahm P, (2010), A Review of Wildland Fire and Air Quality Management. In: Qu, Rebau, Yang, And Sommers (eds) Remote Sensing and Modeling Applications to Wildland Fires. Springer-Verlag, Tsinghua University Press (this publication)

Gavazzi, MJ, McNulty, SG, Boggs, JL, Strickland, SE, Chojnacky, DC, (2010), Dead fuel loads in North Carolina's Piedmont and Coastal Plain and a small scale assessment of NFDRS fuel models. In: Qu, Rebau, Yang, And Sommers (eds) Remote Sensing and Modeling Applications to Wildland Fires. Springer-Verlag, Tsinghua University Press (this publication)

Hanley, DE, Cunningham, P, Goodrick, SL, (2010), Interaction between a Wildfire and the Sea-Breeze Front. In: Qu, Rebau, Yang, And Sommers (eds) Remote Sensing and Modeling Applications to Wildland Fires. Springer-Verlag, Tsinghua University Press (this publication)

Hom, J, Clark, K, Tuyl, SV, Skowronski, N, Heilman W, (2010), Research in the New Jersey Pine Barrens. In: Qu, Rebau, Yang, And Sommers (eds) Remote Sensing and Modeling Applications to Wildland Fires. Springer-Verlag, Tsinghua University Press (this publication)

Ji, Y, Stocker, E, (2010), Diurnal and Seasonal Cycles of Land Fires from TRMM Observations. In: Qu, Rebau, Yang, And Sommers (eds) Remote Sensing and Modeling Applications to Wildland Fires. Springer-Verlag, Tsinghua University Press (this publication)

Jolly, WM, (2010), Integrating Remote Sensing and Surface Weather Data to Monitor Vegetation Phenology. In: Qu, Rebau, Yang, And Sommers (eds) Remote Sensing and Modeling Applications to Wildland Fires. Springer-Verlag, Tsinghua University Press (this publication)

LaCroix, JJ, Li, Q, Ryu, S, Zheng, D, Chen, J, (2010), Simulating Fire Spread with Landscape Level Edge Fuel Scenarios. In: Qu, Rebau, Yang, And Sommers (eds) Remote Sensing and Modeling Applications to Wildland Fires. Springer-Verlag, Tsinghua University Press (this publication)

Liu, Y, Qu, JJ, Wang, W, Hao, X, (2010), A Review of Conflicting Interests and a Technique for Incorporating the Land Manager into Regional Air Quality Modeling. In: Qu, Rebau, Yang, And Sommers (eds) Remote Sensing and Modeling Applications to Wildland Fires. Springer-Verlag, Tsinghua University Press (this publication)

McNulty, SG, Strickland, SE, Myers, JAM, (2010), Climate Change and Fire Impacts on Ecosystem Critical Nitrogen Load. In: Qu, Rebau, Yang, And Sommers (eds) Remote Sensing and Modeling Applications to Wildland Fires. Springer-Verlag, Tsinghua University Press (this publication)

Mell, WE, Charney, JJ, Jenkins, MA, Cheney, P, Gould, J, (2010), Numerical Simulations of Grassland Fire Behavior from the LANL - FIRETEC and NIST - WFDS Models. In: Qu, Rebau, Yang, And Sommers (eds) Remote Sensing and Modeling Applications to Wildland Fires. Springer-Verlag, Tsinghua University Press (this publication)

Millinor, B, Devine, H, Eastman, E, (2010), Creating a Crosswalk of Vegetation Types and Fire Fuel Models for the National Park Service. In: Qu, Rebau, Yang, And Sommers (eds) Remote Sensing and Modeling Applications to Wildland Fires. Springer-Verlag, Tsinghua University Press (this publication)

Miller, J, Borne, K, Thomas, B, Huang, Z, Chi, Y, (2010), Automated Wildfire Detection through Artificial Neural Networks. In: Qu, Rebau, Yang, And Sommers (eds) Remote Sensing and Modeling Applications to Wildland Fires. Springer-Verlag, Tsinghua University Press (this publication)

Nowacki, GJ, Carr, RA, (2010), Altered Disturbance Regimes: the Demise of Fire in the Eastern United States. In: Qu, Rebau, Yang, And Sommers (eds) Remote Sensing and Modeling Applications to Wildland Fires. Springer-Verlag, Tsinghua University Press (this publication)

Rehm, RG, Evans, DD, (2010), - Based Modeling of Wildland - Urban Interface Fires. In: Qu, Rebau, Yang, And Sommers (eds) Remote Sensing and Modeling Applications to Wildland Fires. Springer-Verlag, Tsinghua University Press (this publication)

Sommers, WT, (2010), Wildland Fire and Eastern States Diversity. In: Qu, Rebau, Yang, And Sommers (eds) Remote Sensing and Modeling Applications to Wildland Fires. Springer-Verlag, Tsinghua University Press (this publication)

Spayd, L, (2010), An Overview of NOAA's Fire Weather, Climate, and Air Quality Forecast Services. In: Qu, Rebau, Yang, And Sommers (eds) Remote Sensing and Modeling Applications to Wildland Fires. Springer-Verlag, Tsinghua University Press (this publication)

Stalling, CM, (2010), Integrating the Social and Biophysical Using a Landscape Modeling System (SIMPPLLE). In: Qu, Rebau, Yang, And Sommers (eds) Remote Sensing and Modeling Applications to Wildland Fires. Springer-Verlag, Tsinghua University Press (this publication)

Stanturf, JA, Wimberly, MC, (2010), Demographic Trends in the Eastern US and the Wildland Urban Interface: Implications for Fire Management. In: Qu, Rebau, Yang, And Sommers (eds) Remote Sensing and Modeling Applications to Wildland Fires. Springer-Verlag, Tsinghua University Press (this publication)

Zheng, D, LaCroix, JJ, Ryu, S, Chen, J, Hom, J, Clark, K, (2010), Fire Spread Regulated by Weather, Landscape Structure, and Management in Wisconsin Oak-dominated forests and New Jersey Pinelands. In: Qu, Rebau, Yang, And Sommers (eds) Remote Sensing and Modeling Applications to Wildland Fires. Springer-Verlag, Tsinghua University Press (this publication)

2 Wildland Fire and Eastern States Diversity

William T. Sommers

Enviromental Science and Technology Center, Department of Geography and Geoinformation Science, College of Science, George Mason University, 4400 University Drive, MS 6C3 Fairfax, VA 22030, USA
Email: wsommers@gmu.edu

Abstract The frequency, severity and extent of wildland fires are largely a function of interactions deriving from ecosystem, atmospheric and demographic processes. Science explains universally applicable characteristics of wildland fire, but practical application of fire science requires knowledge of a diverse array of regionally to locally specific conditions. These include ecosystems and how they have evolved, land use history and land use change, demographic trends, fire history and current risk, and the ability of fire managers to bring resources and experience to emergencies in a timely manner. The 95th meridian divides the continental United States in terms of ecosystems, climate, demographics and fire regimes. Fire management and research funding favors the west, but over half of our forests, 70% of our people and the bulk of wildland urban interface (WUI) lands are in the east. Efficient application of fire science information for eastern fire management will benefit from strategies that account for climate, ecosystem, demographic and fire regime diversity of the eastern United States.

Keywords Wildland fire, WUI, fire regimes, fire information, eastern United States

2.1 Introduction

Wildland fire shares universally applicable characteristics related to the classic triangle of fuel, weather, and ignition sources. Conversely, practical application of fire science knowledge in fire management practices introduces several factors that require a diverse array of additional considerations. Included are knowledge of specific ecosystems and how they have evolved, land use history and land use change, demographic trends, risks and values as visualized by local publics, frequency and severity of wildland fire in shared local memory, and the ability of fire managers to bring resources and experience to emergencies in a timely manner.

Much of the current United States focus of wildland fire management, research and resource allocation is on our Western states. Frequent television coverage of firefighters facing vast Western blazes, in military style campaigns, has heightened public awareness and shaped perceptions of wildland fire. An overwhelming percentage of federal emergency firefighting expenditures are, year in and year out, justified by Western fire conditions and then allocated to fighting a very few large fires in the west.

Emergence of the Wildland-urban interface (Radeloff et al., 2005) concept and a deeper understanding of the differing ecological roles of fire in many ecosystems have begun a reexamination of the costs and benefits (United States government accountability office, 2005) for 21st century America of fire management approaches that were so successfully developed during the second half of the 20th century. That reexamination should include a reinvigorated consideration of how best to meet 21st century wildland fire needs in our Eastern states.

2.2 The Eastern United States

The Eastern states (defined herein as those lands east of the 95th meridian) are different from the West in terms of ecosystems (Fig. 2.1), climate and weather, land use history and change, demographics and intraregional diversity. Nearly three quarters of the 2000 population of the United States lived in these Eastern states (Fig. 2.2). Housing density reflects this population distribution. The Eastern states ecosystems are classified as humid temperate and humid tropical, compared to predominantly dry in the west. This means drought in the east does not have to be prolonged for forest fuels to move into heightened fire danger categories.

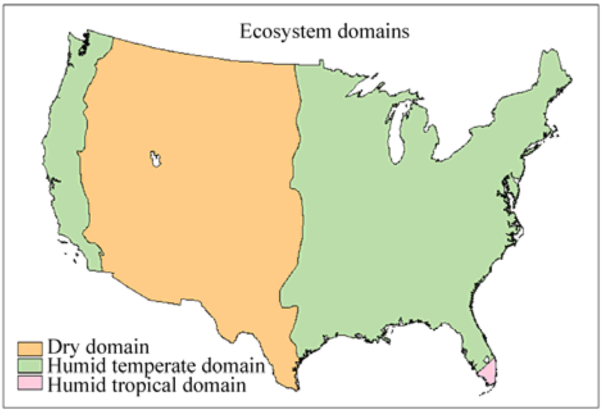

Figure 2.1 Description of the ecoregions of the United States ecosystem domains (Bailey, 1995)

Weather and climate which drive these ecosystem classifications are also clearly divided by the 95th meridian. Land use in the east resulted in the almost complete removal of existing forests by arriving Europeans, with much of the removal tied to land use change from forest to agriculture. Prior to European settlement, native people populated post glacial Eastern forests in increasingly settled communities dependent on agriculture and forest resources. Starting in the post civil war era, conversion of forest lands has been largely reversed in the east.

Today the east is more heavily forested than at any time since the 19th century (USDA Forest Service, 2004), and many of those forests are becoming increasingly mature. Post glacial evolution of Eastern forests has continuously occurred in the presence of human use patterns, and those patterns have shown large and dramatic shifts over the last 300 years. Demographics in the east have shown an increasing trend towards urbanization (Theobald, 2005), particularly through suburban expansion around urban centers, which has contributed to significant increases in tree coverage as agricultural lands are abandoned and converted. Large areas of Eastern forests appear at risk from increased fire activity related to climate change (Bachelet et al., 2004; Breshears et al., 2005).

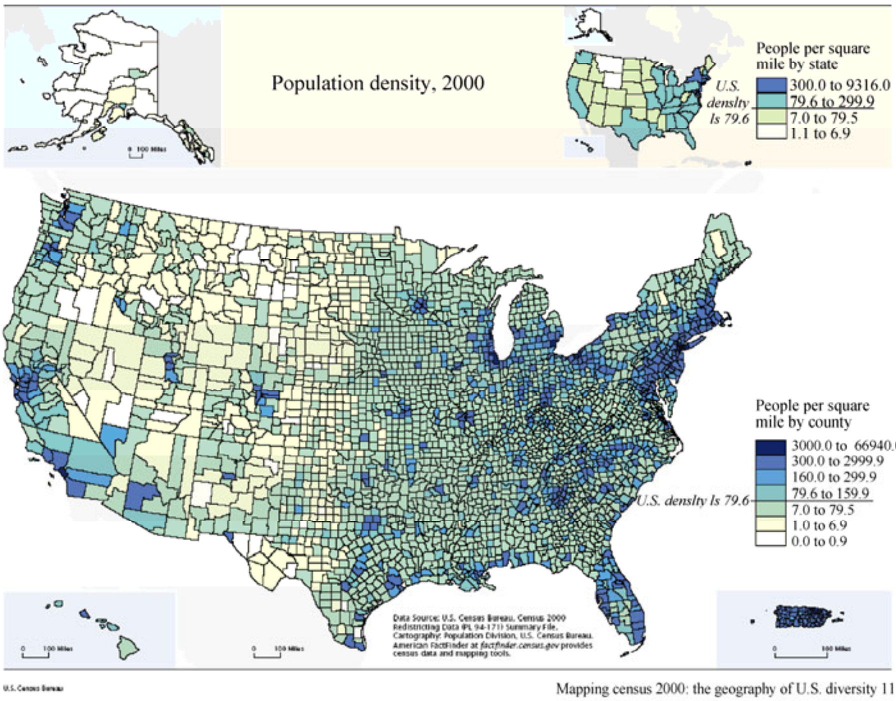

Figure 2.2 Population density of the United States in 2000. http://www.census.gov/population/cen2000/atlas/censr01-103.pdf (last accessed on 06/16/2009)

2.3 Eastern United States Diversity

Generalized statements used to differentiate the east from the west tend to obscure an equally important consideration—the east is internally very diverse in terms of ecosystems, demographics, land use history, social values, and fire management capabilities. For example, the region experienced the worst recorded forest fire in North American history in terms of fatalities (Peshtigo Fire of 1871), the creation of our Nation's first large forest preserve (Adirondack Forest Preserve, 1885), and a renowned restoration of degraded lands through forestry (Southeastern states).

European explorers found the Eastern United States covered with rich forest ecosystems dominated by old growth trees from what is now the Hudson Bay to the Gulf of Mexico (Biodiversity Project, 2003). The Eastern forests found by Europeans had evolved with climate change (Delcourt and Delcourt, 1987) and been shaped by human use of fire (Delcourt and Delcourt, 1997). These Eastern forests fueled the emerging American economy from ship building to iron furnaces. Forest use and clearing for agriculture decimated much of the Eastern forest by the end of the 19th century, leading to passage of the Weeks Act of 1911 which established Eastern National Forests. Eastern forest acreage was reduced from 650 million acres to 400,000 million acres by 1900, with much of the reduction coming in the last 50 years of the 19th century (Heinz Center, 2002). Since then, acreage has remained stable. The Climate Change Atlas for 80 forest tree species of the Eastern United States (Prasad and Iverson, 1999) is an excellent source for viewing the diversity of forest tree species for the Eastern states and how there distributions are likely to change under various climate model scenarios.

Fire regimes are a useful approach for documenting the role of fire in particular ecosystems. While fire regimes have not been extensively studied for all of the Eastern United States, the work of Lafon, Hoss and Grissino-Mayer (2005) on fire regimes and climate variability in the Central Appalachian Mountains is indicative of how important fire is to Eastern ecosystems. They point out the importance of fire regime knowledge to fire management decisions and to understanding the ecological role of fire for any given ecosystem. Much of the area studied appears fire dependent, especially the oak and pine dominated stands. Suppression of fire has lead to species decline and increases in stand density and fuel loads.

2.4 A Fire Information Strategy for the Eastern States

East-west equity in funding of fire management (United States Government Accountability Office, 2006) and fire research is not likely to develop, either in view of currently justified circumstances or a major shift in national priorities. Scientists and managers, therefore, should coalesce around a strategy aimed at providing timely, cost effective, and technically appropriate fire related information to the broad and diverse fire community of the Eastern United States.

There are several key components to such a strategy. ① recognize the diversity of Eastern fire management needs and the limited resources available to meet them. ② utilize the broadly applicable state of art fire science currently flowing from research funded by the joint fire science program (JFSP, 2007) and the national fire plan (NFP, 2007). ③ emphasize decision support technologies to knowledge engineer products designed to meet specific local user needs at very low cost. ④ base the strategy on using available satellite measurements to continuously supply near real time fire information. Developing the mathematical algorithms needed to monitor rapidly changing local fuel conditions from satellite measurements is a technical linchpin to this strategy.

Recognize the diversity of eastern fire management needs and the limited resources available to meet them. One size does not fit all for Eastern fire management. This paper illustrates how fire management needs, and resources, vary from Florida to Maine to Minnesota to east Texas. While florida's State forester deals with acreage burned that exceeds those of many Western states in a typical fire year, New Jersey may face those fire loads on a decadal basis. While a nature conservancy manager needs to introduce prescribed fire on an acre by acre basis to restore the health of the pine bush in Western Albany, New York, wildlife managers will need to burn significant jack pine acreages in Michigan to meet Kirtland Warbler habitat goals. While the supervisor of the superior national forest treats the vast acres of timber blow down in the boundary waters canoe area with prescribed fire to avert disaster, the Supervisor of the Francis Marion national forest in South Carolina must balance fire hazards and red cockaded woodpecker habitat needs following the heavy disturbance caused by Hurricane Hugo. The resources available to meet these diverse and important fire management needs are scarce and must be carefully managed. The incident command system (ICS) which was invented in southern California in the 1970s and has become the backbone of emergency management throughout the much of the country. The ICS is an example of applicable fire research that can and should be tuned to recognize the diverse needs of Eastern fire management.

Utilize the broadly applicable state of art fire science currently flowing from research funded by the joint fire science program (JFSP) and the national fire plan (NFP). A very significant amount of extremely useful research is flowing out of the JFSP and NFP. Concentrated attention should be paid by knowledgeable scientists and technology transfer experts to the task of identifying and applying state of the art fire science to Eastern fire needs. Active utilization of state of the art science is a cost efficient necessity for meeting diverse Eastern fire program needs.

Emphasize decision support technologies to knowledge engineer products designed to meet specific local user needs at very low cost. Most Eastern fire managers can not afford the continuing overhead of technical staff dedicated to ongoing analysis that is possible in the west, based on preparedness for large campaign fires. While many users remain uncomfortable with disembodied machine based guidance, both the user and science communities need to make special efforts to overcome this difficulty. By using improved decision support technologies, including artificial intelligence, low overall program costs can be maintained while providing placed based information designed to meet specific user needs.

Base the strategy on using available satellite measurements to continuously supply near real time fire information. The key to making this strategy successful is the cost effective use of available satellite measurements engineered to meet diverse local needs. As with many other areas of fire research, research on the utility of using remote sensing (RS) measurements is yielding exciting results. In particular, research advances aimed at using remotely sensed fuel measurements that can be directly used in fire danger, fire behavior, smoke management and other real time fire management information needs without the artifice of parameterized fuel models are extremely promising. Advances deriving from research on the utility of satellite measurement for the forest inventory and analysis (FIA) program (USDA Forest Service, 2007) promise significant collateral benefits for Eastern fire programs. FIA data bases for the east can supply the forest vegetation ground truth information needed to rapidly tune applications designed for fire program needs.

The time is now and the technology is here to address the goal of meeting the diverse needs of Eastern fire management by employing state of the art fire science, decision support science and RS data processing technologies to available satellite RS measurements. Carefully tuned knowledge engineered outputs can and should provide useful, timely and geographically specific information to federal, state and local fire managers and other users in the east.

References

Bailey RG, (1995), Description of Ecoregions of the United States. http://www.fs.fed.us/land/ecosysmgmt/ecoreg1_home.html

Bachelet D, Neilson RP, Lenihan JM, Drapek RJ, (2004), Regional Differences in the Carbon Source-Sink Potential of Natural Vegetation in the USA. *Environmental Management*. **33**(1): S23 – S43

Breshears DD, Cobb NS, Rich PM, Price KP, Allen CD, Balice RG, Romme WH, Kastens JH, Floyd ML, Belnap J, Anderson JJ, Myers OB, Myer CW, (2005), Regional vegetation die-off in response to global-change-type drought. Proc. Natl. Acad. Sci. USA 102, 15144 – 15148 doi:10.1073/pnas.0505734102

Biodiversity Project, (2003), A Brief History of Eastern Forest Use and Protection. Biodiversity Project, 214 N. Henry St., Suite 201, Madison, WI 53703 http://www.biodiversityproject.org

Delcourt, P.A. and H.R. Delcourt, (1987), Long-term forest dynamics of the temperate zone. New York: Springer-Verlag. 439

Delcourt, H.R. and P.A. Delcourt, (1997), Pre-Columbian Native American use of fire on southern Appalachian landscapes. *Conservation Biology*. **11**: 1010 – 1014

Heinz Center, (2002), The State of The Nation's Ecosystems. The H. John Heinz III Center for Science, Economics and the Environment, Cambridge University Press. http://www.heinzctr.org/ECOSYSTEMS

JFSP, (2007), Joint Fire Science Program. http://jfsp.nifc.gov/

Lafon, C.W., J.A. Hoss and H.D. Grissino-Mayer, (2005), The Contemporary Fire Regime of the Central Appaclachian Mountains and Its Relation to Climate. *Physical Geography*, **26**(2): 126 – 146

NFP, (2007), National Fire Plan. http://www.fireplan.gov/

Prasad, A. M. and L. R. Iverson. 1999-ongoing. A Climate Change Atlas for 80 Forest Tree Species of the Eastern United States [database]. http://www.fs.fed.us/ne/delaware/atlas/index.html, Northeastern Research Station, USDA Forest Service, Delaware, Ohio

Radeloff VC, Hammer RB, Stewart SI, Fried JS, Holcomb SS, McKeefry JF, (2005), The Wildland-Urban Interface in the United States. *Ecological Applications*, **15**(3): 799 – 805

Theobald D, (2005), Landscape patterns of exurban growth in the USA from 1980 to 2020. *Ecology and Society*, **10**(1): 32, [online].URL, http://www.ecology andsociety.org/vol10/iss1/art32/

United States Government Accountability Office, (2005), Wildland Fire Management Progress and Future Challenges, Protecting Structures, and Improving Communications. GAO-05-627T

United States Government Accountability Office, (2006), Wildland Fire Suppression Lack of Clear Guidance Raises Concerns about Cost Sharing between Federal and Nonfederal Entities. GAO-06-570

USDA Forest Service, (2004), National Report on Sustainable Forests – 2003. USDA Forest Service FS-766. http://www.fs.fed.us/research/sustain/

USDA Forest Service, (2007), Forest Inventory and Analysis (FIA) National Program. http://fia.fs.fed.us/

3 Demographic Trends in the Eastern US and the Wildland Urban Interface: Implications for Fire Management

John A. Stanturf
Center Forest Disturbance Science, US Forest Service, 320 Green St., Athens, GA 30602, USA
Email: jstanturf@fs.fed.us

Michael C. Wimberly
GISc Center of Excellence, South Dakota State University, Brookings, SD 57007-3510, USA
Email: michael.wimberly@sdstate.edu

Abstract Over the last century, the United States has evolved from a predominantly rural to an urbanized society with an exurban area currently referred to as the wildland urban interface (WUI). This WUI is critical as it occupies three to five times as much land area as urban areas with emerging and latent conflicts between traditional resource management and preferences of new residents. The effect of development on wildland fire management has received the most attentions. Increasingly, one of the most effective tools in the manager's kit, fuel reduction by frequent understory burning, is off-limits because of safety and liability risks or public dislike of smoke. Fire risk in the WUI is greater than in wildland because there is a higher risk of catastrophic wildfire. The WUI, however, cannot be defined by simple proximity of forest to urban areas but more realistically is conceptualized as a set of complex social, physical, and biotic gradients. The Southern US exemplifies the problems of mixing urbanized land uses with fire-affected natural vegetation. Remote sensing and geographic information systems, along with spatial information at appropriate scale, will play a critical role in providing managers with monitoring capability that can also be used to educate the public about the wildland urban interface.

Keywords Prescribed burning, hazardous fuel reduction, smoke management, WUI Index, forest land management

3.1 Introduction

Over the last century, the United States has evolved from a predominantly rural to an urbanized society (Hobbs and Stoops, 2002). Since the World War Ⅱ, growth of exurban areas has dominated: beyond the suburbs, not exactly rural and not quite urban. Today this exurban area, currently referred to as the wildland urban interface (WUI) is critical as it occupies three to five times as much land area as urban areas (Theobald, 2001; Radeloff et al., 2005). Although there are many emerging emergent and latent conflicts in the WUI between traditional resource management and preferences of new residents, the effect of development on wildland fire management has attracted the greatest attention from policymakers. As human populations expand farther into fire-affected natural landscapes, more people, more natural ecosystem area, and greater capital investment are at risk from wildfire. Fragmentation of forest land due to land use change driven by population growth constrains many traditional methods of forest management, particularly the use of prescribed burning to manage fuel loads. Prescribed fire is used routinely in conifer forests in the South, Lake States, and Northeast to reduce fuel loads and decrease the risk of catastrophic wildfires, improve forest health, and manage habitat for threatened and endangered species. Increasingly, one of the most effective tools in the manager's kit, fuel reduction by frequent understory burning, is off-limits because of safety and liability risks (Achtemeier et al., 1998; Wade and Brenner, 1995) or public dislike of smoke (Macie and Hermansen, 2002).

Demographic changes in the Eastern United States affect natural resources and the attitudes of the public toward traditional management practices such as prescribed burning (Cordell et al., 1998). The WUI, however, is not a discrete management unit that can be defined, more or less, by simple proximity of forest to urban areas. Because of heterogeneous patterns of both forest cover and human settlement across broad landscapes, the WUI is more realistically conceptualized as a set of complex social, physical, and biotic gradients (Wimberly et al., 2005). Our objectives in this chapter are to briefly describe the changing demographics of the Eastern United States (focusing on the South), characterize the growing WUI, and describe the implications for the land manager of the expansion of dense human settlements into fire-affected forests.

3.2 Demographics

The population of the United States grew 270% over the course of the 20th century, from approximately 76 million to 281 million and growth in the 1990s was the greatest increase in population for any decade in history (Hobbs and Stoops, 2002). The South, defined for our purposes as the 13 states in region 8 of the US forest service, showed a greater percentage increase, 319% (from 22 million to almost 92 million) over the same century (Hobbs and Stoops, 2002; Cordell and Macie, 2002). These growth rates are the combined effect of lowered mortality, longer living, and immigration (Cordell et al., 2004). Population increase was not steady, however, and the post World War II "baby boom" shows clearly when increases are viewed at decadal intervals (Fig. 3.1). Applying the rate of increase for the decade from 1990 – 2000 (13.1%) to future growth, the United States population is predicted by the bureau of census to double in size in the next 100 years, to 570 million (Cordell et al., 2004).

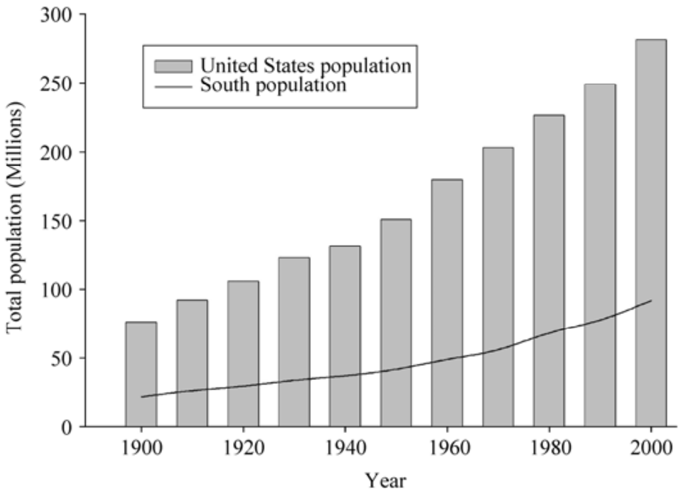

Figure 3.1 Decade to decade population increases for the entire United States and the 13 Southern states in region 8 of the US forest service. Population totals for the United States exclude Alaska and Hawaii through 1950. Source: US census, decennial census of population, 1900 – 2000 presented in Appendix A Table 1 of Hobbs and Stoops (2002)

More than 70% of the current population lives east of the 100th Meridian, i.e. in the East. Increasingly, the US population lives within a metropolitan area. In 1910, only 28% lived in a metropolitan area but by 2000, the US population was 80% metropolitan (Hobbs and Stoops, 2002). The growth of metropolitan population in the South has increased, especially since World War II, and now approaches the national average (Fig. 3.2). Since World War II, growth has been concentrated outside of the central cities; half the US population now lives in suburban areas (Hobbs and Stoops, 2002). In the South, 20.8% of the increase between 1990 and 1999 has been in metropolitan areas outside of the central cities (Mackun and Wilson, 2000).

Increased population levels do not tell the whole story, however. Given a fixed area of land, increasing population means higher population density. The US

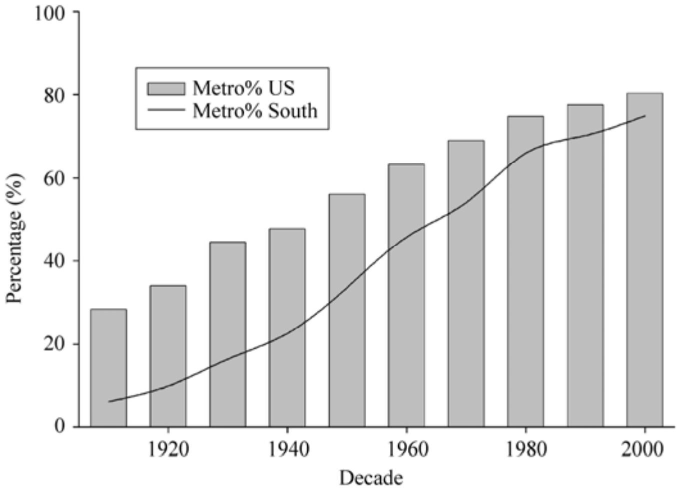

Figure 3.2 Increase in the metropolitan population of the United States and the 13 Southern states in region 8 of the US forest service, 1910 – 2000, shown as the percentage of the total population that lived in metropolitan areas at each decennial census. Population totals for the United States exclude Alaska and Hawaii through 1950. Source: US Census, decennial census of population, 1900 – 2000 presented in Appendix A Table 3 a and b of Hobbs and Stoops (2002)

tripled in density, from 10 people per km^2 at the beginning of the 20^{th} century to 31 people per km^2 at the beginning of the 21^{st} century. The US remains relatively less densely populated, however, in comparison with most countries and is lower than the average world population density of 46 people per km^2 (Hobbs and Stoops, 2002). The average population density in the South exceeds the national average, and has increased more rapidly than the national rate since World War Ⅱ (Fig. 3.3).

Despite the danger of extending past trends into the future, we see no reason to expect that population levels will decline in the United States, or even that the rate of growth will decline (Nowak et al., 2005). Another trend besides the growth of population that is likely to continue is the increase in per capita footprint. Since the 1960s, conversion from rural to urban land use has exceeded the rate of population growth (Hirschorn, 2000), with a preference for non-urban settings (Sullivan, 1994). This trend is due to the combined effects in exurban versus urban areas of lower housing density, larger average lot size, and the expansion of supporting infrastructure such as roads, schools, and commercial area (Cordell et al., 2004). In the decade and a half from 1982 – 1997, developed area in the US increased 34%, with the largest regional increase in the South (Alig et al., 2004). Thus demographics can be visualized through the effect of human population growth on land use, both in terms if the present distribution of people on the landscape in urban, exurban, and rural areas and the likely changes in land use patterns over the next century.

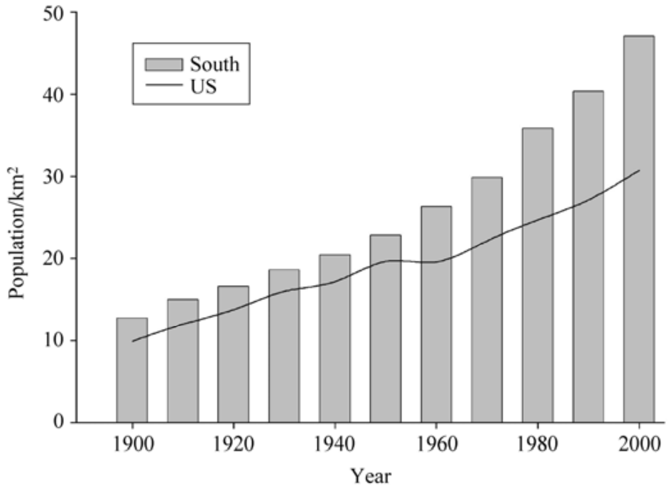

Figure 3.3 Average population density per km^2 of the United States and the 13 Southern states in region 8 of the US forest service, 1910 – 2000, shown as the average density at each decennial census. Density levels for the United States exclude Alaska and Hawaii for 1900 – 1950. Density levels are based on census 2000 land area measurements. Source: US census bureau, geography division; decennial census of population, 1900 – 2000 presented in Appendix A Table 2 of Hobbs and Stoops (2002)

3.3 The Wildland Urban Interface

The traditional concept of the WUI is that of an area of urban sprawl where new housing developments abut large areas of public or private wildland. Recreation managers view this interface in terms of adjacency of people seeking recreational opportunities and access to backcountry. Fire managers view the interface in terms of adjacency of flammable wildland fuels and structures (Long et al., 2005). The federal government defined the interface as "…the area where houses meet or mingle with undeveloped wildland vegetation" and described three types of interface communities: ① the "interface community" where structures about wildland fuels, ② the "intermix community" where structures are dispersed within a wildland matrix, and ③ the "occluded community" where wildland fuels are patches within a matrix of structures, for example a park (USDA and USDI, 2001).

Attempts to map the interface and intermix conditions based on this definition use the threshold set in the Federal register of one house per 40 acres (Radeloff et al., 2005). Further assumptions must be made about the nature of the wildland vegetation. The WUI map for 2000 produced by Radeloff and colleagues (2005) used a 50% threshold for wildland vegetation: greater than 50% for the interface community, less than 50% wildland vegetation but within 1 mile of wildland vegetation for the intermix community type. They estimated that 10% of the area and 33% of the housing units in the conterminous 48 states are in the WUI. As they point out, this approach does not directly map fire risk because wildland vegetation communities vary considerably in their fuel types, fire frequency, and fire regimes. Flammability of construction materials and accessibility to firefighting equipment also must be considered in evaluating fire risk (Cohen, 2000); spatially explicit data on these factors are lacking, except for small areas (e.g., Haight et al., 2004).

Developing fire risk assessments for the WUI is a daunting challenge; most of the needed data are lacking over large areas and such data as exist, primarily from the decennial US Census, provide an incomplete picture. For example, the size of a census block varies with population level, so that rural blocks tend to be of large areas, which limits the spatial precision with which housing units can be mapped (Wimberly et al, 2005). Further, census data do not map associated infrastructure such as schools, hospitals, or industrial sites. Using census housing data to map the WUI is further limited by the omission of second-home, recreational housing; only primary abodes are listed in the census data. Spatial information on the pattern of roads is useful in mapping the WUI, and in combination with census data can overcome some of these limitations. Roads tend to be correlated with housing in rural areas; individual buildings are more likely to be located close to roads, and roads themselves have an impact on probability of ignition (Forman, 2002).

Attempts to map the WUI to date have produced static snapshots of land use and population density. Other predictors of fire risk related to the socioeconomic environment are even harder to map, such as labor markets, law enforcement, and socioeconomic conditions (Prestemon et al, 2002; Mercer and Prestemon, 2005; Butry and Prestemon, 2005). Because it is impractical for managers to redo a WUI map for each fire season, a dynamic view of the WUI is needed, one that identifies where change is most likely to occur (e.g., growth clusters—Hammer et al., 2004). We propose a new typology that defines the WUI along two axes: from wildland to urban land use and private to public land ownership. At one extreme is dispersed urban development within a wildland matrix, typified by second home or summer recreation development, the interface zone. Often these are private in-holdings within large areas of public ownership. The Wildland Island at the other extreme is a park or forest stand within an urban area. These remnant natural areas frequently are rich in plant species; the pine rocklands in South Florida exemplify this form of the WUI (O'Brien, 1998; Snyder et al., 1990).

Between these extremes is the intermix zone of areas undergoing a transition from natural resource uses such as forestry or agriculture to urban uses. We distinguish two types based on the sharpness of the boundary between wildland and urban land uses: the diffuse boundary and defined boundary intermix zones. In both types, developed parcels are small relative to forested land. The diffuse boundary intermix zone occurs where private ownership predominates and parcel sizes are relatively small. Typical leapfrog urban development creates zones of development well beyond the edge of urban development, with land between remaining undeveloped. The undeveloped land may remain in active forest management for a time, unless the patch size is too small to be economical or rising land values push landowners toward development (Wear and Newman, 2004). Another type of intermix occurs where large areas are in public or single private ownership (such as forest industry land); in this case the mixture of forest land with individual private development produces a well-defined boundary between urban and wildland land uses. These two types of intermix zone differ in their dynamism; the diffuse boundary intermix may be unstable over time as individually owned parcels are developed and infrastructure is added. The distinct boundary intermix may remain stable as long as the large publicly or privately owned forestland stays in resource use. The developed side of the boundary likely will be fully developed, however.

We have observed several spatial growth patterns in the WUI. Around small towns and areas of slower growth, a typical pattern is accretion; land at the edge of town is developed, particularly along major roads. Accretion generally develops a defined boundary with wildland. In larger towns undergoing more rapid development, a typical pattern is leapfrog and fill-in; development occurs beyond the outskirts of older development, leaving a sizeable area of undeveloped land between, resulting in a diffuse boundary. Over time, the gap is closed. Analysis of county-level census data illustrates this phenomenon: counties mapped as 40% – 60% urban in the 1990 census saw the greatest increase in urban area in 2000 (Nowak and Walton, 2005). In the southeastern U. S., 35% of the census blocks that converted from rural to WUI between 1990 and 2000 were not adjacent to existing WUI blocks, indicating a leapfrog pattern of development (Zhang and Wimberly, 2007). Another common development pattern seen especially in rapidly developing areas of the South such as Florida and along the Atlantic and Gulf coasts is concentrated development. This is called variously a planned unit development, or a gated or golf course community. Sometimes these developments result from large blocks of forest owned by industry being converted to up-scale real estate development. Vacation home development can occur within the intermix zone on large lots, or be truly dispersed in private forest areas (Stein et al., 2005).

Each type of WUI is dynamic and local factors of economics, access, and proximity to naturalness and scenery largely determine the rate of conversion from wildland to developed land within the national context of capital availability. The types of vegetation communities, stand structures, fuel types and loads vary as well by physiographic province, from the coast to the mountains. There is no single parameter, or simple set of parameters, that adequately describe the WUI environment. As noted by Wear and Bolstad (1998), "…coarse-scale measures of the human drivers of landscape change (for example, population growth measured at the county level) appear to be poor predictors of changes realized at finer scales." The characteristics and significance of the WUI for fire managers at a given location may vary depending upon the spatial scale of the effects considered. Whereas forest patch sizes and interspersion with housing can be assessed at the local level, the potential influences of escaped fires and smoke dispersion must be analyzed over much larger areas. Additionally, fire managers need to be aware of the likelihood of land use changes in intermix areas.

In many ways, the entire South is a WUI. Much of the South was once cleared, farmed, or grazed. Past land use has left many legacies, including an extensive road system (Fig. 3.4). Population growth since the middle of the last century has caused increasing urbanization and fragmentation of the forested landscape (Wear, 2002),

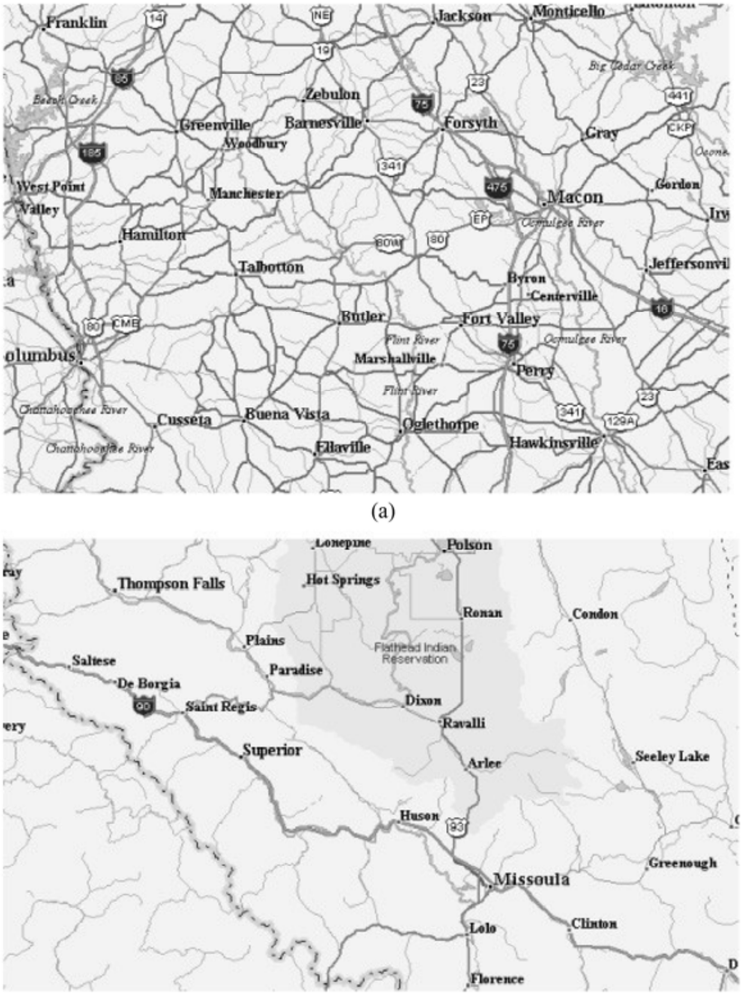

(a)

(b)

Figure 3.4 A legacy of roads in the South as compared to the West: Roads in an approximately 26,000 km^2 area of southwestern Georgia, the Flint River Valley (a), compared to a similar area of the Bitterroot Valley in Montana (b) increasing the size and importance of the WUI. More people now live at the interface and the transportation system is expanding, becoming denser and more pervasive (Riitters and Wickham, 2003). The density of public roads in the US is 0.65 km/km^2 (0.79 km/km^2 for the contiguous US excluding Alaska and Hawaii) and the average for the southern states is 0.98 km/km^2 (US DOT, 2004). The road density in Georgia is 1.22 km/km^2, higher than the national average; the density in Montana is lower than the national average at 0.29 km/km^2. Continuing growth in the South is projected to occur along the Atlantic and Gulf coasts and the Piedmont Crescent, mostly from the conversion of forest to urban land use (Wear, 2002). Besides the physical aspects of the WUI, changing demographic profiles and cultural values (Cordell et al., 1998) have altered attitudes towards natural resource management in general (Bliss et al., 1997; Jacobson et al., 2001; Hull and Stewart, 2002) and prescribed burning in particular (Loomis et al., 2001; Duryea and Hermansen, 2002). In general, Southerners share the same attitudes about the environment as the general population and even small forest landowners are averse to even-aged management practices such as clearcutting and use of herbicides to control competing vegetation (Bliss et al., 1997).

Land ownership in the South and East differs from the West; Eastern forests are predominantly in private ownership, approaching 80% or more in most states. Forest land ownership differences lead to distinctive land cover patterns (e.g., Turner et al., 1996). A distinctive feature of southern forests is the relatively large industrial ownership, especially coastal plain pine plantations. Forest industry has for many years developed or sold parcels with high amenity values, such as coastal islands and lakeshores, and increasingly a significant proportion of new housing starts are vacation homes on wildland/high contrast edges such as abutting national forest or national park land (Theobald, 2004). The 1990s saw a new phenomenon in the wholesale divestiture of industry land to financial and real estate organizations, the Timber Investment Management Organization (TIMO) and Real Estate Investment Trust (REIT) (Ravenel et al., 2002; Stanturf et al., 2003). Although purchased and managed in the short-term for their timber value (Caulfield, 1998; Yin et al., 1998), the long-term fate of this land base is uncertain (Clutter et al., 2005); the question is whether the land will be reforested once the standing value is harvested, or sold for urban development. Again, local and national economics will influence such decisions (Wear and Newman, 2004). Large contiguous blocks of industrial ownership are not limited to the South, and there is concern throughout the Eastern US for the uncertainty of future uses of forest industry land (e.g., Hagan et al., 2005).

3.3.1 Georgia Case Study

To further explore the characteristics of the WUI in the southeastern US, we carried out a GIS modeling exercise for the state of Georgia, in which digital maps of forest cover, housing density, and road density were combined to map the spatial pattern of the WUI. A vector dataset containing housing density from the 2000 census, mapped at the census block level, was obtained from the SILVIS website (Radeloff et al., 2005). The road layer was derived from 1:100,000 digital line graphs (DLGs) originally produced by the USGS. A 18-class land cover map of Georgia, developed by the Institute of Ecology for the Georgia Gap Analysis Project and the Georgia Land Use Trends program, was used to map forest cover (Kramer et al., 2003). This 30 m raster dataset characterized land cover in 1998 and was developed by classifying Landsat TM images from 2 dates representing leaf-on and leaf-off conditions. For this study, cells mapped as deciduous forest, conifer forest, mixed forest, and forested wetlands were reclassified with a value of 1 (forested), and all other pixels were reclassified with a value of 0 (non-forested). Our WUI map for Georgia was developed using the methodology of Zhang (2004). These data sets were transformed spatially using a moving-window analysis. The housing densitymap was converted toa raster dataset with a 30 m cell size to match the land cover dataset. A new housing density value was then assigned to each cell, based on the average housing density within a 2.4 km^2 radius circular neighborhood (Fig. 3.5(a)). This radius was chosen to match the buffer zone for WUI identification that had been used in previous mapping efforts (Radeloff et al., 2005). Road density, computed as km of road per km^2, was also summarized within a 2.4 km^2 circular neighborhood with the output stored in a 30 m raster dataset (Fig. 3.5(b)). Forest cover for each cell was similarly computed as the proportion of forested cells within the surrounding 2.4 km^2 circular neighborhood (Fig. 3.5(c)).

Each spatial variable was converted into an index between 0 and 1 using a scaling function. These functions were based on the assumption that areas with a high WUI index (WUI_I) value should contain both high levels of wildland vegetation (predominantly forests in Georgia), and also have high levels of human habitation and utilization. Thus, both the forest index (F_I) and the road index (R_I) increased linearly with increasing densities. The housing index (H_I) increased logarithmically with housing density, based on the assumption that differences in the index at lower housing densities are more important for defining the WUI than differences at higher housing densities.

These input layers were combined using an enhanced version of the favorability function (O'Sullivan and Unwin, 2003). The final WUI index was computed for each 30 m cell as:

$$WUI_I = FI^{0.5} \times HI^{0.25} \times RI^{0.25} \tag{3.1}$$

This function was a weighted geometric mean of the three indices defined previously, with equal weighting assigned to wildland characteristics (the forest index) and to the combined urban characteristics (the housing and road indices). The value of the WUI index was zero whenever one or more of the component indices was zero, and equaled one only when all three of the component indices were equal to one. Thus, the resulting WUI index was lowest at the extremes of

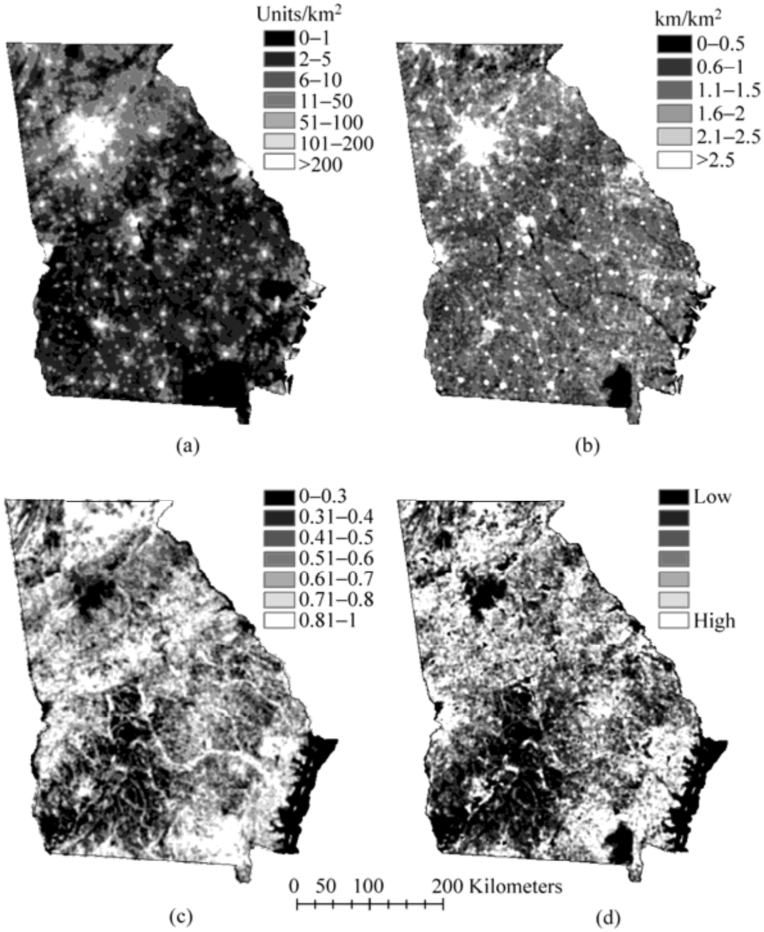

Figure 3.5 Georgia example. (a) Housing density in residential units per square km. (b) Road density in km of road per square km of land area. (c) Forest cover in Georgia as a proportion of total land area. (d) Calculated WUI Index; high index indicates local juxtaposition of housing and natural vegetation, low index value indicates either urban or wildland conditions

the urban-wildland gradient and highest for landscapes falling near the middle of this gradient.

Almost all the areas in Georgia that had high forest cover also had a high WUI index, reflecting the ubiquity of diffuse, low-density development on private lands and extensive road systems (Fig. 3.5(d)). The major exception was the Okefenokee national wildlife refuge, located in the southeastern corner of the state. Another large concentration of the public land in Georgia is in the Chattahoochee national forest, located in the southern Appalachians of Northeast Georgia. However, much of this land was heavily roaded and interspersed with private property, resulting in high WUI indices associated with defined intermix patterns in this portion of the state. The Piedmont region northeast of Atlanta had comparatively low forest cover, but also had high WUI indices because of high housing and road densities. Another large concentration of high WUI indices was found along the Atlantic Coast, resulting from the defined intermix patterns of large areas of industrial timberland juxtaposed with scattered population centers and extensive roads. WUI indices were much lower in other portions of South Georgia, particularly in southwest Georgia where agriculture remains the dominant land use.

In additional to these statewide trends, the WUI index also exhibited finer-grained local variability. In South Georgia, linear patterns reflected the association between forested wetlands and bottomland habitats. Circular patterns around numerous small cities reflected the accretion pattern of development, which created rings of high WUI index values where increasing forest cover intersected suburban housing densities on the urban fringes. Local variability in the relative dominance of forest and agricultural land cover also influenced WUI index patterns across much of Central and South Georgia.

Although road and housing densities were generally correlated, there were several areas where the WUI index was sensitive to our specification of the road index. West of the Okefenokee, housing densities are extremely low but rural road densities were very high. Therefore, this area was assigned high WUI indices rather than being identified as a wildland area. A similar phenomenon was observed at the Fort Stewart military base, which also had low housing densities and high road densities. Our decision to weight all types of roads equally in the road density calculations influenced these outcomes. Areas with high densities of unimproved roads had a similar influence on the final WUI index as areas with similar densities of highways. This decision can be justified on the contention that smaller roads provide direct human access to forested areas for camping, hunting, dumping, and other activities that can have a strong environmental impact. For the standpoint of fire risk assessment, road density may be correlated with the density of ignitions from human sources (Cardille et al., 2001; Zhai et al., 2003).

This example demonstrates that the results of this type of deductive modeling exercise are highly sensitive to the assumptions that underlie the variable selection, scaling, and weighting. However, this sensitivity is advantageous in that it allows the WUI index to be “tuned” to specific objectives. Consider a WUI index intended to identify areas where human infrastructure is likely to limit the applicability of prescribed fire as a fuel management treatment. Potential liability for traffic accidents caused by smoke is a major concern in this regard. Because the potential for such an accident would increase with traffic volume and speed, it would make sense to develop a weighted road density function based on road size.

Additional sources of spatial data can also be readily incorporated into a WUI model. In particular, more detailed information on historical fires, fuels and potential ignitions sources would help to identify forested areas where uncontrolled wildfire is most likely to occur. Detailed information on the locations, of hospitals, schools, utilities, and other infrastructure would be also useful for evaluating the

WUI from the standpoint of potential wildfire risks, as well as managing smoke away from these facilities during prescribed burns. Although our current model presents a static picture of the WUI, it could be enhanced to investigate patterns of development, leading to a more dynamic view of the interface.

3.4 Implications for Managers

Growth of the WUI has many influences on forests and their management (e.g., Duryea and Hermansen, 2002; Zipperer, 2002). Tourism, recreation, and amenity migration are prime examples of these influences. Here we will concentrate on the relationships with fire and smoke. The issues can be generalized into a primary effect on fire risk and a secondary effect on traditional forest management, which includes the use of prescribed burning to manage hazardous fuels. The values at risk are substantial: recent wildfire seasons have seen high costs for suppression ($1.5 billion nationwide in 2002, NIFC, 2001) and damage (the 1998 wildfires in Florida alone cost close to $800 million in damage, Butry et al., 2001). The growing WUI increases both the risk of wildfire occurring and the cost of wildfire by placing higher values at risk than in wildland areas.

Fire behavior is understood at its simplest as the interaction of fuels, weather, and an ignition source. People in the WUI can affect fire behavior by altering natural plant communities as well as by placing artificial fuels (i.e., structures) in the landscape Doolittle, 1978; Donoghue and Main, 1985; Prestemon and Butry, 2005). Natural ignition sources are generally lightning but humans introduce arson, accidents, and transportation as ignition sources. Estimating actual wildfire risk introduces broader spatial and temporal considerations than are used for predicting fire behavior. For example, the devastating 1998 fire season in Florida was below average in number of fires, but double the average number occurred during the summer (Butry et al., 2001). Anomalous weather patterns associated with El Niño-Southern Oscillation (ENSO) caused a build-up in fuels during the preceding year and there was an unusually sharp transition to the dry La Niña phase (Brenner, 1991; Butry et al., 2001). Broad scale modeling of the 1998 Florida fires validated that temporal dynamics are important to effectively estimating wildfire risk (Prestemon et al., 2002) and including socioeconomic conditions of communities improves the understanding of underlying causes of wildfires (Mercer and Prestemon, 2005). At the rural end of the WUI, at least in Florida, there were fewer wildfire ignitions and lower aggregate area burned, probably because forest management was active and prescribed burning frequent. In more densely populated areas with higher property values, prescribed burning was rare and ignitions and the area burned were higher (Mercer and Prestemon, 2005).

Managing hazardous fuel loads in the WUI will be critical for reducing the risk of catastrophic wildfires. Even though land ownership changes and land use is converted from forestry to housing development, the land cover often remains in forest, albeit a less dense forest cover than if managed for timber. In the South, especially in the rapidly urbanizing areas along the coasts, long growing seasons and usually abundant moisture cause those potentially hazardous fuels re-grow within a few years of burning (Brose and Wade, 2002). Prescribed burning remains the most effective treatment of potentially hazardous fuels in southern forests (Haines et al., 2001) and there are many guidelines for conducting prescribed burns in wildland areas (Wade et al., 1989). Land managers use prescribed burning to treat 6 million – 8 million acres of forest and agricultural land annually in the South. Use of prescribed burning in the WUI is still practical but calls for an even higher level of planning and preparedness, safe conduct, and communication to neighboring landowners and local officials (Miller and Wade, 2003; Wade and Mobley 2007).

Even when continued forest management is feasible, there will be further constraints on use of prescribed burning in the WUI due to smoke. In fact, smoke is probably the key issue in suitability of prescribed burning as a way to manage fuel loads in the interface. Concerns with smoke are several: local and regional air quality (Achtemeier 2001 and 2003), visibility on roads (Mobley, 1989), health impacts especially on sensitive segments of the population with respiratory problems (Sorenson et al., 1999), and nuisance effects (Monroe, 2002). Problem smoke is not confined to the South and reduced visibility from smoke on highways has caused fatalities in Western states such as Oregon, as well as in the South (Achtemeier et al., 1998; Achtemeier, 2002). Nevertheless, smoke from prescribed burning is a critical issue in the South due to a combination of physical (meteorology, climate, topography), biological (fire-affected vegetation and hazardous fuels), and social (population density, road network) factors. While smoke can be a problem at any time during a wildland fire, the worst conditions are in valley bottoms and drainages during the night (Achtemeier, 2002) and smoke can combine with moist air masses to produce exceptionally dense "superfog" that reduces visibility to fractions of a meter (Achtemeier, 2003).

Managing hazardous fuel loads across the wildland to urban gradient is a complex problem of many facets without obvious solution. The location within the WUI, time since last fire, stand density, and the quality of woody material affects the range of treatment options available. Not all ecosystems within the WUI are susceptible to ignition, except under extreme drought conditions. If fuels have accumulated by fire exclusion (lack of prescribed burning or suppression of wildfires), overly dense forest stands will have developed that require mechanical reduction of overstory and midstory woody stems before understory woody and herbaceous material can be treated. If the stand to be treated is in the wildland, conventional timber harvesting equipment may be used, and the operation may be economically feasible if there is sufficient timber value. If the operation is conducted in the intermix zones, mechanical reductions (i.e., thinning) may be feasible as a one-time treatment to bring fuel loads into balance. Forest operations selected for WUI applications must be appropriately matched to the terrain and stand conditions, the unique constraints of operating in the WUI, the product specifications of any extracted materials, and the prescription requirements of the treatment. Conventional mechanical reduction equipment is designed to operate effectively on large areas so high speed and maximum cutting width are common design goals. Operations for the WUI, on the other hand, should be lightweight to minimize soil impacts and road transportation problems. Cutting width and speed may not be as important as minimizing thrown debris and operating in tight quarters near structures and the public.

Suitability of an area for continued forest management is affected by exurbanization due to parcelization of the forest estate, reduction of tract size, and diseconomies of scale. Conventional forest operations face significantly increasing costs as tract size drops below 25 acres (Greene et al., 1997). This is primarily due to the increasing overhead of move-in costs and delay time associated with large capital-intensive equipment. In the diffuse boundary intermix zone where individual ownerships are small or in the distinct boundary zone where forest land is becoming parcelized into smaller ownerships, conventional economics may not apply (Wear and Newman, 2004). In the WUI, operations that involve a single machine performing multiple functions will have lower move-in costs (Wilhoit and Rummer, 1999). A small forwarder with a harvester head on the crane (a harwarder) would be a unique multi-function machine for WUI extraction needs. Smaller equipment where multiple machines can be moved on a single transport trailer may also be advantageous. Harvesting equipment mounted on all-terrain vehicles (ATV) can be easily transported from site to site. In dense, overstocked stands resulting from fire suppression, individual stems may be too small for conventional products and biomass thinning for energy wood may be appropriate. In such cases, combining a small chipper with cut-to-length harvesting systems may be feasible (Bolding and Lanford, 2001). Biomass material that has no product value may have to mulched and left in the stand to minimize costs. New technology to collect and bundle small material in the woods for transport to processing facilities and the development of bioenergy conversion technologies may provide additional options in the future. A complete fuel reduction treatment in the WUI will thus require an integrated system of several machines to achieve stand management goals while minimizing costs and maximizing fiber recovery and utilization.

Once woody fuels have been reduced, there remains the need to establish and maintain a low-risk herbaceous understory and prevent development of higher-stature woody fuels. In the South, the need for re-treatment can be as frequent as every 2 – 5 years in some fuel types (e.g., coastal flatwoods; Brose and Wade, 2002). Alternatives to use of fire to manage understory fuel loads over large areas are few, due to higher cost of mechanical and chemical alternatives and the required frequency of application. In localized areas protecting high-value structures or resources, alternatives to prescribed burning may involve mechanical reduction such as mowing or bush-hogging (Windell and Bradshaw, 2000; Rummer et al.,

2002) of current fuel loads and maintenance of low-risk understory through repeated mechanical treatments or herbicides, although such options may not be acceptable to some landowners (Loomis et al., 2000). At the urban end of the WUI gradient and throughout the WUI where individual home sites abut wildland, application of defensible space concepts and use of fire-resistant building and landscaping materials are critical to minimizing losses due to wildfires (Monroe, 2002; Long et al., 2005). In some states, local regulations are beginning to reflect these needs (Haines et al., 2005).

3.5 Conclusion

The rapid expansion of the US population since World War Ⅱ into formerly rural areas has caused significant shifts in land use and land cover that present the natural resource manager not only with constraints on traditional land management but also a new class of resource and people management problems in the interface zone where urban and wildland uses must co-exist. This rapidly expanding and changing WUI is more than a boundary or discrete class of land use, and can best be understood as a set of complex social, physical, and biologic gradients. Where the WUI mixes people with fire-affected forest vegetation, particular problems arise. Fire risk problems in the WUI are greater than in wildland because there is a higher risk of catastrophic wildfire; ignitions by humans increase and fuel loads generally are greater because of lack of on-going management. By placing higher values at risk (i.e., structures built within fire-affected forests), the potential costs of wildfires are greater. The cost of wildfires goes well beyond damage to structures, as scenic viewscapes can remain damaged for years and affect tourism-based economies (Butry et al., 2001).

The Southern US exemplifies the problems of mixing urbanized land uses with fire-affected natural vegetation. Because of an extensive road system, the entire South must be regarded as a WUI, at least in terms of managing smoke from prescribed burning. Even highly urbanized areas such as Atlanta, Georgia have been affected by smoke from wildfires and prescribed burning. Urbanization constrains traditional forest management and use of prescribed burning even at the wildland end of the WUI gradient because of concerns for liability from escaped fire, transportation safety, and regional air quality. Moving toward the urban end of the gradient, these concerns greatly increase and pose the dilemma of the lack of fuel management increasing the risk of occurrence and severity of inevitable wildfire.

Managers need additional tools to define the current WUI and affordable methods for monitoring land use change and updating the WUI. Such tools will provide managers with improved ability to estimate wildfire risk at a scale that permits them to plan appropriately to attack wildfire when it occurs to minimize property losses and insure firefighter safety. Individuals living in the WUI need to be educated as to their risk and their responsibility for reducing that risk. Remote sensing (RS) and geographic information systems, along with spatial information at appropriate scale, will play a critical role in providing managers with monitoring capability that can also be used to educate the public about the WUI: nothing says it like a map.

Acknowledgements

Discussions with many people helped shape the ideas presented here. Special mention goes to Scott Goodrick, Gary Achtemeier, and Yongqiang Liu for broadening our understanding of the issues surrounding smoke management. We also profited from discussions with Joe O'Brien, Tom Waldrop, Ken Outcalt, Dale Wade, and Yangjian Zhang. Helpful reviews were provided by Ken Cordell, Jeff Prestemon, Wayne Zipperer, and two anonymous reviewers.

References

Achtemeier GL, (2001), Simulating nocturnal smoke movement. *Fire Management Today*, **61**: 28 – 33

Achtemeier GL, (2002), Problem smoke. In: Hardy C, Ottmar RD, Peterson JL, et al. (eds) Smoke management guide for prescribed wildland fire. Boise, ID: National Wildfire Coordinating Group

Achtemeier GL, (2003), On the origins of "Superfog"—a combination of smoke and water vapor that produces zero visibility over roadways. In: Proc. 2nd Intl. Wildland Fire Ecology and Fire Management Congress and 5th Symposium on Fire and Forest Meteorology, held 16 – 20 November 2003, Orlando, FL; American Meteorological Society, Boston, MA; J8.9, 4

Achtemeier GL, Jackson W, Hawkins B, Wade DD, McMahon C, (1998), The smoke dilemma: A head-on collision! In: Wadsworth KG (ed), Transactions of the 63rd North American Wildlife and Natural Resources Conference, held 20 – 24 March 1998, Orlando, FL. Wildlife Management Institute, Washington, DC: 415 – 421

Alig RJ, Kline JD, Lichtenstein M, (2004), Urbanization on the US landscape: looking ahead in the 21st century. *Landscape and Urban Planning*, **69**: 219 – 234

Bliss JC, Nepal SK, Brooks RT, Larsen MD, (1997), In the mainstream: environmental attitudes of mid-South landowners. *Southern Journal of Applied Forestry*, **21**(1): 37 – 43

Bolding MC, Lanford BL, (2001), Forest fuel reduction through energy wood production using a small chipper/CTL harvesting system. Proceedings of 24th Annual Meeting Council on Forest Engineering, 15 – 19 July 2001, Snowshoe, West Virginia. Council on Forest Engineering, Corvallis, OR; CD-ROM

Brenner J, (1991), Southern oscillation anomalies and their relation to Florida wildfires. *Fire Management Notes*, **52**(1): 28 – 32

Brose P, Wade DD, (2002), Potential fire behavior in pine flatwood forests following three different fuel reduction techniques. *Forest Ecology and Management*, **163**: 71 – 84

Butry DT, Mercer DE, Prestemon JP, Pye JM, Holmes TP, (2001), What is the price of catastrophic wildfire? *Journal of Forestry*: 9 – 17

Butry DT, Prestemon JP, (2005), Spatio-temporal wildland arson crime functions. Paper presented at the Annual Meeting of the American Agricultural Economics Association, 26 – 29 July 2005, Providence, Rhode Island. Published on the Internet at http://agecon.lib.umn.edu/cgi-bin/pdf_view.pl?paperid=16442&ftype=.pdf (last accessed 9 October 2007)

Cardille JA, Ventura SJ, Turner MG, (2001), Environmental and social factors influencing wildfires in the upper Midwest, United States. *Ecological Applications*, **11**: 111 – 127

Caulfield JP, (1998), A fund-based timberland investment performance measure and implications for asset allocation. *Southern Journal of Applied Forestry*, **22**(3): 143 – 147

Cohen JD, (2000), Preventing disaster: Home ignitability in the wildland-urban interface. *Journal of Forestry*, **98**(3): 15 – 21

Cordell HK, Bergstrom JC, Betz CJ, Green GT, (2004), Socioeconomic forces shaping the future of the United States. In: Manfredo MJ, Vaske JJ, Bruyere BL, Field DR, Brown PJ (eds). Society and natural resources: A summary of knowledge. Jefferson, MO: Modern Litho. 361

Cordell HK, Bliss JC, Johnson CY, Fly M, (1998), Voices from Southern forests. In Wadsworth, K.G., editor, Transactions of the 63rd North American Wildlife and Natural Resources Conference, held 20 – 24 March 1998, Orlando, FL. Wildlife Management Institute, Washington, DC: 332 – 347

Cordell HK, Macie EA, (2002), Population and demographic trends. In: Macie EA, Hermansen LA (eds) 2002. Human influences on forest ecosystems—the Southern wildland-urban interface assessment. USDA Forest Service Southern Research Station General Technical Report SRS-55. Asheville, NC: 11 – 35

Clutter M, Mendell B, Newman D, Wear D, Greis J, (2005), Strategic factors driving timberland ownership changes in the U.S. South. Report to the Southern Group of State Foresters, November 2005. Retrieved January 7, 2006 from http://www.srs.fs.usda.gov/econ/pubs/southernmarkets/strategic-factors-and-ownership-v1.pdf

Duryea ML, Hermansen LA, (2002), Challenges to forest resource management. In: Macie EA, Hermansen LA (eds) 2002. Human influences on forest ecosystems—the Southern wildland-urban interface assessment. USDA Forest Service Southern Research Station General Technical Report SRS-55. Asheville, NC: 93 – 113

Donoghue LR, Main, WA, (1985), Some factors influencing wildfire occurrence and measurement of fire prevention effectiveness. *Journal of Environmental Management*, **20**: 87 – 96

Doolittle ML, (1978), Analyzing wildfire occurrence data for prevention planning. *Fire Management Notes*, **39**(2): 5 – 7

Forman RTT, (2002), Road Ecology. Island Press, Washington, D.C

Greene WD, Harris TG, DeForest CE, Wang J, (1997), Harvesting cost implications of changes in the size of timber sales in Georgia. *Southern Journal of Applied Forestry*, **21**(4): 193 – 198

Hagen JM, Irland LC, Whitman AA, (2005), Changing timberland ownership in the Northern Forest and implications for biodiversity. Manomet Center for Conservation Sciences, Report #MCCS-FCP-2005-1, Brunswick, Maine, 25

Haight RG, Cleland DT, Hammer RB, Volker CR, Rupp TS, (2004), Assessing fire risk in the wildland-urban interface. *Journal of Forestry*, **102**(7): 41 – 48

Haines TK, Busby RL, Cleaves DA, (2001), Prescribed burning in the South: Trends, purpose, and barriers. *Southern Journal of Applied Forestry*, **25**(4): 149 – 153

Haines T, Renner C, Reams M, Granskog J, (2005), The national database of wildfire mitigation programs: state, county and local efforts reduce wildfire risk. p 1 – 7 in Proceedings of the joint meeting of the Society of American Foresters and Canadian Institute of Foresters "One Forest Under Two Flags", held Edmonton, Alberta, Canada: Society of American Foresters, Bethesda, MD

Hammer RB, Stewart SI, Winkler RL, Radeloff VC, Voss PR, (2004), Characterizing dynamic spatial and temporal residential density patterns from 1940 – 1990 across the North Central United States. *Urban and Landscape Planning*, **69**: 183 – 199

Hirschhorn JS, (2000), Growing pains: Quality of life in the new economy. National Governors' Association, Washington, DC

Hobbs F, Stoops N, (2002), Demographic trends in the 20th Century. Census 2000 Special Reports, CENSR-4. US Census Bureau, Washington, DC

Hull RB, Stewart SI, (2002), Social consequences of change. In: Macie EA, Hermansen LA (eds) 2002. Human influences on forest ecosystems—the Southern wildland-urban interface assessment. USDA Forest Service Southern Research Station General Technical Report SRS-55. Asheville, NC: 115 – 129

Jacobson SK, Monroe MC, Marynowski S, (2001), Fire at the wildland interface: the influence of experience and mass media on public knowledge, attitudes, and behavioral intentions. *Wildlife Society Bulletin*, **29**(3): 929 – 937

Kramer EA, Conroy MJ, Elliott MJ, Anderson EA, Bumback WR, Epstein. J, (2003), A Gap Analysis of Georgia. U.S. Geological Survey, Reston, VA

Long AJ, Wade DD**,** Beall FC, (2005), Managing for fire in the interface: Challenges and opportunities. Chapter 13 in Vince SW, Duryea, ML, Macie EA, Hermansen LA. Forests at the Wildland-Urban Interface. CRC Press, Boca Raton. 201 – 223

Loomis JB, Bair LS, Omi PN, Rideout DB, González-Cabán A, (2000), A survey of Florida residents regarding three alternative fuel treatment programs. Report to the Joint Fire Science Program, July 26, 2000. 88

Loomis JB, Bair LS, González-Cabán A, (2001), Prescribed fire and public support: knowledge gained, attitudes changed in Florida. *Journal of Forestry*, **99**(11): 18 – 22

Macie EA, Hermansen LA (eds), (2002), Human influences on forest ecosystems—the Southern wildland-urban interface assessment. USDA Forest Service Southern Research Station General Technical Report SRS-55. Asheville, NC: 160

Mackun PJ, Wilson SR, (2000), Population trends in metropolitan areas and central cities, 1990 to 1998. Retrieved January 7, 2006 from http://www.census.gov/prod/2000pubs/p25-1133.pdf

Mercer DE, Prestemon JP, (2005), Comparing production function models for wildfire risk analysis in the wildland-urban interface. *Forest Policy and Economics*, **7**: 782 – 795

Miller SR, Wade D, (2003), Re-introducing fire at the urban/wild-land interface: planning for success. *Forestry*, **76**: 253 – 260

Mobley HE, (1989), Summary of smoke-related accidents in the South from prescribed fire (1979 – 1988). American Pulpwood Association Technical Release 90-R-11

Monroe M, (2002), Fire. In Macie EA, Hermansen LA (eds) 2002. Human influences on forest ecosystems—the Southern wildland-urban interface assessment. USDA Forest Service Southern Research Station General Technical Report SRS-55. Asheville, NC: 133 – 150

NIFC, (2001), National Fire News, Wildland Fire Season 2000 At A Glance, updated June 14, 2001. National Interagency Fire Center, Boise, ID. Retrieved January 7, 2005 from http://www.nifc.gov/fireinfo/2000/

Nowak DJ, Walton JT, (2005), Projected urban growth (2000 – 2050) and its estimated impact on the US forest resource. *Journal of Forestry*, **103**(8): 383 – 389

Nowak DJ, Walton JT, Dwyer JF, Kaya LG, Myeong S, (2005), The increasing influence of urban environments on US forest management. *Journal of Forestry*, **103**(8): 377 – 382

O'Brien JJ, (1998), The distribution and habitat preferences of rare Galactia species (Fabaceae) and Chamaesyce deltoidea subspecies (Euphorbiaceae) native to southern Florida pine rockland. *Natural Areas Journal*, **18**(3): 208 – 222

O'Sullivan D, Unwin DJ, (2003), Geographic Information Analysis. John Wiley & Sons, Hoboken, NJ

Prestemon JP, Butry DT, (2005), Time to burn: Modeling wildland arson as an autoregressive crime function. *American Journal of Agricultural Economics*, **87**: 756 – 770

Prestemon JP, Pye JM, Butry DT, Holmes TP, Mercer DE, (2002), Understanding broadscale wildfire risks in a human-dominated landscape. *Forest Science*, **48**(4): 685 – 693

Radeloff VC, Hammer RB, Stewart SI, Fried JS, Holcomb SS, McKeefry JF, (2005), The wildland-urban interface in the United States. *Ecological Applications*, **15**: 799 – 805

Ravenel R, Tyrrell M, Mendelsohn R (eds), (2002), Institutional timberland investment. Yale Forest Forum Vol. 5 No. 3. Global Institute of Sustainable Forestry, Yale University, New Haven, CT

Riitters KH, Wickham JD, (2003), How far to the nearest road? *Frontiers in Ecology and Environment*, **1**(3): 125 – 129

Rummer R, Outcalt K, Brockway D, (2002), Mechanical mid-story reduction treatments for forest fuel management. 2002. In: New century: new opportunities: 55th annual Southern Weed Science Society meeting; 28 – 30 January 2002; Atlanta, GA. Champaign, IL: Southern Weed Science Society: 76 [Abstract]

Snyder JR, Herndon A, Robertson WB, (1990), South Florida rockland. 230 – 277 in Myers RL, Ewel JJ (eds), Ecosystems of Florida. University of Central Florida Press, Orlando, FL. 765

Stanturf JA, Kellison RC, Broerman FS, Jones SB, (2003), Productivity of southern pine plantations: where are we and how did we get here? *Journal of Forestry*, **101**(3): 26 – 31

Stein SM, McRoberts RE, Alig RJ, Nelson MD, Theobald DM, Eley M, Dechter M, Carr M, (2005), Forests on the edge: Housing development on America's private forests. General Technical Report PNW-GTR-636. Portland, OR: USDA Forest Service, Pacific Northwest Research Station. 16

Sorenson B, Fuss M, Mulla Z, Bigler W, Wiersma S, Hopkins R, (1999), Surveillance of morbidity during wildfires—central Florida 1998. *Morbidity and Mortality Weekly Report*, **48**(4): 78 – 79

Sullivan WC III, (1994), Perceptions of the rural-urban fringe: citizen preferences for natural and developed settings. *Landscape and urban Planning*, **29**: 85 – 101

Theobald DM, (2001), Land-use dynamics beyond the American urban fringe. *The Geographical Review*, **91**(3): 544 – 564

Theobald DM, (2004), Placing exurban land-use change in a human modification framework. *Frontiers in Ecology and Environment*, **2**(3): 139 – 144

Turner MG, Wear DN, Flamm RO, (1996), Land ownership and land-cover change in the Southern Appalachian Highlands and the Olympic Peninsula. *Ecological Applications*, **6**(4): 1150 – 1172

Turner MG, Pearson SM, Bolstad P, Wear DN, (2003), Effects of land-cover change on spatial pattern of forest communities in the Southern Appalachian Mountains (USA). *Landscape Ecology*, **18**: 449 – 464

USDA and USDI, (2001), Urban wildland interface communities within vicinity of Federal lands that are at high risk from wildfire. *Federal Register*, **66**: 751 – 777

US DOT, (2004), Highway statistics 2003, Public Road Length (Table HM-10). Federal Highway Administration website accessible at http://www.fhwa.dot.gov/policy/ohim/hs03/htm/hm10.htm; last accessed January 24, 2006

Wade DD, Brenner J, (1995), Florida's solution to liability issues. In Weise DR, Martin RE (technical coordinators), Proceedings of the Biswell Symposium: fire issues and solutions in urban interface and wildland ecosystems. USDA Forest Service, Pacific Southwest Research Station General Technical Report PSW-158. Berkeley, CA: 131 – 138

Wade DD, Custer G, Thorsen J, Kaskey P, Kush J, Twomey B, Voltolina D, (1998), Reintroduction of fire into fire-dependent ecosystems: Some southern examples. In Pruden TL, Brennan LA (eds), Fire in ecosystem management: shifting the paradigm from suppression to prescription. Tall Timbers Ecology Conference Proceedings No. 20. Tall Timbers Research Station, Tallahassee, FL: 94 – 98

Wade DD, Lunsford JD, (1989), A guide for prescribed fire in southern forests. Tech. Pub. R8-TP11, USDA Forest Service Southern Region, Atlanta, GA

Wade D, Mobley H, (2007), Managing smoke at the wildland urban interface. General Technical Report SRS-103, USDA Forest Service Southern Research Station, Asheville, NC. 28

Wear DN, (2002), Land use. In: Wear, D.N. and Greis, J.G. eds. Southern forest resource assessment. General Technical Report SRS-53. USDA Forest Service Southern Research Station, Asheville, NC: 153 – 173

Wear DN, Bolstad P, (1998), Land-use changes in Southern Appalachian landscapes: spatial analysis and forecast evaluation. *Ecosystems*, **1**: 575 – 594

Wear DN, Liu R, Foreman JM, Sheffield RM, (1999), The effects of population growth on timber management and inventories in Virginia. *Forest Ecology and Management*, **118**: 107 – 115

Wear DN, Newman DH, (2004), The speculative shadow over timberland values in the U.S. South. *Journal of Forestry*, **102**(8): 25 – 31

Wilhoit J, Rummer B, (1999), Application of small-scale systems: evaluation of alternatives. Presented at the 1999 ASAE/CSAE-SCGR Annual International Meeting, Paper No. 99-5056. ASAE, 2950 Niles Road, St. Joseph, Ml 49085-9659 USA

Wimberly MC, Zhang Y, Stanturf JA, (2005), GIS Application in the wildland-urban interface. Chapter 9 in Shao G, Reynolds K (eds) Computer Applications In Sustainable Forest Management. Springer, Heidelberg. In Press

Windell K, Bradshaw S, (2000), Understory biomass reduction methods and equipment. USDA Forest Service, Technology & Development Program 0051-2828-MTDC. Missoula, MT. [Partial document summarizing the full version, Understory Biomass Reduction Methods and Equipment Catalog 0051-2826-MTDC]

Yin R, Caulfield JP, Aronow ME, Harris TG Jr, (1998), Industrial timberland: current situation, holding rationale, and future development. *Forest Products Journal*, **48**(10): 43 – 48

Zhai YS, Munn IA, Evans DL, (2003), Modeling forest fire probabilities in the South Central United States using FIA data. *Southern Journal of Applied Forestry*, **27**: 11 – 17

Zhang Y, (2004), Identification of the Wildland-Urban Interface at Regional and Landscape Scales. Ph.D. Dissertation. University of Georgia, Athens

Zhang Y, Wimberly MC, (2007), The importance of scale in using hierarchical census data to identify the wildland-urban interface. *Southern Journal of Applied Forestry*, **31**: 138 – 147

Zipperer WC, (2002), Urban influences on forests. In: Macie, E.A. and Hermansen, L.A., editors. 2002. Human influences on forest ecosystems—the Southern wildland-urban interface assessment. USDA Forest Service Southern Research Station General Technical Report SRS-55. Asheville, NC: 73 – 91

4 An Overview of NOAA's Fire Weather, Climate, and Air Quality Forecast Services

Elliot Jacks and Heath Hockenberry

Office of Climate, Water, and Weather Services, NOAA National Weather Service, 1325 East West Highway, Silver Spring, MD 20910, USA

Email: {Elliot.Jacks, Heath.Hockenberry}@noaa.gov

Abstract Among the many products and services NOAA provides include those oriented towards supporting prediction of fire danger and spread, climate prediction with a focus on drought, and air quality predictions with regard to ozone and smoke. The National Weather Service (NWS) Fire Weather program supports two main areas of concern, fire suppression and resource management, with NWS Fire Weather Planning Forecasts, NWS Fire Weather Watch and Red Flag Warning program, site specific spot forecasting, and onsite support services by specially trained incident meteorologists (IMETs). The NWS recently began the implementation of the national digital forecast database (NDFD) that features an interactive map. NWS Climate Services are leading the development of the management structure for the national integrated drought information system (NIDIS) Implementation Team to lead improved monitoring and prediction of drought. The NWS Climate Prediction Center took an active role in the implementation of the new climate forecast system (CFS), a coupled model which represents the interaction between the Earth's atmosphere and oceans. NOAA and the Environmental Protection Agency (EPA) have developed a national air quality forecasting capability to improve the basis for EPA's air quality alerts and to provide a broad spectrum of air quality information, including with respect to smoke. NOAA's products and services to support predictions for Fire Weather, Air Quality and Climate all share the common thread of evolving towards a higher degree of specificity and accessibility.

Keywords Fire weather watch, red flag warning, IMET, NDFD, NIDIS, CFS, AQF System

Among the many products and services National Oceanic and Atmospheric Administration (NOAA) provides include those oriented towards supporting prediction of fire danger and spread, climate prediction with a focus on drought, and air quality predictions with regard to ozone and smoke. In particular, the fire-based products used heavily by Incident Commanders at fire scenes to direct daily fire fighting operations, as well as fire managers to support planning and placement of fire fighting resources.

Figure 4.1 An engine crew scouts a dangerously active crown fire

NOAA's drought and air quality products also support fire planning and mitigation in advance of and in the wake of fires, respectively. This chapter provides an overview of these products and services, including an overview of NOAA's new digital databases which make these products and services increasingly available to a wide spectrum of users.

4.1 NWS Fire Weather

The vision of NOAA's national weather service's (NWS) fire weather program is to provide timely data and forecasts to support wildland firefighters in minimizing fire fatalities, injuries, and loss of property; and to reduce fire suppression and land management costs by providing more timely and accurate weather information. The role served by the NWS is of critical importance to fire managers, who rely heavily on the most timely fire weather planning and forecast information. The NWS uses the latest available technology to continuously advance fire weather forecasting systems and services.

4.2 Products and Services

There are two main areas of concern for NWS customers; these include suppression and resource management. NWS fire weather planning forecasts provide site-specific, detailed information critical to the suppression of a wildfire or a federal prescribed burn. These vital forecast elements include temperature, humidity, wind speed and direction, and dispersion. NWS forecasters focus on weather events such as dry thunderstorms, erratic wind conditions, dangerous lightning, and dry cold fronts which endanger the firefighters and crews on the line. The planning forecast provides 147,000 elements per day. This takes into consideration the 100 forecast offices which each cover 15 zones, twice daily, for a seven-day forecast with seven elements included in each.

For resource management, the NWS takes an active role in forecasting conditions for prescribed burns. Prescribed burning is defined as "fire applied in a knowledgeable manner to forest fuels on a specific land area under selected weather conditions to accomplish pre-determined, well-defined management objectives." Prescribed burns are a safe and cost-effective way to reduce fuels that could lead to destructive, unplanned fires during the next fire season. Prescribed burning is also essential to the maintenance of many healthy ecosystems by creating the necessary changes for habitat manipulation.

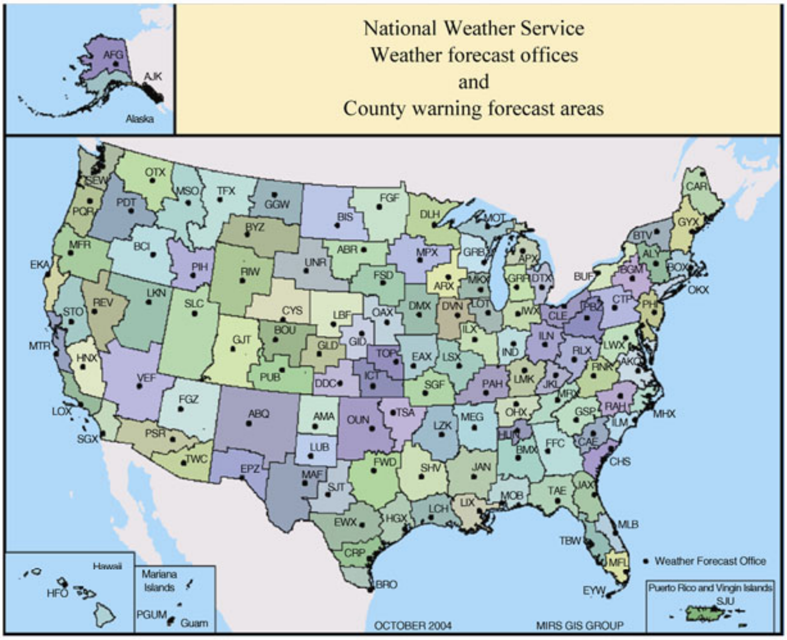

Figure 4.2 Figure indicates the distribution of NOAA's Weather Forecast Offices throughout the country

Figure 4.3 An ominous scene of the glow from a wildland urban interface (WUI)

The NWS fire weather watch and red flag warning program is the nationally recognized federal warning system used to alert wildland firefighters when conditions are favorable for fire weather activity. This program is essential to the safety of fire management crews. A fire weather watch is issued when red flag conditions are expected within the next 72 hours. A watch is upgraded to a red flag warning if the red flag criterion is expected to occur within the next 24 hours. By definition, a red flag event includes weather conditions which could sustain extensive wildfire activity, including sustained surface winds or high gusts, unusually hot and dry conditions or dry thunderstorm activity during a dry period. The NWS issues over 8,000 red flag warnings and fire weather watches throughout the course

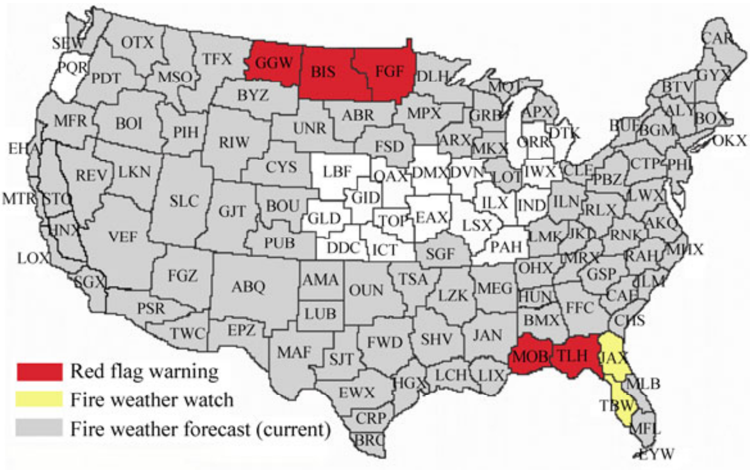

Figure 4.4 A graphic from the National Fire website, highlighting areas of critical fire weather

of a year. These warnings and watches are issued with an 85% rate of accuracy and a false alarm rate of only 22%. The NWS averages a lead-time of 7.8 hours for these warnings.

Site specific spot forecasting is another service provided by the NWS to support fire weather management for wildfires and prescribed burns. Spot forecasts are defined as non-routine forecasts that include skycover/weather, maximum/minimum temperature, maximum/minimum relative humidity, 20-foot winds, wind shifts/gusts and instability. Optional elements provided in a spot forecast include Haines index, transport wind, missing depth, lightning activity level (LAL) and chance of wetting rain. The NWS policy states that any public safety official is permitted to request a spot forecast for non-wildfires if it is deemed a threat to life and or property. The NWS issues over 15,000 fire weather spot forecasts, annually.

The storm prediction center (SPC) produces operational guidance products for fire weather each day. The products are designed to provide forecasting guidance to each weather forecast office (WFO) on the possibility of significant fire weather activity. SPC assesses dry lightning, low relative humidity, and significant wind potential. Areas are then highlighted to emphasize where these dangerous fire weather elements will occur. SPC plans on extending this product to highlight significant fire weather areas up to 8 days in advance.

The NWS also provides onsite support services for wildfires, Federal Prescribed Burns, and hazardous material (HAZMAT) incidents. The NWS currently employs 65 specially trained incident meteorologists (IMETs), who are professionally qualified in fire weather forecasting and onsite assistance. Each IMET receives at least three years of forecaster training and over 225 hours of fire weather classroom and on-the-job training, prior to becoming certified. In addition, IMETs are required to complete over 25 hours of fire weather refresher training annually, throughout the course of their careers and are sent to remote locations across the country to support hundreds of wildfire incidents every year. NOAA plans to continue expansion of IMET capabilities to new cities, and to train its forecasters on how to effectively respond to a wide variety of Incident Support needs from all of its WFOs. This may include supporting response to toxic spills, chemical releases, or other events of national significance such as large public gatherings. Also, IMETs will continue to support emergency managers at local emergency operations centers by utilizing their specialized equipment and expertise.

IMETs use a collection of specialized equipment when issuing on-site fire weather forecasts. The atmospheric theodolite meteorology unit (ATMU) consists of a theodolite, which is used in tracking weather balloons to calculate wind aloft, and various other instruments including a thermometer, anemometer, tools to measure humidity, and a first aid kit. This device gives IMETs the capability to efficiently operate at remote locations while providing close meteorological support to the fire management team. The all-hazards meteorological response system (AMRS) is another tool used by IMETs for data assimilation. The AMRS is comprised of high-tech computer software and satellite communications which make it possible for the IMETs to access accurate and timely weather data while in the field. IMETs also utilize laptop computers with FX-NET software, developed by NOAA's forecast systems laboratory (FSL) in Boulder, CO. This software provides IMETs with the capability to process weather observations and forecast data using an interface which is identical to their home office.

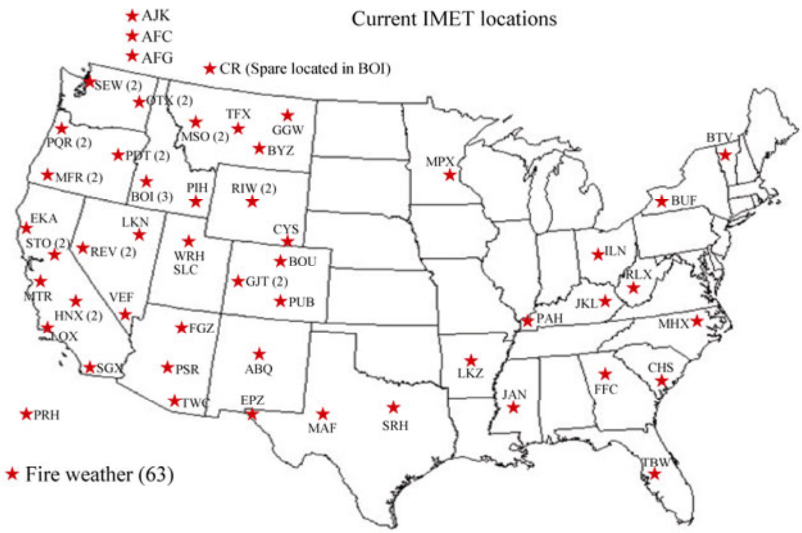

Figure 4.5 IMETs are strategically positioned to quickly meet the threat of wildfires and other hazardous, life-threatening incidents

Figure 4.6 Two NWS IMETs set up a mobile communications dish at an area command in Oregon

While the IMET concept has generally been intended to support wildland fires, IMETs are also used to support non-fire events which require weather support. For example, IMETs were deployed to assist in the Challenger Space Shuttle Recovery Mission, and also to assist with Hurricane Katrina when weather data were unavailable. The expanded use of IMETs is anticipated in support of non-fire events and Homeland Security needs.

NOAA operates two geostationary operational environmental satellites (GOES), one centered over the equator and 75° west and the other positioned at the equator and 135° west, providing images of atmospheric moisture and thermal structure over the continental U.S. at least every fifteen minutes. Each GOES satellite has a 3.9 μm infrared channel that can be used to detect forest fires. They also have high-resolution visible channels that can detect smoke from fires.

Figure 4.7 An example of the visible imagery showing the smoke from fires is shown. The red areas indicate the location of fires detected on the 3.9 μm of infrared imagery

4.3 Making Optimal Use of NWS Technology

4.3.1 Digital Services

The NWS recently began implementation of the national digital forecast database (NDFD) to track and display forecast elements. The database features an interactive map, which allows the user to "point and click" on a specific location and display forecast information for virtually any point across the entire United States. The database, which currently operates at a 5 km resolution, features two different types of forecasts. The forecast for the upcoming 1 – 3 days is updated every 3 hours and the forecast for days 4 – 7 is updated every 6 hours.

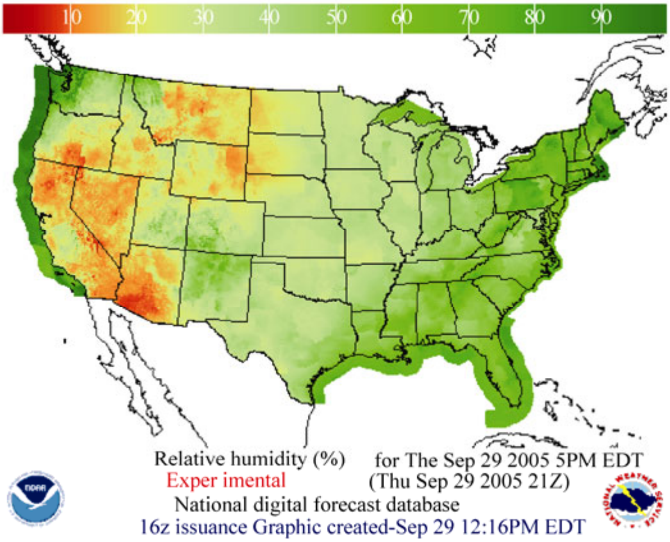

Figure 4.8 An example national mosaic of relative humidity for the continental U.S. generated from the NDFD

The forecaster on duty at each of the local WFOs is responsible for making updates to their segment of the digital database. In order to make the most accurate projection, the forecaster first looks at each of the models, and determines which appears to be the most accurate, based on current conditions and observations in combination with their forecasting experience. The forecaster then "populates" the grids using one of the models or keeping the previous forecast and adjusting it. Smart tools, which were developed to ensure grid consistency, are then run to ensure that forecast elements are consistent. The NDFD currently features six operational elements that are functional in the continental United States. These elements are maximum and minimum temperature, probability of precipitation over a 12 hour period, temperature, dew point, and weather. There are a number of forecast elements that are currently being tested and considered to be "experimental." These elements are evaluated for accuracy, timeliness, and consistency before they are deemed operational. The current experimental elements for CONUS are wave height, wind speed and direction, quantitative precipitation forecast (QPF), snow amount, sky cover, relative humidity and apparent temperature. More elements are scheduled to become operational in 2006.

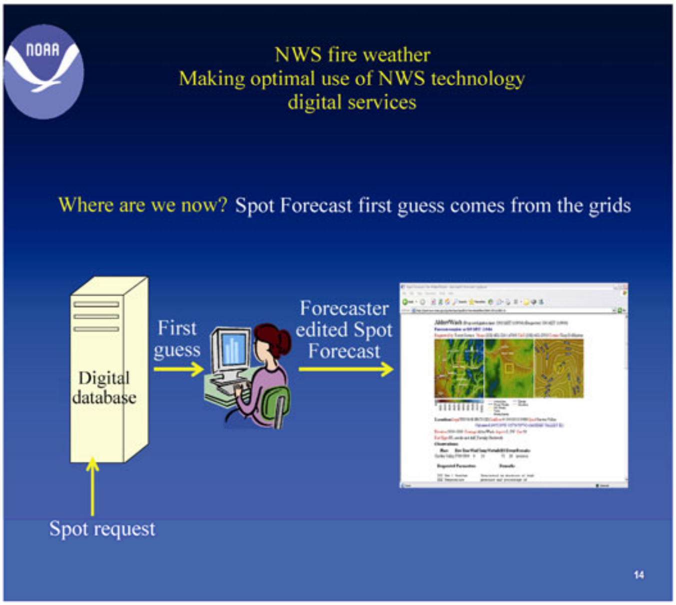

Figure 4.9 Flow chart illustrating how spot forecasts are generated

4.4 NWS Climate Services

NWS Climate Services are leading the development of the management structure for the national integrated drought information system (NIDIS) Implementation Team. The goal of the NIDIS Team is to create a comprehensive system to compile and incorporate data on the major indicators of drought including ground water levels, soil moisture, snow pack, stream flow, climate and forecasts. This early-warning system will enable users to efficiently determine appropriate mitigation efforts. The objective of the NIDIS Team is to lead to improved prediction, in addition to improved monitoring of drought.

4.4.1 Product Improvements

The NWS Climate Prediction Center took an active role in the implementation of the new climate forecast system (CFS). The CFS was developed at NOAA's environmental modeling center in conjunction with NOAA's office of oceanic and atmospheric research (OAR). CFS is a coupled model approach, which represents the interaction between the Earth's atmosphere and oceans. The study of this data is critical to the accurate determination of climate on seasonal time scales. This new system is expected to improve the accuracy and precision of climate forecasting.

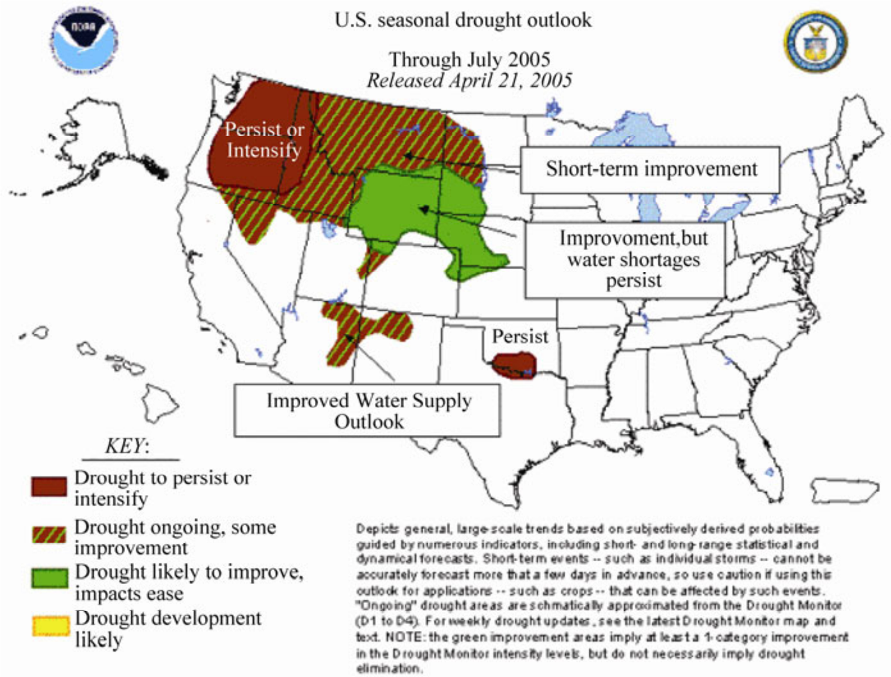

Figure 4.10 An example of the U.S. seasonal drought outlook generated by NOAA's NWS climate prediction center

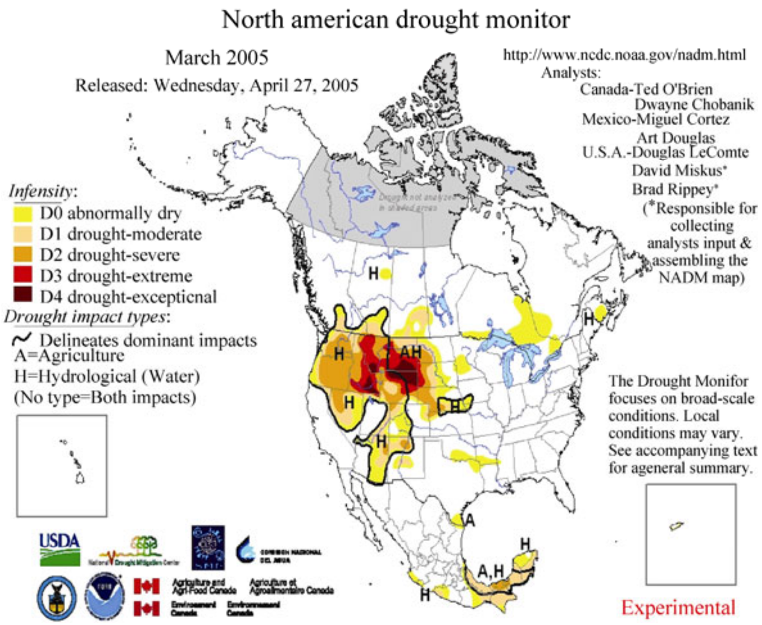

Figure 4.11 A sample of the interagency North American Drought Monitor product

Drought monitoring is a fundamental element in the planning and preparation stages for droughts and the necessary mitigation efforts that often follow. The NWS climate prediction center (CPC) is an integral part of the team developing international drought products and services, including the north american drought monitor (NA-DM). The NA-DM is a collaborative effort among drought experts in the United States, Mexico and Canada, to implement a system for monitoring drought conditions across the continent on a continual basis. The NA-DM is following the path of the already incepted and greatly successful united states drought monitor (US-DM). Since implementation in 1999, the US-DM has proven to be a highly effective tool in drought assessment and reporting on a weekly basis throughout the U.S. The CPC also manages the hazard assessment website which includes information concerning potential hazards in the areas of temperature, wind, precipitation, and soil/wildfire conditions. The purpose of the hazards assessment is to provide emergency managers and the general public with advance notice of potential hazards related to climate, weather and water events. These assessments are formulated by integrating NWS forecasts with long-range seasonal predictions, using state-of-the-art technology and science.

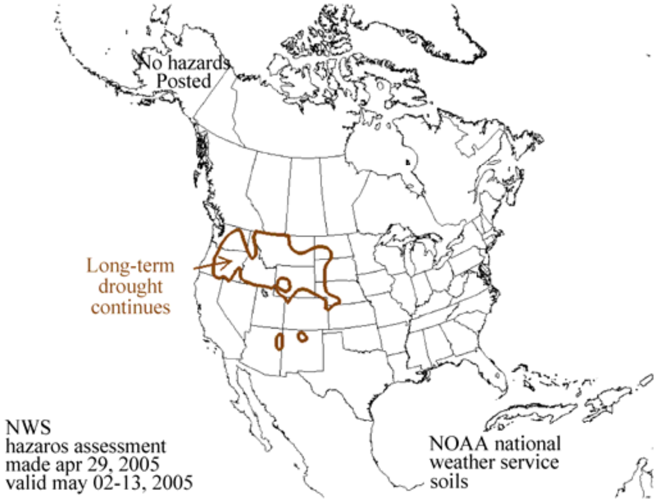

Figure 4.12 An example of the NWS hazard assessment for Soil/Wildfires drought monitoring product

4.5 National Air Quality Forecasting

4.5.1 Planned Capabilities

Under the direction of Congress, NOAA and the environmental protection agency

(EPA) have teamed up with State and local agencies to develop a national air quality forecasting (AQF) system. The goal of this AQF team is to limit harmful effects from poor air quality by forecasting ozone, PM and other pollutant levels with enough advance notice and accuracy for the public to make informed decisions when potentially harmful conditions exist. The initial deployment of NOAA's air quality forecast occurred in September of 2004 in the Northeastern United States. Since then, the AQF system has been expanded to include the entire U.S., east of the Rockies. The current system provides 1-day forecast guidance in 1-hour and 8-hour average concentrations for ground-level ozone. Nationwide deployment of the AQF system is expected to take place by 2008. NOAA plans to improve and expand the AQF system capabilities over the next decade. For example, in the next five to seven years, NOAA and the EPA plan to develop and test the possibility of forecasting concentrations of PM size, less than 2.5 microns. Also, within the next ten years, NOAA plans to extend the AQF range to 48 – 72 hours and include a broader range of significant pollutants.

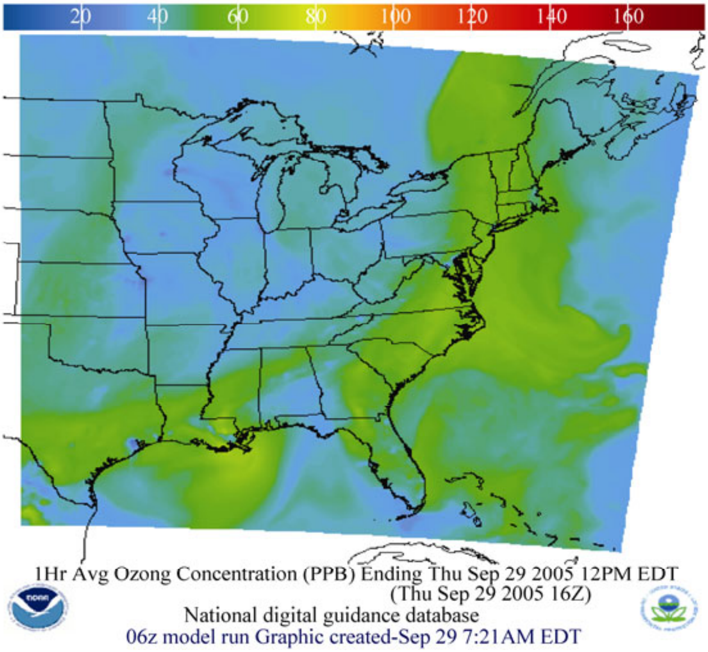

Figure 4.13 The above figure indicates average ozone concentrations over the entire Eastern U.S., east of the Rockies

The AQF system is managed by the national center for environmental prediction (NCEP) in the Environmental Modeling Center (EMC). The AQF system includes weather observations from the NWS and emissions inventory from the EPA, which is operationally integrated on NCEP's "Supercomputer." This collaboration of data, which is referred to as the community multiscale air quality model (CMAQ), is run twice daily, at 6Z and 12Z. Users are able to access this information on the NWS and EPA websites.

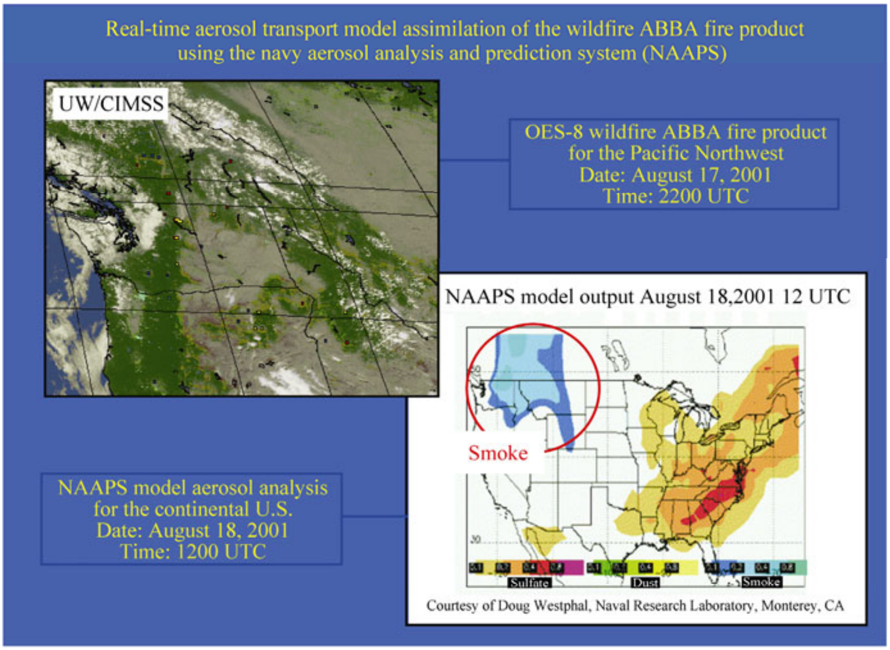

Figure 4.14 An example of how air quality and aerosol levels are now detectable by GOES satellite. (University of Wisconsin, CIMSS)

In conjunction with its federal, state and local government agencies, the NWS strives to meet its mission statement as outlined in NOAA's 2005 – 2010 strategic plan, which is "to understand and predict changes in the Earth's environment and conserve and manage coastal and marine resources to meet our Nation's economic, social, and environmental needs." The NWS and its partners continue to progress by utilizing the latest, state of the art technology and science to produce fire weather, climate, and air quality digital and graphical products.

4.6 Summary

NOAA's products and services to support predictions for fire weather, Air quality and climate all share the common thread of evolving towards a higher degree of specificity and accessibility to support an increasingly sophisticated user base. This evolution includes (but is not restricted to) the provision of on-site and spot forecast services to support fire fighting and planning, access to real time models and other predictive information in digital formats, collaborative operational research geared towards improving predictions in critical areas such as climate and air quality to support public health and preparedness.

References

Office of Climate, Water and Weather Services, Meteorological Services Division.
http://www.weather.gov/om/msd/index.shtml#Fire

National Weather Service National Digital Forecast Database.
http://www.weather.gov/ndfd/

National Weather Service Operations Digital Services Concept – June 2004.
http://www.nws.noaa.gov/ndfd/resources/dsconops0604-3.pdf

National Integrated Drought Information System.
http://www.drought.gov/index.html

Climate Prediction Center's United States' Seasonal Drought Outlook.
http://www.cpc.ncep.noaa.gov/products/expert_assessment/seasonal_drought.html.

NOAA's Air Quality Forecast System.
http://www.noaawatch.gov/themes/air_quality.php.
http://www.weather.gov/ost/air_quality/

National Weather Service Strategic Plan, 2005 – 2010, January 3, 2005.
http://www.weather.gov/sp/NWS_strategic_plan_01-03-05.pdf

NOAA Office of Program, Planning and Integration.
http://www.ppi.noaa.gov/strategic_planning.html

5 A Review of Wildland Fire and Air Quality Management

Douglas G. Fox, Ph.D.
Nine Points South Technical Pty, Ltd., P.O. Box 2419 Clarkson,
Western Australia 6030, Australia
Email: dgfox@comcast.net Phone: 970-221-0800

Allen R. Riebau, Ph.D.
Nine Points South Technical Pty, Ltd., P.O. Box 2419 Clarkson,
Western Australia 6030, Australia
Email: ariebau@ninepointsouth.com.au

Abstract This chapter reviews relationships between wildfire fire and air quality management in the US. Smoke fire emissions contribute to fine particulate concentrations for which there is a national ambient air quality standard (NAAQS) and to regional haze. The status of US regulatory programs for NAAQS and for regional haze are briefly reviewed along with the estimated contribution made by fire to each of these. We suggest that fire emissions can be best managed using emissions management systems adapted to smoke management and recommend that fire management agencies formally adopt such tools.

Keywords Air pollution management, fire smoke and air quality, visibility impairment, smoke management plans, smoke and environmental management plans

5.1 Introduction

5.1.1 Smoke Contributes to Air Pollution

Forest, range and agricultural burning contribute to air pollution, locally, regionally, nationally and globally. Global emissions estimates from biomass burning are quite uncertain but the latest studies suggest that fires may contribute up to 40% – 50% of fine particulate and carbon in the atmosphere (Andreae and Merlet, 2001; IPCC, 2001; Hoelzemann et al., 2004).

Locally, regionally and nationally in the United States emissions are equally significant. Figure 5.1 shows an estimate of the regional emissions of $PM_{2.5}$ for the Western United States for the year 1996 taken from the work of the Western regional air partnership (WRAP) and a projection of how these are anticipated to grow by 2018. This inventory was developed considering a variety of different sources with a significant effort to estimate and quality control fire sources. The total emissions of $PM_{2.5}$ are 1, 630,185 tons. Fire sources account for 760,733 or approximately 47% of the total emissions. (WRAP, 2003). For the same baseline year, fire represents approximately 9% of VOC and NO_x emissions, 3% of SO_2, and 27% of CO emissions.

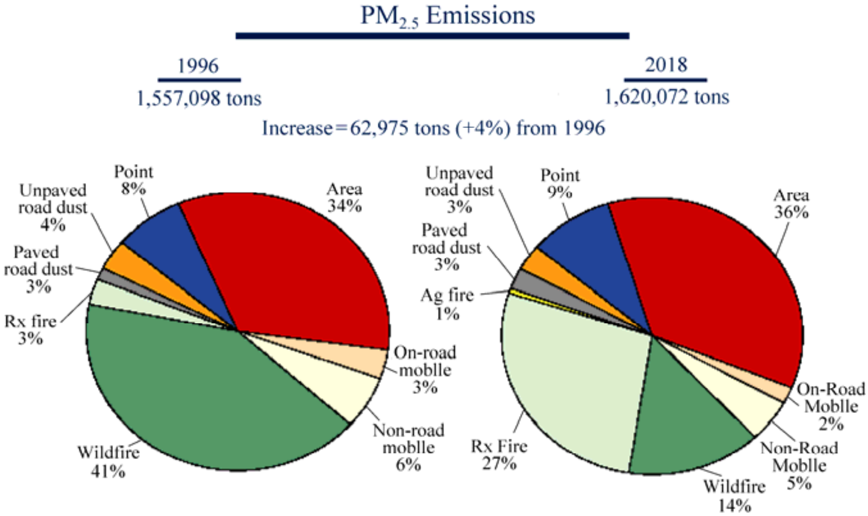

Figure 5.1 The change in $PM_{2.5}$ emissions in the Western US in 1996 and projected emissions for 2,018, assuming wildfire emissions are typical and prescribed burning programs are functioning

* From Regional Technical Support Document for the Requirements of §309 of the Regional Haze Rule (64 Federal Register 35714 – July 1, 1999) WRAP Technical Oversight Committee. December 15, 2003. Available at: http://www.wrapair.org/ 309/031215Final309TSD.pdf

Since smoke makes a significant contribution to air quality it has to be considered in the mix of sources that contribute to regional and local pollution. Smoke from forest burning is, to some extent, natural in as much as it would be present with or without human intervention. However, the “natural” amount of smoke is difficult to determine. Humans have influenced forests through management practices and agricultural burning cannot be considered natural in any way. One might argue wildfire is natural; however, wildfire burning in a forest that has had 75 years of fire exclusion and suppression is hardly natural. Prescribed fire for the purpose of restoring a “natural” fire regime is different from prescribed fire for the purpose of maintaining a natural fire regime. Prescribed fire as a silvacultural tool to enhance production similarly is not natural. Thus, from the air quality perspective, it is no longer sufficient to fall back on the "natural" label for all smoke. Fire and smoke can lead to significant regional air quality impacts. Smoke emissions, especially the fraction of them that are not "natural" need to be planned for, managed, and to the extent possible, mitigated in much the same way as other air pollution sources (for a more in depth discussion of these factors, the reader is referred to the WRAP Fire Emissions Joint Forum and their discussions (http://www.wrapair.org/forums/fejf/index.html).

5.2 Regulatory Considerations Relating to Smoke

5.2.1 Regional Haze Rule

In 1999, the US implemented a new Regional Haze Rule (see http://vista.cira.colostate.edu/improve/Overview/hazeRegsOverview_files/frame.htm for a thorough review of the provisions of the regulations). These regulations protect class I area visibility, specifically 156 federal Wilderness and National Park locations in the US. The regulations are based on the IMPROVE monitoring network (http://vista.cira.colostate.edu/improve/).

IMPROVE measures the dominant chemical species that make up ambient atmospheric aerosols so that their relative contribution to visibility reduction can be evaluated. Aerosols both scatter and absorb light which can be quantified by the extinction coefficient. Specifically, the relationship between visibility and atmospheric aerosols is, for the purposes of the regional haze rule, defined by the IMPROVE equation, a relationship between measured aerosol concentrations, the extinction coefficient and visibility reduction (see http://vista.cira.colostate.edu/improve/Tools/ReconBext/reconBext.htm). This allows the regional haze rule to focus on reducing the ambient concentration of atmospheric aerosols, specifically on their sulfate, nitrate and organic components.

Under the regional haze rule, all states (and participating Indian tribes) are required to develop a "state (or tribal) implementation plan" to reduce emissions of the most appropriate visibility degrading aerosols. By far sulfate is the most significant contributor to poor visibility in the United States (http://vista.cira.colostate.edu/views/). However, the regulations specifically require States to identify for each class I area in their State, what is the natural background for visibility, what is the mean of the 20% haziest and 20% cleanest days (based on a 5 year average) and establish a program of emissions limitations to reduce the haziest days to natural background conditions (whilst not reducing the cleanest days) over the next half century, measuring progress in 10 year increments.

Natural background is a complex concept but it is specifically identified in the regulations to be: reflective of contemporary conditions and land use patterns (not historical, pre-European conditions); a long-term average condition analogous to the 5-year average best-and worst-day conditions that are tracked under the regional haze program, and; estimated for each class I area in the absence of human-caused impairment. For the purposes of the RHR, a document exists that defines the natural condition (USEPA, 2003).

In many class I areas, especially in the cleanest areas of the US, the northern Rocky Mountains and intermountain west, organic carbon is the pollutant responsible for over 50% of the visibility impairment. Figure 5.2 shows IMPROVE data from 2002 to illustrate this point. Organic carbon comes from a variety of sources, namely biogenic (including all forms of fire as well as secondary organic aerosol generated from VOC emissions from vegetation) and from fossil fuel combustion (oil and gas). There are research activities underway to better determine exactly how much of this organic carbon aerosol comes from forest and other fire smoke. However, since forest fire smoke is generally recognized as a significant contributor to regional haze and, at the same time is different from other pollution sources (e.g. industrial and transportation activities), the RHR calls upon States to implement Smoke Management Programs (SMP) as part of their S/TIPS. The WRAP has issued policy guidance on what constitutes a SMP (see http://www.wrapair.org/forums/fejf/documents/esmptt/policy/030115_ESMP_Policy.pdf).

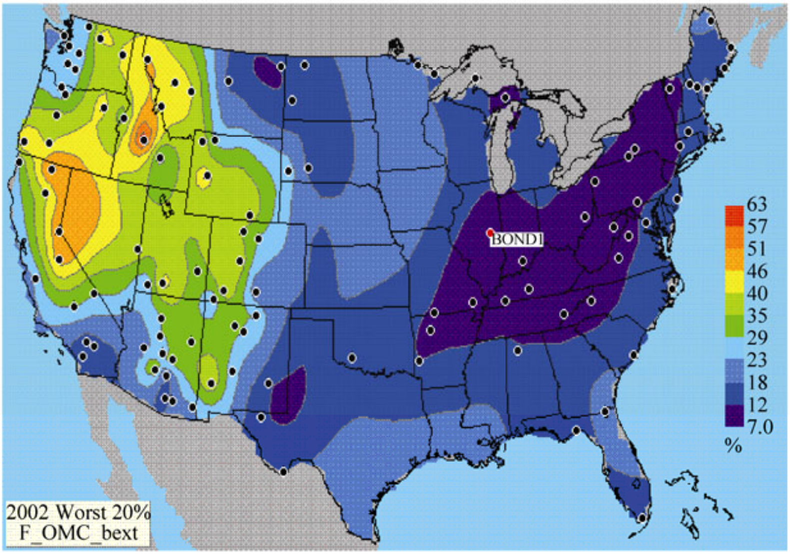

Figure 5.2 On the 20% of days that exhibited the poorest visibility in 2002, this contour shows the percentage of total extinction caused by fine organic particulates. Downloaded from the Visibility Information Exchange Web System (VIEWS) on 7 October, 2005. at http://vista.cira.colostate.edu/views

5.2.2 National Ambient Air Quality Standards for PM

At present (October, 2005), the US EPA is reviewing its national ambient air quality standard for particulate material. This review, part of the required review process for NAAQS, may result in changes of both the numerical value and averaging methods of the standard. At present there are 120 counties that are in non-attainment for annual $PM_{2.5}$. Figure 5.3 shows EPA data from 2000 – 2002. It is likely that any revision of the standard will be more restrictive than the current values (see http://www.epa.gov/ttn/naaqs/standards/pm/s_pm_index.html for more information about the current status of the particulate standard). At any rate, the message here is simply that conducting burning programs in any of the counties shown in Fig. 5.3 is likely to be subject to added complexity and possible limitations in the future.

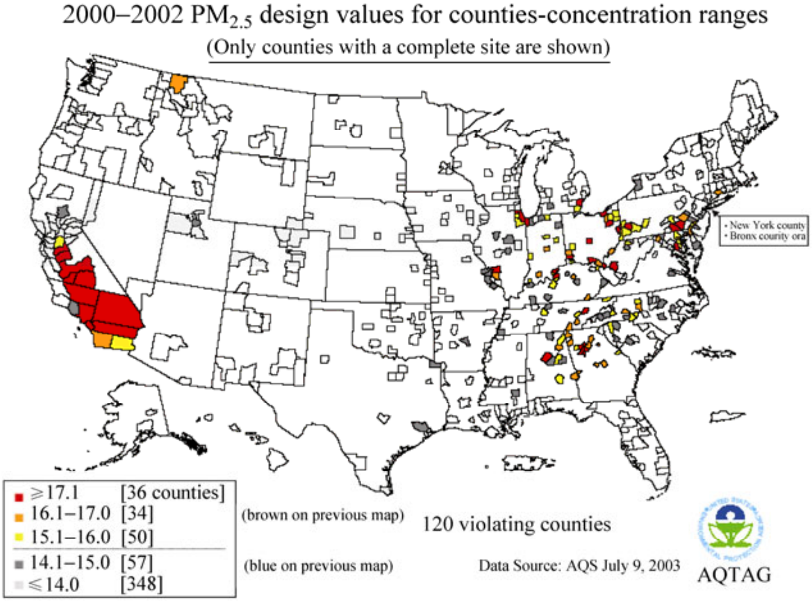

Figure 5.3 Illustration of counties in the US which are not in attainment of the $PM_{2.5}$ annual standard of 15 μg/m^3. This standard is currently under going review and may change in the near future taken from http://epa.gov/oar/oaqps/pm25/pmfinedesignvalues2000 – 2002.pdf

5.2.3 Managing Smoke from Wildfire

As a result of advances in computing and remote sensing (RS) technologies, there have been significant advances over the past decade in the ability to monitor and to predict smoke from burning activities. There are a number of satellites and sensor packages allowing steadily improved temporal, spatial, and spectral monitoring of smoke. Similarly, the cost and accessibility of computers allows simulations of fire events in predictive and real time modes, including all the burning in a region and comparison with other pollution sources to discern the relative contribution of the burning.

5.3 A Review of the TASET Report—Tools Available to Manage Smoke

Under funding from the joint fire sciences program in 2000, the authors completed a study addressing technically advanced smoke estimation tools (TASET) (Fox and Riebau, 2000). The study made 9 specific recommendations for research activities associated with both strategic and tactical planning, operations and evaluation of smoke management activities. It is useful to review these recommendations in light of recent accomplishments and the current research program in smoke management.

Recommendation 1 was for the fire community to collaborate with universities and other partners to develop consortia for advancing land manager's capability to simulate weather and smoke. This recommendation was taken up and funded within the National Fire Plan (NFP) with the result being a national network of fire consortia for advanced modeling of meteorology and smoke (FCAMMS.) At present there are consortia (http://www.fs.fed.us/fcamms) operating in East Lansing MI (USFS Northern Station); Athens, GA (USFS Southern Station); Ft. Collins, CO (and Missoula, MT. USFS Rocky Mountain Station); Seattle, WA (USFS Pacific Northwest Station) and Riverside, CA (and Reno, NV Pacific Southwest Station).

Figure 5.4 illustrates where the FCAMMS are operating. These regions represent the domain of a 12 km (or higher resolution) simulation of hourly weather. The weather simulation represents the basis for calculation of fire weather relevant indices, smoke dispersion from prescribed fire operations and a host of other special weather related parameters.

Recommendation 2 was to conduct a national smoke and visibility conference because of the potential for impacts by the RHR on fire applications. The need for this conference has been supplanted by the development of active fire emissions related activities on the part of the regional planning organizations (RPO). RPOs are state level organizations created by the EPA for the purpose of doing the technical work needed to support the RHR and associated S/TIPS. Specifically, many of the things we were recommending were also accomplished at the National Fire Emissions Technical Workshop held in May of 2004, under the auspices of the RPOs (see http://www.wrapair.org/forums/fejf/documents/wildland_fire/index.html).

Recommendation 3 was to design and implement a national smoke emissions data structure or database system. The call for this was based on the new regulatory programs mentioned above for $PM_{2.5}$ and regional haze, and the feeling that a national record keeping on fire emissions is needed. We felt that these data will

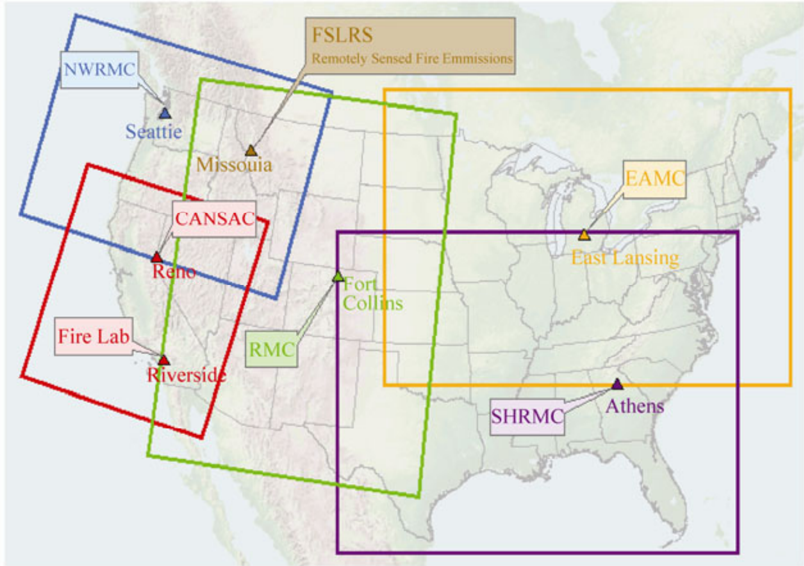

Figure 5.4 The figure shows the high resolution modeling domains of the USDA Forest Service FCAMMS. FCAMMS are primarily research activities located as shown who are engaged in weather, fire behavior and smoke research based on real time simulation of meteorology at spatial and time resolutions that are needed to advise fire management and improve research products. (http://www.fs.fed.us/fcamms)

need to be accessible to many parties including the federal EPA, state air agencies, researchers, fire managers, and the interested public. Smoke emissions will also need to be available for use in regional scale modeling using such systems. Data in such a system would need to be easy to up-date, provide for documentation of the sources of data, provide information on the quality of data, provide explicit geographic reference information, and allow data to be preprocessed for use in modeling. This still exists as a need for this although the RPOs have taken on the responsibility of developing the immediate inventories needed for their modeling. The WRAP has also developed an emissions data management system (EDMS) and specifically designed a fire module for this system. (http://www.wrapair.org/forums/fejf/documents/edms/041005EDMS_Fire_Module_Data.pdf)

Recommendation 4 was to use RS to characterize fuels and fire area for the purpose of improving emissions inventories. There is a recognized need for fuels inventory at state, regional, and national scales. Such information as amount of fuel loading, fuel temperature, and fuel moisture would be extremely useful in calculation of potential for fire. For emissions calculation, accurate estimates of fire area and fuel consumed are also needed. Meaningful spatial resolution for this information would be 100 meters or less. Time resolution for this information would be at several days to daily resolution. New multi-spectral sensor/platform combinations are continuing to become available with the potential to provide significantly enhanced information for fire managers. RS products, preferably from space based platforms, can solve fuels inventory and classification needs if spectral, spatial and temporal resolution are high enough. This information when coupled with burn area estimates can give regional to national emissions estimates for all fires. To achieve this level of information it will require new techniques for data collection, management, and analysis. In 2000 we said that we thought that technology may not exist at the present time to reach the level of spatial and temporal resolution we desire, we should strive to work to develop the framework for methodologies/processes will allow both useful products now and improved technology management as RS advances as a practice. The EASTFire Conference is one result of this sort of recommendation; this volume will advance our level of knowledge in RS for fire.

Recommendations 5, 6 and 7 all related to the need for national fire smoke modeling products. Without going into the details here the functionality being rapidly developed and deployed by the BlueSkyRAINS system (http://www.blueskyrains.org) is exactly what we were calling for to be developed. BlueSkyRAINS is a smoke modeling framework allowing specific fire emissions to be input to a dispersion model (the EPA regulatory CALPUFF model) that is driven by high resolution weather predictions. The system is packaged with an interactive web-based GIS to allow identification of smoke sensitive areas and thus anticipate problems. This fire season (2005) the system is being deployed throughout the Western US at a spatial resolution of 12 km and with predictions for 48 hours in advance. BlueSkyWEST is undergoing an evaluation of its ability and utility for managers (see http://www.fs.fed.us/rmc/). In addition, the Southern high resolution modeling center (SHRMC) is deploying BlueSky for the Southern US, especially in support of the clean up efforts in the wake of the hurricanes that impacted the Gulf States in september 2005. As well other FCAMMS are all implementing versions of BlueSky for their own needs as determined by their user communities.

Recommendation 8 called for the development and deployment of improved on-site fire emissions measurements. Although fire emissions modeling are improving, we need to improve our ability to accurately measure emissions at the fire site. Accurate measurements of emissions at fire sites will become more important as the regulatory programs discussed above start to ramp up. One extremely useful measurement would be the total amount of $PM_{2.5}$ emitted during the course of the fire. Currently, some fire managers are attempting to measure particulate concentrations at fires and near fires using portable light scattering measurements. The limitations of these devices are well known; inability to provide accurate measurements at high concentrations and point rather than spatial measurements being two that are often cited. The Forest Service Missoula Fire Laboratory is investigating LIDAR technologies that can produce fire emission species concentrations and plume volume measurements to calculate total emissions from fires. Work is on-going in this important field.

Recommendation 9 called for the development of apportionment tools to smoke contributions at specific locations. Development of these tools was the subject of a recent joint fire science program (JFSP) call of research proposals. Thus, assuming the research progresses successfully, in the next few years such tools will be available in the literature.

There are a wide variety of tools available for managing smoke from wildfire. Many of these tools, as described above, have developed over the past five years. They add to a rich assortment of tools that have been available from some time for smoke management (Riebau and Fox, 2001).

Technically, these tools provide the needed support for smoke management. The tools are not perfect; they represent approximations of various sorts with varying degrees of accuracy. The next phase of smoke management requires the fire community to step forward and start to use these tools. The context for applying tools is the Smoke Management Program and, more generally, the implementation of a Smoke Management System by the wildland fire community.

5.4 Smoke Management—Programs and Systems

Smoke management programs are identified in the regional haze regulations as being required in selected States to ensure that smoke from managed fire is properly managed. The Western regional air partnership (WRAP) has proposed that the smoke management program should specifically include requirements to: ① minimize fire emissions; ② evaluate smoke dispersion; ③ identify alternatives to fire; ④ notify the public; ⑤ monitor resulting air quality; ⑥ provide surveillance and enforcement of burning programs; ⑦ evaluate the program; ⑧ specific burn authorizations, and; ⑨ coordinate regional burning. (WRAP, 2001; 2002).

This idealized form of a smoke management program shares much in common with the international standard (ISO 14001) for environmental management systems (EMS) (Savage-Tate, 2005; http://www.iso.org/iso/en/iso9000-14000/index.html).

ISO 14000 concerns environmental management in general. It identifies what an organization does to:

(1) Minimize harmful effects on the environment caused by its activities;

(2) Achieve continual improvement of its environmental performance.

It is a "generic management system standard" meaning that the same standards can be applied:

(1) To any organization, large or small, whatever its product;

(2) Including if its "product" is actually a service;

(3) In any sector of activity, and;

(4) Whether it is a business enterprise, a public administration, or a government department.

No matter what the organization's scope of activity, if it wants to establish an environmental management system, then such a system has a number of essential features identified by the ISO standard. "management system" refers to the organization's structure for managing its processes - or activities - that transform inputs of resources into a product or service which meet the organization's objectives, such as complying with regulations, meeting environmental objectives, or accomplishing the job in a professional manner. The components of an EMS are illustrated in Fig. 5.5.

We propose that the fire community consider developing and implementing a formal "smoke management system (SMS)" based on the ISO 14001 standard and built on the generic elements outlined in Fig. 5.5.

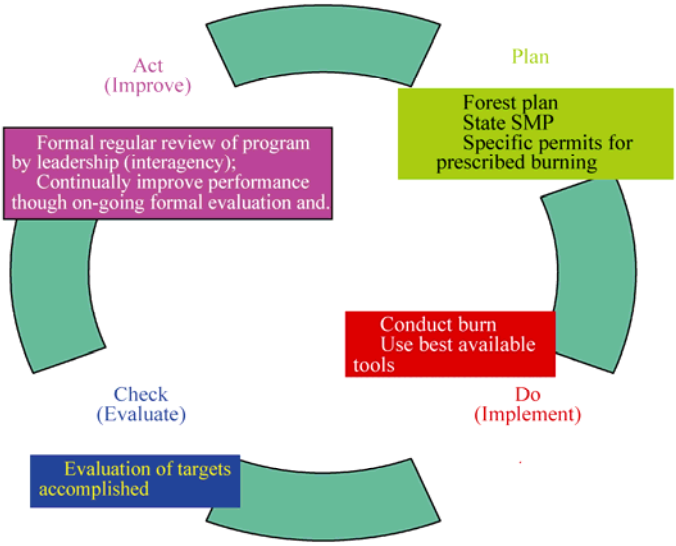

Figure 5.5 Generic environmental management plan with notations associated with a wildland burning application

5.4.1 Plan

In smoke management there are a number of planning activities that occur. These range from management planning at the broadest possibly level, namely the forest plan which might identify general fuel management targets, to specific accomplishment targets for a particular burning season. An important aspect of planning is permitting. Permitting is specifically identified in several of the existing state smoke management programs and takes a variety of different formats. In general it requires identification of a prescription for the burn, which includes windows of wind speed, direction, fuel moisture, humidity and other meteorological parameters, a location and a specific time frame for it. However, in the context of an SMS, this planning needs to take a step or two back and look at the Agency policy with regard to its broadest goals, i.e. wishing to maximize the health and productivity of the forest, to maintain the urban interface as a safe place for people to live, maintain firefighter safety, minimize negative impacts from forest burning, etc. A SMS will also need to identify the environmental "aspects" of the Agency. These "aspects" include positive as well as negative effects of the Agency activity on the environment. Finally, the SMS should specify goals for the Agency, as specifically as possible.

5.4.2 Do (Implement)

This of course represents the actual conduct of the burning activity. Burning should be carried out in as safe and environmentally benign manner as possible. The implementation phase includes utilization of many of the tools we have mentioned, i.e. BlueSkyRAINS, to best manage the burning.

5.4.3 Check (Evaluate)

This involves the evaluation of the burning program. It requires post fire monitoring, evaluation utilizing for example satellite RS and ground based monitoring networks to evaluate the effectiveness of smoke management activities, to evaluate the quality of the smoke modeling estimates and the overall accomplishments of identified targets. This is phase of the current fuel management program that might be considerably enhanced by formal identification of requirements and activities through a formal SMS.

5.4.4 Act (Improve)

This is a critical component of the SMS, and one which traditionally is not formally identified and commissioned. Thus, it may be the single most important contribution that adopting a formal SMS can generate. This element would require formal management review of the fuel management activity, a formal comparison with identified goals and an evaluation of accomplishment, identification of inadequacies and developing plans for improving next year.

5.5 Summary

It seems appropriate for the fire and fuel management communities to start to think in terms of developing and establishing formal SMS at appropriate levels in the agencies. In the forest service, for example, this might be at a district or a forest level. It will require resources to be developed, to be monitored and to be evaluated. We feel the potential benefits of adopting such a SMS will be significant. For one, it will place the forest manager in a definite leadership position with regard to smoke management issues. It will serve to communicate to the public as well as to State and local regulators, that the agency is responsible and professional. Further, it will clearly identify that the Agency is trying to do the right thing. Finally, the bottom line will be better burning programs, better smoke management and fewer negative outcomes.

Acknowledgements

Intergovernmental panel on climate change (IPCC) (2001), Climate Change 2001: The Scientific Basis, Contribution of Working Group I to the Third Assessment Report of the Intergovernmental Panel on Climate Change, edited by J. T. Houghton et al., Cambridge Univ. Press, New York.

References

Andreae MO, Merlet P, (2001), Emission of trace gases and aerosols from biomass burning, *Global Biogeochemical Cycles*, **15**(4): 955 – 966

Fox DG, Riebau AR, (2000), Technically Advanced Smoke Estimation Tools (TASET). Final Report submitted to: National Park Service and Joint Fire Science Program Under agreement number CA 1268-2-9004 TA CSU-187. September 2000. available at: http://www.cira.colostate.edu/smoke/TASETfinalREPORT.pdf

Hoelzemann JJ, Schultz MG, Brasseur GP, Granier C, Simon M, (2004), Global Wildland Fire Emission Model (GWEM): Evaluating the use of global area burnt satellite data, *J. Geophys. Res*. **109**: D14S04, doi:10.1029/2003JD003666

Riebau AR, Fox DG, (2001), The New Smoke Management, International Journal of Wildland Fire, **10**: 415 – 427

Savage-Tate T, (2005), Getting the Most Value from your Environmental Management System. EM March 2005. 12 – 17. Air and Waste Management Association. Pittsburgh, PA

USEPA, (2003), Guidance for Estimating Natural Visibility Conditions Under the Regional Haze Rule, EPA-454/B-03-005. September 2003. available at: http://www.epa.gov/ttn/oarpg/t1/memoranda/rh_envcurhr_gd.pdf

WRAP, (2001), Wildland Fire: Elements of a Basic Smoke Management Program, WRAP Fire Emissions Joint Forum. July 2001 DRAFT available at: http://www.wrapair.org/forums/fejf/documents/task2/BSMP_WF_dft.pdf

WRAP, (2002), WRAP Policy on Enhanced Smoke Management Programs for Visibility, WRAP Fire Emissions Joint Forum. November, 2002. available at: http://www.wrapair.org/forums/fejf/documents/esmptt/policy/030115_ESMP_Policy.pdf

WRAP, (2003), Section 309 Technical Support Document, available from http://www.wrapair.org/309/index.html

6 High-Resolution Numerical Models for Smoke Transport in Plumes from Wildland Fires

Philip Cunningham
Earth and Environmental Sciences Division, Los Alamos National Laboratory
Los Alamos, New Mexico 87545, USA
Email: pcunning@lanl.gov

Scott L. Goodrick
Center for Forest Disturbance Science, US Forest Service
Athens, Georgia 30602, USA
Email: sgoodrick@fs.fed.us

Abstract A high-resolution large-eddy simulation (LES) model is employed to examine the fundamental structure and dynamics of buoyant plumes arising from heat sources representative of wildland fires. Herein we describe several aspects of the mean properties of the simulated plumes. Mean plume trajectories are apparently well described by the traditional two-thirds law for plume rise; however, the spatial structure of the mean plume is significantly different from the Gaussian distributions typically assumed in simple plume models. This discrepancy arises from the fact that entrainment properties of a buoyant plume in a cross wind are significantly different from those of a buoyant plume in the absence of a cross wind, a result of the interaction of the buoyancy-generated vorticity in the plume with the vorticity in the ambient wind. The depth of the crosswind shear layer at the surface also appears to play a role in both the horizontal and vertical spread of the plume boundaries downwind, and in particular the increase in horizontal spread acts to increase the departure from a Gaussian distribution seen in the plume cross sections.

Keywords Fire plumes, large-eddy simulations, smoke transport, plume rise, turbulent kinetic energy, vorticity and entrainment

6.1 Introduction

Predicting the impacts on air quality due to the smoke from prescribed fires and wildfires represents a central problem in smoke management, particularly for many locations in the Eastern United States where wildfire-prone regions are often located near populated areas. A variety of models and tools are available for the purpose of modeling smoke impacts from wildland fires, and in many cases these models are appropriate and provide valuable information. These tools typically fall into three categories: simple Gaussian plume models, Lagrangian puff models, and Eulerian grid models.

Gaussian plume models, such as VSmoke (Lavdas, 1996) are frequently used by land managers during the planning phase of a prescribed burn. VSmoke assumes Gaussian dispersion in both the horizontal and vertical directions from a straight-line trajectory for each independent period of the simulation. VSmoke is designed to provide the best estimate of maximum concentrations of smoke at the surface, rather than accurate concentrations of smoke within the plume. To achieve this estimate, VSmoke allows the user to partition emissions between a component subject to plume rise, following the formulation of Briggs (1975), and a surface component that lacks the buoyancy to achieve significant rise.

As computing power has increased, the use of more complex descriptions of plume behavior, such as Lagrangian puff models, has become more widespread. Lagrangian puff models operate by releasing a series of puffs that are transported by spatially and temporally varying weather conditions. While within-puff dispersion is still handled in a Gaussian manner, puffs are allowed to split when subject to high levels of vertical wind shear. CALPUFF (Scire et al., 2000) is a Lagrangian puff model that is an integral component of the BlueSky smoke modeling framework (Ferguson, 2003). Plume rise from area sources in CALPUFF follows the derivation of Weil (1988), with the exception that the Boussinesq approximation employed by Weil (1988) is not made. CALPUFF assumes that the plumes will have a circular cross section despite evidence that fire plumes are often dominated by a pair of counter-rotating vortices; however, this may be an acceptable approximation since the presence of the counter-rotating vortices does not appear to impact plume rise calculations (Zhang, 1993; Zhang and Ghoniem, 1993).

Eulerian grid models are frequently used in air quality modeling for assessing the cumulative impact of a wide variety of emission sources at a regional scale and can include complex chemical transformations. Although the scale of these models is generally much larger than the scale of a wildland fire plume, air quality models such as the United States environmental protection agency (EPA) community multiscale air quality (CMAQ) modeling system (Byun and Ching, 1999) can contain subgrid-scale parameterizations for representing smaller scale features such as plumes from individual sources. In CMAQ this is handled by the plume-in-grid (PinG) formulation (Gillani and Godowitch, 1999), which behaves in the manner of a hybrid of the Gaussian and puff models. Transport is handled by the mean wind throughout the depth of the plume, similar to the use of a layer-mean wind in the Gaussian models. The plume itself is constructed as a succession of slabs perpendicular to the flow. The lateral spread of these slabs is governed by turbulence, wind shear and a background entrainment value, while the vertical spread of the plume is governed predominantly by turbulence. Each crossflow slab is divided into a series of columns with an initially Gaussian lateral distribution of pollutants. After initialization, the lateral distribution of concentration is controlled by a series of mass balance equations, transferring concentration between columns through parameterized diffusion and entrainment processes.

Although these models have been applied with general success over a wide range of atmospheric conditions, they are all based on simplifications to the governing equations, and none of them is able to represent accurately the 3D turbulent dynamics of the plume itself and its interaction with the ambient atmosphere. It is of particular interest, then, to explore the fundamental dynamics of buoyant plumes arising from intense heat sources (e.g., plume trajectory, lateral and vertical spread, entrainment) to assess the utility and accuracy of the models currently in use for air quality assessment, and in particular to identify situations in which these models may have significant errors.

In a recent study, Cunningham et al. (2005) employed a high-resolution LES model to explore the dynamics of buoyant plumes arising from a heat source representative of wildland fires. This model was designed to resolve the majority of the turbulent eddies in the plume and its environment, and thus does not suffer from the approximations inherent to the models discussed above. The simulations shown by Cunningham et al. (2005) suggest that, even for simple configurations, plume behavior is highly complex and dominated by a variety of coherent vortex structures that may have a significant impact on smoke transport. In the present chapter, we continue and extend this investigation of the fundamental dynamics of buoyant plumes in a cross wind by describing the mean properties of the simulated plumes for different heat source intensities and different ambient wind conditions.

In the following section, the details of the numerical model are described briefly. In Section 6.3, the basic time-averaged properties of the simulated plumes and their dependence on the heat source strength and the ambient wind are shown, while Section 6.4 presents a summary of these results and directions for future research.

6.2 Numerical Model

For this study we utilize the LES model described by Cunningham et al. (2005). The governing equations are those for 3D, compressible flow in a density-stratified atmosphere forced by a prescribed volumetric heat source, Q:

$$\frac{\partial}{\partial t}(\rho u_i) + \frac{\partial}{\partial x_j}(\rho u_i u_j) + \frac{\partial p'}{\partial x_i} + g\rho'\delta_{i3} = \frac{\partial \tau_{ij}}{\partial x_j} - D_i \tag{6.1}$$

$$\frac{\partial}{\partial t}(\rho\theta) + \frac{\partial}{\partial x_j}(\rho\theta u_j) = \frac{\partial H_j}{\partial x_j} + \frac{Q\theta}{c_{\mathrm{p}}T} \tag{6.2}$$

$$\frac{\partial \rho}{\partial t} + \frac{\partial}{\partial x_j}(\rho u_j) = 0 \tag{6.3}$$

where ρ is the density, u_i is the wind velocity in the x_i direction with $i, j, k =$ 1, 2, or 3 representing streamwise (x), spanwise (y), or vertical (z) directions, respectively, p' and ρ' are the departures of pressure and density, respectively, from a hydrostatic base state, D_i is a drag term intended to represent the effects of a vegetation canopy, T and θ are the temperature and potential temperature, and c_p is the specific heat at constant pressure.

A conventional approach to subgrid-scale modeling (e.g., Deardorff, 1973; Moeng and Wyngaard, 1988) is employed for the LES model, in which the subgrid-scale stress tensor, τ_{ij}, and the subgrid-scale heat flux, H_j, are represented respectively by

$$\tau_{ij} = \rho K_m \left(\frac{\partial u_i}{\partial x_j} + \frac{\partial u_j}{\partial x_i} \right) - \frac{2}{3} \rho K_m \frac{\partial u_k}{\partial x_k} \delta_{ij} \tag{6.4}$$

and

$$H_j = \rho K_h \frac{\partial \theta}{\partial x_j} \tag{6.5}$$

where K_m is the eddy viscosity and K_h is the eddy diffusivity.

The eddy viscosity is taken to depend on the subgrid-scale turbulent kinetic energy (TKE), e, as follows

$$K_m = C_k e^{1/2} \Delta \tag{6.6}$$

where C_k is a constant and Δ is the grid spacing. The eddy diffusivity is then related to the eddy viscosity via a turbulent Prandtl number, $Pr = K_m / K_h$, which is assumed to be equal to 1/3 herein. An additional equation for the subgrid-scale TKE is then required, and is given by

$$\frac{\partial}{\partial t}(\rho e) + \frac{\partial}{\partial x_j}(\rho e u_j) = -\tau_{ij} \frac{\partial u_i}{\partial x_j} + 2 \frac{\partial}{\partial x_j} \left(\rho K_m \frac{\partial e}{\partial x_j} \right) - \frac{\rho g K_h}{\theta} \frac{\partial \theta}{\partial z} - \frac{\rho C_e e^{3/2}}{\Delta} \tag{6.7}$$

where the last term on the right hand side represents the dissipation of subgrid-scale TKE. Following Moeng and Wyngaard (1988), values for the constants in Eq. (6.6) and Eq. (6.7) are chosen to be $C_k = 0.1$ and $C_e = 0.93$.

The heat source, Q, in Eq. (6.2) is intended to represent in an idealized manner the heating due to a fire of moderate intensity, and has the form of a smoothed top-hat distribution, as given by Eq. (6.10) in Cunningham et al. (2005). The heat source is centered at point (x_h, y_h), which is (450 m, 600 m) from the origin. The total heat release rate (HRR) is given by the volume integral of Q, and is taken to be constant after a ramp-up period of 10 s at the beginning of each simulation.

The governing equations are solved using the dynamical core of the weather research and forecasting (WRF) model (Skamarock et al., 2001). The computational domain is a rectangular box with spatial dimensions of 1,800 m in the streamwise direction (x), 1,200 m in the spanwise direction (y), and 1,800 m in the vertical direction (z). A uniform grid spacing of 10 m is employed in all directions. The ambient potential temperature is taken to be uniform and equal to 300 K in all simulations. For additional details of the numerical solution procedure, refer to Cunningham et al. (2005).

In an effort to explore the dependence of plume dynamics on the intensity of the heat source and on the nature of the ambient wind, several simulations have been performed for different heat source intensities, and different ambient wind profiles specified by

$$U(z) = U_0 \tanh(z/z_0) \tag{6.8}$$

Parameters employed for each simulation described here, along with the identifying label for each case, are provided in Table 6.1.

Table 6.1 Parameters for the simulations

Case	Heat source (MW)	U_0 (m·s^{-1})	z_0 (m)
*Q*2*U*3*H*50	350	3	50
*Q*2*U*3*H*100	350	3	100
*Q*2*U*5*H*50	350	5	50
*Q*2*U*5*H*100	350	5	100
*Q*3*U*5*H*50	525	5	50
*Q*3*U*5*H*100	525	5	100

In an effort to explore further the dynamics of buoyant plumes in a crossflow, in Chapter we examine the basic structure of various mean properties of simulated plumes. To explore these mean properties, simulations were performed for each case for 20,000 time steps, with statistical properties evaluated over the last 10,000 steps. Herein we examine the mean plume trajectories for each case, the mean structure of temperature and wind, and the mean TKE.

6.3 Dynamical Properties of Simulated Plumes

Instantaneous snapshots of potential temperature, vorticity magnitude, and vertical component of vorticity from the simulation *Q*2*U*5*H*100 are shown in Fig. 6.1, and illustrate the characteristic plume structure as well as the highly vortical nature of the flow. It is apparent from these images that even in such simple initial configurations, the plume is highly turbulent and dominated by coherent vortical structures. These structures include the counter-rotating vortex pair aligned with the plume trajectory that may be associated with bifurcation of the plume, transverse shear-layer vortices on the upwind face of the plume, and vertically oriented wake vortices that form downwind of the heat source and that extend from beneath the bent over plume down to the surface. These vortical structures are described and discussed in more detail by Cunningham et al. (2005).

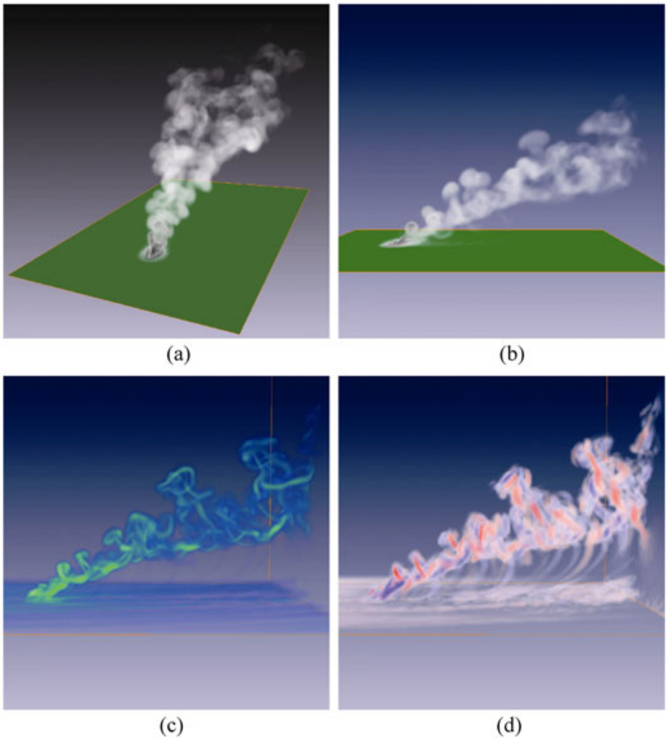

Figure 6.1 Instantaneous fields from the $Q2U5H100$ simulation. (a) and (b) Potential temperature from different view perspectives, (c) total vorticity magnitude, and (d) vertical component of vorticity (blue – positive values; red – negative values)

6.3.1 Mean Plume Trajectories

Mean plume trajectories for each case are depicted by the black and green lines in Fig. 6.2; these plume trajectories are calculated based on the maximum potential temperature deviation from ambient at each location downwind of the heat source along the plume centerline (i.e., the $x-z$ plane that intersects the center of the heat source). Also shown in Fig. 6.2 are trajectories predicted (based on heat source intensity and the magnitude of the ambient cross wind) by the traditional two-thirds law plume rise model of Briggs (1975) and its modification by Mills (1987) to account for finite-area sources.

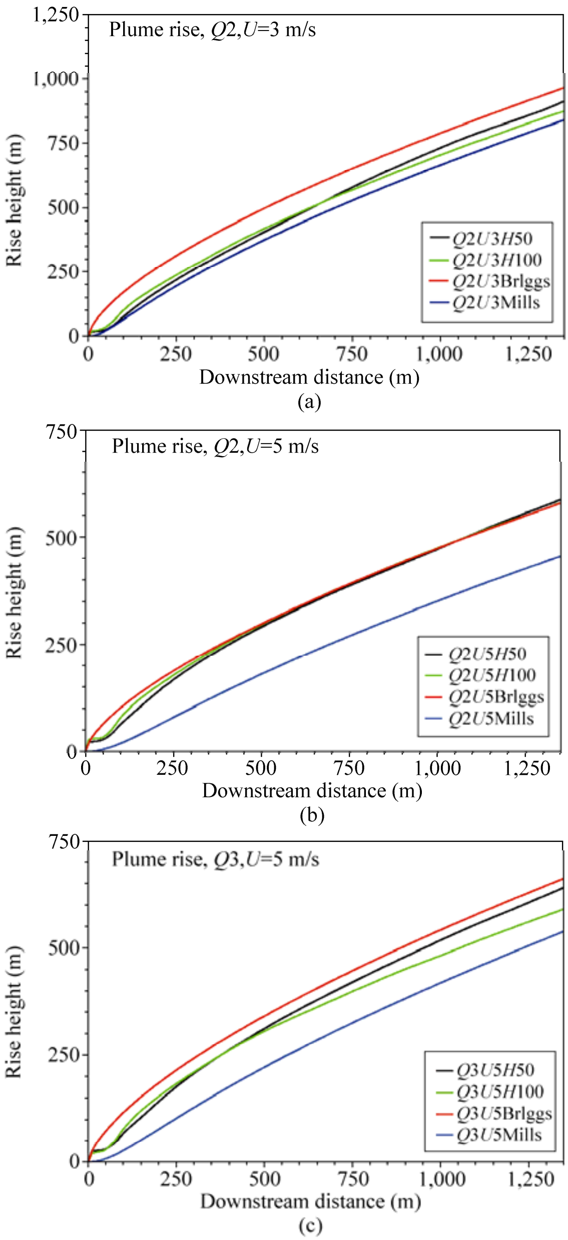

Figure 6.2 Simulated mean plume trajectories for (a) *Q2U*3 cases, (b) *Q2U*5 cases, and (c) *Q*3*U*5 cases. Trajectories for the shallow shear layer ($z_0 = 50$ m) are shown by black lines, while trajectories for the deeper shear layer ($z_0 = 100$ m) are shown by green lines. Also shown are plume rise calculations based on equations of Briggs (1975) and Mills (1987), depicted as red and blue lines, respectively

Following Briggs (1975), the rise height, h_B, for buoyancy-dominated plumes in a neutrally stratified atmosphere is given by

$$h_B = \left(\frac{3}{2\beta^2} \right)^{1/3} \frac{F_B^{1/3} x^{2/3}}{U_0} \tag{6.9}$$

where β is an empirically derived entrainment rate, typically chosen to have a value of 0.6, U_0 is the (constant) ambient wind speed, x is the distance downwind from the center of the source, and F_B is the buoyancy flux, given by

$$F_B = \frac{g Q_{tot}}{\pi \rho_a c_p T_a} \tag{6.10}$$

In Eq. (6.10), Q_{tot} is the total HRR, and ρ_a and T_a are an ambient air density and temperature, respectively. Trajectories calculated via Eq. (6.9) for a given heat source and ambient wind speed are shown by the red lines in Fig. 6.2.

Equation (6.9) assumes that the plume evolves from a point source, and it can be modified to account for a finite diameter, d, of the source (e.g., Mills, 1987; Zhang and Ghoniem, 1993), such that the plume rise height, h_M, is given by

$$h_M = \left(h_B^3 + \left(\frac{d}{2\beta} \right)^3 \right)^{1/3} - \frac{d}{2\beta} \tag{6.11}$$

Trajectories calculated via Eq. (6.11) for a given heat source and ambient wind speed are shown by the blue lines in Fig. 6.2.

It is apparent that several fire diameters downstream of the heat source the mean plume rise seen in the simulations is well described by a power-law trajectory, and is in reasonably good agreement with the simple plume rise calculations. Nevertheless, the trajectories of the simulated plumes do exhibit some dependence on the depth of the shear layer in the ambient cross wind, as evidenced by the difference between the black and green lines. In particular, plume trajectories are slightly lower when the crosswind shear layer is deeper (e.g., Fig. 6.2(c)).

6.3.2 Mean Plume Structure

Despite the fact that the mean plume trajectories appear to be consistent with the well established two-thirds law for plume rise, the mean structure of the simulated plumes departs from the Gaussian or top-hat distribution often assumed in plume models. Indeed, as shown in Fig. 6.3, all of the simulated plumes exhibit a kidney-shaped, or even bifurcated, structure with a local minimum along the plume centerline resulting from the presence of the counter-rotating vortex pair.

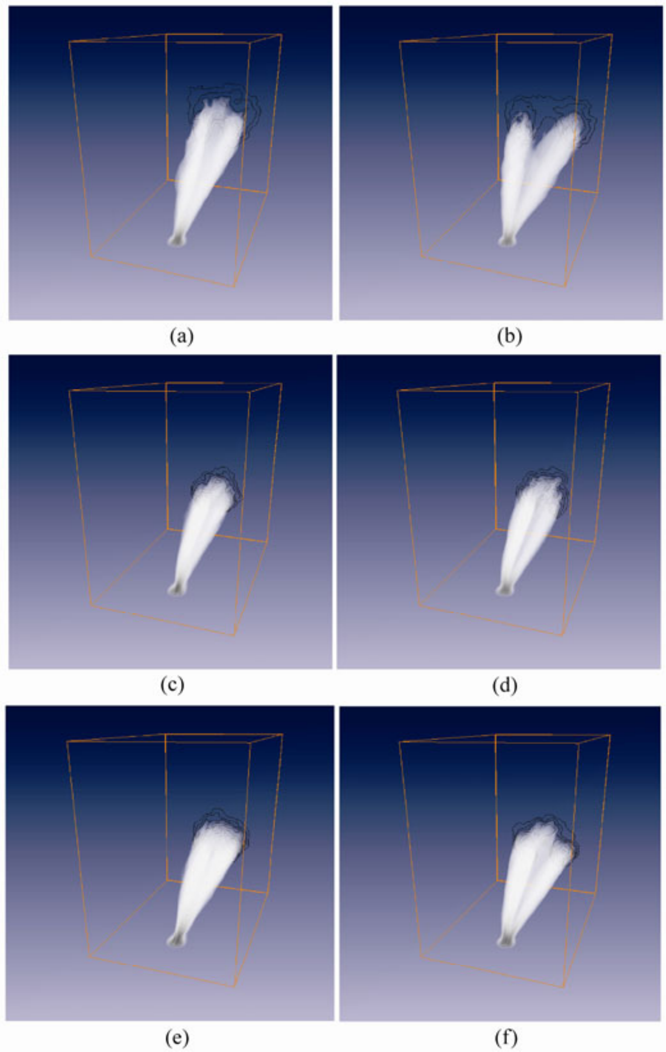

Figure 6.3 Mean potential temperature for case: (a) $Q2U3H50$, (b) $Q2U3H100$, (c) $Q2U5H50$, (d) $Q2U5H100$, (e) $Q3U5H50$, and (f) $Q3U5H100$

Figure 6.3 also illustrates the fact that the depth of the cross wind shear layer also has a significant impact on the mean structure of the plume, as discussed by Cunningham et al. (2005). Specifically, the lateral spread of the plume and the separation of the plume branches are greater for the deeper ambient shear layer. This property appears to result from the enhanced entrainment of ambient cross wind vorticity into the plume for the deeper shear layer, but this process requires further study and quantification.

Mean streamlines in the $y-z$ plane 1000 m downstream of the heat source are shown in Fig. 6.4; these streamlines illustrate clearly the presence of the counter-rotating vortex pair in the time-averaged plume, and the associated upward vertical motion along the plume centerline. This upward motion may be important for PM transport, and may result in different downwind distributions for PM of different sizes (e.g., fine particles with smaller terminal velocities may be kept aloft along the centerline longer than larger particles).

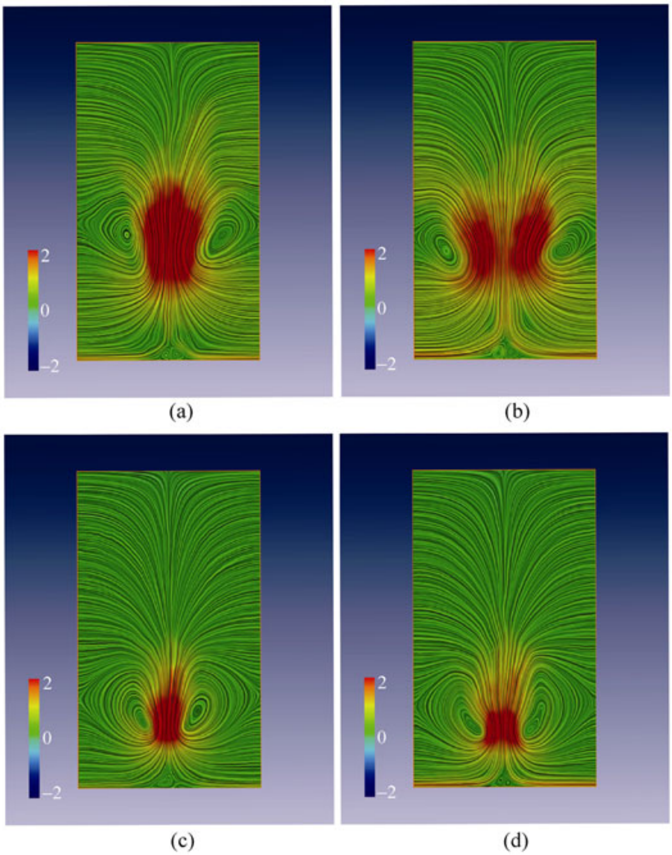

Figure 6.4 Mean streamlines in the $y-z$ plane at $x = 1{,}600$ m for case: (a) $Q2U3H50$, (b) $Q2U3H100$, (c) $Q2U5H50$, and (d) $Q2U5H100$. Color shading corresponds to vertical velocity in m·s^{-1}

6.3.3 Turbulent Kinetic Energy (TKE)

Figure 6.5 shows mean subgrid and total (subgrid plus resolved) TKE for the $Q2U3H100$ case, both in the $x-z$ plane along the plume centerline (Figs. 6.5(a) and (b)), and in the $y-z$ plane 1,000 m downstream of the heat source (Figs. 6.5(c) and (d)).

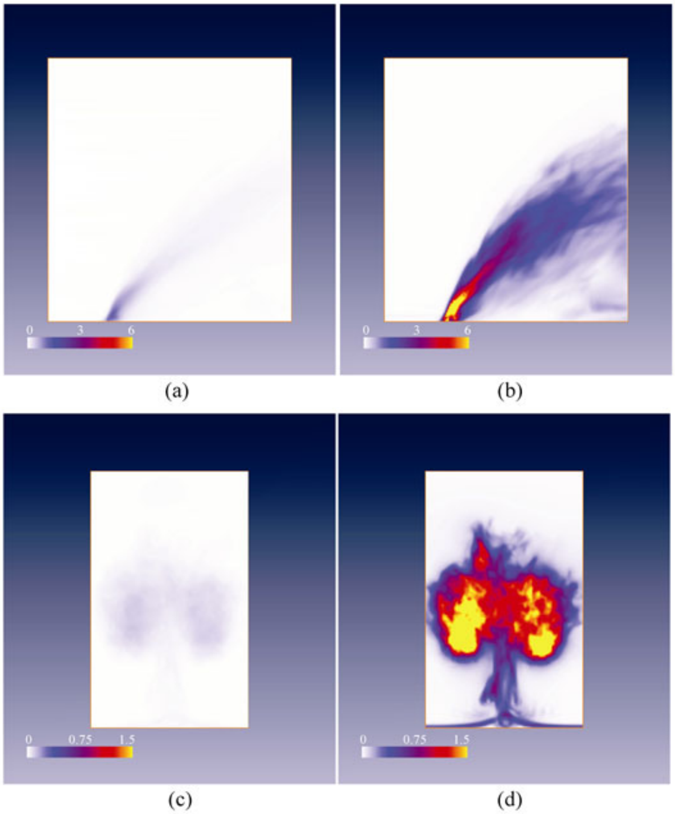

Figure 6.5 Mean turbulent kinetic energy ($m^2 \cdot s^{-2}$) for the $Q2U3H100$ case: (a) subgrid TKE along centerline, (b) total TKE along centerline, (c) subgrid TKE at $x = 1{,}600$ m, (d) total TKE at $x = 1{,}600$ m

First, it is apparent from these figures that the subgrid TKE is significantly smaller in magnitude than the total TKE, indicating that the energy containing eddies in the plume are well resolved on the grid employed in these simulations. Second, it is apparent that the turbulence seen in the simulations is dominated by the mean effect of the vortical structures seen in the instantaneous images. In particular, turbulence, and thus entrainment and mixing, along the centerline (Fig. 6.5(b)) is associated with the repeated passage of shear-layer vortices seen on the upwind face of the plume, whereas farther downwind the turbulence is dominated by the counter-rotating vortex pair (Fig. 6.5(d)).

It is of considerable interest to examine the dynamics of the transition between these turbulence regimes, and specifically how the distance downwind from the heat source at which this transition occurs depends on the parameters of the simulation, such as the intensity of the heat source and the depth of the crosswind shear layer. Investigation of this transition is part of future research.

6.4 Summary and Conclusions

Several simulations have been performed using a high-resolution LES model to examine the dynamics of buoyant plumes arising from heat sources representative of wildland fires. This model is capable of representing the 3D turbulent eddies characteristic of such plumes, and is being employed in an effort to understand the fundamental structure and dynamics of buoyant plumes, including the nature and importance of the coherent vortical structures that are common to these flows.

In this Chapter we describe several aspects of the mean properties of the simulated plumes. It is apparent that the mean plume trajectories (based on potential temperature along the plume centerline) are well described by the traditional two-thirds law for plume rise; however, the spatial structure of the mean plume is significantly different from the Gaussian distributions typically assumed in simple plume models. This discrepancy arises from the fact that entrainment properties of a buoyant plume in a cross wind are significantly different from those of a buoyant plume in the absence of a cross wind, a result of the interaction of the buoyancy-generated vorticity in the plume with the vorticity in the ambient wind.

While the two-thirds plume rise formulation appears to agree well with the simulations of buoyant plumes in a neutral atmosphere presented herein, the modeling results raise several questions for further investigation. The depth of the crosswind shear layer at the surface appears to play a role in both the horizontal and vertical spread of the plume boundaries with downwind distance, and in particular the increase in horizontal spread acts to increase the departure from a Gaussian distribution seen in the plume cross sections. Source strength, or fire intensity, as well as shear layer depth influence the vertical spread of the plume, with intense fires and deeper shear layers providing enhanced vertical plume spread. How well these plume spread results agree with those predicted by current plume formulations is an open area for research.

Ongoing and future research is focused on the continued analysis of these simulations in an attempt to: ① quantify further the nature of the turbulent entrainment in these plumes, and how the entrainment depends on the vortical structures seen in the simulations; and ② examine the nature of turbulent transport in the plume (e.g., of PM of a range of sizes).

Acknowledgements

This research was partially supported by the USDA Forest Service, via a cooperative agreement with the USDA Forest Service Southern Research Station, and by the FSU School of Computational Science, via a grant of resources on the IBM SP Series 690 Power4-based supercomputer “Eclipse”.

References

Briggs GA, (1975), Plume rise predictions. In: Lectures on Air Pollution and Environmental Impact Analysis, Haugen DA (Ed.), American Meteorological Society: 59 – 111

Byun DW, Ching JKS, (1999), Science algorithms of the EPA Models-3 Community Multiscale Air Quality (CMAQ) Modeling System, EPA-600/R-99/030, U.S. Environmental Protection Agency, Research Triangle Park, NC

Cunningham P, Goodrick SL, Hussaini MY, Linn RR, (2005), Coherent vortical structures in numerical simulations of buoyant plumes from wildland fires, *Int. J. Wildland Fire*, **14**: 61 – 75

Deardorff JW, (1973), The use of subgrid transport equations in a three-dimensional model of atmospheric turbulence, *J. Fluids Eng.* **95**: 429 – 438

Ferguson SA, (2003), Real-time mesoscale model forecasts for fire and smoke management: Preprints, Fifth Symp. on Fire and Forest Meteorology, Orlando, FL, American Meteorological Society

Gillani NV, Godowitch JM, (1999), Plume-in-grid treatment of major point source emissions. In: Science algorithms of the EPA Models-3 Community Multiscale Air Quality (CMAQ) Modeling System, Byun DW and Ching JKS (Eds.), EPA-600/R-99/030, U.S. Environmental Protection Agency, 9-1 – 9-39

Lavdas LG, (1996), Program VSMOKE – Users Manual, General Technical Report SRS-6, USDA Forest Service, Southern Research Station

Mills MT, (1987), Modelling the release and dispersion of toxic combustion products from pool fires, Proceedings, Int. Conf. on Vapor Cloud Modeling, Cambridge, MA

Moeng C-H, Wyngaard JC, (1988), Spectral analysis of large-eddy simulations of the convective boundary layer, *J. Atmos. Sci.* (45): 3573 – 3587

Scire JS, Strimaitis DG, Yamartino RJ, (2000), A User's Guide for the CALPUFF Dispersion Model, Earth Tech, Inc., Concord, MA

Skamarock WC, Klemp JB, Dudhia J, (2001), Prototypes for the WRF (Weather Research and Forecasting) model, Preprints, Ninth Conf. on Mesoscale Processes, Fort Lauderdale, FL, American Meteorological Society, J11 – J15

Weil JC, (1988), Plume rise. In: Lectures on Air Pollution Modeling, Venkatram A and Wyngaard JC, (Eds.), American Meteorological Society: 119 – 166

Zhang X, (1993), A computational analysis for the rise, dispersion and deposition of buoyant plumes, Ph D. Thesis, Massachusetts Institute of Technology, Cambridge

Zhang X, Ghoniem AF, (1993), A computational model for the rise and dispersion of wind-blown, buoyancy-driven plumes—I. Neutrally stratified atmosphere, *Atmos. Env.* **15**: 2295 – 2311

7 Interaction between a Wildfire and the Sea-Breeze Front

Deborah E. Hanley
AWS Truepower, LLC, 463 New Karner Road, Albany, NY 12205, USA
Email: dhanley@awstruepower.com Phone: 518-213-0044 X 1027

Philip Cunningham
Earth and Environmental Sciences Division, Los Alamos National Laboratory, Los Alamos, New Mexico 87545, USA
Email: pcunning@lanl.gov Phone: 505-667-5092

Scott L. Goodrick
Center for Forest Disturbance Science, USDA Forest Service, Athens, Georgia 30602, USA
Email: sgoodrick@fs.fed.us Phone: 706-559-4237

Abstract Florida experiences sea breezes, lake breezes, and bay breezes almost every day during the year, and there are frequently complex interactions between many of these breezes. Given the often-rapid changes in temperature, humidity and wind speed that accompany these breezes, most wildfires and prescribed fires in Florida are affected in some way by their interaction with these circulations. In this paper, we explore the interaction between sea breezes and wildland fires from both an observational and an idealized modeling perspective. The progression of the sea-breeze front and its interaction with the smoke plume from a 26,000 acre wildfire are tracked using a variety of data sources including surface and upper-air observations as well as NEXRAD radar imagery. Idealized numerical simulations of a thermally buoyant plume interacting with a density current are performed in an effort to enhance our understanding of the dynamics of the interaction between sea breeze circulations and the convective column of the fire. Our observational analysis and idealized modeling results suggest that the arrival of a sea breeze front induces a temporary, but significant, increase in fire intensity. This intensification precedes the arrival of the sea-breeze front at the location of the fire, such that the fire intensity is at a maximum at the time of, and slightly after, the passage of the front, and decreases gradually thereafter as cooler and moister air behind the front arrive.

Keywords Sea-breeze, fire behavior, fire weather, numerical modeling

7.1 Introduction

Weather is one of the most important factors leading to extreme wildfire behavior. Rapid changes in wind can quickly affect the rate and direction of fire spread, and may have a significant impact on fire intensity. Changes in temperature and humidity also may cause unexpected changes in fire behavior. Florida coastlines experience sea-breezes, lake breezes, and bay breezes almost every day during the year, and there are frequently complex interactions between many of these breezes. Given the often-rapid changes in temperature, humidity and wind speed that accompany these breezes, most wildfires in Florida are affected in some way by their interaction with these circulations. Nevertheless, despite the importance of sea-breeze circulations for fire behavior, the nature of the interaction between sea-breezes and wildfires remains relatively poorly understood.

Previous studies of sea-breezes depended upon a network of observation sites in the area of the sea-breeze (e.g., Atkins and Wakimoto, 1997), or used numerical models to simulate the sea-breeze (e.g., Pielke, 1974; Sha et al., 1991; Rao et al., 1999; Colby, 2004). Radar and satellite imagery have been shown to be useful in tracking the structure, evolution and timing of the movement of sea-breeze fronts (e.g., Atlas, 1960; Wakimoto and Atkins, 1994; Atkins et al., 1995; Atkins and Wakimoto, 1997), and have also been used to observe smoke plumes from fires (e.g., Banta et al., 1992; Rogers and Brown, 1997; Hufford et al., 1998), as well as from other sources of particulate emissions such as volcanoes, dust storms, and industrial emissions.

In this Chapter, we explore the interaction between sea-breezes and wildfires in more detail from both an observational and an idealized modeling perspective. The progression of the sea-breeze front and its interaction with the smoke plume from the fire are tracked using a variety of data sources including surface observations from the remote automated weather station (RAWS) network, surface and upper-air observations from the national oceanic and atmospheric administration/national weather service (NOAA/NWS), and imagery from the Weather Surveillance Radar-1988 Doppler (WSR-88D) site in Tallahassee, Florida. Given that the sea-breeze may be represented by a density current, idealized numerical simulations of a thermally buoyant plume interacting with a density current are performed in an effort to enhance our understanding of the dynamics of the interaction between sea-breeze circulations and smoke plumes. Although these idealized simulations do not allow us to determine directly the impact of the sea-breeze on fire behavior, which would require a fully coupled atmosphere–fire model (e.g., Clark et al., 1996ab, 2004; Linn, 1997; Linn and Cunningham, 2005), they do provide insight into the interpretation of fire behavior observations, and allow us to make inferences as to how the fire behavior would likely change in response to the simulated changes in atmospheric circulations. The combination of observations, idealized modeling results and inferences on fire behavior lead to the development of an initial conceptual model of how the sea-breeze impacts wildfire behavior.

7.1.1 Sea-Breeze Structure and Characteristics

Simpson (1994) provides a detailed overview of the structure and evolution of the sea-breeze front derived from observations as well as numerical and laboratory studies. It is generally observed that the development of the sea-breeze is dependent both upon the temperature difference between the land and the adjacent water surface and upon the strength of any prevailing offshore winds. Offshore flow can often have a dramatic effect on the depth of the sea- breeze circulation. The depth of the sea-breeze circulation may be less than 50 m with winds above this level blowing in the opposite direction. As time progresses, the depth of the sea breeze may reach 1,000 m or more.

The inland penetration of the sea-breeze can vary from 30 – 300 km depending upon the location. Typical distances in Florida are about 50 km, although strong prevailing winds that are in the same direction as the sea-breeze can often result in much deeper penetration, almost to the opposite coast. Florida also has a unique geographic design, being surrounded by water on the east and west coast of the peninsula as well as along the Panhandle coastline. Sea-breezes are observed along all the coasts as well as along the bays, inlets and large lakes like Lake Okeechobee in central Florida. These lake and bay breezes interact with the coastal sea-breezes and result in very complicated wind patterns. Forecasting the winds associated with the sea-breeze passage is also made more difficult by the presence of convex and concave coastlines, resulting in additional convergence and divergence effects (Simpson et al., 1977).

Wakimoto and Atkins (1994) and Atkins and Wakimoto (1997) showed that there were significant differences between the sea-breezes observed under offshore and onshore flow conditions. The offshore flow case exhibited stronger low-level convergence, larger vertical velocities, and higher radar reflectivity values at the sea-breeze front, also known as a radar thin line. The sea-breeze thin line and the kinematic sea-breeze frontal boundary are found to be co-located and easily identifiable on offshore flow days. Onshore flow days typically have a much weaker front and the radar thin line is often hard to detect. In the offshore flow case, the radar thin line is found to increase in intensity during the day and gradients of temperature and moisture are strongest on these days.

It is generally accepted that sea-breeze circulations are dynamically similar to density currents (e.g., Simpson, 1994), which are predominantly horizontal flows driven by density differences. Atkins et al. (1995) note that in the case of an offshore flow sea-breeze, there was a kinematic frontal structure similar to that found in density currents produced in the laboratory. Wakimoto and Atkins (1994) calculated the speed of sea-breeze fronts and found them to be closely matched to the theoretical speeds of comparable density currents. Further study by Atkins and Wakimoto (1997) showed Froude numbers for offshore and parallel flow sea-breeze events, as well as for gust fronts, compared well to values calculated from laboratory density current experiments. This comparison was not as well defined on the onshore flow days where the sea-breeze was moving slower than would be expected using density current theory. It is not clear why this discrepancy exists for onshore flow sea-breezes, although it is suggested that it may be related to the difficulty in locating the location of the frontal zone in these cases.

7.1.2 Radar Observations of Smoke Plumes and the Sea-Breeze

Many wildfires occur in remote regions where observations are limited; as a result, the use of satellite and radar imagery is becoming more prominent in fire detection and monitoring. It has been suggested that remotely sensed data might also be useful in fire behavior prediction (Hufford et al. 1998). Both smoke plumes from fires (e.g., Banta et al., 1992) and sea-breeze fronts (e.g., Wilson et al., 1994) are clearly visible on radar, especially when the radar is in clear-air mode.

Previous studies of the signals returned from the radar during clear-air mode operation have suggested that the echoes are most likely that of birds or insects (Crawford, 1949; Hardy and Katz, 1969; Wilson et al., 1994). Wilson et al. (1994) found that the thin line echoes commonly seen in association with sea-breezes correlated to updraft regions and result from insects actively flying downward to avoid being carried to colder regions of the atmosphere. Atlas (1960) discounts the idea of echoes resulting from birds or insects since they would have to fly along in a very narrow beam, lowering their flight as the beam lowered, or fly in broad waves normal to the beam with the same speed as the beam. Instead, Atlas suggests the pattern seen is a result of a sharp increase in the refractive index. The contrast on the radar is highest when the offshore flow is dry so the contrast is high, leading to higher refractive discontinuities. This would require a sharp vertical lapse rate. Battan (1973) suggests both insects and refractive gradients could be responsible for the radar echoes. Despite some uncertainty regarding exactly what causes the echoes, the sea-breeze signature is readily apparent on the radar for the present case and can be used to follow the inland propagation of the sea-breeze front.

Plumes of smoke have also been observed using radar and satellite imagery in remote locations such as Alaska (Hufford et al., 1998), where plumes from a large wildfire were readily apparent on radar. The plumes from smaller fires were not visible, and it was suggested that the plumes in these cases were concentrated below the level of the radar beam. High reflectivities (i.e., 20 – 25 dBZ) were noted near the head of the fire, however, and Hufford et al. (1998) suggested that radar imagery can be used to provide information on fire location, intensity and growth, smoke plumes and fire weather.

Smoke from a major industrial fire in Montreal, Canada, was observed on three radars operated by McGill University on 23 May 1996 (Rogers and Brown, 1997). They suggested that fires produce particulate matter (PM) and create fluctuations in the refractive index, both of which are potentially detectable by the radar. In this case, they concluded that the echoes are the result of scattering by the particles. Banta et al. (1992) also support the idea that particles in smoke are responsible for the echoes, with the particles having a flat or needle shape (ash platelets or pine needles).

7.1.3 Effect of Sea-Breezes on Fires

There are three main factors that affect fire behavior: fuel, weather and topography. Weather is by far the most variable and arguably the most important of the three. Wind is a strong driver of the rate and direction of fire spread and can also alter fire intensity as well. Changes in wind direction can transform a low intensity backing fire (moving into the wind) or a moderate intensity flanking fire (moving laterally to the wind) into an intense head fire (moving with the wind) capable of overrunning fire fighters who thought they were located in a safe area.

Firefighters typically monitor weather conditions regularly for any changes in wind speed or direction at the scene of the fire using hand-held instruments or portable weather stations. On days where there is adequate moisture, a line of approaching clouds and a gust front may indicate the approach of the sea-breeze front. On dry days, there may be no clouds to warn of the impending frontal passage and the first indication may be the arrival of the gust front. Most fire personnel do not have direct access to radar or satellite data while on a fire scene. Local knowledge of the behavior of the sea breeze is extremely important on both wildfires and prescribed fires as the onset and structure of the sea breeze are typically highly regular in Florida in spring and summer months. One case of a springtime wildfire that is of interest is the East fork fire because of the array of data that was available during the incident and the opportunity it provided to study the sea-breeze–wildfire interaction in a novel way.

7.1.4 East Fork Fire

The East fork fire began either late on 4 April 2004, or early on 5 April 2004, in the Bradwell Bay Wilderness area of the Apalachicola national forest. This area is located in the Florida Panhandle, just southwest of Tallahassee. It is believed that the fire was human-caused, either arson or accidental. The fire ultimately burned over 26,000 acres of the wilderness area. Fire fighting was made difficult due to the restriction on the use of heavy equipment in the wilderness area itself. The fire was considered 90% contained by April 16, 2004.

The sea-breeze was a major factor in fighting the East fork fire. Winds shifted direction on most afternoons, and these wind shifts resulted in varying directions of fire spread. Firefighters had to be aware of these possible weather changes and be able to adjust tactics as the weather changed. Conditions during this period were generally dry, and the daily sea-breeze circulations did not bring any beneficial rains and for the most part were dry events. Because of the dry conditions, the WSR-88D radar site in Tallahassee was operating in clear-air mode at the time of the fire. During clear-air mode periods, the sea-breeze front is often clearly visible on the radar; moreover, smoke plumes can often be seen if they are close enough to the radar. In this case, both the sea-breeze and the smoke plume were noted together and the resulting interaction between the plume and the sea-breeze front could be observed.

The plan of the present Chapter is as follows: in the following section, the data and methodology for both the case study and the idealized numerical simulations are described, while Section 7.3 presents the results of the case study. In Section 7.4, idealized numerical simulations are presented that explore the interaction between a buoyant plume and a density current, and Section 7.5 summarizes the main results of the present investigation and presents a conceptual model for sea-breeze–fire interactions.

7.2 Data and Methodology

7.2.1 Case Study

The goal of this study is to provide an improved understanding of the interactions between wildfires and sea-breeze circulations. The foundation of this understanding is based upon specific observations of one event that will be augmented by idealized numerical simulations. The atmospheric component can be adequately described through a combination of surface observations, upper-air soundings and radar data (both base reflectivity and radial velocity). Description of the fire is considerably more problematic, as no direct measurements of the fire are available, except for daily estimates of area burned. As an alternative, we focus on the behavior of the smoke plume as observed by the Tallahassee WSR-88D radar as a surrogate, since Hufford et al. (1998) found high reflectivities to be associated with more intense burning.

The East Fork Fire burned over a period of approximately two weeks in early April of 2004; however, this study only focuses on the early stages of the fire, specifically the afternoon of April 5. The location of the East fork fire and the four nearby weather stations are shown in Fig. 7.1. Observations of temperature, relative humidity, wind speed and direction are used to track the passage of the sea-breeze front. A high-pass filter was applied to the temperature and relative humidity time series to remove waves with periods greater than or equal to 24 h. The high-pass filter was accomplished using a Fourier decomposition of a 96 h time series for each station and recomposing the time series with the longer wave periods excluded.

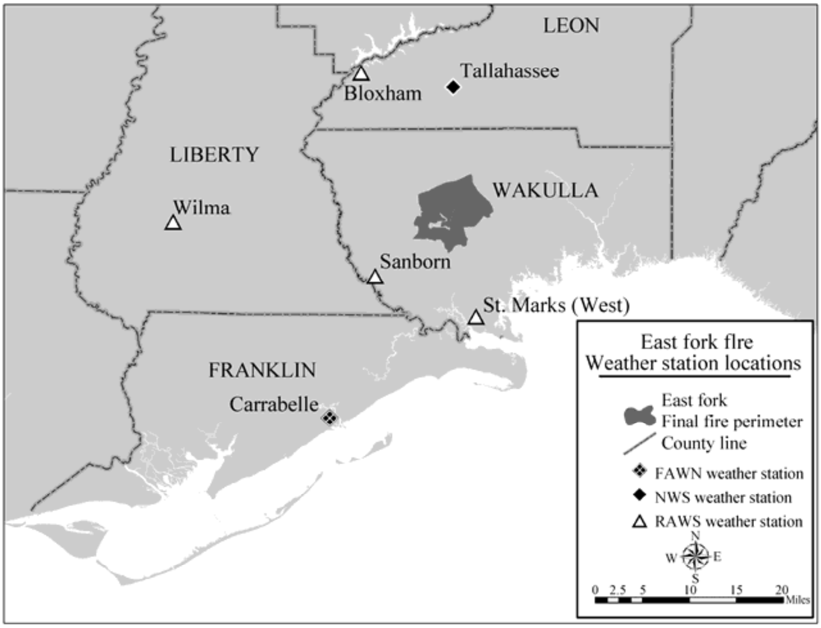

Figure 7.1 Fire perimeters and observation locations

As noted above, the Tallahassee WSR-88D radar was operating in clear-air mode during this period, which is its most sensitive mode of operation (Crum and Alberty, 1993). The antenna has a slower rotation rate than in precipitation mode that increases the radar sensitivity, and therefore its ability to sense smaller objects in the atmosphere. Most of the signal in this mode will be the result of airborne dust and PM. In this mode, the radar scans five different elevation angles (0.5° – 4.5°, in 1° increments) and takes about 10 minutes to complete each scan. In this study we will focus our attention on the three lowest elevations (0.5°, 1.5°, and 2.5°) of the base reflectivity and radial velocity fields.

7.2.2 Idealized Numerical Simulations

The sea-breeze has been studied extensively in the past, and many studies have involved the use of numerical models to simulate sea-breeze circulations, both in an effort to simulate observed cases and in an idealized context to explore their structure and dynamics. From the perspective of idealized simulations of the sea-breeze, Dailey and Fovell (1999), Fovell and Dailey (2001), and Fovell (2005) used a 3D cloud-resolving numerical model with horizontal resolutions as high as 500 m to explore various aspects of the interactions between sea-breeze fronts and horizontal convective rolls in the boundary layer. Several investigators have employed even higher resolution in 2D configurations to explore the parallel between sea-breeze fronts and density currents (e.g., Sha et al., 1991), and in this regard, simulations exploring the dynamics of thunderstorm outflow boundaries are also relevant (e.g., Droegemeier and Wilhelmson, 1987; Xu et al., 1996; Xue et al., 1997).

As discussed further below, our approach follows these studies in that the sea-breeze is idealized as a density current; however, we employ a large-eddy simulation (LES) model focusing solely on the atmospheric boundary layer, with model grid spacing on the order of 10 m in all three dimensions, to explore the dynamics of the interaction of this density current with a buoyant plume that is representative of the smoke plume from a wildland fire. Since it is expected that the most significant interaction between the sea-breeze and a fire and its attendant plume will occur primarily with the passage of the sea-breeze front, this approach appears to be justified, although we acknowledge that there are several details of observed sea-breeze circulations that cannot be represented by the present model.

The LES model to be used is described by Cunningham et al. (2005), and is based on the dynamical core of the weather research and forecasting (WRF) model in physical height coordinates (Skamarock et al., 2001). The domain size used in these simulations is a rectangular box of size $800 \times 3{,}200 \times 1{,}000$ m in the x, y, and z directions, respectively, with a uniform grid spacing of 10 m in all three directions. Boundary conditions are periodic in the x-direction and open-radiative in the y-direction. Other details of the LES model are identical to those described by Cunningham et al. (2005).

As noted previously, there is significant evidence that a sea-breeze front can be interpreted as a density current, particularly when the ambient wind is in the offshore direction. Density currents have been explored extensively by numerical models, in an atmospheric context primarily in connection with thunderstorm outflows (e.g., Droegemeier and Wilhelmson, 1987; Xu et al., 1996; Xue et al., 1997), but also in oceanographic (e.g., Özgökmen et al., 2004) and general fluid mechanics (e.g., Härtel et al., 2000) contexts, and even with respect to the backdraft phenomenon in building fires (e.g., Fleischmann and McGrattan, 1999). Here we initialize the density current with a cold pool that is uniform in the y-direction in the presence of an opposing flow, to simulate the advance of a sea-breeze front in the presence of offshore winds.

As a final comment concerning the modeling approach, we emphasize that the goal of the idealized modeling portion of this study is not to reproduce the behavior in the observed case, but rather to gain insight into the basic dynamical processes associated with the interaction between a sea-breeze front and a buoyant plume representative of those seen with wildland fires.

7.3 Case Study Analysis

The East fork fire began late on April 4, 2004, or early on April 5, 2004, and is suspected to have been started by human causes, either accidental or arson. The fire burned in timber and southern rough fuel groups. According to the National Interagency Coordination Center reports, by April 7 the fire reached 7,000 acres (28.3 km^2) and was only 20% contained. Spotting of up to 0.25 mile (0.4 km) ahead of the main fire front was observed with rates of spread of 20 – 30 chains per hour (0.11 – 0.17 $m \cdot s^{-1}$) reported. This observed fire activity continued and by April 8, the area burned had increased to over 8,400 acres (34.0 km^2). By April 13, the fire had consumed almost 20,000 acres (80.9 km^2) and was only 70% contained. The fire ultimately consumed over 26,000 acres (105.2 km^2) of wilderness area and was 90% contained by April 15. The total area burned was increased by back burning activities of the fire suppression crews. Back burning is used to remove fuels ahead of the active fire front and impede the spread of the fire and help in containment.

Hourly surface observations were used to provide an estimate of the passage of the sea-breeze front. Unfiltered time series of temperature and relative humidity data from four stations near the fire (not shown) indicate that Sanborn, the closest of the four stations to the coast, shows the earliest peak in temperature (1,400 EDT), while the peak at the other stations is delayed by approximately 2 h. Following the temperature maximum is a decrease in temperature spanning 6 – 8 h, which is hardly indicative of the passage of the sea-breeze front, and more closely resembles the normal diurnal cycle. The unfiltered relative humidity time series does not show a marked change in air mass either. Using a high-pass filter to remove the diurnal signal as described in the previous section reveals a stronger sea-breeze signal in both the temperature and relative humidity time series (Fig. 7.2). It is apparent that Sanborn shows the earliest start to humidity recovery around 1,700 EDT with the other stations following rather sharply an hour later.

The sea-breeze front can be seen clearly on the Tallahassee 0.5° elevation base reflectivity imagery at 1828 UTC (Fig. 7.3). The East Fork Fire is visible approximately 40 km southwest of the radar location and is indicated by a reflectivity of approximately 18 dBZ with the smoke plume traveling toward the southeast (Fig. 7.3(a)). The sea-breeze front continues to move inland over the next several hours and by 1927 UTC (Fig. 7.3(b)) the smoke plume from the fire can be seen to increase in intensity with reflectivities reaching 28 – 32 dBZ for a brief period prior to the arrival of the sea-breeze front. By 2025 UTC the sea-breeze is just reaching the fire and the plume is displaying reflectivities in the range of 20 – 25 dBZ near the fire (Fig. 7.3(c)), consistent with values observed by Hufford et al. (1998) near the head of a rapidly moving wildfire. At 2124 UTC, the sea-breeze front has reached the fire, as evidenced by the humidity recovery indicated by the Sanborn RAWS site. Despite the start of humidity recovery the

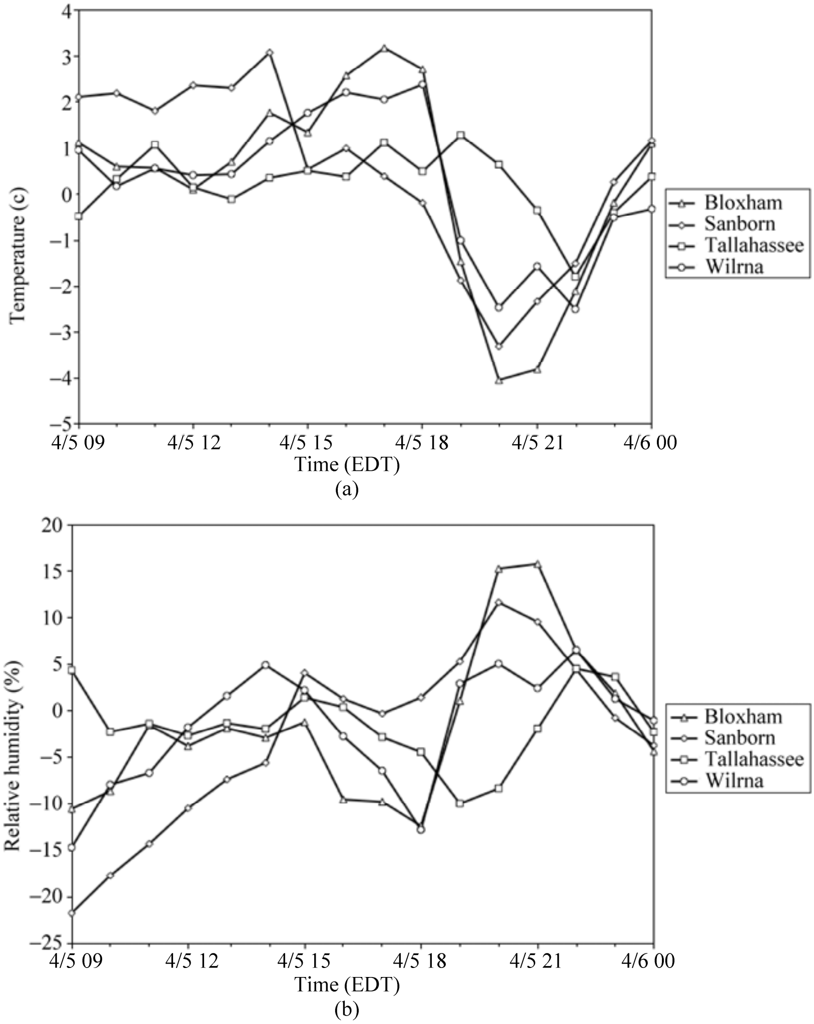

Figure 7.2 High-pass filtered time series of (a) temperature and (b) relative humidity at the surface for the period starting at 0900 EDT 5 April 2004 and ending at 0000 EDT 6 April 2004, for several stations identified in Fig. 7.1

plume intensifies to levels not previously seen with a large core of the plume now displaying reflectivities in the 28 – 32+ dBZ range (Fig. 7.3(d)). Upper-level winds at this time are carrying the plume back toward the coast, aided by the upper-level return flow of the sea-breeze circulation. The reflectivity of the plume decreases from this peak over the next several hours as the fire begins to respond to the decreased temperature and increased moisture of the marine air, leading to a decline in fire intensity (Figs. 7.3(e) and (f)).

Base reflectivities from the 0.5°, 1.5° and 2.5° elevations are used to examine the vertical structure of the plume at 2,124 UTC, the time of greatest intensity

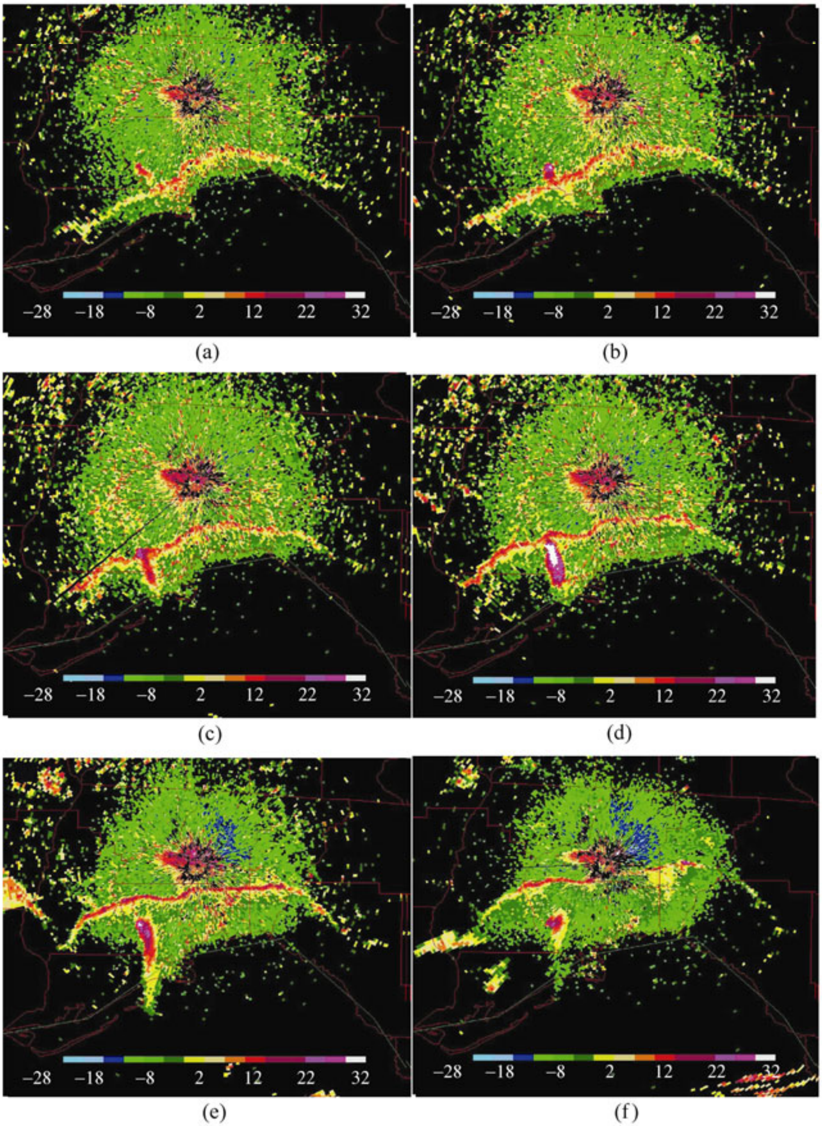

Figure 7.3 Radar reflectivity (dBZ, shaded as indicated) at a scan elevation of 0.5° at (a) 1828 UTC, (b) 1927 UTC, (c) 2025 UTC, (d) 2124 UTC, (e) 2223 UTC, and (f) 2323 UTC for 5 April 2004

(Fig. 7.4). At the lowest elevation, the overall plume is 21.25 km in length with the region of reflectivity >28 dBZ having a length of 8.75 km. The approximate heights of the centroids of the ends of the plume at this elevation are 453 m and 638 m, well within the 800 m deep mixed layer (estimated from the 1200 UTC sounding and observed high temperature). At the 1.5° elevation, the plume is slightly longer, 23.75 km (length of the 28+ dBZ core has shrunk to 3.75 km), ranging in height from 1,151 – 1,637 m. At this elevation the plume is clearly above the mixed layer and in the return flow of the sea-breeze circulation. The 2.5° elevation reveals a considerably smaller plume, 8.75 km in length (2.5 km for the 28+ dBZ core), and spanning elevations of 1,849 – 2,157 m. The northwest corners of the plumes at each level are collocated, indicating that the plume has a rather strong vertical core immediately above the fire that would be consistent with an intensely burning fire producing a strong buoyancy flux.

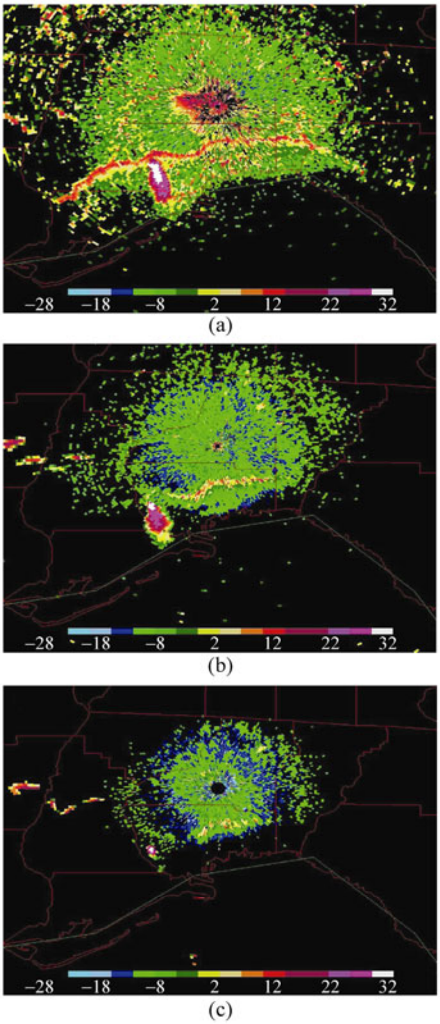

Figure 7.4 Radar reflectivity (dBZ, shaded as indicated) at 2124 UTC for 5 April 2004 at scan elevations of (a) 0.5°, (b) 1.5°, and (c) 2.5°

The radial velocity field from the WSR-88D is a useful tool in identifying areas of convergence and divergence. The 0.5° elevation radial velocity field from Tallahassee shows a well defined convergence zone along the sea-breeze front as it pushes inland against the prevailing northwesterly flow in the region (Fig. 7.5). Near the fire the pattern is more complex as the rising plume generates a region of divergence oriented along the axis of the plume, possibly marking the return flow of the thermal circulation generated by the intense heating of the fire. At the 1.5° elevation, a divergence pattern is still discernible along the plume axis although its extent is limited to the area near the peak in base reflectivity.

It should be noted that we have avoided making any direct comments as to the magnitudes of the velocities shown. This is due to the relatively broad spectrum width observed by the radar in the vicinity of the plume which is indicative of a highly turbulent environment, and thus renders the magnitudes of the radar-derived velocities less reliable.

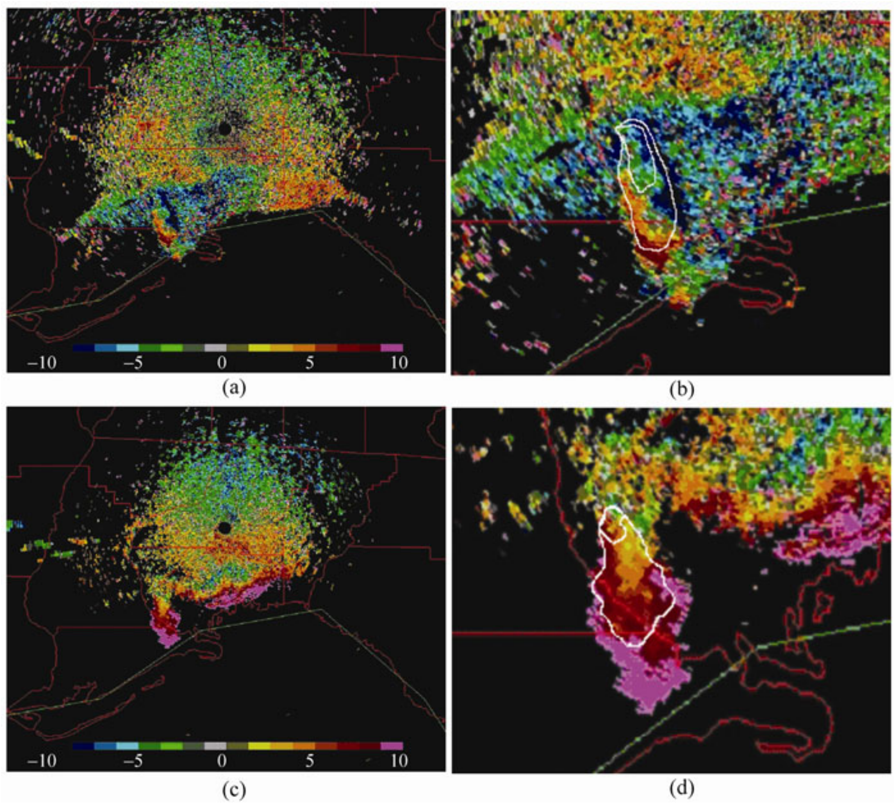

Figure 7.5 Radial velocity ($m \cdot s^{-1}$, shaded as indicated) at 2,124 UTC for 5 April 2004 at scan elevations of (a) 0.5° and (c) 1.5°. Panels (b) and (d) provide close-up representations of panels (a) and (c), respectively, with base reflectivities of 12 dBZ and 28 dBZ indicated by the solid contours

7.4 Numerical Simulations

In this Section, we present results from three numerical simulations to explore the nature of the interaction between a density current and a buoyant plume: two simulations in which a density current and a plume are examined in isolation, respectively, and one in which both are present and are allowed to interact.

The density current is initialized with a cold pool at one end of the domain (Fig. 7.6). When the simulation is started, the cold pool adjusts under gravity and initiates a density current that travels in the positive *y*-direction. The ambient winds are directed in the negative *y*-direction, thus representing an offshore flow situation. The cold pool is initially uniform in the *x*-direction, but rapidly becomes 3D with the development of lobe and cleft instabilities (not shown), consistent with laboratory experiments and previous numerical investigations using three-dimensional models.

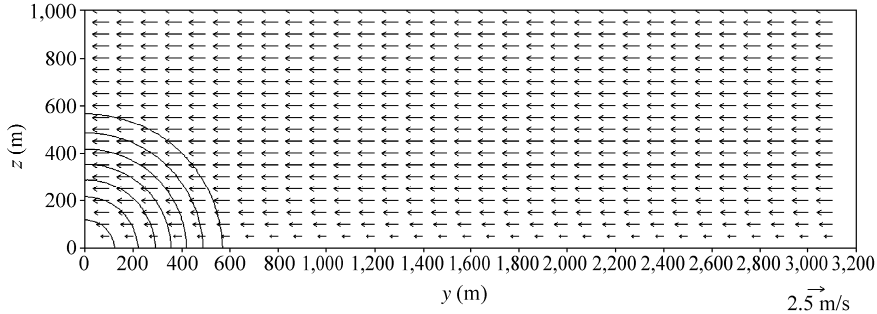

Figure 7.6 Model initial conditions in the $y-z$ plane at $x=480$ m of potential temperature (contour interval 1 K) and wind vectors in the plane of the section (in $m \cdot s^{-1}$, vector scale shown at bottom right)

Figure 7.7(a) depicts the potential temperature, vertical velocity, and wind field in the $y-z$ plane. The Kelvin–Hemholtz billows characteristic of the interface between the density current and the ambient atmosphere are apparent, as is the enhanced vertical motion and return flow associated with the density current.

Figure 7.7(b) illustrates the simulation of the plume only. The plume is initiated by a heat source centered at $y=2{,}700$ m, the spatial configuration of which is a smoothed top-hat function. Characteristic features of the plume are similar to those described in more detail in the simulations by Cunningham et al. (2005).

The simulation in which both the plume and the density current are present is depicted in Fig. 7.7(c). It is evident that the interaction between the density current and the plume results in an apparent intensification of the plume, particularly in the vertical velocity field, in conjunction with the arrival of the circulation associated with the current, and that this intensification occurs before the head of the density current reaches the heat source. The intensification apparently occurs in response to the pressure perturbation that precedes the head of the current: this pressure perturbation, which can impact the plume for a period of time before the arrival of the colder, more dense air behind the head of the current, counteracts the ambient flow at low levels such that the plume becomes more vertical (compare Fig. 7.7(b) with Fig. 7.7(c)), resulting in vertical velocities that are significantly stronger than those seen in the plume in isolation.

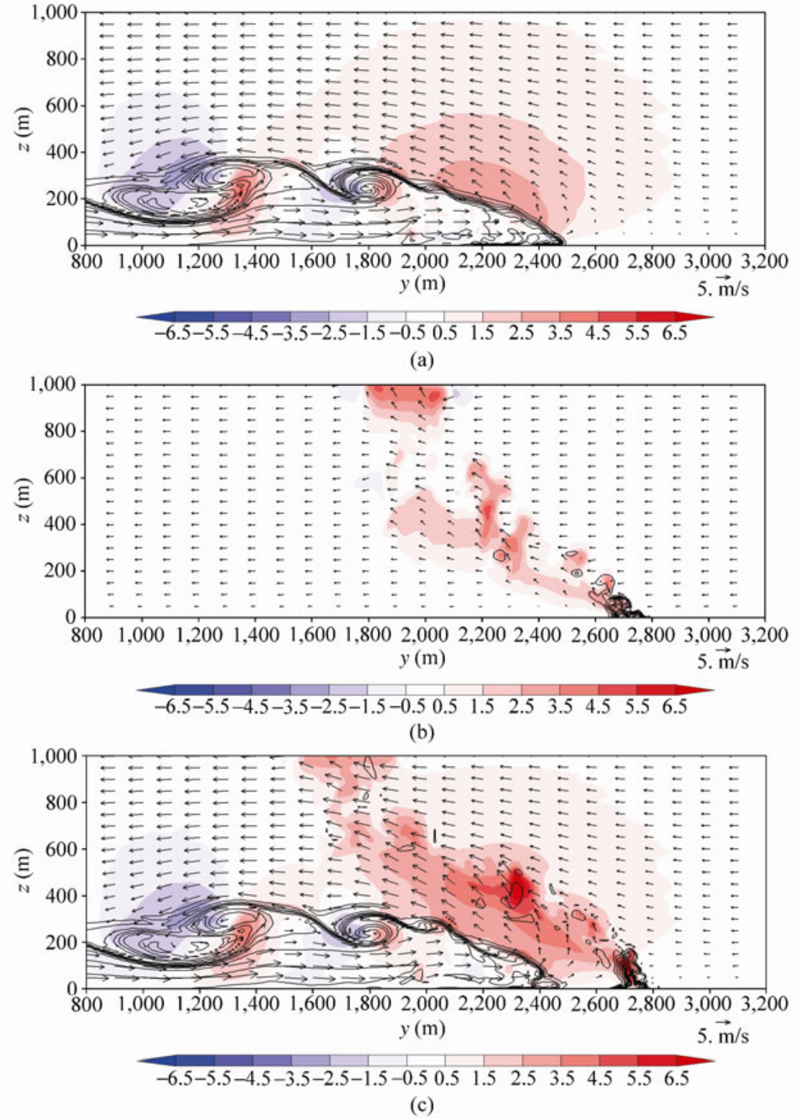

Figure 7.7 Vertical velocity (in m·s^{-1}, shaded as indicated) and potential temperature (contour interval 1 K) in the $y-z$ plane for (a) the density current only, (b) the plume only, and (c) the density current and the plume. Vectors depict velocity in the plane of the section, with the scale in m·s^{-1} at the bottom right

7.5 Summary and Conclusions

Sea-breeze circulations are frequently observed to have a significant impact on fire behavior; however, the nature of the interaction between wildfires and the sea-breeze is poorly understood, and has not been studied extensively. In this Chapter, radar observations of a plume associated with a wildfire in Florida were presented that suggest that the arrival of a sea-breeze front results in a temporary, but significant, increase in fire intensity. This intensification precedes the arrival of the sea-breeze front at the location of the fire, such that the fire intensity is a maximum at the time of, and slightly after, the passage of the front, and decreases gradually thereafter with the arrival of cooler and moister air behind the front.

There is insufficient evidence to explain this intensification; however, the idealized numerical simulations presented in Section 7.4 suggest that the period of interaction preceding the arrival of the current may result in the temporary intensification of vertical velocity in the plume. This increase in vertical velocity appears to result from the interaction of the plume with a pressure perturbation that precedes the head of the density current. The direct impact of this interaction on fire behavior is uncertain, however, and requires further study, particularly using coupled atmosphere-fire models to explore the details of this interaction. Another aspect of the wildland fire-sea-breeze system that warrants investigation is how these interactions influence local and regional air quality.

Acknowledgements

The authors gratefully acknowledge Pam Brown of the USDA Forest Service in Tallahassee for providing the RAWS data for this study, and Scott Taylor of the Florida Division of Forestry for creating Fig. 7.1. We also thank Dr. Rodman Linn for insightful discussions on various aspects of the Chapter. DEH acknowledges support from the Florida Department of Agriculture and Consumer Services. PC acknowledges support from the USDA Forest Service, via a cooperative agreement between the Florida State University and the USDA Forest Service Southern Research Station, and from the FSU School of Computational Science, via a grant of resources on the IBM SP Series 690 Power4-based supercomputer “Eclipse”.

References

Atkins NT, Wakimoto RM, (1997), Influence of the synoptic-scale flow on sea breezes observed during CaPE. *Mon. Wea. Rev.*, **125**: 2112 – 2130

Atkins NT, Wakimoto RM, Weckwerth TM, (1995), Observations of the sea-breeze front during CaPE. Part II: Dual-Doppler and aircraft analysis. *Mon. Wea. Rev.*, **123**: 944 – 969

Atlas D, (1960), Radar detection of the sea breeze. *J. Meteor.*, **17**: 244 – 258

Banta RM, Olivier LD, Holloway ET, Kropfli RA, Bartram BW, Crupp RE, Post MJ, (1992), Smoke-column observations from two forest fires using Doppler lidar and Doppler radar. *J. Appl. Meteor.*, **31**: 1328 – 1349

Battan LJ, (1973), Radar Observation of the Atmosphere. University of Chicago Press, 324

Clark TL, Jenkins MA, Coen JL, Packham DR, (1996a), A coupled atmosphere–fire model: Convective feedback on fire line dynamaics. *J. Appl. Meteor.*, **35**: 875 – 901

Clark TL, Jenkins MA, Coen JL, Packham DR, (1996b), A coupled atmosphere–fire model: Role of the convective Froude number and dynamic fingering at the fire line. *Int. J. Wildland Fire*, **6**: 177 – 190

Clark TL., Coen JL, Latham D, (2004), Description of a coupled atmosphere–fire model. *Int. J. Wildland Fire*, **13**: 49 – 63

Colby FP, (2004), Simulation of the New England Sea Breeze: The effect of grid spacing. *Wea. Forecasting*, **19**: 277 – 285

Cunningham P, Goodrick SL, Hussaini MY, Linn RR, (2005), Coherent vortical structures in numerical simulations of buoyant plumes from wildland fires. *Int. J. Wildland Fire*, **14**: 61 – 75

Dailey PS, Fovell RG, (1999), Numerical simulation of the interaction between the sea-breeze front and horizontal convective rolls. Part I: Offshore ambient flow. *Mon. Wea. Rev.*, **127**: 858 – 878

Droegemeier KK, Wilhelmson RB, (1987), Numerical simulation of thunderstorm outflow dynamics. Part I: Outflow sensitivity experiments and turbulence dynamics. *J. Atmos. Sci.*, **44**: 1180 – 1210

Fisher EL, (1960), An observational study of the sea breeze. *J. Meteor.*, **17**: 645 – 660

Fleischmann CM, McGrattan KB, (1999), Numerical and experimental gravity currents related to backdrafts. *Fire Safety J.*, **33**: 21 – 34

Fovell RG, (2005), Convective initiation ahead of the sea-breeze front. *Mon. Wea. Rev*., **133**: 264 – 278

Fovell RG, Dailey PS, (2001), Numerical simulation of the interaction between the sea-breeze front and horizontal convective rolls. Part II: Alongshore ambient flow. *Mon. Wea. Rev.*, **129**: 2057 – 2072

Härtel C, Meiburg E, Necker F, (2000a), Analysis and direct numerical simulation of the flow at a gravity-current head. Part 1. Flow topology and front speed for slip and no-slip boundaries. *J. Fluid Mech*., **418**: 189 – 212

Härtel C, Carlsson F, Thunblom M, (2000b), Analysis and direct numerical simulation of the flow at a gravity-current head. Part 2. The lobe-and-cleft instability. *J. Fluid Mech.*, **418**: 213 – 229

Hufford GL, Kelley HL, Sparkman W, Moore RK, (1998), Use of real-time multisatellite and radar data to support forest fire management. *Wea. Forecasting*, **13**: 592 – 605

Linn RR, (1997), A transport model for prediction of wildfire behavior. Scientific Report LA-13334-T, Los Alamos National Laboratory, 195

Linn RR, Cunningham P, (2005), Numerical simulations of grass fires using a coupled atmosphere–fire model: Basic fire behavior and dependence on wind speed. *J. Geophys. Res.*, in press

Linn RR, Reisner JM, Colman JJ, Winterkamp J, (2002), Studying wildfire behavior using FIRETEC. *Int. J. Wildland Fire*, **11**: 233 − 246

Özgökmen TM, Fisher PF, Dian J, Iliescu T, (2004), Three-dimensional turbulent bottom density currents from a high-order nonhydrostatic spectral element model. *J. Phys. Oceanogr.*, **34**: 2006 − 2026

Pielke RA, (1974), A three-dimensional numerical model of the sea breezes over south Florida. *Mon. Wea. Rev*., **102**: 115 − 139

Rao PA, Fuelberg HE, Droegemeier KK, (1999), High-resolution modeling of the Cape Canaveral area land–water circulations and associated features. *Mon. Wea. Rev*., **127**: 1808 − 1821

Rogers RR, Brown WOJ, (1997), Radar observations of a major industrial fire. Bull. *Amer. Meteor. Soc*., **78**: 803 − 814

Sha W, Kawamura T, Ueda H, (1991), A numerical study on sea/land breezes as a gravity current: Kelvin–Helmholtz billows and inland penetration of the sea-breeze front. *J. Atmos. Sci.*, **48**: 1649 − 1665

Simpson JE, (1994), Sea Breeze and Local Winds. Cambridge University Press, 234

Simpson JE, Mansfield DA, Milford JR, (1977), Inland penetration of sea-breeze fronts. *Quart. J. Roy. Meteor. Soc*., **103**: 47–76

Skamarock WC, Klemp JB, Dudhia J, (2001), Prototypes for the WRF (Weather Research and Forecasting) model. Preprints, Ninth Conf. On Mesoscale Processes, Fort Lauderdale, FL, *Amer. Meteor. Soc*., J11 − J15

Wakimoto RM, (1982), The life cycle of thunderstorm gust fronts as viewed with Doppler radar and rawinsonde data. *Mon. Wea. Rev.*, **110**: 1060 − 1082

Wakimoto RM, Atkins NT, (1994), Observations of the sea-breeze front during CaPE. Part I: Single-Doppler, satellite, and cloud photogrammetry analysis. *Mon. Wea. Rev.*, **122**: 1092 − 1114

Wilson JW, Weckwerth TM, Vivekanandan J, Wakimoto RM, Russell RW, (1994), Boundary layer clear-air radar echoes: Origin of echoes and accuracy of derived winds. *J. Atmos. Oceanic. Technol.*, **11**: 1184 − 1206

Xu Q, Xue M, Droegemeier KK, (1996), Numerical simulations of density currents in sheared environments within a vertically confined channel. *J. Atmos. Sci.*, **53**: 770 − 786

Xue M, Xu Q, Droegemeier KK, (1997), A theoretical and numerical study of density currents in nonconstant shear flows. *J. Atmos. Sci.*, **54**: 1998 − 2019

8 Prescribed Fire and Air Quality in the American South: A Review of Conflicting Interests and a Technique for Incorporating the Land Manager into Regional Air Quality Modeling

Gary L. Achtemeier
Center for Forest Disturbance Science, USDA Forest Service,
320 Green Street, Athens, GA 30602
Email: gachtemeier@fs.fed.us

Abstract In this paper, conflicting interests in prescribed burn practice and improving air quality in the South are reviewed. Conflicting societal interests and legislative actions threaten to curtail the use of prescribed fire to manage for endangered species and for other land management objectives in the South. This comes at a time when efforts are being made to increase prescribed burning on existing forest land and to initiate prescribed burning on tracts of old agricultural land that are being restored to forest land. Regulatory interests regarding impacts of regional haze on visibility and impacts of fine particulate matter on health are increasingly in conflict with management objectives driven by natural resource management. The air quality community is increasingly relying on computer air quality models for understanding the movement of pollutants across regions and for the chemical interactions of airborne materials. The success of air quality/air chemistry models depends on the availability of accurate source inventories. Wildland burning in the South is considered a significant contributor to the organics inventory. Because prescribed fires are managed, the timing and locations of burns and where in the atmosphere fire products are distributed must be taken into account. Therefore land managers become active players in local and regional air quality.

A technique for incorporating the land manager into regional air quality modeling is described. The core of the technique is two modeling tools for dealing with the conflicting interests, that is, a dynamical-stochastic smoke model, Daysmoke, and a "modeling framework", the SHRMC-4S. Daysmoke distributes smoke in the atmosphere after the manner the burns are "engineered" by land managers. SHRMC-4S is constructed by linking an atmospheric chemical model, CMAQ, with Daysmoke. Applications of the two modeling tools to a prescribed burn case are illustrated. Daysmoke produces a ground

PM level close to the measured value if complex plume structures are correctly modeled. CMAQ simulations of ground-level PM for a single prescribed fire suffer from grid resolution.

Keywords Prescribed burning, smoke, air quality, modeling, daysmoke, SHRMC-4S

8.1 Introduction

The American South comprises one of the most productive forested areas in the United States with approximately 200 million acres (81 million ha) or 40% of the nation's forests in an area occupying only 24% of the U.S. land area (SRFRR, 1996). Furthermore, Southern forests are dynamic ecosystems characterized by rapid growth and hence rapid deposition of fuels within a favorable climate, and a high fire-return rate of every 3 – 5 years (Stanturf et al., 2002).

Research efforts in investigating the air quality effects of prescribed fires in the South have been made in the Southern high-resolution modeling consortium (SHRMC). SHRMC was established as one of the USDA forest service fire consortia for advanced modeling of meteorology and smoke (FCAMMS) centers funded by the national fire plan (NFP).

As the air quality community relies more on high-resolution air quality/air chemistry models such as CMAQ, it is critical that emissions inventories from prescribed burns supplied to these models are accurate. The timing and locations of burns and where in the atmosphere fire products are distributed must be taken into account.

Prescribed burns are managed fires. Land managers choose the day and time to conduct their burns under favorable dispersion conditions. Land managers determine how much fire to place on the landscape and how the fire is to be distributed. Therefore, land managers are active players in local and regional scale air quality.

Our objective is to design a regional scale air quality "modeling framework" that gives land managers a "say" in how their land management practices are incorporated into air quality/air chemistry models. The framework is called Southern High-Resolution Modeling Consortium Southern Smoke Simulation System SHRMC-4S (Achtemeier et al., 2003; Liu et al., 2004). SHRMC-4S includes models to simulate fire emissions, local smoke movement (including plume rise), high-resolution meteorological processes (MM5) and air chemistry (CMAQ). SHRMC-4S, in comparison with the modeling framework, Bluesky (O'Neill et al., 2003), is designed specifically for assessing air quality impacts from prescribed burning in the South through CMAQ.

The impact of prescribed burn "engineering" by the land manager is modeled through plume rise—how high the plume goes and the vertical distribution of smoke particles. The plume model determines the fraction of smoke left in the atmospheric boundary layer (mixed layer) that can be transported to the ground locally and the fraction of smoke partitioned at higher altitudes. Smoke carried to higher altitudes will be transported regionally or beyond by prevailing winds. The national ambient air quality standards (NAAQS) apply to the ground-level pollutant concentrations. When more smoke is injected at higher altitudes and dispersed to remote areas, the chances for exceeding the NAAQS standards locally and regionally are reduced. Specification of plume rise is thus crucial for evaluating the air quality effects of prescribed burning. Many efforts have made to develop smoke plume rise schemes (e.g. Pouliot et al., 2005).

In this Chapter, issues on the air quality effects of prescribed fire are discussed. The development of the modeling tools and their applications to simulating the air quality effects are described.

8.2 Conflicts over the Airshed of the American South

One of the adverse consequences of prescribed burning is degradation of air quality (Ward and Hardy, 1991; Sandberg et al., 1999; Riebau and Fox, 2001). Air pollution from smoke has led to conflicts between interest groups involved with clean air and forest management. Issues of human health, nuisance smoke, visibility, and transportation hazard often stand against issues of forest health and safety, wildlife management, ecosystem restoration, timber production, and carbon sequestration. In some instances, the clean air act conflicts with the threatened and endangered species act.

Prescribed burning is extensively used, treating 6 – 8 million acres (2 – 3 million ha) of forest and agricultural lands each year (Wade et al., 2000). Prescribed fire has long been recognized as the most economical means for managing timberlands for fiber production. Prescribed fire eliminates species that compete for nutrients and reduces buildup of dead and live fuels that increase the hazard of destructive wildfire.

The mild, mostly snow and ice free winters make the Southern climate ideal for the development of retirement communities. Thousands of older people, some with respiratory problems, have relocated into these communities. Many of these retirees have little or no experience with forestry practices and therefore may not be receptive to frequent incursions of smoke into their communities. Human health concerns and issues of nuisance have created a need for regulation of smoke.

The South has some of the highest levels of PM and ozone in the nation. Fires have been found to be an important contributor (Zheng et al., 2002). Smog, regional haze, and visibility impairment are air quality issues addressed by the U.S. EPA. Prescribed burning releases $PM_{2.5}$ and PM_{10} (particulate matter (PM) with a size not greater than 2.5 μm and 10 μm, respectively), NO_2 and volatile organic compounds (VOC), which are either direct contributor or precursors of O_3. Prescribed burning also emits CO, SO_2, which together with PM, NO_2, and O_3 are the criteria air pollutants subject to the U.S. NAAQS (EPA, 2003).

The EPA has issued the interim air quality policy on wildland and prescribed fire to protect public health and welfare by mitigating the impacts of air pollutant emissions from wildland fires on air quality (EPA, 1998). Among various issues of concern in the South is the contribution of burning to $PM_{2.5}$ concentrations. $PM_{2.5}$ is a risk to both human health and the environment. It is able to penetrate to the deepest parts of the lungs. It is also a major cause of visibility impairment and a contributing factor for acid rain. EPA established NAAQS for $PM_{2.5}$ in 1997 and Biomass burning is one of the major sources for the atmospheric $PM_{2.5}$.

These air quality regulatory concerns conflict with growth in the need for prescribed burning of Southern forest lands. The Endangered Species Act, requires land managers to manage habitat to preserve or increase populations of threatened and endangered species. For example, prescribed fire is used in the coastal plains and Piedmont regions of the Southeast to improve habitat for the red-cockaded woodpecker (Picoides borealis Vieillot)—a species listed as endangered under the endangered species act (Achtemeier et al., 1998).

An example of conflicting legislation is to be found in the Southern Appalachians. There, a low-growing shrub species called Hudsonia montana Nuttall is listed as a threatened species under the endangered species act. H. montana is dependent upon fire for survival. Including prescribed burning in a recovery plan would be straightforward except that the largest populations of H. montana are found within and adjacent to the Linville Gorge Wilderness, a Class I area, governed by clean air regulations (Achtemeier et al., 1998).

The conflict between managing for natural resources and managing for air quality has placed Southern land managers in the difficult position of "getting it right all of the time." Through careful monitoring of fuel moisture and weather conditions land managers have learned to "engineer" prescribed burns to accomplish natural resource objectives while minimizing (though not eliminating) impacts on local air quality. Although the vast majority of prescribed burns are done without incident, there are occasions when weather conditions are not as expected and local and regional air quality is compromised.

8.3 Daysmoke

The southern burn program is threatened by nuisance complaints, litigation, and lowering of 24 hour fine particulate ($PM_{2.5}$) air quality standards. Land managers need to have accurate downwind fine particulate predictions if they are to continue burning at the same levels as they have in the past or increase their burning programs. The daysmoke plume model incorporates a human factor—how burns are engineered by land managers through burning techniques/ignition methods—in modeling smoke from prescribed burns. Therefore daysmoke may provide land managers with a tool that will assist in achieving their burn programs.

Daysmoke (Achtemeier et al., 2006) is a dynamical-stochastic plume model designed to simulate smoke from prescribed burns in a manner consistent with how the burns are engineered by land managers. It is an extension of ASHFALL, a plume model developed to simulate deposition of ash from sugar cane fires (Achtemeier, 1998). Daysmoke consists of four models (Fig. 8.1): ① Entraining turret plume model. The plume is assumed to be a succession of rising turrets. The rate of rise of each turret is a function of its initial temperature, vertical velocity, effective diameter, and entrainment. ② Detraining particle trajectory model. Movement within the plume is described by the horizontal and vertical wind velocity within the plume, turbulent horizontal and vertical velocity within the plume, and particle terminal velocity. Detrainment occurs when stochastic plume turbulence places particles beyond plume boundaries, plume rise rate falls below a threshold vertical velocity, or absolute value of large eddy velocity exceeds plume rise rate. ③ A large eddy parameterization. Eddies are 2D and oriented normal to the axis of the mean layer flow. Eddy size and strength are proportional to depth of the planetary boundary-layer (PBL). Eddy growth and dissipation are time-dependent and are independent of growth rates of neighboring eddies. Eddy structure is vertical. Eddies are transported by the mean wind in the PBL. ④ Relative emissions production model. Particles passing a "wall" three miles downwind from a burn are counted for each hour during the burning period.

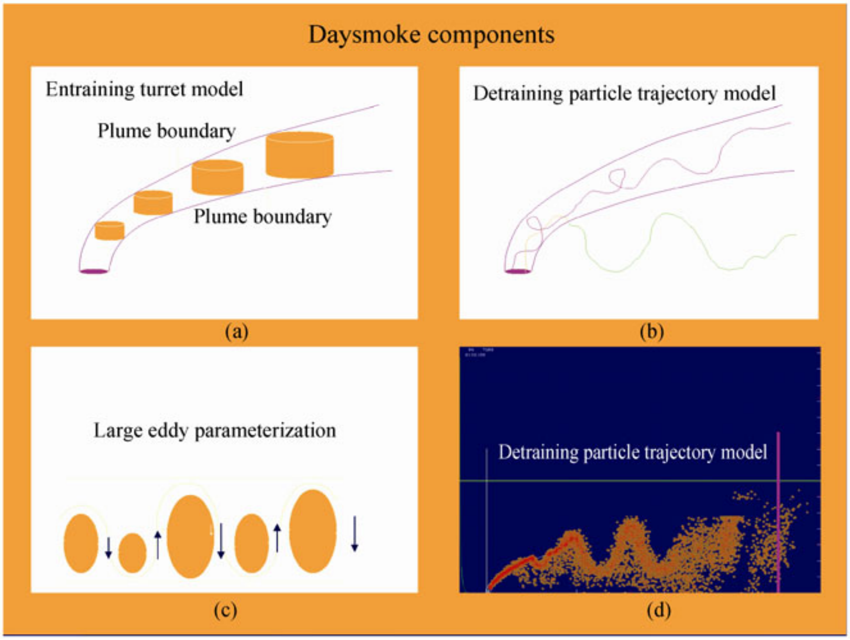

Figure 8.1 An overview of daysmoke, including Entraining turret plume model (a), Detraining particle trajectory model (b), Large eddy parameterization (c), and Relative emissions production model (d)

Daysmoke has many unique features in comparison with some existing smoke transport tools used by land and fire managers in determining downwind transport of $PM_{2.5}$. The ventilation index (VI) is the product of the depth of the atmospheric boundary layer (mixing layer) with the transport wind speed (the mean wind speed within the mixing layer). The VI is used to regulate the amount of fuel consumed on a given day according to ambient weather conditions. However, the VI is limited by the inherent assumptions that the horizontal dimension of the burn site normal to the wind speed is of infinite length and that all smoke remains within the mixed layer. The dispersion index (Lavdas, 1986) modified the VI for an ensemble of finite burn areas and explicitly incorporates atmospheric stability; although the dispersion index also maintains the assumption that all smoke remains within the mixed layer. Lavdas (1996) linked fuels information with meteorological data through VSMOKE, a smoke "screening" model for local smoke dispersion. The Florida fire management information system (Goodrick and Brenner, 1999; Brenner and Goodrick, 2005) merges the cross flow Gaussian horizontal dispersion properties of VSMOKE with 3D trajectories produced by HYSPLIT (Draxler and Hess, 1997) to estimate smoke plume movement and the ground-level impact of $PM_{2.5}$ concentrations on potentially hazardous visibility reductions.

However, none of the existing tools includes the "human element"—how the burns are engineered by land managers. By the choice of firing method—head fire, back fire, mass ignition (where, when, and how much fire is dropped from helicopters)—land managers can influence the timing of heat production and how much heat is produced over the course of the burn. Thus fire ignition timing and pattern can be a major contributor to how high smoke rises and how much is released during a period of evolving mixing layer height within a time-dependent wind field.

Daysmoke includes theory for particulate detrainment from the smoke plume. Daysmoke removes a restrictive assumption inherent in VSMOKE and the Ventilation Index namely that all smoke is contained within the mixed layer. Daysmoke also removes the imposed vertical distribution of smoke in VSMOKE and the instantaneous even distribution of VI. If the convective smoke plume is relatively weak, all or part of it may be captured, torn apart, and dispersed by turbulence within the mixed layer before it rises to an altitude of thermal equilibrium. If the convective smoke plume is strong, most of the smoke may be ejected into the free atmosphere far above the top of the mixed layer with little or no smoke remaining to be dispersed within the mixed layer.

The primary application of daysmoke is simulating local scale smoke concentrations for planning and regulatory purposes. A secondary application is acting as a "smoke-injector" for regional scale air quality models by replacing current plume rise formulations and providing a more representative vertical smoke distribution for wildland fires. Daysmoke is also intended as a training tool to increase our understanding of how ground-level concentrations of $PM_{2.5}$ can be manipulated by burn technique/ignition strategies.

8.4 SHRMC-4S

An overview of SHRMC-4S is shown in Fig. 8.2. Each box along the blue arrow represents steps needed to accomplish the objective of including emissions from wildland fires in regional scale air quality models. The first box, Fire Data, gets SHRMC-4S started. Information on the size of the tract of land to be burned, the date and time of the burn, the location of the burn, plus pertinent data on the kinds and state of fuels is supplied by the land manager. Fire activity data is processed through combustion models that calculate emissions inventories for the burns (the Emissions Calculation box). The outputs are hourly productions of heat and the masses of gases and particulate compounds—fire products. The sparse matrix operator kernel emissions modeling system (SMOKE) (Houyoux et al., 2002) processes emission data and provides initial and boundary chemical conditions for the community multiscale air quality (CMAQ) model (Byun and Ching, 1999) for chemical modeling (fourth box). Then a visualization for illustrating modeling results is the last step. The NCAR/Penn State mesoscale model (MM5) (Grell et al., 1994) is used for providing meteorological conditions for emission calculation and SMOKE and CMAQ simulation.

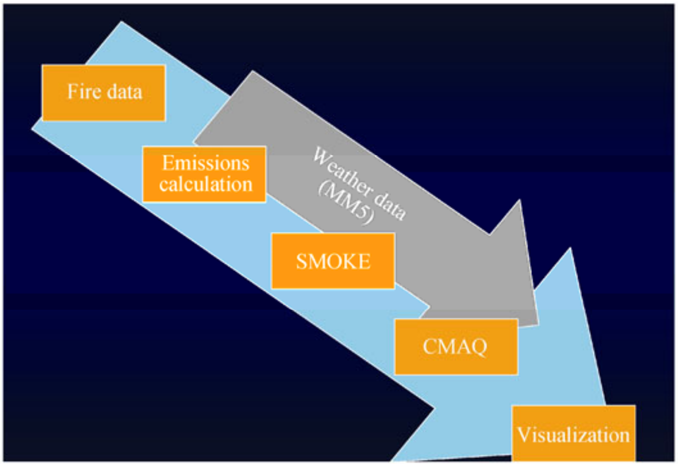

Figure 8.2 An overview of the SHRMC-4S framework

Several modifications were made to SMOKE for prescribed burning applications (Liu et al., 2006a). Area and point sources are among the various emission categories in SMOKE. Area source emissions are annual amounts (or converted to daily averages) from counties, and are put only at the lowest model level, whereas point source emissions are emitted daily or hourly amounts from certain locations like power plants, and are partitioned to multiple levels. Fires have been traditionally regarded as an area source, but they are more likely a point source because they occur as individual events geographically with hourly and daily variability, and smoke may be partitioned through a depth of a few kilometers. To include fire emissions as a point source in SHRMC-4S, fire emission files for SMOKE were created. A fire is identified through its latitude and longitude in an emission file in the inventory data analyzer (IDA) format. All fire properties (height, diameter, exit temperature, exit velocity, and flow rate) are included in this file. Day- or hour-specific emissions of various chemical species are stored in separate files in the emissions modeling system'95 (EMS-95) format.

The other modification was to link daysmoke to SMOKE as an addition to the laypoint algorithm for estimating plume rise and specification of plume vertical profiles. The fourth component of daysmoke, the relative emissions production model, counts particles passing a "wall" three miles downwind from a burn for each hour during the burn period. A percent of particle number at each layer at each hour relative to the total particle number is assigned to SMOKE/CMAQ simulations.

Prescribed fire data is obtained from the existing systems or those to be developed. The portion of this total fuel load consumed by the fire is determined using the single parameter regression equations of CONSUME 3.0 (Ottmar et al., 1993). Fire emissions are calculated by multiplying the consumed fuel by an emission factor appropriate for the fuel type and ignition plan (Mobley et al., 1976). These total emission values are transformed into hourly values using equations provided in Sandberg and Peterson (1984).

8.5 Application

Daysmoke and SHRMC-4S have been used for simulating smoke movements and the air quality impacts of a number of prescribed burns in the South. Simulations with the two modeling tools of a burn case at the Tennessee /North Carolina border on March 18, 2006 have been conducted (Achtemeier et al., 2006; Liu et al., 2006b). They are briefly illustrated here.

8.5.1 Burn

The Cherokee national forest conducted the Brush Creek prescribed burn on 743 ha of woodland near the Tennessee/North Carolina State line (upper left hand corner of Fig. 8.3) approximately 50 km northwest of Asheville, NC on 18 March 2006. Approximately 670 ha or 90% of the land area was expected to be burned. The site had never had a prescribed fire nor had a wildfire occurred recently. The district staff estimated 26.9 metric tons of fuel would be consumed for each hectare burned. Aerial ignition at Brush Creek began along the main and spur ridges between 1,220 and 1,400 EST then further ignition was done between 1,620 and 1,710 EST. During the active burning phase, fire would have spread down the side slopes until no fuels were available to ignite. Hourly estimates of area consumed were used by the REM to model the history of the burn.

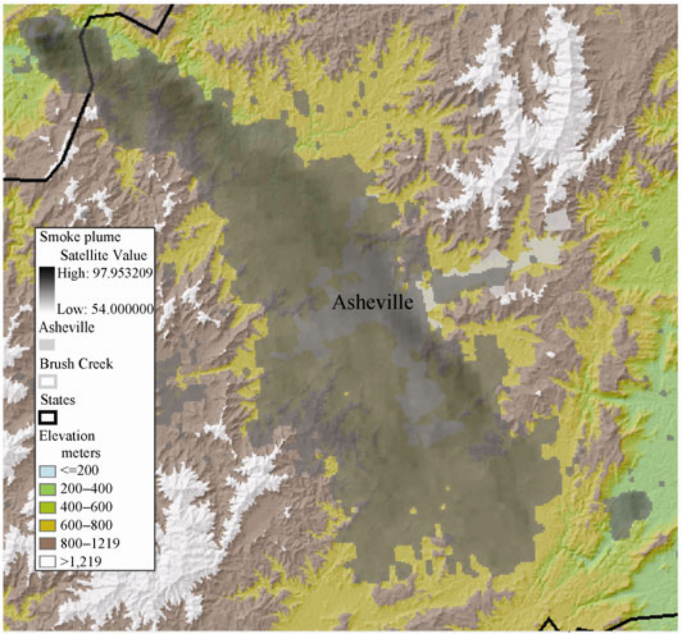

Figure 8.3 Smoke plume image processed from the Polar satellite (received from National Oceanic and Atmospheric Administration) showing the cloud of smoke from the Brush Creek prescribed fire at 1,715 EST (Provided by William A. Jackson, Air Resource Specialist, Cherokee National Forest)

The leading edge of the smoke plume from the Brush Creek burn passed Asheville, NC, between 1,515 and 1,530 EST. Shortly after 1,600, elevated fine PM concentrations were measured at a particulate monitor in Asheville operated by the Western North Carolina Regional Air Quality Agency (Fig. 8.4). Concentrations of $PM_{2.5}$ rose from near zero to 106 $\mu g \cdot m^{-3}$ at 1,700 EST and to 130 $\mu g \cdot m^{-3}$ by 1,800 EST. These PM levels could cause some people who are sensitive to air pollutants to experience short-term health problems. The concentrations fell back to 30 $\mu g \cdot m^{-3}$ by 2,100 EST.

8.5.2 Daysmoke Simulation

Even though the smoke plume shown in Fig. 8.3 is a simple plume, with the implication of a simple plume updraft, the plume structures can be complex. Many smoke plumes are supported by multiple-core updrafts—subplumes rising from the flaming areas and merging into a single plume. Daysmoke allows for the simulation of multiple-core updraft plumes.

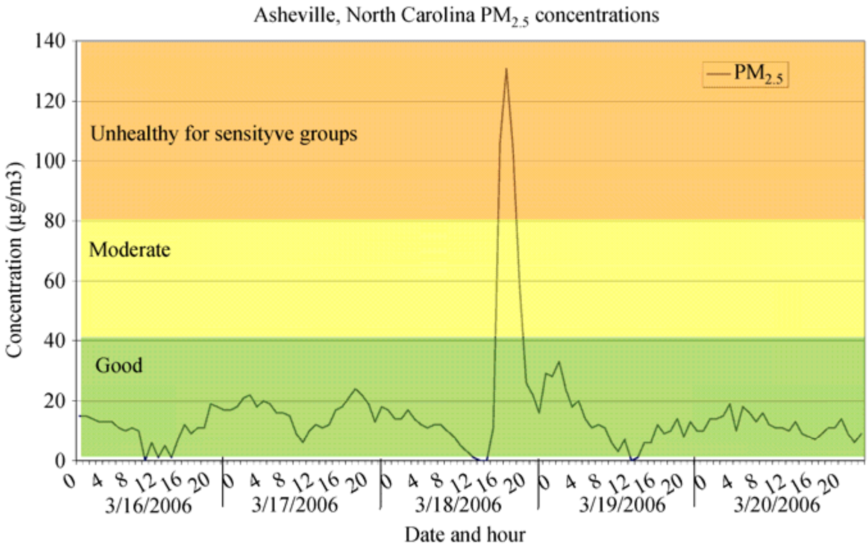

Figure 8.4 Fine PM concentrations (μg·m^{-3}) measured at the Buncombe County Board of Education monitoring site in Asheville, North Carolina between March 16 and March 20, 2006 (Provided by William A. Jackson, Air Resource Specialist, Cherokee National Forest)

Figure 8.5 shows the hourly $PM_{2.5}$ concentration at Asheville as calculated by daysmoke. Each line represents a ten-simulation average. Maximum hourly concentrations range from 42 μg·m^{-3} for a one-core plume updraft to 244 μg·m^{-3} for a ten-core plume updraft.

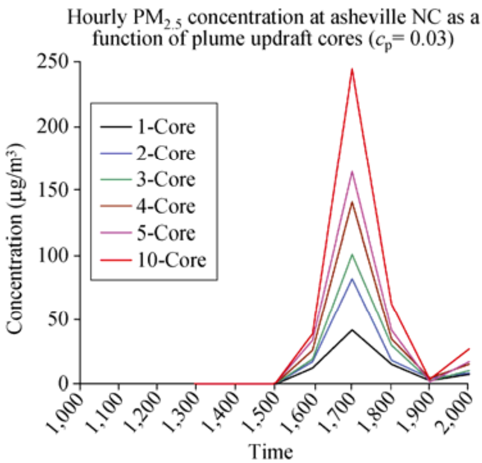

Figure 8.5 Hourly $PM_{2.5}$ smoke concentrations for Asheville, NC, for six multiple-core updraft simulations by daysmoke. (from Achtemeier et al., 2006)

Daysmoke is a combined dynamic-stochastic model. Stochastic terms control small scale turbulence within the plume and within the ambient atmosphere. The large eddy parameterization model is linked to clock-time so that large eddy magnitudes and distributions will be different each time daysmoke is executed (averages of ten simulations for each updraft core were used to calculate the concentrations shown in Fig. 8.5). Therefore, individual simulations by daysmoke vary according to the stochastic terms. The average peak concentration for the one-core updraft is 42 $\mu g \cdot m^{-3}$ but varies between 30 – 60 $\mu g \cdot m^{-3}$. The ensemble average for the 10-core updraft is 244 $\mu g \cdot m^{-3}$ with a range between 211 – 279 $\mu g \cdot m^{-3}$.

Figure 8.6 compares the means and distributions of daysmoke-predicted ground-level $PM_{2.5}$ concentrations at 1,700 hours as a function of the number of updraft cores in a prescribed burn plume. $PM_{2.5}$ concentrations from the 1-core solutions were all under-predictions of observed levels at Asheville (130 $\mu g \cdot m^{-3}$—dashed line). Furthermore, concentrations from the 10-core solutions were all over-predictions of observed levels. Although the mean of the 4-core solution (141 $\mu g \cdot m^{-3}$) was closest to the Asheville observation, some results from the 3-core and 5-core solutions also bracketed the 130 $\mu g \cdot m^{-3}$ concentration.

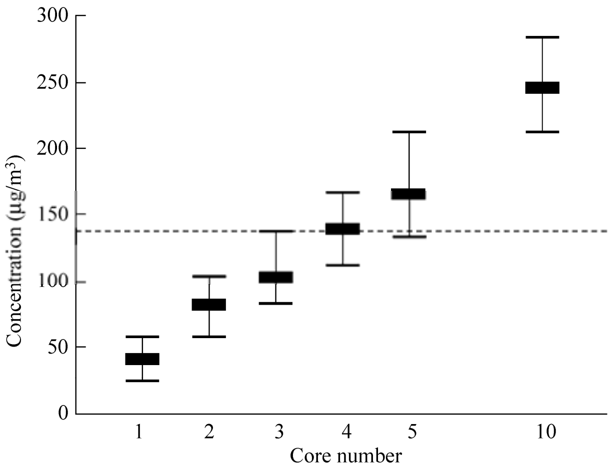

Figure 8.6 The means and distributions for each updraft core number compared with the maximum hourly $PM_{2.5}$ concentration (dashed line) observed at Asheville, NC (from Achtemeier et al., 2006)

8.5.3 CMAQ Simulation

The model domain is configured with a 40×30 horizontal grid with 21 vertical layers. The horizontal resolution is 12 km. This resolution is too low to accurately simulate smoke concentration from a single burn with a size of approximately

1 km. The emission intensity for the grid box that includes the burn site is about two-orders of magnitude smaller than that at the burn site. This simulation provides an example of application of daysmoke in CMAQ. The Carbon Bond-Ⅳ (CB-Ⅳ) chemical mechanism is used to simulate gas-phase chemistry in CMAQ. Daysmoke is used to estimate plume rise and vertical distribution.

Figure 8.7 shows the height of smoke plume (plume rise) and vertical profile of the smoke particle simulated with Daysmoke for 1-core and 10-core updrafts. For the 1-core updraft (Fig. 8.7(a)), plume rise is about 1.5 km from 1,200 to 1,600 LST and increases to 2.1 km at 1,700. For the 10-core updraft (Fig. 8.7(b)), plume rise is about 0.75 km at 1,200 LST with the largest percentage occurring at about 0.6 km. Plume rise gradually increases to 1.1 km at next hour and remains there until 1,700. It reduces to 0.92 km at 1,800. These results indicate two differences between 1- and 10-core updrafts. First, plume rise is usually smaller for multiple-core. Thus, more smoke particles are distributed at lower levels in the atmosphere. Second, plume rise simulations for 1-core updrafts place most smoke high above the PBL, while simulations for 10-core updrafts place smoke close to or slightly higher than the PBL. This results in significant impacts on the ground concentrations when daysmoke smoke profiles are linked to CMAQ.

Figure 8.8 shows the geographic distribution of ground-level $PM_{2.5}$ at 1,700, when largest concentrations were observed at Asheville. The smoke plume spreads from the burn site south-southeastward to the North Carolina-South Carolina border. The transport track is close to what shows in the satellite image (Fig. 8.3) but with too much lateral spread. For both simulations, the magnitudes of concentrations are too small in comparison with the measurements at Asheville. The underprediction by CMAQ is primarily due to the 12 km resolution of the model domain which causes a laterally wider spread of the plume. In comparison, the magnitudes of the concentrations for the 10-core updraft are about 2 – 3 times of that for the 1-core updraft.

Figure 8.9 shows time-height cross sections of $PM_{2.5}$ concentrations over Asheville as simulated by daysmoke/CMAQ. The plume reaches Asheville after 1,500. Both simulations show two peaks in concentrations (an outcome of a 1-hour lapse in aerial ignition) the first arriving at 1,600 and the second arriving at 1,800. This result compares with the PM measurements at Asheville which show a general peak between 1,700 and 1,900. The main difference between the 1- and 10-core updraft simulations is in the vertical distributions of smoke. Large concentrations are found between 1.1 km and 1.5 km above ground for 1-core updraft, and within about 1 km above ground for 10-core updraft. The one-core simulation placed most smoke far enough above the PBL that few particles were transported to the ground (Fig. 8.9(a)). As Fig. 8.9(b) shows, most particles are found within the PBL for the 10-core updraft simulation and these are nearly uniformly distributed from the ground to the top of PBL by strong turbulent mixing.

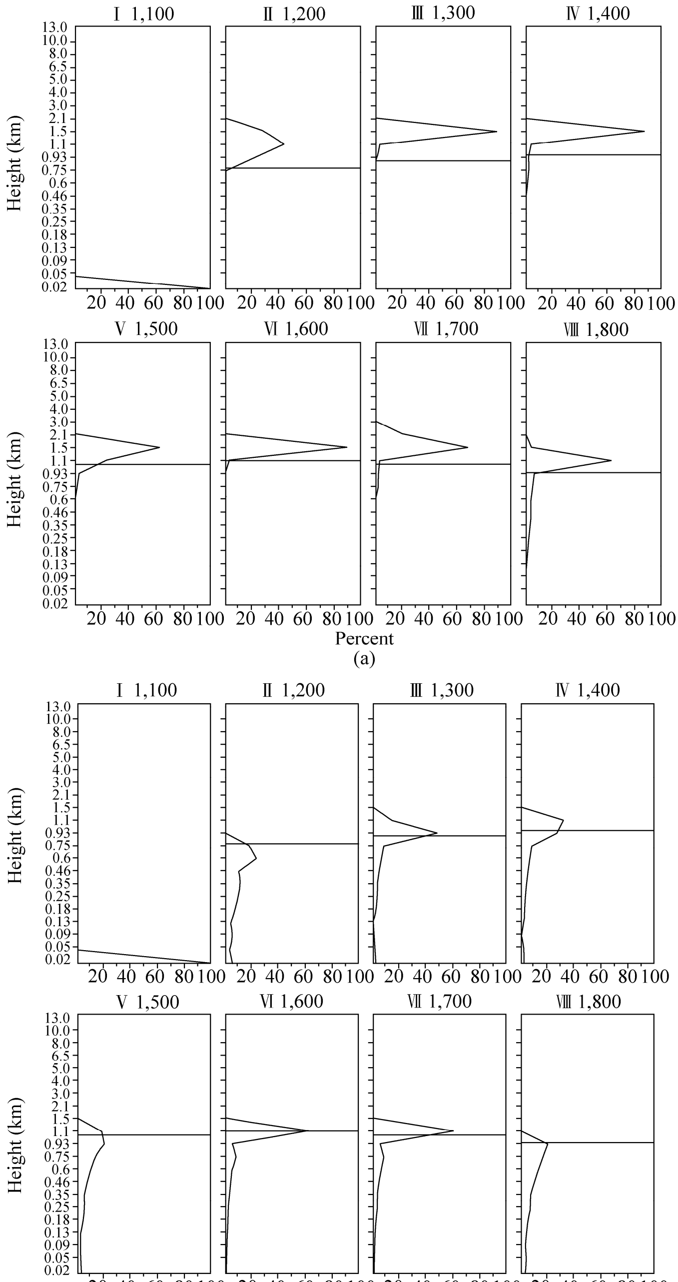

Figure 8.7 The vertical distribution of smoke particles (in %) at the hours from 1,100 throughout 1,800 LST calculated using Daysmoke. The light horizontal lines indicate the top of planetary boundary layer. (a) one-core updraft. (b) 10-core updraft. (from Liu et al., 2006b). The light horizontal lines indicate the top of planetary boundary layer

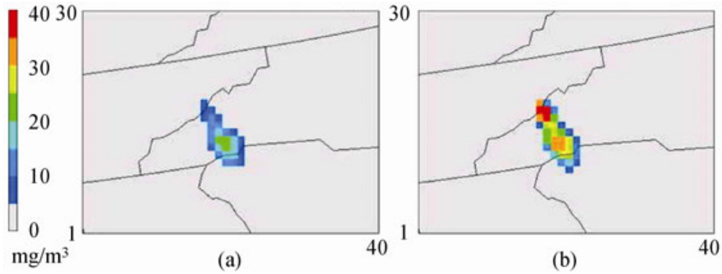

Figure 8.8 Spatial distribution of ground $PM_{2.5}$ concentration ($\mu g \cdot m^{-3}$) at 1,700 LST simulated with CMAQ using plume rise and smoke particle vertical profile specified with daysmoke. (a) one-core updraft. (b) 10-core updraft (from Liu et al., 2006b)

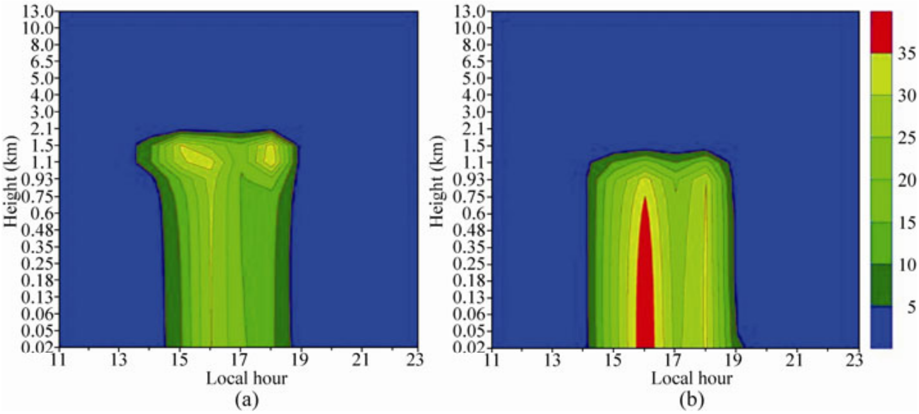

Figure 8.9 Time-height across section of $PM_{2.5}$ concentration ($\mu g\ m^{-3}$) at Asheville simulated with CMAQ with plume rise and smoke particle vertical profile specified with daysmoke. (a) one-core updraft. (b) 10-core updraft (from Liu et al., 2006b)

8.6 Summary and Discussion

Two tools for smoke transport and the regional air quality modeling of prescribed burns, daysmoke and SHRMC-4S, have been described. Their applications have been illustrated by a recent burn case in a National Forest. The daysmoke plume model incorporates a human factor—how burns are engineered by land managers through burning techniques/ignition methods—in modeling smoke from prescribed burns. Therefore daysmoke may provide land managers with a tool that will assist in achieving their burn programs. SHRMC-4S is a framework for smoke and air quality research focused on prescribed fires in the South. daysmoke has been linked as an alternative to the layer fraction method in SMOKE/CMAQ for smoke plume rise calculation and vertical profile specification.

Simulations of a prescribed burn at the Tennessee /North Carolina border on March 18, 2006 indicate that daysmoke and SHRMC-4S are useful modeling tools for understanding smoke transport and the impacts on local and regional air quality. Daysmoke produces a ground PM level that could cause some people who are sensitive to air pollutants to experience short-term health problems. The simulated magnitude is close to the measured one. Daysmoke simulation and the resultant plume rise are dependent on the number of updraft cores. This property has an important impact on CMAQ simulations. The simulated ground PM level with CMAQ is larger for multiple-core updraft than single-core updraft.

Although some measurements were used for the development and validation of daysmoke, more measurements are needed for further validation of this model and comparison with other plume rise schemes. Furthermore, more complete prescribed fire information is needed for improving the performance of SHRMC-4S. Model performance is dependent on accurate specification of burn and other properties such as the number of updraft cores. In addition, the application case of daysmoke to CMAQ simulate presented here was run off-line. The two models need to be coupled to each other to make daysmoke a more practically useful tool for CMAQ simulation.

Daysmoke has shown us that the dynamics of smoke plumes from prescribed burns are complex, often far more complex than dynamics of plumes from industrial stacks. Application of smoke models designed for industrial stacks should not be expected to yield accurate results for smoke plumes from prescribed burns unless the multiple-core updraft issue is taken into consideration.

Acknowledgements

Cherokee national forest personnel associated with the Brush Creek prescribed burn are acknowledged for providing reports and photo images of the burn. The project was conducted as part of the Southern regional models for predicting smoke movement project (01.SRS.A.5) and the prediction of fire weather and smoke impacts in the Southeast project (01.SRS.A.1) funded by the USDA forest service national fire plan (NFP). Funding was also provided through the national research initiative air quality program of the cooperative State research, education, and extension service, U.S. Department of agriculture, under agreement No. 2004-05240.

References

Achtemeier GL, (1998), Predicting dispersion and deposition of ash from burning cane. *Sugar Cane* **1**: 17 – 22

Achtemeier G, Goodrick S, Liu Y-Q, (2003), The Southern High Resolution Modeling Consortium-A source for research and operational collaboration. Proceedings of the 2nd

Int'l Wildland Fire Ecology and Fire Management Congress. Amer. Meteor. Soc. Nov. 16 – 20, 2003, Orlando, FA

Achtemeier G, Goodrick S, Liu Y-Q, Jackson WA, (2006), the Daysmoke plume model for prescribed burns: Model description and application to a multiple-core updraft prescribed burn, *Int'l J. Wildland Fire* (submitted)

Brenner J, Goodrick SL, (2005), Florida's Fire Management Information System. Proceedings of EastFire Conference, Fairfax, VA. May 2005

Byun, DW, Ching J, (1999), Science algorithms of the EPA Model-3 community multiscale air quality (CMAQ) modeling system, Research Triangle Park (NC): EPA/600/R-99/030, National Exposure Research Laboratory

Draxler RR, Hess GD, (1997), Description of the Hysplit_4 modeling system, NOAA Technical Memorandum ERL ARL-224, December, 24

EPA, (1998), Interim Air Quality Policy on Wildland and Prescribed Fire, Office of Air Quality Planning and Standards, Research Triangle Park, NC, USA

EPA, (2003), National Ambient Air Quality Standards (NAAQS), Research Triangle Park, NC, USA (http://www.epa.gov/airs/criteria.html)

Goodrick S, Brenner J, (1999), Florida's Fire management information system. Proceedings of The Joint Fire Science Conference and Workshop, June 15 – 17, 1999 Boise ID. Vol. **1**: 3 – 12

Grell AG, Dudhia J, Stauffer DR, (1994), A Description of the Fifth-Generation Penn State/NCAR mesoscale Model (MM5), NCAR Tech. Note, 398, Boulder, CO, USA, 122

Houyoux M, Vukovich J, Seppanen C, Brandmeyer JE, (2002), SMOKE User Manual, MCNC Environmental Modeling Center

Lavdas LG, (1986), An atmospheric dispersion index for prescribed burning. Research Paper SE-256. Ashville, NC USDA Forest Service Experiment Station. 33

Lavdas LG, (1996), Program VSMOKE–users manual. USDA Forest Service General Technical Report SRS-6. 147

Liu Y-Q, Achtemeier G, Goodrick S, (2004), Air quality effects of prescribed fires simulated with CMAQ, the 2004 CMAQ Workshop, Chapel Hill, NC

Liu YQ, Achtemeier G, Goodrick S, (2006a), Modeling air quality effects of Florida prescribed burning with CMAQ-Daysmoke, *Environ. Pollution* (submitted)

Liu YQ, Achtemeier G, Goodrick S, Jackson WA, (2006b), regional air quality effects of Brush Creek burning simulated with CMAQ-Daysmoke. The Third International Fire Ecology and Management Congress, San Diego, California, USA, 13 – 17 November 2006

Mobley HE, Barden CR, Crow AB, Fender DE, Jay DM, Winkworth RC, (1976), Southern Forestry Smoke Management Guidebook. USDA Forest Service General Technical Report SE-10. Southeastern Forest Experiment Station, Asheville, NC

Ottmar RD, Burns MF, Hall JN, Hanson AD, (1993), CONSUME users guide. USDA Forest Service General Technical Report PNW-GTR-304. Pacific Northwest Research Station, Portland, OR

O'Neill SM, Ferguson SA, Peterson J, Wilson R, (2003), The BlueSky Smoke Modeling Framework. Proceedings of the 5th Symposium on Fire and Forest Meteorology, American Meteorological Society, Orlando, FL, November 2003

Pouliot G, et al., (2005), Wildfire Emission Modeling: Integrating BlueSky and SMOKE. 14th

International. Emission Inventory Conf. “Transforming Emission Inventories Meeting Future Challenges Today”, Las Vegas NV

Prins EM, and Menzel WP, (1990), Geostationary satellite detection of biomass burning in South America, *Int. J. Rem. Sens*. **13**: 2783 – 2799

Riebau AR, Fox D, (2001), The new smoke management. *Int'l J. Wildland Fire,* **10**: 415 – 427

Sandberg DV, Hardy CC, Ottmarn RD, Snell JAK, Acheson A, Peterson JL, Seamon P, Lahm P, Wade D, (1999), National strategy plan: Modeling and data systems for wildland fire and air quality. US Forest Service, PNRS, 60

SRFRR, (1996), Southern Region Forest Research Report, 7th American Forest Congress Feb. 1996

Stanturf JA, et al., (2002), Background paper : Fires in southern forest landscapes, in The Southern Forest Resource Assessment, USDA Forest Service, SRS

Wade DD, Brock BL, Brose PH, et al., (2000), Fire in eastern ecosystems. In: Brown JK, Smith, JK (eds) Wildland Fire in Ecosystems: Effects of Fire on Flora. Gen. Tech. Rep. RMRS-42. Ogden, UT: US. Department of Agriculture, Forest Service, Rocky Mountain Research Station: 53 – 96. Chapter 4. Vol. 2.

Ward DE, Hardy CC, (1991), Smoke emissions from wildland fires, *Environ. Int.,* **17**: 117 – 134

Zheng M, Cass GR, Schauer JJ, Edgerton ES, (2002), Source Apportionment of $PM_{2.5}$ in the Southeastern United States Using Solvent-Extractable Organic Compounds as Tracers. *Environ. Sci. Technol.,* **36**: 2361 – 2371

9 Estimates of Wildland Fire Emissions

Yongqiang Liu
Center for Forest Disturbance Science, USDA Forest Service
320 Green St., Athens, GA 30602, USA
Email: yliu@fs.fed.us

John J. Qu, Wanting Wang and Xianjun Hao
Environmental Science and Technology Center, Department of Geography and Geoinformation Science, College of Science, George Mason University,
Fairfax, VA 22030, USA
Email: jqu@gmu.edu, wwang@gmu.edu, xhao1@gmu.edu

Abstract Wildland fire missions can significantly affect regional and global air quality, radiation, climate, and the carbon cycle. A fundamental and yet challenging prerequisite to understanding the environmental effects is to accurately estimate fire emissions. This chapter describes and analyzes fire emission calculations. Various techniques (field measurements, empirical relations, modeling, and remote sensing) to obtain fuel and fire properties are first reviewed. A calculation of fire emissions across the continental U.S. is then illustrated. In this calculation, an approach recently developed based on high-resolution fuel types from satellite remote sensing is used for fuel loading factors. The burning information is obtained from a historical fire dataset collected by multiple U.S. governmental agencies. The U.S. fire emissions show large spatial and temporal variability. Finally, uncertainties in fire emission estimates are examined by comparing with another method using the traditional AP-42 Table approach for fuel loading. Emissions with the satellite remote sensing approach are mostly reduced in the western U.S., but increased in the eastern coastal regions. A perspective on future fire emission research is given.

Keywords Wildland fire, emission calculation, emission factors, fuel loading, U.S. fire emission results and analyses

9.1 Introduction

Wildlfire is one of the major natural disasters in the United States that threaten human life and property. Millions of acres of forest and other ecosystems are burned annually. In 2000, for example, more than 100 thousand fires consumed 8.4 million acres (3.4 million ha) (NIFC, 2002). Nearly 30 thousand people were involved in wildland firefighting efforts, costing the federal agency fire suppression about $1.4 billion. Prescribed burning, on the other hand, is a forest management technique that temporarily reduces damage from wildfire by removing a portion of the accumulating dead fuels (such as duff and logs on the forest floor) and reducing the stature of the developing understory when burning conditions are not severe (Wade and Outcalt, 1999). These intentional fires also serve as a surrogate for the historical fires by recycling nutrients and restoring/sustaining ecosystem health. The areas burned by prescribed fires have the same order as those by wildfires (Stanturf et al., 2002).

Emissions from wildland fires can cause severe environmental consequences. Fires release large amount of particulate matter (PM) and ozone precursors, adversely affecting regional air quality (Sandberg et al., 1999; Riebau and Fox, 2001). PM and ozone, as well as some other trace gas emissions, are criteria air pollutants subject to the national ambient air quality standards (NAAQS) established by the U.S. Environmental Protection Agency (EPA, 2003a). EPA recently established air quality standards for $PM_{2.5}$ (PM with a diameter of 2.5 μm or smaller) and revised standards for ground-level O_3 and PM_{10} (PM with a diameter of 10 μm or smaller) as an effort to reduce regional haze and smog and to improve visibility. EPA also issued the interim air quality policy on wildland and prescribed fire (EPA, 1998) to protect public health and welfare by mitigating the impacts of air pollutant emissions from wildland fires on air quality.

Smoke particles are one of the atmospheric aerosol sources, which can affect global and regional radiation (e.g., Penner et al., 1992). They can modify earth radiation balance by scattering and absorbing solar radiation (direct radiative forcing) (Charlson et al., 1992), and by changing droplet size and life time of clouds, which are one of the most important factors for atmospheric radiative transfers (indirect radiative forcing) (Twomey et al., 1984). The radiative forcing can further change regional climate, monsoon, and drought (Hansen et al., 1997; Ackerman et al., 2000; Menon et al., 2002; Koren et al., 2004; Liu, 2005a and b).

Fires also affect the carbon cycles. Carbon emissions due to fire increase atmospheric CO_2 concentration. The perturbation of atmospheric chemistry induced by biomass burning is comparable in magnitude to the effect of fossil fuel burning (Lindesay et al., 1996). The 1997 Indonesia Fires emitted as much carbon into the atmosphere as Europe's annual carbon emissions from burning fossil fuel (Page et al., 2002). Thus, biomass burning is an important source for regional atmospheric carbon. On the other hand, fires affect the ecosystem uptake of atmospheric carbon. Biomass accumulates by consuming atmospheric carbon through photosynthetic reaction. The terrestrial ecosystem, therefore, acts as a sink of atmospheric carbon during this process. Fire disturbance will alter the magnitude of this sink.

A fundamental and yet challenging prerequisite to understanding the environmental effects of smoke is to accurately estimate fire emissions. Fire emissions can be calculated using fire and fuel properties such as area burned, fuel loading or consumption factors, and emission factors. Various techniques for calculating these properties have been developed. This Chapter describes calculation and analysis of fire emissions. Fire emission calculation formula and techniques for obtaining fuel and fire properties are reviewed in Section 9.2. A calculation of fire emission in the continental U.S. is presented in Section 9.3. Uncertainty in fire emission estimates is discussed in Section 9.4. Summary and a perspective on future fire emission research are given in Section 9.5.

9.2 Fire Emission Calculation

As indicated in the following formula (Seiler and Crutzen, 1980),

$$E = A\, f\, L\, S \tag{9.1}$$

fire emission E (in mass) is determined by four fuel and fire properties: area burned A, consumption efficiency f (fraction of fuel consumed), fuel loading L (mass of forest fuel per unit area), and emission factor S (mass of the species per unit mass of forest fuel consumed). The product of f and L is also called effective fuel consumption or fuel loading factor (mass of forest fuel per unit area burned). These properties can be obtained using the techniques briefly described below.

9.2.1 Measurements

Burned area has been traditionally obtained from ground measurement and reporting systems. There are a number of regional and national datasets available, in the format of either individual burnings or total burnings of a county or state. The examples are the nation-wide prescribed fires in 1989 (Peterson and Ward, 1993; Ward et al., 1993), wildfires over 11 Western states (Hardy et al., 1998), the data used for developing the EPA the national emission inventory (NEI) for three base years of 1996, 1999, and 2002 (EPA, 2003a), and the federal fire historic dataset (BLM, 2003). The dataset developed by the department of interior bureau of land management (BLM) collects individual fires over the lands owned by five U.S. federal agencies (BLM, Bureau of Indian Affairs, Fish and Wildlife Service, National Park Service, and USDA Forest Service). Besides area burned, this dataset also includes fire information on number, date, location, type, and causes. Figure 9.1 shows wildfire burned areas in each of the contiguous U.S. states.

9.2.2 Empirical relations

Empirical relations have been used extensively to obtain fire emission factors and

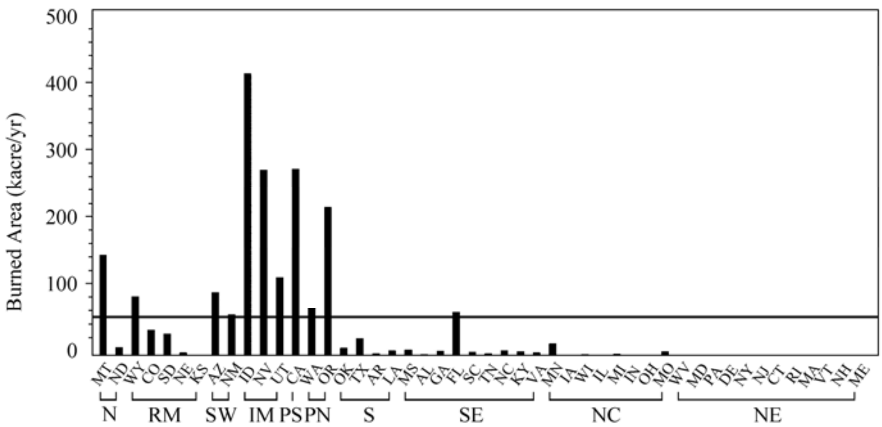

Figure 9.1 Annual burned area by wildfires in the contiguous U.S. states during 1980 – 2002. The horizontal line represents the average over all states. Below the state names are forest service regions (see Fig. 9.2) (redrawn from Fig. 1 in Liu, 2004)

fuel consumption factors. EPA (1995) has formed a table of default values (AP-42 Table) for emission factors of major species. Emission factors in Table 9.1 are adopted from the AP-42 Table for all species except CO_2, which is derived based on the flaming fire emission factor (Battye and Battye, 2002, Table 39) and Hao et al. (2002). The emission factors are geographically independent. Fuel loading factors for the USDA forest service regions (Fig. 9.2) from the AP-42 Table are listed in Table 9.2.

Table 9.1 Emission factor (lbs/ton)

Component	$PM_{2.5}$	PM_{10}	CO	SO_2	NO_x	VOC	CO_2
Factor	11.7	13.0	140.0	0.15	4.0	19.2	3,500.0

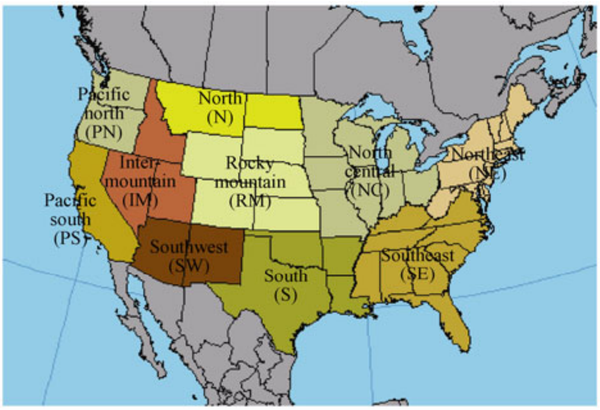

Figure 9.2 The USDA forest service regions (old division)

An effort was recently made to improve the traditionally used AP-42 fuel loading factors. The Western regional air partnership (WRAP, 2002) developed an approach to estimate fuel loading and consumption using the national fire danger rating system (NFDRS) (Cohen and Deeming, 1985) vegetation types for the WRAP states. This approach was extended by EPA (2003b) to the reminder of the contiguous U.S. using the 1999 NFDRS fuel classification map at 1 km resolution derived from a combination of satellite and ground data (Burgen et al., 1998). The state accumulated values from the RS approach are also listed in Table 9.2.

Table 9.2 Fuel loading factor *L* (ton/acre)

Remote sensing approach		**AP-42**		**Remote sensing approach**		**AP-42**	
State	*L*	Region*	*L*	State	*L*	Region	*L*
MT	4.7	N	60	TN	4.3		
ND	0.5			NC	9.6		
WY	5.0	RM	30	KY	3.3		
CO	12.6			VA	7.7		
SD	1.3			MN	13.6	NC	11
NE	1.1			IA	2.8		
KS	1.0			WI	7.4		
AZ	17.7	SW	10	IL	3.1		
NM	14.1			MI	10.1		
ID	8.1	IM	8	IN	2.4		
NV	3.0			OH	3.0		
UT	9.6			MO	2.7		
CA	15.5	PS	18	WV	4.8	NE	11
WA	2.6	PN	60	MD	5.4		
OR	12.5			PA	3.3		
OK	2.7	S	9	DE	7.7		
TX	3.5			NY	20.3		
AR	10.1			NJ	11.6		
LA	9.1			CT	3.1		
MS	9.7	SE	9	RI	3.1		
AL	10.1			MA	24.0		
GA	13.2			VT	51.3		
FL	19.7			NH	33.4		
SC	9.6			ME	27.8		

* See Fig. 9.2 for various regions

9.2.3 Modeling

Numerous fuel models have been developed. Fuel types in NFDRS are represented by 20 fuel models, each of which falls into one of four groups that account for fuels composed mainly of grass, shrub, timber, or slash. In consume, a comprehensive fuel model (Ottmar et al., 1993), separate algorithms are used to calculate consumption of different fuels based on fuel loading, slope, wind, and fuel moisture. In the FCCS (Sandberg et al., 2001), live and dead fuel loadings for 16 types of fuels across 6 layers, from canopy to duff, for 150 fuelbed types defined for the continental U.S. are quantified. The system calculates available fuel potential index between 0 – 9 for each FCCS National or customized fuelbed and provides available consumption of fuels. The fire emissions production simulator (FEPS) is developed to calculate fuel consumption efficiency (PNW, 2005). The FEPS model is run for each of the NFDRS fuel models and for each of the six fuel moisture classes in the model. For each of these combinations the model is used to estimate a unique fuel consumption.

Fire emissions can be simulated using modeling tools such as emission production model (EPM) (Sandberg et al., 1984), first order fire effects model (FOFEM) (Reinhardt et al., 1997), and community smoke emissions modeling (CSEM) (Barna and Fox, 2003). In the recently upgraded version of EPM, FEPS (Anderson et al., 2004), fuel loading, fuel moisture, meteorological conditions, and other parameters are used to obtain hourly fire emissions as well fuel consumption, heat release and plume rise. CSEM, specifically designed to provide historical fire emission estimates for use in air quality models, uses consume and EPM and national GIS coverage for developing a fire inventory, locations, time and size.

A comprehensive modeling tool, BlueSky (O'Neill et al., 2003), was developed as a framework for fire emission and air quality effect simulation and prediction. Regional forecast of smoke concentrations is made using burn information from state and federal agency burn reporting systems, and meteorology, fuel consumption, emission, and dispersion and trajectory models. The southern high-resolution modeling consortium southern smoke simulation system (SHRMC-4S) (Achtemeier et al., 2003) is similar to bluesky but more specifically for prescribed burning in the south. It uses the sparse matrix operator kernel emissions modeling system (SMOKE) (Houyoux et al., 2002) for processing emission data and providing initial and boundary chemical conditions, and the community multiscale air quality (CMAQ) (Byun and Ching, 1999) model for chemical modeling. A unique feature with SHRMC-4S is that it includes a dynamical model (daysmoke) (Achtemeier, 1998) to calcualte smoke plume rise. Figure 9.3 shows a simulation result of SHRMC-4S.

9.2.4 Remote Sensing

Satellite remote sensing (RS) has emerged as a useful technique for fire detection in the past decade. With the unique features of global coverage, high-resolution,

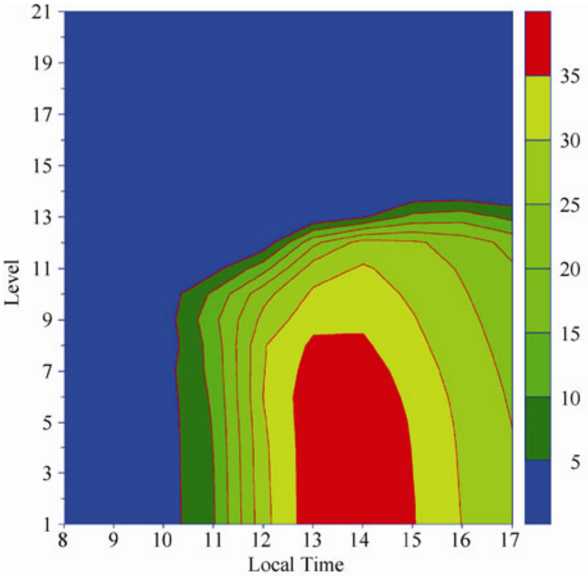

Figure 9.3 Time-height section of $PM_{2.5}$ concentration ($\mu g \cdot m^{-3}$) from prescribed fire emissions in Florida simulated with SHRMC-4S. The horizontal and vertical coordinates represent hour (local time) and height in level (from Liu et al., 2006)

and continuous operation, RS is able to obtain detailed information of fuel type and loading, fire occurrence, extent, structure, and temporal variation (Riebau and Qu, 2004; Qu et al., 2003 and 2005). Satellite instruments such as the advanced very high resolution radiometer (AVHRR) (Kaufman et al., 1990; Justice et al., 1996; Li et al., 1997; Burgan et al., 1998), the geostationary operational environmental satellite (GOES) (Prins and Menzel, 1990), and the moderate resolution imaging spectroradiometer (MODIS) (Kaufman et al., 1998; Justice et al., 2002) have been applied to field experiments and routine monitoring of fuels and wildfires.

AVHRR has daily data over two decades. Algorithms for detecting active fires and mapping burned area (Fraser et al., 2000) have been developed and validated for the fires in North America (Li et al., 2003). With more spectral bands and higher spatial resolution, MODIS measurements can be used to retrieve fire information more accurately (Kaufman et al., 2003). The MODIS rapid response system (MRRS) was recently developed to provide rapid access to MODIS data globally with initial emphasis on 250 m color composite imagery and active fire data. MODIS was found to be able to detect small and cool fires in the South more robustly and accurately (Wang et al., 2005). The Hazard Mapping System (HMS) (NOAA, 2006) was developed to manually integrate data from various automated fire detection algorithms with GOES, AVHRR, MODIS and defense meteorological satellite program/operational linescan system (DMSP/OLS) images. It produces a quality controlled display of the locations of fires and significant smoke plumes detected by meteorological satellites for air quality forecast. Figure 9.4 shows an example of MODIS detection of wildland fires.

Figure 9.4 An example of True-color composite MODIS GeoTiff data (Bands 1, 4 and 3) of the Flathead and Bitterroot Valleys in Montana. Image acquired August 19, 2003 (from Quayle et al., 2003)

In spite of not being a parameter in the formula for fire emissions, fuel moisture is an important property for estimating fuel consumption and fire emissions. Forest fuel consists of live and dead vegetation. Meteorological measurements are traditionally used to estimate fuel moisture. The NFDRS monitors fuel moisture of live vegetation for shrub ecosystem using the normalized difference vegetation index (NDVI) and calculates dead fuel moisture with air temperature, humidity, and cloudiness. The Canadian forest fire danger rating system (CFFDRS) calculates live and dead fuel moisture using various algorithms basically based on meteorological measurements. The limitations with the traditional technique include relatively small spatial resolution of observations, unavailability over part of forest regions, and uncertainties in the relationship between meteorological data and fuel moisture. RS technique has been demonstrated as an efficient means to supplement field measurements for monitoring live fuel moisture, especially in locations not readily accessible by forest rangers. In addition to covering extensive regions, RS also provides values closely related to forest vegetation status such as NDVI and Surface Temperature. Thus, RS data can be directly used to estimate fuel moisture (Chuvieco et al., 1999).

9.3 U.S. Fire Emissions

9.3.1 Parameter Specifications

This section describes a calculation of the U.S. fire emissions. The BLM fire dataset (BLM, 2003) is used. The data used are monthly total acres burned by wildfires for each of the 48 contiguous states during 1980 – 2002. The areas burned by wildfires were about 41,000 acres per year averaged over the contiguous U.S. states (Fig. 9.1). Large emissions occurred in the Western states. Idaho, California, Nevada, Oregon, Montana and Utah had burning areas over hundreds of thousands of acres. Florida was the only state in the East with the emission reaching the national average. A detailed description of the fire statistics is given in Liu (2004). Emission factors are adopted from Table 9.1. Fuel loading factors are adopted from the values for RS approach in Table 9.2.

9.3.2 Spatial Distribution

Figure 9.5 shows geographic distribution of $PM_{2.5}$ emissions from wildfires expressed as emission intensity (kg·km^{-2}). Large emissions are found in the West.

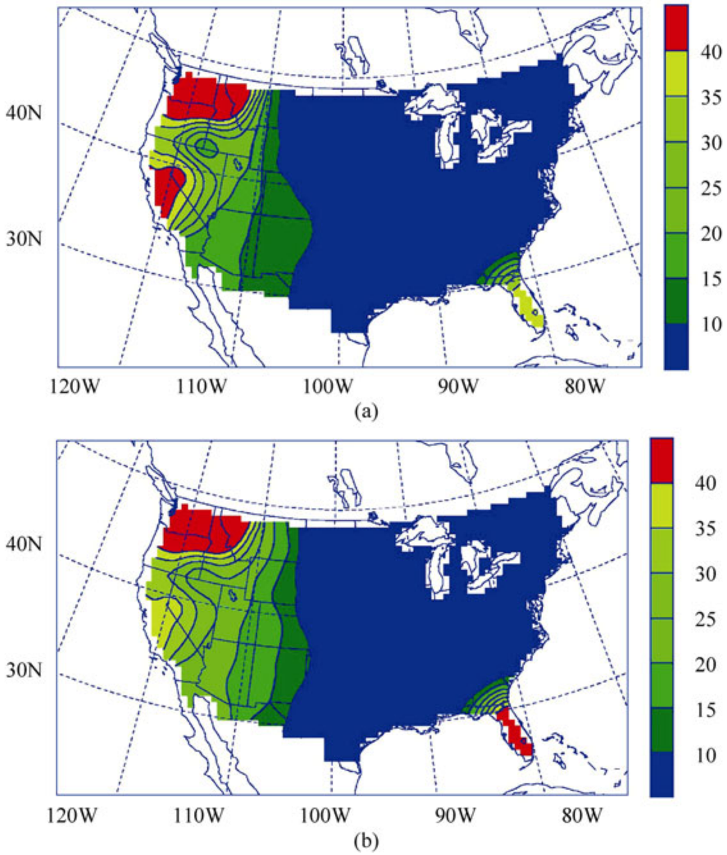

Figure 9.5 Spatial distribution of annual wildfire emissions of $PM_{2.5}$ (kg·km^{-2}) (a) and standard deviation (b)

Two centers with a magnitude of over 40 kg·km^{-2} are located in Pacific South and Pacific North, respectively. Emissions gradually decrease to below 10 kg·km^{-2} east of the Rocky Mountains. Emissions, however, have a center in Florida with a magnitude of about 35 kg·km^{-2}. Emissions decrease rapidly to less than 10 kg·km^{-2} in the surrounding states. Standard deviation of annual emission series has the same magnitude as the average in most states, indicating large inter-annual variability. As shown in Liu (2004), wildfire emissions are characterized by a number of strong emission events and a relatively quiet episode up to a decade long between two strong emission events.

9.3.3 Seasonal Distribution

Figure 9.6 shows total annual emissions of $PM_{2.5}$ of each state and each season. In the West, California, Idaho and Oregon have the emissions around 15,000 tons, a majority of which is during summer. In the East, Florida has the emissions over 5,000 tons. Different from the West, a substantial portion of wildfire emissions in Florida and many other southern states occurs during spring, when the weather is warming up but not very moist yet. The emissions of PM_{10}, VOC and NO_x are roughly comparable to those of $PM_{2.5}$, while the emissions of other components are significantly different. CO and CO_2 are about one and two orders larger, respectively, while SO_2 is about two orders smaller. They reflect the differences in the AP-42 emission factors.

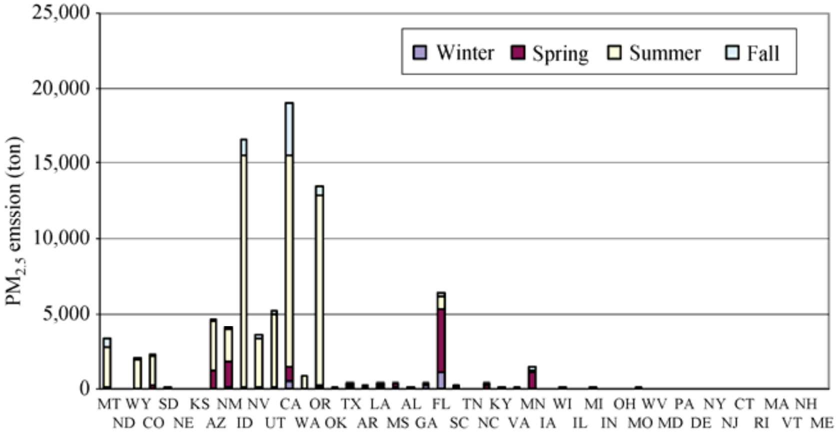

Figure 9.6 Wildfire emissions of $PM_{2.5}$ by state and season

9.4 Uncertainties

Substantial differences in fire emissions are found between the RS and AP-42 Table approaches for fuel loading factors. In general, wildfire emissions from the

RS approach are smaller in the west and larger in Florida than those from the AP-42 Table approach. A quantitative comparison is shown in Fig. 9.7 using the ratio of the difference in emission between the RS and AP-42 Table approaches to emission from the AP-42 Table approach. Remarkable changes ranging from –100%～450% are obtained. The changes display certain geographic patterns. The RS approach leads to overall reduced emissions in the regions from the Pacific coast to Midwest except Southwest. In contrast, overall increased emissions are found in Southeast and Northeast. The largest increase of 200% or more is found in a number of New England states due to the extremely small

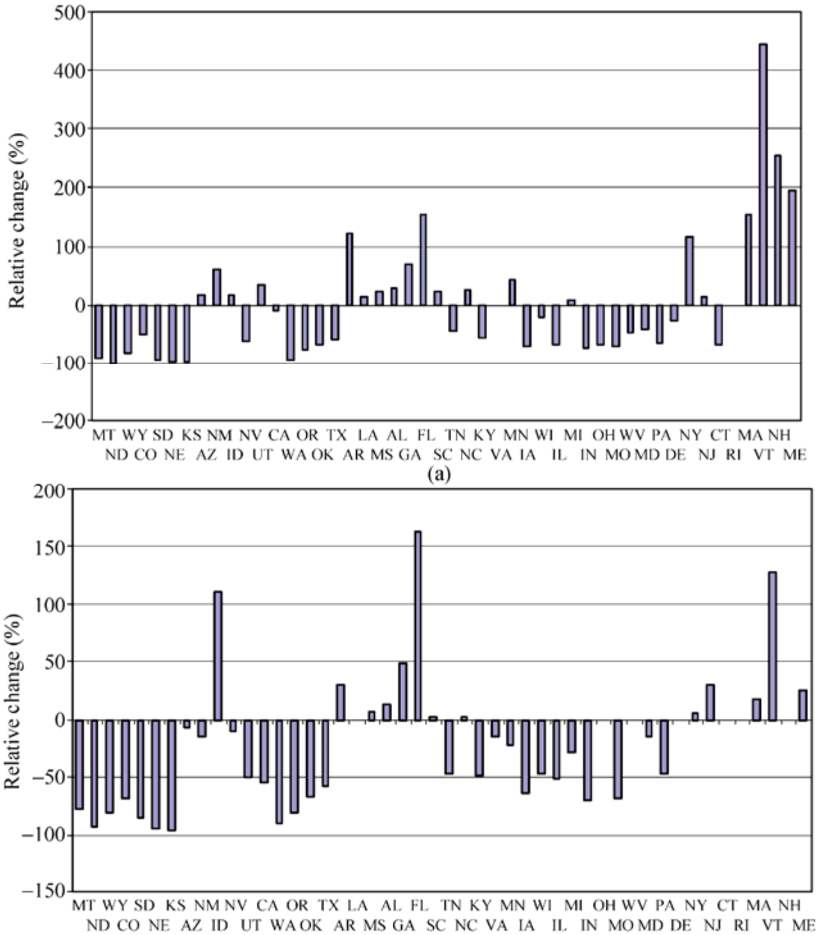

Figure 9.7 Ratio of the difference in fire emissions between RS technique and AP-42 Table to the emission estimated using AP-42 Table for wildfire (a) and prescribed fires (b)

amounts of emission in these states. Among the states with large emissions, the most significant changes happens in Oregon and Florida, where emissions are reduced by about 80% and increased by about 160%, respectively. Changes in California and Idaho are less than 20% in magnitude.

Besides wildfires, fuel loading factors for prescribed burning have also been developed using satellite remote sensed fuel types and loading and consumption of individual fuel types (EPA, 2003b). In Florida, a state with the most extensive prescribed burning in the nation, for example, fuel loading factor is increased from 9 ton/acre in the AP-42 Table to 19.7 ton/acre estimated by the RS approach for wildfire, comparing from 7.1 – 17.2 ton/acre for prescribed burning.

Most fire emission inventories, including fire emissions in the EPA NEIs, have been developed using the AP-42 Table default fuel loading factors. The remarkable changes in the magnitude of fire emissions between this approach and RS approach, including in some states with large fire emissions such as Oregon and Florida, suggest a large uncertainty in estimating fire emissions in these inventories. The result that the fire emissions are reduced in most Westerns states and increased in most Eastern states with RS approach than the AP-42 approach would lead to a reduced geographic contrast between the two regions. Especially, it suggests larger importance of prescribed burning for air quality and other smoke-related environmental issues in the Southeast, which is a major region of such burning.

The changes in fire emission estimates can have some important implications for the environmental effects of wildland fires. A recent modeling study using CMAQ model (Byun and Ching, 1999) with fire emissions estimated using the AP-42 Table fuel loading factors indicated significant impacts of Florida prescribed burning on regional air quality (Liu et al., 2004). The impacts could more serious considering that emissions are about 1.6 times larger if using the RS approach. In addition, a simulation study with a regional climate model indicated the role of wildfires in enhancing drought with emissions estimated using the AP-42 Table fuel loading factors (Liu, 2005b). A better understanding of the role could be achieved by using the RS approach for fuel loading factors.

9.5 Summary and Perspective

Fire emissions are determined by area burned, consumption efficiency, fuel loading, and emission factor. The ground measurement and recording systems have been traditionally used to obtain burned area and fuel loading information. Satellite RS, a new technique developed rapidly in the past decade, is able to provide high-resolution fire and fuel properties. Actual fuel consumption and fire emissions can be determined using modeling and empirical relations.

The U.S. fire emissions estimated using the fuel loading factors recently developed based on satellite RS and ground measurements are found large in Pacific South and Pacific North. A majority of fire emissions occur during summer. In addition, there is an emission center in Florida, which is the largest during spring. There are significant differences in wildfire emissions between the RS and AP-42 Table approaches for fuel loading factors. In general, fire emissions are reduced in the Western U.S. except the Southwest, and increased in the Eastern coastal regions by using the RS approach. The magnitude is up to about 80% in the major Western emission regions and 160 % in the Eastern ones.

It appears that the RS approach is able to detect high resolution properties of fuel type and consumption and therefore is useful for understanding more spatial details of wildfire emissions. The EPA Regional Planning Organizations, for example, has recently decided to re-calculate wildfire emissions in the 2002 NEI using the RS approach (WRAP, 2005).

The following studies in the future are critical to improving our understanding of fire emissions and their environmental effects:

(1) Wildfire data is a key to analyzing fire regimes and the spatial and temporal variability. Continuous efforts are needed to develop historical datasets, and improve the capacity to obtain real or near real time fire information. Some existing datasets such as the one developed by BLM (2003) only include burns occurred on the federal lands, while those of state and private lands and Department of Defense lands, which together contribute to a substantial portion of the acres burned in the South. Expansions to these datasets will make them more valuable.

(2) The lack in systematic prescribed burning information, especially real time burning information, has been one of the major limitations in estimating fire emissions and environmental consequences. The efforts in developing automated reporting systems will provide a capacity in obtaining such information.

(3) More and more RS applications are expected for fire and fuel detection. Further algorithm development and evaluation are needed to solve some technical issues such as false fire signals and cloud interference. The development of the capacity in detecting prescribed fires is of great value. So is the capacity in measuring atmospheric concentrations of fire emissions.

(4) Fuel and fire properties are under constant disturbances from natural processes. Hurricanes, for example, can increase dead fuel loading, which in turn increases wildfire risks. More studies are needed to understand fuel and fire variations in response to environmental forcing.

(5) Decision making support systems are a useful tool for fire and land managers to understand and predict the effects of fire emissions on air quality, radiation, climate, the carbon cycle, and other environmental processes, and to plan and implement plans to migrate possible diverse consequences. Bridging between measurements and monitoring techniques (e.g., satellite RS) and modeling techniques (e.g., fuel, climate, ecosystem, and air quality models) is critical for the development of the systems.

Acknowledgements

This study was supported by the USDA Forest Service National Fire Plan (NFP) through the Southern High-Resolution Modeling Consortium (SHRMC), the USDA Forest Services / Southern Research Station Award (No. SRS 04-CA-11330136-170), and the US EPA STAR program.

References

Achtemeier GL, (1998), Predicting dispersion and deposition of ash from burning cane. *Sugar Cane*, **1**: 17 – 22

Achtemeier G, Goodrich S, Liu Y-Q, (2003), The Southern High Resolution Modeling Consortium-A source for research and operational collaboration. Proceedings of the 2nd Int'l Wildland Fire Ecology and Fire Management Congress. Amer. Meteor. Soc. Nov. 16 – 20, 2003, Orlando, FL

Ackerman AS, Toon OB, Stevens DE, Heymsfield AJ, Ramanathan V, Welton EJ, (2000), Reduction of tropical cloudiness by soot. *Science*, **288**: 1042 – 1047

Anderson GK, Sandberg DV, Norheim RA, (2004), Fire Emission Production Simulator (FEPS) User's Guide. USDA Forest Service. 99

Barna MG, Fox DG, (2003), Combining wildfire emissions from the Community Smoke Emissions Model (CSEM) with a regional-scale air quality model. Proceedings of the 2nd Int'l Wildland Fire Ecology and Fire Management Congress. Amer. Meteor. Soc. Nov. 16 – 20, 2003, Orlando, FL

Battye W, Battye R, (2002), Development of emissions inventory methods for wildland fire (final report). Prepared for U.S. Environmental Protection Agency, Research Triangle Park, NC, USA

BLM (U.S. Bureau of Land Management), (2003), Federal Fire History Internet Map Service User Guide

Burgan RE, Hartford RA, (1997), Live vegetation moisture calculated from NDVI and used in fire danger rating. 13th Conf. on Fire and For. Met., Lorne, Australia, Oct. 27 – 31, 1997. Jason Greenlee, ed. IAWF, Fairfield, WA 99012

Burgan RE, Klaver RW, Klaver JM, (1998), Fuel models and fire potential from satellite and surface observations. *Int'l J. Wildland Fire*, **8**: 159 – 170

Byun DW, Ching J, (1999), Science algorithms of the EPA Model-3 community multiscale air quality (CMAQ) modeling system. RTP, NC: EPA/600/R-99/030

Charlson RJ, Schwartz SE, Hales JM, Cess RD, Coakley JA Jr, Hansen JE, Hoffman DJ, (1992), Climate forcing by anthropogenic sulfate aerosols. *Science*, **255**: 423 – 430

Chuvieco E et al., (1999), Short-term fire risk: foliage moisture content estimation from satellite data. In: Remote Sensing of Large Wildfires in the European Mediterranean Basin, Chuvieco E (ed) Springer, 17 – 38

Cohen JD, Deeming JE, (1995), The National Fire-Danger Rating System: Basic equations. USDA Forest Service, Report PSW-82

EPA, (1995), Compilation of Air Pollutant Emission Factors. AP-42, fifth Edition, 1: Stationary Point and Area Sources

EPA, (1998), Interim Air Quality Policy on Wildland and Prescribed Fire. Office of Air Quality Planning and Standards, Research Triangle Park, NC, USA

EPA, (2003a), Documentation for the Draft 1999 National Emissions Inventory (Version 3.0) for Criteria Air Pollutants and Ammonia (Area Sources)

EPA, (2003b), Data Needs and Availability for Wildland Fire Emission Inventories-Short-term Improvements to the Wildland Fire Component of the National Emissions Inventory. Prepared by EC/R

Fraiser RH, Li Z, Cihlar J, (2000), Hotspot and NDVI differencing synergy (HANDS): A new technique for burned area mapping. *Rem. Sens. Environ*. **74**: 362 – 376

Hansen J, Sato M, Ruedy R, (1997), Radiative forcing and climate response. *J. Geophys. Res*., **102**: 6831 – 6864

Hao WM, Ward DE, Babbitt RA, Susott RE, Baker SP, Ottmar R, Vihnanek RE, Wade D, (2002), Emissions of trace gases and aerosol particles from biomass fires in the southeastern and central United States. USDA Forest Service 6

Hardy CC, Menakis JP, Long DG, Garner JL, (1998), FMI/Westar Emissions Inventory and Spatial Data for the Western United States. USDA Forest Service RMS

Houyoux M, Vukovich J, Seppanen C, Brandmeyer JE, (2002), SMOKE User Manual, MCNC Environmental Modeling Center

Justice CO, Kendall JD, Dowty PR, Scholes RJ, (1996), Satellte remote sensing of fires during the SAFARI campaign using NOAA Advanced Very High Resolution Radiometer data. *J. Geophy. Res*. **101**(23): 851 – 863

Justice CO, Giglio L, Korontzi S, Owens J, Morisette JT, Roy D, Descloitres J, Alleaume S, Petitcolin F, Haufman Y, (2002), The MODIS fire products. *Rem. Sens. Environ*. **83**: 244 – 262

Kaufman YJ, (1990), Remote sensing of biomasss burning in the tropics. *Journal of Geophysical Research*, **95**(D7): 9927 – 9939

Kaufman YJ, Justice C, (1998), MODIS Fire Products, Algorithm Theoretical Background Document (ATBD) (http://eospso.gsfc.nasa.gov/atbd/ modistables.html)

Kaufman Y, Ichoku C, Giglio L, Korontzi S, Chu DA, Hao WM, Li R-R, Justice CO, (2003), Fires and smoke observed from the Earth Observing System MODIS instrument: products, validation, and operational use. *Int'l J. Remote Sensing*, **24**: 1765 – 1781

Koren I, Kaufman YJ, Remer LA, Martins JV, (2004), Measurement of the effects of Amazon smoke on inhibition of cloud formation. *Science*, **303**: 1342 – 1345

Li Z, Cihlar J, Moreau L, Huang F, Lee B, (1997), Monitoring fire activities in the boreal ecosystem. *J. Geophys. Res*. **102**: 29611 – 29624

Li Z, Fraser R, Jin J, Abuelgasim AA, Csiszar I, Gong P, Pu R, Hao W, (2003), Evaluation of algorithms for fore detection and mapping across North America from satellite. *J. Geophys. Res*. **108**(D2): 4076, 10-1029/2001JD001377

Lindesay J, Andreae M, Goldammer J, Harris G, Annegarn H, Garstang M, Scholes R, Wilgen B, (1996), International Geosphere-Biosphere Programme/International Global Atmospheric Chemistry SAFARI-92 field experiment: Background and overview. *J. Geophy. Res*. **101**(D19): 23,521 – 23,530

Liu Y-Q, (2004), Variability of wildland fire emissions across the continuous United States, *Atmos. Environ*. **38**: 3489 – 3499

Liu Y-Q, Achtemeier G, Goodrick S, (2004), Air quality effects of prescribed fires simulated with CMAQ. The 2004 CMAQ Workshop, Chapel Hill, NC. 4

Liu Y-Q, (2005a), Atmospheric response and feedback to radiative forcing from biomass burning in tropical South America. *Agri. Forest. Meteor*. **133**: 40 – 53

Liu Y-Q, (2005b), Enhancement of the 1988 Northern U.S. drought due to wildfires. Geophy. *Res. Let*. 32 (No. 10). L1080610.1029/2005GL022411

Liu Y-Q, Achtemeier G, Goodrick S, (2006), Simulation and Experiment of air quality effects of prescribed fires in the South. (to be submitted)

Menon S, Hansen JE, Nazarenko L, Luo Y, (2002), Climate effects of black carbon aerosols in China and India. *Science*, **297**: 2250 – 2253

NIFC (National Interagency Fire Center) (2002) Wildland Fire Statistics, (2002), NOAA NESDIS (2006) Hazard Mapping System Fire and Smoke Product. (http://www.ssd.noaa.gov/PS/FIRE/hms.html)

O'Neill SM, Ferguson SA, Peterson J, Wilson R, (2003), The BlueSky Smoke Modeling Framework. Proceedings of the 5th Symposium on Fire and Forest Meteorology, American Meteorological Society, Orlando, FL, November 2003

Ottmar RD, Burns MF, Hall JN, Hanson AD, (1993), Consume Users Guide. Version 1.00, Ge. Tech Rep., PNW-GTR-304, Portland, OR, USDA Forest Service, PNRS, 118

Page SE et al., (2002), The amount of carbon released from peat and forest fires in Indonesia during 1997. *Nature*, **420**: 61 – 65

Penner JE, Dickinson RE, O'Neill CS, (1992), Effects of aerosol from biomass burning on the global radiation budget. *Science*, **256**: 1432 – 1434

Peterson JL, Ward DE, (1993), An Inventory of Particulate Matter and Air Toxics from Prescribed Fires in the USA for 1989. IAG-DW 12934736-01-1989

PNW, (2005), Fire Emissions Production Simulator, www.fs.fed.us/pnw/fera/feps

Prins EM, Menzel WP (1990) Geostationary satellite detection of biomass burning in South America. *Int. J. Rem. Sens*. **13**: 2783 – 2799

Quayle B, Lannom K, Finco M, Norton J, Warnick R, (2003), Monitoring wildland fire activity on a national-scale with MODIS imagery. Proceedings of the 2nd Int'l Wildland Fire Ecology and Fire Management Congress. Amer. Meteor. Soc., Nov. 16 – 20, 2003, Orlando, FL

Qu J, Hao X, Kafatos M, Liu Y, Riebau A, (2003), Estimating Ecosystem System Changes from Space using MODIS measurements. Proc. of ISPRS (CD-publication)

Qu J, Hao XJ, Yang RX, Dasgupta S, Bhoi S, Wang WT, Xie Y, Wang LL, Li ZT, Wolf H, Kafatos M, (2005), A System for Monitoring Fire Characteristics and Fire Danger Potential in the Eastern States Using Remote Sensing Techniques. EastFire Conf. 2005, Fairfax, VA, May 11 – 13

Reinhardt ED, Keane RE, Brown JK, (1997), First Order Fire Effects Model: FOFEM 4.0, Users Guide. USDA Forest Service General Technical Report INT-GTR-344

Riebau AR, Fox D, (2001), The new smoke management. *Int'l J. Wildland Fire*, **10**: 415 – 427

Riebau A, Qu JJ, (2004), Application of remote sensing and GIS for analysis of forest fire risk and assessment of forest degradations in the Southwest Pacific Region. Springer-Vergleg (in press)

Sandberg DV, Peterson J, (1984), A source-strength model for prescribed fires in coniferous logging slash. In: Proceedings, 21st Annual Meeting of the Air Pollution Control Association, Pacific Northwest International Section. Pittsburgh, PA: Air Pollution Control Association

Sandberg DV, Hardy CC, Ottmar RD, Snell JAK, Acheson A, Peterson JL, Seamon P, Lahm P, Wade D, (1999), National strategy plan: Modeling and data systems for wildland fire and air quality. US Forest Service, PNRS, 60

Sandberg DV, Ottmar RD, Cushon GH, (2001), Characterizing fuels in the 21st century. *Int'l J. Wildland Fire*, **10**: 381 – 387

Seiler W, Crutzen PJ, (1980), Estimates of gross and net fluxes of carbon between the biosphere and the atmosphere from biomass burning. *Clim. Change*, **2**: 207 – 247

Stanturf JA et al., (2002), Fires in southern forest landscapes, in The Southern Forest Resource Assessment. USDA Forest Service, SRS

Twomey S, Piepgrass M, Wolfe TL, (1984), An assessment of the impact of pollution on global cloud albedo. *Tellus*, **36B**: 356 – 366

Wade DD, Brock BL, Brose PH et al., (2000), Fire in eastern ecosystems. In: Wildlandfire in ecosystems: effects of fire on flora, Brown JK, Smith JK (eds), Gen. Tech. Rep. RMRS-42. Ogden, UT: U.S. Department of Agriculture, Forest Service, Rocky Mountain Research Station: 53 – 96 Chapter 4. Vol. 2

Wang W, Qu JJ, Liu Y, Hao X, Sommers W, (2006), A preliminary study for improving MODIS small and cool fire detection over the southeastern United States. Remote sensing of Environment (in revision)

Ward DE, Peterson JL, Hao WM, (1993), An inventory of particulate matter and air toxic emissions from prescribed fires in the USA for 1989, 93-PM-6.04. Proc. the Air and Waste Management Association 1993 Annual Meeting and Exhibition, Denver, CO, June 14 – 18

WRAP, (2002), 1996 Fire Emission Inventory. Prepared by Air Sciences, INC

WRAP, (2005), Inter-PRO National 2002 Wildfire Emissions Inventory (Final Work Plan). Prepared by Air Sciences and EC/R

10 Integrating Remote Sensing and Surface Weather Data to Monitor Vegetation Phenology

W. Matt Jolly

Rocky Mountain Research Station Fire Sciences Laboratory,
US Forest Service, 5775 Hwy 10 W, Missoula, MT 59808, USA
Email: mjolly@fs.fed.us

Abstract The US national fire danger rating system (NFDRS) generates daily estimates of fire potential throughout the United States. A key component of this system is the condition of live vegetation. Currently, there are no objective methods for determining vegetation condition. Inter-annual climatic variability causes the onset of spring green-up and fall leaf senescence to vary substantially from year-to-year. Therefore, methods used to assess live vegetation condition must be robust to these climatic changes. We present a system designed to integrate both remote sensing and surface weather-derived metrics of foliar greenness. This system provides two independent metrics that are meaningful representations of landscape level greenness responses and are suitable for use in verifying NFDRS greenup dates and greenness factors.

Keywords Phenology, fire danger rating, green-up dates, greenness factors, NDVI

10.1 Introduction

Foliar phenology significantly influences the exchange of mass, energy and momentum between the Earth's surface and its atmosphere. Canopy timing and duration constrain annual plant productivity and alter global seasonal cycles of atmospheric CO_2 (Keeling et al., 1996). Plant canopies lose water to the atmosphere through transpiration. Leaf area alters the boundary layer and changes the coupling between the land surface and the atmosphere. As such, we see many connections between plant foliar dynamics, the global carbon cycle and the global water cycle. Understanding plant phenology is a requisite for a proper understanding of these cycles.

Many methods exist to characterize vegetation foliar phenology across the landscape. Mathematical models driven by both satellite data and / or surface weather data are common tools for assessing seasonal changes in phenology (Schwartz, 1999). Although these tools are useful, there has never been an integrated system that publicly offers multiple resources for the assessment of seasonal changes in leaf cover. Such a system would be useful to a variety of disciplines including fire managers who need live vegetation conditions to initialize the live fuel moisture model of the US national fire danger rating system (NFDRS). NFDRS is used to make fire danger assessments across the United States and is the foundations for many wildland fire management decisions. There are currently two operational versions of NFDRS and each version requires different information about the condition of live vegetation. The 1978 version of NFDRS requires the bud break or green-up date (Deeming et al., 1977) while the 1988 revision to NFDRS added greenness factors which are required daily inputs to NFDRS and are used to express the seasonal greenup and curing rates of live vegetation (Burgan, 1988).

Currently, there are no mechanistic models that can be used to derive both greenup dates and greenness factors from prevailing weather data. Thus, there are no means to examine historical fire potential or to project the fire danger under changing climates. Such a model and the means to estimate it operationally would benefit land managers by providing standardized estimates of vegetation greenness conditions across the entire country. Here we present a phenology monitoring system that combines satellite and surface derived phenology proxies into a simple, automated system. The system assesses phenology across the continental United States and Alaska. It is the first of its kind to provide multiple phenology proxies in near real-time to the general public. The system combines data from point-source surface weather data and satellite-derived vegetation indices from the advanced very high resolution radiometer (AVHRR). Surface weather data are interpolated and used to drive a generalized foliar phenology model which provides estimates of phenology that are interdependent of the satellite-derived metrics. The model combines temperature, water and light constraints into one simple daily metric that can be continually assessed across large regions. The web-based system provides both spatial and temporal phenological metrics across the landscape. This phenology monitoring system will be integrated into the wildland fire assessment system (WFAS) to provide fire managers with quick access to live fuel conditions (http://www.wfas.net) (Jolly et al., 2005a).

10.2 Methods

10.2.1 System Introduction

The phenology monitoring system is composed of two components: the surface weather-based phenology model and the satellite-derived vegetation indices.

These two sources provide independent assessments of phenology spatially.

10.2.2 Surface Weather-Based Phenology Monitoring System

10.2.2.1 Surface Observations Gridding System (SOGS)

This system uses station weather data from multiple obtained automatically from multiple sources to create surfaces of weather variables using the methods described by Jolly et al., (2005b). This system automatically retrieves, stores, and interpolates surface weather observations to create spatially continuous estimates of key meteorological data fields across a region of interest. Interpolation grids are user-defined and can be generated at any spatial resolution. This system is used to generate daily gridded weather data for minimum temperature, vapor pressure deficit and daylength which are provide spatial inputs to a generalized phenology model to estimate greenness conditions of live vegetation across the landscape. The system is configured to make use of multiple mathematical interpolators. For this operational system we chose to use the Truncated Gaussian Filter because it is efficiently calculated and results were similar to other more complicated interpolation schemes (Jolly et al., 2005b).

10.2.2.2 Growing Season Index (GSI)

These interpolated weather grids are then used to spatially estimate the GSI, a relative index of the bioclimatic constraints on plant functioning (Jolly et al., 2005c). This index relates well to plant foliar phenology and can be estimated daily from available surface weather data. The index is calculated as the product of three indicators which express the relative constraints of temperature, evaporative demand/water availability and light on plant functioning. The index uses indicator functions of three weather variables as good surrogates for each of these three constraints: minimum temperature, vapor pressure deficit and photoperiod. Each of these variables is assumed to have a value where below which it completely limits plant functioning (1) and a value where above which it does not constrain plant function (2). The upper and lower limits of the indicator functions for each of these three variables are shown in Table 10.1. The GSI is calculated as the product of these three daily indicator functions.

Table 10.1 GSI meteorological data indicator function parameters used in PhenMon

Variable	Units	Indicator minimum value (fully constrained)	Indicator maximum value (unrestricted)
Minimum temperature	℃	–2.0	5.0
Vapor pressure deficit	Pas	900	4,100
Daylength (photoperiod)	s	36,000 (10 h)	39,600 (11 h)

These daily data provide two potential sources of information to land managers for use with both the 1978 version and the 1988 revisions of the NFDRS. First, the time series can be monitored in the spring or throughout the year to approximate a green-up condition. When the index value exceeds a pre-defined threshold, green-up can be declared and the users can make the appropriate entry into NFDRS. This threshold method has been evaluated at a long-term research site and does well at detecting inter-annual difference in green-up dates (Jolly et al., 2005c). GSI is unique for this application because it is a continuous measure of greenness. This means that it can predict multiple green-up and curing events within the same year. Therefore, it can be monitored continuously throughout the season to understand how bioclimatic limitations are likely affecting vegetation vigor across the landscape for an area of interest. In addition to estimating a green-up date for the 1978 version of NFDRS, GSI can provide estimated greenness factors for the 1988 NFDRS revision. Greenness factors vary as whole numbers from zero to twenty. They are meant to express greenup and curing of live vegetation in a relative context where zero is completely cured and twenty is completely green (Burgan, 1988). GSI is an identical metric but it is scaled continuously from 0 – 1 and requires the definition of a simple threshold value of greenup. GSI can thus be used to calculate greenness factors by a simple linear transformation as follows:

$$\mathrm{GF88}_t = \begin{cases} 0 & \text{if } \mathrm{GSI}_t < 0.5 \\ \mathrm{GSI}_t \cdot 40 - 20 & \text{if } \mathrm{GSI}_t \geqslant 0.5 \end{cases}$$

Where $\mathrm{GF88}_t$ is the greenness factor for the 1988 version of NFDRS at time t and GSI_t is the GSI at time t and assuming a GSI greenup threshold of 0.5 (Jolly et al., 2005b). Greenness factors are rounded to the nearest whole number.

10.3 Satellite-Derived Vegetation Index Data

10.3.1 AVHRR Normalized Difference Vegetation Index (NDVI)

Weekly AVHRR NDVI data are obtained from the wildland fire assessment system (WFAS) (Jolly et al., 2005a). These data are produced operationally each week by the USGS at NC EROS and they are used to calculate two products that are commonly used by fire managers to assess the condition of live vegetation: relative greenness and departure from average greenness (Burgan and Hartford, 1993; Burgan et al., 1996). Although these products are useful in providing spatial assessments of vegetation across the landscape, to date there has been no system to extract time-series data from the raster images for points. This hinders their utility because fire management decisions are often based on data derived from point-sources such as remote automated weather stations.

10.3.2 Point Retrieval Interface

PhenMon provides two separate point retrieval interfaces. The first point retrieval interface provides time-series of GSI for any point within either of the two regions of interest. This interface provides land managers with a tool to assess both the current and short-term changes in greenness at a given location such as an NFDRS station. The second point retrieval interface provides time-series data for AVHRR NDVI. This point summary includes the historical minimum and maximum NDVI value, the historical mean for the current period and the current NDVI value in addition to time series plots of the last year's data along with the mean. Both interfaces provide options for either data values served as text or time-series plots of data for the entire period of record.

The interface is built around a raster extraction tool written using the USGS general cartographic transformation package (GCTP: ftp://edcftp.cr.usgs.gov/pub/software/gctpc/). This tool extracts a given value from a projected raster based on geographic coordinates. The tool can extract either the coincident pixel value from a raster or the values from a user-defined window around the point.

10.3.3 PhenMon: The Phenology Monitoring System

PhenMon uses the interpolated surface weather data from SOGS to run GSI across the regions of interest. A system flow diagram is shown in Fig. 10.1. SOGS is run daily using weather data from the remote automated weather stations (RAWS) and the temperature and precipitation summary from the climate prediction center. SOGS interpolates these data at an eight kilometer resolution for two regions: the continental United States and Alaska. These interpolated data are used as inputs to GSI in addition to the previous twenty days of data. Daily GSI rasters are produced as the 21 day average of daily GSI values (Jolly et al., 2005c). Images suitable for display on the world wide web are created by a custom image generator and the data rasters are archived for use in the point retrieval interface. The system also automatically retrieves the most current AVHRR NDVI data for the continental United States and stores these data in an archive to provide access to data for at least the past year. In addition to these real-time data sources, the system also maintains rasters of long-term weekly mean NDVI as well as the historical minimum and maximum values for each pixel.

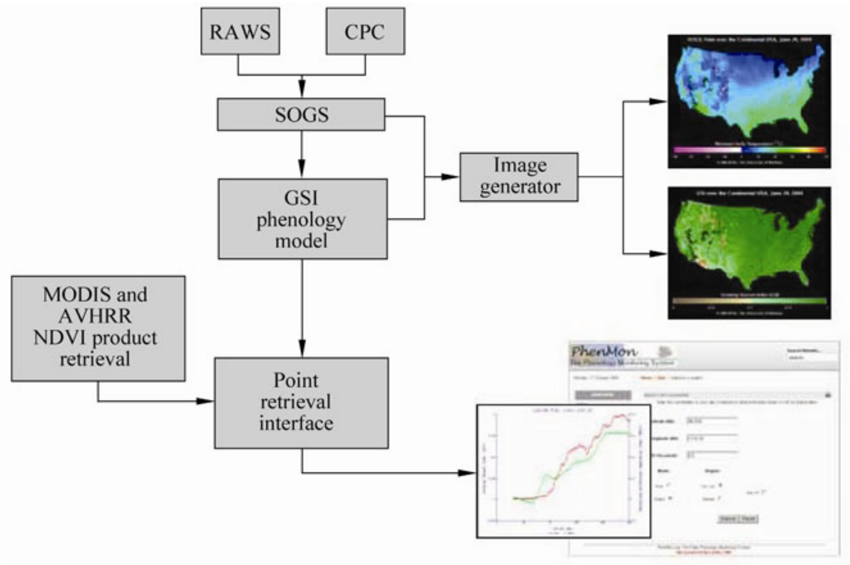

Figure 10.1 PhenMon phenology monitoring system flow diagram

10.4 Results and Discussion

10.4.1 Surface Observations Gridding System

Example images of interpolated surface weather data from SOGS for both the continental United States and Alaska are show in Fig. 10.2. These surfaces of minimum temperature and vapor pressure deficit are generated daily. Photoperiod (daylength) is also calculated each day as a function of site latitude and julian day. These rasters are used as inputs to calculate the GSI. The accuracy of this method has been verified in a previous study. In general, minimum temperature predictions are accurate to within ~2.0℃ and vapor pressure deficit is accurate to within approximately 168 pascals (Jolly et al., 2005b).

10.4.2 Growing Season Index

GSI data are produced daily using the interpolated weather data from SOGS for both the continental United States and Alaska. Example spatial images for each region are shown in Fig. 10.3. An example time-series plot derived from the point retrieval tool is shown in Fig. 10.4.

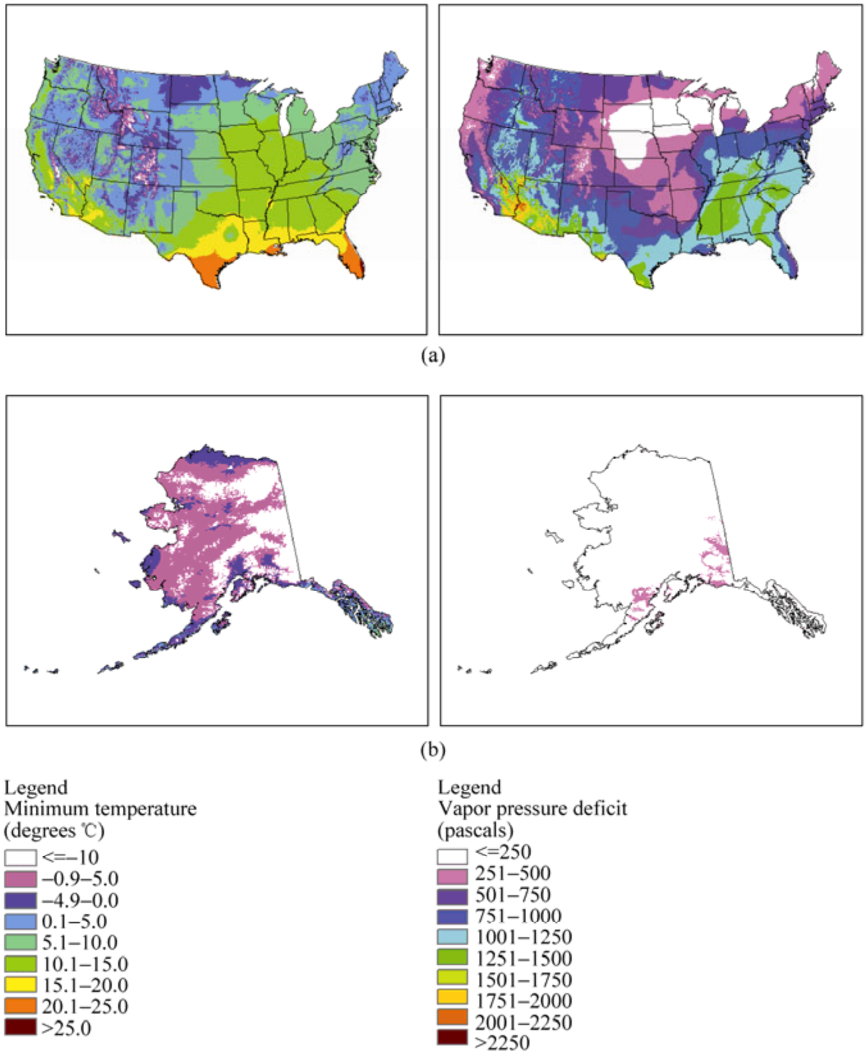

Figure 10.2 Example surfaces of minimum temperature (left column) and vapor pressure deficit (right column) generated with the SOGS for the continental United States (a) and Alaska (b) for October 15, 2007. These rasters of weather data are generated daily using point-source information from both the remote automated weather stations (RAWS) and the Climate Prediction Center's Temperature and Precipitation Summary

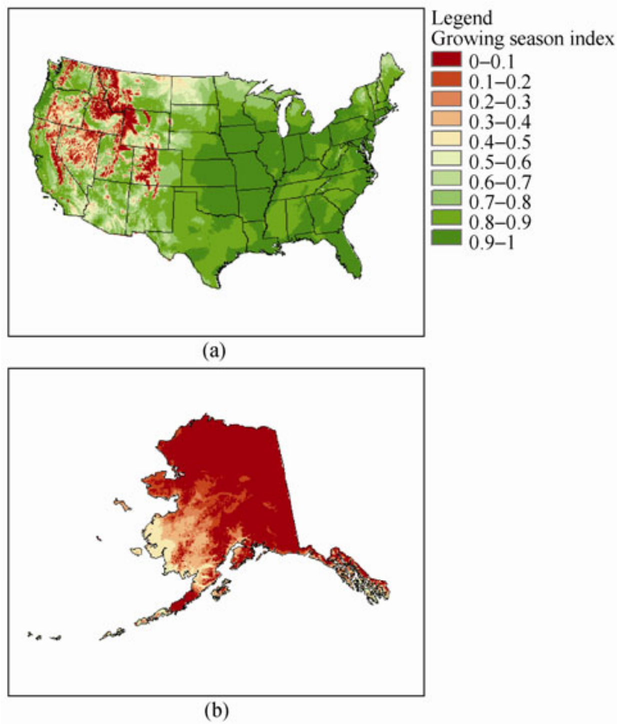

Figure 10.3 Example raster images of the GSI for October 15, 2007 for both the continental United States (a) and Alaska (b), calculated daily as part of the phenology monitoring system (PhenMon). This index integrates temperature, water and light limitations into a single metric that expresses the relative bioclimatic constraints on plant functioning across the landscape

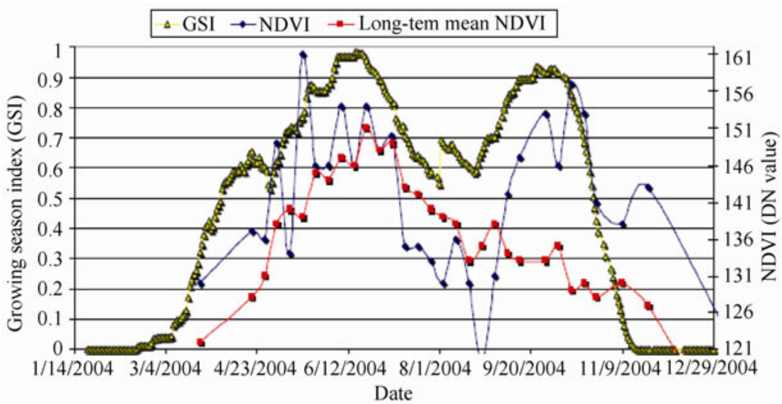

Figure 10.4 Time-series plots of the GSI, current NDVI and the long-term mean NDVI for a point in Western Montana. These data were derived from the PhenMon point retrieval interface. There is generally a good temporal correlation between GSI and NDVI

10.4.3 AVHRR NDVI Data

An example image of the weekly NDVI data is shown in Fig. 10.5. These images are generated each week by the EROS Data Center of the USGS as part of the wildland fire assessment system (WFAS). PhenMon retrieves these images and stores them in the archive for use in the point retrieval tool. Graphic images of the rasters are not produced to avoid duplication of processing already being done by WFAS. An example time series of NDVI along with the long-term weekly mean values and the GSI for the same point is shown in Fig. 10.4. We see good agreement between the satellite derived and the surface weather-derived metrics of greenness for the same location. In a previous study, the GSI has been compared more extensively to NDVI for different vegetation types throughout the world (Jolly et al., 2005c). In addition to the standard point retrieval interface which plots the time-series or provides access to the data via a text output, there is also another feature which allows the users to view the most current NDVI for a given point. This value is also expressed as a function of the historical range of variability for

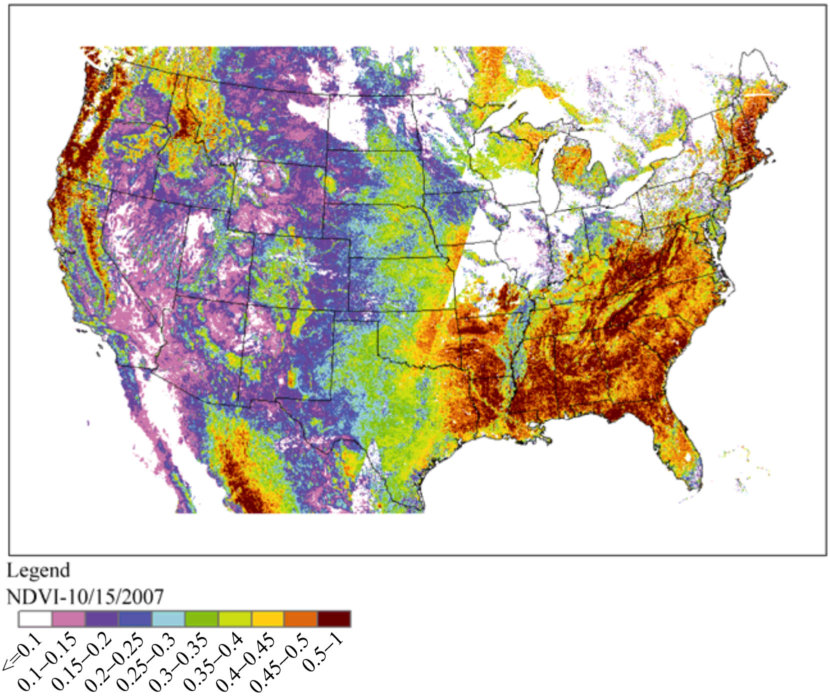

Figure 10.5 Example AVHRR NDVI composite for the continental United States at one kilometer resolution for the weekly composite period ending October 11, 2005. These data are produced weekly by the EROS data center as part of the wildland fire assessment system (WFAS) (Jolly et al., 2005a). White areas show regions with extensive cloud cover during the week

that point as both relative greenness and departure from average greenness (Burgan and Hartford, 1993; Burgan et al., 1996). This interface can be used for a quick summary around an NFDRS weather station to verify green-up conditions predicted using GSI. NDVI data can be used to provide estimates of greenup dates by comparing the current NDVI value to the long-term mean. Greenup can be declared when NDVI exceeds half its seasonal maximum or relative greenness exceeds 50% (White et al., 1997).

10.4.4 General Discussion

This is the first system to its kind to integrate RS and surface weather-derived metrics of canopy greenness into a single, simple interface suitable for use by the general public. The tool is unique because it provides point-wise access to two independent metrics of canopy foliar phenology. This system is not intended to replace field observations but rather to supplement those observations with resources that are standardized across different geographic areas. Greenup conditions are somewhat arbitrary when observed from the field because different species and even similar species within different canopy positions do not green-up at the same time (Gill et al., 1998; Sawada et al., 1999; Augspurger and Bartlett, 2003). Both GSI and NDVI represent the areal-average greenness conditions rather than the green-up dates of a single species in time. Land managers can then use these data to verify observations prior to “greening up” a fire danger rating station.

It is important to note that RS data alone cannot meet the needs of land managers. Passive RS requires temporal compositing to remove the effects of clouds and aerosols that are present in daily images (Holben, 1986). Temporal aggregation reduces this impact but also limits their applicability to systems that require more timely data. The weekly composite period NDVI data that are used in WFAS and integrated into PhenMon are some of the timeliest RS data available. More advanced sensors commonly use longer composite periods which result in longer delays for data delivery. For example, vegetation index data for MODIS use sixteen day composites (Huete et al., 2002). These data are rarely available even as much as a week after the end of the composite period due to the intensive processing and quality control that the data undergo prior to public distribution.

Land managers are not concerned with state values at a given time, they are more concerned with the state transitions of vegetation over time such as the greening up of vegetation in spring or the drying (curing) of vegetation in the summer and the leaf senescence in the fall. These represent rates of change rather than snapshots in time. RS can be used examine these states transitions but this means that at a minimum, users must look at two composite periods to see where NDVI has changed greatly. In reality, it often takes three or four composite periods to adequately depict the change due to problems such as cloud contamination that are present in the weekly images. Studies thus often use running averages of several composite periods before attempting to examine state transitions (Jolly and Running, 2004). This significantly hinders the utility of satellite data as the sole resource for determining greenness conditions especially when greenness can change rapidly with the season, especially in vegetation with shallow roots.

In summary, this system is the first of its kind to integrate RS and surface weather-based models into a simple, user friendly interface that is suitable for use by land managers to remotely determine greenness conditions across the landscape. It provides estimates of both greenup dates and greenness factors for both versions of NFDRS that are currently in operation. Although satellite data themselves do not solely meet the needs of land managers, they do provide independent verification of greenness conditions that are estimated from methods with higher temporal resolution. This system will be useful in standardizing greenness assessment throughout the United States.

Acknowledgements

This research was supported in part by funds provided by the joint fire science program (JFSP) and the Rocky Mountain Research Station, Forest Service, U.S. Department of Agriculture.

References

Augspurger CK, Bartlett EA, (2003), Differences in leaf phenology between juvenile and adult trees in a temperate deciduous forest. *Tree Physiology*, **23**: 517 – 525

Burgan RE, (1988), 1988 Revisions to the 1978 National Fire Danger Rating System. SE-273, USDA, Forest Service, Asheville, SC

Burgan RE, Hartford RA, (1993), Monitoring vegetation greeness with satellite data. INT-297, USDA Forest Service, Intermountain Research Station

Burgan RE, Hartford RA, Eidenshink JC, (1996), Using NDVI to assess departure from average greenness and its relation to fire business. USDA Forest Service, Intermountain Research Station General Technical Report INT-GTR-333

Deeming JE, Burgan RE, Cohen JD, (1977), The National Fire Danger Rating System. USDA Forest Service, Intermountain Forest and Range Experiment Station General Technical Report INT-39: 63

Gill DS, Amthor JS, Bormann FH, (1998), Leaf phenology, photosynthesis, and the persistence of saplings and shrubs in a mature northern hardwood forest. *Tree Physiology*, **18**: 281 – 289

Holben BN, (1986), Characteristics of maximum-value composite images from temporal AVHRR data. *International Journal of Remote Sensing*, **7**: 1417 – 1434

Huete A, Didan K, Miura T, Rodriguez EP, Gao X, Ferreira LG, (2002), Overview of the radiometric and biophysical performance of the MODIS vegetation indices. *Remote Sensing of Environment*, **83**: 195

Jolly WM, Andrews PL, Bradshaw LS, (2005a), The Wildland Fire Assessment System (WFAS): A web-based resource for decision support. in EastFire Conference, Fairfax, VA

Jolly WM, Graham JM, Michaelis A, Nemani R and Running, SW. 2005b. A flexible, integrated system for generating meteorological surfaces derived from point sources across multiple geographic scales. *Environmental Modeling and Software*, **20**(7):873 – 882

Jolly WM, Nemani RR and Running SW. 2005c. A generalized, bioclimatic index to predict foliar phenology in response to climate. *Global Change Biology* **11**(4):619 – 632

Jolly WM, Running SW, (2004), Effects of precipitation and soil water potential on drought deciduous phenology in the Kalahari. *Global Change Biology*, **10**: 303 – 308

Keeling CD, Chin JFS, Whorf TP, (1996), Increased activity of northern vegetation inferred from atmospheric CO_2 measurements. Nature, **382**: 146 – 149

Sawada S, Harada A, Asari Y, Asano S, Kuninaka M, Kawamura H, Kasai M, (1999), Effects of micro-environmental factors on photosynthetic CO_2 uptake and carbon fixation metabolism in a spring ephemeral, Erythronium japonicum, growing in native and open habitats. *Ecological Research*, **14**: 119 – 130

Schwartz MD, (1999), Advancing to full bloom: planning phenological research for the 21st century. *International Journal of Biometeorology*, **42**: 113 – 118

White MA, Thornton PE, Running SW, 1997, A continental phenology model for monitoring vegetation response to interannual climatic variability. *Global Biogeochemical Cycles*, **11**: 217 – 234

11 Creating a Crosswalk of Vegetation Types and Fire Fuel Models for the National Park Service

Bill Millinor

Jones Edmunds & Associates Inc., 730 Northeast Waldo Road, Gainesville, FL 32641-5699, USA
Email: wmillinor@jonesedmunds.com Phone: (352) 377-5821

Abstract The US national fire danger rating System (NFDRS) generates daily estimates of fire potential throughout the United States. A key component of this system is the condition of live vegetation. Currently, there are no objective methods for determining vegetation condition. Inter-annual climatic variability causes the onset of spring green-up and fall leaf senescence to vary substantially from year-to-year. Therefore, methods used to assess live vegetation condition must be robust to these climatic changes. We present a system designed to integrate both remote sensing and surface weather-derived metrics of foliar greenness. This system provides two independent metrics that are meaningful representations of landscape level greenness responses and are suitable for use in verifying NFDRS greenup dates and greenness factors.

Keywords Phenology, fire danger rating, green-up dates, greenness factors, NDVI

11.1 Introduction

With more and more people moving into the wildland urban interface, wildfires have become an increasing concern for the National Park Service and other land-management agencies. According to the National Interagency Fire Center, almost 7 million acres and over 1,000 structures burned in 2004 (National Interagency Fire Center, 2005). This is nearly a 2-million-acre increase over the previous 10-year average and it came with an estimated $890-million-dollar fire-suppression price tag. These increases have generated expanded interest among fire managers and scientists developing more robust fire-behavior models. Key to the performance of these models is an accurate depiction of the spatial arrangement of fire fuel loads.

Current fire-behavior models (e.g., FARSITE) rely heavily on National Fire Fuel Laboratory (NFFL) fuel-classification procedures. These procedures, in turn, are based on litter (downed woody material), vegetation type, and overall vegetation structure (Anderson, 1982). Previous work in two national parks (Booker T. Washington National Monument and George Washington National Monument) found that there was a one-to-one relationship between vegetation type and NFFL fuel models for Mid-Atlantic Eastern United States forests (Devine, et al., 2003). This chapter expands those findings by further exploring this vegetation type-fuel model relationship in eight additional Northeastern national parks from East central Maine to SOUTH central Virginia. The national parks are listed below:

(1) Acadia National Park

(2) Appomattox Court House National Historical Park

(3) Colonial National Historical Park

(4) Fire Island National Seashore

(5) Fredericksburg and Spotsylvania County Battlefields Memorial National Military Park

(6) Petersburg National Battlefield

(7) Richmond National Battlefield Park

(8) Thomas Stone National Historic Site

This chapter focuses on the development of a comprehensive database that could be used to crosswalk formation-level vegetation maps to NFFL fuel-model maps. The process involved developing digital aerial photograph mosaics and using three-dimensional GIS procedures to combine these mosaics with vegetation information. This was followed by the development of techniques to produce complacent and available live fire-fuel-load maps. This chapter is divided into three sections describing the methods and results of the digital orthophoto mosaic production, the formation-level vegetation databases, and the fire fuel mapping.

11.2 Digital Orthophoto Mosaics

For this research we created digital orthophoto mosaics from color infrared, stereo pair 1:6,000-scale aerial photography with airborne global positioning system (GPS) and inertial mapping unit (IMU) data for eight national parks in the NPS Northeast Region. In the first step, the air photos were scanned at 600 dpi with 24-bit color depth on flatbed 11-x-17 scanners with transparency adapters. We found that these scanner settings resulted in manageable file sizes while maintaining a high level of detail.

During this multi-year research project we refined and improved our procedures. The final methodology included five basic steps:

(1) We imported scanned images of the air photos in tiff format to ERDAS' Imagine (.img) format (Erdas, 2004).

(2) We created a photo block in Leica's Photogrammetry Suite (LPS), using airborne GPS and IMU data and a digital elevation model from the United States Geological Survey (USGS, NED) (Leica, 2004).

(3) We triangulated each mosaic photo block with a root mean square error (RMSE) of less than 1. We then generated single frame orthophotos (one for each air photo) within Imagine.

(4) We exported the single frame orthophotos to Imagine .lan format and then imported the .lan files into ER Mapper's native (.ers) format (ER Mapper, 2004). An ER Mapper algorithm was created for color balancing, manual cutline creation, and final mosaicking.

(5) In ER Mapper we generated a band interleaved by line (.bil) image and header file for the final orthophoto mosaic. We imported the .bil image into Imagine .img format and compressed the .img image using MrSid software with a 20:1 target compression ratio (Lizardtech, 2001).

Figures 11.1 and 11.2 illustrate the visual improvements obtained with our final methodology using ER mapper for cutlines and color balancing. Figure 11.1 shows the Green Springs area of Colonial National Park. The left half of the image is the original mosaic and the right half shows the recreated mosaic. In the newer mosaic on the right, the red tint is substantially reduced, photo seamlines are nearly invisible, and the overall color balancing is much improved.

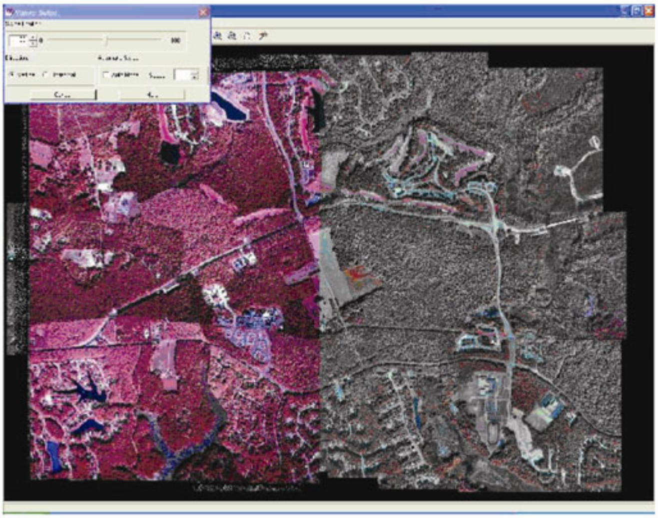

Figure 11.1 Imagine screenshot of initial (left half of image) and final (right half of image) mosaics of the Green Springs area of Colonial National Park

Figure 11.2 shows mosaics of the five forks area of Petersburg National Battlefield that illustrate similar improvements to those shown in Fig. 11.1. The mosaic created with the newer methodology using ER Mapper has better overall color balance, less noticeable seam lines, and less pronounced red tint.

The horizontal positional accuracy of each mosaic was then assessed following guidelines of the NBS/NPS vegetation mapping program (ESRI, NCGIA, and

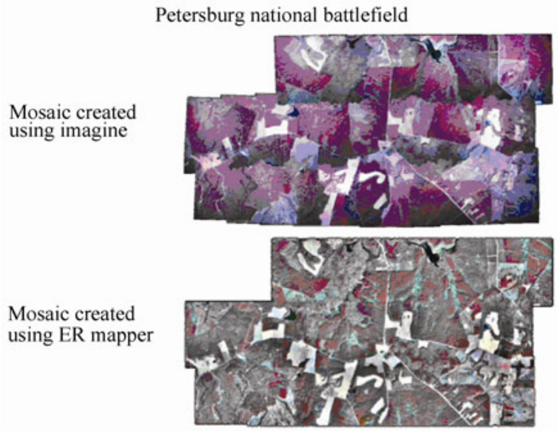

Figure 11.2 Initial and final mosaics of the five forks area of Petersburg National Battlefield

TNC, 1994). At least 20 well-defined positional accuracy ground control points were placed throughout all quadrants of the mosaic in ArcMap. Ground control points and zoomed in screenshots of each point were plotted on hard copy maps with the mosaic as a background. These maps and plots were used to locate the ground points in the field. For each ground-control point, field staff noted any alterations to the locations in the field and then recorded the coordinates with a Trimble Pro XR/XRS or GeoXT. Mapped ground-control points that were physically inaccessible were also noted. The coordinate data were collected with real-time GPS and post processed with differential correction using Trimble's Pathfinder Office software (Trimble, 2004).

Before positional accuracy was calculated, we excluded ground-control points identified by SAS's JMP program as outliers (SAS, 2004). Following USGS/NPS vegetation mapping guidelines, no more than 10 percent of the ground control points for any one mosaic were excluded. We then entered the field-collected GPS coordinates and the coordinates obtained from the mosaic viewed in ArcMap into a spreadsheet designed to calculate horizontal positional accuracy (in meters).

At the beginning of this project, the accepted method of calculating horizontal positional accuracy was based on Euclidean distance. Subsequently, a method based on root mean square error became the accepted procedure for assessing horizontal positional accuracy (FGDC, 1998b; Minnesota Governor's Council on Geographic Information and Minnesota Land Management Information Center, 1999). A positional accuracy handbook and a copy of the spreadsheet that contains the RMSE accuracy calculation formulas (horizontal.xls) can be downloaded from the Minnesota Department of Administration, Office of Geographic and Demographic analysis website (Minnesota Dept. of Administration, 2005).

Horizontal positional accuracy of the 15 mosaics[1] created for this project

[1] For some of the national parks involved in this research, we created two mosaics—a spring/leaf-off mosaic and a fall/leaf-on mosaic.

ranged from 0.815 – 1.580 meters. Thirteen of the 15 mosaics meet the class 1 national map accuracy standard (NMAS) of 1.5 meters or better for 1:6,000-scale photography and the other two mosaics failed to meet that standard by only 0.08 and 0.04 meters.

11.3 Formation-Level Vegetation Databases

The USGS and the NPS have standardized on the use of the hierarchal national vegetation classification system (NVCS) (FGDC, 1997) for their national vegetation characterization program. The formation-level is the lowest of the five physiognomic levels in the NVCS and it identifies ecological groupings of vegetation units with similar broadly defined environmental and physiognomic factors.

We created formation-level vegetation databases by interpreting the digital orthophoto mosaics for each park to delineate vegetation polygons to the formation-level defined in the NVCS. Table 11.1 displays the basic hierarchy of the system as well as some class examples.

Table 11.1 Hierarchy of the U.S. national vegetation classification (from Grossman et al., 1998)

	Level	Primary basic for classification	Example
Physio-gnomic	Class	Growth form and structure of vegetation	Woodland
	Subclass	Growth form characteristic, e.g., leaf phenology	Deciduous woodland
	Group	Leaf types, corresponding to climate	Cold-deciduous woodland
	Subgroup	Relative human impact (nature/ semi-natural, or cultural)	Natural/Semi-natural
	Formation	Additional physiognomic and environ-mental factors, including hydrology	Temporarily flooded Cold-deciduous Woodland
Floristic	Alliance	Dominant/diagnostic species of uppermost or dominant stratum	Populus deltoids Temporarily flooded Woodland Alliance
	Association	Additional dominant/diagnostic species from any strata	Populus deltoids – (Salix amygdaloides) / Salix exigua Woodland

Formation-level vegetation databases were created within ESRI's ArcMap using the orthophoto mosaics (both leaf-off and leaf-on, when available) as basemaps (ESRI). Photo interpreters viewing the mosaic(s) in two-dimensions delineated visible areas of homogeneous vegetation (i.e., vegetation polygons) using ArcMap's onscreen digitizing tools. Although the minimum mapping unit was 0.5 hectare, the photo interpreters were usually able to delineate polygons as small as 0.5 acre. After vegetation polygons were delineated for the entire park area, the photo interpreters created and populated three fields in the attribute table, entering a unique polygon identification number, the formation-level vegetation class code, and notes when they were unsure of the appropriate vegetation class code or could not assign a code. The photo interpreters relied on their experience to attribute the proper vegetation class. In some cases, digital raster graphics and existing spatial vegetation data were used to supplement the photo interpreters vegetation classification. The photo interpreters then examined each polygon in three-dimensions using Leica's Stereo Analyst software to verify the formation-level vegetation class code entered in the attribute table, and they entered a new or corrected code if appropriate (Leica, Stereo Analyst, 2003). Delineating the vegetation polygons in three dimensions is very time consuming. After considerable testing, the methodology was finalized to delineate in two-dimensions and perform validation and accuracy checks in three dimensions. This greatly increased productivity while conserving accuracy over a strictly three-dimensional approach. The final formation-level vegetation databases are archived in ESRI shapefile and geodatabase formats.

Sample field data were collected to assess the thematic accuracy of the formation-level vegetation databases at Booker T. Washington National Monument and George Washington National Monument.[1] These two databases were made up of 68 and 262 vegetation polygons and the final estimated thematic accuracy was 97% and 83%, respectively, based on field accuracy assessment data collected at 64 of the 68 polygons in the first park and at 96 of the 262 polygons in the other.

11.4 Fire Fuel Mapping

After each vegetation database was completed, we collected fire fuel load data at each of the 10 parks. Within each park the data-collection points were stratified by vegetation type to ensure that data would be collected for vegetation types for which we had little or no previous fire fuel data. The number of data-collection points per park ranged from 4 to 101, depending on the size of the park. At each point field crews measured downed woody debris using a modified Brown's transect line technique (Brown, 1974) developed by Shenandoah National Park (Carmichael and Cass, 2001) and an ocular estimation procedure (Burgan and Rothermel, 1984). Additional data that were collected include transect slope measurements, amounts of fine and coarse woody debris intersects, duff and litter depth measurements, canopy cover, average stand height, and height to live crown base (Smith, 2003). Sample forms used to record these data are included in Appendices A and B. On average, it took a two-person field crew 2 hours to take and record downed woody debris and Burgan/Rothermel measurements at each field location. Field plot photos were very helpful in crosswalking the vegetation to the fire fuel models. In future work we will take an additional field photo, looking up at the canopy, to help characterize canopy closure and crown bulk density.

[1] For the other parks, thematic accuracy assessment will be performed for alliance-level vegetation databases to be created in the future.

Analysis of the fire fuel load data included comparing the field data to standard NFFL fire fuel model values following Brown's procedures (1974). We found that fuel loads in the parks were consistently lower than fuel loads reported by Anderson (1982). This is undoubtedly because Anderson's work is based exclusively on data from the western United States, where vegetation and forest characteristics are different from those in the Eastern states. Therefore, we worked closely with NPS personnel to crosswalk vegetation to fire fuel models based on their experience and Anderson's narrative descriptions.

We produced final fire fuel load databases by assigning complacent and available live fuel fire fuel model values to each vegetation polygon. Distinguishing between complacent and available live fuel conditions is important because fire behavior is affected by seasonal differences in vegetation. The available live fuel model represents the fall period when previously unavailable fuels are available due to seasonal curing and drying of vegetation. For example, many shrub fields are considered to be a barrier to fire spread until a critical live fuel moisture threshold is reached. Figure 11.3 shows a completed complacent fire fuel map for the Western Front Unit of Petersburg National Battlefield.

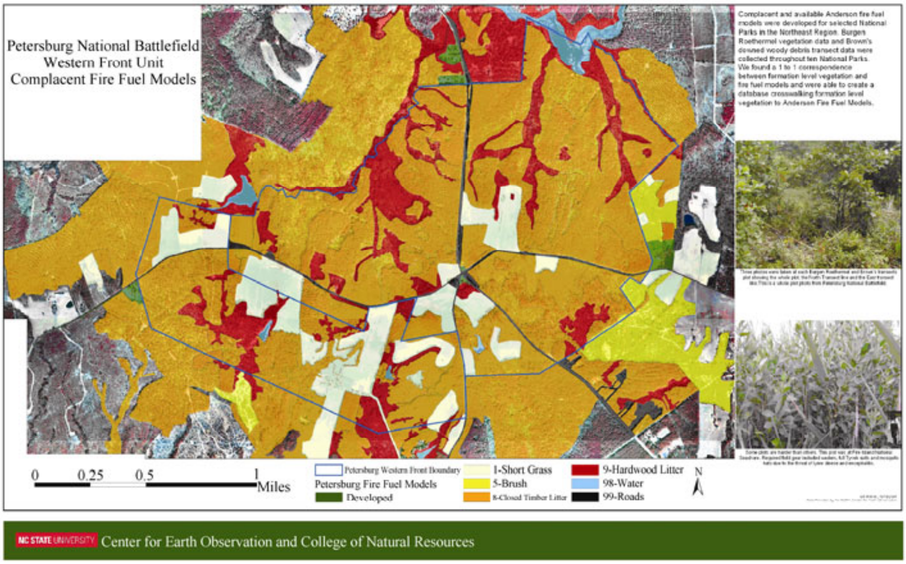

Figure 11.3 Complacent NFFL map of the Western Front of Petersburg National Battlefield

11.5 Discussion

As a result of this research, we have created a fairly comprehensive database of complacent and available fuel loads by vegetation type that could be used to easily crosswalk formation-level vegetation from other areas to NFFL fuel models without the need for the time consuming fire fieldwork (Appendix C). We also have a large database of Brown's and Burgan and Rothermel data that could be used to create custom fire fuel models for Eastern landscapes or, at the least, to generate numbers more useful in determining fire fuel models for national parks in the east. These data have become standard elements in the new fire behavior modeling program of the National Interagency Fire Center.

Based on our experience, we strongly recommend collecting airborne GPS and IMU data with aerial photography that will be used to create digital orthophoto mosaics. Use of these data, as opposed to external reference sources such as USGS digital orthophoto quadrangles (DOQQs), for ground control substantially reduces the time required to create the mosaics and increases their positional accuracy.

Table 11.2 compares the horizontal positional accuracy of four mosaics orthorectified with airborne GPS and IMU data with the positional accuracy of four mosaics orthorectified with DOQQs. The first four mosaics shown in Table 11.2 were orthorectified with airborne GPS and IMU data that were collected at the time the photography was acquired. The other four mosaics were orthorectified using external reference sources such as DOQQs and hand selected ground control points. The externally referenced DOQQS have a much poorer average accuracy. Additionally, the use of airborne GPS and IMU data substantially decreases the time needed to create an orthophoto mosaic because there is no need to place manual tie points or manual ground control points. Finally, airborne GPS/IMU data have been essential for creating mosaics in areas with little or no development, which describes many of our National Parks. When using DOQQs or other external reference sources, we must find recognizable, accurate landmarks throughout the entire area for control. With largely forested and/or uninhabited areas, this is often very difficult, if not impossible. The use of airborne GPS and IMU data eliminates this issue.

Table 11.2 Comparison of horizontal positional accuracy of mosaics orthorectified with airborne GPS and IMU data versus external reference source data

Park	Photography	Horizontal Positional Accuracy (m)	
		RMSE X	RMSE Y
Mosaics orthorectified with airborne GPS and IMU data:			
APCO	Leaf-on (Fall 2001)	0.859952	0.756570
GEWA-1	Leaf-on (Fall 2001)	1.068192	1.276164
GEWA-2	Leaf-off (Spring 2002)	0.826132	0.908170
HOFU	Leaf-off (Spring 2002)	1.188310	0.764670
Average		**0.985647**	**0.926392**
Mosaics orthorectified with external reference source data:			
PETE-MU	Leaf-off (Spring 1992)	1.624120	2.811615
PETE-FF	Leaf-off (Spring 1992)	1.885895	3.674856
VAFO	Leaf-on (Fall 1999)	1.184401	2.894345
APCO	Leaf-off (Fall 2000)	0.603000	2.415000
Average		**1.324354**	**2.948954**

Appendix A

Brown's Transects Field Data Collection Sheets

NCSU Vegetation Map Fuels Inventory Data Sheet

Plot ID: ________ District: __________ Date: ___/___/___

Recorder (s): ________________________ Photo Numbers: _____________ Total # Taken: _____

Transect Lengths (ft): 0-0.25______ 0.25-1: ______ 1-3 ______ 3+r: ______

UTMs: _________________ e _________________ n _________________ +/-m

NORTH
Compass

Direction ______

Slope ______%

[illegible]			Diameter (in)			Litter and Duff Depth						
0-0.25" (1-hr)	0.25-1" (10-hr)	1-3" (100-hr)	3+s (1000-hr)	3+r		L	D	Note		L	D	Note
					1				25			
					5				30			
					10				35			
					15				40			
					20				45			

NOTES:

EAST
Compass

Direction ______

Slope ______%

[illegible]			Diameter (in)			Litter and Duff Depth						
0-0.25" (1-hr)	0.25-1" (10-hr)	1-3" (100-hr)	3+s (1000-hr)	3+r		L	D	Note		L	D	Note
					1				25			
					5				30			
					10				35			
					15				40			
					20				45			

NOTES:

1

CANOPY COVER	
Overstory	
Can. Code:_____(%)	
Species	% Species

Canopy Codes: 1 = 0-20, 2 = 21-50, 3 = 51-80, and 4 = 81-100

HEIGHT TO LIVE CROWN BASE (FT) SEE FIGURE 1				
	Bottom	Base	Ht Lv Crwn	Notes
Canopy				

Height (**Ht Lv Crwn**)= **Bottom** of the live crown + **Base** of the tree
(% = Feet) and degrees actually = Feet

AVERAGE TREE HEIGHT (FT) SEE FIGURE 2				
	Top	Base	Height	Notes
Canopy Distance:_____				

Height = **Top** of the tree + **Base** of the tree *(distance is 100', 50', 66', or 33')

Formation for the plot area:___________

Figure 1

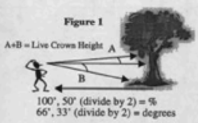

100', 50' (divide by 2) = %
66', 33' (divide by 2) = degrees

Figure 2

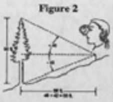

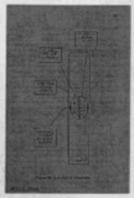

2

Appendix B

Burgan Rothermel Field Data Collection Sheets

16

Figure 9. Burgan and Rothermel Datasheet (front)

Fuel Data Entry Form
Shenandoah National Park

District:__________ Plot:__________

Recorders:__________ Date:__________

UTMs:__________e__________n__________+/-m

Grass

Model Type 1. Dynamic
2. Static

Grass Type 1. Fine – colonial bent, poverty, oat grass
2. Medium – fescue, orchard, japanese bromegrass
3. Coarse – sedges and rushes
4. Very Coarse – sawgrass, tall oatgrass

Bulk Density Class (1-6)________

Total Grass Load (0-30 tons/arce)________ or Grass Depth (0-10 ft)________

Dynamic Models enter maxium % that can be live (0-100%)________

Static Models enter current % live (0-100%)________

Percentage of area covered by grass (0-100%)________

Shrub

Shrub Type 1. Fine stem, thin leaves – Huckleberry, Gooseberry
2. Medium stem, thin leaves – Chiquapin, Alder, Spicebush
3. Medium stem, thick leaves – Ceanothus, Vaccinium
4. Densley packed fine stems and leaves – Spirea, Rubus
5. Thick stems and leaves – Mt. Laurel, Rhododendron

Bulk Density Class (1-6)________

Total Shrub Load (0-80 tons/acre)________ or Shrub Depth (0-10 ft)________

Percentage of total shrub load in each size class. Enter as whole % (must tot. 100%)
1. 1-HR dead (0-1/4 inch) ________
2. 10-HR dead (1/4-1 inch) ________
3. 100-HR dead (1-3 inches) ________
4. Live leaves and twigs (0-1/4 inch) ________

Percentage of area covered by shrubs (0-100%) ________

Oils and Waxes Yes or No

NOTES

17

Figure 10. Burgan and Rothermel Datasheet (back)

Plot:__________ Date:__________

Litter

Litter Source 1. Conifers
2. Hardwoods ________
3. Both but atleast 30% of lessor type

Needle length if conifers or both (1-2) ________
1. Medium/ Long
2. Short

Litter Compactness 1. Loose (freshly fallen) ________
2. Normal
3. Compact (older compressed)

Total litter load (0-100 tons/acre) ________
or
Litter Depth (0-5ft) (ft=cm/30.48) ________

Percentage of total litter load in each size class. Enter as whole % (must tot. 100%)
1. 1-HR (0-1/4 inch) ________
2. 10-HR (1/4-1 inch) ________
3. 100-HR (1-3 inches) ________

Percentage of area covered by litter (0-100%) ________

NOTES

Appendix C

Formation-Level Vegetation and Associated Fire Fuel Models

	Fire Fuel Model	
Formation-Level Vegetation Class	**Complacent**	**Available Live**
NVCS formation codes:		
I.A.4.N.a	8	9
I.A.8.C.x	8	9
I.A.8.N.b	8	9
I.A.8.N.c	8	9
I.B.2.N.a	9	9
I.B.2.N.d	9	9
I.B.2.N.e	9	9
I.B.2.N.g	9	9
I.C.3.N.a	8	9
I.C.3.N.b	8	9
I.C.3.N.d	8	9
II.A.4.N.a	8	9
II.A.4.N.b	8	9
II.A.4.N.f	8	9
II.B.2.N.a	9	9
II.B.2.N.f	9	9
III.A.2.N.a	5	6
III.A.2.N.f	5	5
III.A.2.N.g	5	5
III.B.2.N.a	5	6
III.B.2.N.d	5	5
III.B.2.N.e	6	6
III.B.2.N.f	5	5
III.B.2.N.g	6	6
III.B.2.N.h	1	1
IV.A.1.N.a	2	3

(Continued)

	Fire Fuel Model	
Formation-Level Vegetation Class	**Complacent**	**Available Live**
IV.A.1.N.b	5	5
IV.A.1.N.g	5	5
IV.B.2.N.a	5	5
V.A.5.N.c	1	1
V.A.5.C.x	1	1
V.A.5.N.c	1	1
V.A.5.N.e	1	1
V.A.5.N.k	1	1
V.A.5.N.l	1	1
V.A.5.N.n	1	1
V.A.7.C.a	1	2
V.B.2.N.d	1	3
V.B.2.N.g	1	3
V.C.2.N.a	1	3
VI.B.1.N.c	1	1
V.I.C.2.N.a	98[1]	98
VII.A.2.N.a	1	1
VII.C.2.N.d	98	98
VII.C.4.N.d	98	98
Water	98	98

References

Anderson Hal E, (1982), Aids to determining fuel models for estimating fire behavior. USDA Forest Service General Technical Report INT-122. Ogden, Utah. 22

Brown JK, (1974), Handbook for inventorying downed woody material. USDA Forest Service General Technical Report INT-16. Ogden, Utah. 24

Burgan RE, Rothermel RC, (1984), BEHAVE: Fire prediction and fuel modeling system-FUEL subsystem. USDA Forest Service General Technical Report INT-167. Ogden, Utah. 126

Carmichael BJ, Cass W, (2001), Vegetation Fuel Mapping Protocol. SHEN-N-021.001. Assessment of Vegetation Communities

[1] 98 is a FARSITE code for water.

Devine Hugh A, William A. Millinor, Mark P. Smith, (2003), Wildfire GIS research and technical support. Unpublished final technical report for Task Agreement 003, Cooperative Agreement 4560C0027. Raleigh, NC. 9

Environmental Systems Research Institute (ESRI), National Center for Geographic Information and Analysis (NCGIA), and The Nature Conservancy (TNC) November 1994. Accuracy assessment procedures, NBS/NPS Vegetation Mapping Program. Retrieved October 2001 from http://biology.usgs.gov/npsveg/aa/aa.html

ESRI, (2004), ArcMap 9.0. San Diego, CA: Environmental Systems Research Institute

Erdas, (2004), Imagine v8.7. Atlanta, GA: Leica Geosystems Geospatial Imaging, LLC

ER Mapper, (2004), ER Mapper 6.4. San Diego, CA: Earth Resource Mapping

FARSITE, (2004), FARSITE. Missoula, MT: Systems for Environmental Management. Retrieved 2004 from http://farsite.org/index.php?option=com_content&task=category&sectionid=2&id=8&Itemid=25

Federal Geographic Data Committee, (FGDC), June 1997. Vegetation classification standard (FGDC–STD–005). Retrieved October 2001 from http://www.fgdc.gov/standards/status/sub2_1.html

Federal Geographic Data Committee, (1998a), Content standard for digital geospatial metadata (FGDC-STD-001-1998). Retrieved October 2001 from http://www.fgdc.gov/metadata/contstan.html

Federal Geographic Data Committee (FGDC), (1998b), Geospatial positioning accuracy standards, Part 3: National Standard for Spatial Data Accuracy. (FGDC-STD-007.3-1998). Retrieved October 2001 from http://www.fgdc.gov/standards/status/sub1_3.html

Grossman DH, Faber-Langendoen D, Weakley AS, Anderson M, Bourgeron P, Crawford R, Goodin K, Landaal S, Metzler K, Patterson KD, Pyne M, Reid M, Sneddon L, (1998), International classification of ecological communities: terrestrial vegetation of the United States. Volume 1. The National Vegetation Classification System: development, status, and applications. The Nature Conservancy, Arlington, Virginia, USA

Leica, (2004), Leica Photogrammetry Suite. Atlanta, GA: Leica Geosystems Geospatial Imaging, LLC

Leica, Stereo Analyst, (2003), Stereo Analyst. Atlanta, GA: Leica Geosystems Geospatial Imaging, LLC

Lizardtech, (2001), MrSID Geospatial Encoder 1.4, Seattle, WA: Celartem Technology Inc

Minnesota Department of Administration, Office of Geographic and Demographic Analysis. Positional accuracy handbook: using the national standard for spatial data accuracy to measure and report geographic data quality. http://server.admin.state.mn.us/resource.html?Id=1852 (27, September, 2005)

Minnesota Governor's Council on Geographic Information and Minnesota Land Management Information Center. October 1999. Positional accuracy handbook, using the National Standard for Spatial Data Accuracy to measure and report geographic data quality. Retrieved October 2001 from: http://server.admin.state.mn.us/resource.html?Id=1852

National Interagency Fire Center (2005) http://www.nifc.gov/fireinfo/2004/ (27 September, 2005)

SAS (2004) JMP Statistical Discovery Software 5.1, Cary, NC: SAS Institute Inc

Smith M P, (2003), Predicting fuel models and subsequent fire behavior from vegetation classification maps. M. S. thesis, North Carolina State University. 141 pp. http://www.lib.ncsu.edu/theses/available/etd-08122003-152132/

Trimble, (2004), GPS Pathfinder Office Software 3.0, Sunnyvale, CA: Trimble Navigation Limited

United States Geological Survey (USGS), (2004), Tools for creation of formal metadata, a compiler for formal metadata. Retrieved June 2004 from http://geology.usgs.gov/tools/metadata/tools/doc/mp.html

USGS, NED. Seamless Data Distribution. http://seamless.usgs.gov/website/seamless/viewer.php

12 Diurnal and Seasonal Cycles of Land Fires from TRMM Observations

Yimin Ji
Wyle Information System, 1651 Old Meadow RD, McLean, VA 22102, USA
Email: yimin.ji-1@nasa.gov

Erich Franz Stocker
NASA/GSFC, Code 610.2, Greenbelt, MD 20771, USA
Email: Erich.F.Stocker@nasa.gov

Abstract This Chapter summarizes methodologies of detecting land fires from the TRMM/VIRS measurements. The TRMM science data and information system (TSDIS) fire products include global images of daily hot spots and monthly fire counts at $0.5°\times0.5°$ resolution, as well as text files that details necessary information of all fire pixels. These products have been archived since January 1, 1998. Diurnal and seasonal cycles of TRMM land fire products in the Eastern United States, Africa, as well as the South America and Asia, are discussed and compared to other satellite products. Statistical methods were applied to the TSDIS fire products as well as to the total ozone mapping spectrometer (TOMS) aerosol index products for a period of seven years from January 1998 to December 2004. The variability of global atmospheric aerosol is consistent with the fire variations during this period. The TRMM fire products were also compared to the coincident TRMM rainfall and other rainfall products to investigate the interaction between rainfall and fire.

Keywords Land fires, diurnal and seasonal cycles, TRMM

12.1 Introduction

During the last several decades, satellite fire products have been playing an increasingly important role in the environment monitoring and predictions. The visible infrared spin scan radiometer and atmospheric sounder (VAS) on board the geosynchronous operational environmental satellites (GOES) has been used to monitor biomass burnings in many selected regions since 1980 (Dozier, 1981; Matson and Dozier, 1981). The GOES/VAS provides unique high temporal resolution products that are useful in determining the diurnal variations of intense fires. But the coarse spatial resolution (4 – 13.8 km at nadir) of the products can significantly affect the accuracy of locations and extents of the fire.

The advanced very high resolution radiometer (AVHRR) of the national oceanic and atmospheric administrator (NOAA) satellite series has been able to provide fire monitoring at a higher spatial resolution (1.1 km at nadir) for various areas (Flannigan and Vonder Haar, 1986; Kaufman et al., 1990; Justice et al., 1996). Unfortunately, the full resolution AVHRR data (LAC) are only recorded for selected regions. The available daily AVHRR data is the reduced resolution Global Area Coverage (GAC) for which every third scan of the full resolution orbit data is processed and four out of every five pixels along the third scan are averaged. Therefore, the GAC has a resolution of 1.1×4.4 km at nadir with a 3 km gap between pixels across the scan. While the long history and global coverage of GAC data are very attractive for the study of seasonal cycle and interannual fire variability, the GAC re-sampling scheme would result in unreliable characterization as well as bias in the detection of fire. Since there is no long-term global GAC fire product readily available, substantial efforts may be needed to further analyze the quality of GAC fire.

Pioneering studies based upon GOES/VAS and NOAAA/AVHRR data have provided scientific fundamentals on fire retrieving using remote sensed data. New network techniques have demonstrated the potential for providing real time and long term fire products using operational satellites. The satellite fire detection has been further advanced due to the recent launch of Terra and Aqua. The sophisticated MODIS is on board both Terra (EOS AM-1) and Aqua (EOS PM-1). The MODIS 1 km 4 μm high gain channel with a saturation level of 500 K is specifically designed to improve the fire detection (Kaufman and Justice 1998). MODIS data have been available since early 2000. The MODIS thermal anomalies product provides fire occurrence (day/night), fire location, the logical criteria used for the fire selection, and an energy calculation for each fire. The product also includes composite 8-day-and-night fire occurrence (full resolution), composite monthly day-and-night fire occurrence (full resolution), gridded 10 km summary per fire class (daily/8-day/monthly), and a gridded 0.5° summary of fire counts per class (daily/8-day/monthly). Further, the coincident fire observation from high resolution ASTER on board Terra can provide instantaneous validation for MODIS. It is expected that better global fire products may also emerge in the near future from the visible infrared imager radiometer suite (VIIRS) of national polar-Orbiting operational environmental satellite system (NPOESS) and the NPOESS preparatory project (NPP). Fire is one of the major parameters in both EOS and NPOESS missions. Other satellite sensors being used for fire detection include defense mapping satellite program (DMSP), Landsat Thematic Mapper, the advance along track scanning radiometer (AATSR) onboard the European Space Agency's ENVISAT-1.

While the main objective of tropical rainfall measuring mission (TRMM) is to improve observations and understanding of the tropical rainfall variability

(Kummerow et al., 1998), the visible infrared scanner (VIRS) on board the TRMM, one of the three primary TRMM sensors, is similar to the NOAA/AVHRR. The VIRS data are well calibrated and recorded at its full resolution (2.11 km at nadir, 3.02 km at edge of scan) globally. Therefore, TRMM/VIRS provides the capability of producing a continuous global fire data set over tropics and subtropics. The local overpass time of TRMM satellite drift each day completing a daily cycle in 46 days. This feature provides a good opportunity to derive mean diurnal cycles for land fires over tropics. However, a diurnal cycle aliasing may seriously affect the retrieval of seasonal and intra-seasonal variations.

This Chapter summarizes methodologies of detecting land fires from the TRMM/VIRS measurements. The TRMM science data and information system (TSDIS) fire products include global images of daily hot spots and monthly fire counts at $0.5^\circ \times 0.5^\circ$ resolution, as well as text files that details necessary information of all fire pixels. These products have been archived since January 1998. Diurnal and seasonal cycles of TRMM land fire products in the Eastern United States, Africa, as well as the South America and Asia, are discussed and compared to other satellite products. Statistical methods were applied to the TSDIS fire products as well as to the total ozone mapping spectrometer (TOMS) aerosol index products for a period of seven years from January 1998 to December 2004. The variability of global atmospheric aerosol is consistent with the fire variations during this period. The TRMM fire products were also compared to the coincident TRMM rainfall and other rainfall products to investigate the interaction between rainfall and fire.

12.2 TSDIS Fire Algorithms

Using measurements of VIRS 3.75 μm and 11 μm bands, the TSDIS fire product algorithm was built on heritage algorithms of NOAA/AVHRR (Kaufman et al., 1990; Flasse and Ceccato, 1996). The TRMM/VIRS and NOAA/AVHRR have five channels with similar center wavelengths and bandwidths across visible and infrared spectrums (0.63 μm, 1.61 μm, 3.75 μm, 10.8 μm, and 12 μm). VIRS scans a 45° swath with a 2.11 km instantaneous field of view (IFOV) at nadir and 3.02 km IFOV at the edge of scan from the non-sun-synchronous 350 km TRMM orbit. The VIRS geometric registration has an uncertainty about 0.5 – 0.8 of the pixel size. VIRS provides twice daily observation over most of the tropical and subtropical areas (180°W – 180°E and 40°S – 40°N).

The fundamental physics of the fire algorithm using VIRS 3.75 μm and 11 μm bands is the Wien displacement law:

$$\lambda_{\max} = C / T \tag{12.1}$$

where $\lambda_{\max}$ is the wavelength at which the radiation is at a maximum if the radiative temperature is at T. $C = 2{,}898$ μm·K is a constant. Thus, the vegetated surface over tropics and sub-tropics, with a radiative temperature about 300 K, has a peak around the 11 μm band. Fire pixels, with radiative temperatures about 800 K, have a radiative peak around the 3.75 μm band. Therefore, if fires occur in a portion of a pixel, the radiant energy of 3.75 μm band increases much more rapidly than that of 11 μm band, resulting in a larger than normal difference of brightness temperatures between the two bands.

If a large part of a pixel is filled with fires, the 3.75 μm band could be saturated because the saturation temperature of VIRS 3.75 μm band is only around 322 K. We have not observed saturation of the VIRS 11 μm although the saturation temperature of this band is similar to that of 3.75 μm band. The 11 μm band is not as sensitive as the 3.75 μm band to the thermal anomalies happening within a pixel. The saturation temperature is the maximum output brightness temperature for a thermal infrared channel of the sensor. The NOAA/AVHRR sensors have saturation temperatures between 320 K – 330 K. ATSR, which is designed to measure seas surface temperatures, has a saturation temperature of 312 K only. However, the recent MODIS has a saturation temperature of 500 K for 4 μm band.

The TSDIS nighttime algorithm is basically a traditional threshold method using only the VIRS thermal band brightness temperatures (Tbs). Based on careful studies over various regions globally using VIRS data as well as examining the results of AVHRR experiments (Matson and Dozier, 1981; Kaufman et al., 1990), the TSDIS fire algorithm uses the following criteria to detect nighttime fire pixels:

(1) Channel 3 (3.75 μm) is saturated or

(2) Tb3 > 315 K and Tb3-Tb4 > 15 K

In general, only a small portion of a pixel may be occupied by the fire when a fire occurs. Because the environmental Tb3 (Tb3env) is about 300 K and the fire Tb3 is about 800 K, the criteria presented above may reject a pixel that has less than 2% of its area occupied by fire. Compared to the current existing algorithms (Table 12.1), TSDIS algorithm is reasonable. Table 12.1 shows typical threshold of various sensors. For some of these sensors, multi-algorithms may exist.

Table 12.1 Typical Threshold of Sensors

Sensor	Tb3	Tb3-Tb4	Tb3 Saturation	IFOV
AVHRR	>316 K	>10 K	322 K	1 km
ATSR	>312 K		312 K	1 km
MODIS	>315 K	>10 K	500 K	0.5 km
VIRS	>315 K	>15 K	322 K	2 km

The daytime algorithm uses a contextual approach described by Flasse and Ceccato (1996). The contextual approach uses certain threshold to determine a hot spot pixel and then uses various ancillary data and a series of tests to exclude false alarm. The TSDIS daytime algorithm first uses the thermal band Tbs to choose candidate of fire pixels. After that, additional tests are performed to make final choices. These tests use VIRS visible/near-infrared data as well as ancillary data sources.

Compared to the nighttime retrieval, the daytime fire detection is much more difficult and complicated as the 3.75 μm band is affected by solar radiation in many aspects. The reflected solar radiation from the surface may significantly increase the 3.75 μm channel radiances. Studies over desert, open shrub and other bare ground area indicated that the VIRS 3.75 μm band might be saturated when solar radiation was at its maximum. In a vegetated area, the increase in Tb3 due to solar radiation was not as significant. As a result, the TSDIS daytime fire algorithm uses a 1 km resolution (Townshend et al., 1994) global surface type data to exclude bare ground pixels and other thermal anomalies related to the solar radiation and surface properties. The land type data set was generated by the UMD using near nadir AVHRR data. The uncertainty of geometric registration of this data is about 0.8 km. Therefore, significant number of false fire pixels may exist over areas with mixed surface types in summer or spring season.

Another problem for daytime fire retrieval is the occurrence of sun glint. When sun glint occurring, the 3.75 μm pixels become saturated or have Tbs similar to that of fire pixels. The sun glint pixels have been observed from VIRS measurements in the oceanic area. The sun glint can be detected using variations of reflectance of VIRS Channel 1 and Channel 2 (Flasse and Ceccato, 1996; Kaufman and Justice, 1998). Sun glint may also occur in the cloud surface and cloud edges. Discussion of such problems is beyond the scope of this Chapter. In daytime detection, the algorithm also calculates background Tb3 and Tb4 by scanning an area of 25 pixels and 25 scans with the target pixel as the center. The purpose of this calculation is to further exclude false fire pixels. In the final product, a fire pixel may be rejected if the difference between Tb3 and the background Tb3 is less than 8°.

Based on these analyses, the TSDIS daytime fire algorithm uses the following criteria to identify daytime fire pixels:

(1) Channel 3 (3.75 μm) is saturated and Tb4 > 285 K or
Tb3 > 320 K and Tb3-Tb4 > 20 K and Tb4 > 285 K

(2) Pixel is not a bare ground, or open shrub pixel

(3) Tb3-Tb3env > 8 K.

The Tb4 requirement is used to exclude cloud and heavy aerosol pixels. Under these conditions, the algorithm is unable to detect fire pixels. Both criteria 2 and 3 may reject real fire pixels. However, our day/night fire product comparison showed that the fire occurrence under these two conditions was rare while a large number of false fire pixels might be generated without these daytime constrains. Table 12.2 shows typical threshold of various sensors in daytime. However, most important thing for daytime algorithm is to exclude false fire pixels. Except the contextual threshold, manual methods are often used for regional retrieval. Further discussion of daytime false alarm removal will be discussed in Section 12.5.1.

Table 12.2 Daytime Fire Algorithm Comparison

Sensor	Tb3	Tb3-Tb4	Tb3 Saturation	IFOV
AVHRR	>320 K	> 15 K	322 K	1 km
ATSR				
MODIS	>320 K	> 20 K	500 K	0.5 km
VIRS	>320 K	> 20 K	322 K	2 km

12.3 TSDIS Fire Products

TSDIS fire algorithm routinely creates global daily and monthly fire products. The daily product is a hot spot map with VIRS pixel resolution (2.1 km at nadir). The processing of daily products starts as soon as the production of the VIRS L1B files for the current day is completed. There are typically 16 orbits, or L1B files daily. The operational L1B creation lags real-time by about 12 hours. Therefore, the global fire product has a lag time of approximately 14 hours. The daily products include two files. The first file, the basic file of all products, is a text file that details necessary information for all fire pixels. The information includes date, orbit number, pixel number, solar zenith angle, latitude, longitude, UTC time, reflectance of Channel 1 and Channel 2, brightness temperatures and background brightness temperatures of Channel 3 and Channel 4. This text file is then used to create daily global hot spot.

Figure 12.1 shows a typical daily hot spot image of April 12, 2005. The upper panel displays the distribution of global fire pixels. The three lower panels show enlarged area maps over Northern America, Southern America, and the Indonesian area. On this particular day, a large number of fire pixels were detected over the Southeast Asia and sub-Sahara.

The monthly image is a 0.5°×0.5° resolution composite of fire counts for the month. The monthly text files provide information for all fire pixels observed within the month. Any information missed in daily text files due to operational delays is displayed in the monthly file. The monthly product may be useful for understanding of the effect of fires on the variations of aerosol (Hsu et al., 1996) ozone and other greenhouse gases (Levine, 1991). The description of algorithm, as well as the daily and monthly products (image and data) can be downloaded from TSDIS home page or anonymous ftp site: ftp-tsdis.gsfc.nasa.gov in pub/yji/MONTHLY and pub/yji/DAILY. However, as described above, daytime hot spots contained in these files may contain a large number of false fire pixels. A typical way for user to further exclude false alarms is day/night screening. Such screening may reject most false fires in non-fire season. The detailed description of TRMM fire algorithm and products can be found in Ji and Stocker (2002a).

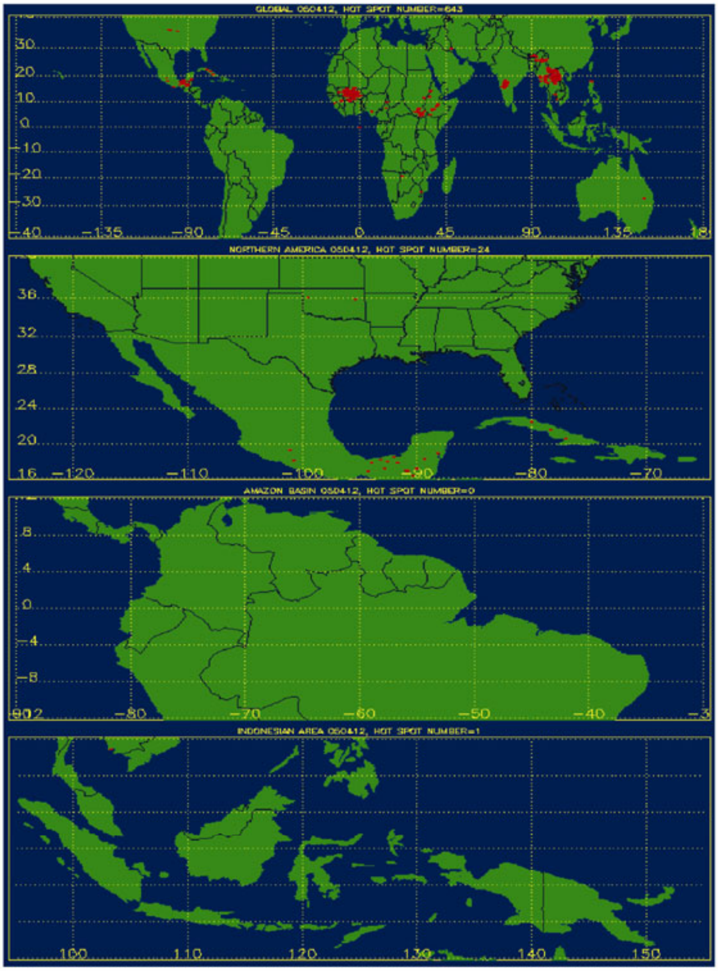

Figure 12.1 TSDIS daily fire image of April 12, 2005

12.4 Seasonal and Interannual Variability

Fires may occur randomly but are constrained by the regional climate and vegetation state. The TRMM yearly mean fire count of 1998 – 2003 years (Fig. 12.2(a)) showed intensive fires in South America, Africa, Australia, Southeast Asia, and Indonesia. Moderate fires occurred in China, Northern and Central America. In February, March, April, and May (FMAM) season, most fires occurred in the Northern hemisphere (Fig. 12.2(b)), especially in Southeast Asia, sub-Saharan Africa and Central America. In June, July, August, and September (JJAS), fires were observed in the southern hemisphere and northern America (Fig. 12.2(c)).

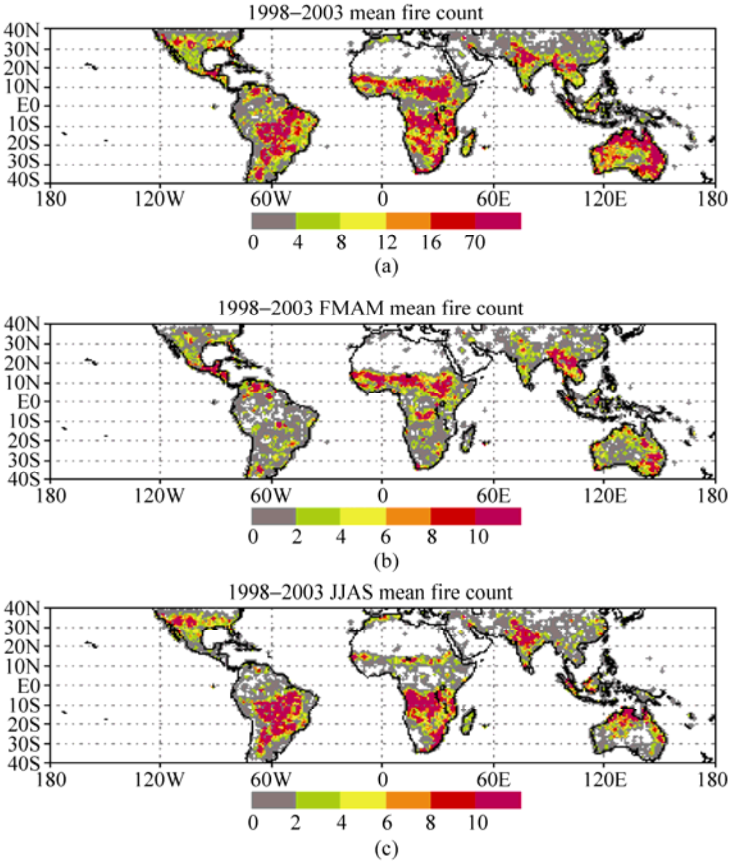

Figure 12.2 Global distribution of fire count (resolution: 0.5°×0.5°). (a) annual mean from 1998 – 2003 (unit: count/year). (b) FMAM mean from 1998 – 2003 (unit: count/4-month). (c) JJAS mean from 1998 – 2003 (unit: count/4-month)

The dominant pattern of aerosol index from TOMS data (Hsu et al., 1996; Ji and Stocker, 2002b) is the Sahara dust (Fig. 12.3(a)). However, the contribution of intensive fires is evident. Since fires occur only in certain season while the Sahara dust is almost a static feature, the magnitude of mean aerosol index in burning areas is significantly smaller than that of the Sahara dust. In FMAM season, the magnitude of aerosol index over fire centers of Southeast Asia and Indonesia is comparable to that over Sahara desert area (Fig. 12.3(b)). Fires in these areas have been very serious in the recent decade (Malingreau, 1990; Giri and Shrestha, 2000). Almost no aerosols were observed over the southern hemisphere in this season. In JJAS season (Fig. 12.3(c)), the strength of aerosol index in southern Africa and Southern America is quite strong but still considerably weaker than that of Sahara dust. There were moderate aerosols in northern America in this season.

The TOMS aerosol index maps (Hsu et al., 1996; Ji and Stocker, 2002b) are generally in agreement with the fire maps except the desert area. Since the smoke

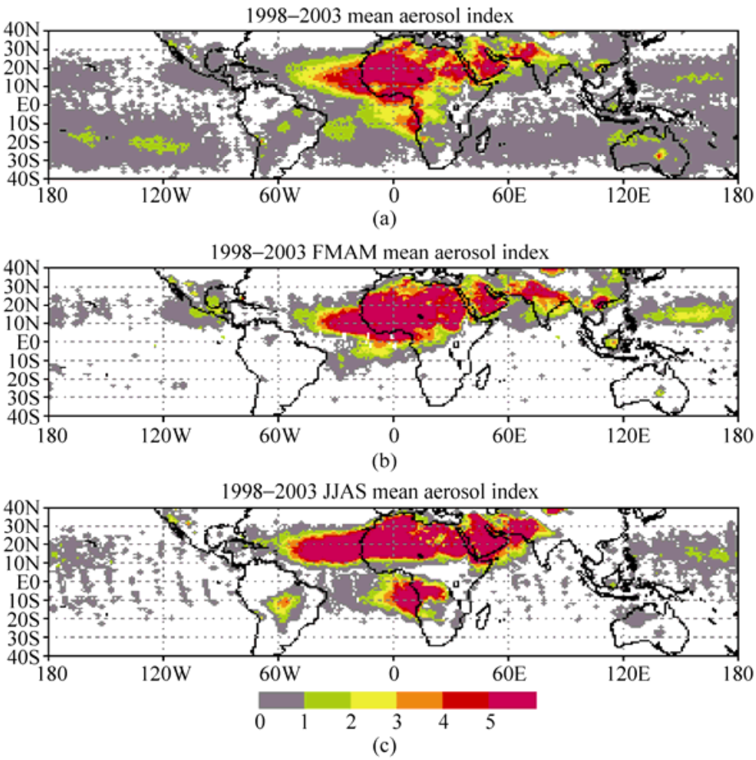

Figure 12.3 Global distribution of aerosol index (resolution 1.25°×1.0°). (a) annual mean from 1998 – 2003. (b) FMAM mean from 1998 – 2003. (c) JJAS mean from 1998 – 2003

can be transported far beyond its fire origin, the unconditional correlation between fire count and aerosol index is only about 0.22. For conditional (only compare pixels where fire exists) cases, the correlation between aerosol index and fire count is as high as 0.55 if the Australia is excluded. In Australia, there were virtually no aerosols observed while substantial fires were observed. This inconsistency may reflect false fire in TRMM fire algorithm for vegetation/desert mixed pixels. The false fire pixels have also been noticed in sub-Saharan and other areas. However, the decreasing sensitivity of TOMS algorithm toward lower altitudes may also contribute to this difference. The depth of smoke in Southwestern Australia fire during winter season may be quite small.

Interannual variations were significant in Indonesia and the Central America. For example, in FMAM 1998, an El Niño season, intensive fires and aerosols in the two regions were observed by TRMM and TOMS, respectively (Figs. 12.4(a) and 12.5(a)). The magnitude of aerosol index in Indonesia and Central America in 1998 FMAM season is comparable to that of Saharan dust. However, in FMAM 1999, a normal season, fires were moderate and no aerosols were observed (Figs. 12.4(b) and 12.5(b)).

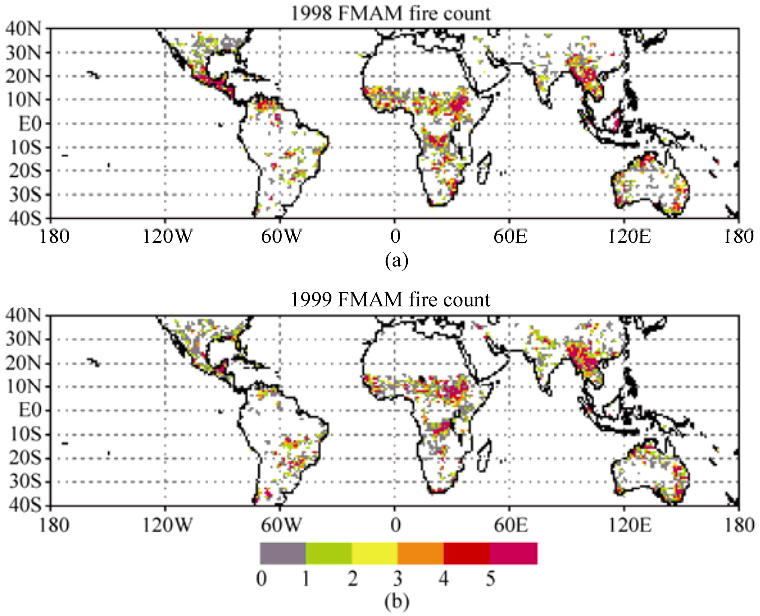

Figure 12.4 FMAM mean fire count (unit: count/4-month, resolution 0.5°×0.5°). (a) 1998. (b) 1999

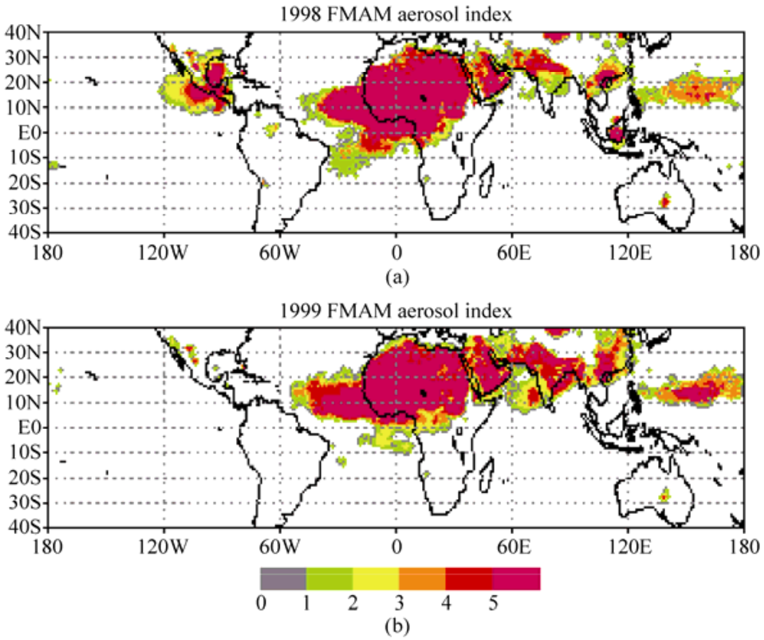

Figure 12.5 FMAM mean aerosol index (resolution 1.25°×1.0°). (a) 1998, (b) 1999

12.5 Diurnal and Seasonal Cycles

12.5.1 Diurnal Cycle of TRMM Observation

In order to use daily hot spot products, the diurnal cycle must be carefully studied because a large number of false fire pixels may exist in the operational data in either burning season or off-fire season, especially over sand/vegetation mixed land cover (Ji and Stocker, 2002). False fire in off-fire season may impact the fire seasonality significantly. We have looked into a number of fire regions for the past six years and found that in fire seasons, the fires are often observed during nighttime during an off-fire season, the satellite observation may show hot spots in daytime but not in nighttime. As shown in Table 12.3, in Southeast Asia, South America, and Africa, the numbers of fire pixels in daytime and nighttime do not differ substantially in fire seasons. The ratios are about 1 – 1.5. In Indonesia, the nighttime fire pixels are outnumbered the daytime fires pixels. However, in non-fire season, there are normally no nighttime fire pixels.

Table 12.3 Comparison of Day/Night Fire Observations

Region	Longitude	Latitude	Time Period	Day Count	Night Count
Indonesia	110°E – 120°E	10°S – 0°S	03/01 – 04/30 1998	152	157
Southeast Asia	90°E – 110°E	5°N – 25°N	02/1 – 03/31 1999	717	612
Southeast Asia	90°E – 110°E	5°N – 25°N	02/1 – 03/31 1999	744	640
South America	70°E – 50°W	25°S – 5°S	07/1 – 08/31 1998	2136	1450
South America	70°W – 50°W	25°S – 5°S	07/1 – 08/31 1999	2149	2078
South America	70°W – 50°W	25°S – 5°S	07/1 – 08/31 2000	658	592
South America	70°W – 50°W	25°S – 5°S	07/1 – 08/31 2001	790	630
Africa	25°E – 35°E	0° – 10°N	01/01 – 03/31 1998	709	559
Africa	25°E – 35°E	0° – 10°N	01/01 – 03/31 1999	850	540

Figure 12.6 shows typical fire diurnal cycle in Southeast Asia from February – March 1998 – 1999 data and South America from July – August 1998 – 2001 data. The maximum fire counts appears between noon to almost mid-night. In East and West USA, the non-fire seasons show strong diurnal cycle with a peak in noon, while the fire seasons have fire peaks between noon and 6 pm and last into midnight (Fig. 12.7). The situation is similar for other areas across the world (Fig. 12.8).

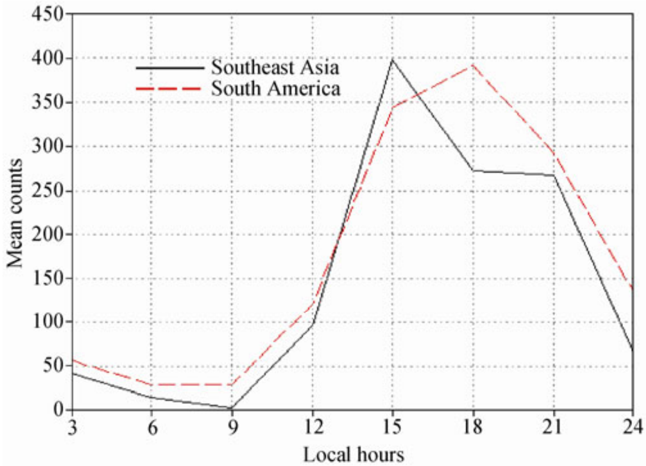

Figure 12.6 Typical diurnal cycles in Southeast Asia and South America

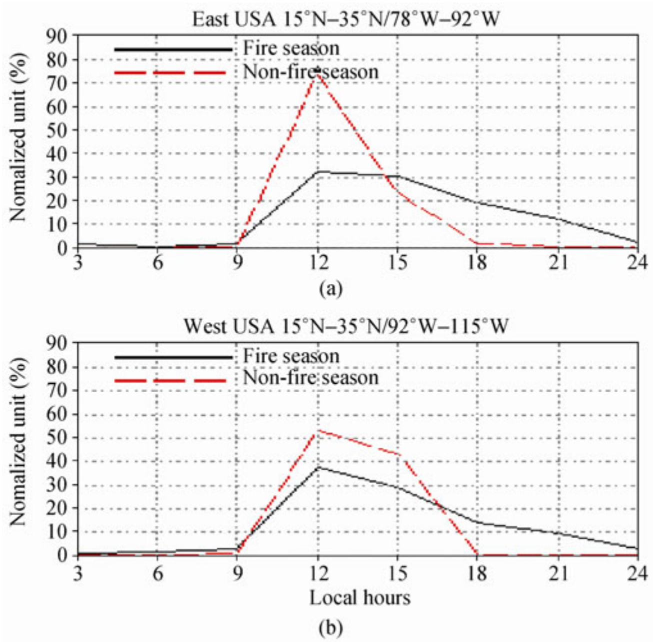

Figure 12.7 Diurnal cycles during fire and non-fire seasons in East USA (a) and West USA (b)

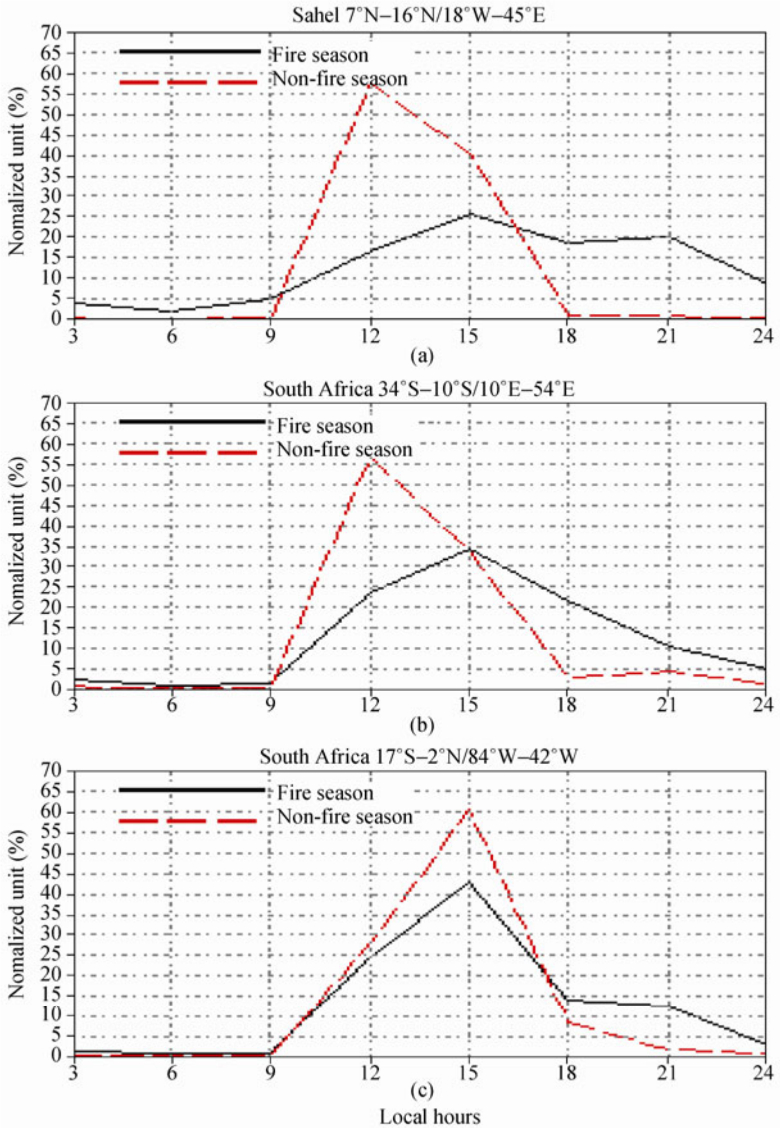

Figure 12.8 Diurnal cycles during fire and non-fire seasons in Sahel (a), South Africa (b) and South America (c)

Different pictures of seasonal cycles may appear by using daytime and nighttime satellite fire data (Fig. 12.9). In the Eastern USA, the nighttime product shows peaks around April for each year, while the daytime product showed much stronger seasonal cycle. In the Western USA, the nighttime fire counts do not show evidence of seasonal cycle, but the daytime counts indicate a strong annual cycle with peaks in summer time.

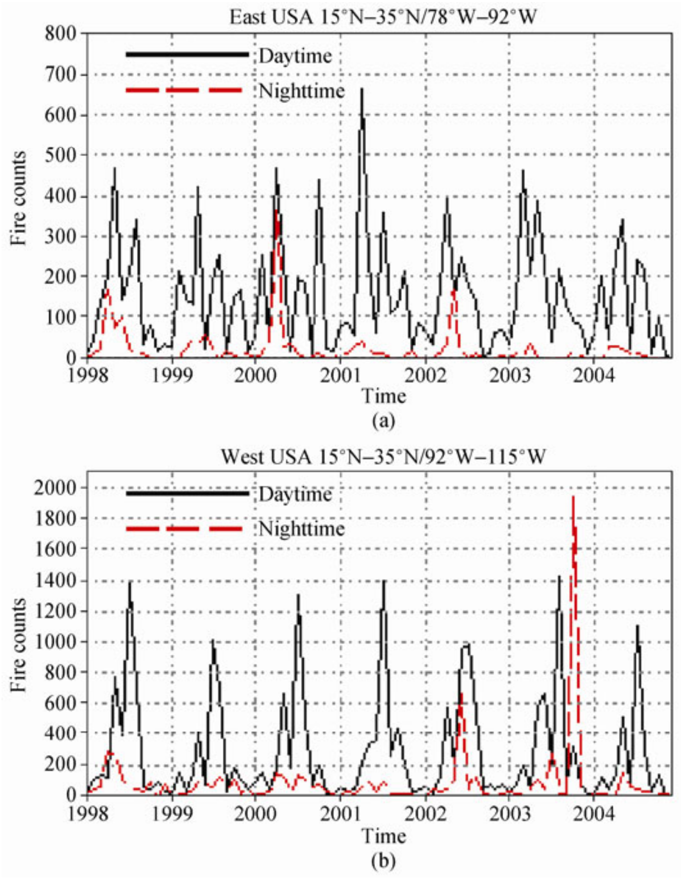

Figure 12.9 Variations of fire counts in East USA (a) and West USA (b)

In order to reduce the effect of aliasing of diurnal cycle on the seasonal and intraseasonal fire variability, a simplified model is developed to transform the TRMM fire data. Only nighttime results are presented in this Chapter to avoid discussions of issues such as false fire and day/night screening although the methods can be used for daytime too. In the prototype, the nighttime period is divided into four particular time windows (Table 12.4) and the model assumes one overpass for each window for all pentads. Multi-overpasses are normalized before processing. The model then calculates the average fire counts per overpass within each window using TRMM observations during major fire seasons. As an example, the ratios for each window and each fire season in Southeast Asia (90°E – 110°E, 5°N – 25°N) are listed in Table 12.4. Since each pentad of this region has observations that cover about 2/3 of the daily cycle, TRMM overpasses for at least one of the four windows in all pentads are guaranteed. Available observations within certain windows and pre-calculated ratio look-up tables are then used to extrapolate fire counts for windows with no observed overpasses.

Table 12.4 Count Per Overpass for Time Windows in Southeast Asia

Year (time)	6 pm – 9 pm	9 pm – 12 pm	12 pm – 3 am	3 am – 6 am
1998 (1/1 – 5/20)	5.10	1.64	1.09	1.11
1999 (1/1 – 4/5)	6.59	1.92	1.42	0.94
2000 (1/1 – 4/10)	2.52	0.26	0.35	0.13
2001 (1/1 – 4/15)	2.35	0.82	0.22	0.10

Time series of TRMM observed fire count (count/day) and transformed fire count (count/day) in Southeast Asia is displayed in Fig. 12.10. In the observed time series, the effect of satellite aliasing can be seen from a number of dips during certain fire episodes. Such dips are largely eliminated in the transformed time series. The fire time series in Southeast Asia are also compared with the Global Precipitation Climatology Project Janowiak and Arkin (1991) rainfall over land. The results (Fig. 12.10) indicate that the fire intraseasonal variability is indeed closely related to the rainfall variations. The intraseasonal fire variability is dominated by fire episodes relative to the rainfall variability rather than a few dips relative to the aliasing. The transformation does not substantial change the pattern of time series. The comparison also indicates that the onset and duration of fire season are also related to the intraseasonal variability of rainfall. The 15 – 30 day and 30 – 60 day intraseasonal oscillations of tropical rainfall have been well defined. Further discussion about the diurnal cycle aliasing can be found in Ji and Stocker (2003).

12.5.2 Seasonal Variation

Genoroso et al. (2003) compared the ATSR nighttime products to the daily fire products from TRMM, AVHRR etc. in nine selected regions. Their analyses demonstrate that in most cases, the nighttime products show a seasonal cycle that is

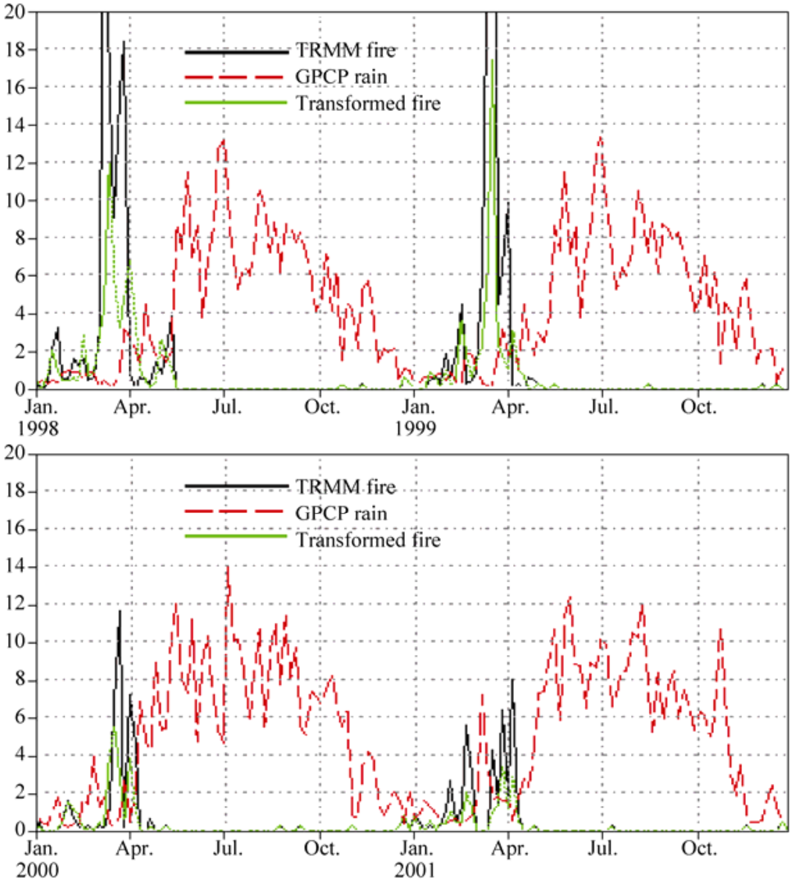

Figure 12.10 Time series of TRMM fire count(count/day, solid line), TRMM transformed fire count (count/day, dotted line), and GPCP rainfall (mm/day) in Southeast Asia (90°E – 110°E, 5°N – 25°N)

consistent with the daily observations. However, they noticed significant discrepancies in biomass seasonality between ATSR nighttime product and TRMM daily product in Sahel and other two selected regions. Since the normalized nighttime fire count units for the three selected regions (Fig. 12.11) showed consistent seasonality, it is believed that the daytime false alarm would be the major contributor to such differences.

We used day/night screening to filter the daytime false alarm. The discrepancies of seasonality between ATSR nighttime data and TRMM daily data noted in Generoso et al. (2003) are avoided (Fig. 12.12).

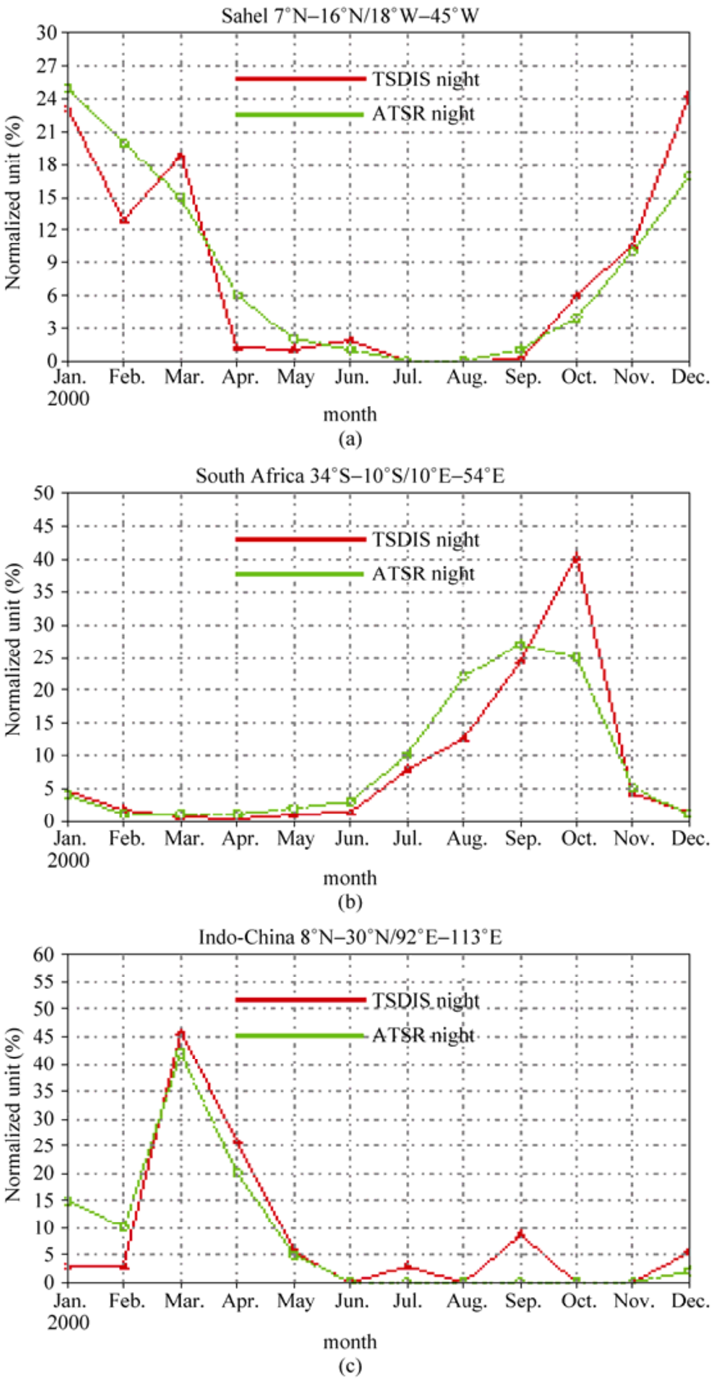

Figure 12.11 Time series of normalized nighttime fire count units for Sahel (a), South Africa (b) and Indo-China (c)

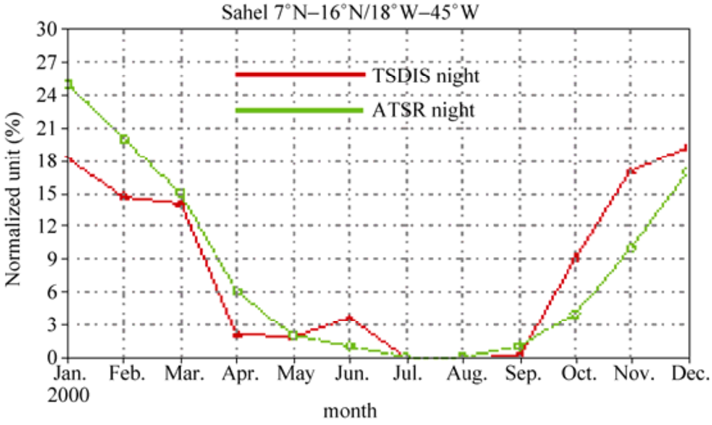

(a)

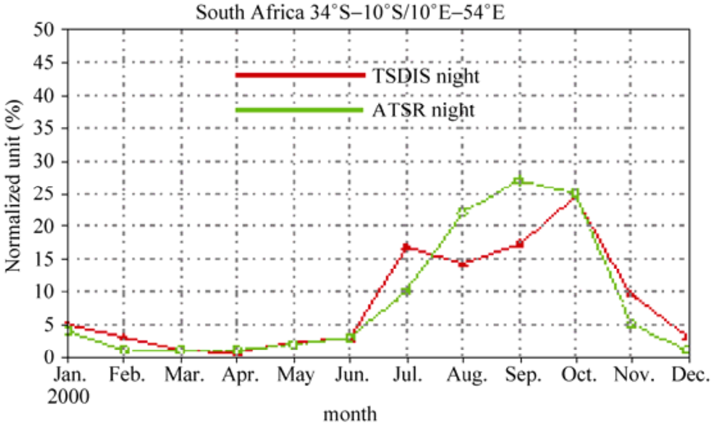

(b)

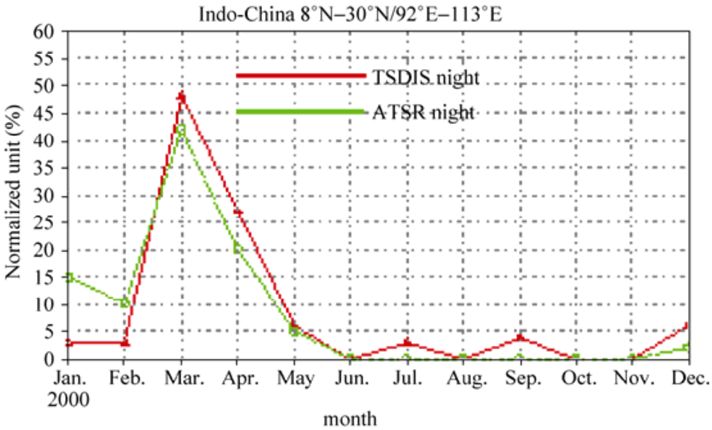

(c)

Figure 12.12 Normalized ATSR nighttime and TRMM daily fire count units for Sahel (a), South Africa (b) and Indo-China (c)

12.6 Summary

The TSDIS fire product has provided global fire information since January 1998 and will continue to do so for the TRMM lifetime. The results presented in this paper indicate a strong seasonal cycle of fire occurrences over Southeast Asia with peaks in March and over South America and Africa with peaks in northern summers. The fire occurrences in the Indonesian region and Central America were dominated by the ENSO cycles. The false alarms from daytime observations may seriously affect the accuracy of diurnal cycle, as well as seasonal and intra-seasonal cycles. A day/night screening method was used to filter out the daytime false alarm and improve the description diurnal and seasonal cycles of satellite observed land fire.

References

Dozier J, (1981), A method for satellite identification of surface temperature fields of sub pixel resolution. *Remote Sensing of Environment*, **11**: 221 – 229

Flannigan MM, Vonder Haar TH, (1986), Forest fire monitoring using the NOAA satellite AVHRR. *Can. J. of For. Res.*, **16**: 975 – 982

Flasse SP, Ceccato PS, (1996), A contextual algorithm for AVHRR fire detection. *Int. J. of Remote Sensing*, **17**: 419 – 424

Hsu NC, Herman JR, Bhartia PK, Seftor CJ, Torres O, Thompson AM, Eck TF, Holben BN, (1996), Detection of biomass burning smoke from TOMS measurements. *Geophysical Research Letters*, **23**: 745 – 748

Janowiak JE, Arkin PA, (1991), Rainfall variations in the tropics during 1986-1989, as estimated from observations of cloud-top temperature. *J. Geophys. Res*. **96**: 3359 – 3373

Ji Y, Stocker E, (2002a), An overview of the TRMM/TSDIS fire algorithm and products. *Int. J. of Remote Sensing*, **23**: 3285 – 3303

Ji Y, Stocker E, (2002b), Seasonal, Intra-seasonal, and Interannual Variability of Land Fires and their effect on the Atmospheric Aerosols. *J. Geophys. Res.*, **107**: 4697, doi: 10 1029/2002JDoo2331

Ji Y, Stocker E, (2003), Reply to comment by Giglio et al. on "Seasonal, intra-seasonal, and interannual Variability of Global Land Fire and Their Effects on Atmospheric Aerosol Distribution". J. of Geophys. Res. **108**: 4697, doi: 10 1029/2003JD004115

Justice CO, Kendell JD, Dowty PR, Scholes RJ, (1996), Satellite remote sensing of fires during the SAFARI campaign using NOAA-AVHRR data. *Journal of Geophysical Research*, **23**: 851 – 863

Kaufman YJ, Justice CO, (1998), MODIS fire products algorithm technical background document. EOS ID# 2741, USA, http://modis.gsfc.nasa.gov/MODIS/ATBD/atbd_mod14.pdf.

Kaufman YJ, Tucker CJ, Fung I, (1990b), Remote sensing of biomass burning in the tropics. *J. Geophys. Res.*, **95**: 9927 – 9939

Kummerow C, Barnes W, Kozu T, Suiue J, Simpson J, (1998), The tropical rainfall measuring mission (TRMM) sensor package. *Journal of Atmospheric and Oceanic Technology*, **15**: 808 – 816

Matson M, Dozier J, (1981), Identification of sub resolution high temperature sources using a thermal IR sensor. *Photo. Engr. Remote Sensing*, **47**: 1311 – 1318

Townshend JR, Justice CO, Skole D, Malingreau JP, Cihlar J, Teillet PM, Sadowski F, Ruttenberg S, (1994), The 1 km resolution global dataset: needs of the International Geosphere-Biosphere Programme. *Int. J. Remote*, **15**: 3417 – 3441

13 Fire Research in the New Jersey Pine Barrens

John L. Hom

Northern Research Station, USDA Forest Service, Newtown Square, PA 19073, USA
Email: jhom@fs.fed.us

Abstract A multi-disciplinary research program to enhance fire research in New Jersey and the Eastern coastal plain has been re-established at the USDA Forest Service—Silas Little in New Lisbon, New Jersey. The goals are to provide fire managers better tools for predicting fire danger, quantifying hazardous fuels and their accumulation rates, and mitigating air quality issues at multiple scales. Research products and applications are described, including a network of towers reporting real-time fire weather data and indices, mesoscale fire weather modeling, vegetation mapping by LIDAR and remote sensing, and validation activities using field plots for estimates of forest productivity, fuel dynamics, and ecosystem modeling. The tower infrastructure is also used to monitor smoke emissions and carbon flux from prescribed fires and wildfires. These data will help determine best management practices for reducing hazardous fuels, maintain cleaner air, and increase carbon sequestration following fires. Close interaction with state and federal fire managers facilitates the integration of new results with current decision support tools.

Keywords Silas little experimental forest, New Jersey, multi-disciplinary studies, fire danger, vegetation mapping, hazardous fuels, smoke emissions, carbon flux, fire management tools

13.1 Introduction

Twenty-three percent of New Jersey's land area (500,000 ha) is occupied by the Pine Barrens, a complex mosaic of upland (47%) and wetland forests (29%), with the balance comprised of primarily developed and agricultural areas (Fig. 13.1; Lathrop and Kaplan, 2004). Much of the upland forests are dominated by highly flammable stands composed of Pitch Pine (Pinus rigida), dense scrub oaks (Quercus marlandica, Q. ilicifolia) and Ericaceous shrubs. Large (+40,000 ha) fires were common prior to fire suppression activities.

Wildfire behavior and fire danger prediction in the New Jersey Pinelands are complex, due to highly dynamic meteorological conditions and the wide range of biophysical factors that prevail in the region. Meteorological conditions are strongly influenced by the Appalachians to the West and the Atlantic Ocean to the East. Frequent passage of frontal systems followed by windy, dry conditions occurs during the spring and fall, and scattered convective thunderstorm activity occurs in the summer. Biophysical factors that impact fire behavior include the presence of sandy, rapidly-draining soils in upland forests, which contrast with wet histosols in wetland forests. All forest types are characterized by moderate rates of productivity (Pan et al. 2006), abundant sub-canopy and understory vegetation (Skowronski et al. 2007), and the rapid accumulation of 1-hr and 10-hr fuels on the forest floor.

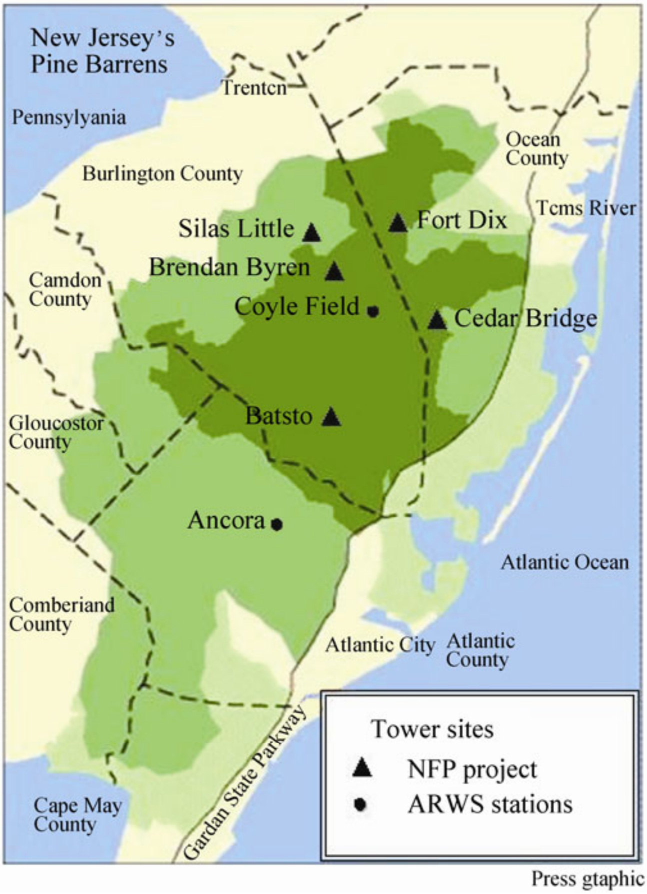

Figure 13.1 The Pinelands of New Jersey. Fire weather stations installed by the NFP project are indicated with a ▲, and new RAWS are indicated with a ●

This combination of meteorological and biophysical factors can produce fire danger conditions and fire behavior that are difficult to predict using standard fire danger indices and models, complicating wildfire suppression activities across the region.

As part of the USDA Forest Service research efforts in New Jersey funded by the national fire plan (NFP), we developed an integrated network of fire weather stations, above-canopy atmospheric sampling towers, remotely sensed estimates of forest composition and structure, and field sampling plots to better estimate fire danger, quantify fuel loads, and evaluate fuel models. Collectively, data also are used to validate predictive fire weather and forest ecosystem models. Our framework provides the basis for a "model forest" system with the infrastructure and tools that can address fire management issues at multiple scales. This framework has been extended to parallel studies in Eastern coniferous forest in Florida, New York, North Carolina and Wisconsin. This Chapter provides the rationale and an overview of the interdisciplinary study and monitoring program initiated in 2002 to support NFP research in the Eastern US.

13.2 Regional Fire Weather and Climate Modeling

Fire managers have identified the need for a more reliable fire danger rating system for the Eastern coastal plain that would augment the national fire danger rating system (NFDRS), because it does not always capture rapid changes in fire weather conditions or the dynamics of fuel moisture content in these ecosystems. Fuel moisture contents can drop dramatically following the passage of cold fronts and the onset of dry, windy conditions during the spring in the Pine Barrens. For example, frontal passage on May 11, 2007 resulted in RH levels >20% and windy conditions, driving a rapid decrease in 10-hr fuel moisture content to <7% (Fig. 13.2). On May 15th and 16th, the Warren Grove wildfire burned 8,200 ha and damaged or destroyed 41 structures. During this period, the NFDRS showed low fire danger, and the keetch byram drought index (KBDI) was reported to be <200 (out of a maximum value of 800; WFAS archive for May 15 and May 16, 2007 at http://www.wfas.net/).

Analysis of long-term (1930-present) weather records and wildfire history data indicates that wildfire occurrence in spring is largely decoupled from fire severity indices such as the KBDI and Buildup Index, commonly used by the New Jersey Forest Fire Service (NJFFS; Skowronski et al., submitted). Rather, wildfires correspond to these events characterized by low RH and high windspeeds, and to a recently- documented seasonal depression in moisture content of Pitch Pine foliage in the spring. Such fire weather conditions are predicted accurately by the MM5 model.

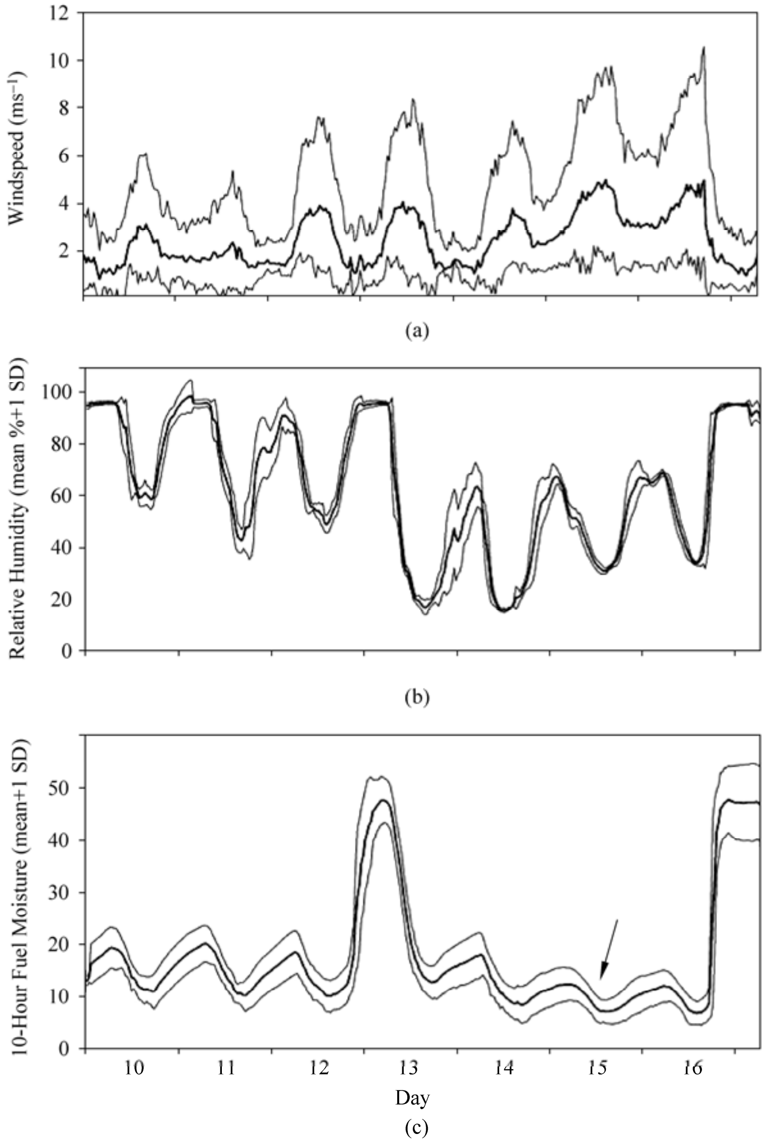

Figure 13.2 The passage of a cold front in mid-May 2007 resulted in windy conditions with very low atmospheric humidity levels, which drove 10-hour fuel moisture contents down rapidly (b). On May 15 – 19th, the Warren Grove Wildfire burned 18,300 acres of Pitch/ Scrub Oak and Pine/Oak Forests, and damaged or destroyed 44 structures

We have established a network of ten canopy level and understory meteorological towers for improved fire weather monitoring (Figs. 13.1 and 13.3). Towers are located in the three major upland forest types (Oak/Pine, Pine/Oak, Pine/Scrub Oak; McCormick and Jones, 1973; Lathrop and Kaplan, 2004, Skowronski et al.

2007), two of which are in high fire risk areas, and measure incoming solar radiation, net radiation, air temperature, relative humidity, wind speed and direction, precipitation and 10-hour fuel moisture. Hourly data are sent via wireless modems to the New Jersey State Climatologist Office, for posting on their website (http://climate.rutgers.edu/stateclim; fast-loading fire weather page at http://climate.rutgers.edu-usfs-monitoring.php), making this information accessible to fire managers and other users in real-time. In addition to these variables, atmospheric turbulence and fluxes of energy, water vapor and carbon dioxide are measured above the forest canopy using sonic anemometers and fast response gas analyzers (see below). A SODAR (Sonic Detection and Ranging) system, which measures 15-minute average windspeed and direction profiles up to 700 m height, also has been operated on a walk-up tower at the Silas Little Experimental Forest since July 2004.

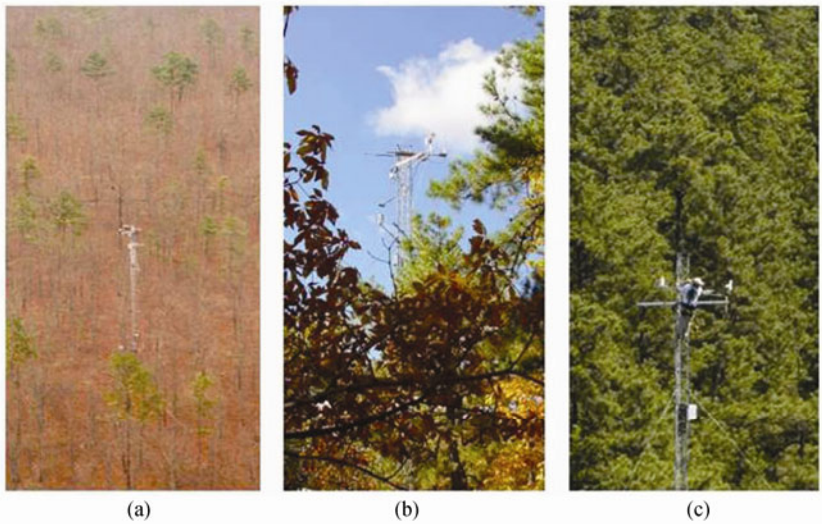

Figure 13.3 Above canopy towers located in (a) Oak/Pine, (b) Pine/Oak, and (c) Pine/Scrub Oak forests in the Pinelands of New Jersey. In addition to real-time fire weather variables, these towers are used to measure eddy fluxes of sensible heat, water vapor, and carbon dioxide above the canopy

The Eastern area modeling consortium (EAMC) in East Lansing, MI has run the MM5 atmospheric mesoscale model twice daily in real time since the summer of 2002 (Heilman et al., 2005). High-resolution fire weather indices (1 km for New Jersey) predicted using the MM5 are available on an operational basis (http://fs.fed.us/fcamms).

The MM5 has proven to be a valuable tool for predicting severe fire conditions. For example, case studies like the 2002 Jake's Branch fire and the 2007 Warren Grove wildfire illustrate its ability to accurately predict fire weather conditions up to 48 hours in advance (Fig. 13.4). MM5 predictions are also being linked to a variety of products such as fuel moisture models, fire behavior models such as FARSITE, and fuel prescription models such as CONSUME.

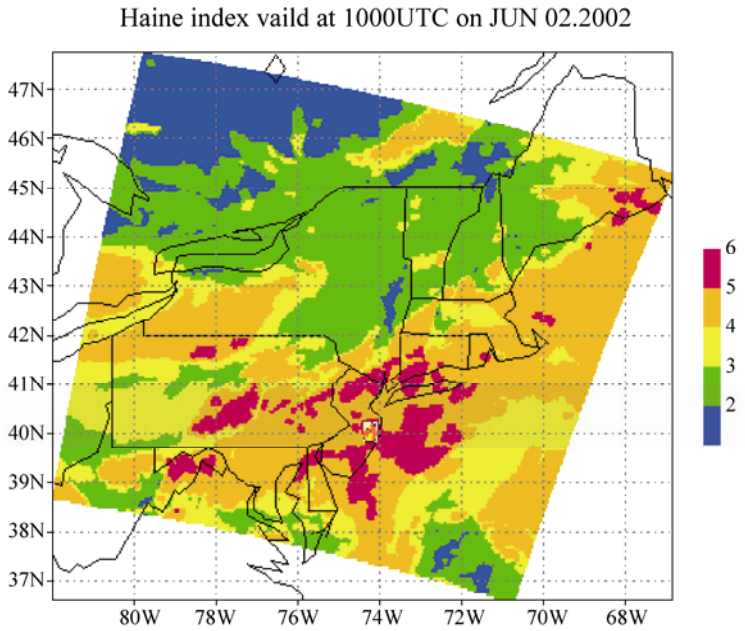

Figure 13.4 MM5 predictions of the Haines index 48 hours previous to a 1,400 acre wildfire in the NJ Pine Barrens. Box with flame indicates site of Jake's Branch fire that closed the New Jersey Parkway

The EAMC simulations are archived every three hours for validation purposes, and data collected by networks such as described above can be used to evaluate MM5 fire weather predictions. For example, landscape level variation in meteorological variables measured from fire weather towers was low for air temperature and RH (mean CV's 2.4% and 4.6%, respectively) and greater for windspeed (mean CV = 21.2%) (Fig. 13.5(a)). The MM5 predicted weather events and trends very well, but hourly data occasionally under predicted daily maximal temperature values (Fig. 13.5(b)). Model evaluation such as this has led to the recent incorporation of more realistic algorithms for surface-atmosphere exchange, and a better fit to measured fire weather variables.

We are developing a new drought stress index, based on forest energy balance measurements made from the three above-canopy towers instrumented to measure eddy fluxes (Figs. 13.1 and 13.3). Specifically, the ratio of sensible heat to absorbed radiation (S/R_{ibs}) is typically < 0.4 during summer daytime hours (10:00 – 17:00) when soil water is abundant. During periods of drought stress, S/R_{ibs} >0.5, and reaches >0.7 during periods of very high to extreme fire danger. Ratios of S/R_{ibs}

are calculated at half hourly intervals, and characterize 1 – 5 km^2 of forest, depending upon measurement height and meteorological conditions.

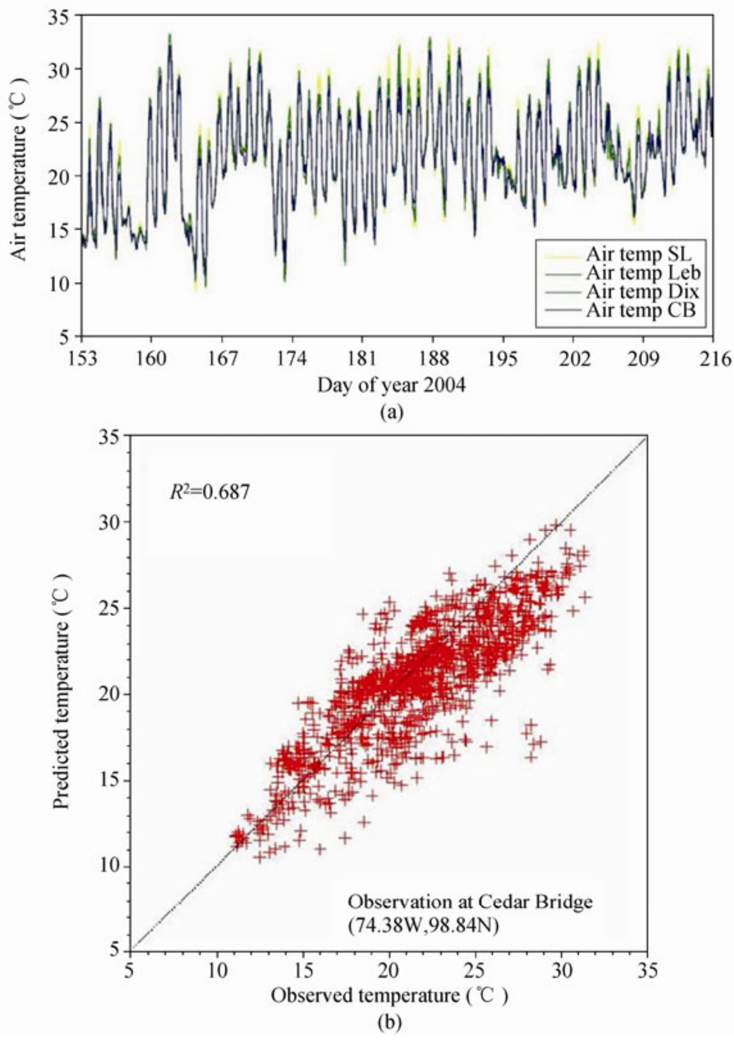

Figure 13.5 (a) Air temperature measured at four of the above-canopy fire weather towers from JD 153 – 215, 2004. (b) Relationship between measured and predicted air temperature

13.3 Fuel Mapping, Forest Biomass and Forest Dynamics

The Eastern LANDFIRE Prototype was initiated in 2004 to enhance the national LANDFIRE effort by developing fire regime maps that accurately characterize the historic fire frequency, severity, and patterning at multiple scales in the Eastern US. This effort complements the ongoing efforts of LANDFIRE-US, to provide a cohesive and consistent national fire management strategy for the conterminous US (Keane et al., 2003). The Eastern Prototype region covers 3.6 million ha, and includes the Delaware River Basin Watershed (DRB) in Pennsylvania, New Jersey, Delaware and New York, in addition to the New Jersey Pine Barrens. Biometric measurements from field plots and LIDAR measurements of biomass and fuel structure have been used to evaluate LANDFIRE models and products for the region.

Vegetation maps derived from LANDSAT and digital orthophotos (Lathrop and Kaplan, 2004), LIDAR (Light Detecting and Ranging) measurements of stand height and canopy density made by helicopter and fixed-wing aircraft (Skowronski et al., 2007, Clark et al, submitted), Forest Inventory and Analysis census data (FIA; http://fia.fs.fed.us), fuel photo series plots (Wright et al. 2007), and our intensive forest inventories have been used to obtain accurate estimates of fuel loads for approximately 500,000 acres of the Pinelands in public ownership. LIDAR metrics are highly correlated with plot-based measurements of canopy height and biomass across the major upland forest types ($r=0.79$ and $r=0.69$, respectively). LIDAR data also are being used to evaluate the arrangement of branches and foliage within the forest to detect the presence of “ladder fuels”, which increase probability of understory fires becoming crown fires (Fig. 13.6; Skowronski et al. 2007). Collectively, these data are used to produce maps of forest structure and fuel loading across the Pinelands, and to evaluate the effectiveness of fuel reduction treatments implemented by the NJFFS. Along with observations of fire behavior, these data are being used to select the appropriate fire behavior models for the region (Scott and Burgan, 2005).

During prescribed fire season in spring, we evaluate fuel reduction treatments in collaboration with the NJFFS and federal fire managers by sampling fuel depths and mass on the forest floor pre- and post-prescribed fire. Prescribed fires typically range from 20 to + 500 ha per fire, and a target of + 10,000 ha is treated per year. On average, 2.2 ± 0.3 t ha^{-1} (mean ± 1 SD, $n=16$) of 1-hr and 10-hr fuels on the forest floor are consumed in a single prescribed fire, and biomass of understory vegetation is reduced considerably. These measurements help quantify fuel reduction treatments for fire managers, and contribute to an understanding of the tradeoffs between hazardous fuel reduction and carbon sequestration by forests in the Pinelands.

Validated ecosystem models, MODIS satellite products and carbon flux measurements have been used to characterize rates of forest productivity and fuel accumulation at the research forest stands with flux towers (Silas Little, Fort Dix, and Cedar Bridge; Figs. 1 and 3; Pan et al. 2006). In conjunction with fuel loading measurements, models and flux measurements lead to an understanding of the dynamics of fuel accumulation. For example, field measurements were similar to model predictions for 1-hr (3.2 ± 0.3 vs. 3.0 ± 0.3 t ha^{-1} yr^{-1}; mean ± 1 SD) and 10-hr (0.6 ± 0.2 vs 0.6 ± 0.1 t ha^{-1} yr^{-1}) fuel accumulation rates.

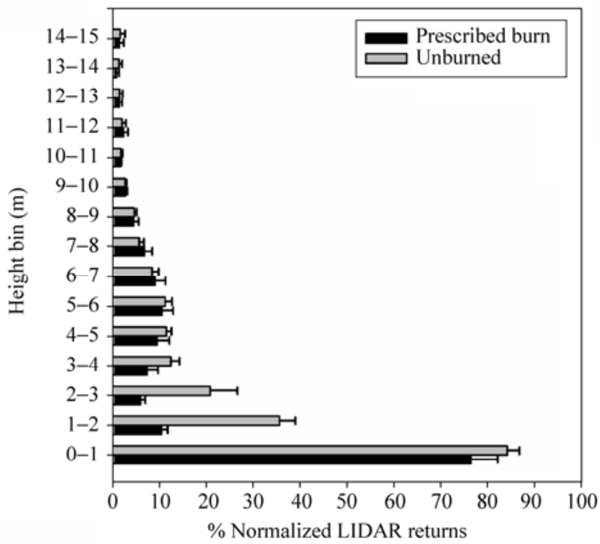

Figure 13.6 Percent normalized LIDAR returns in 1 m height bins in a Pitch Pine/Scrub oak stand near the Cedar Bridge fire tower. The recently burned area was the site of a prescribed fire 2 months previously, and the unburned site has not burned since 1995. Data are binned in 1 m increments, ± 1 SD. Differences between normalized fraction of LIDAR returns are significant for 1 − 2 m and 2 − 3 m height class bins at $P < 0.05$. Data are adapted from Skowronski et al. 2007

LIDAR and plot-based measurements help guide transitions among different fuel models. We compared forest productivity at different scales with MODIS satellite estimates of net primary productivity (NPP), predictions using forest ecosystem models, eddy flux estimates of NPP, and FIA data. We determined that MODIS (MOD17) overestimated NPP in conifer-dominated stands, and underestimated NPP in deciduous hardwood stands in the Eastern Prototype region. We were able to correct the underestimates in coniferous forests using an algorithm for soil water availability, but deciduous forests may need better estimates for physiological parameters (Pan et al., 2006).

13.4 Air Quality

The current network of towers monitoring fire weather and fluxes of energy, water and carbon dioxide can be use to monitor smoke emissions and carbon flux from prescribed fires and wildfires. In conjunction with measurements of fuel consumption during prescribed fires, these data will help determine best management practices for reducing hazardous fuels, maintain cleaner air, and increase carbon sequestration following fires.

We have instrumented a mobile eddy covariance tower to measure carbon dioxide and water fluxes during and immediately following wildfires and prescribed burns. Turbulence, SODAR and fuel consumption data collected during prescribed fires are used in conjunction with BlueSky to model air quality (http://ncrs.fs.fed.us/eamc/products/bluesky/).

The Silas little experimental forest is part of New Jersey's Atmospheric Deposition monitoring network. Wet bulk deposition and air quality monitoring are located at the site. The air quality work will continue at the Silas little experimental forest as part of a Forest Service Research initiative to implement the international cooperative programme (ICP) on Assessment and Monitoring of Air Pollution Effects on Forests Level Ⅱ monitoring protocols (www.icp-forests.org) at selected experimental forests and long term ecological research (LTER) sites to determine the flux of air pollutants, such as ozone, that is taken up by the forests in this region.

In conjunction with particulate research conducted by the NJ Department of Environmental Protection, Rutgers Coastal Ocean Research Laboratory, and the EAMC BlueSky modeling effort, new $PM_{2.5}$ samplers (Met One Inst., E-BAM) have been placed on existing fixed towers and the mobile trailer. The meteorological and SODAR data will be used to run a high resolution WRF mesoscale model with a plume model, CalPuff, to model the distribution of pollen/air pollutants/smoke and the sea-breeze effects on human health and air quality.

We anticipate that there will be a need for air quality and flux research to address the effects of hazardous fuels reductions (under the healthy forest restoration act) and air quality standards ($PM_{2.5}$, ozone) in problem regions such as the mid-Atlantic, and the desire to maximize forest productivity (carbon sequestration) following disturbance.

13.5 Conclusions

A multi-disciplinary research program to enhance fire research in New Jersey and the East has been re-established at the Silas little experimental forest. National Fire Plan (NFP) research has established a regional network of ground plots, meteorological stations, above-canopy sampling towers, RS data layers, and validated weather and forest ecosystem models. This provides a "model forest system" with the infrastructure and tools for an integrated fire research program to address fire management issues in the East.

References

Clark K L, Hom J L, Skowronski N, Duveneck M, Van Tuyl S, Cole J, Patterson M, (2007), Decision support tools to optimize the effectiveness of hazardous fuel reduction treatments (abstract). EastFIRE Conference 2007, June 5 – 8, 2007

Heilman WE, Potter BE, Charney JJ, Bian X, (2005), FIRE-Weather and air-Quality research and product development in the Eastern Area Modeling Consortium. EastFire Conference, 11 – 13 May 2005, Fairfax, VA

Keane RE, Rollins M, Parsons R, (2003), Developing the spatial programs and models needed for the implementation of the LANDFIRE project. In: Second international wildland fire ecology and fire management congress and fifth symposium on fire and forest meteorology; 2003 November 16 – 20; Orlando, FL. Boston, MA: American Meteorological Society. J10D.2. 6 p http://ams.confex.com/ams/FIRE2003/techprogram/program_160.htm

Lathrop R, Kaplan MB, (2004), New Jersey land use/land cover update: 2000-2001. New Jersey Department of Environmental Protection, 35 p. http://www.nj.gov/dep/dsr/landuse/landuse00-01.pdf

McCormick J, Jones L, (1973), The Pine Barrens: Vegetation Geography. Research Report Number 3, New Jersey State Museum, 76

Pan YR, Birdsey R, Hom J, McCullough K, Clark K, (2006), Improved estimates of net primary productivity from MODIS satellite data at regional and local scales. *Ecological Applications*, **16**: 125 – 132

Scott JH, Burgan RE, (2005), Standard fire behavior fuel models: A comprehensive set for use with Rothermel's surface fire spread model. USDA Forest Service General Technical Report RMRS-GTR-153

Skowronski N., Clark K, Hom J. Evaluation of Historic NFDRS indices as predictors of hazardous fire weather in the New Jersey Pine Barrens. Submitted to International Journal of Wildland Fire, EastFire 2007

Skowronski N, Clark K, Nelson R, Hom J, Patterson M., (2007), Remotely sensed measurements of forest structure and fuel loads in the Pinelands of New Jersey. *Remote Sensing of Environment*, **108**: 123 – 129

Wright CS, Ottmar RD, Vihnanek RE, (2006), Stereo photo series for quantifying natural fuels. Volume Ⅷ: Hardwood, pitch pine, and spruce/balsam fir types in the Northeastern United States. PMS 840. Boise, ID: National Wildfire Coordinating Group, National Interagency Fire Center. 91

14 Dead Fuel Loads in North Carolina's Piedmont and Coastal Plain and a Small Scale Assessment of NFDRS Fuel Models

Michael J. Gavazzi
Eastern Forest Environmental Treat Assessment Center
USDA Forest Service, Raleigh, NC 27606, USA
Email: mgavazzi@fs.fed.us

Steven G. McNulty
Eastern Forest Environmental Treat Assessment Center
USDA Forest Service, Raleigh, NC 27606, USA
Email: smcnulty@fs.fed.us

Johnny L. Boggs
Eastern Forest Environmental Treat Assessment Center
USDA Forest Service, Raleigh, NC 27606, USA
Email: jboggs@fs.fed.us

Sara E. Strickland
Eastern Forest Environmental Treat Assessment Center
USDA Forest Service, Raleigh, NC 27606, USA
Email: sstrickland@fs.fed.us

David C. Chojnacky
Department of Forestry, Virginia Tech., Falls Church, VA 22046, USA
Email: dchoj@cox.net

Abstract Dead fuel loads were measured on six distinct forest management compartments in North Carolina's Uwharrie national forest, Croatan national forest and the Alligator River National Wildlife Refuge. Average 1-, 10-, 100- and 1000-hour fuels loads were analyzed within and between each of the three research areas and compared to National Fire Danger Rating System fuel model estimates of dead fuel load. Mean dead fuel load measurements were significantly different within and between most research areas and differences tended to increase with fuel class size. While there was good agreement within and between research areas for woody fuels, the addition of litter and duff generally resulted in larger variability and significantly different dead fuel load measurements. NFDRS fuel load estimates compared well with some classes of measured fuel load, but no one model provided estimates comparable with measured fuel load across all fuel size classes within a site. The models tended to estimate 1- and 10-hour fuels well, but generally underestimated 100- and 1000-hour fuels. Large differences between 100- and 1000-hour fuels were mostly the result of high duff and litter measurements, especially on the sites with deep peat soils. This important component of forest fuel loads may not be well represented in the current NFDRS. As forests become more fragmented and managed for different resource objectives, finer scale fuel load estimates may be necessary to accurately assess fire danger and minimize the loss of life and property.

Keywords Wildfire, fuel load, fuel model, NFDRS, woody material

14.1 Introduction

Wildfires burn only a small percentage of forestland in the southern US every year, but the potential for loss of life and property has increased as urban development moves closer to forested areas, especially those with high fuel loads. Fuel loads are one of the major factors associated with wildfire risk, yet there is little data available to support local and regional estimates. The U.S. Government Accountability Office identified the need for improved fuel data as a prerequisite to meeting the goal of reducing wildfire risk (GAO, 2005). The report concluded that if fuel loads are not reduced there will be an increased risk to communities and ecosystems, and fighting wildfires could cost tens of billions of dollars in coming years. To reduce this threat and comply with the president's healthy forests initiative, land managers need to be able to better identify areas at a high risk of wildfire.

Wildfire danger rating systems have existed since the early 1920's (Schlobohm and Brain, 2002). In 1972 the USDA Forest Service began using the national fire danger rating system (NFDRS) to identify areas at high risk to wildfire and to plan suppression tactics (Deeming and Brown, 1975). NFDRS fuel models are designed to encompass large areas (tens of thousands of acres) and rely on local knowledge of observed or predicted conditions, including fuel load (Schlobohm and Brain, 2002). The original NFDRS was comprised of nine fuel models, but increased to twenty models in 1978 (Anderson, 1982). A drought index was added in 1988 to improve fire danger rating in the southeastern US (Burgan, 1988). The index accounts for litter and duff that serve as fuels when drought conditions progress. The NFDRS dead fuel load estimates double when periods of maximum drought exist.

Under the current system, only one to three fuel models may be appropriate for a given forest cover type. Due to the limited options available from the NFDRS and other fuel models, Scholl and Waldrop, (1999) developed their own fuel loading estimates across eight representative southern pine ecosystems and reported dead fuel loads two to three times greater than those in the NFDRS, depending on the model selected. Litter made up over half of the fine dead fuel load at 6 of the 8 sites. While the NFDRS was never intended to be used at the forest stand level, assumptions about fuel load and fire danger over broad and diverse areas in the South may be underestimating the risk of wildfire for forest stands. As forests become more fragmented and managed to achieve different resource objectives, finer scale fuel load models may be necessary to better assess fire danger.

Dead fuel load in the NFDRS is classified into 1-, 10-, 100- and 1000-hour fuels, and each class is defined by the amount of time, or time lag, that it takes a fuel to reach moisture equilibrium with the environment. The 1- to 100- hour fuels include litter, duff and down deadwood, termed fine woody material (FWM), less than 7.6 cm in diameter. The 1000-hour fuels include duff and down deadwood, termed coarse woody material (CWM), larger than 7.6 cm in diameter. FWM decomposes relatively fast and influences how quickly a fire spreads. Fire managers are primarily concerned with the 1- and 10-hour fuels that influence diurnal changes in wildfire danger as moisture content fluctuates (Schlobohm and Brain, 2002). While the ecological role of CWM in forest ecosystems has been well documented (Harmon et al., 1986; McMinn and Crossley, 1996) there are only a few studies that quantify dead fuel load biomass in southern forest ecosystems (Wendel et al., 1962; Hough and Albini, 1978; Scholl and Waldrop, 1999; Chojnakcy et al., 2004).

With the creation of the National Fire Plan (NFP) in 2000, emphasis was placed on quantifying down deadwood in an effort to identify areas that are at high risk of wildfire and better understand the temporal dynamics of forest fuels. Federal and state agencies, such as the USDA's Forest Service and the multi-partnered LANDFIRE project, are working to provide fine resolution data that will aid in the creation of more accurate fuel load models. While it may be years before this research can be incorporated into a fire danger rating system, the end result will help land managers allocate limited resources toward areas with the greatest wildfire risk. The objectives of this Chapter were to compare dead fuel load estimates across six North Carolina forest communities with different management objectives and to assess NFDRS dead fuel load estimates for these forest types. An assessment of NFDRS dead fuel load estimate accuracy will assist researchers in determining if additional study is needed to better quantify wildfire risk across these important southern US ecosystems.

14.2 Materials and Measures

14.2.1 Site Descriptions

This study was conducted in North Carolina's Alligator River national wildlife refuge, Croatan national forest, and Uwharrie national forest. Prescribed fire is used in each of these forests to reduce understory fuels. Study areas included two pond pine woodlands (commonly called high pocosins), two longleaf-loblolly pine stands, one oak-hickory and one mixed pine hardwood stand.

The Alligator River (AR) national wildlife refuge is located in Dare County and contains a mix of high and low pocosins, pond pine woodlands, hardwood swamps and Atlantic white cedar swamps. Like many managed Coastal Plain forests, much of the area was ditched to promote tree growth. Two 36 hectare research sites were established in 80-year old high pocosin management areas. One area (AR-B) was severely burned during a prescribed fire in 2000 and the other area (AR-NB) has not been burned (NB) in recent memory. Both areas are commonly referred to as high pocosins, but their species composition and structures are more closely related to pond pine woodland (Schafale and Weakley 1990). Each site is dominated by pond pine (pinus serotina Michx.) with lesser amounts of biomass found in swampbay (Persea borbonia L.), sweetbay (Magnolia virginiana L.) and red maple (Acer rubrum L). The dominant understory species is inkberry (Ilex glabra L.), but Vaccinium sp., greenbrier (Smilax sp.) and lesser amounts of fetterbush (Lyonia lucida Lam.) are found throughout both areas. The primary difference between the two sites resulted from the prescribed fire in 2000. This fire crowned many of the pond pine in AR-B, creating large gaps and a thick growth of understory species in the openings. Dead fuel load measurements were collected between June and July 2002 in AR-B, and between December 2002 and January 2003 in AR-NB.

Croatan national forest (CNF) is located in Jones County. Forest land in this Coastal Plain ecosystem is primarily composed of longleaf pine (Pinus palustris Mill.), loblolly pine (Pinus taeda L.) and bottomland hardwoods, with a mixed pine-hardwood transition found between the managed pines and unmanaged bottomland hardwoods. Two longleaf-loblolly pine stands, each with different prescribed burn cycles, were selected as study sites. CNF-3 is a 27 hectare stand on a 3-year burn cycle, with an understory dominated by gallberry (Ilex coriacea Pursh), Vaccinium species, greenbrier, swamp pepperbush (Clethra alnifolia L.) giant cane (Arundinaria gigantean Walt.), waxmyrtle (Myrica cerifera L.) and hardwood saplings. This site was last burned in 2002. CNF-1 is an annually burned stand that comprises approximately 6 fragmented hectares. The understory is dominated by gallberry, fetterbush (Lyonia lucida Lam.), waxmyrtle, and hardwood saplings. Both sites were planted with longleaf pine in the 1930s, and managed for sawtimber. This has created open canopied stands where longleaf and loblolly pine are codominant species. Dead fuel load measurements were collected from both sites in June 2004.

The two sites in Uwharrie national forest (UNF) are located in Randolph and Montgomery counties. UNF is a patchwork of publicly owned lands, surrounding and bordering privately owned lands. As a result of this land fragmentation, wildfire risk at the WUI is an important management concern. Both research sites are representative of typical Piedmont forests. One site (UNF-O) is a 21 hectare, 88-year old oak-hickory mix (O), and the other (UNF-P) is a 77 hectare loblolly pine stand (P) planted in 1964. Loblolly and shortleaf pine (Pinus echinata Mill.) make up approximately 61% of the basal area in UNF-P, with the other 39% comprised of hardwoods. Each site is burned on a 3 – 4 year cycle and dead fuel load measurements were collected from both sites in July 2004.

14.2.2 Methods

Field plots were established on two sites in each research area (UNF, CNF, AR) to measure fuel loads. Protocols followed those used by the USDA Forest Inventory and Analysis Program to measure down woody debris and fuels (FIA, 2005). Field plots at AR and CNF-3 consisted of four 7.3 m radius clustered subplots 35.6 m apart and 0, 120° and 240° from the central subplot. A singular plot design was used at both UNF sites and CNF-1. Hereinafter, plots and subplots will be referred to as plots. Three 7.3 m transects at 30°, 150° and 270° from plot center were used to tally and measure fine and coarse woody material.

FWM was classified as 1-, 10- and 100-hour fuels equating to less than 0.6 cm, 0.6 – 2.5 cm, and 2.5 – 7.6 cm in diameter at the line intersect, respectively. FWM less than 2.5 cm in diameter was tallied along a 1.8 m length of each transect. FWM 2.5 – 7.6 cm in diameter was tallied along a 3.1 m length of each transect. The diameter of FWM was measured along random transects to determine the mean diameter squared for each size class. Down deadwood was classified as CWM if it was greater than 7.6 cm in diameter and 0.9 m in length at the point of intersect along any of the transects. Species, decay class, length, and large and small end diameters were recorded for each piece of CWM. Species decay was classified on a 1 – 5 scale, 1 for undecayed CWM and 5 for heavily decayed CWM.

Litter depth was measured at the end point of each transect and included undecomposed foliage in the A_e soil horizon. Duff was measured at the same point below the litter layer and was defined as partially decomposed litter below the A_e horizon. The percentage of forest floor covered by litter was estimated using a 2.1 m radius mircoplot 90 degrees east and 3.7 m from the plot center. Fine and coarse woody material biomass were combined with litter and duff biomass to estimate dead fuel load in each size class. The 1-hour fuels included litter biomass to a depth of 0.6 cm and 10-hour fuels included litter biomass from a depth of 0.6 – 1.9 cm. 100- and 1000-hour fuels included litter and duff from a depth of 1.9 – 10.2 cm and from 10.2 – 30.5 cm, respectively. These criteria were derived from definitions used in the NFDRS as described by Schlobohm and Brain (2002) and Deeming et al. (1977). In situations where the litter depth did not exceed 1.9 cm, duff biomass was classified as a 100-hour fuel.

Biomass was calculated based on line intercept theory developed by Van Wagner (1968) and de Vries (1973) and later improved upon by Howard and

Ward (1972) and Brown (1974). The basic concept, as detailed by Waddell (2002), is that multiple attributes can be summed across transects to estimate per-unit-area volume. FWM biomass (Eq.14.1) was calculated in tons/acre as;

$$\mathrm{FWM}=\sum_{i=1}^{n}\frac{f\,\mathrm{dia}_i^2\,\rho\,d\,a\,c}{L} \qquad (14.1)$$

where n is the total pieces of FWM tallied per size class and transect, f is the units conversion factor (11.64); dia is the mean squared diameter for each class of FWM (in^2); ρ is the average green specific gravity of species know to exist in each forest type; d is a decay class reduction factor that accounts for biomass loss through decay (assumed to be 0.9); a is the correction factor for orientation (assumed to be 1.13); c, slope correction factor, $=\sqrt{1+(\mathrm{slope}\%/100)^2}$; and L is the transect length (ft). CWM biomass (Eq. 14.2) was calculated in tons/acre as;

$$\mathrm{CWM}=\sum_{i=1}^{n}\frac{f\,(d_s^2+d_1^2)\,\rho\,d\,c}{L} \qquad (14.2)$$

where n is the total pieces of CWM sampled along each transect; f is the units conversion factor (5.8); d_s and d_l are the small and large end diameter squared (in^2) of each piece of CWM measured, respectively; ρ is the green specific gravity of each piece of CWM measured; d is a decay class reduction factor for conifers (class 1 = 1.0, class 2 = 0.84, class 3 = 0.71, class 4 = 0.45, class 5 = 0.35) and hardwoods (class 1 = 1.0, class 2 = 0.78, class 3 = 0.45, class 4 = 0.42, class 5 = 0.35) (Waddell (2002); c and L are the same as for FWM.

Site-specific variables included green wood specific gravity, average diameter for each FWM class, and litter and duff bulk density (Table 14.1). Litter and duff biomass were calculated by multiplying the average depth times site-specific bulk density times the percentage of forest floor covered in litter (unpublished data from Gavazzi and Chojnacky, 2005). Specific gravity values were obtained from Markwardt and Wilson (1935) and Jenkins et al. (2003). If pieces of CWM were

Table 14.1 Site specific parameters for calculating dead fuel load

Site	FWM Diameter Squared [in^2]			FWM Specific Gravity	Litter Bulk Density [lb/ft^3]	Duff Bulk Density [lb/ft^3]
	1-hour	10-hour	100-hour			
AR	0.014	0.190	2.38	0.49	2.0	3.7
UNF-O	0.019	0.182	3.03	0.55	0.9	4.6
UNF-P	0.021	0.223	2.34	0.56	2.2	3.6
CNF-1	0.020	0.216	2.83	0.53	1.3	4.2
CNF-3	0.013	0.187	2.63	0.53	1.4	3.5

FWM Fine Woody Material, AR Alligator River National Wildlife Refuge, UNF Uwharrie National Forest, CNF Croatan National Forest.

not identifiable, an average specific gravity value for hardwoods or softwoods was assigned.

NFDRS model estimates of dead fuel load in each forest cover type (Table 14.2) were compared with measured dead fuel load to determine if there was good agreement and identify any trends. Minimum and maximum fuel loads across model size classes were based on drought indexes of 100 and 800, respectively. This resulted in minimum fuel loads equal to the NFDRS estimate and a maximum fuel loads equal to the NFDRS estimate times two. A model was considered to have good fit within and across size classes if the measured 95% confidence intervals for woody material and dead fuel load overlapped the minimum and maximum model estimates, respectively. This method was also used to determine if there was a best-fit fuel model for each study area.

Table 14.2 National Fire Danger rating system (NFDRS) fuel models, forest association and dead fuel load estimates[1]

NFDRS Fuel Model	Forest Type Description	1-hour Fuel Load [t/ac]	10-hour Fuel Load [t/ac]	100-hour Fuel Load [t/ac]	1000-hour Fuel Load [t/ac]
C	Longleaf Pine	0.4 – 0.8	1.0 – 2.0	*	*
G	Dense Conifer stands with high fuel loads	2.5 – 5.0	2.0 – 4.0	5.0 – 10.0	12 – 24
K	Slash Fuels	2.5 – 5.0	2.5 – 5.0	2.0 – 4.0	2.5 – 5.0
O	High Pocosin	2.0 – 4.0	3.0 – 6.0	3.0 – 6.0	3.0 – 6.0
P	Long Needled Southern Pines	1.0 – 2.0	1.0 – 2.0	0.5 – 1.0	*
R	Oak-Hickory and Mixed SE US Forests (before leaf fall)	0.5 – 1.0	0.5 – 1.0	0.5 – 1.0	*

[1] NFDRS fuel loads range from a minimum typical fuel load (drought index = 100) to a maximum fuel load (drought index = 800).
[*] Listed model has no NFDRS estimate for this fuel load class.

Biomass estimates were calculated using SAS statistical software. Systat (Version 9.0) was used to calculate statistical differences within and between sites and estimate mean biomass confidence intervals.

14.3 Results

14.3.1 Dead Fine and Coarse Woody Fuel Load

FWM and CWM were analyzed by size class to determine the variability between and within research areas (Table 14.3). Results are reported in tons/acre since this is the standard unit used by fire managers to estimate fuel loads. There were no significant differences within the Croatan and Uwharrie national forest research areas across sites and fuel classes. This was not the case at Alligator River (AR) where fuel loads were significantly larger in AR-B compared to AR-NB across all FWM fuel classes. CWM fuel loads were not significantly different between these two sites.

Table 14.3 Within size class fine and coarse woody dead fuel load at each site

Site	Forest Type (treatment)	FWM 1-hour Fuel Load [t/ac]	FWM 10-hour Fuel Load [t/ac]	FWM 100-hour Fuel Load [t/ac]	CWM 1000-hour Fuel Load [t/ac]
AR-B	Pond Pine-Pocosin (burned/wildfire)	0.4 (0.1)	1.8 (0.2)	2.3 (0.3)^{a}	1.3 (0.4)^{a}
AR-NB	Pond Pine-Pocosin (no burn)	0.2 (0.0)^{a}	0.9 (0.1)^{a}	1.4 (0.2)^{bc}	2.5 (0.6)^{ab}
UNF-O	Oak-Hickory (3 to 5-year burn)	0.2 (0.0)^{ab}	0.7 (0.1)^{ab}	2.2 (0.5)^{ac}	5.4 (2.7)^{bc}
UNF-P	Loblolly Pine (3 to 5-year burn)	0.2 (0.0)^{ab}	0.9 (0.1)^{ac}	2.3 (0.5)^{a}	2.5 (1.0)^{abc}
CNF-1	Longleaf-Loblolly Pine (annual burn)	0.1 (0.0)^{b}	0.5 (0.2)^{bc}	1.1 (0.6)^{b}	2.1 (1.6)^{abc}
CNF-3	Longleaf- Loblolly Pine (3-year burn)	0.1 (0.0)^{b}	0.5 (0.1)^{b}	0.6 (0.2)^{b}	5.2 (2.0)^{bc}

FWM Fine Woody Material, CWM Coarse Woody Material, AR Alligator River National Wildlife Refuge, UNF Uwharrie National Forest, CNF Croatan National Forest.
Numbers in parentheses are the 95% confidence interval limit.
^{abc} Fuel class means not significantly different, $P < 0.05$.

Mean dead woody fuel load increased with class size at all sites, but there was very little difference between 1- and 10-hour fine woody fuels across sites with the exception of AR-B. Mean 1- and 10-hour woody fuels at AR-B were significantly different and two times greater than the other sites. AR- B had the largest FWM fuel load (4.5 t/ac), but the smallest CWM fuel load. Mean 100-hour FWM fuel loads at UNF were similar to the AR-B site, but approximately 60% larger than AR-NB and 100% – 280% larger than the CNF sites. UNF-O had the largest mean coarse and total dead woody fuel load. There were no significant differences between UNF and CNF for 1-hour FWM and 1000-hour CWM, but 100-hour FWM was significantly larger at UNF compared to CNF.

14.3.2 Total Dead (Woody, Litter and Duff) Fuel Load

Mean dead fuel load measurements were significantly different within and between most research areas and differences tended to increase with fuel class size (Table 14.4). While there was good agreement within and between research areas for woody fuels, the addition of litter and duff generally resulted in larger variability and significantly different dead fuel load measurements. CNF was the only research area where dead fuel loads were significantly different across all size classes. Mean 1- and 10-hour dead fuel loads were significantly larger at UNF-P compared to UNF-O, but only by 0.1 (10%) and 0.4 t/ac (18%), respectively. There were significant differences between the two AR sites for 1- to 100-hour dead fuels, but not for 1000-hour fuels.

Table 14.4 Within size class dead fuel load at each site

Site	Forest Type (treatment)	1-hour Fuel Load [t/ac]	10-hour Fuel Load [t/ac]	100-hour Fuel Load [t/ac]	1000-hour Fuel Load [t/ac]
AR-B	Pond Pine-Pocosin (burned/wildfire)	1.2 (0.1)	3.3 (0.3)	17.1 (0.6)	48.8 (0.6)[c]
AR-NB	Pond Pine-Pocosin (no burn)	1.0 (0.0)[ab]	2.5 (0.1)[ab]	14.3 (0.5)	47.9 (1.0)[c]
UNF-O	Oak-Hickory (3 – 5 year burn)	1.0 (0.0)[b]	2.2 (0.2)[b]	7.8 (1.0)[a]	5.4 (2.7)[ab]
UNF-P	Loblolly Pine (3 – 5 year burn)	1.1 (0.0)[a]	2.6 (0.1)[a]	8.8 (1.2)[a]	2.5 (1.0)[a]
CNF-1	Longleaf-Loblolly Pine (annual burn)	0.4 (0.1)	0.9 (0.3)	2.6 (1.0)	2.1 (1.6)[a]
CNF-3	Longleaf- Loblolly Pine (3 year burn)	0.7 (0.0)	1.6 (0.1)	7.4 (0.8)[a]	6.3 (2.2)[b]

AR Alligator River National Wildlife Refuge, UNF Uwharrie National Forest, CNF Croatan National Forest.
Numbers in parentheses are the 95% confidence interval limit.
[abc] Fuel class means not significantly different, $P < 0.05$.

Measured dead fuel loads were smallest in the CNF-1 site and largest in the AR-B site across all fuel size classes with total dead fuel loads of 6 t/ac and 71 t/ac, respectively. The annually burned site (CNF-1) had significantly smaller dead fuel loads compared to all other sites, with the exception of 1000-hour fuels at UNF-P. Both AR sites had nearly 2 and 9 times the amount of 100- and 1000-hour fuels, respectively, compared to the other sites. The AR sites also had the deepest litter and duff which accounted for most of the dead fuel load. While litter and duff accounted for over 95% of 1000-hour fuel load at the AR sites, they contributed only 4 and 17% at UNF-P and CNF-3, respectively, and 0% at UNF-O and CNF-1. Mean litter and duff biomass measurements were similar across size classes in AR and UNF. With the exception of CNF-1 and AR-B 10-hour fuel loads, litter and duff contributed 59% – 92% of the 1- to 100-hour fuels.

14.3.3 Comparison between Measured and NFDRS Dead Fuel Load Estimates

14.3.3.1 Alligator River National Wildlife Refuge

Measured woody and dead fuel loads were compared with minimum and maximum NFDRS model estimates of dead fuel load to assess model accuracy in each forest cover type. Model O, a high pocosin fuel model and the most appropriate model for the AR pond pine-pocosin sites, accurately estimated 10-hour dead fuel load at AR-B (burn/wildfire) and 1000-hour woody fuel load at AR-NB (no burn). Woody fuels were overestimated across all other size classes, and 100- and 1000-hour dead fuels were underestimated at both AR sites. Only the 100-hour NFDRS model O fuel load estimate was within 1 t/ac of measured woody fuel load. While model O overestimated 100-hour fine woody fuels at both sites and 1000-hour coarse woody fuels at AR-B, the model underestimated dead fuels in these size classes by 8 – 42 t/ac.

Models G and K, developed for dense conifer and slash stands with high fuel loads, respectively, were also compared with measured fuel loads at AR since these sites had higher fuel loads. Like model O, these models tended to overestimate woody fuels in the 1- and 10-hour size classes and underestimate dead fuel loads in the 100- and 1000-hour size classes. Model G 10-hour and Model K 100-hour dead fuel load estimates did compare well with measured woody fuel load at the AR-B site, but not the AR-NB site. Overall, there was poor agreement between NFDRS model estimates and measured fuel loads at the AR sites. While woody and smaller sized classes of dead fuels were overestimated by the models, 100 and 1000-hour dead fuels were underestimated by 58% – 88%.

14.3.3.2 Uwharrie National Forest

NFDRS fuel models P and R matched the forest cover types at UNF-P (loblolly pine) and UNF-O (oak-hickory, respectively. Model R, used in oak-hickory and mixed SE US forests prior to leaf fall, was also considered for use in UNF-P since nearly 40% of the site is composed of hardwoods. Model P, used in long needled southern pine stands, overestimated 1-hour woody and dead fuel load at UNF-P by 0.8 t/ac (400%) and 0.9 (82%) t/ac, respectively. There was good agreement between this model and 10-hour woody fuels, but 10-hour dead fuels were underestimated by 0.6 t/ac (23%). Model P underestimated both 100-hour woody and dead fuels by 1.8 t/ac (78%) and 7.8 t/ac (89%), respectively, and does not estimate 1000-hour fuels.

Model R provided reasonable estimates of 1-, 10- and 100-hour woody fuels and 1-hour dead fuels at UNF-P. While the 1-hour and 10-hour woody fuel estimates did not overlap the measured confidence interval, the estimates were only 0.3 t/ac (150%) larger and 0.4 t/ac (44%) smaller, respectively. Model R underestimated

10- and 100-hour dead fuel load by 1.6 t/ac (62%) and 7.8 t/ac (89%), respectively. Like model P, model R does not provide estimates for 1000-fuels.

Model R estimated 1- and 10-hour woody fuels and 1-hour dead fuels reasonable well at UNF-O, but only the 1-hour dead fuel load estimate overlapped the measured confidence interval. The NFDRS overestimated 1-hour woody fuels by only 0.3 t/ac (150%), and underestimated 10-hour woody fuels by 0.2 t/ac (29%) compared to measured fuel load. Model R underestimated 100-hour woody fuels and 10- and 100-hour dead fuels by 55% – 87%.

14.3.3.3 Croatan National Forest

Measured fuel load at the CNF sites, dominated by longleaf and loblolly pines, were compared with fuel models C and P. Model C, developed for longleaf pine ecosystems, gave reasonable estimates of 1- and 10-hour woody and dead fuel loads at both CNF sites, with the exception of 10-hour dead fuel load at CNF-1. Model C does not provide estimates of 100- and 1000-hour fuel loads, but these fuels represented at least 84 and 78% of the total woody and dead fuel load, respectively. Model P, developed for long needled southern pine ecosystems, overestimated 1- and 10-hour woody and dead fuel loads at both sites, but 10-hour dead fuels were only 0.4 (25%) t/ac higher compared to measured dead fuel load at CNF-3. This model provided reasonable estimates of 100-hour woody fuel load at both CNF sites, but underestimated 100-hour dead fuel load by 1.6 (62%) – 6.4 (86%) t/ac.

14.4 Discussion and Conclusions

14.4.1 Woody Fuel Load Variability

Woody fuel loads (FWM and CWM) were not significantly different within the CNF (longleaf-loblolly pine) and UNF (oak-hickory and pine-hardwood) research areas, but were significantly different between the two sites at AR (pond pine-pocosin). There was nearly twice as much FWM at AR-B (burned/wildfire) compared to AR-NB (no burn), and a large proportion of these fuels were from dead inkberry stems (personal observation), possibly a product of the wildfire in 2000. Surprisingly, there was nearly twice as much CWM at AR-NB compared to AR-B, though the confidence intervals nearly overlap. While mean CWM fuel loads differed by 2.9 – 3.1 t/ac at the UNF and CNF sites, respectively, they were not significantly different due to the large confidence intervals associated with these measurements.

Mean 1- and 10-hour woody fuel loads differed by no more than 0.2 and 0.4 t/ac between sites, respectively, with the exception of AR-B. The small differences between these fuels across sites with different forest cover types and management regimes were unexpected. Litter fall generally covers the previous year's FWM indicating that annual production of these fuels was similar across these sites. While natural and human disturbances influence the production of FWM at a given site, their effect on our sites is beyond the scope of this research. Fuel load variability, as well as the confidence intervals associated with these measurements, increased with fuel class size across all sites. While mean 100-hour fine and CWM fuel loads differed by as much as 3.3 t/ac, the heterogeneous distributions of these fuels resulted in few significant differences. This was especially true for CWM.

14.4.2 Dead Fuel Load Variability

The addition of litter and duff to fine woody fuels resulted in larger differences and variability between mean dead fuel loads across sites compared to woody fuels alone. Mean 1- and 10-hour dead fuel loads were lowest at CNF and highest at AR-B. These results were expected given the wildfire disturbance at AR-B and the open canopied stands at the CNF sites. The UNF and AR-NB sites had similar mean 1- and 10-hour dead fuel loads, suggesting a good relationship between these fuels and sites with closed canopies and little disturbance, regardless of cover type. Mean 100- and 1000-hour dead fuel loads were much higher at AR compared to the other sites, with litter and duff contributing the majority of these fuels. This was expected and underscores the potential of larger sized classes of dead fuels to significantly impact fire danger on sites with organic soils during periods of extended drought.

It was difficult to compare our results with other studies due to different definitions used to derive fuel load. The 1- to 100-hour woody fuel and litter biomass estimates reported by Scholl and Waldrop (1999) were similar to those in this study, but 1000-hour woody fuels were generally lower or not reported. Wade and Ward (1973) reported that fine fuel loads in AR commonly reach 15 t/ac, and can double when deep organic soils lose moisture during drought conditions. Fine fuel loads (1- to 100-hour fuels) at AR-B and AR-NB were 22 t/ac and 18 t/ac, respectively.

14.4.3 Comparison between Measured and NFDRS Dead Fuel Load Estimates

While some NFDRS fuel model estimates compared well with measured woody and dead fuel loads, no one model accurately estimated measured fuel load across all fuel size classes within a site. Model O, the high pocosin fuel model most appropriate in AR (pond pine-pocosin), generally overestimated woody and 1-hour dead fuels, but underestimated 100- and 1000-hour dead fuels. Results were similar when models G and K were compared with measured fuel loads, and these models are designed for areas with higher fuel loads.

NFDRS fuel models did a better job of estimating fuel loads at the UNF (oak-hickory and pine hardwood) and CNF (longleaf-loblolly pine) sites. There was good agreement between model R, the oak-hickory and mixed hardwood model, and measured fuel loads at both UNF sites. While this model overestimated 1-hour woody fuel loads and underestimated 10-hour woody fuels, differences were small. Model R estimates and measured 1-hour dead fuels were almost identical at both UNF sites, but 100-hour woody and dead fuel loads were underestimated. Model R did a better job of estimating fuel loads at UNF-P than model P, a NFDRS fuel model developed for long needled southern pine ecosystems. While UNF-P is classified as a loblolly pine stand, nearly 40% of the stand is an oak-hardwood mix indicating that model P may be better suited for pine stands with less of a hardwood component.

NFDRS fuel load estimates for model C, developed for longleaf pine ecosystems, compared relatively well with 1- and 10-hour measured fuel load in the longleaf-loblolly pine stands at CNF. While estimates did not overlap the measured confidence interval, differences were small except for 10-hour dead fuel loads at CNF-1. The annual burn cycle at CNF-1 likely resulted in a loss of litter and the lower dead fuel load measurement for this size class compared to the model estimate. Model C does not have estimates for 100- or 1000-hour fuels. Since these fuel classes are not represented by the NFDRS, model P may be considered as a substitute for 100-hour woody fuels. While model P overestimated 1- and 10-hour fuels at the CNF sites, it did provide good estimates of 100-hour woody fuels. However, model P underestimated 100-hour dead fuel loads at both sites, indicating that the model does a poor job of capturing the litter and duff fuels at these sites.

The NFDRS fuel models in our analysis tended to overestimate 1- and 10-hour woody and dead fuels at the AR and CNF sites and while differences were sometimes small, model estimates were generally over 100% larger than measured mean fuel load. The models tended to underestimate 100- and 1000-hour fuels, and in many cases did not provide an estimate of 1000-hour fuel loads. Litter and duff made up a large percentage of dead fuels and this important component of forest fuel loads may not be well represented in the current NFDRS, especially in the 100- and 1000-hour fuels. Our measurements, and those reported by Wendel et al. (1962) and Scholl and Waldrop (1999), indicate that litter and duff can make up the majority of the dead fuel load in southern US forests. With the exception of CNF-1 and AR-B 10-hour fuels, litter and duff contributed 59% – 92% of the 1- to 100-hour fuel load. The smaller contribution of litter to the AR-B 10-hour fuel load (45%) is due to the higher mean FWM biomass at this site compared to the other sites. Litter at CNF-1 only contributed 38% of the total 10-hour fuel load due to the reduced litter layer from the previous year's burn.

A drought index was added to the NFDRS in 1988 to account for the drying of deep litter and duff in the absence of precipitation and can as much as double the dead fuel load. Our results indicate that this has improved estimates of 1- and 10-hour dead fuel loads, but estimates of 100- and 1000-hour dead fuels are still being underestimated. Fire managers are generally more concerned with 1- and 10-hour dead fuels since they have the biggest influence on fire ignition and spread. This may be sufficient for initial wildfire assessments, but drought conditions coupled with underestimates of larger sized classes of fuel will result in higher available fuel loads and increase the vulnerability of sites to more intense wildfires.

This research indicates that: ① there is little difference between 1- and 10-hour dead woody fuels across forest types in the absence of major disturbances such as wildfire; ② litter and duff can make a significant contribution to the total dead fuel load and results in greater differences and variability between forest types; ③ NFDRS model O, developed for high pocosin sites, generally overestimates woody fuels and underestimates dead fuels at the AR pond pine-pocosin sites indicating that this model does not capture the deep litter and duff component found at these sites; ④ NFDRS model R, developed for oak-hickory mixed hardwood forests before leaf fall, reasonably estimates 1- and 10-hour dead fuels in the oak-hickory stand at UNF, but underestimates 100-hour fuels and lacks 1000-hour fuels; ⑤ NFDRS model R is a better fit than model P, developed for long needled southern pine ecosystems, at UNF-P, a loblolly pine site with a 40% hardwood component; and ⑥ NFDRS model C, developed for longleaf pine ecosystems, does a good job of estimating 1- and 10-hour fuel loads for the two longleaf-loblolly pine stands in CNF, but lacks estimates for 100- and 1000-hour fuels.

The comparison between measured and NFDRS dead fuel loads was done with the understanding that NFDRS fuel models were designed for use over large areas and to only provide a reasonable representation of typical fuel loads (Deeming and Brown, 1975). While results from the six sites in this study are not sufficient enough to assess the NFDRS for use in all southern forests, this and other studies indicate that dead fuel loads can be highly variable within similar forest cover types. Management regimes including prescribed burning along with other disturbances have created a patchwork of forestland that complicates fire danger assessments. As forests become more fragmented and managed for different objectives, finer scale fuel load estimates may be necessary to accurately assess fire danger and minimize the loss of life and property.

References

Anderson HE, (1982), Aids to determining fuel models for estimating fire behavior. US Department of Agriculture, Forest Service, GTR-INT-122, Ogden, UT, 22

Brown JK, (1974), Handbook for inventorying downed woody material. US Department of Agriculture, Forest Service, GTR-INT-16, Ogden, UT, 24

Burgan RE, (1988), 1988 revisions to the 1978 national fire-danger rating system. US Department of Agriculture, Forest Service, Research Paper SE-273, Asheville, NC, 39

Chojnacky DC, Mickler RA, Heath LS, Woodall CW, (2004), Estimates of down woody materials in Eastern US forests. *Environ Mgmt*, **33**: 44 – 55

Deeming JE, Brown JK, (1975), Fuel Models in the national fire-danger rating system. *J For*, **73**: 347 – 350

Deeming JE, Burgan RE, Cohen JD, (1977), The national fire danger rating system-1978, US Department of Agriculture, Forest Service, GTR-INT-39, Ogden, UT, 63

de Vries PG, (1973), A general theory on line-intersect sampling with application to logging residue inventory. Mededdlingen Landbouw Hogeschool No. 73 – 11, Wageningen, The Netherlands, 23

FIA, (2005), US Department of Agriculture, Forest Service, Forest Inventory and Analysis Program website, available at http://fia.fs.fed.us/libary/ (accessed November 27, 2007)

GAO, (2005), Wildland Fire Management: important progress has been made, but challenges remain to completing a cohesive strategy. US Governement Accountability Office, Report to the Chairman, Subcommittee on Forests and Forest health, Committee on Resources, House of Representatives, GAO-05-147, Washington DC, 33

Harmon ME, Franklin JF, Swanson FJ, Sollins P, Gregory SV, Lattin JD, Anderson NH, Cline SP, Aumen NG, Sedell, JR, Lienkaemper GW, Cromack K, Cummings KW, (1986), Ecology of coarse woody debris in temperate ecosystems. In: Macfadyen A, Ford DE (eds) Advances in Ecological Research, vol 15. Academic Press, Orlando, FL, 133 – 302

Hough, WA, Albini, FA, (1978), Predicting fire behavior in palmetto-gallberry fuel complexes. US Department of Agriculture, Forest Service, Southeastern Forest Experiment Station, Research Paper SE-174, Asheville, NC, 44

Jenkins JC, Chojnacky DC, Heath LS, Birdsey RA, (2003), Comprehensive database of diameter-based biomass regressions for North American tree species. US Department of Agriculture, Forest Service, GTR-NE-319, Newtown Square, PA, 45

Markwardt LJ, (1930), Compartive strength properties of woods grown in the United States. US Department of Agriculture, Forest Service, Technical Bulletin 158, Washington, DC

McMinn JW, Crossley DS Jr (eds), (1996), Biodiversity and coarse woody debris in southern forests, proceedings of the workshop on coarse woody debris in southern forests: effects on biodiversity, 1993 October 18-20; Athens, GA. US Department of Agriculture, Forest Service, Southern Research Station, GTR- SE-94, Asheville, NC, 146

Schafale MP, Weakley AS, (1990), Classification of the natural communities of North Carolina. NC Department of Environment, Health, and Natural Resources, NC Natural Heritage Program, Division of Parks and Recreation, Raleigh, NC

Schlobohm P, Brain J, (2002), Gaining a better understanding of the National Fire Danger Rating System. National Interagency Fire Center, National Wildfire Coordinating Group, NFES 2665, Boise, ID, 71

Scholl ER, Waldrop TA, (1999), Photos for estimating fuel loadings before and after prescribed burning in the upper coastal plain of the southeast. US Department of Agriculture, Forest Service, GTR-SRS-26. Ashville, NC, 25

Van Wagner CE, (1968), The line-intersect method in forest fuel sampling. *Forest Sci* **14**: 20 − 26

Waddell KL, (2002), Sampling coarse woody debris for multiple attributes in extensive resource inventories. *Ecol Indicators*, **11**: 1 − 15

Wade DD, Ward DE, (1973), An analysis of the Air Force Bomb Range fire. US Department of Agriculture, Forest Service, Research Paper SE-105, Asheville, NC, 38

Wendel GW, Storey TG, Byram GM, (1962), Forest fuels on organic and associated soils in the coastal plain of North Carolina. U.S. Department of Agriculture, Forest Service, Southeastern Forest Experiment Station, Station Paper 144, Asheville, NC, 47

15 Numerical Simulations of Grassland Fire Behavior from the LANL-FIRETEC and NIST-WFDS Models

William Mell
Engineering Laboratory, National Institute of Standards and Technology, Boulder, CO, USA
Email: William.mell@nist.gov

Joseph Charney
Northern Research Station, USDA Forest Service, East Lansing, MI, USA
Email: jcharney@fs.fed.us

Mary Ann Jenkins
Department of Earth and Space Science and Engineering, York University, Toronto, Canada
Email: maj@yorku.ca

Phil Cheney
Australian Commonwealth Scientific Research Organization ACT, Australia (retired)
Email: phil.cheney@gmail.com

Jim Gould
Australian Commonwealth Scientific Research Organization ACT, Australia
Email: Jim.Gould@csiro.au

Abstract Grassland fires on level terrain offer a good basic scenario for test wildland fire behavior models, due to the simplicity and homogeneity of the fuels and terrain. Two physics based models, FIRETEC and WFDS, are briefly described, applied fire spread in grassland fuel, followed by a discussion of the results. It is important to note that both models have undergone appreciable development since the writing of this conference paper in 2005.

Keywords Fire models, grass fire, wildland fire, computational fluid dynamics, CFD

15.1 Introduction

Two physics-based computational fire models (FIRETEC and WFDS), capable of predicting time dependent fire behavior and fire-atmosphere interactions in 3D are applied to wind driven grassland fires over flat terrain. Because these are surface fires (i.e., relatively little vertical flame spread) in a single, homogeneous fuel they are a good choice for the first stage in model evaluation. By "physics-based model" we mean that all modes of heat transfer (conduction, convection, radiation) present in both the fire-fuel and the fire-atmosphere interactions are modeled (in some approximation). These models are in their initial stages of development and validation. It is unlikely, due to their computational requirements, that they will replace present day operational models and approaches (e.g., McArthur meters, Nobel et al., 1980; BEHAVE, Andrews, 1986; Forest Service Fire Behavior Predictor, Hirsch, 1996; FARSITE, Finney, 1998) in the near future, at least in their present form. However, they do have the potential, in the near term, to provide reliable and detailed predictions of the behavior and effects of fire over a much wider range of conditions than operational models. Examples of near term research orientated applications include assessing the effect of fire on vegetation during prescribed burns, the response of a fire to a given fire break or thinning strategy, and furthering our understanding of the behavior and spread of fires through the intermix of structural and vegetative fuels that characterize the wildland urban interface (WUI).

Fire models can be classified into three types (e.g., see Pastor et al., 2003): empirical, semi-empirical, or physics based (here we use "physical" and "physics based" interchangeably). Empirical models involve no physical modeling since they are based on statistical correlations of a given experimental data set. Semi-empirical models are based on energy conservation but do not distinguish between the different modes of heat transfer (conductive, convective, radiative). Physics-based models (such as FIRETEC and WFDS) attempt to solve (in some approximation) the equations governing fluid dynamics, combustion, and heat transfer. A complete, physics-based, wildland fire simulation must include approximations for the fire/atmosphere and the fire/fuel interactions

Section 15.2 provides an overview of the approaches used in the FIRETEC and WFDS models. Measurements from Australian (AU) grassland fire experiments can be used for model evaluation. These experiments are described in Section 15.3. WFDS predictions of the head fire spread rate and fire perimeters are compared to the AU grassland fire experiments in Sections 15.4.1 – 15.4.3. To date similar comparisons have not been made with FIRETEC. For this reason, in Section 15.4.4 WFDS simulations were conducted of tall grass fires that match, as much as possible, the conditions of FIRETEC simulations reported in Linn and Cunningham (2005). This allowed a comparison of to be made of the two models. Finally, in Section 15.5 a summary of the findings is given.

15.2 Overview of the FIRETEC and WFDS Numerical Models

FIRETEC has been developed at Los Alamos National Laboratory (LANL) by Linn and colleagues (Linn 1997, Linn et al. 2002). FIRETEC provides fire spread predictions over landscape and requires significant computational resources (multiple processors). The governing model equations are based on ensemble averaging of the conservation equations for mass, momentum, energy, and chemical species. This results in additional closure equations which require a number of turbulence modeling assumptions. The numerical time stepping scheme explicitly handles the high frequency acoustic waves (Reisner, 2000). Chemical heat release from the combustion process occurs only in computational grid cells that contain the solid fuel (Linn et al., 2002). For grid cell dimensions that are smaller than the flame length this is unrealistic and improvements are underway (Colman and Linn, 2003). Combustion is the result of a reaction rate that is a function of the density of both the solid fuel and the gas phase reactants, and an ad-hoc Gaussian-shaped probability density function (PDF) of the temperature. The use of this PDF is physically motivated but not yet validated. An assumed fraction of the heat produced by combustion is deposited in the solid fuel to help sustain pyrolysis. The solid fuel is assumed to be thermally thin. Thermal radiation transfer is computed using a diffusional transport approximation adapted from Stephens (1984). There is not, in the results reported to date, a model for the solid phase that handles pyrolysis which is coupled, through resolved heat fluxes, to a separate model for the gas phase which handles combustion. Instead, the pyrolysis of the solid phase and heat release from combustion in the gas phase are lumped together. This is the most significant difference (from a physical modeling point of view) between FIRETEC and other approaches, including WFDS.

WFDS is an extension of Fire Dynamics Simulator (FDS), a product of the National Institute of Standards and Technology (NIST) (McGrattan, 2004; McGrattan and Forney, 2004). The development of FDS started in the 1980's and it was created to simulate structural fires in a computationally efficient manner. It can be run on single processor desktop computers or on multiple processors and on a range of operating systems. FDS is currently used worldwide by 100s of fire protection engineers for structural fires and can be downloaded free. Smokeview, a companion software package, was also developed at NIST to interactively visualize FDS results (Forney and McGrattan, 2004). A survey of validation studies of FDS given in McGrattan (2004). The solution of the governing equations is based on basic large eddy simulation concepts as first presented by Smagorinsky (1963). Recently, modifications to FDS were begun to handle fire spread through vegetative fuels (Rehm et al., 2003; Mell et al., 2007a) with the goal of simulating fire spread in an intermix of vegetative and structural fuels (i.e., WUI fires). This modified version of FDS is called WFDS and is used here to simulate grassland fires. Application of WFDS to elevated fuels has also begun (e.g., Mell eta al., 2007c). A websie, Mell et al. (2007b), provides information on the ongoing experimental and modeling work at NIST in WUI fires. WFDS uses a low Mach number approximation to the governing equations developed by Rehm and Baum (1978. This approximation, which has been applied successfully to a wide range of fire and combustion problems, and the use of a fast direct solver for the pressure, results in computational speeds that are 10 – 100 times faster than many other methods. The gas and vegetative phases are handled separately on different grids. The combustion model uses the well established mixture fraction based approach that assumes the fuel and oxygen react instantaneously over time scales characteristic of the flow (Bilger, 1980). The solid fuel is assumed to be thermally thin. Radiative and convective heat transfer within the fuel bed is directly modeled in manner similar to Albini (1985) and Morvan and Dupuy (2004). The pyrolysis model of Morvan and Dupuy (2004) is used. Char oxidation is not included. Thermal radiation transfer in the gas phase is computed with a finite volume based solver (Raithby and Chui, 1990). In the fuel bed a forward-reverse approximation (Ozisk, 1973; Mell and Lawson, 2000) is used for radiation transfer. Details on the model equations, numerical algorithm, and the approach used for igniting the solid fuel are given in Mell and Jenkins. (2007a), as are additional simulation results. Mell et al. (2007a) also provide a review of other physics-based models.

15.3 Overview of Grassland Fire Experiments

The experimental results and data used here were reported in Cheney et al. (1993) and Cheney and Gould (1995). The grassland fires were started by line fires, of varying lengths, along a fire break on the upwind edge of a grassland plot. One of two types of grass was present on a given plot: either Eriachne burkittii (kerosene grass) or Themeda australis (kangaroo grass). These two grasses differed in their structural and growth characteristics. In the models, however, physical differences in the fuel bed are accounted for only by the solid phase parameters listed in Table 15.1. The grassland plots measured 100×100 m, 200×200 m, or 200×300 m and were surrounded by fuel breaks. At each corner of a plot the wind magnitude was measured every 5 s at a height of 2 m above the ground. Aerial photos and ground observations were used to obtain fire perimeters, head fire widths, and quasi-steady head fire spread rates. Figure 15.1(a) shows a photo of experiment F19 (see Section 15.4.3) and Fig. 15.1(b) shows a snapshot from a WFDS prediction of the experiment.

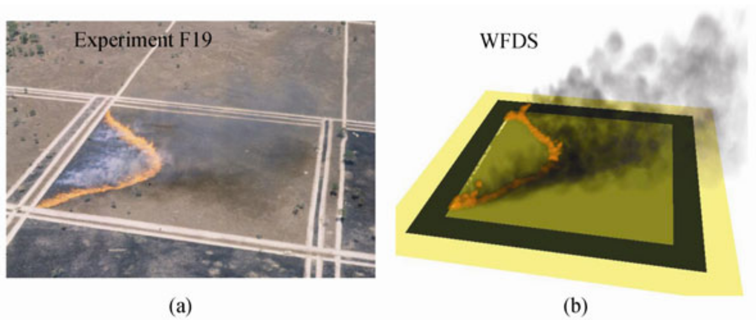

Figure 15.1 (a) Photograph of experimental fire F19 (see Section 15.4.3) at $t=56$ s. (b) Snapshot of WFDS simulation of the same experimental fire at $t=56$ s

The following empirically based formula (Equation 4 in Cheney et al., 1998) relates the experimentally observed head fire spread rate R_o ($m \cdot s^{-1}$), to the wind speed U_2 ($m \cdot s^{-1}$) at a 2 m height, the head fire width W (m), and the fuel moisture content M (%):

$$R_o = (0.165 + 0.534 \times U_2) \times \exp[(-0.859 - 2.036 \times U_2)/W)] \times \exp(-0.108 \times M). \quad (15.1)$$

Cheney et al. (1998) defined the effective head fire width as the width of the fire, measured at right angles to the direction of head spread (and thus at right angles to direction of the wind at the head fire), which influenced the shape and size of the head fire during the next period of spread measurement (Cheney and Gould, 1995). The effective width of the head fire can also be defined as that portion of the perimeter where the flames are leaning towards unburnt fuel. In WFDS the head fire width was defined to be the distance between the flank fires one fire depth upwind of the trailing edge of the head fire. Figure 15.2 is a schematic showing, for an arbitrary fire perimeter, the head width, head-fire depth, and ignition line fire. For a sufficiently large head fire width the observed spread rate, R_o, obtained

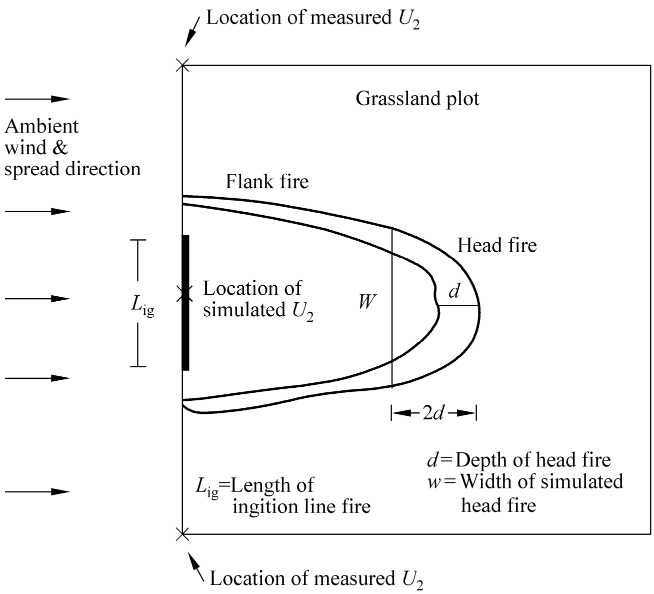

Figure 15.2 A schematic of a grassland fire. The ambient wind flows from left to right. The value of the wind speed, U_2, in the experiments is obtained by averaging the magnitude of the horizontal velocity measured at a height of $z = 2$ m positioned at the upper and lower left-hand-side corners of the grassland plot. The value of the wind speed in the simulation is obtained from the computed component of the velocity vector parallel to the ambient wind at a height of approximately $z = 2$ m positioned above the center of the ignition line fire

its potential quasi-steady value, R_{ss}. This spread rate is obtained from Eq. (15.1) for $W \rightarrow \infty$

$$R_{ss} = (0.165 + 0.534 \times U_2) \times \exp(-0.108 \times M). \qquad (15.2)$$

In this Chapter, simulated spread rates and head fire location from WFDS were compared to their experimentally observed values through the use of these empirical relations.

15.4 Approach and Results

This is the first comparison of FIRETEC and WFDS. As such, the primary objective is to assess how well the models predict experimentally observed trends of macroscopic behavior. FIRETEC simulations of the AU grassland experiments are not available at this time, so only comparisons of WFDS simulations and AU grassland fires appear here (see Sections 15.4.1 – 15.4.3). Comparisons between FIRETEC and WFDS were accomplished by running simulations of fire spread in the tall grass fuels reported by Linn and Cunningham (2005) (see Section 15.4.4). The authors feel it is important to compare both models against the AU grassland fire data in future experiments, and consider that such a comparison is a logical next step in the comparison of the models.

Table 15.1 lists the environmental parameters used in the simulations of fire in AU grasslands and tall grass. Parameters that were not measured in the AU experiments were determined from sources in the literature (Mell Jenkins., 2007a).

Table 15.1 Gas and solid properties used in the simulations

	Property	**AU Experiments**		**WFDS AU exp.**	**FIRETEC[a] Tall Grass**	**WFDS Tall Grass**
		F19	**C064**			
Gas phase	heat of combustion of volatiles, kJ·kg^{-1}	*n*/a	*n*/a	15,600	8,914	15,600
	radiation fraction	*n*/a	*n*/a	0.35	*n*/a	0.35
	soot fraction	*n*/a	*n*/a	0.02	*n*/a	0.02
Solid phase	surface area to-volume ratio, m^{-1}	12,240	9,770	from exp	4,000	4,000
	char mass fraction	*n*/a	*n*/a	0.20	*n*/a	0.2
	grass height, m	0.51	0.21	from exp	0.7	0.7
	fuel element density, kg·m^{-3}	*n*/a	*n*/a	512	*n*/a	512
	fuel loading, kg·m^{-2}	0.313	0.283	from exp	0.7	0.7
	moisture, %	5.8	6.3	from exp	5.0	5.0

[a] Linn and Cunningham (2005)

Two AU experiments, each with a different grass, were considered. In Table 15.1, and in the following text, the two experiments are denoted F19 (natural Themeda grass) and C064 (cut, with cuttings removed, Eriachne grass).

15.4.1 Head Fire Spread Rate Dependence on Wind Speed in AU Grassland Fuel (WFDS only)

Four wind speeds, U_2, were used in the simulations: $U_2 = 1$ m·s^{-1}, 3 m·s^{-1}, 4 m·s^{-1}, 5 m·s^{-1}. For each wind speed there were four different ignition line fires were used (a total of 16 cases) lengths: $L_{ig} = 8$ m, 25 m, 50 m, 100 m. Ignition lines with lengths of $L_{ig} = 8$ m and 25 m had a depth of 6.7 m; ignition lines $L_{ig} = 50$ m and 100 m had a depth of 3.3 m. The grassland fuel characteristics were those of experiment F19 in Table 15.1. The initial wind speed depends on height, z, above the ground according to a power law to approximate a boundary layer (Morvan and Dupuy, 2004):

$$u(x, y, z, t = 0) = U_{2,\mathrm{I}}(z/2)^{1/7}. \tag{15.3}$$

Here $U_{2,\mathrm{I}}$ is the value in WFDS of the initial wind speed at a height of 2 m. As the simulation proceeds, the wind speed at this height is modified by the fire (due to both entrainment and blockage effects) and by drag from the grass. When comparing head fire spread rates from WFDS simulations and from Eq. (15.1) a consistent value of U_2 must be used. In WFDS U_2 is the average value of the windward velocity, over the course of the simulation, in the first cell above the vegetation at the center of the ignition line-fire. The height of this velocity location is within $z = 1.95 - 2.1$ m for the simulation cases reported here. Simulations with a number of grid resolutions and domain sizes were conducted to ensure that the results were not significantly influenced by grid resolution or boundary effects. All the WFDS simulations used an overall computational domain area of 1500×1500 m with a 200×200 m grassland plot in the center. The height of the computational domain was 200 m. The horizontal grid for a central 300×300 m area containing the grassland plot was $\Delta x = \Delta y = 1.66$ m; outside this central area $\Delta x = \Delta y = 3.33$ m. The vertical grid was stretched from $\Delta z = 1.4 - 5.5$ m at a height of 200 m throughout the computational domain. Figure 15.3 is a plot of head fire spread rate versus wind speed. The physical parameters of the fuel are listed in Table 15.1. Spread rates from WFDS (symbols), BEHAVE (Andrews, 1986) (solid line) and Eq. (15.2) (dashed line) are shown.

As will be seen below, in Fig. 15.4, WFDS spread rates for $L_{ig} = 50$ m quickly reached a quasi-steady value. The linear dependence of the spread rate on the wind speed is well predicted by WFDS. The quantitative agreement of WFDS is also good, however it is important to note that the sensitivity of WFDS to realistic variations in environmental variables (wind speed, moisture content, etc.) has not yet been assessed. Another important issue is how the value of the wind speed, U_2, is obtained. WFDS and both Eqs. (15.1) and (15.2) use a value of U_2 that is the average wind speed at a height of approximately 2 m. This value of the wind speed was used to obtain BEHAVE results in Fig. 15.3. However, in BEHAVE the default height of the wind speed is at the mid-flame height. Experimentally observed flame heights, for $U_2 = 5$ m·s^{-1}, were 2.7 m for this fuel. This suggests that the wind speed input into BEHAVE should be larger, leading to a prediction of even faster spread rates than plotted in Fig. 15.3. BEHAVE's over prediction of the spread rate for fuels with a surface-to-volume ratio of 13100 m^{-1}, which is a relatively fine fuel similar to the fuel used here, has been noted before, Gould (1988).

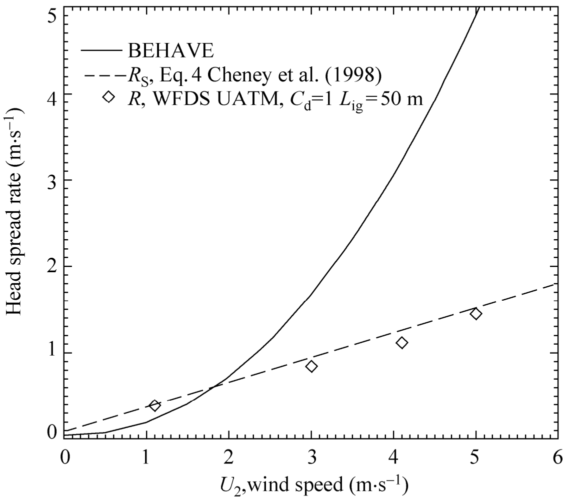

Figure 15.3 Spread rate versus wind speed from WFDS (symbols), BEHAVE (solid line) and Eq. (15.2) (dashed line)

15.4.2 Head Fire Spread Rate Dependence on the Head Fire Width in AU Grassland Fuel (WFDS only)

Figure 15.4(a) below shows the fire spread rate versus the head fire width on the left from WFDS simulations with $U_2 = 1$ m·s^{-1} and the four different lengths (Figs. 15.4(b) – 15.4(e)) of the ignition line fire. The solid line is the spread rate from Eq. (15.1). The simulations reproduced the trend of an increasing head fire spread rate with an increasing width of the head fire. All L_{ig} cases reach a quasi-steady spread rate that is within 25% of the Eq. (15.2) value. The experimental fires, as described by Eq. (15.1), reached a quasi-steady spread rate at narrower head fires than the simulated fires. Figures 15.4(b) – 15.4(e) are sequential snapshots of the burning region (shaded contours of the burning rate are shown) for each of the ignition line fire lengths used. Note that for the $L_{ig} = 50$ m and 100 m cases, Figs. 15.4(d) and 15.4(e) respectively, the flank fires reach the upper and lower fire breaks.

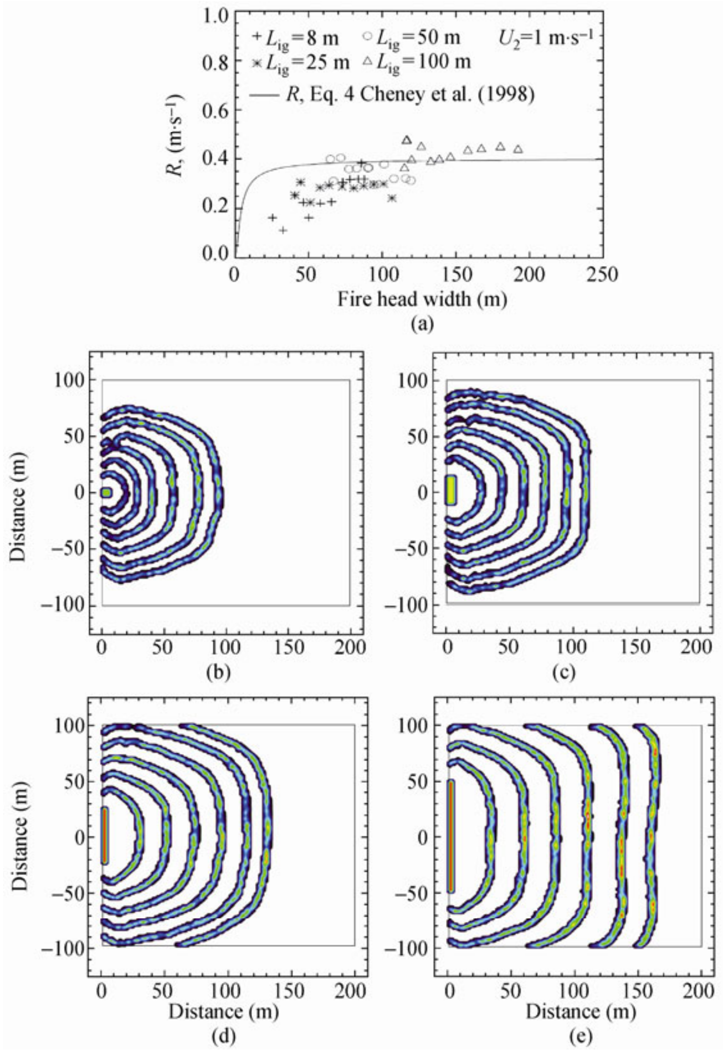

Figure 15.4 (a) Spread rate versus head fire width from WFDS for a wind speed of 1 m·s^{-1} and four different ignition line fires is shown. The fire lines from which the spread data was determined shown on the right. The four ignition line lengths are (b) 8 m, (c) 25 m, (d) 50 m, (e) 100 m. The fire perimeters are plotted at times 0 s, 60 s, 120 s, 180 s, 240 s, 300 s, and 350 s. The fire spreads in a 200×200 m grassland plot

In Fig. 15.5 (left column) the location of the leading edge of the head fire versus time, from both WFDS (solid line) and from the Eq. (15.1) (circles) with $U_2 = 5$ m·s^{-1}, is shown in the left column. Each row in Fig. 15.5 corresponds to a

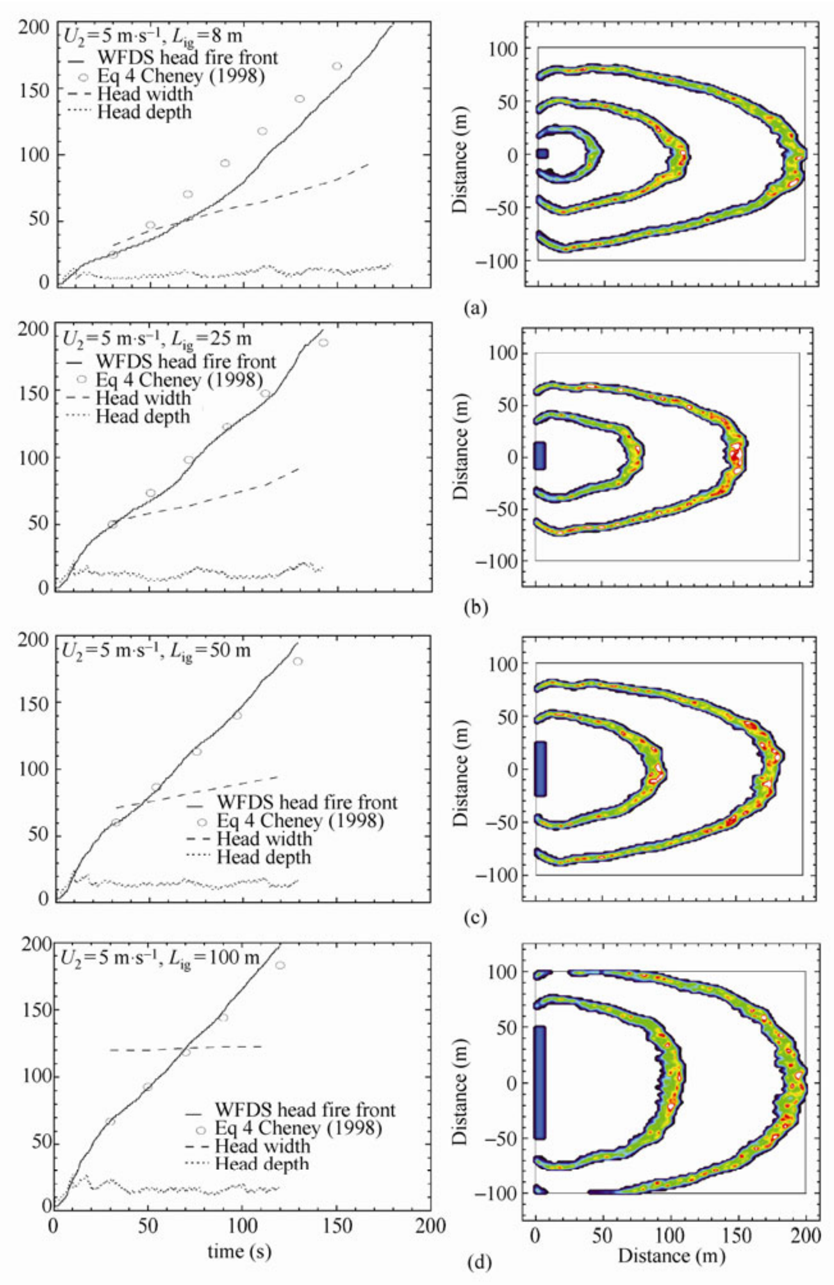

Figure 15.5 Left column shows the location of the leading edge of the head versus time from WFDS (solid line) and Equation 4 of Cheney et al. (1998) (circles) for a wind speed of 5 m·s^{-1} and the four ignition line fires are used 8 m (a), 25 m (b), 50 m (c), and 100 m (d) long (same as Fig. 15.4). The width (dashed line) and depth (dotted line) of the head fire are also plotted. The fire lines for each case are shown in the right column at 60 s intervals, starting at 0 s

different L_{ig}. Also shown in the left column are the width (dashed line) and depth (dotted line) of the head fire. In each case an initial time period of relatively rapid spread is present, followed by a slower spread rate. This initial rapid spread may depend on the ignition procedure. This issue needs to be investigated. Equation (15.1) is implemented, using head fire widths from WFDS, to determine the location of the head fire (circle symbols) at the end of the initial time period of rapid spread. For the cases with $L_{ig} = 25$ m, 50 m, and 100 m WFDS predictions of the head fire location agree well with Eq. (15.1). When $L_{ig} = 8$ m there is a period of time during which the head fire spread rate increases before reaching a quasi-steady value. The quasi-steady spread rate agrees well with Eq (15.1) at around $t = 110$ s (i.e., the solid line and a line through the circles become roughly parallel). The head width (dashed line) at which the simulated head fire spreads in a quasi-steady manner is approximately $W \geqslant 65$ m (note Fig. 15.4(a) shows similar results for $U_2 = 1$ m·s^{-1}). This is consistent with experimental observations that spread rates are relatively unaffected by L_{ig} when L_{ig} is sufficiently large. The head fire width is constant with time for $L_{ig} = 100$ m. Cheney and Gould (1995) noted at their highest wind interval between 4.7 m·s^{-1} and 7.1 m·s^{-1} the head fire width of more than 125 m in open grassland is required to get spread rates within 10% of the quasi-steady rate of forward spread.

Figure 15.5 (right column) shows the fire perimeter at 60 s intervals. The relatively high wind speed results in head fire depths (10 – 12 m) that are greater than the flank fire depths (5 – 7 m). This does not occur in the weak wind case ($U_2 = 1$ m·s^{-1} in Figs. 15.4b – e). This behavior is consistent with field observations. Field measurements of the head fire depth for $L_{ig} = 175$ m and $U_2 = 4.9$ m·s^{-1} range from 6.5 – 10. 5 m. Fire depths were interpreted from oblique photographs which were corrected and plotted onto a planar map of time isopleths of fire perimeter and fire depth.

15.4.3 Case Studies—Fire Perimeter in AU Grassland Fuel (WFDS only)

The mechanism of fire spread can change along the fire perimeter depending on the wind speed. In zero ambient wind, entrainment by the fire creates a local wind into which the entire fire line spreads (backing fire). In the presence of an ambient wind the downwind portion of the fire perimeter spreads with the wind (heading fire), the upwind portion of the fire perimeter spreads into the wind (backing fire), and the sides or flanks of the fire perimeter spread under conditions that can alternate between heading and backing fires. Note that in the cases considered here there are no backing fires since ignition occurred along the fire break at the upwind border of the plot. Backing fires, in which the flame tends to tilt away from the unburned fuel, can consume the fuel from the base upward, resulting in more complete fuel consumption. Heading fires, in which the flame tilts toward the unburned fuel, can be associated with lower fuel consumption because the grass ignites at the top and burns downward, covering the unburned fuel beneath with a protective coating of ash. The spread mechanism in flank fire can involve, depend on the fire/wind interaction, both the burning downward mechanism of head fires and the burning upward mechanism of backing fires. Thus, predicting the evolution of the entire fire line is much greater challenge, due to variation along the fire line of the fire/wind interaction and spread mechanisms, than predicting the behavior of just the head fire.

Neither FIRETEC nor WFDS can directly resolve the details in the grass fuel bed that differentiate a backing fire from a heading fire since the entire fuel bed is unresolved on the computational grid. For example, the height of the first grid cell in WFDS is 1.4 m while the height of the grass is 0.51 m. However, the fire/atmosphere interactions that occur over scales on the order of a few meters can be resolved. It is hoped that this level of resolution of the fire physics will be sufficient to capture the dynamics of the entire fire perimeter. It is important that a three-dimensional model predict the behavior of the entire fire perimeter. Otherwise, the overall heat release rate (HRR), fuel consumption, and smoke generation will be (to some degree) incorrectly predicted. These global fire characteristics are particularly important inputs to regional smoke transport models. In addition, the mechanisms behind extreme fire behavior (such as blow ups) are still poorly understood. A model that simulates the behavior of the entire fire perimeter, as opposed to only the head fire, is more likely to shed light on these issues.

In this section, model predictions of fire perimeters from two experimental cases are presented. In the first experiment, called F19, the ignition line fire is 175 m long. This line fire was created with drip torches carried by two field workers walking for 56 s (87.5 m) in opposite directions from the center point to the ends the line fire. The average wind speed, measured at the corners of the 200×200 m plot and not including measurements influenced by the fire, equaled 4.9 $m \cdot s^{-1}$. In the second experiment considered, called C064, the ignition line is 50 m long. The average wind speed was 4.6 $m \cdot s^{-1}$. Fuel bed characteristics are given in Table 15.1 for both experiments. Figure 15.6 shows the leading edge of the fire perimeter from the experiments (symbols) and the entire fire bed from WFDS (shaded contours of the burning rate) at three different times.

Experiment F19 is shown in Fig. 15.6 (a). A wind shift occurs in the experiment after $t = 86$ s which breaks the symmetry of the fire perimeter, this does not occur in WFDS since a constant wind orientation is assumed at the inflow boundary. As expected from the previous results, the spread of the head fire is well predicted at all times. Before the wind shift, the predicted fire perimeter closely matches the measured fire perimeter. After $t = 86$ s it's not clear how well WFDS performs because the wind shift significantly changes the observed fire perimeter. Also, long flanking fires (as, for example, those shown in Fig. 15.5) do not develop for this case because the flank fires reach the fire breaks relatively quickly.

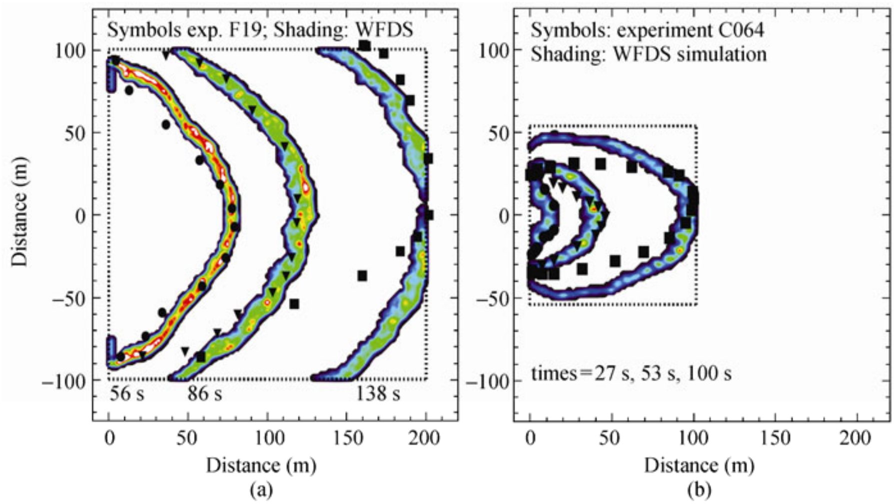

Figure 15.6 Fire perimeters from experiments (symbols) and WFDS simulations (shaded contours). Experiment F19 (a) and experiment C064 (b). See text for details and Table 15.1 for fuel/environmental parameters

Experiment C064 is shown in Fig. 15.6(b). Extended flank fires do develop in this case. WFDS over predicts the spread rate of the flank fires. The reasons for this are the subject of ongoing model development efforts. The current version of WFDS does not faithfully model the upward spread mechanism that can be present in flank fires. Instead, the fire burns downward through the grassland fuel bed everywhere along the perimeter. Also, in the field the depths of flank fires are significantly smaller than head fire depths for this experiment. The horizontal grid resolutions used here (1.66 m) adequately resolve the head fire depth but this may not be the case for the flank fires.

15.4.4 Simulation of Tall Grass (FIRETEC and WFDS)

Linn and Cunningham (2005) simulated fire spread in a fuel similar to the tall grass NFFL standard model 3. The parameters of this grass fuel are listed in Table 15.2. Two different lengths of an ignition fire line were used, $L_{ig} = 16$ m, 100 m and four different ambient wind speeds, constant with height, $U = 1$, 3, 6, 12 m·s^{-1}. Six WFDS simulations were made: $U = 1$, 3, 12 for each of the two L_{ig} values. The results are listed in Table 15.2. The most significant difference in the two models was that backing fires (spreading upwind) and flank fires are more likely to occur, in a manner consistent with field observations, in WFDS. Figures 15.7(a) and 15.7(b) show plots of the fire perimeter at different times for $U = 3$ m·s^{-1} and $L_{ig} = 16$ m and 100 m, respectively. Velocity vectors corresponding to the latest time, at a height of $z = 2$ m, overlie the fire perimeters. Figures 15.8(a) and 15.8(b)

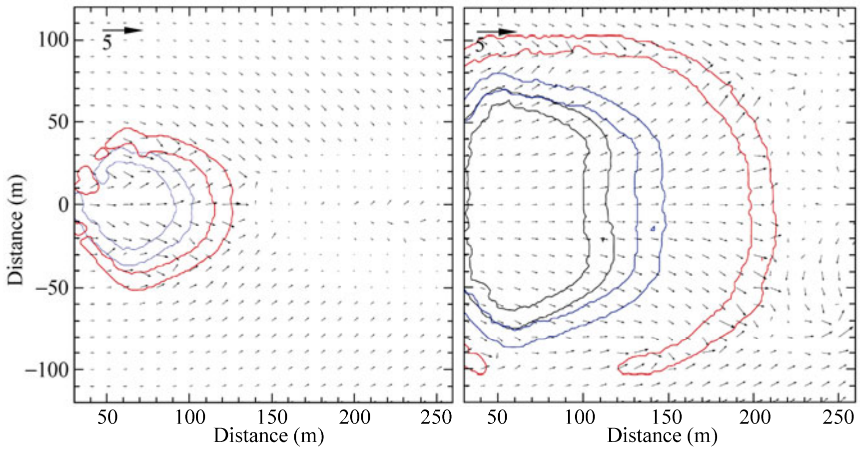

Figure 15.7 Fire perimeters (at different times) and velocity vectors (at a height of $z = 2$ m) for two different ignition line fire lengths and a constant ambient wind speed of $U = 3$ m·s^{-1}. Velocity vectors are from the same time as the latest fire perimeter. (a) Length of initial line fire is $L = 16$ m. Times of fire perimeters are $t = 150$ s, 250 s. (b) Length of initial line fire is $L = 100$ m. Times of fire perimeters are $t = 100$ s, 150 s, 250 s

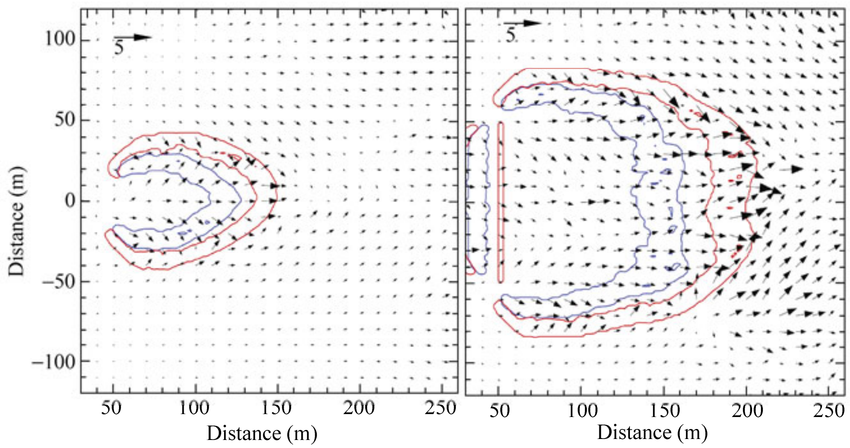

Figure 15.8 Fire perimeters (at different times) and velocity vectors (at a height of $z = 2$ m) for two different ignition line fire lengths and a constant ambient wind speed of $U = 6$ m·s^{-1}. Velocity vectors are from the same time as the latest fire perimeter. (a) Length of initial line fire is $L = 16$ m. Fire perimeters are at times $t = 90$ s, 150 s. (b) Length of initial line fire is $L = 100$ m. Fire perimeters are at times $t = 90$ s, 150 s

are plots for a higher ambient wind speed of $U = 6\ \text{m·s}^{-1}$. Figures similar to Figs. 15.7 and 15.8 here are provided by Linn and Cunningham (2005). Their Figs. 3(a,b) and 4(a,b) correspond to Figs. 15.7(a,b) and 15.8(a,b) here. Backing fires are clearly seen in the WFDS for the slower wind speed cases in Fig. 15.7(a) and Fig. 15.7(b). Backing fires are also present in the faster wind speed cases of Fig. 15.8(a) and Fig. 15.8(b). However, for the shorter ignition line case (Fig. 15.8(a)) the backing fire was extinguished after $t = 50$ s due to diminished heat transfer to the upwind fuel.

For both FIRETEC and WFDS backing fires, when present, were more robust for the longer ignition lines. Field observations of backing fire behavior suggest that they are less likely to survive at higher wind speeds. This trend is not reproduced by FIRETEC, which was recognized by Linn and Cunningham (2005) and is under investigation. When a backing fire is not present in WFDS, as in case $L_{ig} = 16$ m, $U = 6\ \text{m·s}^{-1}$ after $t = 50$ s, a similar head fire shape, which is necked inward toward the centerline, is predicted by both WFDS and FIRETEC. Head fire spread rates could not be compared because the presence of backing fires in WFDS influence the wind at the head fire locations

Table 15.2 Summary of results from FIRETEC and WFDS simulations of fire spread in tall grass

U	L_{ig}	Backing fire		Flank fire	
		FIRETEC	WFDS	FIRETEC	WFDS
1	16	no	yes/no*	no	yes/no*
1	100	no	yes	no	yes
3	16	no	yes	yes	yes
3	100	no	yes	yes	yes
12	16	yes	yes/no**	yes	yes
12	100	yes	yes	yes	yes

* fire spread erratically and eventually extinguished due to the weak ambient wind
** backing fire survived for approximately 50 s before it was extinguished due to convective cooling

15.5 Conclusions

Findings from Australian grassland experiments were used to evaluate the physics based fire model, WFDS. Whenever possible, fuel and atmospheric parameters measured in the experiments were used in the simulation. The spread rates of head fires were well predicted by WFDS. Spread rates of flank fires appear to be over predicted, but only one AU grassland experiment with freely spreading flank fires has been considered to date. Backing fires were not present in the experiments because ignition occurred just downwind of a fuel break. FIRETEC simulations for the AU grassland fuels were not available. However, WFDS simulations for fuels and conditions matching tall grass FIRETEC simulations (Linn and Cunningham, 2005) were run in order to compare results of the two models. Qualitatively the models produced similar results. The general trend, in observed grassland fires, of backing fires spreading more slowly as the ambient wind speed increased was not reproduced by FIRETEC. Both of these models are in their first stages of development and application to wildland fires. There is a great need for well documented full scale fires to aid further development in more complex fuel beds.

Acknowledgements

This work was sponsored in part by the USDA Forest Service Joint Venture Agreement 03-JV-11231300-088.

References

Albini FA, (1985), Wildland fire spread by radiation—a model including fuel cooling by natural convection. *Combust. Sci. Tech.* **45**: 101 – 113

Andrews PL, (1986), BEHAVE: Fire behavior prediction and modeling system—BURN subsystem part 1. USDA For. Serv. Gen. Tech. Rep. INT-194. See also http://www.fire.org

Bilger RW, (1970), Turbulent Reacting Flows. Chap. 4 in Turbulent Flows with Nonpremixed Reactants, Springer-Verlag

Cheney NP, Gould JS, Catchpole WR, (1993), The influence of fuel, weather and fire shape variables on fire spread in grasslands. *Int. J. Wildland Fire*, **3**: 31 – 44

Cheney NP, Gould JS, (1995), Fire growth in grassland fuels. *Int J. Wildland Fire*, **5**: 237 – 347

Cheney NP, Gould JS, Catchpole WR, (1998), Prediction of fire spread in grasslands. *Int. J. Wildland Fire*, **8**: 1 – 13

Colman JJ, Linn RR, (2003), Non-local chemistry implementation in HIGRAD/FIRETEC. 2nd Intnl. Wildland Fire Ecology and Fire Manage. Congress and 5th Symp. on Fire on Forest Meteorology, 16-20 November, Orlando, FL, American Meteorological Society

Fons WL, (1946), Analysis of fire spread in light forest fuels. *J. Agricultural Res.*, **72**: 93 – 121

Forney GP, McGrattan KB, (2004), User’s Guide for Smokeview Version 4: A Tool for Visualizing Fire Dynamics Simulation Data. NIST Special Publication 1017, http://fire.nist.gov/bfrlpubs/

Finney MA, (1998), FARSITE: Fire Area Simulator-Model, Development and Evaluation. USDA Forest Service, Rocky Mountain Research Station Paper, RMRS-RP-4

Hirsch KG, (1996), Canadian forest fire behavior prediction (FBP) system: user's guide. Canadian Forest Service, Special Report 7, Northwest Region, Northern Forestry Centre

Larini M, Giroud F, Porterie B, Loraud J-C, (1998), A multiphase formulation for fire propagation in heterogeneous combustible media. *Int. J. Heat Mass Trasfer*, **41**: 881 – 897

Linn RR, (1997), A transport model for prediction of wildfire behavior. Ph. D. thesis, New Mexico State University, also published as Los Alamos Report, LA-13334-T

Linn R, Reisner J, Colman JJ, Winterkamp J, (2002), Studying wildfire behavior using. FIRETEC, *Int. J. Wildland Fire*, **11**: 233 – 246

Linn R, Cunningham P, (2005), Numerical simulations of grass fires using a coupled atmosphere-fire model: Basic fire behavior and dependence on wind speed. J. Geophysical Research, 110

McGrattan KB, (2004), Fire Dynamics Simulator (Version 4), Technical Reference Guide. NISTIR Special Publication 1018, McGrattan K (ed), http://fire.nist.gov/bfrlpubs/

McGrattan KG, Forney G, (2004), Fire Dynamics Simulator (Version 4), Users Guide. NISTIR Special Publication 1019, http://fire.nist.gov/bfrlpubs/

Mell WE, Lawson JR, (2000), A Heat Trasfer Model for Firefighters' Proctective Clothing. *Fire Technology*, **36**: 39 – 68

Mell W, Jenkins MA, (2007a), A physics based approach to modeling grassland fires. *Int. J. Wildand Fire*, **16**: 1 – 22

Mell W, Rehm R, Maranghides A, Manzello S., Forney, G., (2007b), Wildland-Urban Interface and Wildland Fires. http://www2.bfrl.nist.gov/userpages/wmell/public.html

Mell W, Maranghides A, McDermott R, Manzello S, (2007c), Numerical simulation and experiments of burning Douglas fir trees. Submitted to Combustion Theory and Modeling.

Morvan D, Dupuy JL, (2004), Modeling the propagation of a wildfire through a Mediterranean shrub using a multiphase formulation. *Comb. Flame*, **138**: 199 – 210

Nobel IR, Bary GAV, Gill AM, (1980), McArthur's fire-danger meters expressed as equations. *Aus. J. of Ecol.*, 5: 210 – 203

Ozisk MN, (1973), Radiative Heat Transfer and Interactions with Conduction and Convection. John Wiley & Sons, 1st Edition

Pastor E, Zarate L, Planas E, Arnaldos J, (2003), Mathematical models and calculations systems for the study of wildland fire behavior. *Prog. Energy. Combust. Sci*. **29**: 139 – 153

Rehm RG, Baum, HR, (1978), The Equations of Motion for Thermally Driven, Buoyant Flows. *Journal of Research of the NBS*, **83**: 297 – 308

Rehm R, Evans D, Mell W, Hostikka S, McGrattan K, Forney G, Bouldin C, Baker E, (2003), Neighborhood-Scale Fire Spread. 5th Symposium on Fire and Forest Meteorology, November 16-20, American Meteorological Society, J6.7

Raithby GD, Chui EH, (1990), A Finite-Volume Method for Predicting Radiant Heat Transfer in Enclosures with Participating Media. *J. Heat Transfer*, **112**: 415 – 423

Reisner J, Wynne S, Margolin L, Linn R, (2000), Coupled Atmosphere-Fire Modeling Employing the Method of Averages. *Monthly Weather Review* **128**: 3683 – 3691

Rothermel RC, (1972), A mathematical model for predicting fire spread in wildland fuels. Research Paper INT-115, Intermountain Forest and Range Experiment Station, Odgen, Utah, USA

Smagorinksy J, (1963), General Circulation Experiments with the Primitive Equations I. The Basic Experiment. *Monthy Weather Reivew* **91**: 99 – 164

Stephens GL, (1984), The parameterization of radiation for numerical weather prediction and climate models. *Monthly Weather Review* **112**: 826 – 867

16 Physics-Based Modeling of Wildland-Urban Interface Fires

Ronald G. Rehm
RGR Consulting, LLC, 405 W. Montgomery Ave., Rockville, MD 20850, USA
Email: rehmro@comcast.net

David D. Evans
Home Safety Foundation, 3 Magnolia Parkway, Chevy Chase, MD 20815, USA
Email: devans@smartsafety.org

Abstract This paper addresses the development of a practical physics-based model for fires in the wildland-urban intermix. These fires arise when wildland burning invades the built environment. Fire models for ignition and spread must consider individual fuel elements of both vegetation and structures in order to assess fire risk of developed properties. The potential fuel loadings for various land uses demonstrates that structures can provide much higher loadings than wildlands do. However, the time scales for ignition and the heat release rates for the wildland fuel and the fuel in the structures will be widely disparate, influencing both the spread rate of the fire and its persistence. The NIST computational model known as the Fire Dynamic Simulator (FDS) was developed to study building fires. Its potential use to study community-scale fire spread is discussed.

Keywords Computational fluid dynamics; fire spread; firewise; mathematical models; potential fuel loads; wildland/urban interface fires; WUI

16.1 Introduction

The protection of structures in a community from destruction by fire is a national concern. Building codes and standards reduce the threat of fire by addressing the ways in which our communities can be built and the materials that can be used. Annually in the U.S. there are more than 300,000 fires that originate in homes. In addition, nearly 10% of the land and over one-third (42 million) of the homes in the U.S. today belong to the Wildland Urban Interface (WUI). The WUI is used to refer to both areas where housing abuts heavily vegetated areas (interface) and those areas where houses and vegetation are intermingled (intermix). If current trends in housing continue, the WUI will grow rapidly.

Experiments and case studies of WUI fires conducted by Cohen (2000), (2001) have shown that, under the conditions of these experiments, fuels, either vegetation or structures, within about 40 meters distance from a home constitute a major threat for ignition. At this “neighborhood scale,” models and the computational resources are adequate to allow simulation of many of the details of fire behavior. These models require detailed data on the topography, local meteorology, building layouts and elevations, three-dimensional distributions of natural fuels, and the material properties of both the natural fuels and the structures. Predictions of fire spread that threaten structures is the goal. The results can be used to understand the risk to communities on a property-by-property basis.

16.2 WUI Fuels

In the WUI, structures and vegetation are intermixed and their 3D distribution must be taken into account. As both the duration and intensity of burning structures is much greater than for vegetation, WUI fires cannot be studied accurately as a type of 2D fuel bed through which fire spreads. Furthermore, the intense burning of WUI fires cannot be characterized as burning along a line or boundary. WUI fires are area fires in which structures can burn independently from the vegetation. Figures 16.1(a) and (b) show respectively a damaged area from the Oakland Hills, CA fire and burning during the Summerhaven, AZ fire. In both fires, it is obvious that trees and structures ignite and spread fire differently. In some areas homes burn while surrounding trees are uninvolved. The report of Murphy et al (2007) on the Angora Fire near Lake Tahoe, 24 – 26 June, 2007, shows that fire behavior at the WUI is different than it is in wildland fuels alone. It describes ignition of

(a) (b)

Figure 16.1 (a) Spotty damage to homes and vegetation at the periphery of the 1991 Oakland Hills fire area. (b) Homes in Summerhaven, AZ burn amid tall trees during 2003 Aspen fire. (Photo Courtesy of KTVK NewsChannel 3, Phoenix, Arizona) structures by brands and by ground fire while nearby tree crowns remain untouched even under the prevailing very dry conditions. The fact that it is common in WUI fires to find homes totally destroyed adjacent to vegetation that is untouched illustrates the complicated nature of the WUI fire events.

Only two references were found that discuss substantive technical issues related to wildland and community fires (Maranghides, 1993) and (Chandler et al., 1983). Maranghides attempts for the first time to combine analyses of ignition and spread of a fire in a vegetation fuel bed, commonly employed in current operational models, with a model for ignition of a structure. This simple and interesting physics-based approach is found to be limited by a lack of data, a problem also discovered by the authors of the present study.

In the second, Chandler et al., (1983), in Chapter 8 entitled, "Fire at the Urban-Forest Interface," make several very important observations. First, the authors note that fuel loadings in buildings are typically many times those in a forest: "the heaviest likely fuel load in the forest is less than the lightest load for a structure." Next they observe that fuels in buildings include a variety of combustibles whereas forest fuels are exclusively cellulosic. The authors also point out several important differences between burning in a structure and burning forest fuels. Moisture, which is a very important factor in ignition and burning intensity, is controlled within a building, but is determined in wildlands by environmental factors such as the sun, wind and precipitation. Radiation from an indoor fire is trapped inside the building whereas most radiation in a wildland fire escapes. Similarly, most convective heat is trapped in an indoor fire whereas it is lofted into the atmosphere in a wildland fire. Finally, oxygen is severely limited in an indoor fire whereas it is virtually unlimited in a wildland fire.

The first point concerning the potential fuel loading differences between structural and wildland fuels is illustrated in Fig. 16.2. In this figure, land use has been divided into four basic categories: wildland, rural, suburban and urban. The number of structures per hectare is plotted as the abscissa, and the ratio of the estimated vegetation energy load to the structure energy load is the ordinate. In this diagram, wildland covers the upper left corner of the diagram, where the number of structures is small and the vegetation energy load is relatively high, whereas the urban area occupies the lower right corner. Also shown on this plot are several fires for which we estimated, from information available, the potential energy load per hectare where the fires did their greatest damage to the built environment, whether the fires began there or elsewhere. Note that the Oakland Hills fire of 1991 and the Los Alamos/Cerro Grande fire of 2000 fall directly in the category of suburban fires and are good examples of community-scale or WUI fires. Greater details about this analysis are available from (Rehm et al., 2002).

In the suburban and urban setting, the key quantity is the density of houses—together with the combustible material in these houses and the ignition propensity—in determining fuel loading and fire behavior, see Rehm (2006). One of the most important parameters governing the physics of fire spread in wildland

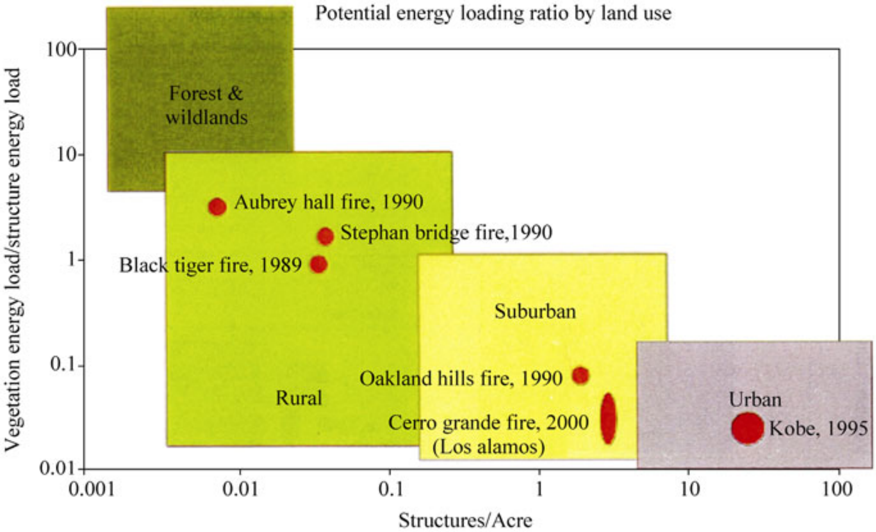

Figure 16.2 Potential energy loading by land use. Also shown are six specific fires including the Oakland Hills fire of 1991 and the Los Alamos/Cerro Grande fire of 2000

material is the heat release rate (HRR) of all burning materials, including structural and wildland fuels. The density of trees, shrubs and ground cover (grass) is important for determination of the fire behavior, but clearly house density is critical.

An estimate of the HRR during a house fire in the Oakland and Berkeley Hills fires was made by Trelles (1995) and by Trelles and Pagni (1997). According to these estimates, a house burns at a peak rate of 45 MW for 1 hour (yielding about 160 GJ), and then dies down over another 6 hour period. The die-down of the fire is approximated as two steps, one 10 MW for 3 h and the last as 5 MW for 3 more hours. The total burn time is 7 hours, and the total energy released by the house is 324 GJ. If the house is assumed to have a 15 m by 15 m footprint, then we estimate the total potential fuel loading per unit area to be 1.4 GJ/m^2 and the peak HRR per unit planview area to be 0.20 MW/m^2.

For comparison Figs. 16.3(a) and 16.3(b) show the burning of a small (6.2 m by 5 m by 2.5 m) wood frame out building in Odenton, MD ignited by burning vegetation. Measurements of the total heat flux were made 16.6 m from the building. Assuming uniform hemispherical heat flux and 30 percent radiative fraction from the fire a preliminary estimate of the total heat production of the fire was calculated. From this analysis, the building fire was found to produce a sustained HRR of about 23 MW for approximately 5 minutes. The peak HRR per unit planview area was then approximately 0.74 MW/m^2. The peak value for the HRR per unit area is much greater than the value estimated for homes in the Oakland Hills fire, but the fire duration is much shorter.

The widely different burning characteristics of petroleum based home furnishing materials (shingles, foam, plastics and synthetic fabrics and carpets) compared to

Figure 16.3 (a) Small building ignition. (b) Full involvement

wood materials can change the characteristic HRR for a home by an order of magnitude. Chandler et al (1983) describe the concept of an “ideal” burning rate, which was first introduced by Tewarson and Pion (1976). The “ideal” burning rate is the rate at which the energy required to produce a unit mass of fuel gas is equal to the energy released by burning the fuel gases in air. At the “ideal” burning rate, energy lost from the burning surface equals that supplied from the flame and other sources. Tewarson and Pion (1976) tabulate the ideal burning rates for several fuels. Liquid hydrocarbons have ideal HRRs per unit area ranging between 0.7 MW/m^2 and 3.0 MW/m^2. The corresponding rate for wood is about 0.26 MW/m^2.

The fuel-bed burning used in operational models suggests the use of the plan view area basis for comparing the burning of structures and wildland fuel. However, characterization of burning structures for WUI fire modeling remains to be resolved.

16.3 Fire Model

For wildland fires, mathematical models are regularly used to predict the likely burn development for expected meteorological conditions. These models, which are known as operational models, have largely developed through empirical correlations over the past few decades. In the United States, they include the Rothermel model, (Rothermel, 1972), and models known as BEHAVE, (Andrews and Bevins 1999), and FARSITE, (Finney and Andrews, 1999), with the last one being the most recent and most highly developed.

Generally, these operational models have served well as long as the fires are confined to wildland fuels alone. They are based on the assumption that the fuels can be represented by continuum 2D beds, which may be inhomogeneous and anisotropic, but nevertheless are continuous. Thus these models can address horizontal variation of fuel beds, but cannot address 3D structure of fuels. Fire spread in fuels that include buildings and transitions from ground to crown fires are among the fire phenomena that cannot be analyzed using these models. For example, in the report on “Standard Fire Behavior Fuel Models…,” by Scott and Burgan (2005), urban development in the context of wildland fire models is regarded as “nonburnable” with “expected fire behavior: no fire spread.” There is no mention of fire spread in suburban areas where both wildland and structural fuels exist.

When the built environment becomes involved in a fire, as in the Oakland and Berkeley Hills fire of October 21, 1991, or more recently the Los Alamos fires of May 2000 and Summerhaven, AZ of June 2003, these operational models are ineffective. The operational models cannot predict the spread of fire because the building fuel loads are larger and discrete. In these community-scale fires, buildings must be treated as discrete fuel elements. At a fundamental level, the physical mechanisms controlling fire spread are very different than those in wildland fires. The empirical correlations upon which the wildland-fire models have been developed are no longer valid, in part because the heat released by the burning structures influences how the fire spreads even in the wildland fuel, see Rehm (2006). No validated predictive models of fires in an urban or urban/wildland setting exist to our knowledge.

Over the past 25 years, the Building and Fire Research Laboratory (BFRL) at the National Institute of Standards and Technology (NIST) has been developing a physics-based mathematical and computational model, the current version known as the fire dynamics simulator (FDS), to predict fire spread in a structure. Over the past few years, it has also been used to predict smoke and hot gas plume behavior produced by outdoor fires. FDS is well documented and is widely used by fire protection engineers around the world. BFRL is extending the model to include fire spread from structure to structure and generalizing FDS to include a means to predict fire spread in both continuous and discrete natural fuels. The current model, as well as its generalization, is both computationally and data intensive. For any specified region, the model requires high-resolution, 3D data to describe the geometry, fuels, and the ignition and burning characteristics. In addition, more recently, it has been used to predict wind fields in the built environment with one to ten meter resolution over regions measuring up to one kilometer or so on a side. All of these simulations require only a current high-end PC running overnight. The code can be downloaded free of cost from the URL: http://fire.nist.gov. It consists of two components, a computational fluid dynamics (CFD) code, called FDS, written in Fortran 90 for computation of fire-driven flows, and an OpenGL graphics program known as Smokeview for visualization of results, see McGrattan et al. (2000), McGrattan and Forney (2000), and Forney and McGrattan et al. (2000).

A second fire modeling effort for wildland fuels alone is underway at the Los Alamos National Laboratory under the direction of Dr. Rodman Linn (2002). Both models can address the 3D structure of fuels. Linn’s model is currently being used to understand fire behavior in wildland fuels. Both models will need extensive 3D data on the properties of wildland fuels in order to calibrate and validate the model assumptions.

FDS has been used to construct a simulation of burning and fire spread in the WUI that is useful for analyzing the fire hazards associated with a structure and its surroundings. In FDS, structures and vegetation must be characterized as separate fuel elements with individual ignition and burning properties. As each element in the model can be modified, the value of actions taken by owners or land managers to reduce hazards can be analyzed. It is expected that when properly validated, using data yet to be obtained, FDS will be able to duplicate the well known fire spread characteristics in ground fuels, but will also have the capabilities of quantifying transitions of fire spread between fuel types. This includes the phenomena of transitions from ground fire to tree-crown fires as well as ignition and burning of structures intermixed with vegetation. Such a tool will be of value to community planners, building code authorities and firefighters.

The capabilities of the FDS model can be demonstrated by an example. Figure 16.4 shows a series of frames from an FDS simulation of fire spread on a parcel of land. These frames were obtained using the Smokeview visualization software, also developed at NIST. Four structures, many trees, and shrubs have all been included in this simulation. It can be seen that simulations of fire events on the

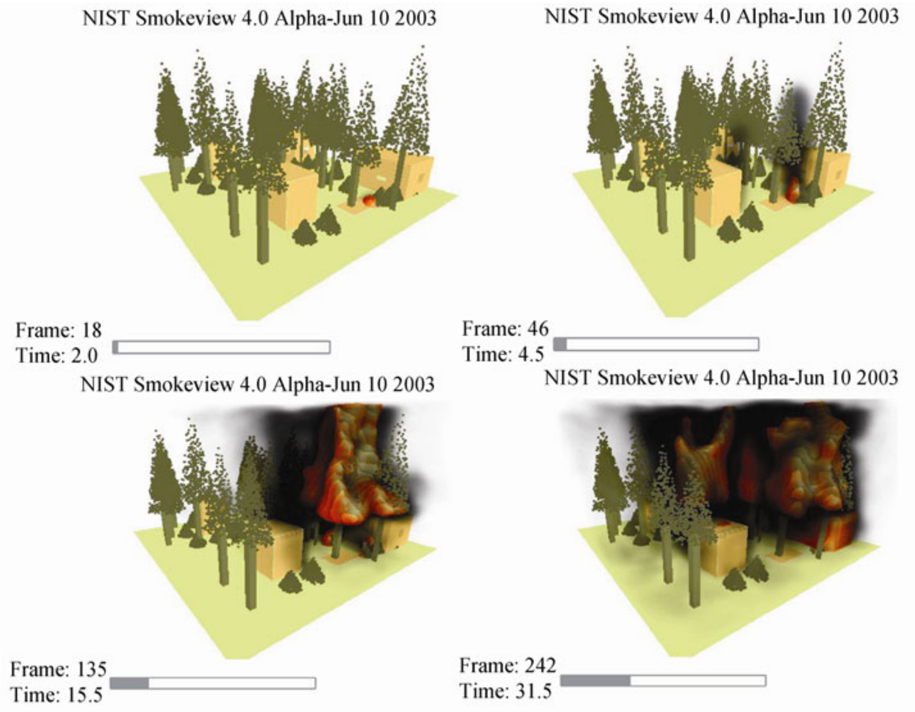

Figure 16.4 Selected frames from FDS / Smokeview simulation of "neighbourhood scale" fire spread from a single ignition. The fire spreads from ground fuels (grass), through ladder fuels (shrubs around houses) to the tree-crowns. Structures are ignited by heat flux from the burning vegetation. The time shown is the burn time for extremely dry fuels

“neighborhood scale” are now possible. For the simulation, ignition and burning characteristics for each of the fuel elements–ground surface, shrubs, trees and the homes were selected. The selection of these properties was guided by experiments and other experience. From a single ignition point, the model predicts where and how rapidly the fire will spread. It considers heat transfer by convection and radiation, sensible and latent heat of pyrolysis absorption by material, ignition conditions for materials, the consumption of mass by burning, smoke generation, smoke blocking of radiation from fires, and the effect of wind. Fire spread by brands is not included in the current model. It is known that structures have a greater ignition delay time and total burning time than wildland fuels. The long burning structures distributed over an extended area produce plumes that can substantially change the wind patterns and therefore the spread of the fire front at some distance from the structures (Trelles and Pagni, 1997), (Rehm, 2006).

Even though the graphical representation of the result is realistic, it should be remembered that underlying the pictures at every position (to the limit of the cell size in the computation) the gas and surface temperatures, gas velocity, heat flux, and materials burning can be quantified for each time step in the simulation. There is an enormous amount of detailed information available from the model. It is common to view the results as computer generated simulations and gain insight from the viewing as one would from seeing an actual fire event.

The “neighborhood scale” fire simulations using FDS have the capability to provide authorities with insight about the fire safety in communities. The simulations can also be used to assess the impact of changing local regulations. The physical science basis for the FDS model provides confidence that even without the benefit of comparison with full-scale urban fire experiments, it is capable of providing relative quantitative results between alternatives and accurate predictions of trends.

16.4 Conclusions

Through the capabilities to simulate the major features of WUI fires, we are beginning to develop an understanding of the mechanisms by which fires progress in a community where both structures and wildland fuels exist. Except for investigations of actual community fires, we have not previously had a technology that was capable of providing the fire safety insight that can be obtained from physics-based, high temporal and spatial resolution simulations. Many fire-properties of vegetation and structures remain to be measured in ways that permit the description of the ignition and burning of individual trees, shrubs, and structures. All methods of fire propagation, including spread by brands, need to be quantified to build a complete and accurate model of the WUI fire. Experimental data for ignition and fire spread for individual elements and the collective fuel layout are needed to calibrate and validate such high-resolution fire models.

References

Andrews PL, Bevins CD, (1999), BEHAVE Fire Modeling System: Redesign and Expansion. *Fire Management Notes*. **59**: 16 – 19, http://fire.org/

Chandler C, Cheney P, Thomas P, Trabaud L, Williams D, (1983), Fire in Forestry: Volume Ⅱ Forest Fire Management. Wiley-Interscience, John Wiley & Sons, New York

Cohen JD, (2000), Preventing Disasters, Home Ignitability in the Wildland-Urban Interface. Journal of Forestry 15 – 21, March 2000

Cohen JD, (2001), Wildland-urban fire—a different approach. In: Proceedings of the Firefighter Safety Summit, Nov. 6 – 8, 2001, Missoula, MT. Fairfax, VA: International Association of Wildland Fire. http://www.umt.edu/ccesp/wfs/proceedings/Jack D. Cohen.doc

Finney MA, Andrews PL, (1999), FARSITE - A Program for Fire Growth Simulation. *Fire Management Notes*. **59**: 13 – 15; http://fire.org/

Forney GP, McGrattan KB, (2000), User's Guide for Smokeview Version 1.0—A Tool for Visualizing Fire Dynamics Simulation Data. NISTIR 6513, National Institute of Standards and Technology

Linn R, Reisner J, Colman J, Winterkamp J, (2002), Studying Wildfire Behavior using FIRETEK. *International Journal of Wildland Fire*. **11**: 233 – 246

Maranghides A, (1993), Wildland-Urban Interface Fire Models. MS Thesis to Worchester Polytechnic Institute, December 8, 1993, 139

McGrattan KB, Baum HR, Rehm RG, Hamins A, Forney GP, (2000), Fire Dynamics Simulator - Technical Reference Manual. NIST Report NISTIR 6467, National Institute of Standards and Technology

McGrattan KB, Forney GP, (2000), Fire Dynamics Simulator—User's Manual. NIST Report NISTIR 6469, National Institute of Standards and Technology

Murphy K, Rich, T. and Sexton, T, (2007), An Assessment of Fuel Treatment Effects on Fire Behavior, Suppression Effectiveness, and Structure Ignition on the Angora Fire, USDA Report R5-TP-025

Rehm RG, Hamins A, Baum HR, McGrattan KB, Evans DD, (2002), Community-Scale Fire Spread. NIST Report NISTIR 6891, National Institute of Standards and Technology

Rehm, RG, (2006), The Effects of Winds from Burning Structures on Ground-Fire Propagation at the Wildland-Urban Interface, NIST Report NIST GCR 06-892. http://fire.nist.gov/bfrlpubs/

Rothermel RC, (1972), A Mathematical Model for Predicting Fire Spread in Wildland Fuels. USDA Forest Service Research Paper INT-115, Intermountain Forest and Range Experiment Station

Scott, JH. and Burgan, RE, (2005), Standard Fire Behavior Fuel Models: A Comprehensive Set for Use with Rothermel's Surface Fire Spread Model USDA Forest Service Report RMRS-GTR-153. http://www.firemodels.org/downloads/behaveplus/publications/Scott_and_Burgan_RMRS-GTR-153_2005.pdf

Tewarson A, Pion RF, (1976), Flammability of Furnishings. *Combustion and Flame*, **26**: 85 − 103

Trelles J, (1995), Mass Fire Modeling of the 20 October 1991 Oakland Hills Fire. Ph.D. Thesis in Mechanical Engineering, University of California at Berkeley

Trelles J, Pagni PJ, (1997), Fire-Induced Winds in the 20 October 1991 Oakland Hills Fire. Fire Safety Science-Proceedings of the Fifth International Symposium, 3 − 7 March 1997, Melbourne, Australia, Yuji Hasemi (ed) 911 − 922

17 Climate Change and Fire impacts on Ecosystem Critical Nitrogen Load

Steven G. McNulty*, Sara E. Strickland, Erika Cohen, Jennifer A. Moore Myers

Eastern Forest Enviornmental Threat Assessment Center, USDA Forest Service, 920 Main Campus Drive, Suite 300. Raleigh, NC 27606. (919)515-9489

*primary contact Email: steve_mcnulty@ncsu.edu

Abstract The federal agencies of the United States (US) are currently developing guidelines for critical nitrogen loads for US forest ecosystems. These guidelines will be used to establish regulations designed to maintain nitrogen inputs below the level shown to damage forests and streams. Traditionally, an ecosystem is considered to be at risk for health impairment when the critical nitrogen load exceeds a level known to impair forest health. The excess over the critical nitrogen load is termed the exceedance, and the larger the exceedance, the greater the risk of ecosystem damage. This definition of critical nitrogen load applies to a single, long-term pollutant exposure. Unfortunately, a single critical nitrogen load level may not accurately reflect ecosystem health risk when an ecosystem is subjected to multiple environmental stresses. In other US regions, fire is a major component of the forest ecosystem. Fire volatilizes organic nitrogen, reduces plant nitrogen uptake, increases nitrogen mineralization and nitrification, and can change the pH level of surface horizons. If multiple stress impacts (i.e., drought and fire) are included in critical nitrogen load assessments, critical nitrogen load may need to be lowered in many areas. This paper explores how fire and climate change and variability influence ecosystem critical nitrogen loads.

Keywords Critical load, nitrogen, United States, forests

17.1 Introduction

Air borne nitrogen (N) from industry and automobile exhaust has been falling across Europe and New England for over 60 years in the form of acid rain. Heavily polluted areas can receive over 50 $kg{\cdot}N{\cdot}ha^{-1}$ each year (Holland et al., 2005). The environmental impacts of air pollutants have been studied since nitrogen was first suspected to cause forest damage and decline across the region in the mid 1980s. High pollutant levels and forest mortality can lead to leaching of soil aluminum (Al) and nitrate (NO_3) (Cronan and Schofield, 1979; Berg, 1986; Johnson et al., 1994) and subsequent increases in stream Al and NO_3. Increased Al and NO_3 stream concentrations can have negative health impacts on fish populations and human water supplies (Baker et al., 1996). Too much nitrogen in trees can also cause aluminum toxicity in roots (Shortle and Smith, 1988), foliar nutrient imbalance (Zoettl and Huettl, 1986; Cronan and Grigal, 1995), reduced tree cold tolerance (Sheppard, 1994), and tree freezing injury (DeHayes, 1992). Each of these stressors can lead to tree mortality (Aber et al., 1989; McNulty et al., 2005).

Traditionally, an ecosystem is considered to be at risk for health impairment when its critical nitrogen load exceeds a level known to impair forest health. Deposition in excess of the critical nitrogen load is termed the nitrogen exceedance, and the larger the nitrogen exceedance, the greater the risk of ecosystem damage. This definition of critical nitrogen load applies to a single, long-term pollutant exposure. However, a static critical nitrogen load level may not accurately assess ecosystem risk to damage when an ecosystem is subjected to multiple, episodic environmental stresses. If multiple stress impacts (i.e., climate change and variability and fire) are included in critical nitrogen load assessments, critical nitrogen load may need to be lowered in many areas to maintain long-term ecosystem health.

Various methods have been designed to test the critical nitrogen load of an ecosystem. One of the most popular methods for determining an ecosystem's critical load is the use of a simple mass balance equation. The simple model uses static soil, climate, vegetation, and pollutant deposition data to estimate an ecosystem's critical load. We will examine how climate change and fire could alter each of the ecosystem parameters used in a simple mass balance equation for critical nitrogen loading.

17.2 Climate Change Impacts on Critical Loads

Climate change is a generic termed used to define a host of changing environmental conditions associated with the atmospheric increase of "greenhouse" gases and global warming. Climate change is characterized by both climatic shifts and increased climate variability. Both inter-decadal shifts in climate and inter-annual climate variability can influence the critical nitrogen load of an ecosystem.

17.2.1 Drought

Water is one of the principle determinants of ecosystem type. Average annual precipitation in temperate forests ranges from 50 – 250 cm per year. Deserts, scrubland, and woodlands receive between 0 cm and 125 cm of precipitation per year (Whittaker, 1970). Millennia of plant competition have favored vegetative species that best adapt to limited resources (including water).

Short-term (i.e., less than two years) drought can cause reduced ecosystem productivity (Hanson, 2000), reduced leaf longevity in deciduous species (Jonasson, 1997), and reduced leaf area (Gholz, 1990). These factors reduce biological demand for nitrogen. Under extreme drought, reduced soil moisture can cause reduced nitrogen mineralization and nitrification that then result in reduced ammonium and nitrate availability. These conditions will cause little short-term impact on critical nitrogen load if both nitrogen demand and supply are reduced. However, nitrogen deposition will continue to accumulate in the ecosystem, and a nitrate pulse could occur following a drought if nitrogen mineralization and nitrification rates respond more quickly to available water than plant demand for nitrogen.

Long-term (i.e., greater than two years) droughts can cause additional ecosystem disruptions, and therefore have the potential to significantly lower ecosystem critical nitrogen load levels. Long-term droughts have all of the characteristics of short-term drought (described above) plus the potential for tree mortality due to water stress (Kloeppel, 2003), increased insect outbreak potential (Mattson, 1987), and increased fire risk (Flannigan and Wotton, 2001). As with the short-term drought, long-term drought may reduce biological nitrogen demand and supply. Additionally, the potential for terrestrial vegetation mortality could lead to a significant decrease in biological nitrogen demand. If tree mortality is severe, a large nitrate pulse could occur following the drought, similar to the nitrogen pulse observed following forest harvesting (Vitousek, 1985).

The critical nitrogen load may be significantly reduced for several years after drought-induced forest mortality, because new growth cannot fully utilize existing water, light, and nutrients. For example, in the Southern Appalachian Mountains a combination of drought, increased air temperature, and insects likely caused the mortality of mature high elevation red spruce (Picea rubens) trees. The critical pollutant load level for this area will be reduced until new growth can fill in gap openings and increase biological nitrogen demand.

17.2.2 Climate Change Shifts in Water Availability

Both short- and long-term droughts are transient weather events. However, climate change is a permanent shift in the amount and timing of precipitation for a region. Changes in tree species, nutrient cycling, and water flow are all likely with climatic shifts. Reductions in precipitation would cause a shift toward more open, drought tolerant woodlands (Hansen, 2001). As tree density decreases, nitrogen demand and uptake by vegetation decreases. Therefore, the critical nitrogen load for an ecosystem receiving less precipitation would likely decrease. Conversely, the critical nitrogen load could increase if climate change causes an increase in precipitation, along with a shift toward more dense forests with higher nitrogen demands.

Long-term precipitation change-induced forest species shifts can also change the nitrogen cycle. Mesic tree species have a tendency to be more nitrogen demanding (Watmough, 2004). Therefore, increased precipitation could gradually shift a forest toward a higher critical nitrogen load.

17.2.3 Increased Air Temperature

During the next century, substantial changes are expected to occur in a variety of environmental variables including temperature. The magnitude of these changes is expected to vary temporally and spatially. The intergovernmental panel on climate change (IPCC) concluded that average global surface temperature is projected to increase by between 1.4℃ and 5.8℃ above 1990 levels by 2100 (Houghton et al., 2001).

While all general circulation models predict that the earth will warm over the next century, the degree and distribution of the warming is not clear (Houghton et al., 2001). The disagreement about warming is largely due to uncertainty regarding reductions in green house gas emissions and model design and use (Thorning, 1998; USGCRP, 2001).

Biological processes accelerate as air temperature increases. Increases in tree respiration and metabolism can shorten leaf retention time as temperature increases. Litter decomposition, soil nitrogen mineralization, and soil nitrification also increase with increasing temperature. Increases in both nitrogen demand and supply can offset each other, and the critical nitrogen load may not change. However, if tree nitrogen demand does not keep pace with nitrogen availability, then critical nitrogen loads could decrease with increasing air temperature.

17.3 Fire Impacts on Critical Pollutant Loads

Fires can be either controlled or wild; both types can impact an ecosystem’s critical pollutant load, but in different ways. Therefore, the critical nitrogen load impact of each type of fire will be discussed separately.

17.3.1 Wildfire Impacts on Critical Loads

From 1994 – 2004, an average of 4 million acres of forestland was burned by wildfire every year, and most of these fires occurred in the Western US (NIFC, 2005). Over 50 years of fire suppression have led to a significant accumulation of fire fuels across the Eastern US (Brown et al., 2004). Climate change can impact the likelihood of wildfires due to warmer air temperatures (Fried et al., 2004), increased lightning strikes (Price and Rind, 1994) and changed atmospheric synoptic patterns (i.e., movement of the jet stream, Heilman et al., 1997). Increased fuel loads and global warming have resulted in an increase in area burned, with over 8 million acres burned in both 2004 and 2005 (NIFC, 2005). Both controlled burns and wildfires significantly impact forest structure and function, which in turn affect the critical nitrogen load of the ecosystem.

Low impact wildfires can influence critical load levels in ways similar to a controlled burn. High impact wildfires can significantly alter ecosystem structure and function for many years (NWCG, 2001) and can have both positive and negative impacts on ecosystem critical load levels.

Short-term (i.e., less than 5 years) negative impacts of wild fires include the loss of soil cation exchange capacity (CEC) and organic matter (see Table 17.1) that reduce the ecosystem critical nitrogen load. Wildfires can burn hot enough to sterilize the soil and volatilize organic nitrogen, which then greatly reduces soil processes such as nitrogen mineralization (Table 17.1). Under these conditions, ammonium (NH_4) deposition may be a significant source of nitrogen needed for plant regeneration while nitrate (NO_3) deposition may be rapidly leached through the soil.

Table 17.1 Effects of controlled fire, wildfire, and climate change on critical loads. (+) represents increase in critical load, (–) represents decrease in critical load, (→) represents possible increase or decrease in critical load

CL Factor	Disturbance	Trend	Source	Site	Notes
Soil pH	controlled fire	→	Vose et al. 1999	pine-hdwd forest, southern appalachians	
		+	Boerner et al. 2004	mixed-oak forest, southern Ohio	
		+	Lynham et al. 1998	immature jack pine forest, Ontario	still elevated after 10 yrs in organic layer
		+	McKee 1982	southern pine forests, SE coastal plain	in mineral soil, coastal plain pine sites, short-term, increased effects with increased fire intensity
		→	Masters et al. 1993	oak-pine forest, Ouachita Mtns, OK	
		+	NWCG 2001	increase more significant on low pH sites	
		+	Knoepp et al. 2004	mixed oak-pine forest, southern appalachians	

(Continued)

CL Factor	Disturbance	Trend	Source	Site	Notes
	wildfire	+	Amirbahman et al. 2004	heterogeneous predom hdwd forest, Arcadia NP, ME	long-term, in all horizons
		+	Simard et al. 2001	boreal forest, Quebec	in organic, no difference in mineral layer
		+	Alauzis et al. 2004	Nothofagus forest in Patagonia, Argentina	sampled at 10 cm, still high 4 yrs after burn
		+	Hernandez 1997	Mediterranean pine forest	still slightly higher 9 mos after burn
		+	Baird et al. 1999	coniferous forest, Cascades, WA	in mineral layers
	climate change	+	Smith et al. 2002		
		+	Ryan et al. 1998	spruce forest in Ireland, maritime climate	drought followed by rewetting (to simu-late climate change effects of drought then intense rainfall)
Soil organic matter	controlled fire	→	Boerner et al. 2004	mixed-oak forest, southern Ohio	
		–	Phillips et al. 2000	deciduous forest, Tennessee	on annually burned plots, little change on periodically burned plots
		–	NWCG 2001		
		–	Neary et al. 1999		loss increases with fire severity
		+	Waldrop et al. 1987	pine forest, SC	in mineral layers
	wildfire	–	Baird et al. 1999	coniferous forest, Cascades, WA	
		–	Neary et al. 1999		
		–	Hernandez et al. 1997	Mediterranean pine forest	
Soil bulk density	controlled fire	+	Phillips et al. 2000	deciduous forest, Tennessee	on annually burned plots, little change on periodically burned plots
	wildfire	→	Baird et al. 1999	coniferous forest, Cascades, WA	for mineral layers

(Continued)

CL Factor	Disturbance	Trend	Source	Site	Notes
N mineral-ization	controlled fire	→	Boerner et al. 2004	mixed-oak forest, southern Ohio	
		+	Bell & Binkley 1989	loblolly pine plantation	
		+	Covington & Sackett 1992	ponderosa pine forest, Flagstaff, AZ	
		+	Christensen 1973		
		+	Rapp 1990	pine forest, Mediterranean	in organic layers
	wildfire	+	Neary et al. 1999		citing Klopatek
	climate change	+	Williams et al. 1998	in alpine CO	
		+	Verburg & van Breemen 2000	with elevated temp & CO_2	
		+	Ryan et al. 1998	spruce forest in Ireland, maritime climate	drought followed by rewetting (to simulate climate change effects of drought then intense rainfall)
		+	Hart & Perry 1999	old-growth forest, Oregon	more than doubled for soils transferred from high elevation to low elevation site
		+	Pastor & Post 1988		
Nitrifi-cation	controlled fire	→	Boerner et al. 2004	mixed-oak forest, southern Ohio	
		+	Covington & Sackett 1992	ponderosa pine forest, Flagstaff, AZ	
		+	White 1985	ponderosa pine forest, New Mexico	
		+	Pietikainen & Fritze 1995	spruce forest, NE Finland	
		+	Bauhus et al. 1993	Australia	
	wildfire	+	Neary et al. 1999		citing Klopatek
		+	Hernandez et al. 1997	Mediterranean pine forest	

(Continued)

CL Factor	Disturbance	Trend	Source	Site	Notes
	climate change	–	Smith et al. 2002		
		+	Williams et al. 1998	in alpine CO	
		→	Verburg & van Breemen 2000	increased, but not significantly, with elevated temp & CO_2	
		+	Hart & Perry 1999	old-growth forest, Oregon	more than doubled for soils transferred from high elevation to low elevation site
Total soil N	controlled fire	→	Knoepp & Swank 1993	pine hdwd forest, s. Appalachians	
		–	Vose et al. 1999	pine-hdwd forest, s. Appalachians	slight decrease
		+	Lynham et al. 1998	immature jack pine forest, Ontario	in mineral layers, still elevated after 10 yrs
		–	Lynham et al. 1998	immature jack pine forest, Ontario	in organic layers
Total soil N		→	Wan et al. 2001	meta-analysis	meta-analysis, for surface layers
		–	Binkley et al. 1992	pine forest, coastal plain of SC	in organic layers
		→	Binkley et al. 1992	pine forest, coastal plain of SC	in mineral layers
		+	Covington & Sackett 1992	ponderosa pine forest, Flagstaff, AZ	in mineral layers
		+	McKee 1982	southern pine forests, SE coastal plain	in mineral layers
		→	Waldrop et al. 1987	pine forest, SC	in mineral layers; increased slightly due to increased abundance of N-fixing legumes & forbs
		+	Knoepp et al. 2004	mixed oak-pine forest, southern Appalachians	
	wildfire	–	Alauzis et al. 2004	Nothofagus forest in Patagonia, Argentina	sampled at 10 cm, still low 4 yrs after fire
		–	Baird et al. 1999	coniferous forest, Cascades, WA	in all horizons
		–	Fernandez et al. 1997	pine forest in NW Spain	

(Continued)

CL Factor	Disturbance	Trend	Source	Site	Notes
		–	Parker et al. 2001	spruce & hdwd stands in ME	for organic layer, 50 yrs after wildfire
		+	Parker et al. 2001	spruce & hdwd stands in ME	for upper mineral layer, 50 yrs after wildfire
		–	Kutiel & Naveh 1987	pine forest in Israel	
	climate change	–	Smith et al. 2002		
N availa-bility	controlled fire	+	Knoepp & Swank 1993	pine-hdwd forest, s. appalachians	still elevated after 1 yr
	climate change	–	Yin 1992		decreases with increasing January & July temps
		+	Bonan & Van Cleve 1992	black spruce forest	model prediction
		+	Schimel et al. 1990	grassland ecosystems	due to higher decomposition rates
Soil ammo-nium	controlled fire	+	Knoepp & Swank 1993	pine-hdwd forest, s. appalachians	still elevated after 1 yr
		+	Wan et al. 2001	meta-analysis	meta-analysis, back to original values 1 yr later
		+	Covington & Sackett 1992	ponderosa pine forest, Flagstaff, AZ	substantial increase immediately after burn, returned to original levels in all stands except old-growth after 1 yr
		+	Rapp 1990	pine forest, Mediterranean	in organic layer, still much higher 6 wks after burn, no change in mineral layer
	wildfire	+	Hernandez et al. 1997	Mediterranean pine forest	still high 9 mos after fire
		+	Kutiel & Naveh 1987	pine forest	still high 8 mos after fire
	climate change	+	Smith et al. 2002		
Soil ammo-nium		+	Ryan et al. 1998	spruce forest in Ireland, maritime climate	drought followed by rewetting (to simu-late climate change effects of drought then intense rainfall)

(Continued)

CL Factor	Disturbance	Trend	Source	Site	Notes
Soil nitrate	controlled fire	→	Knoepp & Swank 1993	pine-hdwd forest, s. appalachians	
		+	Wan et al. 2001	meta-analysis	meta-analysis, increase small at first, increased at 0.5-1 yr after fire, then declined
		+	Covington & Sackett 1992	ponderosa pine forest, Flagstaff, AZ	→ immediately after burn, increase found 1 yr later (in old-growth stands)
		+	Rapp 1990	pine forest, Mediterranean	in organic layers: decrease after fire, increase 6 weeks later
	wildfire	+	Hernandez et al. 1997	Mediterranean pine forest	
		+	Kutiel & Naveh 1987	pine forest	still high 8 mos after fire
	climate change	+	Williams et al. 1998	in alpine CO	
Soil CEC	controlled fire	–	Vose et al. 1999	pine-hdwd forest, s. appalachians	
		–	Gimeno-Garcia et al. 2000	shrubland in Mediterranean Spain	organic layer
	wildfire	–	Fernandez et al. 1997	pine forest in NW Spain	
Soil S	controlled fire	–	Binkley et al. 1992	pine forest, coastal plain of SC	2.0 to 5.3 g/m^2 lower in burn sites (in organic hor)
		–	Richter et al. 1982	pine forest, southeast	0.2 to 0.8 g/m^2 for burn sites
		→	Binkley et al. 1992	pine forest, coastal plain of SC	in mineral layers
	wildfire	→	Amirbahman et al. 2004	heterogeneous predom hdwd forest, Arcadia NP, ME	long-term
Soil P	controlled fire	+	Lynham et al. 1998	immature jack pine forest, Ontario	still elevated after 10 yrs
		+	McKee 1982	southern pine forests, SE coastal plain	
		→	Binkley et al. 1992	pine forest, coastal plain of SC	in organic layers
		+	Gimeno-Garcia et al. 2000	shrubland in Mediterranean Spain	organic layer
		+	Waldrop et al. 1987	pine forest, SC	in mineral layers

(Continued)

CL Factor	Disturbance	Trend	Source	Site	Notes
	wildfire	+	Simard et al. 2001	boreal forest, Quebec	
		+	Alauzis et al. 2004	Nothofagus forest in Patagonia, Argentina	sampled at 10 cm, still high 4 yrs after burn
		+	Hernandez et al. 1997	Mediterranean pine forest	
		+	Kutiel & Naveh 1987	pine forest	still high 10 mos after burn
C mineral-ization	wildfire	+	Fernandez et al. 1997	pine forest in NW Spain	
	climate change	+	Williams et al. 1998	in alpine CO	
Soil C	controlled fire	–	Vose et al. 1999	pine-hdwd forest, s. appalachians	slight decrease
		–	Thornley & Cannell 2004	boreal forest, from Edinburgh Forest Model	
		+	Wells et al. 1979		
	wildfire	+	Amirbahman et al. 2004	heterogeneous predom hdwd forest, Arcadia NP, ME	long-term
		–	Alauzis et al. 2004	Nothofagus forest in Patagonia, Argentina	sampled at 10 cm, still low 4 yrs after fire
		–	Wardle et al. 2003	boreal forest, Swedish lake islands	
		–	Thornley & Cannell 2004	boreal forest, from Edinburgh Forest Model	
		–	Prieto-Fernandez et al. 1998	pine forest in temperate, humid NW Spain	still lower 13 yrs after fire
		–	Fernandez et al. 1999	pine forest in temperate, humid NW Spain	
		–	Fernandez et al. 1997	pine forest in NW Spain	
		–	Hernandez et al. 1997	Mediterranean pine forest	still low 9 mos after fire
		–	Parker et al. 2001	spruce & hdwd stands in ME	for organic layer, 50 yrs after wildfire
		+	Parker et al. 2001	spruce & hdwd stands in ME	for upper mineral layer, 50 yrs after wildfire

(Continued)

CL Factor	Disturbance	Trend	Source	Site	Notes
		–	Baird et al. 1999	coniferous forest, Cascades, WA	for all horizons
		–	Groeschl et al. 1993	pine forest	
		–	Smith et al. 2002		
C:N ratio	controlled fire	+	Binkley et al. 1992	pine forest, coastal plain of SC	in organic horizons
		–	Klopatek et al. 1991	pinyon-juniper ecosystem	
	wildfire	–	Fernandez et al. 1999	pine forest in temperate, humid NW Spain	
		–	Fernandez et al. 1997	pine forest in NW spain	
		–	Parker et al. 2001	spruce & hdwd stands in ME	for organic and upper mineral layers, fifty yrs after wildfire
Soil Mg	controlled fire	–	Vose et al. 1999	pine-hdwd forest, s. appalachians	
		+	Lynham et al. 1998	immature jack pine forest, Ontario	
		+	McKee 1982	southern pine forests, SE coastal plain	in coastal plain pine sites, mineral soil
		→	Binkley et al. 1992	pine forest, coastal plain of SC	
		+	Gimeno-Garcia et al. 2000	shrubland in Mediterranean Spain	organic layer
Soil Mg		+	Knoepp et al. 2004	mixed oak-pine forest, southern appalachians	
	wildfire	+	Alauzis et al. 2004	Nothofagus forest in Patagonia, Argentina	sampled at 10 cm
Soil Ca	controlled fire	–	Vose et al. 1999	pine-hdwd forest, s. appalachians	slight decrease
		+	Boerner et al. 2004	mixed-oak forest, southern Ohio	
		+	Lynham et al. 1998	immature jack pine forest, Ontario	
		+	McKee 1982	southern pine forests, SE coastal plain	in coastal plain pine sites, mineral soil
		+	Binkley et al. 1992	pine forest, coastal plain of SC	in organic soils

(Continued)

CL Factor	Disturbance	Trend	Source	Site	Notes
		–	Gimeno-Garcia et al. 2000	shrubland in Mediterranean Spain	organic layer
		+	Waldrop et al. 1987	pine forest, SC	in mineral layers
		+	Knoepp et al. 2004	mixed oak-pine forest, southern appalachians	still elevated after 5 yrs in B horizon but not A horizon
	wildfire	+	Simard et al. 2001	boreal forest, Quebec	
		+	Alauzis et al. 2004	Nothofagus forest in Patagonia, Argentina	sampled at 10 cm
Soil K	controlled fire	–	Vose et al. 1999	pine-hdwd forest, s. appalachians	
		+	Lynham et al. 1998	immature jack pine forest, Ontario	still elevated after 10 yrs
		→	McKee 1982	southern pine forests, SE coastal plain	in coastal plain pine sites, mineral soil
		→	Binkley et al. 1992	pine forest, coastal plain of SC	
		+	Gimeno-Garcia et al. 2000	shrubland in Mediterranean Spain	organic layer
		+	Knoepp et al. 2004	mixed oak-pine forest, southern appalachians	still elevated 2 yrs after burn, then decreased
	wildfire	+	Simard et al. 2001	boreal forest, Quebec	
		+	Alauzis et al. 2004	Nothofagus forest in Patagonia, Argentina	sampled at 10 cm
		+	Hernandez et al. 1997	Mediterranean pine forest	
Soil Na	controlled fire	+	Gimeno-Garcia et al. 2000	shrubland in Mediterranean Spain	organic layer
		→	McKee 1982	southern pine forests, SE coastal plain	in coastal plain pine sites, mineral soil
	wildfire	+	Alauzis et al. 2004	Nothofagus forest in Patagonia, Argentina	sampled at 10 cm
Insects	controlled fire	+	Sullivan et al. 2003	longleaf pine forest in SC	for secondary beetles (not harmful to trees) in longleaf pine stands in SC
Insects		→	Sullivan et al. 2003	longleaf pine forest in SC	for harmful beetles
		→	Boyle et al. 2004	southern pine forests infested with SPB	no short term change

(Continued)

CL Factor	Disturbance	Trend	Source	Site	Notes
		–	Boyle et al. 2004	southern pine forests infested with SPB	long term change because of increased tree vigor and reduction in stand density
		–	Ferry et al. 1995	ponderosa, lodgepole and southern pine forests	for fire-adapted ecosystems
		–	Mutch et al. 1993	Blue Mtns	for fire-adapted ecosystems
		→	Elkin & Reid 2004	lodgepole pine forest, Banff & Kootenay NPs	for mountain pine beetles
		→	McHugh et al. 2003	ponderosa pine forest in n Arizona	for bark beetle
		→	Amman & Ryan 1991	pine forests in Yellowstone	
	wildfire	+	Furniss 1965	Doug-fir forests in southern Idaho	for Doug-fir & w. pine beetle in s. Idaho
		+	Yanovsky & Kiselev 1996	boreal forests	
		→	Hanula et al. 2002	pine forest in FL	for pine bark beetles
		+	Dixon et al. 1984	slash pine forest	for black turpentine beetles on slash pine
		+	Rasmussen et al. 1996	pine forests in Yellowstone	
	climate change	+	Williams et al. 2000	depends on spp, area	
		+	Porter et al. 1991		
		+	Cammell & Knight 1992		
		+	Williams & Liebhold 1995		
		+	Straw 1995		
		+	Sutherst 1996		
		+	Logan et al. 1995	for SPB	
		+	Whittaker 2001		
		+	Volney & Fleming 2000		
		+	Oechel & Vourlitis 1994		

(Continued)

CL Factor	Disturbance	Trend	Source	Site	Notes
Disease	controlled fire	–	Zimmerman & Laven 1984	lodgepole pine forests	for dwarf mistletoe in lodgepole pine
		–	Hardison 1976	longleaf pine forest in Southern US	for brown spot needle blight in longleaf pine, fusiform rust in southern pines, dwarf misteltoe
		+	Hardison 1976	conifer forests	for Rhizina in fir, blister rust in white pines
		+	Piirto et al. 1998	giant sequoia forests, Sierra Nevadas, CA	for fungi in giant sequoia
		+	Sullivan et al. 2003	longleaf pine forest in SC	levels of fungi increased as burn severity increased
	wildfire	+	Hanula et al. 2002	pine forest in FL	
		+	Ferguson et al. 1960	pine forest	
	climate change	+	Williams et al. 2000	depends on spp, area	
		+	Brasier 1996	for P. cinnamomi	
Disease		–	Lonsdale & Gibbs 1996	for spot fungi such as Marrsonina spp. on poplars	
		–	Neely & Weber 1976	for spot fungi such as Cristulariella pyramidalis on black walnut	
		+	Hall 1995	for Discula campestris after tent caterpillar attack	
		+	Coakley 1995		
		+	Sutherst 1996		
Freeze/ thaw dieback	climate change	+	Winnett 1998		
		+	Bassow et al. 1994		
		+	Auclair et al. 1990		
		+	Auclair et al. 1996		
		+	Auclair et al. 1992		

(Continued)

CL Factor	Disturbance	Trend	Source	Site	Notes
Tree nutrient uptake	controlled fire	+	Van de Vijver et al. 1999		short-lived, 3 mos after fire, back to normal
		→	Tuininga et al. 2002	greenhouse study with pitch pine seedlings covered with burned/ unburned litter	
	climate change	+	Cole et al. 2002	increased N and P contents in blanked peat ecosystem plant	
NPP	controlled fire	–	Thornley & Cannell 2004	boreal forest, from Edinburgh Forest Model	
		–	Lynch & Wu 2000		in model simulation
	wildfire	–	Thornley & Cannell 2004	boreal forest, from Edinburgh Forest Model	
	climate change	–	Lynch & Wu 2000	in model simulation, unless very moist	
		→	Cao & Woodward 1998	globally	increase in north offsets decrease in tropics
		+	Verburg & van Breemen 2000	because of increased N min & CO_2 fertilization, esp. in areas where N is limiting NPP	
		+	Schimel et al. 1990	grassland ecosystems	
Tree N uptake	controlled fire	→	Boerner et al. 1988	oak-pine forest, New Jersey pine barrens	
		+	Van de Vijver et al. 1999		
		+	Harris & Co-vington 1983	ponderosa pine forest, Flagstaff, AZ	
		+	Covington & Sackett 1990	ponderosa pine forest, Flagstaff, AZ	measured 1 yr after fire
		+	Kranabetter & Yole 2000	high-elevation pine plantation, British Columbia	still high after 7 yrs
Tree N uptake		→	Tuininga et al. 2002	greenhouse study with pitch pine seedlings covered with burned/ unburned litter	

(Continued)

CL Factor	Disturbance	Trend	Source	Site	Notes
	wildfire	+	Baird et al. 1999	coniferous forest, Cascades, WA	
	climate change	+	Van Cleve et al. 1990	cold black spruce forest	after heating soil up 8℃–10℃
		+	Pastor & Post 1988		
		–	Smith et al. 2002		
Growth rates	controlled fire	+	Boerner et al. 1988	oak-pine forest, New Jersey pine barrens	in oaks in NJ
		→	Waldrop et al. 1987	pine forest, SC	
		+	Sackett 1984	ponderosa pine forest, Flagstaff, AZ	
		+	Launonen et al. 1999	greenhouse study with mountain ash seedlings in Australia	
		–	Thornley & Cannell 2004	boreal forest, from Edinburgh Forest Model	
		–	Lynch & Wu 2000		in model simulation
	wildfire	–	Thornley & Cannell 2004	boreal forest, from Edinburgh Forest Model	
	climate change	–	Woodbury et al. 1998	model prediction for loblolly pine	
		–	Olszyk et al. 1998	for Douglas fir seedlings; increased temps reduced canopy growth but not woody growth	
		–	Reams & Van Deusen 1998	for mature baldcypress in southeastern US	
		–	Cook 1998	for loblolly pine seedlings, in response to increased growing-season drought	
		+	Bonan & Van Cleve 1992	black spruce forest, birch forest	model prediction showed increased production lasted for 10 yrs, then leveled off
		–	Lynch & Wu 2000	in model simulation, unless very moist	

(Continued)

CL Factor	Disturbance	Trend	Source	Site	Notes
		→	Cao & Woodward 1998	globally	increase in north offsets decrease in tropics
		+	Verburg & van Breemen 2000	because of increased N min & CO_2 fertilization, esp. in areas where N is limiting NPP	
		+	Schimel et al. 1990	grassland ecosystems	

However, over the long-term (i.e., more than 5 years), intense wildfires can significantly increase the critical load limit of an ecosystem. Other macronutrients (e.g., magnesium (Mg), calcium (Ca), potassium (K), phosphorus (P)) generally increase with fire (both controlled and wild) (Table 17.1) as biomass is consumed and the inorganic elements are returned to the soil. An increase in macronutrients can stimulate plant growth, which increases plant demand for nitrogen and increases the long-term critical nitrogen load limit. For example, in Yellowstone national park wildfires initially destroyed much of the forest in 1988. Several years were required to re-establish the ecosystems, but now species diversity and forest growth have been restored to pre-burn conditions (Turner et al., 2003). Therefore, it is likely that critical load limits are now higher across the park than before the fire.

17.3.2 Controlled Burn Impacts on Critical Loads

To restore the natural ecosystem balance that existed before widespread fire exclusion in the United States, many land managers routinely implement controlled or prescribed burning on their forests. These burns can help to reduce fuel loads (Waldrop et al., 1987; Clinton et al., 1998), curb insect and disease infestations (McCullough et al., 1998), and release and recycle forest nutrients (Wan, 2001; Knoepp et al., 2004). Between 1995 and 2000, an average of over 1.4 million acres of controlled burning was conducted by federal agencies (NIFC, 2005). Air quality concerns, land fragmentation, and the integration of housing developments into forestland hamper land managers' ability to effectively reduce fuel loads using controlled burns (Cleaves et al., 2000). Controlled burns can be very beneficial to an ecosystem.

Over time, much of the macronutrients (e.g., Ca, Mg, P) needed to sustain forest growth can become incorporated into dead twigs, branches and wood, or in underbrush (McClaugherty et al., 1985). Controlled burns can reduce the amount of dead material and underbrush in an ecosystem and return nutrients back to the soil, allowing tree roots to take up the returned nutrients. Increased macronutrient supply can significantly increase forest productivity (Thornton et al., 2000; Albaugh et al., 2004) and therefore increase the ecosystem's critical nitrogen load. Reductions in underbrush can also increase the available soil water for the remaining forest trees. Increased water availability can also increase forest productivity and critical nitrogen load (Churkina, 1999).

Unlike wild fires, controlled burns have little likelihood of significantly affecting soil organic matter, reducing soil CEC, sterilizing the soil, or significantly reducing forest nitrogen demand. Controlled burns have far fewer negative critical nitrogen load impacts compared to wild fires, while exhibiting the positive aspects of fire. Therefore, controlled burns should be considered as a tool for (generally) increasing ecosystem critical nitrogen load, whenever air quality would not exceed regulatory standards.

17.4 Combined Impacts on Critical Pollutant Loads

Thus far, we have only examined how climate change and fires can impact individual ecosystem parameters (e.g., soil pH, CEC and nitrogen mineralization, and tree nitrogen uptake). Now we will examine how combinations of changing ecosystem parameters impact an ecosystem's critical load. Not all impacts from wild fires, controlled burns, or climate change and variability have a universally negative or positive impact on critical nitrogen loads (Table 17.2). For example, wildfires negatively impact critical nitrogen loads by generally reducing soil organic matter content and soil CEC. However, wildfires can also positively impact critical nitrogen loads by increasing soil pH and macronutrient content (Table 17.2). Also, the stress impacts are not universally negative or positive in all areas. For example, Binkley et al. (1992) found that controlled burns increased the C:N ratio in coastal pine organic horizon ecosystems (Table 17.1). However, Klopatek et al. (1991) found that controlled fire reduced the soil C:N ratio in pinyon-juniper ecosystems (Table 17.1). Therefore, controlled burns may increase the critical nitrogen load in one ecosystem while reducing it in another. This example illustrates the need to assess the impact of fire and climate change and variability on an individual ecosystem basis. Generalities are useful only in understanding how critical nitrogen loads of most ecosystems respond to fire and climate change and variability, not in predicting specific ecosystem impacts.

It should not be surprising that the impacts of combinations of environmental stresses on critical nitrogen load limits are difficult to assess given the variability in individual ecosystem critical nitrogen load response to environmental stress.

A single ecosystem may have a large change in its critical nitrogen load depending on the type and severity of non-nitrogen ecosystem stresses. For example, the base critical nitrogen load for an ecosystem, as calculated from a simple mass

Table 17.2 Summary table of effects of controlled burn, wildfire, and climate change on critical loads. (+) represents increase in critical load, (–) represents decrease in critical load, (→) represents possible increase or decrease in critical load, (NA) represents no significant impact

CL Factor	Controlled Burn	Wildfire	Climate Change
Soil pH	+	+	+
Soil organic matter	–	–	NA
Soil bulk density	+	→	NA
N mineralization	+	+	+
Nitrification	+	+	→
Total soil N	→	–	–
N availability	+	NA	+
Soil ammonium	+	+	+
Soil nitrate	+	+	+
Soil CEC	–	–	NA
Soil S	–	→	NA
Soil P	+	+	NA
Soil Na	+	+	NA
Soil C	→	–	NA
C mineralization	NA	+	+
C:N ratio	→	–	NA
Soil Mg	+	+	NA
Soil Ca	+	+	NA
Soil K	+	+	NA
Insects	→	+	+
Disease	→	+	+
Freeze/thaw dieback	NA	NA	+
Tree cation uptake	+	NA	+
Tree N uptake	+	+	→
Growth rates	→	–	→

balance equation, could equal 15 kg N ha^{-1} yr^{-1} (Fig. 17.1(a)). However, drought can significantly reduce available soil water and plant growth. In turn, reductions in plant growth reduce nitrogen uptake, which then reduce the ecosystem's ability to use and store nitrogen. Therefore, under a drought, the same ecosystem may have its critical nitrogen load reduced to 10 kg N ha^{-1} yr^{-1} (Fig. 17.1(b)).

Prolonged drought can reduce trees' ability to produce secondary compounds such as oleoresin (Lorio, 1977). Without resin, insects have a much greater potential for successfully colonizing and causing tree mortality (Nebeker et al., 1993). In combination, a prolonged drought and subsequent insect attack could further reduce the critical nitrogen load of the ecosystem to 8 kg N ha^{-1} yr^{-1} (Fig. 17.1(c)).

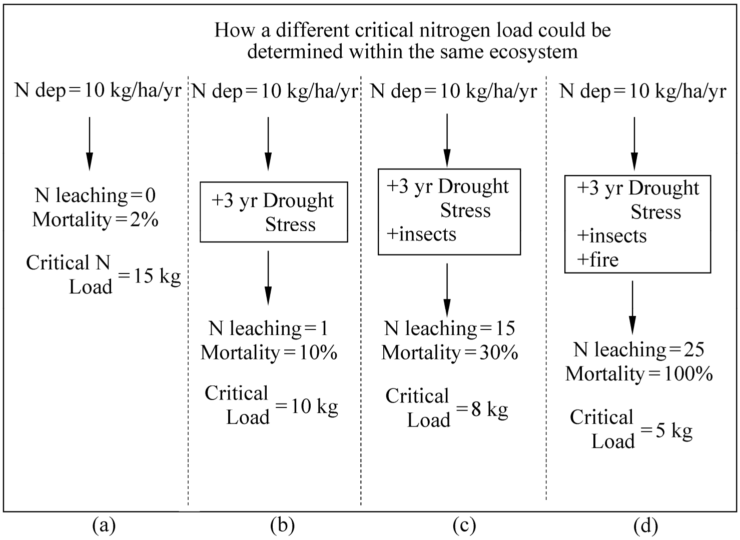

Figure 17.1 Different critical nitrogen loads could be determined within the same ecosystem, given the type and severity of stress

Dry conditions created by a drought and scattered dead trees (due to insect attack) are two important predisposing components for increasing wildfire risk (Mattson, 1987; Flannigan and Wotton, 2001). As previously discussed, wildfires can significantly reduce the critical nitrogen load of an ecosystem. Therefore, the same ecosystem that experiences drought, insect, and wildfire impacts may now only have a critical nitrogen load of 5 kg N ha^{-1} yr^{-1}.

As demonstrated by this example, there is no single critical nitrogen load level for any given ecosystem, even if nitrogen deposition levels remain constant. Land managers and policy makers need to recognize that whole ecosystem management is necessary if we wish to avoid exceeding an ecosystem's ability to absorb nitrogen. A national scale critical nitrogen load assessment has yet to be completed. Therefore, it may be unrealistic to address the issue of a variable critical nitrogen load before a basic critical nitrogen load map is even available. However, we should begin to develop the research tools that will eventually allow state and federal policy makers to better assess the impacts of nitrogen deposition on ecosystem health and function.

17.5 Conclusions and Future Research

The impacts of climate change, and the associated increase in wild fire frequency and severity will very likely increase in coming years and decades. Cooler regions will likely see increases in forest productivity and nitrogen uptake as warming favors a longer growing season, increased nitrogen mineralization and other factors favorable for plant growth. Conversely, currently warm or hot ecosystems will become even hotter. Increased evapotranspiration could reduce available soil moisture more quickly, and lead to reductions in forest growth, especially when coupled with the potential for increased fire.

Without a steady state baseline of environmental conditions, the development of a ecosystem CL will be very difficult. Even simple mass balance equation estimates of critical nitrogen loads have been difficult to apply across large spatial scales. Accurate estimates of nitrogen mineralization and plant uptake are two of the most vexing problems. However, several forest process models (e.g., PnET, MAGIC) are now available for calculating these critical nitrogen loads. Forest process models may be very useful in increasing our ability to examine how multiple critical load parameters interact to affect an ecosystem's critical nitrogen load. Continued progress in the development of more dynamic critical load estimates will reduce the potential for unexpected ecosystem degradation in the future.

References

Aber JD, Nadelhoffer KJ, Steudler P, Melillo JM, (1989), Nitrogen saturation in northern forest ecosystems. *Bioscience*, **39**(6): 378 – 286

Alauzis M, Mazzarino M, Raffaele E, Roselli L, (2004), Wildfires in NW Patagonia: long-term effects on a Nothofagus forest soil. *For Ecol Manage* **192**: 131 – 142

Albaugh TJ, Allen HL, Dougherty PM, Johnsen KH, (2004), Long term growth responses of loblolly pine to optimal nutrient and water resource availability. *For Ecol Manage* **192**: 3 – 19

Amirbahman A, Ruck P, Fernandez I, Haines T, Kahl J, (2004), The effect of fire on mercury cycling in the soils of forested watersheds: Acadia National Park, Maine, *U.S.A. Water Air Soil Pollut*, **152**: 313 – 331

Amman G, Ryan K, (1991), Insect infestation of fire-injured trees in the Greater Yellowstone area. Research Note INT-398. USDA Forest Service Intermountain Research Station. 9

Auclair A, Martin H, Walker S, (1990), A case study of forest decline in western Canada and the adjacent United States. *Water Air Soil Pollut*, **53**: 13 – 31

Auclair A, Worrest RC, Lachance D, Martin HC, (1992), Climatic perturbation as a general mechanism of forest dieback. In: Manion PD, Lachance D (eds) Forest Decline Concepts. APS Press, St Paul, MN, 38 – 58

Auclair A, Lill J, Revenga C, (1996), The role of climate variability and global warming in the dieback of northern hardwoods. *Water Air Soil Pollut*, **91**: 163 – 186

Baird M, Zabowski D, Everett R, (1999), Wildfire effects on carbon and nitrogen in inland coniferous forests. *Plant Soil*, **209**: 233 – 243

Baker JP, Van Sickle J, Gagen CJ, DeWalle DR, Sharpe WE, Carline RF, Baldigo BP, Murdoch PS, Bath DW, Krester WA, Simonin HA, Wigington PJ Jr, (1996), Episodic acidification of small streams in the northeastern United States: effects on fish populations. *Ecol Appl*, **6**: 422 – 437

Bassow S, McConnaughay K, Bazzaz F, (1994), The response of temperate tree seedlings grown in elevated CO_2 to extreme temperature events. *Ecol Appl* **4**(3): 593 – 603

Bauhus J, Khanna P, Raison R, (1993), The effect of fire on carbon and nitrogen mineralization and nitrification in an Australian forest soil. *Aust J Soil Res*, **31**: 621 – 639

Bell R, Binkley D, (1989), Soil nitrogen mineralization and immobilization in response to periodic prescribed fire in a loblolly pine plantation. *Can J For Res*, **19**: 816 – 820

Berg B, (1986), The influence of experimental acidification on nutrient release and decomposition rates on needle and root litter in the forest floor. *Forest Ecol Manage*, **15**: 195 – 213

Binkley D, Richter D, David M, Caldwell B, (1992), Soil chemistry in a loblolly/longleaf pine forest with interval burning. *Ecol Appl*, **2**(2): 157 – 164

Boerner R, Brinkman J, Sutherland E, (2004), Effects of fire at two frequencies on nitrogen transformations and soil chemistry in a nitrogen-enriched forest landscape. *Can J For Res*, **34**: 609 – 618

Boerner R, Lord T, Peterson J, (1988), Prescribed burning in the oak-pine forest of the New Jersey pine barrens: effects of growth and nutrient dynamics of two Quercus species. *Amer Midl Nat*, **120**(1): 108 – 119

Bonan GB, Van Cleve K, (1992), Soil temperature, nitrogen mineralization, and carbon source-sink relationships in boreal forests. *Can J For Res* **22**: 629 – 639

Boyle M, Hedden R, Waldrop T, (2004), Impact of prescribed fire and thinning on host resistance to the southern pine beetle: preliminary results of the National Fire and Fire Surrogate Study. In: Connor, K., ed. Proceedings of the 12th biennial southern silvicultural research conference. General Technical Report SRS-71. Asheville, NC: USDA Forest Service, Southern Research Station. 60 – 64

Brasier C, (1996), Phytophthora cinnamomi and oak decline in southern Europe. Environmental constraints including climate change. *Ann For Sci*, **53**: 347 – 358

Brown TJ, Hall BL, Westerling AL, (2004), The impact of twenty-first century climate change on wildland fire danger in the western United States: an applications perspective. *Clim Change* **62**: 365 – 388.h

Cammell M, Knight J, (1992), Effects of climatic change on the population dynamics of crop pests. *Adv Ecol Res*, **22**: 117 – 162

Cao M, Woodward FI, (1998), Dynamic responses of terrestrial ecosystem carbon cycling to global climate change. *Nature*, **393**: 249 – 252

Christensen NL (1973) Fire and nitrogen cycle in California chaparral. *Science*, **181**: 66 – 68

Cleaves DA, Martinez J, Haines TK, (2000), Influences on prescribed burning activity and costs in the National Forest System. USDA Forest Service: GTR SRS-37. 1 – 34

Clinton BD, Vose JM, Swank WT, Berg EC, Loftis DL, (1998), Fuel consumption and fire characteristics during understory burning in a mixed white pine-hardwood stand in the southern Appalachians. US Dept of Agric For Serv Res Pap SRS-12

Coakley S, (1995), Biospheric change: will it matter in plant pathology? *Can J Plant Pathol*, **17**: 147 – 153

Cook ER, Nance WL, Krusic PJ, Grissom J, (1998), Modeling the differential sensitivity of loblolly pine to climatic change using tree rings. In Mickler RA, Fox S (eds) The Productivity and Sustainability of Southern Forest Ecosystems in a Changing Environment.

Springer, New York. 717 – 739
Cole L, Bardgett R, Ineson P, Hobbs P, (2002), Enchytraeid worm (Oligochaeta) influences on microbial community structure, nutrient dynamics and plant growth in blanket peat subjected to warming. *Soil Bio Biochem,* **34**: 83 – 92
Covington W, Sackett S, (1990), Fire effects on ponderosa pine soils. US Dep Agric For Serv, Rocky Mount For Range Exp Stn, Fort Collins, CO, Gen Tech Rep RM-191. 105 – 111
Covington W, Sackett S, (1992), Soil mineral nitrogen changes following prescribed burning in ponderosa pine. *For Ecol Manage*, **54**: 175 – 191
Cronan CS, Grigal DF, (1995), Use of calcium/aluminum ratios as indicators of stress in forest ecosystems. *J Environ Qual*, **24**(2): 209 – 226
Cronan CS, Schofield CL, (1979), Aluminum leaching response to acid precipitation: effects on high-elevation watersheds in the northeast. *Science*, **204**: 304 – 306
Dixon W, Corneil J, Wilkinson R, Foltz J, (1984), Using stem char to predict mortality and insect infestation of fire-damaged slash pines. *South J Appl For*, **8**: 85 – 88
Elkin CM, Reid ML, (2004), Attack and reproductive success of mountain pine beetles (Coleoptera: Scolytidae) in fire damaged lodgepole pines. *Environ Entomol*, **33**(4): 1070 – 1080
Ferguson E, Gibbs C, Thatcher R, (1960), Cool burns and pine mortality. *Fire Contr Notes*, **21**: 27 – 29
Fernandez I, Cabaneiro A, Carballas T, (1997), Organic matter changes immediately after a wildfire in an Atlantic forest soil and comparison with laboratory soil heating. *Soil Biol Biochem*, **29**(1): 1 – 11
Fernandez I, Cabaneiro A, Carballas T, (1999), Carbon mineralization dynamics in soils after wildfires in two Galician forests. *Soil Biol Biochem*, **31**: 1853 – 1865
Ferry G, Clark R, Montgomery R, Mutch R, Leenhouts W, Zimmerman G, (1995), Altered fire regimes within fire-adapted ecosystems. In: LaRoe E, Farris G, Puckett C, Doran P, Mac M (eds). Our living resources: a report to the nation on the distribution, abundance, and health of U.S. plants, animals, and ecosystems. U.S. Dept. Interior, National Biological Service.
Flannigan MD, Wotton BM, (2001), Climate, weather and area burned. In: Johnson, E.A. and K. Miyanishi (eds). Forest Fires. New York: Academic Press. 351 – 373
Fried JS, Torn MS, Mills E, (2004), The impact of climate change on wildfire severity: a regional forecast for northern California. *Clim Change*, **64**: 169 – 191
Furniss M, (1965), Susceptibility of fire-injured Douglas-fir to bark beetle attack in southern Idaho. J For 8 – 11
Gimeno-Garcia E, Andreu V, Rubio J, (2000), Changes in organic matter, nitrogen, phosphorous and cations in soil as a result of fire and water erosion in a Mediterranean landscape. *Eur J Soil Sci*, **51**: 201 – 210
Groeschl D, Johnson J, Smith D, (1993), Wildfire effects on forest floor and surface soil in a table mountain pine-pitch pine forest. *Int J Wildland Fire*, **3**: 149 – 154
Hall T, (1995), Effect of forest tent caterpillar and Discula campestris on sugar maple in Pennsylvania. *Phytopathol*, **85**: 1129
Hanula J, Meeker J, Miller D, Barnard E, (2002), Association of wildfire with tree health and numbers of pine bark beetles, reproduction weevils and their associates in Florida. *For Ecol Manage*, **170**: 233 – 247

Hardison J, (1976), Fire and flame for plant disease control. *Annual Reviews in Phytopathol*, **14**: 355 – 379

Harris GR, Covington WW, (1983), The effect of a prescribed fire on nutrient concentration and standing crop of understory vegetation in ponderosa pine. *Can J For Res*, **13**: 501 – 507

Hart SC, Perry DA, (1999), Transferring soils from high- to low-elevation forests increases nitrogen cycling rates: climate change implications. *Glob Ch Biol*, **5**: 23 – 32

Heilman WE, Potter BE, Zerbe JI, (1997), Regional climate change in the southern United States: the implications for wildfire occurrence. In: R. Mickler and S. Fox. The Productivity and Sustainability of Southern Forest Ecosystems in a Changing Environment. *Ecological Studies,* **128**: 683 – 699

Hernandez T, Garcia C, Reinhardt I, (1997), Short-term effect of wildfire on the chemical, biochemical and microbiological properties of Mediterranean pine forest soils. *Biol Fertil Soils*, **25**: 109 – 116

Holland EA, Braswell BH, Sulzman J, Lamarque J-F, (2005), Nitrogen deposition onto the United States and western Europe: synthesis of observations and models. *Ecol Appl*, **15**(1): 38 – 57

Houghton JT, Ding Y, Griggs DJ, Noguer M, van der Linden PJ, Dai X, Maskell K, Johnson CA (eds), (2001), Climate Change 2001: The Scientific Basis, Contribution of Working Group 1 to the Third Assessment Report of the Intergovernmental Panel on Climate Change (IPCC). Cambridge Univ Press, Cambridge, UK and NY, NY USA, 881

Johnson AH, Schwartzman TN, Battles JJ, Miller R, Miller EK, Friedland AJ, Vann DR, (1994), Acid rain and soils of the Adirondacks. II. Evaluation of calcium and aluminum as causes of red spruce decline at Whiteface Mountain, New York. *Can J For Res*, **24**: 654 – 662

Klopatek J, Klopatek C, DeBano L, (1991), Fire effects on nutrient pools of woodland floor materials a dsoils in a pinyon-juniper ecosystem. In Fire and the Environment: Ecological and Cultural Perspectives (Nodvin S, Waldrop T, eds.), 154 – 159. Proceedings of an International Symposium, 1990, Knoxville, TN. General Technical Report SE-69, USDA Forest Service, Southeastern Forest Experimental Station

Knoepp J, Swank W, (1993), Site preparation burning to improve southern Appalachian pine-hardwood stands: nitrogen responses in soil, soil water, and streams. *Can J For Res*, **23**: 2263 – 2270

Knoepp J, Vose J, Swank W, (2004), Long-term soil responses to site preparation burning in the southern Appalachians. *For Sci*, **50**(4): 540 – 550

Kranabetter J, Yole D, (2000), Alternatives to broadcast burning in the northern interior of British Columbia: short-term tree results. *For Chron*, **76**(2): 349 – 353

Kutiel P, Naveh Z, (1987), The effect of fire on nutrients in a pine forest soil. *Plant Soil*, **104**: 269 – 274

Launonen T, Ashton D, Keane P, (1999), The effect of regeneration burns on the growth, nutrient acquisition and mycorrhizae of Eucalyptus regnans F. Muell. (mountain ash) seedlings. *Plant Soil*, **210**: 273 – 283

Logan J, Bolstad P, Bentz B, Perkins D, (1995), Assessing the effects of changing climate on mountain pine beetle dynamics. In: Tinus R (ed.), Report of Interior West Global Change Workshop. USDA Forest Service General Technical Report RM-GTR-262. USDA, Fort Collins, CO, 92 – 105

Lonsdale D, Gibbs J, (1996), Effects of climate change on fungal diseases of trees. In: Proceedings, Fungi and Environmental Change Symposium of the British Mycological Society, March 1994, Cranfield Univ, Cambridge. Cambridge University Press, Cambridge, UK, 1 – 19

Lynch A, Wu W, (2000), Impacts of fire and warming on ecosystem uptake in the boreal forest. *J Clim*, **13**: 2334 – 2338

Lynham T, Wickware G, Mason J, (1998), Soil chemical changes and plant succession following experimental burning in immature jack pine. *Can J Soil Sci*, **78**: 93 – 104

Masters R, Engle D, Robinson R, (1993), Effects of timber harvest and periodic fire on soil chemical properties in the Ouachita Mountains. *South J Appl For*, **17**(3):139 – 145

McClaugherty, C.A., J. Pastor, J.D. Aber, and J.M. Melillo, (1985), Forest litter decomposition in relation to soil nitrogen dynamics and litter quality. *Ecology*, **66**(1): 266 – 275

McCullough DG, Werner RA, Neumann D, (1998), Fire and insects in northern and boreal forest ecosystems of North America. *Annu Rev Entomol*, **43**: 107 – 127

McHugh C, Kolb T, Wilson J, (2003), Bark beetle attacks on ponderosa pine following fire in northern Arizona. *Env Entom*, **32**: 510 – 522

McKee W, (1982), Changes in soil fertility following prescribed burning on coastal plain pine sites. USDA Forest Service Research Paper SE-234

McNulty S, Boggs J, Aber J, Rustad L, Magill A, (2005), Red spruce ecosystem level changes following 14 years of chronic N fertilization. *For Ecol Manage*, **219**: 279 – 291

Mutch R, Arno S, Brown J, Carlson C, Ottmar R, Peterson J, (1993), Forest health in the Blue Mountains: a management strategy for fire-adapted ecosystems. U.S. Forest Service General Technical Report PNW-310. 14

National Interagency Fire Center (NIFC), (2005), Wildland Fire Statistics http://www.nifc.gov/stats/index.html

National Wildfire Coordinating Group (NWCG), (2001), Fire Effects Guide. National Interagency Fire. http://www.nwcg.gov/pms/RxFire/FEG.pdf

Neary DG, Klopatek CC, DeBano LF, Ffolliott PF, (1999), Fire effects on belowground sustainability: a review and synthesis. *For Ecol Manage*, **122**: 51 – 71

Nebeker TE, Hodges JD, Blance CA, (1993), In Beetle-Pathogen Interactions in Conifer Forests, In: Schowalter TD, Filip GM (eds) Academic, London. 76 – 91

Neely D, Weber B, (1976), Cristulariella leaf spot associated with defoliation of black walnut plantations in Illinois. *Plant Dis Rep*, **60**: 587 – 590

Oechel W, Vourlitis G, (1994), The effect of climate change on land-atmosphere feedbacks in arctic tundra regions. *Trends Ecol Evol*, **9**: 324 – 329

Olszyk D, Wise C, VanEss E, Tingey D, (1998), Elevated temperature but not elevated CO_2 affects long-term patterns of stem diameter and height of Douglas-fir seedlings. *Can J For Res*, **28**: 1046 – 1054

Parker J, Fernandez I, Rustad L, Norton S, (2001), Effects of nitrogen enrichment, wildfire, and harvesting on forest-soil carbon and nitrogen. *Soil Sci Soc Amer J*, **65**: 1248 – 1255

Pastor J, Post WM, (1988), Responses of northern forests to CO_2-induced climate change. *Nature*, **334**: 55 – 58

Phillips D, Foss J, Buckner E, Evans R, FitzPatrick E, (2000), Response of surface horizons in an oak forest to prescribed burning. *Soil Sci Soc Amer J*, **64**: 754 – 760

Pietikainen J, Fritze H, (1995), Clear-cutting and prescribed burning in coniferous forest: comparison of effects on soil fungal and total microbial biomass, respiration activity and nitrification. *Soil Biol Biochem*, **27**(1): 101 – 109

Piirto D, Parmeter J, Cobb F, Piper K, Workinger A, Otrosina W, (1998), Biological and management implications of fire-pathogen interactions in the giant sequoia ecosystem. In: Pruden T, Brennan L (eds). Fire in ecosystem management: shifting the paradigm from suppression to prescription, pp 325 – 336. Tall Timbers Fire Ecology Conference Proceedings, No. 20. Tall Timbers Research Station, Tallahassee, FL

Porter J, Parry M, Carter T, (1991), The potential effects of climate change on agricultural insect pests. *Agric For Manage*, **57**: 221 – 240

Price C, Rind D, (1994), The impact of a 2 x CO_2 climate on lightning-caused fires. *J Clim*, **7**: 1484 – 1494

Prieto-Fernandez A, Acea M, Carballas T, (1998), Soil microbial and extractable C and N after wildfire. *Biol Fert Soils*, **27**: 132 – 142

Rapp M, (1990), Nitrogen status and mineralization in natural and disturbed Mediterranean forests and coppices. *Plant Soil*, **128**: 21 – 30

Rasmussen L, Amman G, Vandygriff J, Oakes R, Munson A, Gibson K, (1996), Bark beetle and wood borer infestation in the greater Yellowstone area during four postfire years. USDA Forest Service Intermountain Research Station Research Paper INT-RP-487, Ogden, UT, 1 – 10

Reams GA, Van Deusen PC, (1998), Detecting and predicting climatic varation from old-growth baldcypress. In: Mickler RA, Fox S (eds) The Productivity and Sustainability of Southern Forest Ecosystems in a Changing Environment. Springer, New York. 701 – 716

Richter D, Ralston C, Harms W, (1982), Prescribed fire: effects on water quality and nutrient cycling. *Science*, **215**: 661 – 663

Ryan MG, O'Toole P, Farrell EP, (1998), The influence of drought and natural rewetting on nitrogen dynamics in a coniferous ecosystem in Ireland. *Environ Pollut*, **102**(S1): 445 – 451

Sackett SS, (1984), Observations on natural regeneration in ponderosa pine following a prescribed fire in Arizona. US Dep Agric For Serv, Rocky Mount For Range Exp Stn, Fort Collins, CO, Res Note RM-435. 8

Schimel DS, Parton WJ, Kittel TGF, (1990), Grassland biogeochemistry: links to atmospheric processes. *Clim Change*, **17**: 13 – 25

Shortle WC, Smith KT, (1988), Aluminum-induced calcium deficiency syndrome in declining red spruce. *Science*, **240**: 1017 – 1018

Simard D, Fyles J, Pare D, Nguyen T, (2001), Impacts of clearcut harvesting and wildfire on soil nutrient status in the Quebec boreal forest. *Can J Soil Sci*, **81**: 229 – 237

Smith J, Halvorson J, Bolton H, (2002), Soil properties and microbial activity across a 500 m gradient in a semi-arid environment. *Soil Biol Biochem*, **34**: 1749 – 1757

Straw N, (1995), Climate change and the impact of green spruce aphid, Elatobium abietinum (Walker), in the U.K. *Scot For*, **49**: 134 – 145

Sullivan B, Fettig C, Otrosina W, Dalusky M, Berisford C, (2003), Association between severity of prescribed burns an dsubsequent activity of conifer-infesting beetles in stands of longleaf pine. *For Ecol Manage*, **185**: 327 – 340

Sutherst R (ed), (1996), Impacts of climate change on pests, diseases and weeds in Australia. Report of an International Workshop, 9 – 12 October 1995, Brisbane, Australia. CSIRO Division of Entomology, Canberra, Australia

Thornley J, Cannell M, (2004), Long-term effects of fire frequency on carbon storage and productivity of boreal forests: a modeling study. *Tree Physiol*, **24**: 765 – 773

Thornton FC, Bock BR, Behel DA, Houston A, Tyler DD, (2000), Utilization of waste materials to promote hardwood tree growth. *Southern Journal of Applied Forestry*, **24**(4): 230 – 237

Tuininga A, Dighton J, Gray D, (2002), Burning, watering, litter quality and time effects on N, P, and K uptake by pitch pine (Pinus rigida) seedlings in a greenhouse study. *Soil Biol Biochem*, **34**: 865 – 873

Turner MG, Romme WH, Tinker DB, (2003), Surprises and lessons from the 1988 Yellowstone fires. *Front Ecol Environ*, **1**(7): 351 – 358

US Global Change Research Program (USGCRP), National Assessment Synthesis Team, (2001), Climate Change Impacts on the United States: The Potential Consequences of Climate Variability and Change. Cambridge Univ Press, Cambridge, UK

Van Cleve K, Oechel WC, Hom JL, (1990), Response of black spruce (Picea mariana) ecosystems to soil temperature modification in interior Alaska. *Can J For Res*, **20**: 1530 – 1535

Van de Vijver C, Poot P, Prins G, (1999), Causes of increased nutrient concentrations in post-fire regrowth in an East African savanna. *Plant Soil*, **214**: 173 – 185

Verburg PSJ, van Breemen N, (2000), Nitrogen transformations in a forested catchment in southern Norway subjected to elevated temperature and CO_2. *For Ecol Manage*, **129**: 31 – 39

Volney W, Fleming R, (2000), Climate change and impacts of boreal forest insects. *Agric Ecosyst Environ*, **82**: 283 – 294

Vose JM, Swank WT, Clinton BD, Knoepp JD, Swift LW, (1999), Using stand replacement fires to restore southern Appalachian pine-hardwood ecosystems: effects on mass, carbon, and nutrient pools. *For Ecol Manage*, **114**: 215 – 226

Waldrop T, Van Lear D, Lloyd F, Harms W, (1987), Long-term studies of prescribed burning in loblolly pine forests of the southeastern coastal plain. General Technical Report SE-45. Asheville, NC: USDA Forest Service, Southeastern Forest Experiment Station. 23

Wan S, Hui D, Luo Y, (2001), Fire effects on nitrogen pools and dynamics in terrestrial ecosystems: a meta-analysis. *Ecol Appl*, **11**(5): 1349 – 1365

Wardle D, Hornberg G, Zackrisson O, Kalela-Brundin M, Coomes D, (2003), Long-term effects of wildfire on ecosystem properties across an island area gradient. *Science*, **300**: 972 – 975

Wells C, Campbell R, DeBano L, Fredriksen R, Franklin E, Froelich R, Dunn P, (1979), Effects of fire on soil. USDA Forest Service, Washington, DC. 34

White CS, (1985), Effects of prescribed fire on factors controlling nitrogen mineralization and nitrification in a ponderosa pine ecosystem. Ph.D. Diss, Univ New Mex, Albuquerque, NM

Whittaker JB, (2001), Insects and plants in a changing atmosphere. *Journal of Ecology*, **89**: 507 – 518

Williams D, Liebhold A, (1995), Forest defoliators and climatic change: potential changes in spatial distribution of outbreaks of western spruce budworm and gypsy moth. *Env Entom*, **24**: 1 – 9

Williams D, Long R, Wargo P, Liebhold A, (2000), Effects of climate change on forest insect and disease outbreaks. In: Mickler R, Birdsey R, Hom J (eds), Responses of Northern U.S. Forests to Environmental Change, 455 – 494

Williams M, Brooks P, Seastedt T, (1998), Nitrogen and carbon soil dynamics in response to climate change in a high-elevation ecosystem in the Rocky Mountains, U.S.A. *Arctic and Alpine Res*, **30**(1): 26 – 30

Winnett S, (1998) Potential effects of climate change on U.S. forests: a review. *Clim Res*, **11**: 39 – 49

Woodbury P, Smith J, Weinstein D, Laurence J, (1998), Assessing potential climate change effects on loblolly pine growth: A probabilistic regional modeling approach. *For Ecol Manage*, **107**: 99 – 116

Yanovsky V, Kiselev V, (1996), Response of the endemic insect fauna to fire damage in forest ecosystems. In: J. Goldammer and V. Furyaev (eds). Fire in Ecosystems of Boreal Eurasia, 409 – 413

Yin X, (1992), Empirical relationships between temperature and nitrogen availability across North American forests. *Can J For Res*, **22**: 707 – 712

Zimmerman G, Laven R, (1984), Ecological interrelationships of dwarf mistletoe and fire in lodgepole pine forests. In: Hawksworth F, Scharpf R (eds). Biology of dwarf mistletoes: Proceedings of the Symposium, 123 – 131. USDA Forest Service General Technical Report RM-111. Rocky Mtn Forest Range Experiment Station, Fort Collins, CO

Zoettl HW, Huettl RF, (1986), Nutrient supply and forest decline in southwest Germany. *Water Air Soil Pollut*, **31**: 449 – 462

18 Simulating Fire Spread with Landscape Level Edge Fuel Scenarios

Jacob J. LaCroix
Scenarios Network for Alaska and Arctic Planning, University of Alaska, Fairbanks, 3352 College Road, Fairbanks, Alaska 99709, USA
Email: jlacroix@alaska.edu

Qinglin Li
Forest Analysis and Inventory Branch, Ministry of Forests and Range, 6th 727 Fisgard St, Victoria, BC V8T 9W3, Canada
Email: Qinglin.li@gov.bc.ca

Soung-Ryoul Ryu
Department of Renewable Resources, University of Alberta, 713C General Services, Edmonton, AB T6G 2H1, Canada
Email: soung.ryu@ualberta.ca

Daolan Zheng
Department of Natural Resources & the Environment, University of New Hampshire, Durham, NH 03824
Email: daolan.zheng@unh.edu

Jiquan Chen
Department of Environmental Sciences, University of Toledo, Bowman-Oddy Laboratories, Mail Stop 604, Toledo, OH 43606
Email: Jiquan.Chen@utoledo.edu

Abstract Area-of-edge influence (AEI) is sometimes the dominant element of many forested landscapes. Patch vegetation dynamics can create a different fuel loading at the edge relative to the interior. We used the computer simulation model FARSITE to examine a fuel edge structural feature with scenarios from three levels of edge fuel loading to determine what impacts fuels in AEI have on fire spread by ranking all of the landscape scenarios. The mean burned area (ha) was significantly different among the landscapes after seven days. Fire spread increased by 38% with a high fuel loading assigned to the designated edge structure; while it decreased by 20% with medium edge fuel loading and 44% with low edge fuel loading. The landscape without edge structure (i.e., control) produced burned areas between the medium and the high edge fuel loading scenarios. The daily rate of fire spread was also significantly affected by edge fuel loading. We encourage model users to include edge fuel in FARSITE fuel maps of highly fragmented forests. This study suggests that with on the ground fuel treatments, AEI can be manipulated to change the spread potential of large fires.

Keywords Area-of-Edge influence, fire spread, edge effects, FARSITE, Chequamegon National forest

18.1 Introduction

Area-of-edge influence (AEI, Chen et al, 1992) is common, and is sometimes the dominant element of many landscapes due to increased timber harvesting, road building, urbanization, and other land-use activities that cause fragmentation (Reed et al., 1996; Saunders et al., 2002; Watkins et al., 2003). Assessing the functional role of AEI's for conservation and management can be difficult (Murcia, 1995). Recent research on AEI's suggests that edges are an important landscape structural element for plants (Brosofske et al., 1999 and 2001; Euskirchen et al., 2001), birds and mammals (Yahner, 1988; Gustafson and Crow, 1994), and the biophysical environment (Chen et al., 1995). Edges have distinct microclimate and biomass from the interior forest (Matlack, 1993; Brosofske et al., 1997; Chen et al., 1999; Saunders et al., 1999). As a result edges could have a different fuel loading than the interior of forest patches. This unique fire fuel source may influence fire spread in a landscape. However, edges have rarely been examined with respect to their influence on larger ecosystem processes, such as fire spread, which can interact with many edges on a landscape scale (Harper et al., 2005). This study is designed to advance understanding of edge influence on fire spread by focusing on AEI as a unique fuel source in a fire simulation model.

Patch dynamics in managed landscapes can create a different fuel loading at the edge relative to the interior, and are unique in space and time. From the time forest edges are created following disturbances (i.e., natural or from clear cutting) there are many primary and secondary processes, and plant structural responses occurring, including increases in decomposition, downed wood, recruitment, growth, mortality and understory cover. As forest edges age, the magnitude and depth-of-edge influence (DEI) change as the abiotic and biotic gradients between patch edge and interior seal, soften, or expand (Harper et al., 2005). Edge dynamics are also influenced by location, contrast, and orientation with respect to the sun and the direction of the prevailing winds (Geiger, 1965; Matlack, 1994; Zheng and Chen, 2000). Edge dynamics may result in situations were fuel loading may be increasing or decreasing relative to the interior of the forest patches. Capturing these differences of AEI is obviously important if we want to model precise simulations of fire spread across the landscape. Since measuring the fuel loading in every AEI is labor intensive, we used the FARSITE (Finney, 1998) model in this study with different fuel loading scenarios within the AEI to illustrate the importance of AEI in a managed landscape. Working on a FARSITE fuel map, a layer in a geographic information system (GIS), edges were delineated around four major fuel categories.

At landscape scales, modeling fire spread is a preferable approach because fire is a destructive process, and field experiments can be prohibitive. Early on with the development of computers, modeling fire was found to be helpful in examining fire spread and behaviors (Rothermel, 1972; Frandsen, 1973; Albini, 1976). Since then, fire simulation models have advanced and include models of succession, such as FIRE-BGC (Keane et al., 1996), and models of fire behavioral prediction such as BEHAVE (Burgen, 1996). FARSITE is a powerful fire area simulation model that incorporates a GIS map so that fire spread can be studied at a larger landscape scale with spatial precision (i.e., spatially explicit). The model has been used to successfully examine fire at the landscape scale (Keane et al., 1999), and to examine various forest fuel treatment scenarios as management options in order to attenuate rates of fire spread and the levels of heat produced from wildfires in the Western United States (Finney, 2001; Stratton, 2004; Ryu et al., 2004), and to construct visualizations of fire/forest interactions in development of alternative landscape management options for decision makers (Wang et al., 2006).

Model application, defined as using an existing model to address specific management questions about a particular case, is a good way to help guide management decisions (Ginzberg and Akcakaya, 2003). This study seeks to bring forest edge structure into the ecological simulation model FARSITE, where it has not been used before, as an example of model application to answer the management question: How would various fuel loading scenarios in the edge effect fire spread? To help understand the effects of AEI as a fuel structure on fire spread, FARSITE model simulations of surface fire in the Chequamegon national forest (CNF) in Northern Wisconsin were performed using existing databases of vegetation, weather, and topography. The CNF is an ideal landscape for studying edges because it is highly fragmented from long-term timber harvesting and recreational activities (Bresee et al., 2004) and has a rich field database (http://research.eeescience.utoledo.edu/lees/data/).

The CNF has been used as a research landscape in numerous studies, such as field (Euskirchen et al., 2001), remote sensing (RS) (Bressee et al., 2004; Zheng et al., 2004), modeling (Zheng and Chen, 2000; Wang et al., 2005), and road effects (Sunders et al., 2002; Watkins et al., 2003). Edges are a particularly strong focus of study in this forest, including the effects of edges on soil respiration (Zheng et al., 2005), carbon storage (Rademacher, 2004), microclimate (Saunders et al., 1999), and plant distribution (Brosofske et al., 1999; Euskirchen et al., 2001). However, the effect of edges as an additional fuel source on fire spread has not yet been undertaken. As a result this study was intended to make improvements to fire spread projections in the CNF by adding edge to the fuel classification map.

We hypothesized that adding edge fuels would significantly influence fire spread across the landscape, as measured by burned area. This hypothesis was developed not only because of the different possible fuel loading within the AEI, but also because the AEI has unique structure (i.e., linear and connected) in a landscape (Zheng and Chen, 2000). The results provided us with information on edges as a landscape element and their influences in a large fire event.

Our overall objective was to use FARSITE to examine a fuel edge structural feature with scenarios from three levels of edge fuel loading to determine what impacts fuels in AEI have on fire spread by ranking all of the landscape scenarios. Additionally, the simulation results help mangers and modelers to make inferences about other landscape features with high connectivity, which may also be included in a modeled landscape such as roadsides, power line corridors, railroads, trails, or riparian zones.

18.2 Methods

18.2.1 Study Area

The study area is located in the Washburn Ranger District of the Chequamegon national forest (CNF) in Northern Wisconsin (46°30' – 46°45'N, 91°02' – 91°22'W) USA. A previously classified Landsat land cover map was used as the study area, which is approximately 39,381 ha in size (Bresee et al., 2004). The landscape was reclassified into four nationally recognized fire fuel categories: 5 (brush), 8 (Red Pine Pinus resinosa Ait.), 10 (northern hardwoods) and 11 (light logging slash) (Anderson, 1982). The topography is flat with gently rolling hills with elevations ranging from 232 – 459 m above sea level. This relatively flat topography helps eliminate elevational influences on fire spread and allows us to emphasize the effects of landscape structure (Fig. 18.1).

18.2.2 Model Inputs

FARSITE simulations require three major classes of variables: topography, vegetation properties and weather. Topographic variables include elevation, slope, and aspect and were obtained from the digital elevation model (DEM). Vegetative variables are canopy openness and fuel type. Canopy openness was derived by rescaling the normalized difference vegetation index (NDVI) values (0 – 1), calculated from the red and infrared channels of landsat 7 data (Rouse et al., 1973) to 0% – 100% by multiplying by a factor of 100. The fuel type was created by reclassifying the major habitats at the CNF (Bresee et al., 2004) into four nationally recognized fire fuel categories 5, 8, 10, and 11 (Anderson, 1982).

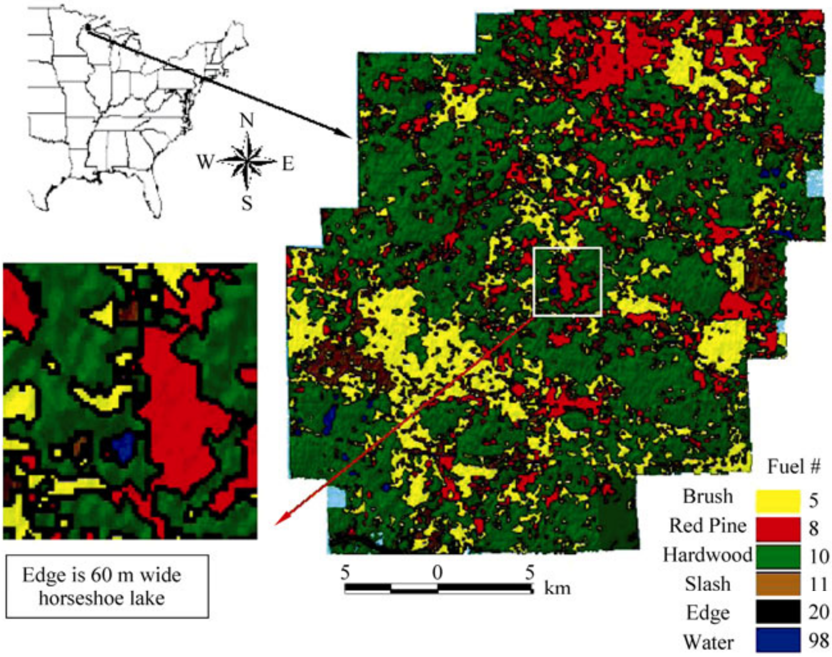

Figure 18.1 Study site location in the Washburn Ranger District of the Chequamegon national forest, Wisconsin, USA, showing the model map with its fuel categories. Number 5 represents brush, 8 is used for Red Pine, 10 is hardwood, 11 is light logging slash, 20 is edge, and 98 is water

The weather data were from a micrometeorological station located in the mixed northern hardwood habitat, which is the dominant habitat type in the CNF. The weather data was recorded on site for the month of April 2004, including temperature, precipitation, relative humidity, and wind (Noormets et al., 2004). Wind speed and direction at noontime was applied in our simulations (Bessie and Johnson, 1995). There was no precipitation during this seven-day period from April 3rd to the 10th. This eliminated any rain effects. In addition no roads, streams, barriers or fire suppression were used to impede fire spread.

18.2.3 Simulations

In the fuel layer all patches that were equal to or less than 0.36 ha in size (60×60 m) were aggregated by using the best neighborhood method. Then we added a 30 m edge buffer on both sides of the patches as was recommended by Euskirchen et al., (2001) for this landscape, creating one edge structural feature, which forms a uniform 60 m wide belt on the simulated landscape. Landscape scenarios were assigned with one of three different custom fuel model numbers 20, 21, or 22 placed in the edge feature. These fuel models were created using

FARSITE's custom fuel editor to produce fuels with various loadings to place in the edge structure and were based on Anderson's (1982) forest fuel model numbers 8 (closed timber litter), 9 (hardwood and conifer litter), and 10 (timber litter and understory), respectively. The custom fuels have the same initial fuel moistures and other basic characteristics as 8, 9, and 10; however, 8 was tuned down by a factor of 0.5 to produce the 1 hr, 10 hr, and 100 hr fuel loadings and the resulting fire spread that were used in custom fuel model number 20, and 9 was tuned down by a factor of 0.5 to produce the loadings and rate of spread that were used in custom model 21, and 10 was tuned up by a factor of 1.5 to produce the loadings and resulting fire spread for model 22. Model numbers 8, and 10 were used in our forest classification to represent non-edge forest patches; therefore the edge fuels represent low, medium, and high fuel loadings compared to these in terms of the resulting fire spread and flame lengths they produced (Table 18.1).

Table 18.1 Fuel loadings for all the fuels used in the FARSITE simulations. Model numbers 5, 8, 10, and 11 are from Anderson (1982) used directly without modification. Numbers 20, 21, and 22 are custom fuels with the same basic characteristics as Anderson's models 8, 9, and 10 respectively but with different loadings that produce rates of spread (m/min) and flame lengths (m) as low, medium and high relative to the forest fuel categories, 8 and 10 used in this classification. Custom fuels (20, 21, and 22) were created using the FARSITE custom fuel editor for moderate fuel moisture levels and midflame wind speeds of 8 km/hr

Model #	Description	Fuel Loading (Mg/ha)			Rate of Spread (m/min)	Flame Length (m)
		1 hour	10 hour	100 hour		
20	Low edge	1.68	1.12	2.80	0.3	0.2
8	Red pine	3.36	2.24	5.60	0.7	0.3
21	Medium edge	3.27	0.46	0.17	1.5	0.5
11	Light slash	3.36	10.11	12.35	2.0	1.1
10	Hardwood	6.75	4.48	11.23	2.5	1.5
22	High edge	10.12	6.72	16.85	3.7	2.1
5	Brush	2.24	1.12	0.00	4.8	1.3

We produced a total of four landscapes, each with different compositions representing various scenarios of fuel loading in the edge: ① The control or no edge fuel landscape classification with larger sized patches but no edge fuel structure defined having a total of four different fuels. ② The low edge fuel loading landscape with the same basic four fuels and an additional low loading custom fuel, number 20 in the edge structure. ③ The medium edge fuel loading landscape applies the medium loading custom fuel, number 21 to the edge structure, and ④ the high edge fuel loading landscape with the high loading custom fuel, number 22 in the edge structure. The landscapes with edge structure have a total of five fuel categories. Separating AEI from other patch types reallocated a portion of each of the four basic fuels and redefined them as edges. With a 30 m DEI on both sides' of the patches, 29% of the landscape is considered edge (Table 18.2). FARSITE was used to simulate 16 surface fires systematically placed to cover as much area as possible. The fire ignition points were kept constant for simulations at all four landscapes. The simulated burned areas were analyzed with ANOVA (SAS V.9) to detect if the burned area was significantly affected by different fuel loadings within AEI after each day of a seven-day long simulation and a 24-hour burn period. The Tukey test was used to determine significant differences between the landscape scenarios.

Table 18.2 Comparison of landscape structure among the four landscapes generated from assigning different custom fuels to 60 m combined patch edges. Control has no edge fuels. Landscapes with edges were created using a 30 m buffer inside and outside of the patches. Fuel area was reallocated from the four main patch types and a portion was put into the edge category. Categories 5, 8, 10, and 11 are Anderson's (1982) fuel types and categories 20, 21, and 22 are custom fuels created using the FARSITE custom fuel editor to create fuel loadings that represented low, medium, and high rates of spread in timber fuel loadings

	Percent Area in Each Classification (%)						
	Anderson's Fuel Model #'s				Custom Edge Fuel Model #'s		
	Brush	Red Pine	Hard-Wood	Slash	Low	Medium	High
Landscape Scenarios	**5**	**8**	**10**	**11**	**20**	**21**	**22**
Control: no edge fuel	25	14	52	9	0	0	0
Low fuel loading	15	9	42	5	29	0	0
Medium fuel loading	15	9	42	5	0	29	0
High fuel loading	15	9	42	5	0	0	29

18.3 Results

Fire spread was significantly affected by the edge fuel structure and the mean burned area (ha) was significantly different ($P < 0.000,1$) among the landscapes after seven days (Table 18.3). Fire spread responded to changes in landscape structure of both the edge feature and its fuel loading. The Tukey test showed each landscape to be significantly different (Fig. 18.2). Fire spread increased by 38% with a high fuel loading assigned to the designated edge structure; while it decreased by 20% with medium edge fuel loading and 44% with low edge fuel loading. Ranking the landscape scenarios shows that the landscape without edge structure (i.e., control) produced burned areas between the medium and the high edge fuel loading scenarios.

Table 18.3 ANOVA results for testing the main effect of four landscape scenarios with different edge fuel loadings on the size of fire spread for each day, for seven days. Dependent variable: Cumulative mean burned area (ha) after each day

Source	DF	Sum of Squares	Mean Square	F-Value	P-Value
Model	3	14,235,150	4,745,050	57.58	< 0.0001
Error	60	4,944,079	82,401		
Corrected total	63	19,179,229			
R – Squared = 0.74					
Source	**DF**	**ANOVA SS**	**Mean Square**	**F-Value**	**P-Value**
Landscape	3				
Day 1	3	974	325	4.56	0.0061
Day 2	3	45,664	15,221	14.02	< 0.0001
Day 3	3	279,130	93,043	16.84	< 0.0001
Day 4	3	1,277,311	425,770	33.83	< 0.0001
Day 5	3	3,456,856	1,152,285	41.75	< 0.0001
Day 6	3	7,400,299	2,466,766	48.46	< 0.0001
Day 7	3	14,235,150	4,745,050	57.58	< 0.0001

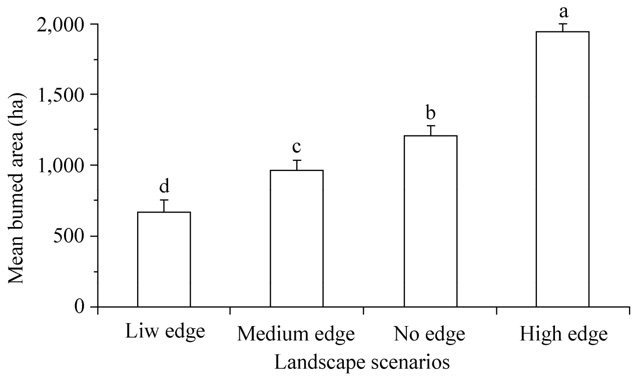

Figure 18.2 Fire size; mean ($n = 16$) burned area (ha) for each of the four landscape scenarios. Low edge represents the landscape with custom fuel # 20, with low fuel loading in the edge. Medium edge represents the landscape with custom fuel # 21, with medium fuel loading in the edge. No edge represents the aggregated landscape with no edge area delineated. High edge represents the landscape with custom fuel #22, with high fuel loading in the edge. Fires lasted seven days with a 24-hour burn period per day with no rain. The error bars represent one standard error. The letters represent significant differences (alpha = 0.05) using the Tukey test

The daily rate of fire spread was also affected by edge fuel loading. The mean burned area (ha) was calculated on a per day basis for each landscape and a daily rate of spread was plotted to show the rate of spread for each landscape as well (Fig. 18.3). Fire spread was significantly ($P = 0.0061$) different after the first day

(Table 18.3). Fire responded to edge structure in just 24 hours but practical size differences between edges scenarios did not show up until after the second day (Fig. 18.3).

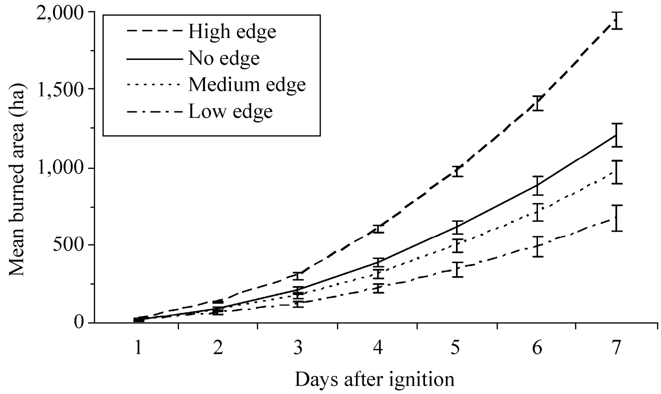

Figure 18.3 Daily rate of fire spread for each landscape, mean ($n = 16$) burned area (ha) per day for each of the four landscapes. Low edge represents the landscape with custom fuel #20, with low fuel loading in the edge. Medium edge represents the landscape with custom fuel #21, with medium fuel loading in the edge. No edge represents the aggregated landscape with no edge area delineated. High edge represents the landscape with custom fuel #22, with high fuel loading in the edge. The error bars represent one standard error

18.4 Discussion

We encourage model users to include edge fuel in FARSITE fuel maps of highly fragmented forests. Edges comprised 29% of our simulated landscape at the CNF (Table 18.2), suggesting a highly fragmented landscape and a large portion of landscape that could be uniquely influencing fire spread. In the CNF we show that almost one-third of the fuel picture was changed, affecting the modeled results. The control landscape (i.e., edges were not considered) produced fires with burned areas between our high and medium edge fuel loading scenarios. As a result, fuel maps without edge may over predict fire spread. With this data we can project what might happen in other landscapes with similar fragmentation, if forest fires encounter edges with high connectivity and comparable fuel loadings.

AEI as a landscape element may not be changeable in a highly fragmented forest like the CNF but the fuel loading within the AEI can be manipulated to increase or decrease the spread potential of large fires. Burned area was significantly different among four contrasting landscapes. This suggests that landscape management focusing on manipulating fuel loading within the AEI could be an effective approach in attenuating fire spread across the landscape. Therefore it is important to understand edge fuel dynamics and if possible manage fuel loading in forest edges because they are potentially a controlling fire fuel source at the landscape level, especially in highly fragmented landscapes, and if the high connectivity which we have modeled here is realized on a large portion of the edges between patches. Through simulations, we showed a 1,500 ha range for which managers could influence the seven-day outcome of fire spread by managing edge fuels alone. Carrying out the manipulation of fuel loading in the AEI could be done at the same time as normal harvesting operations.

Even though daily fire spread response to landscape structural changes from adding and manipulating edge fuel loading were statistically significant ($P=0.0061$) after the first day (Table 18.3) large practical differences in fire size did not start to show up until after the second day (Fig. 18.3). This suggests that fires need to reach a certain size before the effects of the edge structure appear—meaning that if fires are suppressed in the first two days, edge fuels will have less of an impact on overall fire size. Currently, the forest management plans for the Chequamegon-Nicolet national forests call for immediate and complete suppression of all wildfires because of the high intermingling of private lands (USDA Forest Service, 2004). However, large fires do sometimes occur and edge fuel management should attenuate them based on these modeled projections. The fact that the model did find significance after one day of burning between different scenarios points to the importance of edge in the CNF as a fire fuel structure. This supports the conclusion that more edge and fire research should be conducted (Harper et al., 2005).

A 30 m DEI to one side of an edge was chosen because Euskirchen et al. (2001) recommended a DEI of 30 m to both sides of the edge when managing the CNF landscape for understory plants that are unique to an edge after having examined herbaceous and woody plant species diversity across edges in the CNF. Since this was determined to be the size of the edge for plants, we used it as the DEI in this study to represent potentially unique fuel. In addition, further support comes from Harper et al. (2005) who report a synthesis of literature from around the world, including Eastern North America, which measured, among other variables, snag or log abundance in edges, an important fuel, as having mean DEI's of between 5 m and 125 m. Also, Harper and McDonald (2002) reported a range for this in another study as being between 10 m and 20 m.

Understanding fuel structure in a landscape and its potential influence on fire spread will help in managing the size of fire disturbance on the landscape and its resulting renewal of community successional processes. Through this study we demonstrated that separating AEI from other landscape elements clearly produced different projections of fire spread. This suggests that manipulating the fuel loading around edges is an effective activity in determining the rate of fire spread and the total size of burns in the landscape, especially for large fires. When developing landscape management plans for fuel reduction, edge manipulation should be seriously considered because of their significant role in determining fire spread in a landscape (Stratton, 2004).

Acknowledgements

The joint fire science program (JFSP) and the NGCP of the USDA Forest Service provided funding for this study. We thank Thomas Crow, Sari Saunders, Bo Song, and a few others for their thoughtful ideas to initialize the project.

References

Albini DH, (1976), Estimating wildfire behavior and effects. General Technical Report. GTR-INT-30. USDA Forest Service, Intermountain Forest and Range Experiment Station, Ogden, UT USA

Anderson HE, (1982), Aids to determining fuel models for estimating fire behavior. USDA Forest Service, GTR-INT-122

Bessie WC, Johnson EA, (1995), The relative importance of fuels and weather on fire behavior in subalpine forests. *Ecology*, **76**: 747 – 762

Bresee MK, LeMoine J, Mather S, Brosofske KD, Chen J, Crow TR, Rademacher J, (2004), Disturbance and landscape dynamics in the Chequamegon National Forest Wisconsin, USA, from 1972 to 2001. *Landscape Ecology*, **19**: 291 – 309

Brosofske KD, Chen J, Naiman RJ, Franklin JF, (1997), Harvesting effects on Microclimate gradients from streams to uplands in Western Washington, USA. *Ecological Applications*, **7**: 1188 – 1200

Brosofske KD, Chen J, Crow TR, Saunders SC, (1999), Vegetation responses to landscape structure at multiple scales across a northern Wisconsin pine barren landscape. *Plant Ecology*, **143**: 203 – 218

Brosofske KD, Chen J, Crow TR, (2001), Understory vegetation and site factors: implications for a managed Wisconsin landscape. *Forest Ecology and Management*, **146**: 75 – 87

Burgan RE, (1984), BEHAVE: Fire behavior prediction and fuel modeling system-fuel subsystem. General Technical Report. GTR-INT-167. USDA Forest Service, Intermountain Research Station, Ogden, UT

Chen J, Franklin JF, Spies TA, (1992), Vegetation responses to edge environments in old-growth Douglas-fir forests. *Ecological Applications*, **2**: 387 – 396

Chen J, Franklin JF, Spies TA, (1995), Growing season microclimate gradients extending into old-growth Douglas-Fir forests from clearcut edges. *Ecological Applications*, **5**: 74 – 86

Chen J, Saunders SC, Crow TR, Naiman RJ, Brosofske KD, Mroz GD, Brookshire BL, Franklin JR, (1999), Microclimate in forest ecosystem and landscape ecology. *Bioscience*, **49**: 288 – 297

Euskirchen ES, Chen J, Bi R, (2001), Effects of edges on plant communities in a managed landscape in northern Wisconsin. *Forest Ecology and Management*, **148**: 93 – 108

Finney MA, (2001), Design of regular landscape fuel treatment patterns for modifying fire growth and behavior. *Forest Science*, **47**: 219 – 228

Finney MA, (1998), FARSITE: Fire area simulator-model development and evaluation. USDA

Forest Service, RP-RMRS-4. Frandsen, W.H. 1973. Rothermel's fire spread model programmed for the Hewlett-Packard 9820. General Technical Report. GTR-INT-9. USDA Forest Service, Intermountain Forest and Range Experiment Station, Ogden, UT USA

Geiger R, (1965), The Climate Near the Ground. Harvard University Press, Cambridge, Massachusetts

Ginzburg L, Akcakaya HR, (2003), Science and management investments needed to enhance the use of ecological modeling in decision making. In, Ecological Modeling for Resource Management. V.H. Dale (editor) Springer-Verlag, New York, Inc. 249 – 262

Gustafson EJ, Crow TR, (1994), Modeling the effects of forest harvesting on landscape structure and the spatial distribution of cowbird brood parasitism. *Landscape Ecology*, **9**: 237 – 248

Harper KA, Macdonald SE, Burton PJ, Chen J, Brosofske KD, Saunders SC, Euskirchen ES, Roberts D, Jaiteh MS, Esseen P, (2005), Edge influence on forest structure and composition in fragmented landscapes. *Conservation Biology*, **19**: 1 – 15

Harper KA, Macdonald SE, (2002), Structure and composition of edges next to regenerating clear-cuts in the mixed wood boreal forest. *Journal of Vegetation Science*, **13**: 535 – 546

Keane RE, Morgan P, White JD, (1999), Temporal patterns of ecosystem processes on simulated landscapes in Glacier National Park, Montana, USA. *Landscape Ecology,* **14**: 311 – 329

Keane RE, Morgan P, Running SW, (1996), FIRE-BGC- a mechanistic ecological process model for simulating fire succession on coniferous forest landscapes of the Northern Rocky Mountains. Research Paper, INT-RP-484. USDA, Forest Service, Intermountain Forest and Range Experiment Station, Ogden, UT, USA

Matlack GR, (1993), Microenvironment variation within and among forest edge sites in the eastern United States. *Biological Conservation*, **66**: 185 – 194

Matlack GR, (1994), Vegetation dynamics of the forest edge: trends in space and successional time. *Journal of Ecology*, **82**: 113 – 123

Murcia C, (1995), Edge effects in fragmented forests: Implications for conservation. *Trends in Ecology and Evolution*, **10**: 58 – 62

Noormets A, Chen J, LeMoine J, Rademacher J, (2004), Seasonal dynamics of ecosystem carbon fluxes in five managed Northern Wisconsin forests. Journal of Geophysical Research. Submitted

Rademacher JA, (2004), Forest structure and carbon allocation within and between two northern-mixed hardwood edges. M.S. Thesis. Toledo, OH, University of Toledo

Reed RA, Johnson-Barnard J, Baker WL, (1996), Contribution of roads to forest fragmentation in the Rocky Mountains. *Conservation Biology*, **10**: 1098 – 1106

Rothermel RC, (1972), A mathematical model for predicting fire spread in wildland fuels. Research Paper. RP-INT-115. USDA Forest Service, Intermountain Forest and Range Experiment Station, Ogden, UT USA

Rouse JW, Haas RH, Schell JA, Deering DW, (1973), 'Monitoring vegetation systems in the Great Plains with ERTS'. In Third ERTS Symposium

Ryu S, Chen J, Crow TR, Saunders SC, (2004), Available fuel dynamics in nine contrasting forest ecosystems in North America. *Environmental Management*, **34**: 87 – 107

SAS, (2004), Statistical Analyst Software, SAS, Version 9. SAS Institute, Inc. Cary, NC 27513, USA

Saunders SC, Mislivets MR, Chen J, Cleland DT, (2002), The effects of roads on landscape structure within nested ecological units of the Northern Great Lakes Region, USA. *Biological Conservation*, **103**: 209 – 225

Saunders SC, Chen J, Drummer TD, Crow TR, (1999), Modeling temperature gradients across edges over time in a managed landscape. *Forest Ecology and Management*, **117**: 17 – 31

Stratton RD, (2004), Assessing the effectiveness of landscape fuel treatments on fire growth and behavior. *Journal of Forestry*, **102**: 32 – 40

USDA, Forest Service, (2004), Chequamegon-Nicolet National Forests. Forest Plan. Final Environmental Impact Statement. http://www.fs.fed.us/r9/cnnf/natres/final_forest_plan/feis/index.html

Yahner RH, (1988), Changes in wildlife communities near edges. *Conservation Biology* **2**: 333 – 339

Watkins RZ, Chen J, Pickens J, Brosofske KD, (2003), Effects of forest roads on understory plants in a managed hardwood landscape. *Conservation Biology*, **17**: 411 – 419

Wang W, Song B, Chen J, Zheng D, Crow TR, (2006), Visualizing forest landscapes using public data sources. *Landscape and Urban Planning*, **75**: 111 – 124

Zheng D, Chen J, (2000), Edge effects in fragmented landscapes: a generic model for delineating area of edge influences (D-AEI). *Ecological Modeling*, **132**: 175 – 190

Zheng D, Chen J, LeMoine J, Euskirchen E, (2005), Influences of land-use change and edges on soil respiration in a managed forest landscape, WI, USA. *Forest Ecology and Management*, **215**: 169 – 182

Zheng D, Rademacher J, Chen J, Crow T, Bresee M, LeMoine J, Ryu SR, (2004), Estimating aboveground biomass using Landsat 7 ETM+ data across a managed landscape in northern Wisconsin, USA. *Remote Sensing of Environment*, **93**: 402 – 411

19 The Need for Data Integration to Achieve Forest Sustainability: Modeling and Assessing the Impacts of Wildland Fire on Eastern Landscapes

Christine M. Stalling

Missoula Forestry Science Lab, Rocky Mountain Research Station,
800 East Beckwith, Missoula, MT 59801, USA
Email: cstalling@fs.fed.us

Abstract Public concerns regarding wildland fire management in the Eastern United States reflect myriad issues including the costs of fire suppression, landscape rehabilitation under pre- and post-fire conditions, structural damage and loss, health and cultural effects of smoke emissions, effects of insect and disease in association with fire, impacts of fire on aesthetic values, and risk of fire to human life. Because of the complexity of natural resource problems, managers can benefit from an integrated approach to landscape level management using both technologies, such as modeling and satellite imagery, with expert knowledge to better address these concerns. The ability to display the science of landscape change and the influences of natural processes such as fire, insects, and disease as well as prescribed treatments over time can help managers, decisions makers and the public to address complex issues from multiple scales and perspectives. A framework is presented pairing the modeling system SIMPPLLE (SIMulating vegetation Patterns and Processes at Landscape scaLEs), with basic concepts of sustainable forest management for a method to address complex issues in natural resources.

Keywords Fire, complex issues, integrated modeling, expert knowledge, criterion 7, Montreal Process, SIMPPLLE

19.1 Introduction

Public concerns regarding wildland fire management in the United States reflect myriad issues including the high costs of fire suppression, landscape rehabilitation, loss of and damage to homes and other structures, impacts of smoke emissions to human health and activities, effects of insect and disease in association with fire, impacts of fire on aesthetic values, and threats of fire to human life. From the

Eastern United States to West, wildland fire is only one aspect of the many issues natural resource managers and stakeholders must address as people become more concerned about the sustainability of forest resources. Concerns about sustainability expand the globe and have been the topic of discussion among forest managers, policy-makers, and the general population in countless nations for decades, yet there remain more questions than answers as time progresses.

In response to these growing concerns, an international seminar on sustainability for boreal and temperate forests convened in Montreal, Canada in 1993. From this seminar a standard for measuring and tracking progress toward sustainability was developed using a scientifically rigorous set of Criteria and Indicators for assessing forest management (Montreal Process, 1998). Once the international working group formalized its process for characterizing forest sustainability it was named the working group on criteria and indicators for the conservation and sustainable management of temperate and boreal forests, commonly referred to as the montreal process. This working group, composed initially of representatives from 10 nations, produced seven Criteria addressing the biophysical aspects of sustainability as well as the economic and social structures that are key to sustainable forest management; the criteria are associated with a number of measurable indicators for the evaluation of progress toward sustainable forest management (Montreal Process, 2003).

The criteria and indicators articulated in the Montreal process provide a general framework for measuring forest management practices across landscapes. It includes methods of analyzing current forest conditions for sustainability into the future, the maintenance of acceptable current conditions, and guidance for measuring trends to track subsequent changes over time. An important aspect of this framework is that no single criteria or indicator is an absolute indication of sustainability; rather, individual criteria must be considered in the context of the other 6 criteria (Montreal Process, 1995). The criteria and indicators provide a comprehensive overview of forest conditions, a common data source for further analysis, and a basis to discussing forest sustainability across diverse levels of expertise. The fundamental connection between people and forests is at the center of this ecosystem approach to management.

But defining forest sustainability within the context of public values must be broad enough to account for changing societal needs as well as forest conditions into the future and across landscapes of various scales. The U.S. forest service defines sustainable forest management as “the stewardship and use of forests and forest lands in such a way, and at a rate, that maintains their biodiversity, productivity, regeneration capacity, and vitality, and their potential to fulfill, now and in the future, relevant ecological, economic, and social functions at local, national and global levels, and that does not cause damage to other ecosystems” (USDA Forest Service, 2004). Similarly, the Canadian forest service considers the criteria and indicators as useful for assessing forest health since the sustainability of forests are based on the forests being healthy and “in general terms, a healthy forest is one that maintains biodiversity, resiliency, wildlife habitat, aesthetic appeal and resource sustainability" (Canadian Forest Service, 1999). According to Kimmins (1997) a healthy forest ecosystem can by measured by the underlying ecological processes operating within a natural range of variation so that these processes function dynamically and are resilient to disturbance at any temporal or spatial scale.

Given the far-reaching concerns for sustainable forestry, managers, policy-makers, and others are faced with the challenge of deciding the best management practices for sustainability. The number, diversity, and interconnectedness of the criteria and indicators developed in the Montreal process reflect the complexity of managing forests sustainably. This issue of wildland fire, for example, illustrates how social, economic, and ecological aspects of natural resources are intertwined to clearly display where sustainability is not being achieved on many forested ecosystems. While fire, flood, drought, climate change, insect and disease processes historically played key roles in shaping and maintaining the forests of the United States and Canada, human activities such as logging, grazing, fire suppression, introductions of insect and disease, land use changes, atmospheric pollutants, carbon dioxide and other greenhouse gasses, and many other influences all have contributed to forest conditions that are much less resilient to disturbance (Canadian forest service, 1999).

In the Northeastern United States human activities are evident in more recent historical analyses of northeastern forests; records indicate that they were heavily influenced by the setting of fires by Native Americans, although with the arrival of European settlers, fire activity was reduced and logging increased tremendously along with conversion to agriculture (Delcourt and Delcourt, 2000). Today, population growth, changing land uses, and the influences of past land use have altered fire behavior and the associated risks to the ecological, economic, and social integrity of forest ecosystems; private ownership mixed with State and Federal brings a divergence of forest management goals. There is an implicit need to work cooperatively across a diversity of ownership boundaries toward sustainable forest management, but how are these divergent ideas brought together toward a common goal of ecologic, economic, and social integrity across landscapes? Albert Abee, the national coordinator for sustainability, discussed reducing barriers to assessing sustainability in the U.S. (1999) and indicated that the integration of social, economic, and biological indices must include all ownerships across the landscape and promote collaborative stewardship.

Natural resource managers can benefit from an integrated approach to landscape level modeling that incorporates the most recently remotely sensed data available along with the best available knowledge of natural resource sciences to better address these concerns, which are exacerbated by patterns of ownership, population, and housing densities across the Eastern landscapes. The ability to display the science of landscape change and the influences of natural processes and management treatments over time can effectively raise public awareness and address concerns at multiple geographic scales. An integrative approach to landscape level planning and management can be accomplished by bringing together knowledge from many disciplines and effectively communicating that knowledge to stakeholders and the public; public participation is critical to sound environmental policy and decision-making (Videira et al., 2003). The complexity of natural systems, however, is difficult enough to convey even from a single discipline to an audience already familiar with the medium. Integrating knowledge from multiple disciplines and communicating that information to the public introduces yet another level of complexity. Accomplishing the goals of sustainable forest management requires a multi-disciplinary approach; and given the interdependent nature of the variables on which sustainable forestry depends, integration of the knowledge and sciences is a necessity.

An integrative approach to landscape level planning and sustainable management joins knowledge from multiple disciplines to address the myriad values associated with ecosystems. SIMulating patterns and processes at landscape scales (SIMPPLLE) is a management tool developed to help land managers integrate the best available knowledge of vegetation change resulting from disturbance processes such as fire, insects, and diseases as well as fire suppression and management treatment activities (Chew et al., 2004). The system integrates data from many sources, including satellite imagery and stand level database inventories, to represent landscape conditions. By linking with other inventory and assessment techniques such as the structure ignition assessment model (SIAM) (Cohen, 1995), SIMPPLLE can represent the probabilities of landscape scale fire disturbances spreading to specific sites and structures. A treatment optimization and scheduling model, MAGIS (Zuuring, 1995), has been linked to SIMPPLLE to assess the economic efficiency of fuel treatment allocations.

As previously mentioned, there is a need to work across various ownership boundaries toward sustainable forest management, but this is an area that has always been rife with controversy. How do we bring these divergent ideas together toward a common goal of ecologic, economic, and social integrity across landscapes? Our ability to understand the science of ecosystems is limited by our ability to fit divergent variables together as they are represented by massive, disconnected data sets. Bringing information together comprehensively may be the key to understanding and communicating ecosystem concepts and the associated methods of managing for sustainability, “better data leads to better dialog, which leads to better decisions” (USDA Forest Service, 2004). How can knowledge be better understood and shared to attain sustainability?

19.2 The Montreal Process

Long-term sustainable development is a fundamental concern countries worldwide have been debating for at least the last two decades. The United Nation’s

Brundtland Commission Report provided an integrative statement of the many ideas that were generated when participants defined sustainable development as "development that meets the needs of the present without compromising the ability of future generations to meet their own needs" (WCED, 1987). The concept of sustainable forest management, a key factor in reaching the goal of sustainable development, is recognized globally as a necessary end for meeting the social, economic, and environmental needs of present and future generations. At the Rio Earth Summit in 1992, the United States identified sustainable forest management as a priority, yet methods of characterizing and assessing sustainability remained uncertain (USDA Forest Service, 2004). At that time the United States joined the global community to address mounting worldwide concerns regarding sustainable development in which sustainable forestry is a key component (USDA Forest Service, 2004). Following these initial meetings of nations, formal discussions continued among international leaders and the science community focusing on potential methods that could be employed to measure and track progress toward sustainability.

In 1993, an international seminar on sustainability for boreal and temperate forests convened in Montreal, Canada. The seminar of 10 nations including the United States formed the working group on criteria and indicators for the conservation of sustainable management of boreal and temperate forests, best known as the Montreal process (Montreal Process, 1998). As a signatory participant of the Montreal process, which has grown to 12 member nations, the United States recognized the need for measuring the status, trends, and conditions of our nation's forests and grasslands; the forest service developed an action plan for bringing criteria and indicators into operational programs nationwide (Abee, 1998).

From this seminar a standard for measuring and tracking progress toward sustainability was developed using a scientifically rigorous set of criteria and indicators for assessing forest management (Montreal Process, 1998). The final meeting of the working group produced seven criteria, five addressing the biophysical aspect of forests including biological diversity, forest ecosystem productivity, forest ecosystem health, soil and water conservation, forest contribution to global carbon cycles; another criterion addressing socio-economic benefits, and the seventh criterion addressing a social framework for sustainable management; the criteria are associated with a number of measurable indicators for the evaluation of progress toward sustainable forest management (Montreal Process, 2003). Criterion seven addresses the social emphasis which is core to facilitation of the other six criteria and arguably the basis to accomplishing the goals of sustainable forest management since we can assume that a nation cannot reach forest sustainability without the support and understanding of its public (Oliver, 2003; USDA Forest Service, 2004).

The framework provided by the Montreal process criteria and indicators provides an initial step toward understanding current trends in forested systems, baseline information for evaluating whether management activities are being directed toward sustainability, how to get there within the changing boundaries of environmental variables such as warmer, drier conditions compared to recent human history influencing fire behavior, along with changing human use on the landscape.

The importance of addressing sustainability from the social, economic, and ecological perspective is clearly understood by forest managers, stakeholders, and policy-makers worldwide. Land management agencies have recognized the need for managing for ecosystem health for many years, and sustainable forest management is the latest term for taking a holistic approach to managing ecosystems. Despite this recognition managers continue to wrestle with methods of reaching a sustainable approach to landscape level management and have yet to find a way to integrate all aspects of ecological systems to gain better understanding of these systems.

19.3 Sustainable Forest Management (SFM)

The general framework for pinpointing conditions, or "vital signs" (Abee, 1998) and assessing sustainable forest management is provided by the Montreal process which outlines the issues that must be addressed to direct management toward sustainable future conditions or maintenance of acceptable current conditions and some guidance for measuring trends to track subsequent changes over time. The criteria and Indicators provide a source of reference information as a comprehensive overview of forest conditions and a common data source for further analysis and a basis to discussing forest sustainability. But defining forest sustainability within the context of public values must be broad enough to account for changing needs and forest conditions over time and space. Oliver (2003) posits that a "working" definition is required and that a common theme of all definitions of sustainable forestry lies in the concept of environmental justice where people living in one place and time should provide their "fair share" of values neither to the detriment or benefit of people in another place and time. The U.S. Forest service defines sustainable forest management as "the stewardship and use of forests and forest lands in such a way, and at a rate, that maintains their biodiversity, productivity, regeneration capacity, and vitality, and their potential to fulfill, now and in the future, relevant ecological, economic, and social functions at local, national and global levels, and that does not cause damage to other ecosystems" (USDA Forest Service, 2004).

A working definition is necessary because of the changing conditions that are seen across ecosystems. Researchers cannot predict what kind of impacts we can expect from global warming, pollution, changing land uses, and so many other environmental issues. While many people question current activities that will only result in benefits to later generations, a key aspect of sustainable forest management is to manage for both present and future generations. In order to move management activities toward sustainability, the social, ecological, and economic perspectives of the ecosystem must be addressed together. Criterion seven provides the context for bringing together all the pieces of the ecosystem. While ecological conditions may be the platform to forest sustainability, it is the legal, institutional, and economic structures that enable identification of concerns about forest sustainability and ways to address and implement policy and management responses (USDA Forest Service, 2004).

19.4 Northeastern Forests—an Example of Changing Conditions

With world wide concerns for sustainable forestry as a basis to sustainable development, managers, policy-makers, and others are faced with the challenge of deciding the best management practices for sustainability. The number and diversity of criteria and indicators developed in the Montreal process reflect the complexity of managing forests sustainably. The forest management issue of wildland fire is a single instance of how the social, economic, and ecological aspects of natural resources are intertwined into an intricate barrier to achieving sustainable management. The "Sourcebook on criteria and indicators of forest sustainability in the Northeastern Area" (2002) echoes the key features of the Montreal process summing that forests must be managed for continued existence as a healthy organism in order to meet human physical, economic, and social needs now as well as for future generations.

Just as forests of the Western United States have been shaped through time by the presence and then suppression of fire, forests of the Eastern United States have been formed through similar processes. Wildland fire in the Northeastern United States with the associated expansive population densities, diverse economic and ecologic goals, and the many impacts of fire on the landscape typifies a common management problem of escalating concern. The complex knot of private ownership intertwined with State and Federal is fertile ground for controversy. Northeastern temperate forests provide an example of landscapes heavily influenced historically by Native American burning, followed by the arrival of European settlers when fire activity was reduced and harvesting increased tremendously along with conversion to agriculture (Delcourt and Delcourt, 2000). Now, population growth, changing land uses, and the influences of past land use have altered fire behavior and the associated risks to human life and structures; similar to management issues in the Western States in which private ownership mixed with State and Federal brings a divergence of forest management goals (McKinney and Harmon, 2004), Eastern States must consider an even more fragmented landscape of ownerships. Questions regarding management practices present great complexity and an even larger population to communicate with than is seen in the west.

19.5 Modeling Landscape Conditions to Address Sustainable Forest Management

The complexity of natural systems, however, is difficult to convey even from a single discipline to an audience already familiar with the medium. Integrating knowledge from multiple disciplines and communicating that information to the public introduces yet another level of complexity. Further, resource managers and researchers must avail themselves of effective technology transfer approaches to share the ecological and socio-economic information while focusing on the importance of the social and political sense of place to public and stakeholders. Communicating the sciences of ecosystems in the context of social implications is new territory; until managers can better understand how ecosystem values fit together they cannot address sustainability and without public understanding of the issues management cannot be applied at levels that can have an impact on forest conditions.

The premise of criteria and indicators is interdependency; no single criteria is a measure of sustainability alone, each must be considered in the context of the others to fully identify current sustainability trends in forest ecosystems (USDA Forest Service, 2004). And central to this interdependency is the need for local stakeholder participation in forest management assessments because understanding the connections of ecosystem variables sets the stage for better informed decisions for sustainability.

Accomplishing the goals of sustainable forest management requires a multi-disciplinary approach and given the interdependent nature of the variables on which sustainable forestry depends, integration of the knowledge and sciences is a necessity.

Indicators 60 – 62, of criterion seven of the Montreal process details the need to maintain and standardize up-to-date data, data collection, statistics, and other information important to measuring all seven criteria (Montreal process working group, 1998). However, data collection is costly in both time and dollars and national agencies struggle to bring forest inventories up-to-date, as well as to monitor and assess the data for validity. In 1997, the U.S. forest service compiled its first approximation report for sustainable forest management based on the criteria and indicators and although some information was available for most indicators data was completely lacking, or had been only recently collected making it impossible to determine trends, or data collection had been conducted using inconsistent definitions or methodologies across study locations so that conclusions could not be drawn (USDA Forest Service, 1997). More recently, appendix 3 of the National Report on Sustainable Forests—2003 (USDA Forest Service, 2004) discusses continuing data issues and the need for better data management and availability specific to each criterion. While on-line sources continue to increase and become more easily available, the "best" available data changes frequently and will continue to do so into the future.

Since natural resource information is changing regularly, a model must be adaptable to using the best, or sometimes any, available data; it must represent multiple landscape scales (Oliver, 2003) and represent those processes influencing vegetation change such as insects, disease, and fire, as spatially explicit so that interactions of specific vegetation conditions and process probabilities can be displayed as they occur and spread.

An integrative approach to landscape level planning and sustainable management joins knowledge from multiple disciplines to address the myriad values associated with ecosystems. SIMPPLLE is a management tool developed to help land managers integrate the best available knowledge of vegetation change resulting from disturbance processes such as fire, insects, and diseases as well as fire suppression and management treatment activities (Chew et al., 2004). The model uses landscape level vegetation data to represent vegetation change as a result of the interacting disturbance processes and management actions. The model's spatial link to GIS and the dynamic approach to modeling landscapes provide a tool to aid users in visualizing how a landscape can change over time and space with and without the influence of management applications.

Modeling with SIMPPLLE helps quantify the level of resources and the realistically attainable future conditions that meet the goals of sustainable forest management. The model represents landscapes from multiple scales by representing individual plant communities as spatially linked units across the larger landscape. The modeling approach in SIMPPLLE and its tie to GIS provides a valuable visual display, a picture to enhance communication of issues scaling from one acre to millions. Discussions of management activity toward SFM are greatly enhanced by displaying the potential effect on the landscape.

19.6 Conclusions

The framework to sustainable forest management can be derived from the Criteria and Indicators developed in the Montreal process. Managers can refine applications specific to locations world wide. The criteria and indicators are broad yet provide a standard base from which forest managers can make better decisions, enhancing sustainability ranging across a wide variety of landscapes and conditions—from highly populated, industrialized conditions to sparsely populated, non-industrialized conditions.

It is necessary to help managers strive for goals of sustainability by developing a better understanding of how changes within landscapes over time and space influence the management of landscapes on a scale that expands generations. If we want to reach sustainability into the future we must plan for future conditions within a realistic horizon which includes large events such as fire, insect and disease epidemics, climate change, human population growth, and an endless list of alternative possible conditions that can be expected across a landscape. Modeling techniques used in the SIMPPLLE system that are adaptive to changing data, representative of changing conditions, and able to integrate information across disciplines provide a forum to better understand how biophysical processes can be managed sustainably within our social and economic framework.

Criteria and indicators developed in the Montreal process, specifically criterion 7, combined with developing modeling techniques, and ongoing efforts to work cooperatively across a diversity of landownership boundaries, will all go a long way in helping managers promote, protect and maintain sustainable forests across a vast landscape long into the future.

References

Albert A, (1998), Reducing barriers to assessing sustainability. In the U.S. North American Science Symposium: toward a unified framework for inventorying and monitoring forest ecosystem resources, Guadalajara, Mexico, November 1 – 6, 1998

Canadian Forest Service, (1999), Forest health: context for the Canadian Forest Service's science program. Science branch, Canadian Forest Service, Natural Resources Canada, Ottawa

Chew JD, Stalling CM, Moeller K, (2004), Integrating knowledge for simulating vegetation change at landscape scales. *West. J. App For*. **19**(2): 102 – 108

Cohen JD, (1995), Structure ignition assessment model (SIAM). USDA FS Gen. Tech. Rep. PSW-GTR-158. 8

Delcourt HR, Delcourt PA, (2000), Eastern deciduous forests. pp. 358 – 395 in Barbour MG, Billings WD (eds.), North American Terrestrial Vegetation—2nd ed. Cambridge Univ. Press, UK

Kimmins JP, (1997), Biodiversity and its relationship to ecosystem health and integrity. *For. Chron*. **73**(2): 229 – 232

McKinney M, Harmon W, (2004), The western confluence. Island Press. 256

Montreal Process, (1995), Criteria and indicators for the conservation and sustainable management of temperate and boreal forests. Hull, Quebec: Canadian Forest Service, Natural Resources Canada. p27

Montreal Process, (1998), The Montreal Process available only online at: http://www.mpci.org/whatis/whatis_e.html

Montreal Process, (2003), Working Group Criteria for Sustainable Forest Management (Working Group). Available only online at: http://silvae.cfr.washington.edu/ecosystem-management/IntroFrame.html

Oliver CD, (2003), Sustainable forestry: What is it? How do we achieve it? *J. Forest.* **101**(5): 8 – 14

USDA Forest Service, (2004), National Report on Sustainable Forests—2003. FS-766. Washington, DC: USDA FS

USDA Forest Service, (2002), Sourcebook on Criteria and Indicators of forest sustainability in the Northeastern area. NA-TP-03-02. [Newtown Square, PA]: State and Private Forestry, Northeastern Area. 64

USDA Forest Service, (1997), First approximation report for sustainable forest management: report of the United States on the criteria and indicators for the sustainable management of temperate and boreal forests. Washington DC.

Zuuring HR, Wood WL, Jones JG, (1995), Overview of MAGIS: a multi-resource analysis and geographic information system. USDA FS Res. Note. INT-RN-427. 6

Videira N, Antunes P, Santos R, Gamito S, (2003), Participatory modeling in environmental decision-making: the RIA Formosa Natural Park case study. *Journal of Environmental Assessment Policy and Management*, **5**(3): 421 − 447

20 Automated Wildfire Detection Through Artificial Neural Networks

Jerome Miller
NASA/Goddard Space Flight Center, Greenbelt, Maryland 20771
Email: Jerome.Miller-1@nasa.gov

Kirk Borne
George Mason University, Fairfax, Virginia 22030
Email: kborne@gmu.edu

Brian Thomas
University of Maryland, College Park, Maryland 20742
Email: thomas@astro.umd.edu

Zhenping Huang
University of Virginia, Charlottesville, Virginia 22908
Email: zh2a@virginia.edu

Yuechen Chi
George Mason University, Fairfax, Virginia 22030
Email: ychi@mason.gmu.edu

Abstract Satellite observations of wildland, agricultural and prescribed fires are routinely identified by Fire Analysts and software algorithms which are part of NOAA's Hazard Mapping System. However, to more fully automate this operational system, NOAA teamed up with NASA to train a neural network which mimicked the behavior of both analysts and software algorithms in their examination of multi-sensor, satellite imagery. Three spectral channels from GOES, AVHRR and MODIS imagery, spanning the 2003 fire season across the continental United States, was used as training data and JOONE, SNNS and MATLAB software packages generated the NNs. Test results from MATLAB's 147-10-1 feedforward, backpropagation NN are described. Performance analysis consisted of error matrices, Producer's, User's and Overall accuracy, and a Kappa/KHAT.

Keywords Satellite, GOES, AVHRR, MODIS, sensors, imagery, neural network, feedforward, backpropagation

20.1 Introduction

Wildfires have a profound impact upon the biosphere and our society in general. They cause loss of life, destruction of personal property and natural resources and alter the chemistry of the atmosphere. In response to the concern over the consequences of fire and to support the fire management community, the national oceanic and atmospheric administration (NOAA), national environmental satellite, data and information service (NESDIS) located in camp Springs, Maryland gradually developed an operational system to routinely monitor wildland, agricultural and prescribed fire by satellite observations. The hazard mapping system, as it is known today, allows a team of trained fire analysts to examine and integrate, on a daily basis, remote sensing (RS) data from geostationary operational environmental satellite (GOES), advanced very high resolution radiometer (AVHRR) and moderate resolution imaging spectroradiometer (MODIS) satellite sensors and generate a 24 hour fire product for North America. Although assisted by automated fire detection algorithms, NOAA has not been able to eliminate the human element from their fire detection procedures. The national aeronautics and space administration (NASA) at goddard space flight center in Greenbelt, Maryland has been collaborating with NOAA to more fully automate the hazard mapping system by training neural networks to mimic the decision-making process of the fire analyst team as well as the automated algorithms.

20.2 Data Archiving

More than four years ago a team of government and (ultimately) University personnel were assembled with the intent of applying artificial intelligence techniques to NOAA's automation problem. NASA began archiving satellite imagery from GOES, AVHRR and MODIS satellite sensors in the summer of 2003. Three spectral channels for each of 3 science instruments were provided by NOAA NESDIS by uploading to a NASA computer within the information systems division at goddard space flight center. The following uploaded spectral bands, being only a subset of those available from each instrument, were found by NOAA NESDIS to be the most useful in fire identification: MODIS Channels 1 (0.66 μm), 2 (0.86 μm), 22 (3.96 μm); AVHRR Channels 1 (0.63 μm), 2 (0.91 μm), 3b (3.7 μm), and GOES Channels 1 (0.62 μm), 2 (3.9 μm), 4 (10.7 μm). Both reflectance and brightness temperature were scaled by NESDIS to a range of 0 – 255. It became apparent almost immediately that the huge volume of satellite imagery which NESDIS provided but did not archive themselves presented a formidable storage problem. Each day, NESDIS processed 96 GOES image files, 25 AVHRR image files and 16 MODIS image files which were uploaded to NASA. Satellite imagery, in lambert conformal conic projections, plus ancillary data required approximately 1.44 gigabytes of storage daily. A Mac G5 with 12 Maxtor external disk drives (250 gigabytes each) was able to handle the enormous storage requirement.

20.3 Preliminary Analysis

The first step in our analysis consisted of a series of scatter plots to help visualize the relationship between pixels in 2 selected spectral bands. We began with the GOES image set in an attempt to determine the separability of fire and non-fire pixels. Refer to Fig. 20.1 for a sample scatter plot. Using data sets over the course of a single day, clusters of background pixels (upper region) and fire pixels (lower region) are clearly distinguishable. All intensity values were background subtracted. This was the first indication, confirmed by subsequent analysis, that different fires types (crown, surface and ground) did not have unique fire signatures and that a simple linear separability existed between the two general classes of fire and background pixels.

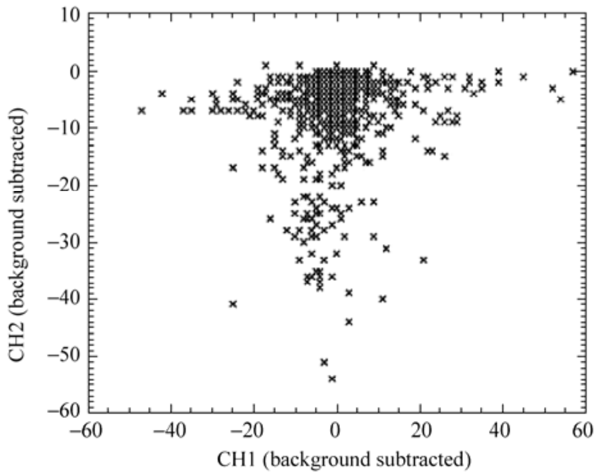

Figure 20.1 Scatter plot of GOES Channels 1 and 2

20.4 Data Reduction

A good deal of effort went into the construction of satisfactory feature vectors for neural network training. Early in the investigation data sets were drawn from specific regions of the country which had more or less uniform land cover characteristics (such as Kansas) as well as specific seasons and time of day in an attempt to confine wildfires to specific types and possibly signatures. Feature vectors which incorporated these components as well as spectral information made neural network convergence difficult. Once it was determined that only a single fire signature was involved, spectral data became the only component of the feature vector. The guiding principle in training set composition was to use NOAA's ASCII data formatted fire product (McNamara et al., 2002), to locate wildfires within satellite imagery, then extract 3-band pixel information at these points. Table 20.1 is exemplary of NOAA's text formatted fire product available at their FTP site. As shown on each line and for each separate fire, the geographic coordinates of the fire are followed by a time stamp, the satellite imagery from which the determination was made and finally the method of detection which may have been a human analyst or one of three automated algorithms: wildfire automated biomass burning algorithm (WF-ABBA) (Prins and Menzel, 1992; McNamara et al., 2002), fire identification mapping and monitoring algorithm (FIMMA) (McNamara, et al., 2002; McNamara et al., 2002) or MODIS MOD14 (NASA, 2005) Fire Product.

Table 20.1 ASCII data format of NOAA fire product

Lon	Lat	Time	Satellite	Method of Detect
–80.597	22.932	1830	MODIS AQUA	MODIS
–79.648	34.913	1829	MODIS	ANALYSIS
–81.048	33.195	1829	MODIS	ANALYSIS
–83.037	36.219	1829	MODIS	ANALYSIS
–83.037	36.219	1829	MODIS	ANALYSIS
–85.767	49.517	1805	AVHRR NOAA-16	FIMMA
–84.465	48.926	2130	GOES-WEST	ABBA
–84.481	48.888	2230	GOES-WEST	ABBA
–84.521	48.864	2030	GOES-WEST	ABBA
–84.557	48.891	1835	MODIS AQUA	MODIS
–84.561	48.881	1655	MODIS TERRA	MODIS
–84.561	48.881	1835	MODIS AQUA	MODIS
–89.433	36.827	1700	MODIS TERRA	MODIS
–89.750	36.198	1845	GOES	ANALYSIS

Using environment for visualizing images (ENVI) software, geographic coordinates of wildfires provided by NOAA's fire product were converted to pixel row and column coordinates for a particular image being processed through a series of ENVI function calls embedded in interactive data language (IDL) code. When examining satellite imagery of wildfires using ENVI in visual mode however it was found that fires were not in the precise location where the geographic coordinates placed them, being offset possibly by several pixels from their expected location. Considering the 1,000 meter spatial resolution of MODIS and AVHRR, the offset error might have been 2,000 or 3,000 meters but for GOES data in the thermal band (4,000 meter resolution) the error could have been as much as 12,000 meters. This offset was attributed to 3 sources: spacecraft navigation errors, the inherent tolerances within NOAA software and operational errors in the point-and-click method of a Fire Analyst identifying fire locations with a mouse. One of the best clues for identifying wildfires that NOAA Fire Analysts employ is to visually inspect the 4 micrometer band for dark spots within NESDIS-processed satellite imagery. NOAA software has been written in such a way that brightness temperatures, which have been scaled to a range of 0 – 255 will assume the lowest values for the hottest fires. This can be seen clearly in Fig. 20.2(a), a satellite image of northern Florida. Here, a wildfire (enclosed in rectangle) at coordinates –82.10° West Longitude, 30.49° North Latitude recorded on Julian day 126 in 2003, appears as a single black spot. Although appearing to be a pinpoint location in the normal view, a zoomed-in view in Fig. 20.2(b) indicates that the fire is actually spread across numerous pixel locations. In order to extract the spectral information around this exemplar fire, using the approximate location as specified by the ASCII data fire product, our software performed a local minima search in the 4 micrometer band in the expected region to pinpoint the hottest fire pixel (lowest intensity value). Spectral information was then collected around that image coordinate in all 3 bands.

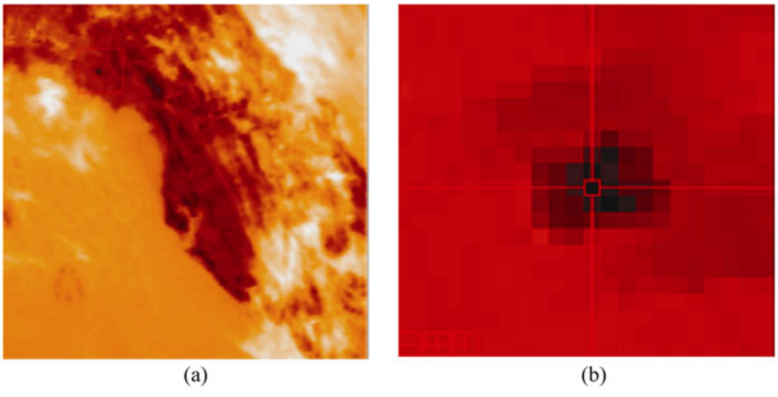

Figure 20.2 (a) GOES Channel 2 Northern Florida fire (normal view), (b) GOES Channel 2 northern Florida fire (zoom view)

In the course of the investigation, three different methods to characterize a fire across 3 spectral bands were attempted: as a single pixel at an instantaneous point of time, a pixel time series demonstrating the time evolution of a fire throughout the day and as a pixel array at an instantaneous point in time. The first two techniques had mixed results in achieving neural network convergence, however the third, a spatial technique consisting of 7×7 pixel arrays with the hottest part of the fire as the central pixel, was successful. In the 4 micrometer band, the approximate locations of hot spots were identified by NOAA's fire product, and then the local minima technique identified the hottest part of the fire. In all 3 bands, using the image coordinates of the hottest fire pixel, pixel arrays of size 7×7 were collected around that central point. A typical spatial fire pattern for the MODIS sensor is shown in Table 20.2. Numeric values represent reflectance or brightness temperature scaled to a 0 – 255 range. In the 3.96 μm band the pattern becomes visually obvious. Moving away from the central pixel, the cooler parts of the fire are represented by rising intensity values (an intentional inversion).

Table 20.2 MODIS Channels spatial fire signature

MODIS Channel 1 Spatial Fire Signature						
70	65	65	73	74	71	66
81	76	80	68	67	61	63
74	75	74	75	75	61	62
63	71	80	81	79	66	63
62	69	77	78	77	69	59
69	75	69	78	77	67	72
85	82	65	69	67	72	79
MODIS Channel 2 spatial fire signature						
139	156	155	125	133	135	145
151	143	141	129	129	137	142
146	143	143	136	129	145	142
144	146	128	127	128	138	142
148	144	138	124	125	134	145
140	145	147	123	123	138	131
129	136	148	141	144	146	136
MODIS Channel 22 spatial fire signature						
46	51	48	35	35	38	38
41	38	35	41	43	51	50
46	41	34	20	42	53	52
52	21	3	0	21	51	51
51	36	4	28	43	49	56
41	42	50	48	41	49	42
28	35	47	47	49	43	37

20.5 Neural Network Architecture

Three bands of 7×7 pixel arrays, formatted as 147 element feature vectors determined the number of network input nodes while the number of hidden nodes was initially determined by the rule-of-thumb to start with the square root of the sum of the inputs and outputs (Eberhart and Dobbins, 1990), which in this case is 12. Even with some experimentation though, the number of hidden nodes did not vary much from the initial value. A single output node was required to discriminate between the 2 classes. The final 147-10-1 feedforward backpropagation neural network configuration used for training and testing is shown in Fig. 20.3. Separate, identical networks were created for each sensor. Mathematical operations performed by network layers are shown in Table 20.3 in terms of: I (induced local field), O (nodal output), W (network weight) and f (hyperbolic transfer function).

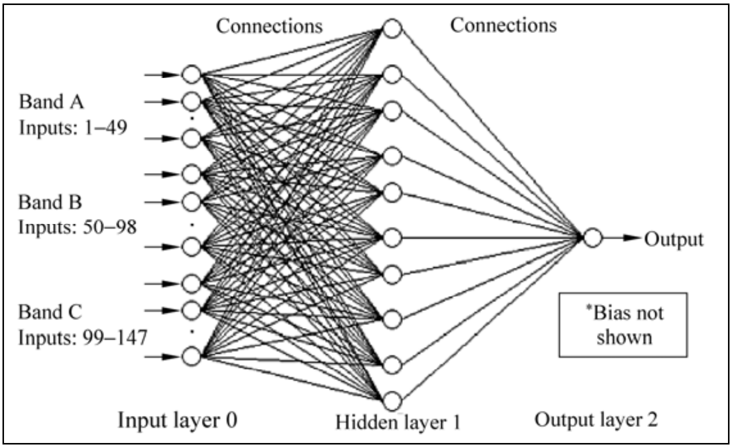

Figure 20.3 MODIS, GOES or AVHRR 147-10-1 neural network

Table 20.3 Defining network equations

Level 0: $O_i^0 = I_i^0$ (no computation)

Level 1: $I_j^1 = s\sum_{i=1}^{N_{i+1}} W_{j,i}^1 O_i^0 \qquad O_j^1 = f(I_j^1)$

Level 2: $I_1^2 = \sum_{j=1}^{N_{h+1}} W_{1,j}^2 O_j^1 \qquad O_1^2 = f(I_1^2)$

where:
I,*O* superscripts = layer number
I,O subscripts = node index number
W superscripts = destination layer
W subscripts = destination and source node index numbers, respectively
N = number of nodes per layer (including bias)
h = number of hidden nodes
i = input node index number
j = hidden node index number

20.6 Training and Testing

Thousands of spatial pattern training samples were extracted from the 3 sensor imagery which spanned the 2003 fire season across the continental United States. Three different neural network modeling tools were used in the course of the investigation: java object oriented neural engine (JOONE), stuttgart neural network simulator (SNNS) and MATLAB Neural Network Toolbox. The first 2 tools were freely downloadable from the Internet (http://www.jooneworld.com and http://www-ra.informatik.uni-tuebingen.de/SNNS, respectively). The following discussion however pertains only to results obtained with MATLAB. The total number of spatial pattern samples for MODIS, AVHRR, GOES-EAST and GOES-WEST was 25,713, 43,758, 73,010 and 53,922 respectively, with the ratio of fires to non-fires being approximately 1:1. A variation of the cross-validation technique (Amari et al., 1997) was employed for training and testing. Total available patterns for each instrument were divided into 4 quarters, each being representative of the entire data set. Training samples constituted 1/2 of the total number of patterns with 1/4 relegated to a validation set and 1/4 a test set resulting in 3 disjoint data sets. Batch training using the gradient descent with momentum algorithm was selected from a suite of available MATLAB routines and generally the early stopping technique was used to avoid overfitting. During training, the mean squared error on the validation set was monitored and when it began to rise, training was automatically halted. Testing was then performed on data that had not been seen by the neural network during the training phase.

20.7 Classification and Analysis

Results of the neural network classification for MODIS, AVHRR and GOES EAST and GOES WEST data are presented in the form of error matrices, the starting point for further analysis techniques, in Tables 20.4. Since this is a 2-class system, empirical data represents true positives (TP), true negatives (TN), false positives (FP) and false negatives (FN) which occupy the upper left hand corner of the error matrices for which marginal totals have been computed. Remaining notations used in these tables are: fires (F), non-fires (NF), marginal column total (MCT) and marginal row total (MRT). Error matrices were analyzed statistically (Congalton and Green, 1999) as shown in Table 20.5 with results tabulated in Table 20.6.

As can be seen, using Congalton's method results in 5 different accuracy measures of neural network performance. Overall accuracy describes the neural network's ability to correctly assign unknown image pixels to either of two classes, fire and background while the producer's and user's accuracy figures account for omission and commission errors, respectively. This somewhat confusing set of results was rectified by a procedure called marginal fitting (Congalton, 1991) in which error matrix rows and columns are iteratively normalized so that marginal totals converge to unity and differences in sample size are accounted for. Normalized error matrices are shown in Tables 20.7. For a 2-class system, normalized error matrices yield identical results for overall accuracy, producer's accuracy and user's accuracy thus a single performance measure was obtained. This was followed by a Kappa analysis (Congalton and Green, 1999). Comparison of normalized accuracy and the KHAT statistic are shown in Table 20.8; as indicated, a high degree of classification accuracy, greater than 95%, was achieved for the MODIS sensor. This tracks well with the KHAT value which measures how well the classification agrees with the reference data. A value greater than 80% indicates strong agreement. ANN classification performance in terms of both measures however becomes progressively worse thereafter for AVHRR and GOES and thus the ANNs became less useful for our intended purpose.

Table 20.4 MODIS, AVHRR, GOES WEST and GOES EAST error matrix

Classified Data	Reference Data		
MODIS	F	NF	MRT
F	2834 (TP)	173 (FP)	3007
NF	318 (FN)	3103 (TN)	3421
MCT	3152	3276	6248
AVHRR	F	NF	MRT
F	5500 (TP)	479 (FP)	5979
NF	624 (FN)	4336 (TN)	4960
MCT	6124	4815	10,939
GOES WEST	F	NF	MRT
F	4826 (TP)	771 (FP)	5597
NF	1451 (FN)	6432 (TN)	7883
MCT	6277	7203	13,480
GOES EAST	F	NF	MRT
F	7445 (TP)	2304 (FP)	9749
NF	1312 (FN)	7191 (TN)	8503
MCT	8757	9495	18,252

Table 20.5 Classification accuracy formulas

Overall Accuracy	(TN+TN) / (TP+TN+FP+FN)
Producer's Accuracy (fire)	TP / (TP+FN)
Producer's Accuracy (non-fire)	TN / (FP+TN)
User's Accuracy (fire)	TP / (TP+FP)
User's Accuracy (non-fire)	TN / (TP+FN)

Table 20.6 Preliminary analysis of neural network classification performance

Statistic	MODIS (%)	AVHRR (%)	GOES WEST (%)	GOES EAST (%)
Overall AA Accuracy	92.362	89.917	83.516	80.188
Producer's Accuracy (fire)	89.911	89.811	76.884	85.018
Producer's Accuracy (non-fire)	94.719	90.051	89.296	75.735
User's Accuracy (fire)	94.247	91.989	86.225	76.367
User's Accuracy (non-fire)	90.704	87.419	81.593	84.570

Table 20.7 Normalized error matrix of MODIS, AVHRR, GOES WEST and GOES EAST

Classified Data	Reference Data		
MODIS	F	NF	MRT
F	0.926703	0.073297	1.000000
NF	0.073297	0.926703	1.000000
MCT	1.000000	1.000000	2.000000
AVHRR	F	NF	MRT
F	0.899319	0.100681	1.000000
NF	0.100681	0.899319	1.000000
MCT	1.000000	1.000000	2.000000
GOES WEST	F	NF	MRT
F	0.840447	0.159553	1.000000
NF	0.159553	0.840447	1.000000
MCT	1.000000	1.000000	2.000000
GOES EAST	F	NF	MRT
F	0.808003	0.191997	1.000000
NF	0.191997	0.808003	1.000000
MCT	1.000000	1.000000	2.000000

Table 20.8 Comparison of normalized accuracy and KHAT statistic

Sensor	Normalized Accuracy (%)	KHAT Statistic (%)
MODIS	96.7	84.7
AVHRR	89.9	79.6
GOES WEST	84.0	66.6
GOES EAST	80.8	60.5

20.8 Conclusions

The original intent of the project was to develop a single neural network that could process sensor data from all 3 satellite instruments, and perform fire classification at least as well as the automated algorithms and human fire analysts currently achieve so that incorporation into NOAA's operational hazard mapping system could reduce the amount of manual intervention. Our research has shown that there was insufficient temporal and spatial overlap between the 3 sensors to process image data with a single ANN. Even excepting this problem, the extreme size of the network, exacerbated by 7×7 pixel arrays to characterize fire patterns, would have made training difficult or impossible for our host platform. Our analysis showed that dividing processing between 3 independent networks was the practical solution; however, except in the case of MODIS, classification accuracy did not achieve the level of performance that would allow the relief of human workload. Improvement in classification accuracy could likely be achieved however by incorporating in the training process additional generalization techniques such as those offered by MATLAB's neural toolbox: modified performance function, and bayesian regularization (Demuth and Beale, 2000). Perhaps then, with further research efforts, our neural designs could be incorporated into NOAA's operational system.

Acknowledgements

This work was supported by NASA's computing, information and communications technology (CICT) Program operating out of the NASA ames research center in Moffett Field, California. Sincere appreciation is extended to George Mason University and University of Maryland for their valuable research support and special thanks is given to the Fire Analysts within the NOAA/NESDIS Satellite Analysis Branch for their consultive services.

References

Amari S, Murata N, Muller K, Finke M, Yang HH, (1997), Asymptotic statistical theory of overtraining and cross-validation. *IEEE Transactions on Neural Networks* **8**: 985 – 996

Congalton RG, (1991), A review of assessing the accuracy of classifications of remotely sensed data. *Remote Sensing of Environment*, **37**: 35 – 46

Congalton RG, Green K, (1999), Assessing the Accuracy of Remotely Sensed Data: Principles and Practices. Boca Raton: CRC Press

Demuth H, Beale M, (2000), Neural Network Toolbox For Use with MATLAB., pp 5-51 – 5-55, Natick: The Math Works, Inc.

Eberhart RC, Dobbins RW, (1990), Neural Network PC Tools a Practical Guide (35 – 58). San Diego: Academic Press, 35 – 58

McNamara D, Stephens G, Ruminski M, (2002), NOAA's multi-sensor fire detection program using environmental satellites. *Earth System Monitor* **13**(1): 1 – 7

McNamara D, Stephens G, Ramsay B, Prins E, Csiszar I, Elvidge C, Hobson R, Schmidt C, (2002), Fire detection and monitoring products at the National Oceanic and Atmospheric Administration. *Photogrammetric Engineering and Remote Sensing*, **68**(8): 774 – 775

National Aeronautics and Space Administration, (2005), MODIS Fire and Thermal Anomalies. http://modis-fire.umd.edu/products.asp#1

Prins EM, Menzel WP, (1992), Geostationary satellite detection of biomass burning in South America," *International Journal of Remote Sensing*, **13**: 2783 – 2799

21 Altered Disturbance Regimes: the Demise of Fire in the Eastern United States

Gregory J. Nowacki and Robert A. Carr

Eastern Regional Office, USDA Forest Service, 626 E. Wisconsin Avenue, Milwaukee, WI 53202, USA
E-mail:gnowacki@fs.fed.us; racarr@fs.fed.us

Abstract We generated a series of maps to help alert and educate people to the pervasiveness of fire regime changes across the eastern United States. Using geographic information systems (GIS), fire regimes were assigned to spatial vegetation databases to depict past and current conditions. Comparisons revealed substantial reductions in fire throughout the East. The most dramatic shifts took place in the former Midwestern grasslands and across a broad swath of southern and central States where pine and oak communities historically dominated. Land-use changes (e.g., agricultural and forest-type conversions) and recent fire suppression largely explain these shifts. Fire regime change was least in northern hardwood systems, in the mixed mesophytic region, and within the Mississippi Embayment. Negative ecological consequences of prolonged fire suppression are mounting while restoration opportunities are waning.

Keywords Fire regime condition class, fire suppression, fire history, Native Americans, oak

21.1 Introduction

Ecosystems are the product of physical settings (e.g., climate, geology, soils), biota (plants and animals), and disturbance regimes. Ecosystems are dynamic (Pahl-Wostl, 1995), shifting states as components interact and change over time and space. Intriguingly, ecological research has been slow to grasp dynamism, focusing instead on equilibrium and stability to explain physical and biotic interactions (especially climate-site-vegetation relations) at the expense of disturbance (Christensen, 1991; Reice, 2001). Indeed, early ecological theories clearly bear this out (e.g., succession towards climax in the absence of disturbance; Clements, 1916). Fortunately, through mounting scientific evidence, perspectives have changed to embrace disturbance as an equally important, actually vital driver of ecological patterns, processes, and diversity (Watt, 1947; Denslow, 1980; Pickett and White, 1985; Oliver and Larson, 1996; Frelich, 2002). Even in climax systems, where autogenic (internal) processes were once thought to reign supreme, the role of allogenic (external) disturbances has been proven instrumental (Henry and Swan, 1974; Oliver and Stephens, 1977).

Disturbances affect biota in a wide variety of ways, from catastrophic extinction events (e.g. asteroid impacts or mass volcanism; Benton and Twitchett, 2003; McElwain and Punyasena, 2007) to chronic, less-destructive disturbances that help guide species evolution, adaptation, and assemblage (Grime, 1977). The term "disturbance regime" refers to the latter, encompassing an array of common, recurrent disturbances within a physical setting over a period of relative constant climate. In this context, species possessing life-history and physiological traits that "match" a given disturbance regime will express dominance, whereas those physiologically "ill equipped" will not (Bazzaz, 1979; Denslow, 1980; Osmond et al., 1987). This explains, in part, why hydrophilic trees grow on floodplains (Jackson and Colmer, 2005), fire-adapted trees dominate fire-prone areas (Lorimer, 1985; Abrams, 1996; Hengst and Dawson, 1994), and shade-tolerant trees proliferate in closed-canopied forests with gap-phase dynamics (Barden, 1979; Runkle, 1981 and 1982).

Humans have long enhanced or facilitated certain types of disturbances through their activities, thus directly affecting disturbance regimes. The global use of fire is most noteworthy (Stewart, 1956; Komarek, 1967; Sauer, 1975). Unfortunately, early North American scientists were slow to grasp the magnitude of Native burning, thus grossly underestimating its impacts on the environment (Stewart, 2002). Ecologists frequently misinterpreted pre-European vegetation as climatic climaxes rather than fire-maintained systems, while anthropologists viewed past cultures as merely reacting to the environment rather than being active participants. As a result, the concept of the environmentally benign Indian was firmly entrenched in science.

The consequences of Indian ignitions are most stark in moist temperate regions not conducive to burning, which is the case over most of the Eastern United States. Here, a long history of Native burning has produced a broad and diverse array of fire-based ecosystems (Little, 1974; Pyne, 1982; Wright and Bailey, 1982; Stewart 2002). As such, many Eastern species are adapted to and dependent on fire, either directly or indirectly (e.g.; jack pine (Pinus banksiana) and Kirtland's warbler (Dendroica kirtlandii); longleaf pine (Pinus palustris) and red-cockaded woodpecker (Picoides borealis)). Some plants actually reinforce fire regimes through the production of volatile compounds and flammable foliage (Mutch, 1970). With over 70 documented uses of fire (Lewis, 1993), Native Americans were an important ignition source, vastly augmenting natural causes (e.g., lightning) in most cases (Fahey and Reiners, 1981; Van Lear and Waldrop, 1989). In this respect, Native Americans were a "keystone species," actively managing the environment with fire over millennia (Sauer, 1975; Cronon, 1983). Due to the prevalence of fire, early European explorers and settlers encountered vast landscapes of fire-adapted (pyrogenic) vegetation, spanning from northern systems of spruce-fir (Picea-Abies), aspen-birch (Populus-Betula), and pine (Pinus) through oak-dominated (Quercus) central hardwoods to southern "pineries" and canebrakes (Wright and Bailey, 1982). Tallgrass prairies scattered throughout owed their existence to Native Americans who, through annual/biennial burning, maintained them for big game forage and hunting (grass → game → meat → satiated and flourishing families!).

European exploration, settlement, and land use fundamentally changed disturbance regimes of the East. Soon after first contact, a wave of Native depopulation, social disintegration, and displacement ensued, greatly changing the disturbance dynamics that formerly operated for thousands of years (Cook, 1973; Cronon, 1983; Denevan, 1992). With westward Euro-American expansion, forestlands were universally cut (aka, the "Great Cutover"), often subsequently burned, and many converted to agriculture (MacCleery, 1996). On areas allowed to reforest, deciduous tree species with disturbance adaptations (light-seeded, fast-growing pioneers; sprouters) often increased in importance at the expense of conifers (Nowacki and Abrams, 1992; Schulte et al., 2003). Natural systems rebounded where ongoing European activities mimicked past disturbance regimes, such as frequent surface burning of oak-hickory (Quercus-Carya) woodlands. In contrast, where European activities largely deviated from past disturbance regimes, wholesale changes in forest conditions occurred. For instance, a sizeable proportion of conifer-northern hardwoods (rich mesophytic systems that infrequently burned) converted to aspen-birch or oak through repeated cutting and burning (Graham et al., 1963; Nowacki et al., 1990; Schulte et al., 2003).

Social attitudes towards fire changed in the early 1900's when outbreaks of destructive wildfires led to aggressive suppression efforts (Pyne, 1982; Stewart, 2002). This campaign with seemingly good intentions had major unforeseen ecological consequences across America. Without fire, open lands (grasslands, savannas, and woodlands) quickly succeeded to closed-canopied forests, followed by the eventual replacement of light-demanding, fire-dependent plants by shade-tolerant, fire-sensitive vegetation. Ground flora diversity in particular was negatively affected by forest conversion as light resources to the understory became limited (Anderson et al., 2000). These compositional and structural changes continue largely unabated today through ongoing fire suppression.

The fire dependency of many native plant communities necessitates that certain landscapes are managed with fire. This is an evolutionary-based principal that can not be ignored (Grime, 1977; Bazzaz, 1979). Indeed, without fire, the ecological integrity of pyrogenic ecosystems is compromised with accumulating species loss and biodiversity reduction. By comparing past and current fire regimes, the authors attempt to document the magnitude and pervasiveness of fire regime change and discuss the ecological consequences of such change in the Eastern United States.

21.2 Methods

Geographic information systems (GIS) and available vegetation data layers were used to depict past and current fire regimes and temporal changes. For consistency, only data layers spanning the entire Eastern United States were considered. Vegetation classes were assigned fire regime groups (Fig. 21.1) according to nation-wide fire regime condition class (FRCC) protocols (http://www.frcc.gov). All maps were uniformly rasterized at 1-kilometer pixels for analytical purposes.

Schmidt's et al., (2002) potential natural vegetation (PNV) map served as the basis to reconstruct past fire regimes (digital cover acquired through Jim Menakis, USDA Forest Service). Fire regime groups were assigned using Cecil Frost's "Presettlement fire frequency regions of the United States" map (Frost, 1998), other relevant literature (e.g.; Heinselman, 1973; Wright and Bailey, 1982; Wade et al., 2000), and expert opinion (see Table 21.1 and Acknowledgements).

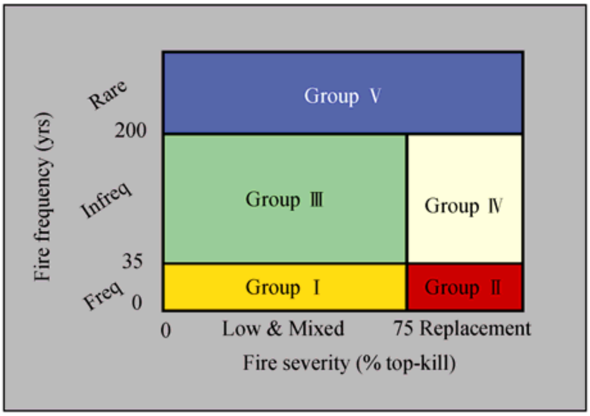

Figure 21.1 Five fire regime groups depicted along axes of fire severity and frequency. Criteria breakpoints are 75% top-kill for fire severity (low & mixed vs. replacement) and 35 yrs and 200 yrs for fire frequency (frequent, infrequent, and rare). Fire regime groups have been colored to reflect a fire gradient from extreme (red; Group II) to rare (blue; Group V)

Advanced very high resolution radiometer (AVHRR) and national land cover dataset (NLCD) layers were used in tandem to map current fire regimes. The individual classification power of the two datasets was capitalized on, maximizing the number of classes to depict current vegetation (theoretically increasing accuracy). As such, AVHRR data were used to classify forestlands (by type and cover class), whereas NLCD data were applied to the remaining lands, primarily non-forested openlands. Fire regime group assignments (Tables 21.2 and 21.3) were applied to produce a current fire regime map.

Table 21.1 Potential natural vegetation codes, titles, and assigned fire regime group

Code	Title	Fire Regime Group
32	Plains grassland	Ⅱ
33	Prairie	Ⅱ
36	Wet grassland	Ⅱ
38	Oak savanna (ND)	Ⅰ
39	Mosaic bluestem/oak–hickory	Ⅱ
40	Cross timbers	Ⅰ
41	Conifer bog (MN)	Ⅳ
42	Great Lakes pine forest	Ⅲ
43	Spruce–fir	Ⅳ
44	Maple–basswood	Ⅲ
45	Oak–hickory	Ⅰ
46	Elm–ash	Ⅴ
47	Maple–beech–birch	Ⅴ
48	Mixed mesophytic forest	Ⅲ
49	Appalachian oak	Ⅰ
50	Oak–northern hardwoods	Ⅲ
51	Northern hardwoods	Ⅴ
52	Northern hardwoods–fir	Ⅴ
53	Northern hardwoods–spruce	Ⅴ
54	Northeastern oak–pine	Ⅰ
55	Oak–hickory–pine	Ⅰ
56	Southern mixed forest	Ⅰ
57	Loblolly–shortleaf pine	Ⅰ
58	Blackbelt prairie	Ⅱ
59	Oak–gum–cypress	Ⅲ
60	Northern Floodplain	Ⅲ
61	Southern Floodplain	Ⅴ
62	Barren	Ⅱ

Table 21.2 Advanced very high resolution radiometer (AVHRR) vegetation class titles and assigned fire regime group by tree cover class

Title	0%—9%	10%—24%	25%—59%	≥60%
White-red-jack pine	Ⅱ	Ⅰ	Ⅲ	Ⅳ
Spruce-fir	Ⅱ	Ⅰ	Ⅲ	Ⅳ
Longleaf-slash pine	Ⅱ	Ⅰ	Ⅲ	Ⅳ
Loblolly-shortleaf	Ⅱ	Ⅰ	Ⅲ	Ⅳ
Oak-pine	Ⅱ	Ⅰ	Ⅲ	Ⅲ

(Continued)

Title	0%—9%	10%—24%	25%—59%	≥60%
Oak-hickory	Ⅱ	Ⅰ	Ⅲ	Ⅲ
Oak-gum-cypress	Ⅱ	Ⅰ	Ⅲ	Ⅲ
Elm-ash-cottonwood	Ⅱ	Ⅴ	Ⅴ	Ⅴ
Maple-beech-birch	Ⅱ	Ⅴ	Ⅴ	Ⅴ
Aspen-birch	Ⅱ	Ⅰ	Ⅲ	Ⅲ
Ponderosa pine	Ⅱ	Ⅰ	Ⅲ	Ⅳ
Lodgepole pine	Ⅱ	Ⅰ	Ⅳ	Ⅳ
Pinyon-juniper	Ⅱ	Ⅰ	Ⅳ	Ⅳ

Table 21.3 National land cover data (NLCD) vegetation codes, titles, and assigned fire regime group

Code	Title	Fire Regime Group
21	Low-intensity residential	Ⅴ
22	High-intensity residential	Ⅴ
23	Commercial/industrial/ transport	Ⅴ
31	Bare rock/sand/clay	Ⅴ
32	Quarries/strip mines/gravel pits	Ⅴ
33	Transitional	Ⅴ
41	Deciduous forest	Ⅴ
42	Evergreen forest	Ⅳ
43	Mixed forest	Ⅲ
51	Shrubland	Ⅰ
61	Orchards/vineyards/other	Ⅴ
71	Grasslands/herbaceous	II
81	Pasture/hay	Ⅳ
82	Row crops	Ⅴ
83	Small grains	Ⅳ
84	Fallow	Ⅴ
85	Urban/recreational grasses	Ⅳ
91	Woody wetlands	Ⅴ
92	Emergent herbaceous wetlands	Ⅳ

To spatially depict fire regime change over time, fire regime groups were reassigned Arabic numerals reflecting a fire gradient from hottest (most frequent and severe; ① to coolest (least frequent and severe; ② This Roman-to-Arabic conversion was not direct as the former did not best capture this fire gradient; which strikes diagonally from lower right (hottest) to upper left (coolest) in Fig. 21.1. Thus, the following values were applied: FRG Ⅰ =2, FRG Ⅱ =1, FRG Ⅲ =4, FRG Ⅳ =3 and FRG Ⅴ =5.

A fire regime change map was then generated on a pixel-by-pixel basis using the following equation:

$$\text{Fire regime change} = \text{Past fire regime group} - \text{Current fire regime group} \quad (21.1)$$

This formula projects past-to-current fire regime change over 9 classes from -4 through 0 to +4. Negative values represent reductions of fire (in terms of fire frequency and severity) on the landscape over time, whereas positive values indicate increased fire. The more negative or positive the values are, the more dramatic the trend.

21.3 Results and Discussion

Past and current fire regime maps are shown in Figs. 21.2 and 21.3, respectively. Color palettes reflect a fire regime gradient from highly "pyrogenic" systems that

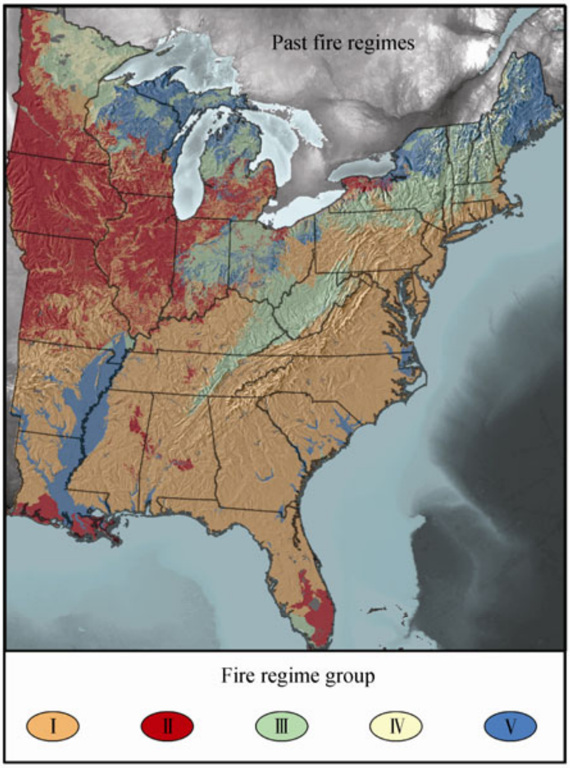

Figure 21.2 Past (presettlement) fire regimes by group based on potential natural vegetation (Schmidt et al., 2002). Fire regime group assignments of vegetation types are listed in Table 21.1

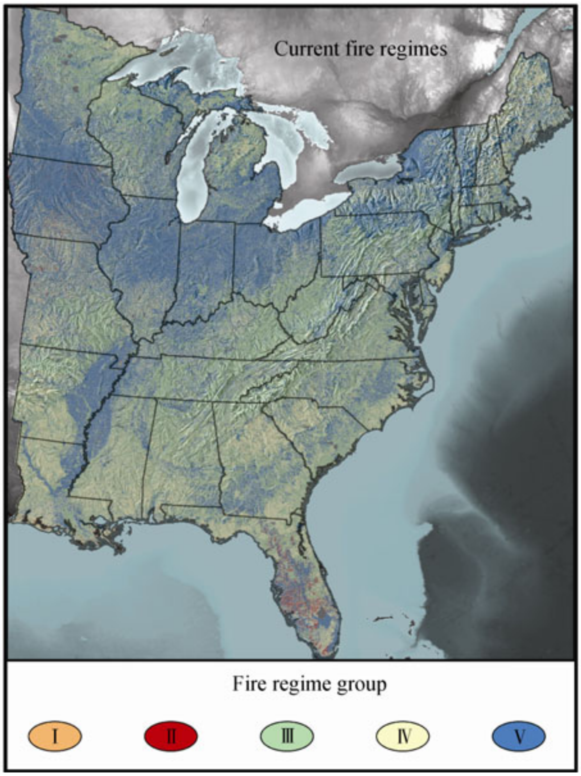

Figure 21.3 Current fire regimes by group based on the advanced very high resolution radiometer (AVHRR)-national land cover data (NLCD) hybrid map. Fire regime group assignments of vegetation types are listed in Table 21.2

burn most frequently and intensely (FRG Ⅱ; red) to “asbestos” systems that rarely burn (FRG Ⅴ; blue). Note that the color spectrum (red hot to cool blue) differs somewhat from fire regime group enumeration (FRG Ⅰ − Ⅴ).

Past fire regimes differed distinctly across the eastern United States as inferred from potential natural vegetation (Fig. 21.2). Historic fire regimes reflected a complex interaction among climate, vegetation, and topo-edaphic factors buoyed by human and natural ignitions (Jackson, 1968; Anderson, 1991). Fittingly, fire was most pronounced (FRG Ⅱ; red) within the Eastern, wedge-shaped extension of the Great Plains, known as the “Prairie Peninsula” (Transeau, 1935). Here, a large expanse of highly flammable grasses with few natural topographic barriers fostered hot, fast-spreading, near-complete burns (Jackson, 1965; Komarek, 1965; Anderson, 1991). Warm, dry conditions during dormant seasons (spring and fall) were especially favorable for fire outbreaks. Since tallgrass prairies are wholly dependent on burning for persistence, fires were undoubtedly frequent, probably occurring every year or so (Wells, 1970; Stewart, 2002). Rivers, lakes and dissected topography afforded some protection from fire such that surrounding lands, particularly on the lee side of prevailing winds, probably burned at lower severities allowing woodlands to develop (McComb and Loomis, 1944; Zicker, 1955; Grimm, 1984; Ebinger and McClain, 1991; Bowles et al., 1994). Correspondingly, a network of lower fire severity (FRG Ⅰ; orange) clearly appears along larger rivers across the former Prairie Peninsula (Fig. 21.2).

A fire regime of frequent, light surface burns (FRG Ⅰ; orange) historically extended south and east of the Prairie Peninsula, interrupted only by the Mississippi Alluvial Plain (FRG Ⅴ; blue) and the mixed mesophytic region of West Virginia and Eastern Kentucky (FRG Ⅲ; green). Here, on uplands, fire occurred in a variety of intensities and patchworks, creating mixes from grass and shrub openings to savannas, woodlands, and forests of oak and pine. Throughout the south, native forbs and wiregrass (Aristida) were well suited for light mosaic burning (Lemon, 1967; Walker and Peet, 1983), as were the southern pines (Greene, 1931; Chapman, 1932ab; Wright and Bailey, 1982; Landers, 1991; Wade et al., 2000). Stand-replacing, crown fires undoubtedly occurred under favorable fuel and weather (drought) conditions, adding to the landscape mosaic of age classes and vegetative types. Topographically protected areas, riparian zones, and swamps burned much less readily and harbored a greater collection of fire-sensitive plants. These areas occurred along larger coastal rivers and wetlands (FRG V; Fig. 21.2).

A fire regime of infrequent, mosaic-like surface burns (FRG Ⅲ; green) formed a historic interface between the "hotter" systems of the south and central states and cool, largely incombustible hardwoods to the north (Fig. 21.2). Here, a mix of fire-tolerant and fire-sensitive vegetation types occurred according to topography, landscape position, soils, and firebreaks (Grimm, 1984; Seischab, 1990; Cogbill et al., 2002; Whitney and DeCant, 2003). On drier uplands (coarse-textured soils, interfluves, ridgetops) periodic surface burns favored fire-dependent species of pine, oak, aspen, and birch. This burning regime allowed the famed northern pineries of jack, red (P. resinosa), and white pine (P. strobus) to develop on sandy outwash plains (Kilburn, 1960; Whitney, 1986; Cleland et al., 2004). On moister portions of the landscape (fine-textured soil, coves, riparian areas), fire impacts were much less, favoring mesophytic trees of beech (Fagus), maple (Acer), elm (Ulmus) and ash (Fraxinus) (Kaatz 1955).

Infrequent, stand-replacement fire regimes (FRG Ⅳ; yellow) were best represented by sub-boreal conifer forests (black and white spruce (Picea mariana and glauca), jack pine, balsam fir (Abies balsamea), tamarack (Larix laricina)) that extended southward from Canada into northern Minnesota and Maine. Fire was rare (FRG Ⅴ; blue) in certain northern landscapes where mesic ice-contact tills and wet-mesic glacio-lacustrine deposits supported beech-maple, elm-ash, northern hardwoods, and conifer-northern hardwoods. Fire was also limited in the Mississippi Alluvial Plain where flooding was the primary disturbance agent (Grimmett, 1989; Nelson, 1997; Foti, 2001; Tingle et al., 2001). Here, hydrophilic species dominate, such as bald cypress (Taxodium distichum), tupelo (Nyssa aquatica), and sweet gum (Liquidambar styraciflua).

Contemporary fire regimes are vastly more subdued across the Eastern United States (Fig. 21.3). Extensive stretches of FRG Ⅴ (blue) correspond with highly productive agricultural regions of the Midwest (Iowa and Southern Minnesota eastward through Ohio), the Mississippi Alluvial Plain, and along the Southeast Piedmont. The largely fire-resistant northern hardwood systems of Northern Wisconsin, Upper Peninsula of Michigan, Northern Pennsylvania, and New England also fall in this group. The remainder of the East was principally classified as FRGs Ⅲ (green) and Ⅳ (yellow) that burn infrequently, every 35 – 200 yrs.

There has been a dramatic "cooling" of the Eastern U.S. landscape when comparing past and current fire regimes (Fig. 21.4). This trend is consistent with the historical record, which points towards wholesale fire reduction, both spatially and temporally, across the East (Pyne, 1982; Abrams, 1992; Cutter and Guyette, 1994; Stewart 2002). The suppression of fire was due to convergence of events, including elimination of Native burning, building of road networks (providing fire breaks and access), forest/prairie conversion to croplands (fuel change/reduction), and aggressive 20th century fire fighting.

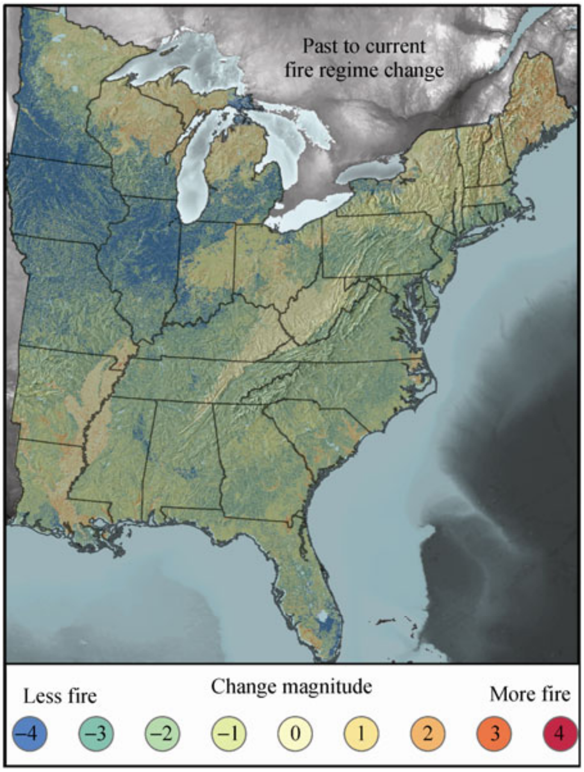

Figure 21.4 Past-to-current fire regime change map based on spatial analysis of PNV (past) and AVHRR-NCLD (current) fire regime maps. Positive values represent shifts towards more fire, whereas negative values represent shifts to less fire. The departure from zero relates to the extent of fire regime change

The largest reductions of fire (depicted in blue) were centered in the Midwest forming a crescent from southern Minnesota through northern Ohio. Here, the conversion of historic grasslands and open woodlands to an agriculture-dominated landscape largely explains this abrupt change (Wells, 1970; Iverson and Risser, 1987). The few areas not converted to agricultural production (cropland or pasturage) were quickly occupied by trees due to fire suppression (Loomis and McComb, 1944; Cottam, 1949). Agricultural conversion and fire exclusion, in concert, largely explain why tallgrass prairies and oak savannas are now considered the rarest ecosystems of North America (Nuzzo, 1986). Success of restoring open systems quickly diminishes upon conversion to closed-canopied forests (Anderson et al., 2000).

Substantial reductions of fire (represented by aqua-greens) stretched across the southern two-thirds of the Eastern United States, excluding the Mississippi Alluvial Plain and the mixed mesophytic region of West Virginia and eastern Kentucky, which remained largely unchanged (yellow). Here, in the absence of fire, pine- and oak-dominated systems are readily converting to fire-sensitive, shade-tolerant species (Chapman, 1932b; Fralish et al., 1991). Eastern oak forests are illustrative of the ecological ramifications of these changes (Appendix A).

Slight decreases in fire regime (light green) were found in northern Minnesota (consistent with Heinselman, 1973) and on the Tipton Till Plain of Indiana and Ohio extending eastward across most of southern and central New England. Here, depending on site conditions, sugar and red maple (Acer saccharum; A. rubrum) have been major benefactors of fire reduction (Abrams, 1992). These mesophytic species further "fire-proof" conditions by deep shading (promoting cooler and moister understory conditions) and producing non-flammable fuel beds (moist, rapidly decaying woody debris; wet, flaccid foliage accumulation in the fall).

Some exceptions to the above trends exist, though fire increases (oranges and reds) were less pronounced and generally scattered in small pockets (Fig. 21.4). The most conspicuous concentrations of increased burning were in Maine and Northern Wisconsin and Michigan. The projected increase in fire in the Upper Great Lakes states is probably an artifact of elevated levels of aspen-birch and off-site pine plantations (both fire-dependent forest types) on former Northern hardwood sites. The fire increase in Maine might be anomaly, given sequential decreases in area burned over the past century (Fahey and Reiners, 1981). However, some of the largest fires in Maine did occur in 1947 (Patterson, 1991), which would reflect in the current vegetation (and thus the current fire regime). Lastly, the generalness of PNV classes used to depict past fire regimes (northern hardwood-spruce forests; FRG V) compared to the preciseness of AVHRR-NLCD classes for current fire regimes (spruce-fir; FRG IV) might further explain this portrayed increase. As such, the coarse-scale maps generated by this analysis must be used with caution and limited to general application and interpretation.

Acknowledgements

We thank Roger Fryar, Beth Buchanan, Bruce Davenport, Melissa Thomas-Van Gundy, and David Cleland for contributing to fire regime group assignments.

Appendix A The Eastern Oak Story

Oaks historically covered a large portion of the Eastern United States, forming common associations with pine, chestnut, and hickory. These fire-dependent systems were maintained by frequent, Native-ignited surface burns. Europeans profoundly altered the disturbance regime through land use and non-native species introduction. The first wave of logging concentrated on Eastern white pine—a preferred timber-producing tree. Thereafter, hardwoods (oaks, chestnut, and hickories) were harvested and oftentimes maintained through repetitive clear cutting, which encouraged sprout regeneration. This intense harvesting regime coupled with recurring wildfires largely favored hardwoods over conifers (i.e. pines). Three significant things happened in the early portion of the twentieth century: ① harvesting eased ② chestnut blight (effectively wiping out American chestnut), and ③ active fire suppression (the "Smokey Bear" campaign). These interrelated phenomena allowed oaks to dominate and form closed-canopied forests. Over the past century, native ground cover largely decreased due to low light levels, lack of surface fires, and unprecedented white-tailed deer foraging. In the meantime, fire-sensitive, shade tolerant mesophytic species (sugar and red maple, beech, black cherry, black gum) have flourished and now dominate understories. Under these conditions, overstory oak is quickly replaced by subordinate mesophytic trees upon death. Gypsy moth (an introduced insect) further accelerates this transition by preferentially attacking and weakening overstory oaks, causing their early demise and replacement. Without ecological restoration in the form of silvicultural treatments (thinning and prescribed burning), these systems will continue to decline (in terms of species richness and ecological function), converting from oak to mesophytic forests within a generation. Effects on native wildlife populations dependent of large-seeded trees producing acorns and nuts are equally imperil.

References

Abrams M, (1992), Fire and the development of oak forests. *BioScience*, **42**: 346 − 353

Abrams M, (1996), Distribution, historical development, and ecophysiological attributes of oak species in the eastern United States. *Ann. Sci. For.*, **53**: 487 − 512

Anderson RC, (1991), Presettlement forests of Illinois. pp.9 – 19 in Burger GV, Ebinger JE, Wilhelm GS (eds.), Proceedings of the Oak Woods Management Workshop, Eastern Illinois University, Charleston, IL, 65 – 73

Anderson RC, Schwegman JE, Anderson MR, (2000), Micro-scale restoration: A 25-year history of a southern Illinois Barrens. *Restoration Ecology*, **8**: 296 – 306

Barden LS, (1979), Tree replacement in small canopy gaps of a *Tsuga canadensis* forest in the southern Appalachians, Tennessee. *Oecologia*, **44**: 141 – 142

Bazzaz FA, (1979), The physiological ecology of plant succession. *Ann. Rev. Ecol. Syst.*, **10**: 351 – 371

Benton MJ, Twitchett RJ, (2003), How to kill (almost) all life: the end-Permian extinction event. *TRENDS in Ecology and Evolution* **18**(7): 358 – 365

Bowles ML, Hutchison MD, McBride JL, (1994), Landscape pattern and structure of oak savanna, woodland, and barrens in northeastern Illinois at the time of European settlement. P. 65 – 73 in J.S. Fralish, R.C. Anderson, J.E. Ebinger, and R. Szafoni (eds), Proceedings of the North American Conference on Barrens and Savannas, October 15 – 16, 1994, Illinois State University, Normal, IL

Chapman HH, (1932a), Is the longleaf type a climax? *Ecology*, **13**: 328 – 334

Chapman HH, (1932b), Some further relations of fire to longleaf pine. *Journal of Forestry*, **30**: 602 – 603

Christensen NL, (1991), Wilderness and high intensity fire: How much is enough? *Tall Timbers Fire Ecology Conference Proceedings*, **17**: 9 – 24

Cleland DT, Crow TR, Saunders SC, Dickman DI, Maclean AL, Jordan JK, Watson RL, Sloan AM, Brosofske KD, (2004), Characterizing historical and modern fire regimes in Michigan (USA): A landscape ecosystem approach. *Landscape Ecology*, **19**: 311 – 325

Clements FE, (1916), Plant succession: An analysis of the development of vegetation. Carnegie Institute Washington Publication No. 242

Cogbill CV, Burk J, Motzkin G, (2002), The forests of presettlement New England, USA: Spatial and compositional patterns based on town proprietor surveys. *Journal of Biogeography*, **29**: 1279 – 1304

Cook SF, (1973), The significance of disease in the extinction of the New England Indians. *Human Biology*, **45**: 485 – 508

Cottam G, (1949), The phytosociology of an oak wood in southwestern Wisconsin. *Ecology*, **30**: 271 – 287

Cronon W, (1983), Changes in the land: Indians, colonists and the ecology of New England. Hill and Wang, New York, NY

Cutter BE, Guyette RP, (1994), Fire frequency on an oak-hickory ridgetop in the Missouri Ozarks. *American Midland Naturalist*, **132**: 393 – 398

Denevan WM, (1992), The pristine myth: The landscape of the Americas in 1492. *Annals of the Association of American Gegraphers* **82**: 369 – 385

Denslow JS, (1980), Patterns of plant species diversity during succession under different disturbance regimes. *Oecologia*, **46**: 18 – 21

Ebinger JE, McClain WE, (1991), Forest succession in the Prairie Peninsula of Illinois. *Illinois Natural History Survey*, **34**:375 – 381

Fahey TJ, Reiners WA, (1981), Fire in the forests of Maine and New Hampshire. *Bulletin of the Torrey Botanical Club*, **108**: 362 – 373

Foti TL, (2001), Presettlement forests of the Black Swamp Area, Cache River, Woodruff County, Arkansas, from notes of the first land survey. P. 7 – 15 in P.B. Hamel, and T.L. Foti (eds), Bottomland hardwoods of the Mississippi Alluvial Valley: Characteristics and management of natural function, structure, and composition. USDA Forest Service General Technical Report SRS-42

Frelich LE, (2002), Forest dynamics and disturbance regimes: Studies from temperate evergreen-deciduous forests. Cambridge University Press, Cambridge, UK

Frelish JS, Crooks FB, Chambers JL, Harty FM, (1991), Comparison of presettlement second-growth and old-growth forest on six site types in the Illinois Shawnee Hills. *American Midland Naturalist*, **125**: 294 – 309

Frost CC, (1998), Presettlement fire frequency regimes of the United States: A first approximation. Tall Timbers Fire Ecology Conference Proceedings, **20**: 70 – 81

Graham SA, Harrison RP Jr., Westell CE Jr., (1963), Aspens: Phoenix trees of the Great Lakes region. University of Michigan Press, Ann Arbor, MI

Greene SW, (1931), The forest that fire made. *American Forests*, **37**: 583 – 584, 618

Grime JP, (1977), Evidence for the existence of three primary strategies in plants and its relevance to ecological and evolutionary theory. *American Naturalist*, **111**: 1169 – 1194

Grimm EC, (1984), Fire and other factors controlling the Big Woods vegetation of Minnesota in the Mid-Nineteenth Century. *Ecological Monographs*, **54**: 291 – 311

Grimmett, HK, (1989), Early plant and animal communities of the Arkansas Delta. *Arkansas Historical Quarterly*, **48**: 101 – 107

Heinselman ML, (1973), Fire in the virgin forests of the Boundary Waters Canoe Area, Minnesota. *Quaternary Research*, **3**: 329 – 382

Hengst GE, Dawson JO, (1994), Bark properties and fire resistance of selected tree species from the central hardwood region of North America. *Canadian Journal of Forest Research*, **24**: 688 – 696

Henry JD, Swan JMA, (1974), Reconstructing forest history from live and dead plant material—an approach to the study of forest succession in southwest New Hampshire. *Ecology*, **55**: 772 – 783

Iverson LR, Risser PG, (1987), Analyzing long-term changes in vegetation with geographic information system and remotely sensed data. *Advances in Space Research*, **7**: 183 – 194

Jackson AS, (1965), Wildfires in the Great Plains grasslands. Tall Timbers Fire Ecology Conference Proceedings **4**: 241 – 259

Jackson MB, Colmer TD, (2005), Response and adaptation by plants to flooding stress. *Annals of Botany*, **96**: 501 – 505

Jackson WD, (1968), Fire, air, water and earth—an elemental ecology of Tasmania. Proceedings of the Ecological Society of Australia **3**: 9 – 16

Kaatz MR, (1955), The Black Swamp: A study in historical geography. *Annuals of the Association of American Geographers* **45**:1 – 35

Kilburn PD, (1960), Effects of logging and fire on xerophytic forests in Northern Michigan. *Bulletin of the Torrey Botanical*, *Club*, **87**: 402 – 405

Komarek EV Sr., (1965), Fire ecology—grasslands and man. Tall Timbers Fire Ecology Conference Proceedings, **4**: 169 – 220

Komarek EV Sr., (1967), Fire—and the ecology of man. Tall Timbers Fire Ecology Conference Proceedings, **6**: 143 – 170

Landers JL, (1991), Disturbance influences on pine traits in the southeastern United States. Tall Timbers Fire Ecology Conference Proceedings, **17**: 61 – 98

Lemon PC, (1967), Effects of fire on herbs of the southeastern United States and central Africa. Tall Timbers Fire Ecology Conference Proceedings, **6**: 113 – 127

Lewis HT, (1993), Patterns of Indian burning in California: Ecology and ethnohistory, pp 55 – 116 in Blackburn TC, Anderson K (eds.), Before the wilderness: Environmental management by Native Californians, Ballena Press, Menlo Park, CA

Little S, (1974), Effects of fire on temperate forests: Northeastern United States, pp 225 – 250 in Kozlowski TT, Ahlgren CE (eds.), Fire and ecosystems. Academic Press, New York, NY

Loomis WE, McComb AL, (1944), Recent advances of the forest in Iowa. *Iowa Academy of Science*, **51**: 217 – 224

Lorimer CG, (1985), The role of fire in the perpetuation of oak forests, pp 8 – 25 in Johnson J (ed.), Challenges in oak management and utilization, University of Wisconsin Cooperative Extension Service, Madison, WI

MacCleery DW, (1996), American forests: A history of resiliency and recovery. Forest History Society Issues Series, Forest History Society, Durham, NC

McComb AL, Loomis WE, (1944), Subclimax prairie. *Bulletin of the Torrey Botanical Club*, **71**: 46 – 76

McElwain, JC, Punyasena JC, (2007), Mass extinction events and the plant fossil record. *Trends in Ecology and Evolution*, **22**: 548 – 557

Mutch RW, (1970), Wildland fires and ecosystems—A hypothesis. *Ecology*, **51**: 1046 – 1051

Nelson, JC, (1997), Presettlement vegetation patterns along the 5th Principal Meridian, Missouri Territory, 1815. *American Midland Naturalist*, **137**: 79 – 94

Nowacki GJ, Abrams MD, (1992), Community, edaphic, and historical analysis of mixed oak forests of the Ridge and Valley Province in central Pennsylvania. *Canadian Journal of Forest Research*, **22**: 790 – 800

Nowacki GJ, Abrams MD, Lorimer CG, (1990), Composition, structure, and historical development of northern red oak stand along an edaphic gradient in north-central Wisconsin. *Forest Science*, **36**: 276 – 292

Nuzzo V, (1986), Extent and status of Midwest oak savanna: Presettlement and 1985. *Natural Areas Journal*, **6**: 6 – 36

Oliver CD, Larson BC, (1996), Forest Stand Dynamics. John Wiley & Sons, Inc., New York, NY

Oliver CD, Stephens EP, (1977), Reconstruction of a mixed-species forest in central New England. *Ecology*, **58**: 562 – 572

Osmond CB, Austin MP, Berry JA, Billings WD, Boyer JS, Dacey JWH, Nobel PS, Smith SD, Winner WE, (1987), Stress physiology and the distribution of plants. *BioScience*, **37**(1): 38 – 48

Pahl-Wostl C, (1995), The dynamic nature of ecosystems: Chaos and order entwined. John Wiley & Sons Ltd., Chichester, England

Patterson WA III, (1991), The 1947 Maine fires: The last great fires in New England? Tall Timbers Fire Ecology Conference Proceedings, **17**: 59

Pickett STA, White PS, (1985), The ecology of natural disturbance and patch dynamics. Academic Press, Inc., San Diego, CA

Pyne SJ, (1982), Fire in America: A cultural history of wildland and rural fire. Princeton University Press, Princeton, NJ

Reice SR, (2001), The silver lining: The benefits of natural disasters. Princeton University Press, Princeton, NJ

Runkle JR, (1981), Gap regeneration in some old-growth forests of eastern United States. *Ecology*, **62**: 1041 – 1051

Runkle JR, (1982), Patterns of disturbance in some old-growth forests of eastern North America. *Ecology*, **63**: 1533 – 1546

Sauer CO, (1975), Man's dominance by use of fire. *Geoscience and Man*, **10**: 1 – 13

Schmidt KM, Menakis, JP, Hardy CC, Hann WJ, Bunnell, DL, (2002), Development of coarse-scale spatial data for wildland fire and fuel management. USDA Forest Service General Technical Report RMRS-GTR-87

Schulte LA, Crow TR, Vissage J, Cleland D, (2003), Seventy years of forest change in the Northern Great Lakes Region, USA. pp 99 – 101 in Buse LJ, Perera AH (comp.), Meeting emerging ecological, economic, and social challenges in the Great Lakes region: Popular summaries. Ontario Forest Research Information Paper No. 155, Ontario Ministry of Forest Research Institute, Sault Ste. Marie, Ontario, Canada

Seischab FK, (1990), Presettlement forests of the Phelps and Gorham Purchase in western New York. *Bulletin of the Torrey Botanical Club*, **117**: 27 – 38

Stewart OC, (1956), Fire as the first great force employed by man. pp 115 – 133 in Thomas WH (ed.), Man's role in changing the face of the earth. University of Chicago Press, Chicago, IL

Stewart, OC, (2002), Forgotten fires: Native Americans and the transient wilderness. University of Oklahoma Press, Norman, OK

Tingle JL, Klimas CV, Foti TL, (2001), Application of General Land Office Survey notes to bottomland hardwood ecosystem management and restoration in the Lower Mississippi Valley—An example from Desha County, Arkansas. pp 16 – 27 in P.B. Hamel, and T.L. Foti (eds), Bottomland hardwoods of the Mississippi Alluvial Valley: Characteristics and management of natural function, structure, and composition. USDA Forest Service General Technical Report SRS-42

Transeau EN, (1935), The prairie peninsula. *Ecology*, **16**: 423 – 437

Van Lear DH, Waldrop TA, (1989), History, uses, and effects of fire in the Appalachians. USDA Forest Service General Technical Report SE-54

Wade DD, Brock BL, Brose PH, Grace JB, Hoch GA, Patterson WA III, (2000), Fire in eastern ecosystems pp 53 – 238 (Chapter 4) in Brown JK, Smith JK (eds.), Wildland fire in ecosystems: Effects of fire on flora. USDA Forest Service General Technical Report RMRS-GTR-42-Vol. 2. (http://www.fs.fed.us/rm/pubs/rmrs_gtr42_2.pdf)

Walker J, Peet RK, (1983), Composition and species diversity of pine-wiregrass savannas of the Green Swamp, North Carolina. *Vegetatio*, **55**: 163 – 179

Watt AS, (1947), Pattern and process in the plant community. *Journal of Ecology*, **35**: 1 – 22

Wells PV, (1970), Historical factors controlling vegetation patterns and floristic distributions in the Central Plains Region of North America, pp 212 – 221 in Dort W, Jones J (eds.), Pleistocene and recent environments of the Central Great Plains. University of Kansas Special Publication No. 3, Lawrence, KS

Whitney GG, (1986), Relation of Michigan's presettlement pine forests to substrate and disturbance history. *Ecology*, **67**: 1548 – 1559

Whitney GG, DeCant JP, (2003), Physical and historical determinants of the pre- and post-settlement forests of northwestern Pennsylvania. *Canadian Journal of Forest Research*, **33**:1683 – 1697

Wright HA, Bailey AW, (1982), Fire Ecology: United States and Southern Canada. John Wiley & Sons, New York, NY

Zicker WA, (1955), An analysis of Jefferson County vegetation using survey's records and present day data. MS Thesis, University of Wisconsin-Madison

22 Fire Spread Regulated by Weather, Landscape Structure, and Management in Wisconsin Oak-Dominated Forests and New Jersey Pinelands

Daolan Zheng
Department of Natural Resources & the Environment, University of New Hampshire, Durham, NH 03824, USA
Email: daolan.zheng@unh.edu

Jacob J. LaCroix
Scenarios Network for Alaska and Arctic Planning, University of Alaska, Fairbanks, 3352 College Road, Fairbanks, AK 99709, USA
Email: jlacroix@alaska.edu

Soung-Ryoul Ryu
Department of Renewable Resources, University of Alberta, 713C General Services, Edmonton, AB T6G 2H1, Canada
Email: soung.ryu@ualberta.ca

Jiquan Chen
Department of Environmental Sciences, University of Toledo, Bowman-Oddy Laboratories, Mail Stop 604, Toledo, OH 43606, USA
Email: Jiquan.Chen@utoledo.edu

John Hom
Northern Research Station, USDA Forest Service, Newtown Square, PA 19073, USA
Email: jhom@fs.fed.us

Kenneth Clark
Northern Research Station, USDA Forest Service, Newtown Square, PA 19073, USA
Email: kennethclark@fs.fed.us

Abstract This study is to predict fire spread behavior and burned area across two fire-prone landscapes with contrasting vegetation (Oak-dominated ecosystem in WI vs. pine-dominated ecosystem in NJ), fuel-type composition, and land-use history regulated by the effects of weather, landscape structure and land management by combining simulations from three models (FARSITE, HARVEST, AND FRAGSTATS) under different scenarios. The results demonstrate: ① substantial differences in fire-spread patterns between the two landscapes were observed when holding weather conditions constant and excluding roads, indicating that landscape fragmentation is a main controlling factor on fire spread at the landscape level; ② roads functioning as barriers could significantly reduce the burned area from fire spread; and ③ Harvesting effects showed different trends, depending on landscape fuel type composition and weather conditions. At 4% harvesting intensity, both clustered and dispersed methods showed no significant impact ($a=0.01$) on reducing the mean burned area across the more fragmented WI landscape, but showed significant effects on fire spread in the less fragmented NJ landscape in summer when weather was hot and dry.

Keywords Fire spread, burned area, landscape, fire model and weather condition

22.1 Introduction

There is a growing concern over catastrophic fires in the U.S. in recent years (http://www.usgs.gov/themes/Wildfire/fire.html). These fires can degrade environmental quality and wildlife habitat, destroy buildings and cost human life, reduce wood production, and increase firefighting costs. For example, the unusual fire season of 2000 consumed 3 million hectares across the country. Nearly a billion and a half dollars alone were spent on fire suppression in 2002—the second largest fire season in the last 50 years (Graham 2003).

At landscape level, wildfire spread and behavior are determined by many factors, including weather, fuel loading and type, topography, landscape structure, road density, and human activities and land use (Pyne et al., 1996; Rollins et al., 2002). While the physics of fire spread are well known at fine spatial and temporal scales (e.g., individual trees and forest stands, seconds to hours) (Rothermel 1983), examination of factors determining the variability of fire spread patterns over entire landscape is more complex and deserves greater attention.

The prediction of burned area (BA) across the landscape is a very important element in planning fire suppression efforts and reducing wildfire damage. Fire effects are often examined at the stand level after a single fire event and are difficult to link with landscape-scale processes without the application of models (Keane et al., 1989). Modeling is an efficient and practical approach to help understand and predict fire effects at landscape scales or larger because models simplify complex processes and systems for improved human understanding (Kercher and Axelrod 1984; Hunt Jr. et al., 1999; Finney and Andrews 1999; Miller and Urban 1999). It also allows us to test various fire cause-and-effect scenarios from economic, physical, social, ecological, and management perspectives that are almost impossible to be discerned in the field.

Timber harvesting is a major human-derived disturbance that alters landscape structure, thus affecting fire spread. Previous reports on the subject have generated conflicting, sometimes contradictory findings. On one hand, some recent data (1980 through 1999) suggest that logging activity increase BA (http://www.wildrockies.org/wildfire/), because logged areas tend to increase rate of fire spread and fire intensity by increasing fuel loading and creating additional corridors (Huff et al. 1995; Anderson 1982). On the other hand, harvesting can fragment the fuel complex and disrupt local fire growth, thereby increasing fire suppression effectiveness (Stratton 2004). Nevertheless, quantifying the effects of different harvesting methods on fire spread across landscapes is rare.

This study will examine the effects of weather, landscape structure, and land management on fire spread in two landscapes. We combine 3 models to conduct hypothetical simulations over a 15-day period to obtain a more-complete picture of how changes in landscape patch heterogeneity and fuel type composition could affect landscape fire spread. This Chapter is designed to answer four specific questions from a landscape perspective: ① How fire spread is affected by landscape structure? ② Does harvest increase or decrease surface fire spread across the landscapes? ③ Is there a significant difference in harvesting methods on fire spread? And ④ does the above influences on fire spread vary by seasonal, and, if so, to what degree?

The definition of landscape structure in this study refers to: ① the heterogeneity and spatial arrangement of different fuel patches across the entire landscape, and ② fuel type compositions across the landscape; because changes in either one can significantly affect the simulation results.

22.2 Methods and Materials

22.2.1 Study Areas

Two temperate forest landscapes in the eastern USA (Fig. 22.1) were selected for examining landscape-level effects on fire spread and behaviors. Both are fire-prone ecosystems with contrasting vegetation (a Oak-dominated ecosystem in WI vs. pine-dominated ecosystem in NJ), fuel-type composition, and land-use history (a highly fragmented and managed landscape in WI vs. a less fragmented landscape without harvesting activity for the last 100 years in NJ).

22.2.1.1 NJ Pinelands

The 38,150 ha sub-area of the Pinelands used in this study is flat with mean elevation of 39 m, ranging from 12 – 65 m. The majority of the study area is State Forest and a NJ wildlife management area, and some land is in federal ownership on Fort Dix Army Base. Thus, recent human interference (e.g. harvesting and urbanization) is minimal. The long-term (1930 – 2004) annual mean temperature of the area is 12.0℃, and annual precipitation is 1123±182 mm. The pine-oak

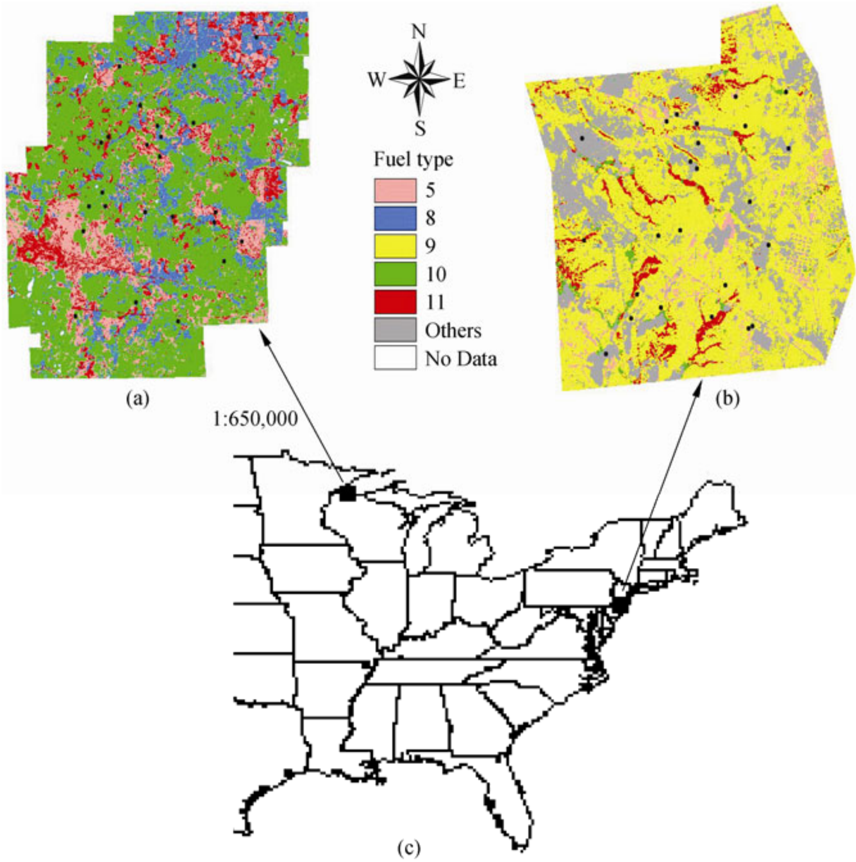

Figure 22.1 Spatial distribution of 24 fire ignition points in relation to fuel types in the Chequamegon National Forest (a) and New Jersey Pinelands (b) USA. Fuel type 5 = Brush < 0.8 m with scattered trees, 8 = Litter layer without under story, 9 = Pinelands/brush, 10 = Litter layer with under story, and 11 = light logging/Swamps. There are 5 more fuel types in the NJP landscape but all were grouped into the category of others to illustrate substantial difference in fuel type composition between the two landscapes

landscape is characterized by highly volatile fuels and sandy soils with a low water holding capacity (http://www.fs.fed.us/ne/global/research/fire.html).

New Jersey's Pinelands occupy 22% of the state (http://www.fs.fed.us/ne/global/pubs/maps_posters/pdfs/firepine.pdf) and depend on fire to regenerate and maintain its composition and structure. Sixty-two percent of the Pinelands are upland forests comprised largely of three communities; ① Oak/Pine, consisting of black oak (Quercus velutina), chestnut oak (Q. prinus), white oak (Q. alba), and pitch (Pinus rigida) and shortleaf pine (P. echinata), ② Pine/Oak, consisting of pitch pine with mixed oaks in the overstory, and ③ Pine/Scrub Oak, consisting of pitch pine with scrub oaks (Q. ilicifolia, Q. marlandica) in the understory (McCormick and Jones

1973, Lathrop and Kaplan 2004). All stands have ericaceous understories, primarily huckleberry (Gaylussacia bacata) and blueberries (Vaccinium spp.). Sedges, mosses and lichens are also present. Wetland forests communities include Pitch Pine lowlands, mixed Oaks, and Atlantic White Cedar (Chamaecyparis thyoides) swamps.

22.2.1.2 Wisconsin Oak-Dominated Forests

The 39,350 ha study area is located in the Washburn Ranger District of the Chequamengon national forest (CNF) in Northern Wisconsin, USA. The topography of the area is flat to gently rolling with elevations ranging from 232 – 459 m. The area in general has deep, coarse-textured soils. The climate is characterized by a short/hot summer with a growing season of 120 – 140 days, and cold winters. Annual precipitation ranges from 660 – 700 mm (Albert 1995) while annual mean temperature is about 4.7℃. Historically, the area was occupied primarily by jack pine (Pinus banksiana Lambert), red pine (Pinus resinosa Aiton), and several oaks (Quercus spp.) and is now dominated by red oak (Quercus rubra L.), sugar maple (Acer succharum Marsh), paper birch (Betula papyrifera Marsh), and aspen (Populus spp.) (Radeloff et al. 1999). Six dominant land-cover types in the study area are Oak, jack pine, red pine, mixed Oak/conifer, regenerating forest/shrub, and non-forested bare ground (Bresee et al. 2004). The dominant fuel type in the area is forest with under story (50.2%) after the cover types were grouped into fuel types following Anderson's (1982) classification system.

22.2.2 Study design

22.2.2.1 Fire Ignition Locations and Fuel Type Assignments

For each landscape, 24 fire ignition points were randomly generated after being stratified by major fuel types (13 nationally recognized fuel categories; Anderson 1982). There were 3 to 6 replicates for each fuel type depending on its weighted area of the total landscape. The fuel maps were developed using the 2001 land-cover map from Bresee et al. (2004) for the CNF and the 2001 land-cover map provided by the Grant F. Walton center for remote sensing and spatial analysis (CRSSA), Rutgers University (Lathrop and Kaplan 2004) for the NJP. Land cover, fuel type composition and patch mosaics differ appreciably between the 2 landscapes (Table 22.1, Fig. 22.1).

22.2.2.2 Management Scenarios and Simulations

We considered roads as fire barriers in our FARSITE simulations and compared these to the results from control runs without road effects. The CNF road map was provided by the USDA Forest Service (http://www.fs.fed.us/r9/cnnf/ftp/forest_files/). We used paved (road level B) and gravel with greater width (road level C) roads for comparison purposes. For the NJP road map, we used primary highway and secondary roads from the US Census Tiger Dataset (www.esri.com/data/download/census2000_tigerline/index.html#datainfo).

To detect effects of landscape structure and fuel type composition on fire spread (Question 1), hypothetical simulations were conducted by applying 15-day weather data collected in August 2 – 17, 2002 in both landscapes (i.e., weather was kept constant while varying the landscapes). In this particular test, roads were excluded to simplify the analysis. Additionally, we created two alternative fuel maps by assigning different fuel types to some land-cover types in the NJP to detect how changes in fuel-type composition could have on BA. One map had a similar mean rate of fire spread (MROS, 173 m/hr) to that in the control landscape of CNF (183 m/hr). The other map had a much higher MROS for NJP (334 m/hr) than that in the control landscape, which we think is closer to reality due to differences in fuel type composition (pine vs. oak) between the two landscapes. The MROS was calculated using the rate of spread defined by Anderson (1982) for various fuel types and multiplying by their corresponding fractions of land area to the entire landscape, then summed up to mean burned area (MBA, ha).

To illustrate how forest practices can affect fire spread across the landscape (Questions 2 and 3), we used the HARVEST 6.1 model (Gustafson and Crow 1996) to generate hypothetical landscapes imposing 4% cutting with two different methods, clustered (clearcuts) and dispersed (select cutting), in both the CNF and the NJP, then compared the results to those in the control landscapes.

To examine seasonal variation of fire spread (Question 4), we used daily weather data in August of 2002 (8/2-8/17) and April of 2004 (4/3-4/18, the April data in 2002 was unavailable and April data in 2003 had missing days) in the CNF recorded by meteorological equipments mounted on an eddy covariance flux tower (Noorments et al. 2004). The meteorological measurements were programmed to record data every 20 seconds and output 30-minute means to a data logger. In the NJP, meteorological data were collected from three weather towers, one located in each of the dominant upland forest communities; an Oak/Pine forest at Silas little experimental forest, a Pine/Oak forest at Fort Dix, and a Pine/Scrub oak forest located at the Cedar Bridge fire tower. Continuous meteorological measurements were made from each tower. Meteorological data was recorded with automated data loggers (CR23x, Campbell Scientific).

The selections of data periods (hereafter referred to as spring and summer, respectively) were determined using our best judgment on usefulness of weather data and its availability at each landscape. For example, August of 2004 in the NJP was affected by the hurricane season and there was a 1000-year storm event on 7/12 (21.7 cm of rain in one day) and consequently, June to July data were used for the NJP landscape. The simulated results from these data are useful for illustrating general patterns of seasonal fire spread and comparison between the two landscapes because fires are affected by weather in addition to other factors. We also conducted sensitivity analyses to examine the effects of wind speed on fire spread by increasing wind speed to 40 km/hr in both landscapes.

22.2.3 Model Linkage and Applications

22.2.3.1 FARSITE

Quantitative understanding of the interactions between landscape structure and disturbances such as fire spread is one of the major focuses of landscape ecology. Three models (FARSITE, HARVEST, and FRAGSTATS) were linked to conduct integrative analyses (Fig. 22.2). We used a fire growth model FARSITE (Finney 1998) to simulate fire spread across our landscapes. The model can predict both surface and crown fires, however surface fire spread was only used to simplify the analyses for comparison because most fires in the CNF are low-intensity surface fires (Sturtevant et al. 2004) and both landscapes are relatively flat. The required inputs for FARSITE include two ASCII files for weather conditions and five grid layers at 30 m resolution representing landscape structure, vegetation and topography. The five layers were: ① elevation, ② slope, ③ aspect, ④ fuel type, and ⑤ degree of canopy closure (Fig. 22.2). The topographic files were derived from 3-arc DEM data. The canopy closure file was developed and rescaled to 0% – 100% based on the Normalized Difference vegetation Index (NDVI) values (0 – 1) that were calculated from the red and infrared channels of the Landsat 7 data (Rouse et al. 1973). The Landsat TM-based fuel maps were developed from the land-cover maps in the CNF (Bresee et al. 2004) and NJP (Lathrop and Kaplan 2004) and categorized by Anderson (1982) fuel type (Table 22.1).

It is also well known that weather and landscape structure interact to affect fire spread. Thus, separating these two effects is desired for increasing our understanding of fire ecology and providing insights for improved fire management at the landscape level. In each landscape, we ran the FARSITE model for 24 randomly selected fire ignition points stratified by major fuel types within a 15-day period.

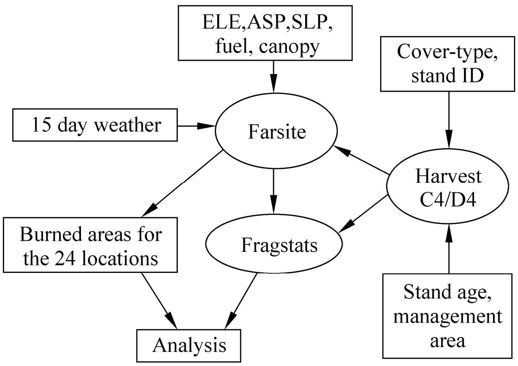

Figure 22.2 General flow chart of model linkages and simulations of fire spread in the Chequamegon national forest WI and New Jersey Pinelands. The rectangular boxes represent inputs and outputs, while the ellipse boxes represent the models used in the analyses

Table 22.1 Landscape percentages in major land-cover types and Anderson (1982) fuel types for the Chequamegon National Forest (CNF, oak-dominated forests), WI and the New Jersey Pinelands (NJP, pine dominated)

Landscape	Cover Type	Fuel Type	Proportion (%)	Definition
CNF	Regenerating forest/shrub, Jack pine	5	23.6	Brush < 0.8 m with scattered trees
	Red pine	8	16.1	Litter layer without under story
	Hardwoods and Mixed forests	10	50.2	Litter layer + under story
	Clearcuts	11	10.1	Light logging slash/Swamps
NJP	Lightly developed/unwooded, managed grasslands	1	0.5	Short grass < 0.3 m
	Lightly developed/wooded	2	1.2	Timber grass with under story, medium grass
	Croplands, tall grasslands	3	4.6	Tall grass > 0.8 m
	Upland Scrub/Shrub	5	7.5	Brush < 0.8 m
	Oak brush/slash	6	14.7	Brush/Cured slash
	Upland Pines/Coast plain	8	0.3	Litter layer without under story
	Upland Pine-Oak	9	61.7	Dense pinelands /under story brush
	Riverine/Palustrine mixed wetland	10	1.0	Litter layer + under story
	Wetland forest	11	2.3	Light logging slash/Swamps
	Moderately & highly developed	28	0.3	Urban

22.2.3.2 HARVEST

The HARVEST model is primarily a landscape-level, harvesting allocation simulator designed to evaluate alternative strategies of forest management and timber harvests and provide comparable predictions of the spatial pattern consequences of these alternative strategies (Gustafson and Crow 1996). Three fuel maps were created for each landscape; a control (fuel map with no harvest), and two fuel maps representing "clustered" and "dispersed" harvests with a cutting level of 4% using the model (http://ncrs.fs.fed.us/4153/Harvest/harvhome.asp). The harvesting units were set with an average of 10 ha with a 5 ha standard deviation, while minimum and maximum units were 1 ha and 20 ha, respectively, without buffer area. For the simulation, the HARVEST model randomly selected a place to clearcut (clustered and dispersed shape) according to the patch size and age of a stand, where dispersed is more irregular shape with more edge. After forest was cleared, the fuel type assignment was simply changed from forest categories 8, 9, or 10 to harvested category 11 (logging slash/swamp).

22.2.3.3 FRAGSTATS

We used FRAGSTATS (McGarical and Marks, 1995), a spatial pattern analysis program, to quantify the landscape structures in the CNF and NJP landscapes. The characteristics of quantified landscape structures were then linked to fire spread across the landscapes.

22.3 Results

Substantial differences in fire-spread patterns between the two landscapes were observed when holding weather conditions constant and excluding roads in our simulations. The MBA of 24 fires after a 15-day burning period was 3,867 ha on the CNF versus 4,177 ha on the NJP using the same weather inputs. This 8% MBA difference was surprising given that the MROS differed by 83% between the two landscapes (183 vs.334 m/hr). Spatial variation in BA across the NJP (930 and 1,773 ha, respectively) was much larger than that in the CNF (795 ha). This strongly indicates that land cover fragmentation is substantially controlling fire spread at the landscape level (Finney 2000) because the topographic differences were minimal between the two landscapes and road effects were excluded. Four landscape-level indices clearly demonstrated that the CNF landscape was roughly twice as fragmented as the NJP landscape (Fig. 22.3).

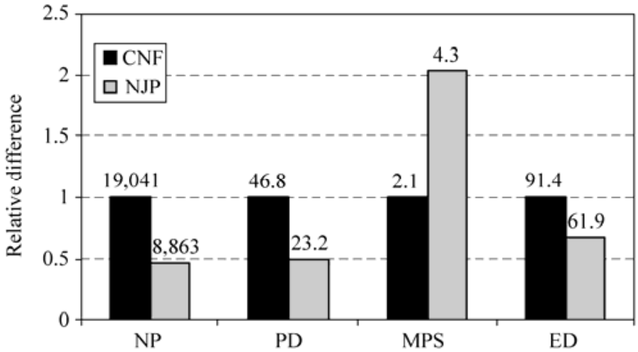

Figure 22.3 Relative differences ($VALUE_{NJP}$ / $VALUE_{CNF}$) of 4 landscape indices in the Chequamegon national forest (CNF) and New Jersey Pinelands (NJP). These were selected to illustrate the relationship between landscape fragmentation and fire spread. The values of indices in the CNF landscape are always expressed as 1. Absolute values are shown on top of each bar: NP = number of patches, PD = patch density (No./100 ha), MPS = mean patch size (ha), and ED = edge density (m/ha). Higher values of NP, PD, and ED or lower values of MPS indicate a higher degree of fragmentation for a given landscape

If the roads were considered as fire barriers during the simulations, the averaged BA in the CNF was 1,319 ha and 1,300 ha, respectively, for spring and summer periods without significant seasonal difference (Fig. 22.4). In the NJP, the averaged BAs were 1,503 ha and 2,515 ha for spring and summer periods, respectively.

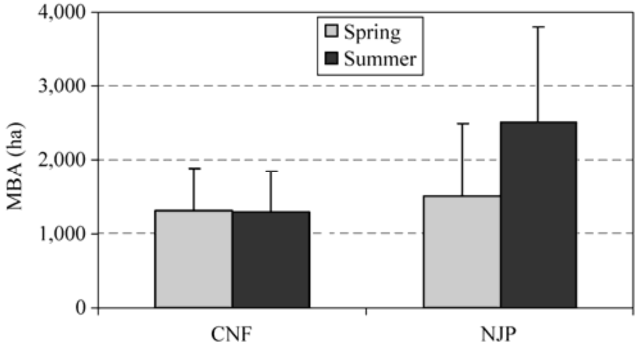

Figure 22.4 Comparison of seasonal changes of mean burned area (MBA, road effects were considered) of 24 fire ignition locations across the landscapes in the Chequamegon National Forest (CNF) and the New Jersey Pinelands (NJP). Vertical bars represent one standard deviation

Our simulations indicated that roads functioning as barriers could significantly reduce the BA of fire spread. In the CNF, road effects reduced the MBA by 71% and 66% for the spring and summer periods, respectively; compared to 25% and 30% for spring and summer, respectively, in the NJP. Much larger road effects in the CNF were partly due to the higher road density (0.63 km/km^2) than that in the NJP (0.33 km/km^2) (Table 22.2). In both landscapes, interacting with weather conditions further complicated the road effects on fire spread. The more favorite weather for fire spread, the larger road effects on reducing BAs are expected (Table 22.2).

Table 22.2 Seasonal weather variables and road density used for FARSITE model simulations of the 24 fires (considering roads as fire barriers) over a 15 day duration in the Chequamegon National Forest (CNF, WI) and New Jersey Pinelands (NJP). Model estimates of seasonal burned area are included. Numbers in the parentheses are the mean burned area (MBA) without considering road effects and the reduction in MBA by% if road effects were considered, separated by comma

	CNF		**NJP**	
	Spring 2004	Summer 2002	Spring 2004	Summer 2004
Mean temperature (℃)	4.6	18.1	10.4	23.1
Total precipitation (mm)	0	48	93	15
Mean wind speed (km/hr)	4.1	7.8	3.3	1.4
MBA (ha)	1,319 (4,561, 71)	1,300 (3,867, 66)	1,503 (2,015, 25)	2,515 (3,599, 30)
Road density (km/km^2)	0.63		0.33	

Harvesting effects showed different trends, depending on landscape fuel type composition and weather conditions. At 4% harvesting intensity, both clustered and dispersed methods showed no significant impact ($a = 0.01$) on reducing the mean burned area across the more fragmented CNF landscape, but showed significant effects on fire spread in the less fragmented NJP landscape in summer (Fig. 22.5) when weather condition (hot/dry) was more favorable to fire spread (Table 22.2). The clustered harvesting resulted in a slight reduction in MBA in NJ during the spring period. Relative changes in MBA caused by harvesting practices in a more fragmented landscape (CNF) were much smaller (< 2.5% in absolute value) than those in the NJP landscape with much less fragmentation and higher MROS (up to 17%, Fig. 22.5).

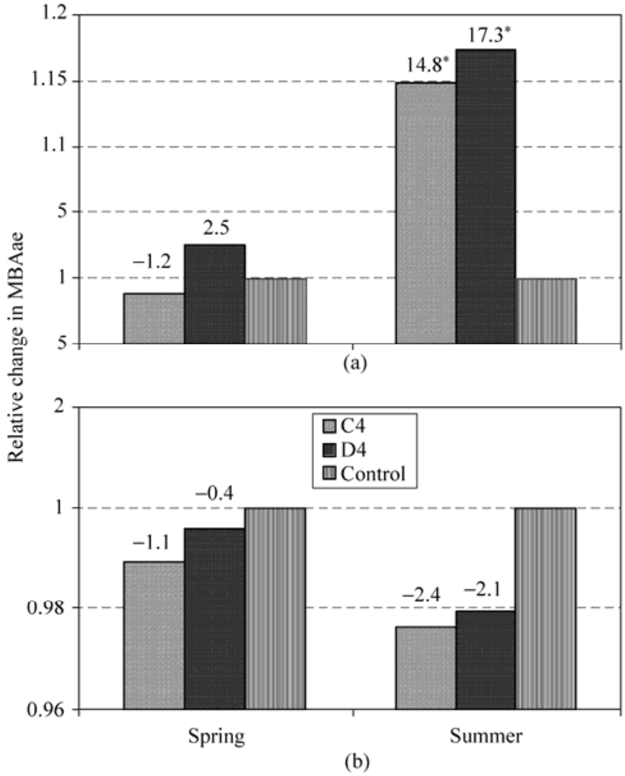

Figure 22.5 Effects of harvesting and harvesting methods on mean burned areas (MBA, relative change) in (a) New Jersey Pinelands; and (b) Chequamegon National Forest, WI; compared to the MBA in spring and summer for the control landscapes. Numbers above the bars indicate relative changes in %, compared to the MBA in control landscapes (scaled to 1). * Indicating that the difference in MBA is significant at level of 0.01

22.4 Discussion

Our simulations revealed that both landscape structure (e.g., spatial arrangement of patches and degree of fragmentation) and fuel type composition can significantly affect fire spread across the landscapes when weather is held constant. Our results clearly indicated that increases in both fragmentation and rate of spread generally increased the size of MBA. However, how these two variables interact across the landscape was the key to determine MBA. For example, the fuel-based MROS in the CNF was 183 m/hr, which resulted in a landscape mean burned area of 3,867 ha (Table 22.2). When we assigned the fuel types in the NJP with a similar MROS (173 m/hr) to that of the CNF, the mean burned area across the landscape was only 1,630 ha, 58% smaller than that in the CNF, reconfirming our previous conclusion that landscape fragmentation was another controlling factor for fire spread across the landscape. Quantified landscape indices showed that the degree of fragmentation in the CNF was, on average, about twice as that in the NJP (Fig. 22.3). If both the degree of fragmentation and fuels' MROS in landscape A is higher than those in landscape B, the difference in burned area should be enhanced between the two landscapes. If one factor is higher while the other is lower in one versus the other landscape, then the effects of the two factors on fire spread will be contradictory, hence moderating each another. Our results have demonstrated such combined effects. Because the NJP landscape was much less fragmented than that of the CNF landscape and the effect of increasing fuels' MROS overcame the effect of decreasing landscape fragmentation in the NJP (Fig. 22.3).

Spatial variation (measured by STD) of fire spread across the NJP landscape was higher than that in the CNF landscape. This is likely because there were 3 additional grass fuel categories (not presented in the CNF) in the NJP that have much faster fire-spread rates. If a fire reaches these fuel types it can greatly increase the size of its perimeter, even with the same weather.

While the combination of temperature and moisture conditions in the weather input was the most influencing environmental factor on fire spread across the landscape, wind speed can also enhance fire spread across the landscapes (Table 22.2). To better understand that relationship, we ran the FARSITE model in the control NJP and CNF landscapes by increasing wind speed to 40 km/hr in spring (when both landscapes had similar mean wind speeds (4.1 km/hr in the CNF vs. 3.3 km/hr in the NJP), Table 22.2) while keeping all other inputs as the same. Consequently, landscape mean fire-spread area increased by about 8 times in the NJP and 5 times in the CNF landscape, suggesting that an increase in wind speed has greater enhancement power on fire spread across landscape that possesses higher fuels' MROS. However, the simulated spread areas using 40 km/hr wind input should be interpreted with caution because in both landscapes it is rare to have such a high wind speed consistently over a 15 day period.

The actual fire-spread areas on the ground within the NJP landscape could be larger than our simulated results for two reasons. First, our simulations dealt with the surface fire only for comparison purposes because most fires in the oak-dominated CNF landscape are low-intensity surface fires (Sturtevant et al. 2004) while crown fires in the pine-dominated NJP landscape could be an influencing factor on fire spread. Second, Anderson's (1982) fuel classification system was primarily developed for the Western USA, thus, it may not quite match the unique characteristics of the vegetation and fuel types in the Eastern USA (http://www.fs.fed.us/ne/global/research/fire.html).

If roads are treated as fire barriers, our results as expected showed an inverse relationship between road density and mean area burned (Table 22.2). However, the degree of reduction in BA related to roads was not proportional to the change in road density between the two landscapes, nor had the same degree of reduction between seasons, even within the same landscape, indicating the road effects on BA are non-linear and complicated other interacting factors such as weather, landscape structure, and fuel characteristics. Furthermore, the road effects on fire spread could go in opposite directions (e.g., increasing fire spread) if human factors are considered. More roads often equates to increased area accessible by people, resulting in higher fire ignition frequency and, thus, increasing fire spread across landscapes (http://www.uecutah.org/where%20there%20is%20smoke.htm). For example, humans caused over 97% of all fire ignitions in the northern forests of the upper Midwest during the 1980's and 1990's (Cardille et al. 2001). Therefore, future studies on fire spread and behavior should incorporate human and social factors, especially in densely populated areas to improve our current understandings on the topic.

Seasonal changes in fire spread should be strongly associated with how energy and water conditions were combined. In the CNF, MBA only differed by 1.5% between spring and summer because the overall effects of whether conditions in spring (dry but cool) and in summer (warm but wet) on fire spread were contradictory to each other (Table 22.2). In the NJP it showed 67% difference in MBA between spring and summer because of sharp weather contrasts, with cool and wet springs vs. warm and dry summers (Table 22.2), thus enhancing the seasonal effects of weather on fire spread (Fig. 22.4). Our results suggested that differences in BAs between seasons should not be necessarily larger than the changes within the season across landscape. Such differences primarily depend on a combination of weather conditions, although climate can be used to differentiate the fire regimes in general. Spatial variations in BA for a given landscape seemed to be determined by landscape mosaic and fuel type composition but not by the variations in weather condition (Fig. 22.4).

The effects of harvesting (e.g., spatial arrangement, treatment method) on fire spread were complicated by interactions with landscape fragmentation, fuel type, and weather. In the CNF, both harvesting practices reduced burned area slightly and the cluster method showed more effects than the dispersed method did on fire spread. In contrast, harvesting practices tended to increase burned area and dispersed method showed more effects than clustered method did on fire spread in the NJP. Such influence was more evident and significant under weather conditions that are favorable to fire spread (Fig. 22.5). Following reasons could cause this inconsistency. When harvesting was conducted within the landscapes, it caused two changes simultaneously: ① the MROS was generally reduced in both landscapes because fuel type 11 (logging slash) had 24% lower fuel intensity than type 10 (occupying 50% in the CNF) and 20% lower than type 9 (occupying 62% in the NJP, Table 22.1), thus slowing fire spread; and ② both landscapes became more fragmented, which could increase fire spread. In the CNF, the effects of reducing MROS seemed to outweigh the effects of increasing fragmentation in an already highly fragmented landscape, resulting in less than expected corridor effects on increasing fire spread. Consequently, harvesting reduced the amount of area burned. In the NJP landscape where has been no harvests conducted in the past 100 years, the effects of increasing fragmentation across the landscape was larger than the effects of reducing MROS, thus, harvesting tended to increase fire spread. Furthermore, harvesting can cause more effects on fire spread under extreme weather conditions that are favorable to fire spread (Fig. 22.5).

Harvests can altered landscape structure in several ways such as fragmenting the fuel complex, creating open areas for easier fire spread, or disrupting local fire growth patterns (Stratton 2004). Some of these changes can be favorable or unfavorable for fire spread depending on the interactions with other contributing factors. In the CNF, our results suggested that the clustered method had greater effects on reducing fire spread than the dispersed method possibly due to the disruption of fuel connectivity in a already fragmented landscape. In the much less fragmented NJP landscape, however, dispersed method showed more effects on fire spread than the clustered method probably due to enhancing the corridor effects and improving the fire ventilation across a landscape having a much higher MROS. In both landscapes, harvesting practices showed more effects on fire spread in summer than in spring (Fig. 22.5). Evaluation of harvesting methods on BA was confounded by varying weather conditions throughout the year and interactions with other factors such as fuel type composition and landscape fragmentation; therefore, it deserves more studies in the future.

22.5 Conclusions

Burned areas in general were larger in the NJP landscape due to highly volatile fuels, compared to the CNF landscape when weather inputs were held constant. Our results indicated that fire spread was associated with landscape fragmentation. The combined effects of fuel-type composition and landscape fragmentation ultimately determined the differences in fire-spread areas and spatial patterns between the two landscapes if other controlling factors are considered constants.

In a more fragmented Oak-dominated landscape in northern Wisconsin, both clustered and dispersed harvesting methods with 4% cutting intensity could reduce burned areas up to 2.4%, compared to those in the control landscape. Although the clustered method reduced more areas both in spring and summer, such reductions were not significantly different ($a = 0.01$). In the less fragmented NJP landscape, 4% cutting could significantly increase burned areas compared to the control landscape, especially under extreme weather conditions that favor fire spread. Seasonal variation in fire-spread area is not necessarily larger than within-season variation in fire-spread area, depending on combinations of weather conditions during the period that fires occurred.

Our results showed that roads as physical barriers could significantly reduce fire spread across the landscape depending on existing road density. However, road effects on fire spread could have the opposite effect (e.g., increasing fire spread) if human factors (ignitions) are considered. Road effects can be enhanced when weather conditions are more favorable to fire spread.

This study suggests that effects of harvesting methods on fire spread are more complicated and vary with other fire controlling factors such as land-use history, fuel type composition and weather conditions. Thus, forest management planning should be flexible and aim to the characteristics of given landscape to minimize fire spread. As such, more studies on this from a landscape-oriented perspective are desired.

Acknowledgements

The joint fire science project (JFSP) and the Northern global change program (NGCP) primarily support this research. We are grateful to Kevin McCullough and Nicholas Skowronski in USDA forest service, newtown square, PA for providing us field data and GIS maps in the New Jersey Pinelands. We thank two anonymous reviewers for their valuable comments on the manuscript.

References

Albert DA, (1995), Regional landscape ecosystems of Michigan, Minnesota, and Wisconsin: a working map and classification. Gen. Tech. Rep. NC-178, USDA Forest Service North Central Forest Experiment Station, St. Paul, MN

Anderson HE, (1982), Aids to determining fuel models for estimating fire behavior. General Technical Report INT-GTR-122, USDA Forest Service

Bresee MK, Le Moine JM, Mather S, Brosofske KD, Chen J, Crow TR Rademacher J, (2004), Disturbance and landscape dynamics in the Chequamegon National Forest, Wisconsin, USA, from 1972 to 2001. *Landscape Ecology*, **19**: 291 − 309

Cardille JA, Ventura SJ, Turner MG, (2001), Environmental and social factors influencing wildfires in the upper midwest, United Stats. *Ecological Applications*, **11**: 111 − 127

Finney MA, (1998), FARSITE: fire area simulator—model development and evaluation. Res. Pap. RMRS-RP-4, USDA, For. Serv. Rocky Mt. Res. Station, Fort Collins, CO, USA

Finney MA, Andrews PL, (1999), FARSITE: Fire area simulator—a model for fire growth simulation. *Fire Management Notes*, **59**: 13 − 15

Finney MA, (2000), A spatial analysis of fire behavior associated with forest blowdown in the Boundary Waters Canoe Area, Minnesota Duluth, MN. USDA Superior National Forest http://www.superiornationalforest.org/ july4thstorm1999/bwcara/bwcawra.html

Graham RT, (2003), Influence of forest structure on wildfire behavior and the severity of its effects: an overview. USDA, Forest Service, North Central Experiment Station, 12

Gustafson EJ, Crow TR, (1996), Simulating the effects of alternative forest management strategies on landscape structure. *Journal of Environmental Management*, **46**: 77 − 94

Huff MH, Ottmar RD, Lehmkuhl JF, Hessburg PF, Everett RL, Alvarado E, Vihanek RH, (1995), Historical and current forest landscapes of eastern Oregon and Washington. Part II: potential fire behavior and smoke production. General Technical Report PNW-GTR-355, USDA Forest Service, Portland, OR

Hunt Jr. ER, Lavigne MB, Franklin SE, (1999), Factors controlling the decline of net primary production with stand age for balsam fir in Newfoundland assessed using an ecosystem simulation model. *Ecological Modelling*, **122**: 151 − 164

Keane RE, Arno SF, Brown JK, (1989), FIRESUM—an ecological process odel for fire succession in western conifer forests. General Technical Report INT-266, USDA Forest Service, Intermountain Research Station

Kercher JR, Axelrod MC, (1984), A process model of fire ecology and succession in a mixed-conifer forest. *Ecology*, **65**: 1725 − 1742

Lathrop R, Kaplan MB, (2004), New Jersey land use/land cover update: 2000-2001. New Jersey Department of Environmental Protection, 35

McCormick J, Jones L, (1973), The Pine Barrens: Vegetation Geography. New Jersey State Museum, 76

McGarical K, Marks BJ, (1995), FRAGSTATS: spatial pattern analysis program for quantifying landscape structure (version 2.0). USDA Forest Service, PNW-GTR-351, Portland, OR

Miller C, Urban DL, (1999), A model of surface fire, climate and forest patter in the Sierra Nevada, California. *Ecological Modeling*, **114**: 113 − 135

Noormets A, Chen J, LeMoine J, Rademacher J, (2004), Seasonal dynamics of ecosystem carbon fluxes in five managed Northern Wisconsin forests. *Global Change Biology*: Submitted

Pyne SJ, Andrews PL, Laven RD, (1996), Introduction to wildland fire. John Wiley & Sons, New York

Radeloff VC, Mladenodd DJ, He HS, Boyce MS, (1999), Forest landscape change in the northwestern Wisconsin Pine Barrens from pre-European settlement to the present. *Canadian J. of Forest Research*, **29**: 1649 − 1659

Rollins MG, Morgan P, Swetnam T, (2002), Landscape-scale controls over 20th century fire occurrence in two large Rocky Mountain (USA) wilderness areas. *Landscape Ecology*, **17**: 539 − 557

Rothermel RC, (1983), How to predict the spread and intensity of forest and range fires. Gen. Tech. Rep. INT-143, USDA Forest Service

Rouse JW, Haas RH, Schell JA, Deering DW, (1973), Monitoring vegetation systems in the Great Plains with ERTS. pp 48 – 62 in Third ERTS Symposium

Stratton RD, (2004), Assessing the effectiveness of landscape fule treatments on fire growth and behavior. *Journal of forestry*, **102**: 32 – 40

Sturtevant BR, Zollner PA, Gustafson EJ, Cleland DT, (2004), Human influence on the abundance and connectivity of high-risk fuels in mixed forests of northern Wisconsin, USA. *Landscape Ecology*, **19**: 235 – 253

23 The GOFC-GOLD Fire Mapping and Monitoring Theme: Assessment and Strategic Plans

Ivan A. Csiszar
NOAA/NESDIS Center for Satellite Applications and Research,
5200 Auth Road, Camp Springs, MD 20746, USA
Email: ivan.csiszar@noaa.gov

Christopher O. Justice
Department of Geography, University of Maryland, 2181 LeFrak Hall,
College Park, MD 20742, USA
Email: justice@hermes.geog.umd.edu

Johann G. Goldammer
Global Fire Monitoring Center, Max Planck Institute for Chemistry,
c/o Freiburg University, Georges-Koehler-Allee 75 D – 79110, Freiburg, Germany
Email: johann.goldammer@fire.uni-freiburg.de

Timothy Lynham
Natural Resources Canada, Canadian Forest Service Great Lakes Forestry Centre,
1219 Queen Street East, Sault Ste. Marie, ON P6A 2E5, Canada
Email: tim.lynham@nrcan.gc.ca

William J. de Groot
Natural Resources Canada, Canadian Forest Service Great Lakes Forestry Centre,
1219 Queen Street, East Sault Ste., Marie, ON P6A 2E5, Canada
Email: bill.degroot@NRCan.gc.ca

Elaine M. Prins
Cooperative Institute for Meteorological Satellite Studies, University of
Wisconsin-Madison, 1225W. Dayton St., Madison, WI 53706, USA
Email: elaine.prins@ssec.wisc.edu

Christopher D. Elvidge
NOAA National Geophysical Data Center, 325 Broadway, Boulder, CO 80303, USA
E-mail: Chris.Elvidge@noaa.gov

Dieter Oertel
Deutsches Zentrum für Luft- und Raumfahrt Optical Information Systems,
Rutherfordstrasse 2, Berlin D-12489, Germany
Email: Dieter.Oertel@dlr.de

Eckehard Lorenz
Deutsches Zentrum für Luft- und Raumfahrt Optical Information Systems, Rutherfordstrasse 2, Berlin D-12489, Germany
Email: eckehard.lorenz@dlr.de

Thomas Bobbe
Remote Sensing Applications Center, USDA Forest Service, 2222 West 2300 South, Salt Lake City, UT 84119, USA
Email: tbobbe@fs.fed.us

Brad Quayle
Remote Sensing Applications Center, USDA Forest Service, 2222 West 2300 South, Salt Lake City, UT 84119, USA
Email: bquayle@fs.fed.us

Diane Davies
Department of Geography, University of Maryland, 2181 LeFrak Hall, College Park, MD 20742, USA
Email: ddavies@hermes.geog.umd.edu

David P. Roy
Geographic Information Science Center of Excellence, South Dakota State University, Wecota Hall, Box 506B Brookings, SD 57007, USA
Email: david.roy@sdstate.edu

Luigi Boschetti
Department of Geography, University of Maryland, 2181 LeFrak Hall, College Park, MD 20742, USA
Email: luigi.boschetti@hermes.geog.umd.edu

Stefania Korontzi
Department of Geography, University of Maryland, 2181 LeFrak Hall, College Park, MD 20742, USA
Email: stef@hermes.geog.umd.edu

Stephen Ambrose
NASA Headquarters, Washington, DC 20546, USA
Email: sambrose@nasa.gov

George Stephens
NOAA NESDIS, 511 Deerfield Ave., Silver Spring, MD 20910, USA
Email: George.stephens@verizon.net

Abstract The objectives of the fire mapping and monitoring theme of the global observation of forest and landcover dynamics (GOFC-GOLD) program are to refine and articulate the international requirements for fire related observations, to increase access to and make the best possible use of existing and future observing systems for fire management, policy decision-making and global change research and to ensure the provision of long-term, systematic satellite observations necessary for the production of the full suite of recommended fire products. The GOFC-GOLD Fire Implementation Team also fostered the development of regional networks of data providers and users to capture regional specific information needs and priorities. This chapter discusses specific goals of the program related to pre-fire evaluation, fire observations and post-fire assessment, and the implementation status of corresponding activities. Examples of contributory programs from US agencies are also presented.

Keywords Satellite fire monitoring; international collaboration; decision making support; global change

23.1 Introduction

The global observation of forest cover- global observation of landcover dynamics (GOFC-GOLD) was initiated in response to the committee on earth observation (CEOS) to develop a stronger linkage between the Space Agencies and the users of earth observation technologies (Townshend et al., 2004). The observation technologies were being developed and research and development undertaken to provide new and improved satellite products for monitoring the earth surface but the full potential of these technologies was not being realized. It was recognized that in some cases there was a mismatch between the information that was being provided and that which was really needed by those responsible for the operational monitoring and management of earth resources and those undertaking global change research. It was recognized that there was the need for a better understanding of the observational requirements from the user community. In other cases potential users were simply unaware of the available technologies and in many cases there were obstacles to accessing and utilizing the data.

GOFC-GOLD is currently a project of the global terrestrial observing system (GTOS), with a project office in Edmonton run by the Natural Resources Canada and the Canadian forest service (GOFC, 2007). The secretariat for GTOS is at the United Nations food and agriculture organization (FAO) in Rome (GTOS, 2005). A more detailed evolution of the GOFC-GOLD program can be found in Townshend et al., (2004).

The fire phase of GOFC-GOLD was initiated in 1998 at a kick-off meeting at the Joint Research Center, Ispra (Ahern et al., 2001). At that meeting it was evident that the satellite fire observations fell largely in the research domain and that the products are often of unknown accuracy. It was also recognized that there is often parallel development of methods and techniques amongst different groups and that there are a number of opportunities for efficiencies through information

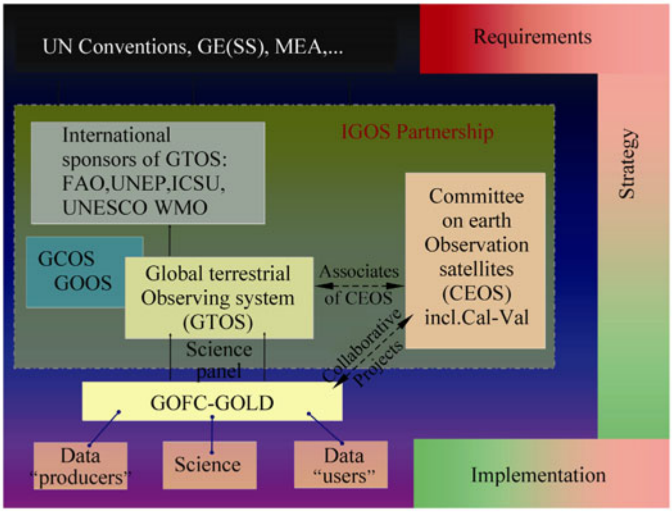

Figure 23.1 GOFC-GOLD within the overall structure of earth observation programs

and data exchange. It was recognized that for fire information users, the products must be reliable with sustained data provision and that there is a need to transition proven techniques in the research domain to the operational agencies. It was also recognized that there are often a number of institutional obstacles to such transition, most often related to funding responsibility. There is also a need for better integration of satellite, aircraft and ground based information. It was strongly recommended at the meeting that GOFC-GOLD Fire establish strategic partnerships with other national and international organizations building on existing programs, addressing other aspects of fire monitoring and management. In particular every effort should be made to also make available information to users beyond the international organizations at the regional to local level.

Since the 1998 kick-off meeting, GOFC-GOLD Fire has developed strategic partnerships with a number of organizations that share some of the program goals, for example with the U.N. Interagency strategy for disaster reduction (UNISDR) working group on wildland fire and its follow-up arrangements, the UNISDR global wildland fire network and the wildland fire advisory group, which is focusing on improving fire management capacity around the world. National fire reporting is inconsistent globally and is often of unknown accuracy. In many countries there is a scarcity of fire information and there is a need for better and timely information. To help coordinate and guide its fire program, GOFC-GOLD established a secretariat and a fire implementation team consisting of data providers and data users (GOFC FIRE, 2008). The aims of this team are to refine and articulate the international requirements for fire related observations, to increase access to and make the best possible use of existing and future observing systems for fire management, policy decision-making and global change research and ensure the provision of long-term, systematic satellite observations necessary for the production of the full suite of recommended fire products (Justice et al., 2003). The team is also involved in a number of global initiatives requiring international cooperation. Following the lead of the land cover component of GOFC-GOLD, the implementation team fostered the development of regional networks of data providers and users to capture regional specific information needs and priorities. Regional Fire Networks have been established in Southern Africa, Northern Eurasia, Southeast Asia and South America. The networks provide a forum for shared experience in fire observation and monitoring and opportunities for lateral transfer of technology. These networks complement and are coordinated with the regional fire management networks being developed by the UNISDR global wildland fire network. The implementation team set out the broad goals for the fire program and near term program objectives.

23.2 GOFC-GOLD Fire Goals and Current Implementation Status

23.2.1 To Increase User Awareness by Providing an Improved Understanding of the Utility of Satellite Fire Products for Resource Management and Policy Within the United Nations and at Regional, National and Local Levels

The challenge for nations and the international community is to develop informed policy and management capabilities that recognize both the beneficial and traditional roles of fire, while reducing the incidence and extent of uncontrolled burning and its adverse impacts. A major impediment for efficient wildland fire management and for strategic planning is the lack of reliable data and information on the occurrence and extent of wildland fires and their effects (Ahern et al., 2001). In most countries of the world there is also a lack of information on precursors of wildfires and fire use, such as weather-related information (wildland fire danger), ecosystem properties that influence fire behavior and fire severity (wildland fire hazard) and the probability of ignition (wildland fire risk). There is also a lack of internationally agreed standards for assessments, reporting and evaluation of the consequences of wildland fires. The development of a standardized wildland fire inventory system is urgently needed. However, even if an international consensus would be reached in future, it is evident that most countries do not have sufficient ground- or aircraft based systems for detection, monitoring and fire damage assessment. Thus, information generated by spaceborne instruments is essential to provide the information required.

The United nations recently have shown an increasing interest to develop informal partnerships, joint projects and formal agreements among governments and between government and non-governmental institutions that are essential to enable nations to develop sustainable fire management capabilities. In 2001 UNISDR provided a mechanism to facilitate a common policy dialogue at inter-agency and international levels. Starting in 2001 a working group on wildland fire was created within the UNISDR inter-agency task force for disaster reduction. Through this group the various UN specialized agencies, programmes and secretariats of conventions that have a direct or indirect responsibility in matters related to wildland fire shared their views and visions for a collective approach (UNISDR, 2008). In this working group the GOFC-GOLD fire implementation team provided concepts and visions for the coordinated use of satellite remote sensing (RS) of wildland fires. While the UN has to agree on a systematic and standardized approach in developing a global database on wildland fire, there is an increasing demand of countries on the other side to receive guidance and support for developing such databases. The UN and other international organizations also require spaceborne fire information—to mention a few examples:

(1) United nations environment programme (UNEP)—for monitoring the environment effects of wildland fire

(2) UN office for the coordination of humanitarian affairs (UN-OCHA)—for response to wildland fire disasters (with UNEP and GFMC)

(3) FAO—for the regular global forest resources assessments

(4) World health organization (WHO)—for providing guidance on response measures to reduce impacts of smoke pollution on human health and security

(5) World meteorological organization (WMO)—for early warning of wildland fire danger and smoke trajectories

(6) The "Rio conventions"—for the implementation of the mandates of the UN conventions on combat desertification (UNCCD), biological diversity (UNCBD) and the UN framework convention on climate change (UNFCCC)

(7) The United nations forum on forests (UNFF)—for including forest fire management into the multi-year plan of work of the "Non-legally binding instrument on all types of forests" (2007)

(8) The UN office for outer space affairs (OOSA) / UN Committee on the peaceful uses of outer space (COPUOS)—for satellite RS technology transfer to developing countries

(9) The earth observation user Liaison Office for the humanitarian community—for providing accurate information updates on fast evolving situations for humanitarian relief and crisis prevention operations

(10) United Nations University (UNU)—for conducting dedicated targeted research and training

Driven by the interests of countries to create synergies in sharing fire management resources—including fire information systems—the Global Wildland Fire Network was established in 2003 as an outreach programme of UNISDR (GWFNa, 2008). Government and non-government institutions actively organized under the Regional Wildland Fire Networks are aiming at strengthening the dialogue between specialists and government agencies of neighbouring countries. Representatives of the Regional Wildland Fire Networks are members of the UNISDR Wildland Fire Advisory Group which is serving as an advisory body to the United Nations. There is a close working relationship with the regional GOFC-GOLD networks which are focussed on fire observations and monitoring. Both networks are interacting in regional consultations and workshops aiming at the preparation of targeted proposals to the international community, notably the UN family.

Regional network consultations conducted in 2004 came up with recommendations directed to a ministerial conference at FAO (Rome, March 2005) to formulate an International Wildland Fire Accord. The ministerial meeting, however, rejected the proposal for an accord and instead recommended the development of "voluntary guidelines"; at the time of writing this Chapter the overall aims of these guidelines have not yet been defined (GWFNb, 2008). FAO also rejected the GOFC-GOLD proposal to utilize satellite RS products for a consistent global fire assessment within the Global Forest Resources Assessment 2005 (FAO, 2006).

So far all proposals to set up a consistent global wildland fire monitoring programme under the umbrella of the UN have failed. However, the GOFC-GOLD Fire Implementation Team, through its involvement in the Wildland Fire Advisory Group and by facilitation through the Global Fire Monitoring Center (GFMC), continues to push the agenda at the UN level.

23.2.2 To Encourage the Development and Testing of Standard Methods for Fire Danger Rating Suited to Different Ecosystems and to Enhance Current Fire Early Warning Systems

23.2.2.1 Early Warning Systems and Fire Danger

Fire danger rating (FAO, 1986) is a mature science and has long been used as a tool to provide early warning of the potential for serious wildfires. Fire danger rating systems (FDRS) utilize basic weather data to calculate wildfire potential. Fire danger is a general term used to express an assessment of both fixed and variable factors of the fire environment that determine the ease of ignition, rate of spread, difficulty of control, and fire impact (Merrill and Alexander, 1987). FDRS early warning information is often enhanced with satellite data such as hot spots for early fire detection, and spectral data on land cover type and indices of vegetation condition. More recently, remote sensed weather data is also being used to enhance the ground-based network of weather stations. Normally, these systems provide a 4 – 6 hour early warning of the highest fire danger for any particular day that the weather data is supplied. However, by using forecasted weather data, as much has 10 days of early warning can be provided. As well, FDRS indices can be calibrated with local data to provide longer term early warning, such as a 30-day early warning tool developed for SE Asia to indicate the potential for disaster-level haze events from peatland fires (Field et al., 2004).

23.2.2.2 Developing a Global Early Warning System

The science to develop a global early warning system for wildland fire currently exists, but there are some technical issues to overcome. A daily operational global system will need large amounts of data and will require considerable processing capability. There are a number of regional examples demonstrating feasibility, and global implementation is essentially a technical issue of providing complete data coverage for all countries and regions, and scaling-up with standardized products. Implementing a global system will also require regional calibration of early warning indicators using danger level boundaries. This can be done using historical ground-based weather data and remotely sensed fire data such as hotspots and burned area maps.

Advances in measuring spatial precipitation from space would offer the single largest improvement to the development of fire danger monitoring systems. Such advances would reduce or eliminate the need for spatial interpolation of precipitation from ground-based point sources, which in some regions has serious limitations. Even some countries that have established fire danger systems do not have a reliable, comprehensive network of ground-based precipitation stations that cover their fire regions. While it is recognized that space-based precipitation estimates also have limitations, combining those estimates with ground-based data as control points is expected to significantly improve the spatial modeling of this critical fire danger parameter.

Establishing an operational global early warning system for wildland fire will require an international partnership of agencies. A weather data stream from WMO could provide the baseline data necessary to calculate fire danger. The WMO could also provide additional weather-based early warning products such as smoke trajectories and air pollution warnings. Such near real-time products are currently being generated from geostationary satellites. The GOFC-GOLD Fire Implementation Team is involved in exploring the use of satellite data for early warning and fire danger purposes including hot spots for early detection, land cover classification of fuel types, and perhaps spatial weather information (e.g., precipitation) for areas where ground-based weather data is sparse. Fire management data system expertise is needed to develop a system that integrates the disparate data sources and generates early warning indicators.

Establishing a global early warning system for wildland fire provides common criteria for comparing burning conditions and wildfire situations internationally. It also provides a globally-consistent method for quantifying fire danger, an important factor for promoting resource-sharing arrangements between nations. Perhaps most importantly, establishing a global early warning system would provide a formal system for the large number of developing countries that would never have the means to develop their own. It would also provide those countries with a substantial base of information to use in developing their own fire management capabilities.

An immediate contribution that GOFC-GOLD can make to expand the international role of wildland fire danger rating. The first step would to be to promote an international fire weather index (FWI) system that is modeled on a working system. A suitable candidate is the Canadian Forest Fire weather index (FWI) System which has already been implemented in several locations around the world including Southeast Asia (de Groot et al., 2007), Mexico, New Zealand and in some states or fire agencies (Michigan, Minnesota, Alaska) within the USA. The FWI system consists of six components that account for the effects of fuel moisture and wind on fire behavior (Van Wagner, 1987). The system requires four continuous inputs (temperature, 24-hour precipitation, wind speed and relative humidity) to monitor the water balance in forests that are characterized by organic soils. However, the system could be adapted to measure fire danger in any wildland zone.

In response to the request by the UN Secretary General, the Hyogo Framework for Action 2005 – 2015: "Building the Resilience of Nations and Communities to Disasters" and the preparation of the upcoming Third International Early Warning Conference (EWC-III, Bonn, Germany, March 2006) a project proposal on the development of Global Early Warning System for Wildland Fire has been submitted to the United Nations in October 2005.

23.2.3 To Develop an Operational Global Geostationary Fire Network Providing Observations of Active Fires in Near Real Time

The international environmental monitoring and scientific research communities have stressed the importance of utilizing operational satellites to produce routine fire products and to ensure long-term stable records of fire activity. Although a number of geostationary systems cover most of the Earths surface and in some cases with considerable overlap, there has been little coordination to date concerning fire monitoring. An operational global geostationary fire monitoring network would enable monitoring of fires as they occur and capture the diurnal signature of fire activity.

Geostationary systems have an important contribution to make in providing multiple observations per day for active fire and smoke detection and characterization with applications in fire management, emissions and air quality studies, and global change research. A global geostationary fire monitoring network is technically feasible, but must be supported by the operational agencies in order to sustain the activity and produce standardized long-term data records and fire inventories of known accuracy.

In an effort to coordinate international geostationary fire monitoring efforts the

GOFC-GOLD fire monitoring and implementation team and the EUropean organization for the exploitation of METeorological SATellites (EUMETSAT) hosted two workshops on geostationary fire monitoring and applications in Darmstadt, Germany in 2004 and 2006. The 2006 workshop was attended by over 45 representatives from 18 countries in Europe, Africa, Asia and the Americas.

23.2.3.1 Current Status

Currently the Imager on the US geostatationary operational environmental satellites (GOES-East and GOES-West) allows for diurnal fire detection and monitoring throughout the Western Hemisphere. The European Meteosat-9 spinning enhanced visible and infrared imager (SEVIRI) provides diurnal fire monitoring capabilities in Western Europe and Africa. FY-2C and MTSAT-1R were launched in 2004 and 2005, respectively, allowing for nearly global geostationary fire monitoring capabilities. Over the past 2 years, FY-2C/2D and MTSAT-1R have been used to some extent for fire detection and monitoring in Asia and Australia.

The number of countries and research and operational groups involved in geostationary fire monitoring has significantly grown in the last two years, with applications in a variety of areas including hazards, air quality monitoring, climate change, and industrial applications. Applications of GOES-E/-W, Met-8/-9, FY-2C/2D, and MTSAT-1 are demonstrating the capabilities of these operational satellites for fire detection, monitoring, and characterization. Furthermore, several operational agencies (e.g., NOAA/NESDIS, EUMETSAT, UK Met Office, China Meteorological Administration, and India) plan to develop or expand existing geostationary fire detection and monitoring programs.

23.2.3.2 Future Plans

The current configuration of geostationary platforms around the globe leaves a gap in coverage over Eastern Europe and Western Asia to monitor burning in India and the boreal forests of Russia. Within the next 2 years additional geostationary instruments with fire monitoring capabilities will be launched by India (INSAT-3D, 2008), Russia (GOMS Elektro L MSU-GS, 2008) and Korea (COMS, 2009) providing coverage of this region as well. Together with the current suite of meteorological geostationary sensors, these upcoming sensors will enable nearly global geostationary fire monitoring. They will be able to detect, monitor, and characterize sub-pixel fires as they occur with high temporal resolution. NOAA/NESDIS and the UK Met Office plan to implement a real-time global geostationary fire monitoring system in 2008 and 2009, respectively. Furthermore fire detection and monitoring is a requirement for the next generation GOES-R Advanced Baseline Imager (ABI) and the Meteosat Third Generation geostationary platforms.

For algorithm development, operational implementation, and validation there is a need for more involvement from all countries, but especially Africa, Eastern Europe, Asia and Australia, with the recent/near-term launches of FY-2C/2D, MTSAT-1R, INSAT-3D, GOMS Elektro L MSU-GS, and COMS. Research and development is needed in the area of fused polar and geostationary fire products with the goal of improved merged products. This includes fire identification and sub-pixel characterization. Validation activities to date have been on an ad-hoc basis and would benefit greatly from more interaction with the CEOS LPV Working Group to establish systematic validation plans that include efforts to understand cross platform differences. In order to implement a global geostationary fire monitoring network with consistent global fire products, it is necessary to characterize the unique fire monitoring capabilities of each sensing system.

23.2.4 To Establish Operational Polar Orbiters with Fire Monitoring Capability to Provide Operational Moderate Resolution Long-Term Global Fire Products and Enhanced Regional Products from Distributed Ground Stations to Meet User Requirements

23.2.4.1 Current Status

Moderate resolution polar orbiters currently provide data used in detection of vegetation condition, active fires and burn scars. The system having the clearest operational status is the National Oceanic and Atmospheric Administration (NOAA) polar orbiting environmental satellites (POES) advanced very high resolution radiometer (AVHRR). Many of the existing national or regional operational systems for detecting active fires rely on AVHRR data downloaded from direct readout stations (GFMC 2008; GOFC FIRE 2008). The National Aeronautics and Space Administration (NASA) Moderate-resolution imaging spectrometer (MODIS) a research instrument, has demonstrated the value that improved spatial resolution, radiometric calibration, geolocation accuracy, and an extended suite of spectral bands can bring to fire RS (Justice et al., 2002). MODIS sensors are currently flying on NASA's Terra and Aqua satellites and fire data from these systems is increasingly used by operational agencies. Data from the European space agency (ESA) (Advanced) Along Track Scanning Radiometer ((A)ATSR) have been processed to produce global compilations of night-time active fire and burn scars (Arino et al., 2001). Data from the European Commission SPOT-VEGETATION, sensor have been used to produce annual compilations of global burn scar. The U.S. air force defense meteorological satellite program (DMSP) operational linescan system (OLS) can detect fires at night via low light imaging in the visible wavelength region (Elvidge et al., 2001), a capability used in conjunction with data from other systems, such as AVHRR and MODIS.

23.2.4.2 Future Plans

In the next three years there will be good continuity of primary moderate resolution systems for global fire monitoring, barring system failures (i.e. AVHRR, MODIS, DMSP and AATSR). The NASA/NOAA/DoD visible infrared imaging radiometer suite (VIIRS) instrument, to be flown on the NPOESS preparatory mission (NPP) in 2009 is designed to provide continuity for the MODIS mission and prototype the operational moderate resolution sensor and product data streams from VIIRS during the national polar-orbiting operational environmental satellite system (NPOESS, Townshend et al., 2002) Importantly, the NPP spacecraft will provide direct broadcast of data, continuing the tradition of the NOAA-POES and NASA Terra/Aqua.

The VIIRS is under construction and will provide fire data similar to that of MODIS. An advantage over MODIS will be the inclusion of a suite of imaging bands, centered at 0.64, 0.86, 1.61, 3.74 and 11.4 microns at 400 meter resolution at nadir. This should enable improvements in both active fire and burn scar mapping. (Note that the VIIRS thermal anomaly product will be based on the moderate resolution bands, not the imaging band set). The major problem with the VIIRS bands in the 10.8 um region is that the saturation temperature is set to maximize the discrimination of cloud top temperatures and saturation is expected on large fires. Upon saturation, it will not be possible to estimate fire characteristics, such as size and temperature using the standard 3.7 versus 10.8 μm band algorithm. In addition, on-board aggregation will average values for saturated and unsaturated pixels. It may be possible to make use of other VIIRS bands, such as those placed at 1.61 and 2.25 to characterize fire size and temperature when saturation occurs in the 10.8 μm bands, but this is currently not planned for the operational thermal anomaly product.

In the next ten years it is anticipated that the NPOESS VIIRS will become the primary operational moderate resolution polar orbiting system used in active fire and burn scar RS. This will be augmented by a continuation of the AVHRR data record on the morning MetOp the first of which was launched in October 2006. It is important that the active fire RS user community effectively establish requirements for unsaturated 3.7 μm data, for all but the very largest and hottest fires.

23.2.5 To Develop Long-Term Fire Data Records by Combining Data from Multiple Satellite Sources

Beginning in the 1980's, various instruments on geostationary and polar platforms have been providing systematic measurements useful for fire mapping and monitoring. The independent development of these systems has led to the generation of a number of single-sensor products. However, the sensors on board operational and experimental satellite platforms have provided data limited to the associated sensor's spatial and temporal coverage and only for the duration of the specific mission or project. The accuracy of the different products also varies due to sensor characteristics, such as spatial resolution, geolocation accuracy and radiometric characteristics, and algorithm. To generate a long-term, science quality, homogeneous fire data record, a number of issues related to inter-satellite and inter-sensor continuity need to be addressed. In this process the advancement of technology and the consequent improvement of data quality and the availability of an increasing number of sensors need to be considered. Specifics of such dynamic continuity for fire products need to be defined. A fundamental component of this process is product validation, which also allows the linkage of products from different sensors.

23.2.5.1 Active Fire Data Record

The longest data record—25 years-applicable for active fire monitoring is available from AVHRR. In many areas, however, for most of the data record full 1km resolution data are not available. The 4 km Global Area Coverage (GAC) data generated by sampling and averaging the 1km data, are of limited use for fire detection and burned area mapping. In addition, inter-satellite changes, the orbital drift of the NOAA satellites and sensor degradation make the creation of a homogeneous AVHRR-based active fire data record difficult (Csiszar et al., 2003). Nighttime data within the ATSR/AATSR World Fire Atlas (Arino et al., 2001) now provide nearly a decade of systematic record. Science quality daytime and nighttime active fire data have been generated from MODIS since late 2000 (Justice et al., 2002). To establish continuity between these products, differences in detection capabilities and temporal sampling of the diurnal cycle of fire activity need to be analyzed. Multi-year data records from GOES (hemispherically) and TRMM (within the tropics) provide an opportunity for such intercomparisons and the normalization of fire counts. Advances have also been made in the use of coincident fire observations from high resolution sensors—primarily Terra/ASTER—for product validation (Morisette et al., 2005a; 2005b, Csiszar et al., 2006). The creation of true multi-sensor fire products via data fusion—defined as the generation of a single, enhanced product using information from various sensors—is currently still in the exploratory phase.

23.2.5.2 Burned Area Data Record

The production of long-term, large-scale burned area datasets has begun only recently. After pilot projects such as GBA-2000 (Tansey et al., 2004) and GLOBSCAR (Simon et al., 2004) multi-year global datasets from several sensors are being generated within the ESA GLOBCARBON project (GLOBCARBON, 2008). Recently most of the Pathfinder AVHRR Land dataset has been processed into a multi-year burned area product, however a systematic validation of the product has yet to be developed (Carmona-Moreno et al., 2005). Production of the standard MODIS burned area product (Roy et al., 2005a) began in early 2007 and reprocessing of the entire MODIS data record will be completed by mid-2008. Validation of the beta-product has been undertaken in close collaboration with the GOFC-GOLD regional fire networks in Africa, Australia and Russia (Roy et al., 2005b). Regional burned area mapping initiatives, such as TerraNorte for the boreal zone of the Northern Hemisphere (TERRANORTE, 2008) also exist.

Major requirements for the creation of the science quality burned area long term data record are the provision of 1km AVHRR observations and the inclusion of burned area among the systematically generated and validated data products by the various space and operational agencies. GOFC-GOLD Fire can be instrumental in advocating and coordinating the adoption of standard validation protocols and sustained product validation activities.

23.2.5.3 Analysis of Global Fire Dynamics

The emerging products have been used for provisional studies on the spatial and temporal dynamics of fire activity at global (e.g. Dwyer et al., 2000; Csiszar et al., 2005a; Giglio et al., 2006) and regional (e.g. Schroeder et al., 2005) scales. These analyses have revealed some important patterns of fire activity, particularly in remote areas, that will result in a better understanding of fire regimes and the role of human activity in fire dynamics. The data record will enable the analysis of long-term interactions between fire, land use, land cover and other components of the climate system (Csiszar et al., 2005b).

23.2.6 To Establish Operational Polar Orbiters with Fire Monitoring Capability to Provide Operational High Resolution Data Acquisition Allowing Fire Monitoring and Post-fire Assessments

23.2.6.1 Advanced Active Fire Detection and Characterization

The German Bi-spectral InfraRed Detection (BIRD) satellite was successfully exploited as an innovative technology development in an end-to-end demonstration for semi-operational fire detection during the FUEGOSAT Consolidation Phase Step 1 within the FIREBIRD / DEMOBIRD projects in 2003 (Briess et al., 2003; Lorenz et al., 2003). The FUEGOSAT Consolidation Phase is part of the ESA Earth Watch initiative and running since 2002 with funding contributions and participation of the ESA Member States: Spain, Italy, France, and Germany.

Work conducted by DLR and partners (Kings College London (KCL), GFMC, Remote Sensing Solution GmbH (RSS), Ingeneria y Servicios Aerospatiales (INSA) and OHB-Systems) for ESA in the ECOFIRE Study on "Scientific Assessment of Space-borne High Temperature Event Observing Mission Concepts" revealed that active fire data nearly simultaneously obtained by MODIS on Terra and by BIRD complement very well (Wooster et al., 2003; Zhukov et al., 2003). There is a high complementary potential of these two types of Low Earth Orbiting (LEO) IR sensors for innovative and quantitative active fire detection. Wide-swath moderate-resolution spectro-radiometers (MODIS type) on major polar orbiting satellites can provide daily global coverage fire detection, whereas moderate-to-high spatial resolution imagers (BIRD type) flown on micro-satellite constellations and / or on medium-scale satellites allow detailed monitoring and validation of the parameters of fires whose occurrence was detected before by the wide-swath and geostationary sensors.

A conclusion from the above European initiatives is that a dedicated fire-detecting and monitoring instrument with ~200 m spatial resolution would complement the fire detection capability of VIIRS. The accommodation of such an instrument on the GMES satellites (Global Monitoring for Environment and Security; GMES, 2008) Sentinel 2 (Land) and Sentinel 3 (Ocean) is still pending. A market study for FIRES—a prospective micro-satellite constellation with BIRD-type IR sensors, real time on-board fire product generation and broadcast—was conducted in 2005.

23.2.6.2 Role of Burned Area Maps from High Resolution RS Data to Support Global Wildland Fire Management

High resolution (20 – 30 m) RS data support a variety of global wildland fire management programs. Local fire managers require fine scale information for applications such as pre-fire vegetation/fuels mapping, fire risk modeling, burn area mapping, and post-fire assessment and monitoring.

Landsat has historically been the primary source of such high resolution imagery since it provides spectral bands in the visible, near infrared, short wave infrared, and thermal infrared regions and a valuable global archive of imagery from 1972 to the present (Sheffner, 1994). Continuity of the Landsat record is critical to accurately monitor regional and local scale temporal changes in vegetation and land cover and land use both for resource monitoring and global change research. The immediate future of the Landsat program is currently at risk due to the current operating conditions of Landsat 5 and Landsat 7, and the delay in the launch of the Landsat Data Continuity Mission (LDCM) in 2011.

Landsat 5, launched in 1984, and Landsat 7 are currently operating past their original design lives. Several critical mission components on Landsat 5 are presently operating without redundancy (Irons 2005) and instrument problems continue to arise. The fuel remaining onboard Landsat 5 is not sufficient to maintain its orbit through to the beginning of the NPOESS era and data can only be directly downlinked in real-time to a limited number of ground stations (Irons and Ochs, 2004). Landsat 7’s ETM+ sensor experienced a failure of the scan line corrector (SLC) in May 2003. The result of this failure causes portions of the area within the scene to be collected redundantly while other areas are missed entirely (Howard and Lacasse 2004). The lost data which are scattered throughout the image except for a narrow central swath, amounts to ~22% of each scene (Irons and Ochs, 2004). In addition to the SLC failure, Landsat 7 lost one of its three gyroscopes in May 2004.

Since the SLC failure, various alternatives have been discussed for Landsat continuity beyond the LDCM, including a free flyer, collocation on the NPOESS platform, a commercial data buy and a micro-satellite imaging constellation. The latter approach which has been proven by the Disaster Monitoring Constellation (DMC) developed by Surrey Satellite Ltd., has considerable appeal as it would enable multiple low cost satellites to be built and launched, increasing temporal coverage and ensuring timely instrument replacement upon failure. With a number of high resolution instruments currently orbit e.g. IRS AWiFS, SPOT, ASTER, EO1, and CBERS, GOFC-GOLD in cooperation with the CEOS Working Group on Information Systems and Services in the framework of the Global Earth Observing System of Systems (GEOSS) is pursuing the coordination of the acquisition from multiple international spaceborne assets to fill this critical gap in global data continuity.

23.2.7 To Enhance Fire Product Use and Access by Developing Operational Multi-source Fire and GIS Data and Making These Available Over the Internet

Recent advances in information technology make it easier integrate RS products and GIS data within web-based GIS systems to provide resource managers with information that is timely, accurate, and delivered in a readily accessible format. Using these technologies NASA Goddard Space Flight Center (GSFC) and the University of Maryland (UMd) are working with GOFC-GOLD partners to improve the way in which active fire locations are disseminated to end users around the world.

23.2.7.1 Delivering MODIS Global Active Fire Data over the Internet

The standard MODIS active fire product can be obtained a few days after satellite data acquisition from the Earth Observation Systems Data Center (EDC) Distributed Active Archive Center (LP DAAC, 2007). However, accessing data from the DAAC requires users to download large files (typically 50 MB), use specialized software, and to possess some expertise to order the data and handle the HDF file format. To better meet the needs of resource managers, two systems were developed as part of NASA's Applications Program, under the umbrella of GOFC-GOLD Fire; the MODIS Land Rapid Response (MLRR) system (MLRR, 2008) and Web Fire Mapper (WFM, 2008).

The MLRR system processes MODIS data in near real-time and serves true color images with active fire locations overlain over the Internet. The active fire locations generated by MLRR are also ingested into Web Fire Mapper and made available to natural resource managers in readily accessible formats; these include interactive Web maps, downloadable GIS layers, and more recently (for selected areas) fire email alerts and cell phone text messages. The development of Web Fire Mapper has been based on an understanding of user needs and providing appropriate delivery systems. Using the Web GIS tools, users can customize a map by selecting from a range of geospatial layers and overlaying them with most recently acquired active fire data. Users can also analyze and query the global database of active fire detections from November 2000 to present. This capacity to integrate fire information with local geospatial information (such as park boundaries, roads and settlements) allows natural resource managers to place active fires in their geographic context.

23.2.7.2 Regional Web Fire Mapping Initiatives

There are a number of regional initiatives that also serve MODIS active fire data from a direct broadcast station. The primary advantage of these initiatives is the reduced time from satellite overpass to data distribution (~40 minutes). Examples of these systems are those operated by: the USDA Remote Sensing Applications Center (USDA, 2005), Sentinel in Australia (SENTINEL, 2007), INPE in Brazil (INPE, 2008), Conabio in Mexico (CONABIO, 2007), Avialesookhrana in Russia (AVIALESOOKHRANA, 2005) and the Satellite Applications Center in South Africa (SACSA, 2008); for a complete list of systems see the monitoring portal of the Global Fire Monitoring Center (GFMC, 2008) and the GOFC-GOLD Fire Implementation Team website (GOFC FIRE, 2008) The regional systems are better placed than centralized, global systems, to combine the active fire locations with regional information such as weather conditions, local GIS datasets and active fire locations from other satellite sensors. For example, INPE integrates fire detections from NOAA-AVHRR and GOES as well as MODIS; the South African system integrates active fire detections from Meteosat-8 G data; and Sentinel adds localized information such as water courses, terrain relief, built up areas and topographic maps.

23.2.7.3 Future

A considerable investment has been made by the space agencies around the World to develop improved satellite monitoring of the planet. To maximize the societal benefit of these systems to support natural resource management and decision-making, there needs to be a continued emphasis on ensuring that the data are converted to useable information and made available in a timely fashion. This process is becoming easier with advances in web technology and improved access to broadband Internet.

Technologies already exist to create interactive web maps that incorporate data from a wide range of servers (in different locations); a key obstacle to improving these maps for active fire managers, is finding suitable data that are up-to-date, accurate, readily available and consistent across regions. For examples, Web Fire Mapper is being updated to serve the MODIS burned area product.

It is expected that future efforts to enhance the delivery of multi-source fire and GIS data will include: XML (extensible markup language) based data feeds (that allow the end user to customize the information they are interested in and have it delivered to them through a web browser), enhanced interoperability (allowing more integration of datasets), improved web technologies (such as Asynchronous JavaScript + XML), emerging open source GIS solutions, and a wider range of Fire Alerts /summary reports in the form of email alerts and cell phone messages, with text only or text and map attachments. Providing these data in a range of formats that are easy to access—even with slow internet connectivity, will continue to improve access to satellite derived information and enhance product use globally.

23.2.8 To Establish an Operational Network of Fire Validation Sites and Protocols, Providing Accuracy Assessment for Operational Products and a Testbed for New or Enhanced Products, Leading to Standard Products of Known Accuracy

The potential research, policy and management applications of satellite fire products place a high priority on providing statements about their accuracy. Inter-comparison of different fire area products provides an indication of gross differences and possibly insights into their causes, however product comparison with independent reference data is needed to determine accuracy (Justice et al., 2000). Validation is defined here, and more generally, as the process of assessing satellite product accuracy by comparison with independent reference data (Morisette et al., 2002; Roy et al., 2002a). Validation is required (i) to provide accuracy information to help users decide if and how to use a product, and (ii) to identify needed product improvements.

Previous studies have revealed large discrepancies in the areal estimates, timing and location among satellite fire products and highlight the need for systematic validation (Korontzi et al., 2004; Boschetti et al., 2004). Despite the large number of experimental and systematically derived satellite fire products, there has been neither rigorous assessment of their accuracy, nor development of systematic methodologies to evaluate their accuracy, arguably because of the limited resources made available for validation and because of the scope and complexity of the task.

Validation of satellite active fire products is difficult because of practical problems in collecting independent reference data that characterize the location and physical properties of actively burning fires. Previous approaches have used data from aircraft observations of prescribed fires and wildfires (Kaufman et al., 1998), but are expensive to undertake in a regionally or globally representative manner and are difficult to coordinate with satellite observations. Similarly, field based measurements are difficult to coordinate and cannot be used to infer active fire product accuracy over large areas (Cardoso et al., 2005). Burned areas identified in high spatial resolution satellite data do not provide a reliable validation if the fires are inactive or cloud-covered at the time of satellite overpass (Pereira and

Setzer, 1996). More recently, high spatial resolution ASTER data collected simultaneously with low resolution MODIS data on the NASA EOS Terra platform have been used to validate the MODIS active fire product (Morisette et al., 2005a; Morisette et al., 2005b; Csiszar et al., 2006).

The validation of burned area products is less sensitive to the need for simultaneous collection of independent reference data with satellite overpasses, as the surface effects of fire persist for a time varying between weeks (grassland ecosystems) to years (typically, forest ecosystems). Consequently, independent reference data derived from high spatial resolution satellite data, such as Landsat, have been used extensively to validate lower spatial resolution burned area products (e.g., Barbosa et al., 1999; Fraser et al., 2000; Roy et al., 2005b; Boschetti et al., 2006).

There are several outstanding issues in the development of robust regional to global scale fire product validation methodologies. These include the need to increase the quality and reduce the cost of validation by developing and promoting an international network of validation sites and by establishing validation standards and protocols (Morisette et al., 2002). Common validation sites would facilitate data sharing and can be expected, with the development of validation protocols, to foster standardization of the validation data and of the product accuracy reporting. Validation protocols are needed not as strict requirements but as suggested baseline approaches (Rasmussen et al., 2001). These issues are more pressing than ever with the prospects of operational fire products, for example from NPOESS data, and with a proliferation of global and regionally generated products.

A strategic GOFC-GOLD fire goal is to advocate and where possible facilitate the development of international validation standards and protocols for the validation of satellite active fire and burned area products, including: independent reference data definition and measurement; validation site selection and exchange of independent reference data collected at validation sites; statistical comparison of independent reference data and products; and product accuracy reporting. Despite the broadening recognition for these needs, and an emerging adoption of validation concepts by the fire product producer community, they have not yet been achieved.

23.2.9 To Operationally Generate Fire Emission Product Suites of Known Accuracy Providing Annual and Near Real-Time Emission Estimates with Available Input Data Sets

23.2.9.1 Current Status

The common approach used in land-based emission quantifications relies on a combination of satellite burned area information, modeled fuel load amounts, estimates of combustion completeness and ground and/or airborne measured emission factors (Hoelzemann et al., 2004; Ito and Penner, 2004; van der Werf et al., 2004). The improvements in spatially and temporally explicit regional to global emissions modeling have been rather incremental and have been hampered by the lack of the reliable underlying datasets. The recent availability of two global satellite-based burned area products, GBA-2000 (Tansey et al., 2004) and GLOBSCAR (Simon et al., 2004) for the year 2000 has provided an opportunity for generating new global emissions estimates. A global MODIS burned area algorithm has also been implemented and validated over several regions in the world (Roy et al., 2002b; 2005a; 2005b). However, several studies have highlighted the pressing need for rigorous validation of these satellite burned area products (see Sect. 23.2.8). Further improvements in the burned area products require biome/regional specific representative information.

Considering the advances in burned area mapping, likely the largest persistent challenge in global emissions modeling is the spatiotemporal quantification of different fuel types available for burning. Interannual variations in fuel loads at regional scales are also largely unknown and require a dynamic modeling approach. Biogeochemical models have been applied to assess fuel loads that are higher when compared with a handful of field measurements in Southern Africa (van der Werf et al., 2003). Satellite measures of global net primary productivity (e.g., MODIS, GLOPEM model) adjusted by region specific available fuel maps (e.g., fuel map of Malaysia and Western Indonesia by Dymond et al., 2004) and validated through regionally representative field measurements can provide the means to estimate fuel loads more accurately.

Current global emission models do not adequately account for burning of organic matter present in peatlands and boreal regions which release significant amounts of carbon into the atmosphere (Page et al., 2002; Soja et al., 2004). The capability to map these low energy peat fires and estimate the fire release energy has been developed locally using the high resolution experimental BIRD Infrared sensor (Wooster et al., 2003; Siegert et al., 2004). Similar mapping methodologies for large scale peatland fire events using suitable operational sensors remain to be developed.

Large woody fuels can be an important fuel load component especially in tropical regions, with significant implications for smoldering emissions (Bertschi et al., 2003). Tree mortality has been incorporated to some extent in current global emissions models but is still highly uncertain. Other forms of potential fuel load alteration whether natural (e.g., herbivory, insects, fuel decay) or anthropogenic (e.g., fuel load removal by humans, forest clearance, agriculture, rangeland management) also warrant improvements in their implementation in fuel load models. Information of fire frequency/return is also pertinent to quantifying fuel accumulation since the last fire event in a particular location. The establishment of consistent time-series of long-term satellite fire records from different sensors is required to investigate fire regimes (see Sect. 23.2.5).

The fire and atmospheric science community has made considerable advances in the knowledge of emission factors for various important atmospheric species from vegetation fires in major biomes (Andreae and Merlet, 2001). Some important gaps exist though. The seasonal variations in emission factors and combustion completeness can be significant and have not been thoroughly addressed in global emissions models partially also due to the very limited number of existing early dry season measurements (Hoffa et al., 1999; Korontzi et al., 2003). The importance of accounting for the seasonal variations in emission factors and combustion completeness has been shown for southern African savanna fires (Korontzi, 2005). A compelling need for the prediction of these seasonal variations is the reliable assessment of the fuel moisture content which can be estimated from satellite observations (Zarco-Tejada et al., 2003; Chuvieco et al., 2004). There is still a lack of adequate field measurements for important compounds, such as acetonitrile and hydrogen cyanide. The improved characterization of nitrogen, sulfur and halogen containing fire emitted compounds requires the development of seasonal fuel chemistry databases.

23.2.9.2 Future Plans

In the future, national or regional fire analysis and data information service centers may provide the institutional environment for the operational production of these emissions model outputs. The methodologies, roles and responsibilities for transferring the experimental emissions estimates to the operational domain are still undeveloped. A critical step in the transition of the emission model outputs to their operational production on a continuous basis will be to determine their accuracy. Rigorous sensitivity analyses at the regional scale can provide explicit information as to which parameters add the most uncertainty (French et al., 2004) and priorities for improvements. The synergistic use of different products made available for the same region has to rely on standard guidelines and protocols for product accuracy assessment intended for optimal use in emissions models. Atmospheric modelers have started to utilize the land based emissions estimates in inverse modeling studies (van der Werf et al., 2004; Arellano et al., 2004). Approaches that integrate land-based emissions models with atmospheric chemistry/transport models will be the key to improve emissions on a global scale and will be most useful to the community. This is especially true considering the still unresolved discrepancy between these two approaches for emissions estimation.

Other currently experimental satellite based measurements of the fire radiative energy may offer an important new way of directly estimating the amount of fuel consumed which needs to be further explored (Kaufman et al., 1998; 2003; Wooster, 2002; Wooster et al., 2003; Siegert et al., 2004; Ichoku and Kaufman, 2005).These techniques have been successfully tested at local to regional scales and are currently being developed at a global scale. Satellite based techniques for direct estimation of trace gases (e.g., CO, CH_4) (McMillan et al., 2005) and aerosol loading (e.g., Kaufman et al., 1998; 2003) are also being developed.

23.3 Example Contributory Activities from US Agencies

23.3.1 NASA Wildfire Activities

NASA's research, analysis, and applied science activities associated with wildfire fall within both the Research and Analysis and Applied Sciences programs. The NASA Earth Science Division is divided into focus areas with wildfire as an important terrestrial process that cuts across a number of these e.g. carbon cycle, ecosystems and land use change, atmospheric composition, water cycle and land cover . The NASA Land Cover and Land Use change program has been a strong supporter of the GOFC-GOLD Fire program, providing outreach for NASA research and data products and assisting the GOFC regional fire networks to access and utilize NASA data. In the NASA science program, satellite fire data are being used for example, to assess recent trends in global fire activity, to model annual trace gas and particulate emissions, to examine the relationship between fire and climate change, to model land use change and project the future changes in fire regimes (Korontzi et al., 2004; van der Werf et al., 2004). From the atmospheric science perspective NASA is studying the role of particulates generated by fires in cloud formation and global radiative forcing. These science studies are couched within the framework of the US Climate Change Science Program (CCSP) and the US Global Earth Observations (USGEO). In support of these science studies, NASA provides funding for algorithm development, product generation, validation and benchmarking of research results e.g. (Justice et al., 2002). Current emphasis within the science program is to develop long-term data records to enable the study of global change. New techniques are also being developed using airborne Lidar to estimate vegetation structure and fuel load in anticipation of a future spaceborne vegetation Lidar missions.

The NASA Applied Science program has two main themes, transitioning NASA research into the operational domain, and using NASA research results to enhance decision support systems and tools for fire management. To help achieve the goal of integrating data and models into decision support systems, NASA is partnering with the USDA Forest Service Remote Sensing and Applications Center (RSAC). With the Forest Service, emphasis has been given to support the provision of NASA data to the National Interagency Fire Center (NIFC), for example through the MODIS Rapid Response System (see Sect. 3.3). Satellite data along with airborne sensors and platforms are being used for assessing fire danger, monitoring fires in near real time and assessing post-fire impacts. New technologies for improving fire observations have been developed under the recent Sensor Web project. The goal of this project is to link the NASA spaceborne systems in an automated way, so that coarse resolution fire detection systems can direct the acquisition of data from the next high resolution sensor overpass. The prototype for this system was developed using MODIS and Earth Observer (EO-1) sensor. NASA has also been experimenting with the use of Unmanned Aerial Systems (UAS) in support of fire management under the Wildfire Research and Applications Partnership (WRAP) funded by NASA's Research Education and Applications Solutions Network (REASoN Cooperative Agreement). Seamless data from the Shuttle Radar Topography Mission (SRTM) are also integrated to improve geo-correction of sub-orbital data sets. Support was given to the U. S. Forest Service this past fire season and created a Western States Fire Mission that coincidently provided support to the Esperanza and Southern California Fire events in 2003 and 2007, respectively.

23.3.2 NOAA Wildfire Activities

The Hazard Mapping System (HMS; NOAA, 2008), developed and run operationally by NOAA's Satellite Services Division (SSD), is a multiplatform RS approach to detecting fires and smoke over the US and adjacent areas of Canada and Mexico. The system utilizes sensors on seven different NOAA and NASA satellites. Automated fire detections are incorporated into the system from GOES through the Wildfire Automated Biomass Burning Algorithm (WF-ABBA) (Prins and Menzel, 1996), AVHRR (Li et al., 2001) and MODIS (Giglio et al., 2003). Automated detection algorithms are employed for each of the satellites for the fire detects while smoke is delineated by an image analyst. Analyses are quality controlled by an analyst who inspects all available imagery and automated fire detects, deleting suspected false detects and adding fires that the automated routines miss. Graphical, text, and GIS compatible analyses are posted to a web site as soon as updates are performed, and a final product for a given day is posted early the following morning. All products are archived at NOAA's National Geophysical Data Center. Daily fire and smoke analyses are available on-line (NOAA, 2008).

Areal extent of detectable smoke is outlined using animated visible imagery, for input to a dispersion and transport model, the HYbrid Single-Particle Lagrangian Integrated Trajectory (HYSPLIT), developed by NOAA's Air Resources Laboratory (ARL). Resulting smoke forecasts will be used as input to NOAA's Air Quality forecasts. The GOES Aerosol and Smoke Product (GASP) is an experimental GOES imagery based aerosol optical depth product developed by the NESDIS Office of Research and Applications, being implemented for operational use by the NESDIS Satellite Analysis Branch for use in smoke and volcanic ash monitoring. GASP products are available on-line (GASP, 2004).

NOAA's Operational Significant Event Imagery (OSEI, 2008) program processes satellite imagery of environmentally significant events, including fire, smoke and volcanic ash, visible in operational satellite data. This imagery is often referred to by fire managers and air quality agencies.

NOAA's future plans include the integration of high resolution global data from the European Space Agency's MetOp satellite, integration of more ancillary data layers, and better characterization of fire emissions for input to air quality models. Ongoing research in NESDIS' Center for Satellite Applications and Research (STAR) will provide means to estimate smoke concentrations and trace gas characterization by incorporating data from RS sources as they become available, such as the Ozone Monitoring Instrument (OMI) and VIIRS.

23.3.3 USDA Forest Service Wildfire Activities

The USDA Forest Service is currently using a combination of satellite and airborne RS systems to map and monitor active wildland fires, and to map burn severity for post-fire rehabilitation. RS systems are used to provide national scale—strategic planning level, and local scale—tactical incident level fire maps and products.

National scale, strategic planning fire maps are developed using the NASA MODIS sensor, direct broadcast capability, and Rapid Response System. The system utilizes Western United States MODIS data acquired in real time by the RSAC MODIS Direct Broadcast receiving station in Salt Lake City, Utah and near real time MODIS data for the Eastern United States and Alaska from the NASA GSFC. Both day and night time data are collected. These data are used to prepare active fire maps and geospatial data continuously for the entire United States and Canada. These maps and data are made available to fire managers and the public through the internet and have proved to be useful for monitoring actively burning fires, assisting in planning, allocating fire suppression resources, and informing the public on current fire activity across the nation (USDA, 2005).

National scale active fire maps are intended to provide accurate and current information to assist wildfire managers in strategic planning. The information is used to make decisions on where and when to allocate critical fire suppression resources, such as high resolution airborne thermal infrared fire mapping systems at NIFC. The national scale active fire maps allow managers to prioritize fire mapping needs and prepare flight plans for airborne thermal infrared systems.

For local planning, fire managers require higher spatial resolution fire map products to support decisions such as where to place fire crews or airborne retardant drops. Tactical scale, finer resolution fire maps, and geospatial data are provided to Incident Command fire suppression teams to assist in tactical level planning. A combination of airborne Forward Looking Infrared (FLIR), thermal imagers, and high resolution thermal infrared line scanner systems are used to acquire detailed imagery and data for quick response fire mapping products. These products are used to brief Incident Command staff and support local decisions on where fire suppression assets should be used.

Satellite and airborne RS systems are used to quickly map burn severity and prioritize areas for re-vegetation and erosion control treatments. To mitigate the effects of wildland fire on soil and duff layers, the Forest Service and other federal land management agencies prepare Burned Area Emergency Response (BAER) plans to stabilize soils and return vegetation cover to the burned areas as soon as possible. One of the first steps in the BAER process is the creation of a map that highlights the areas most in need of immediate erosion control and other protection measures. Traditionally this map was created by airborne sketch mapping in combination with field surveys. Recently, techniques have been developed using airborne and satellite RS imagery to derive base maps to improve the accuracy of the initial burn severity product. These base maps have included mosaicked digital camera images and satellite imagery such as IKONOS, SPOT, Landsat TM, ASTER, and MODIS.

RSAC provides field level BAER team members, arriving at an incident, with remotely sensed imagery, Burn Area Reflectance Classification (BARC) maps, and ancillary data. A BARC map is typically created using change detection on a band ratio such as the Normalized Burn Ratio (NBR) and the Normalized Difference Vegetation Index (NDVI). The BARC output is delivered to the field in two forms. One has four classes: High, Moderate, Low, and Unburned. The other has 255 discrete values and allows field users to make their own classification decisions such as altering the threshold values between burn severity categories. The BARC map, when used in conjunction with other geospatial data, provides a synoptic view of the burned area and allows for more consistent mapping decisions. The BARC data and remotely sensed imagery are commonly used to focus the reconnaissance efforts of the BAER team on areas of greatest concern, develop the BAER burn severity map, create 3-dimensional models of the burned area and visualization products, and prepare graphics for public meetings to show areas with increased erosion potential.

23.4 Conclusion

The GOFC-GOLD program has undertaken an ambitious agenda to improve the availability, accessibility and use of earth observation information. The program started from grass-roots concern amongst practitioners that the potential of satellite RS was not being realized, despite the overwhelming demand for environmental information. Since that time there has been a broadening recognition of the need for effective global earth observation. The program activities and structure established by GOFC-GOLD provide an important contribution to the emerging GEOSS which recognizes that in a rapidly changing world, there is the need for timely and up-to-date earth observations and information (GEOSS, 2005). The emergence of systematically generated and validated global fire products also provides the opportunity for a reliable Global Fire Assessment. Such an assessment is currently being coordinated by the GOFC-GOLD Implementation Team and the regional fire networks. The ultimate goal is to put in place sustained systems which are operational, providing reliable and consistent fire information to meet the needs of decision-makers, resource managers and global change scientists. We are a long way from achieving this goal but GOFC-GOLD is making considerable progress and has highlighted some of the necessary near-term and concrete steps to that end. The challenge in this time of limited budgets is for governments to make the necessary commitment to international coordination, utilizing the international programs such as GOFC-GOLD to facilitate and proceed with implementation.

References

Ahern F, Goldammer G, Justice CO, (2001), Global and Regional Vegetation Fire Monitoring From Space: Planning a Coordinated International Effort. SPB Academic Publishing, The Hague, The Netherlands

Andreae M, Merlet P, (2001), Emission of Trace Gases and Aerosols From Biomass Burning. *Global Biogeochemical Cycles*, **15**(4), 955 – 966

Arino O, Simon M, Piccolini I, Rosaz JM, (2001), The ERS-2 ATSR-2 World Fire Atlas and the ERS-2 ATSR-2 World Burnt Surface Atlas projects. In: Proceedings of the 8th ISPRS conference on physical measurement and signatures in remote sensing, http://shark1.esrin.esa.it/ionia/FIRE / references_fire.html

Arellano AF Jr, Kasibhatla PS, Giglio L, van der Werf GR, Randerson JT, (2004), Top-down estimates of global CO sources using MOPITT measurements, Geophysical. Research Letters, 31, L01104, doi:10.1029/2003GL018609

[AVIALESOOKHRANA] Aerial Forest Protection Service. 2005 Jan 2. Avialesookhrana Fire Monitoring home page: http://www.nffc.aviales.ru/engl/main.sht. accessed 2008 Jan 14

Barbosa PM, Stroppiana D, Grégoire JM, Pereira JMC, (1999), An assessment of vegetation fire in Africa (1981 – 1991): Burned areas, burned biomass, and atmospheric emissions. *Global Biogeochemical Cycles*, **13**: 933 – 950

Bertschi I, Yokelson RJ, Ward DE, Babbitt RE, Susott RA, Goode JG, Hao WM, (2003), Trace gas and particle emissions from fires in large diameter and belowground biomass fuels, *Journal of Geophysical. Research*, **108**(D13): 8472, doi:10.1029/2002JD002100

Boschetti L, Eva H, Brivio PA, Grégoire JM, (2004), Lessons to be learned form the intercomparison of three satellite-derived biomass burning datasets. *Geophysical Research Letters*, **31**(21): L21501 10.1029/2004GL021229

Boschetti L, Brivio PA, Eva H, Gallego J, Baraldi A, JM Grégoire, (2006), A Sampling Method for the Retrospective Validation of Global Burned Area Products. *IEEE Transactions on Geoscience and Remote Sensing*, **44**(7): 1765 – 1773 Digital Object Identifier 10.1109/TGRS.2006.874039

Briess K, Jahn H, Lorenz E, Oertel D, Skrbek W, Zhukov B, (2003), Remote Sensing Potential of the Bi-spectral InfraRed Detection (BIRD) Satellite. *International Journal of Remote Sensing*, **24**: 865 – 872

Cardoso MF, Hurtt GC, Moore B, Nobre CA, Bain H, (2005), Field work and statistical analyses for enhanced interpretation of satellite fire data. *Remote Sensing of Environment*, **96**: 212 – 277

Carmona-Moreno C, Belward A, Malingreau J-P, Garcia-Alegre M, Hartley A, Antonovskiy M, Buchshtaber V., Pivovarov V, (2005), Characterizing Inter-annual Variations in Global Fire Calendar Using Data from Earth Observing Satellites. *Global Change Biology*, **11**(9): 1537 – 1555

Chuvieco E, Cocero D, Riaño D, Martin P, Martínez-Vega J, de la Riva J, Pérez F, (2004), Combining NDVI and surface temperature for the estimation of live fuel moisture content in forest fire danger rating. *Remote Sensing of Environment*, **92**(3): 322 – 331

[CONABIO] Comisión nacional para el conocimiento y uso de la biodiversidad. 2007 Jan 10. CONABIO Fire detection home page: http://www.conabio.gob.mx/conocimiento/hotspots/doctos/puntos_calor.html, accessed 14 Jan 2008

Csiszar I, Abdelgadir A, Li Z, Jin J, Fraser R, Hao WM (2003) Interannual changes of active fire detectability in North America from long-term records of the Advanced Very High Resolution Radiometer. *Journal of Geophysical Research* **108**(D2), 4075. doi:10.1029/2001JD001373

Csiszar I, Denis L, Giglio L, Justice CO, Hewson J, (2005a), Global Fire Activity from two years of MODIS data. *International Journal of Wildland Fire*, **14**: 117 – 130

Csiszar I, Justice CO, McGuire AD, Cochrane MA, Roy DP, Brown F, Conard SG, Frost PGH, Giglio L, Elvidge C, Flannigan MD, Kasischke E, McCrae DJ, Rupp TS, Stocks BJ, Verbyla DL, (2005b), Land use and fires. In: Land Change Science: Observing, Monitoring, and Understanding Trajectories of Change on the Earth's Surface. Kluwer Academic Publishers, 329 – 350

Csiszar I, Morisette JT, Giglio L, (2006), Validation of active fire detection from moderate resolution sensors: the MODIS example in Northern Eurasia. *IEEE Transactions on Geoscience and Remote Sensing*, **44**(7): 1757 – 1764

de Groot WJ, Field RD, Brady MA, Roswintiarti O, Mohamad M, (2007), Development of the Indonesian and Malaysian fire danger rating systems. *Mitigation and Adaptation Strategies for Global Change*, **12**: 165 – 180, doi: 10.1007/s11027-006-9043-8

Dwyer E, Pinnock S, Grégoire JM, (2000), Global spatial and temporal distributions of vegetation fire as determined from satellite observations. *International Journal of Remote Sensing*, **21**:1289–1302. doi:10.1080/014311600210182

Dymond CC Roswintiarti O, Brady M, (2004), Characterizing and mapping fuels for Malaysia and western Indonesia. *International Journal of Wildland Fire*, **13**(3) 323 – 334

Elvidge CD, Nelson I, Hobson VR, Safran J, Baugh KE, (2001), Detection of fires at night using DMSP-OLS data. Global and Regional Vegetation Fire Monitoring from Space: Planning a Coordinated International Effort. Edited by Ahern FJ, Goldammer JG, Justice CO. SPB Academic Publishing, The Hague, The Netherlands, 125 – 144

FAO, (1986), Wildland Fire Management Terminology. Food and Agriculture Organization of the United Nations, FAO Forestry Paper, 70 – 257

FAO, (2006), Global Forest Resources Assessment 2005. Food and Agriculture Organization of the United Nations, FAO Forestry Paper, 147

Field, RD, Wang Y, Roswintiarti O, Guswanto, (2004), A drought-based predictor of recent haze events in western Indonesia, *Atmospheric Environment*, **38**: 1869 – 1878

Fraser RH, Li Z, Cihlar J, (2000), Hotspot and NDVI differencing synergy (HANDS): A new technique for burned area mapping over boreal forest. *Remote Sensing of Environment*, **74**: 362 – 376

French NHF, Goovaerts P, Kasischke ES, (2004), Uncertainty in estimating carbon emissions from boreal forest fires. Journal of Geophysical Research 109 D14S08, doi:10.1029/2003JD003635

[GASP] National Oceanic and Atmospheric Administration. 2004 May 21. GOES Aerosol/Smoke Product home page: http://www.ssd.noaa.gov/PS/FIRE/GASP/gasp.html, accessed 2008 Jan 14

[GEOSS] Global Earth Observation System of Systems. Date of latest revision unknown. GEOSS home page: http://earthobservations.org/, accessed 2008 Jan 14

[GFMC]. Global Fire Monitoring Center. Updated daily. Current & Archived Significant Global Fire Events and Fire Season Summaries. Near-Real Time and Daily Updates by GFMC Partners. http://www.fire.uni-freiburg.de/current/globalfire.htm, accessed 2008 Jan 14

Giglio, L, Descloitres, J, Justice, CO, Kaufman, Y, (2003), An enhanced contextual fire detection algorithm for MODIS. *Remote Sensing of Environment*, **87**: 273 – 282

Giglio, L, Csiszar, I, Justice, CO, (2006), Global distribution and seasonality of active fires as observed with the Terra and Aqua MODIS sensors. *Journal of Geophysical Research—Biogeosciences*, **111**, G02016, doi:10.1029/2005JG000142

[GLOBCARBON] European Space Agency. 2008 Jan 9. GLOBCARBON home page: http://dup.esrin.esa.it/projects/summaryp43.asp, accessed 2008 Jan 14

[GMES] European Space Agency. Date of latest revision unknown. Global Monitoring for Environment and Security Living Planet Programme home page: http://www.esa.int/esaLP/LPgmes.html, accessed 2008 Jan 14

[GOFC] Global Observation of Forest Cover/Global Observation of Landcover Dynamics. 2007 Apr 16. GOFC-GOLD home page: http://www.fao.org/gtos/gofc-gold/index.html, accessed 2008 Jan 14

[GOFC FIRE] University of Maryland. Date of latest revision unknown. GOFC-GOLD Fire Implementation Team home page: http://gofc-fire.umd.edu/, accessed 2008 Jan 14

[GTOS] Global Terrestrial Observing System. 2005 May 18. GTOS home page: http://www.fao.org/gtos/, accessed 2008 Jan 14

[GWFNa] Global Fire Monitoring Center. Date of latest revision unknown. Global Wildland Fire Network home page: http://www.fire.uni-freiburg.de/GlobalNetworks/globalNet.html, accessed 2008 Jan 14

[GWFNb] Global Fire Monitoring Center. Date of latest revision unknown. Global Wildland Fire Network: Rationale and Introduction. http://www.fire.uni-freiburg.de/GlobalNetworks/RationaleandIntroduction. html, accessed 2008 Jan 14

Hoelzemann JJ, Schultz MG, Brasseur GP, Granier C, Simon M, (2004), Global Wildland Fire Emission Model (GWEM): Evaluating the use of global area burnt satellite data, Journal of Geophysical Research 109, D14S04, doi:10.1029/2003JD003666.

Hoffa, E, Ward D, Hao WM, Susott R, Wakimoto R, (1999), Seasonality of carbon emissions from biomass burning in a Zambian savanna. *Journal of Geophysical Research* **104**(D11): 13841 – 13853

Howard SM, Lacasse JM, (2004), An Evaluation of Gap-Filled Landsat SLC-Off Imagery for Wildland Fire Burn Severity Mapping. *Photogrammetric Engineering and Remote Sensing*, **70**(8): 877 – 880

[INPE] Instituto Nacional de Pesquisas Espaciais. Updated daily. INPE Fire home page: http://www.cptec.inpe.br/products/queimadas, accessed 2008 Jan 14

Ichoku C, Kaufman Y, (2005), A method to derive smoke emission rates from MODIS fire radiative energy measurements. *IEEE Transactions on Geoscience and Remote Sensing*, **43**(11): 2636 – 2649

Irons JR, Ochs WR, (2004), Status of the Landsat Data Continuity Mission. 2004 IEEE International Geoscience and Remote Sensing Proceedings. Anchorage, AK, September 20 – 24, 2004

Irons JR, (2005), Status of the Landsat Data Continuity Mission. A presentation at NASA's Land Cover Land Use Change Science Team Meeting. College Park, MD, January 11 – 13, 2005

Ito A, Penner JE, (2004), Global estimates of biomass burning emissions based on satellite imagery for the year 2000, *Journal of Geophysical Research*, **109**: D14S05, doi:10.1029/2003JD004423

Justice CO, Belward A, Morisette J, Lewis P, Privette J, Baret F, (2000), Developments in the 'validation' of satellite sensor products for the study of land surface. *International Journal of Remote Sensing*, **21**: 3383 – 3390

Justice CO, Giglio L, Korontzi S, Owens J, Morisette JT, Roy DP, Descloitres J, Alleaume S, Petitcolin F, Kaufman YJ, (2002), The MODIS fire products. Remote Sensing of Environment **83**: 244 – 262. doi:10.1016/S0034-4257(02)00076-7

Justice CO, Smith R, Gill M, Csiszar I, (2003), Satellite-based Fire Monitoring: current capabilities and future directions. *International Journal of Wildland Fire*, **12**: 247 – 258

Kaufman YJ, Justice CO, Flynn LP, Kendall JD, Prins EM, Giglio L, Ward DE, Menzel WP, and Setzer AW, (1998), Potential global fire monitoring from EOS-MODIS. *Journal of Geophysical Research*, **103**: 32, 215 – 232, 238

Kaufman Y, Ichoku C, Giglio L, Korontzi S, Chu DA, Hao WM, Li RR, Justice CO, (2003), Fires and smoke observed from the Earth Observing System MODIS instrument: products, validation, and operational use. *International Journal of Remote Sensing*, **24**: 1765 – 1781

Korontzi S, Ward DE, Susott RA, Yokelson RJ, Justice CO, Hobbs PV, Smithwick EAH, Hao WM, (2003), Seasonal variation and ecosystem dependence of emission factors for selected trace gases and PM 2.5 for southern African savanna fires. *Journal of Geophysical Research*, **108**(D24): 4758, doi:10.1029/2003JD003730

Korontzi S, Roy DP, Justice CO, Ward DE, (2004), Modeling and sensitivity analysis of fire emissions in southern Africa during SAFARI 2000. *Remote Sensing of Environment*, **92**(2): 255 – 275

Korontzi S, (2005), Seasonal patterns in biomass burning emissions from southern African vegetation fires for the year 2000. *Global Change Biology*, **11**: 1680 – 1700

Li, Z, Kaufman, Y, Ichoku, C, Fraser, R, Trishchenko, A, Giglio, L, Jin, J, Yu, X, (2001), A review of AVHRR-based fire active fire detection algorithm: Principles, limitations, and recommendations, in Global and Regional Vegetation Fire Monitoring from Space, Planning and Coordinated International Effort (Eds. F. Ahern, J.G. Goldammer, C. Justice) SPB Academic Publishing, The Hague, The Netherlands, 199 – 225

Lorenz E, Briess K, Halle W, Kayal H, Oertel D, Skrbek W, Zhukov B, Leibrandt W, (2003), BIRD—A Technology Demonstrator Dedicated to the Fire Hazard Detection and Monitoring. Proceedings of 30th International Symposium on Remote Sensing of Environment, Information for Risk Management and Sustainable Development, Honolulu, Hawaii, November 10 – 14, 2003

[LP DAAC] US Geological Survey. 2007 Jul 25. Land Processes Distributed Active Archive Center home page: http://edcdaac.usgs.gov/main.asp, accessed 2008 Jan 14

McMillan WW, Barnet C, Strow L, Chahine MT, McCourt ML, Warner JX, Novelli PC, Korontzi S, Maddy ES, Datta S, (2005), Daily global maps of carbon monoxide from NASA's Atmospheric Infrared Sounder. *Geophysical Research Letters*, **32**: L11801, doi:10.1029/2004GL021821

Merrill DF, Alexander ME, (1987), Glossary of forest fire management terms. Fourth edition. National Research Council of Canada, Canadian Committee on Forest Fire Management, Ottawa, Ontario, Publication NRCC No. 26516, 91

[MLRR]. National Aeronautics and Space Administration. Updated daily. MODIS Land Rapid Response System home page: http://rapidfire.sci.gsfc.nasa.gov, accessed 2008 Jan 14

Morisette JT, Privette JL, Justice CO, (2002), A framework for the validation of MODIS land products. *Remote Sensing of Environment*, **83**: 77 – 96

Morisette JT, Giglio L, Csiszar I, Setzer A, Schroeder W, Morton D, Justice CO, (2005a), Validation of MODIS active fire detection products derived from two algorithms. *Earth Interactions* **9**: 1 – 25

Morisette JT, Giglio L, Csiszar I, Justice CO, (2005b), Validation of MODIS active fire product over southern Africa with ASTER data. *International Journal of Remote Sensing*, **26**(10): 4239 – 4264

[NOAA] National Oceanic and Atmospheric Administration. Updated daily. Hazard Mapping System home page: http://www.ssd.noaa.gov/PS/FIRE/hms.html, accessed 2008 Jan 14

[OSEI] National Oceanic and Atmospheric Administration Satellite and Information Service. Operational Significant Event Imagery home page: http://www.osei.noaa.gov/, accessed 14 Jan 2008

Page SE, Siegert F, Rieley JO, Boehm HDV, Jaya A, Limin S, (2002), The amount of carbon released from peat and forest fires in Indonesia during 1997. *Nature*, **420** (6911): 61 – 65

Pereira AC, Setzer AW, (1996), Comparison of fire detection in savannas using AVHRR's channel 3 and TM images. *International Journal of Remote Sensing*, **17**: 1925 – 1937

Prins, E.M., and W.P. Menzel, (1996), Investigation of biomass burning and aerosol loading and transport utilizing geostationary satellite data. Biomass Burning and Global Change, edited by J.S. Levine, pp. 65 – 72, The MIT Press, Cambridge, MA

Rasmussen K, Russell-Smith J, Morisette JT, (2001), Establishing a validation site network for remote sensing applications to fire research: a joint activity between GOFC-Fire and the LPV subgroup, White paper available at http://modis.gsfc.nasa.gov/MODIS/LAND/VAL/CEOS_WGCV/GOFC_LPV_fire_sites.pdf

Roy DP, Borak J, Devadiga S, Wolfe R, Zheng M, Descloitres J, (2002a), The MODIS land product quality assessment approach. *Remote Sensing of Environment*, **83**: 2 – 76

Roy DP, Lewis PE, Justice CO, (2002b), Burned area mapping using multi-temporal moderate spatial resolution data—a bi-directional reflectance model-based expectation approach. *Remote Sensing of Environment*, **8**(1 – 2): 263 – 286

Roy DP, Jin Y, Lewis PE, Justice CO, (2005a), Prototyping a global algorithm for systematic fire-affected area mapping using MODIS time series data. *Remote Sensing of Environment*, **97**: 137 – 162

Roy DP, Frost P, Justice CO, Landmann T, Le Roux J, Gumbo K, Makungwa S, Dunham K, Du Toit R, Mhwandagara K, Zacarias A, Tacheba B, Dube O, Pereira J, Mushove P, Morisette J, Santhana Vannan S, Davies D, (2005b), The Southern Africa Fire Network (SAFNet) regional burned area product validation protocol. *International Journal of Remote Sensing*, **26**: 4265 – 4292

[SACSA] Satellite Applications Center South Africa. Updated daily. SACSA home page: http://www.wamis.co.za/eskom/checkboxes/sa.htm, accessed 14 Jan 2008

Schroeder W, Morisette J, Csiszar I, Giglio L, Morton D, Justice CO, (2005), Characterizing Vegetation Fire Dynamics in Brazil Through Multi-Satellite Data: Common Trends and Practical Issues. *Earth Interactions*, **9**: 13

[SENTINEL] Commonwealth Scientific and industrial Research Organization. 2007 Aug 15. Sentinel home page: http://www.sentinel.csiro.au, accessed 14 Jan 2008

Sheffner, EJ, (1994), The Landsat Program: Recent History and Prospects. *Photogrammetric Engineering & Remote Sensing*, LX(6): 735 – 744

Siegert F, Zhukov B, Oertel D, et al., (2004), Peat fires detected by the BIRD satellite. *International Journal of Remote Sensing*, **25**(16): 3221 – 3230

Simon M, Plummer S, Fierens F, Hoelzemann JJ, Arino O, (2004), Burnt area detection at global scale using ATSR-2: The GLOBSCAR products and their qualification. Journal of Geophysical Research 109:D14S02, doi:10.1029/2003JD003622

Soja AJ, Cofer WR, Shugart HH, Sukhinin AI, Stackhouse PW, McRae DJ, Conard SG (2004) Estimating fire emissions and disparities in boreal Siberia (1998 – 2002). Journal of Geophysical Research 109:D14S06, doi:10.1029/2004JD004570

Tansey K, et al., (2004), Vegetation burning in the year 2000: Global burned area estimates from SPOT VEGETATION data. Journal of Geophysical Research **109**: D14S03, doi:10.1029/2003JD003598

[TERRANORTE] Russian Academy of Sciences Space Research Institute. Date of latest revision unknown. TerraNorte home page: http://terranorte.iki.rssi.ru/, accessed 2008 Jan 14

Townshend JRG, Justice CO, (2002), Towards operation monitoring of terrestrial systems by moderate-resolution remote sensing. *Remote Sensing of Environment*, **83**: 351 – 359

Townshend JRG, Justice CO, Skole DL, Belward A, Janetos A, Gunawan I, Goldammer J, Lee B, (2004), Meeting the goals of GOFC: an evaluation of progress and steps for the future. In: Gutman G, Janetos AC, Justice CO et al. (eds) Land Change Science: Observing, Monitoring and Understanding Trajectories of Change on the Earth's Surface. Kluwer Press, pp 31 – 51

[UNISDR] United Nations Interagency Strategy for Disaster Reduction Working Group.

Date of latest revision unknown. Wildland Fire home page: http://www.unisdr.org/eng/task%20force/tf-working-groups4-eng.htm, accessed 14 Jan 2008

[USDA] United States Department of Agriculture. 2005 Aug 8. US Department of Agriculture Forest Service Remote Sensing Application Center MODIS Active Fire Maps page: http://activefiremaps.fs.fed.us, accessed 14 Jan 2008

Van der Werf GR, Randerson JT, Collatz GJ, Giglio L, (2003), Carbon emissions from fires in tropical and subtropical ecosystems. *Global Change Biology*, **9**(4): 547 − 562

Van der Werf, GR, Randerson JT, Collatz GJ, Giglio L, Kasibhatla PS, Arellano AF, Olsen SC, Kasischke ES, (2004), Continental-Scale partitioning of fire emissions during the 1997 to 2001 El Nino/La Nina period. *Science*, **303**: 73 − 76

Van Wagner CE, (1987), Development and structure of the Canadian Forest Fire Weather Index System. Canadian Forest Service, Ottawa, ON. Forestry Technical Report, 35 − 37

[WFM] University of Maryland. Updated daily. Web Fire Mapper home page: http://maps.geog.umd.edu, accessed 14 Jan 2008

Wooster MJ, (2002), Small-scale experimental testing of fire radiative energy for quantifying mass combusted in natural vegetation fires. Geophysical Research Letters, **29**(21): 2027 − 2034

Wooster M, Zhukov B, Oertel D, (2003), Fire radiative energy release for quantitative study of biomass burning: derivation from the BIRD experimental satellite and comparison to MODIS fire products. *Remote Sensing of Environment*, **86**: 83 − 107

Zarco-Tejada PJ, Rueda CA, Ustin SL, (2003), Water content estimation in vegetation with MODIS reflectance data and model inversion methods. *Remote Sensing of Environment*, **85**(1): 109 − 124

Zhukov B, Briess K, Lorenz E, Oertel D, Skrbek W, (2003), BIRD Detection and Analysis of High-temperature Events: First Results. *Proc. SPIE*, **4886**: 160 − 171

Index